2022

Explorations In Novel Photochemical Modes Of Radical-Alkene Reactivity: My Piece Of The Pi

Mark Wesley Campbell
University of Pennsylvania

Explorations In Novel Photochemical Modes Of Radical-Alkene Reactivity: My Piece Of The Pi

Abstract

The formation of Csp3-Csp3 bonds is arguably the most critical yet challenging transformation in organicsynthesis. For many years the Michael addition, which utilizes highly reactivity organometallic carbon nucleophiles which are "poised to react", was used to achieve hydroalkylation of activated alkenes. Furthermore, this mode of reactivity also offered the potential to use other electrophiles to perform vicinal (1,2) alkene difunctionalization. Though effective in many contexts, this reaction is often plagued by functional group incompatibilities, poor 1,2 vs 1,4 addition selectivity and unstable precursors. In contrast to organometallic carbanions, carbon-centered radicals display markedly higher regioselectivly in additions to alkenes and demonstrate much improved chemoselectivity. The Giese addition utilizes carbon radicals, typically generated from alkyl halides via halogen atom abstraction, to engage in radical addition with activated alkenes. Unfortunately, the harsh conditions and reagents required for the radical chain mechanisms employed in Giese reactions restrict the transformation to alkene hydroalkylations with minimal functional group compatibility. However, several modes of photochemical catalysis can be used for radical generation which are significantly milder and more tolerant than typical radical initiation used in classical Giese addition protocols. These catalytic mechanisms offer the potential for further functionalization of radical addition intermediates opening the door a wide variety of alkene difunctionalizations with dramatically improve functional group compatibility compared to classical vicinal difunctionalizations. Herein are reported personal explorations in novel radical alkene reactions facilitated via photochemical modes of catalysis.

Degree Type

Dissertation

Degree Name

Doctor of Philosophy (PhD)

Graduate Group

Chemistry

First Advisor

Gary A. Molander

Keywords

Catalysis, Photochemistry

Subject Categories

Organic Chemistry

EXPLORATIONS IN NOVEL PHOTOCHEMICAL MODES OF RADICAL-ALKENE REACTIVITY:

MY PIECE OF THE π

Mark Wesley Campbell

A DISSERTATION

in

Chemistry

Presented to the Faculties of the University of Pennsylvania

in

Partial Fulfillment of the Requirements for the

Degree of Doctor of Philosophy

2022

Supervisor of Dissertation

_____

Gary A. Molander

Professor of Chemistry

Graduate Group Chairperson

_____

Daniel J. Mindiola

Brush Family Professor of Chemistry

Dissertation Committee

Marissa C. Kozlowski, Professor of Chemistry

Amos B. Smith, Rhodes-Thompson Professor of Chemistry

Jeffery D. Winkler, Merriam Professor of Chemistry

ACKNOWLEDGMENTS

First and foremost, I am grateful for the consistent support and guidance from Ph.D. advisor, Professor Gary A. Molander. Even before I was accepted to the graduate program I was inspired by the research program that Professor Molander had fostered. Throughout my doctoral studies he has pushed me to strive for excellence in my research with constructive criticism and consistent support. Through his leadership he has demonstrated to me how to develop creative solutions for "real-world" chemistry problems. I am especially grateful for the freedom he has given me to pursue my own ideas help guide with his invaluable expertise throughout these explorations.

Furthermore I would like to thank each of my committee members: Professors Marisa Kozlowski, Amos Smith and Jeffery Winkler. I had the opportunity to take courses with each of them during my first year in the graduate program which greatly increased my knowledge of organic chemistry and helped shape my style of research. In the subsequent years each of them has provided me with excellent advice and critiques throughout my studies.

I also want to thank Professor Osvaldo Guterriez and Mingbin Yuan for engaging in excellent collaborations with our research teams. With their computation studies I was able to learn so much more about my reactions and their detailed mechanisms. Both of them worked very hard to provide excellent insight into our chemistry and we had many fruitful discussions over the years.

Next, I must express my deepest gratitude toward all of the past and present members of the Molander group. From my first weeks in lab Dr. Christopher Kelly was a phenomenal mentor. I benefited tremendously not only from his broad knowledge of chemistry, research acumen and eloquent writing but also from his friendship. I would also like to thank Prof. Jun Yi and Dr. Dan Lippincott for being a wonderful friends, coworkers and even better basketball players. Viktor

Polities has been an excellent friend and companion from day one and a great coworker who taught me the value of "attention to detail" for which I am deeply grateful. I would like to thank Juliette Lipson for being a great first mentee whose intelligence and creativity were truly remarkable. I must thank Shivani Patel for being the greatest mentee, coworker and friend I could have asked for; every day in lab was filled with smiles and laughter because of her.

Finally I am forever grateful for the unyielding support from my family. Well before my first day as a Ph.D. student I had been instilled with the most wonderful examples of hard work, endurance and kindness from my father, mother and sisters. Additionally, my mother and father were never more than a phone call or even a day drive away, especially when I needed it most. Both of my sisters were so consistent in reminding me of their confidence in me which helped me get through more days than they know.

ABSTRACT

EXPLORATIONS IN NOVEL PHOTOCHEMICAL MODES OF RADICAL-ALKENE REACTIVITY:

MY PIECE OF THE π

Mark Wesley Campbell

Gary A. Molander

The formation of C_{sp3}-C_{sp3} bonds is arguably the most critical transformation in organic synthesis. For many years the Michael addition which utilizes highly reactivity organometallic carbon nucleophiles which are "poised to react" was used to achieve hydroalkylation of activated alkenes. Furthermore, this mode of reactivity also offered the potential to use other electrophiles to perform vicinal (1,2) alkene difunctionalization. Though effective in many contexts this reaction is often plagued by functional group incompatibilities, poor 1,2 vs 1,4 addition selectivity and unstable precursors. In contrast to organometallic carbanions, carbon radicals display much more selective reactivity, particularly with alkenes, and demonstrate much improved chemoselectivity. The Giese addition utilizes carbon radicals typically generated from alkyl halides via halogen atom abstraction to engage in hydroalkylation with activated alkenes. Unfortunately, the harsh conditions and reagents required for the radical chain mechanisms employed in Giese reactions restrict the transformation to alkene hydroalkylations with minimal functional group compatibility. However, several modes of photochemical catalysis can be used for radical generation which are significantly milder and more tolerance than typical radical initiation used in classical Giese addition protocols. These catalytic mechanisms offer the potential for further functionalization of radical addition intermediates opening the door a wide variety of alkene difunctionalizations with dramatically improved functional group compatibility compared to classical vicinal difunctionalizations. Herein are reported personal explorations in novel radical alkene reactions facilitated via photochemical modes of catalysis.

TABLE OF CONTENTS

List of Tables

List of Figures

Chapter 1: Overcoming challenges in C_{sp3}-C_{sp3} bond formation

1.1 Introduction: Michael and Giese Additions

The formation of new C-C bonds is arguably the most foundational transformation in organic synthesis. Throughout decades of research, the forging of C-C bonds has been mainly accomplished via unstable, functionalized precursors that are "poised to react" (highly nucleophilic or electrophilic) in polar, two-electron mechanisms. Among the most common of these C-C bond-forming processes is the conjugate addition of a carbon nucleophile into an electron-deficient olefin, typically referred to as a Michael addition. This mode of reactivity can be used to construct new C_{sp3}-C_{sp3}, C_{sp3}-C_{sp2} or C_{sp3}-C_{sp} bonds. Soft carbon nucleophiles, such as organocuprates, demonstrate excellent chemoselectivity for 1,4-addition over 1,2-addition into α,β-unsaturated aldehydes, ketones, esters, nitriles etc. (Figure 1.1).[1]

For many years such mechanisms were the standard protocol for the hydroalkylation, - alkenylation, or -arylation of activated alkenes. Later, it was realized that the anionic Michael addition intermediate could be trapped by electrophiles other than a proton. Many so-called "vicinal difunctionalization" strategies were thus performed in a two-step, one pot protocol with a variety of different electrophiles, dramatically increasing the modular nature of conjugate additions.[2] The bond disconnections of vicinal difunctionalizations can be identified in the retrosyntheses of many renowned natural products, offering a more streamlined approach to their total synthesis.[3] Although a remarkably enabling technology, the requisite organometallic nucleophiles employed in Michael additions have several major limitations. The highly reactive nature of these species imposes strict limitations on the functional groups that can be incorporated, necessitating the use of protecting groups and inefficient synthetic routes. Additionally, organocuprate reagents, which are the most commonly used, C_{sp3} nucleophiles, are

challenging to prepare, often unstable and offer a rather inadequate set of readily accessible

substructures as they are derived from organolithium and Grignard precursors.
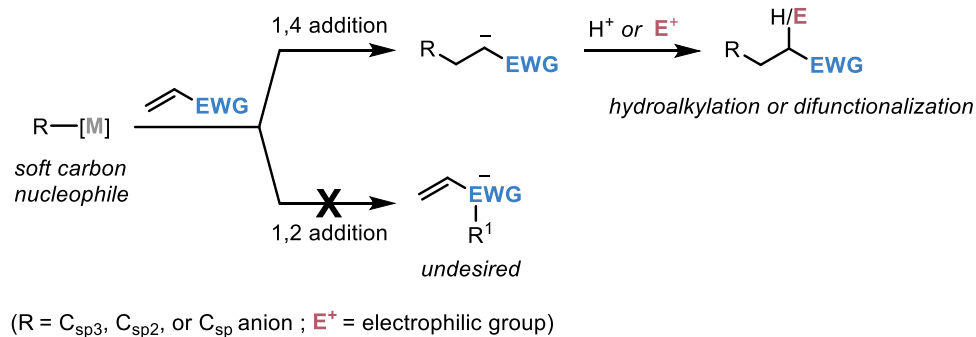
Figure 1.1. C-C bond formation via Michael addition strategies

Similar to stabilized carbanoin reagents used in Michael additions, carbon-centered free

radicals are also considered to be nucleophilic[4] and can undergo rapid conjugate addition into

electron-deficient alkenes in a process that is typically referred to as a Giese addition.[5] In contrast

to two-electron nucleophiles, carbon radicals demonstrate complete regioselectivity for 1,4-

addition rather than 1,2-addition to conjugated alkenes. Additionally, many electrophilic- or

acidic functional groups that are incompatible with organometallic nucleophiles used in Michael

additions provide minimal to no off-target reactivity in radical-mediated Giese additions.

Considering the superior chemoselectivity of carbon radicals it would seem that Giese additions

provide a comprehensive solution to the shortcomings of Michael additions. However, the

significant challenge associated with Giese additions is the generation of the desired carbon

radical. Generally, classical Giese additions are initiated via the homolysis of a catalytic species

(i.e., radical initiators) that commence a radical chain mechanism. Among the most common

modes of initiation are photolysis or thermolysis of labile bonds in precursors such as

azobisisobutyronitrile, di-*tert*-butyl peroxide, benzoyl peroxide or bis(tributyltin). The resulting radical fragments then engage in hydrogen atom transfer (HAT) with a tin- or silicon hydride species (Figure 1.2) which, in turn, performs halogen atom abstraction (HAA) on alkyl halides, producing the desired carbon radical. The alkyl radical will then undergo regioselective addition into an alkene. The radical chain is propagated via HAT between the Giese addition adduct and another molecule of tin hydride.

Though an intriguingly chemoselective mode of reactivity, the conditions employed in classical Giese addition protocols have many unattractive aspects. The radical initiators commonly employed are highly unstable, often expensive, and of varying degrees of purity that impacts reaction reproducibility. Because of explosion hazards, such protocols are impractical to perform on multi-gram scale, thus preventing the utilization of such transformations in industrial synthesis. The use of organostannanes also proves problematic for several reasons. In addition to their acute toxicity, the rate of stannyl radical addition to the alkene often outcompetes the desired halogen atom abstraction, and thus iodides and activated bromides typically are employed to minimize hydrostannylation of the alkene. Additionally, the homolytically labile Sn-H bond readily engages in hydrogen atom transfer with carbon-centered radicals, resulting in protodehalogenation of the alkyl halide radical precursor.[6] To ensure that the rate of carbon-centered radical addition outcompetes protodehalogenation, most classical Giese additions are intramolecular; intermolecular protocols typically require a large excess of either radical precursor or alkene.[7] Beyond alkyl halides there exists only a small set of alternative radical precursors, such as organoselenides[8] and xanthate esters[9], which offer a limited scope of accessible substructures. Finally, the mechanism of these processes requires that each Giese addition adduct engage in HAT with the tin hydride species to regenerate the stannyl radical and

3

sustain the chain, thus eliminating the possibility of performing any type of alkene difunctionalization.
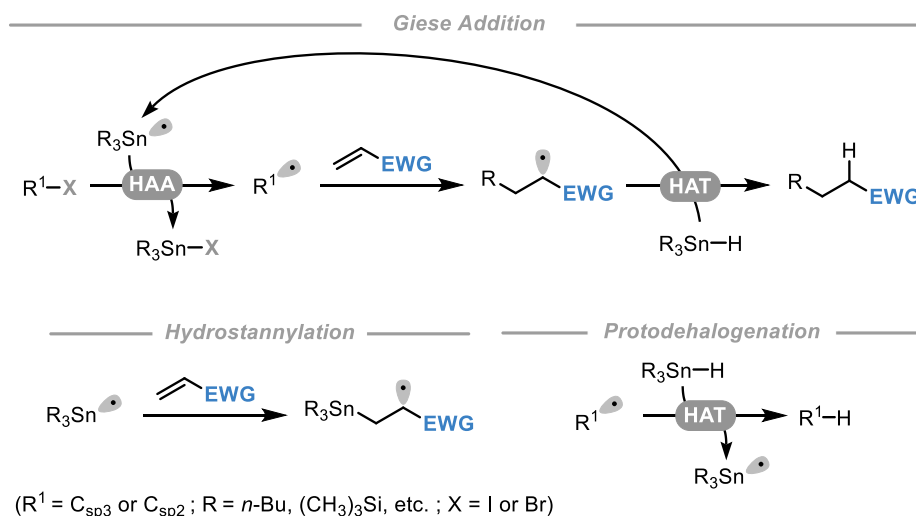
Figure 1.2. C-C bond formation via Giese addition strategies and prevalent side reactions

Though classical Giese additions have driven a significant amount of fundamental investigation into the mechanistic and kinetic aspects of radical-alkene reactivity and could be employed in specific instances in total synthesis, the problematic nature of classical radical generation has restricted the broad applicability of such methods. Although radical-based mechanisms, in theory, appeared to provide the ideal mode reactivity for hydroalkylation of activated alkenes, in reality, these reactions were severely limited because of their harsh conditions, impractical stoichiometry, and limited scope of radical precursors.

1.2. Alkene Hydroalkylation via Photochemical Catalysis

A recent resurgence of interest in photochemical transformations has facilitated the development of protocols that address the shortcomings of classical Giese addition reactions. Mechanisms relying on photoinduced electron-, energy- or atom transfer processes have been

4

developed for the catalytic generation of carbon radicals, circumventing the unattractive modes of radical generation previously employed in hydroalkylation reactions. The improved kinetic profile of such photocatalytic processes limits the off-target reactivity that impaired the efficiency of classical Giese additions. These novel strategies have also opened the door to a diverse suite of readily available, bench-stable radical precursors stemming from a wide range of feedstocks.

The most popular of the aforementioned modes of photochemical radical generation has been photoinduced electron transfer mechanisms, commonly referred to as photoredox catalysis. A general mechanism for the catalytic cycles of photoredox reactions is outline in Figure 1.3A. Following photoexcitation, a chromophore (PC) accesses a unique electronic configuration (PC*) in which single electron oxidation or reduction becomes facile. Chromophoric compounds that exhibit such excited state redox properties are referred to as photocatalysts. These excited state photocatalysts may engage in reductive quenching with an electron donor or via oxidative quenching with an electron acceptor (Figure 1.3). These electron donors/acceptors are typically alkyl fragments bearing functional groups that are susceptible to single electron transfer and subsequently undergo fragmentation, producing a carbon radical. Finally, the oxidized/reduced state photocatalyst will then engage in the inverse electron transfer to return to its original ground state, completing the catalytic cycle.
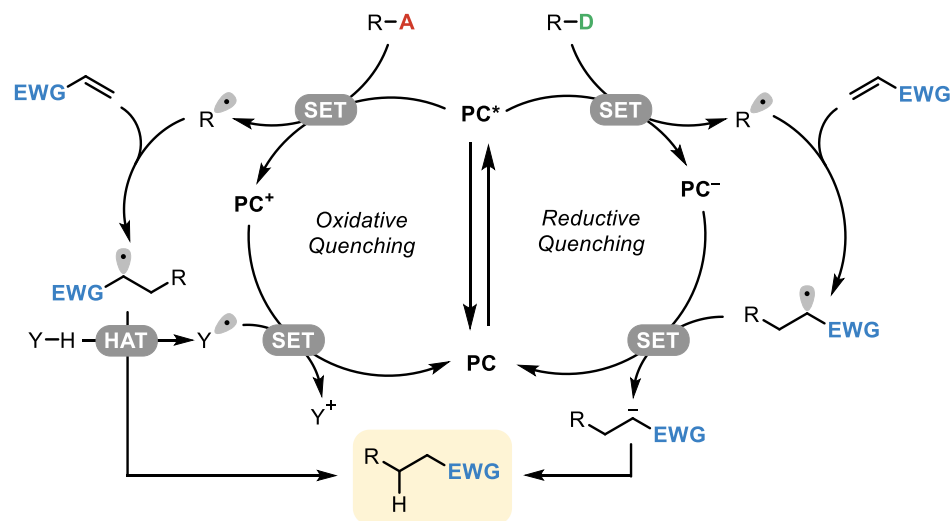
A = electron acceptor group ; D = electron donor group ; PC = photocatalyst ; SET = single electron transfer

Figure 1.3. A general mechanism for the photoredox-catalyzed hydroalkylation of activated alkenes

In the context of Giese additions, most mechanisms operate via reductive quenching of the photocatalyst to generate the desired alkyl radicals. After radical addition to the electron-deficient olefin, the resulting adduct then engages in single electron transfer with the reduced state photocatalyst (Figure 1.3), closing the redox cycle. The resulting anionic intermediate is then protonated, yielding the hydroalkylated product. Alternatively, some mechanisms leverage radical precursors that engage in oxidative quenching with the excited state photocatalyst, such as *N*-hydroxyphthalimide esters and alkyl halides. In these mechanisms, HAT between a labile Y-H bond and Giese adduct followed by oxidation of the radical fragment (Y$^{\bullet}$) with the oxidized state photocatalyst is typically employed to close the catalytic cycle. The non-toxic, bench stable photocatalysts employed in these strategies facilitate strictly regimented catalytic cycles, overcoming many of the limitations associated with the hazardous conditions required to initiate radical chain mechanisms in classical Giese additions. The remarkably functional group tolerant nature of photoredox reactions has fueled the development of many Giese addition protocols that can be employed in the synthesis of complex, functionally dense molecules. Overall, photoredox-

6

mediated hydroalkylations offer the inherent functional group tolerance of Giese additions while circumventing the harsh reaction conditions and off-target reactivity observed with the use of radical initiators and tin hydride radical mediators.

One of the earliest examples of a photoredox-mediated Giese addition was developed by Okada and co-workers in 1991. Utilizing a well-developed organometallic photocatalyst, Ru(bpy)$_3$PF$_6$, in concert with *N*-hydroxyphthalimide esters as a reductively generated source of alkyl radicals, hydroalkylation of methacrylate was accomplished (Figure 1.4A). Critical to the mechanism was the addition of a dihydropyridine, which functioned as an H-atom source and terminal reductant to complete the redox cycle.
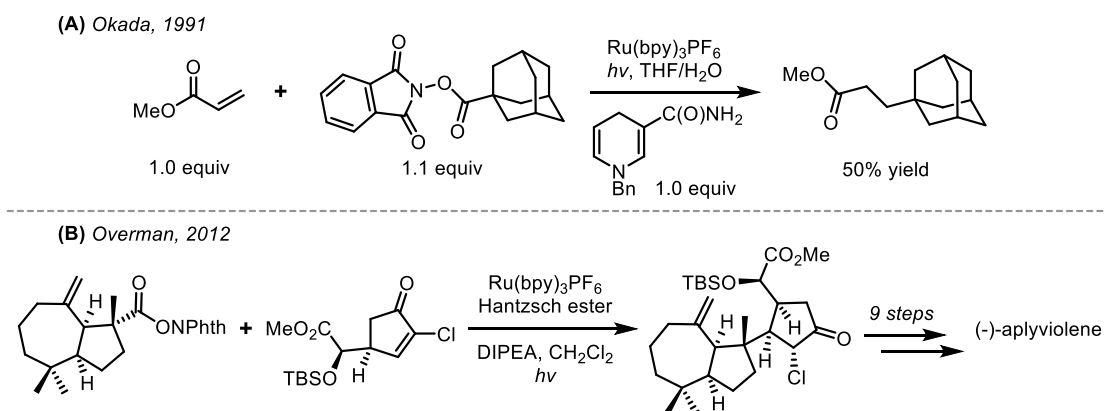
Figure 1.4. Photoredox hydroalkylation reactions using *N*-hydroxyphthalimide esters

This mode of reactivity was expanded by Hu,[10] König,[11] Kong,[12] and others to incorporate more complex and diverse *N*-hydroxyphthalimide esters derived from carboxylic acids in the hydroalkylation of synthetically useful alkenes. Application of this decarboxylative hydroalkylation in the construction of complex molecular architecture was demonstrated by Overman and coworkers in the total synthesis of (-)-aplyviolene (Figure 1.4B).[13] *N*-Hydroxyphthalimide esters are a particularly attractive functional group for the reductive

generation of radicals because the electron transfer occurs in the π-system of the phthalimide group, resulting in an essentially standard reduction potential independent of the alkyl substructure.[14] Another unique feature of *N*-hydroxyphthalimide esters is their ability to undergo reduction via electron donor-acceptor (EDA) complexes through π-π interactions with electron-rich substrates. These "photocatalyst-free" conditions have also been applied to the Giese additions with electron-deficient alkenes in small molecules[15] as well as solid-phase peptides,[16] demonstrating the extraordinary functional group tolerance and broad applicability of photoredox-mediated hydroalkylations.

Alkyl halides have also been employed as radical precursors in photoredox hydroalkylations. As the most common radical feedstock employed in tin hydride-promoted reactions, alkyl halides have been well adapted to photoredox-mediated Giese additions, offering a practical solution for classic radical hydroalkylation strategies. However, because of their more challenging reduction potentials, most substrates are limited to alkyl iodides and activated bromides,[17,18] though some conditions have been developed for radical generation from alkyl chlorides.[19] Perhaps the most dramatic example of an improved set of conditions for a hydroalkylation protocol was demonstrated in a report by Gagné and coworkers (Figure 1.5A).[20] Intermolecular hydroalkylation of α-glucosyl halides to produce C-alkyl glycosides was among the most impactful radical reactions of the 1980s, but typically required a 10-20 equivalent excess of the alkene (Figure 1.5B).[21] However, under the photoredox conditions developed by Gagné, which obviate the need for tin hydride species, only two equivalents of alkene was required to give excellent yields across a diverse range of bromoglycosides and activated alkenes.

(A) *Gagné, 2010*

(B) *Giese, 1983*
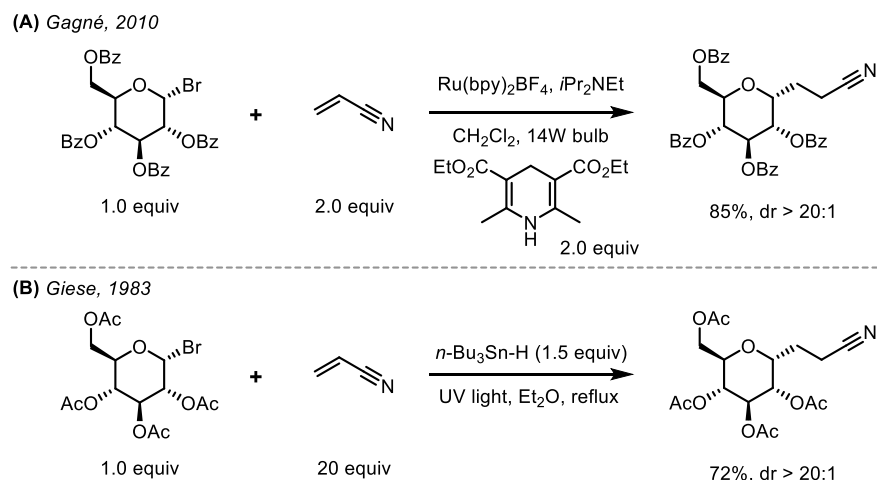
Figure 1.5. Giese additions of glycosyl halides via photoredox and tin hydride protocols

A range of protocols also exist for hydroarylation of activated alkenes with aryl radicals generated via reduction of electron-deficient aryl- and heteroaryl halides.[22] Alternatively, methods have been developed for the photoredox generation of silyl radicals (e.g., TMS$_3$Si$^•$), which can perform HAA from alkyl- or aryl halides, obviating the limitation of structure-based redox potentials.[23,24] More common protocols for radical hydroalkylation of alkenes with alkyl halides involve Ni or Mn catalysts,[25] some of which are photoactive metallic complexes.[26] Finally, a ground-breaking report merging the fields of photoredox and organocatalysis utilized activated bromides to perform the α-alkylation of aldehydes.[27] In this mechanism, reduction of alkyl bromides generated α-ester/ketone radicals, which are more electrophilic than typical alkyl radicals. These species underwent efficient addition into the nucleophilic enamine. This report served as a critical example of how photoredox catalysis offers modular reactivity to perform an umpolung version of the typical Giese addition (nucleophilic radical adding into an electron deficient alkene), which would be much more challenging under classical conditions.

9
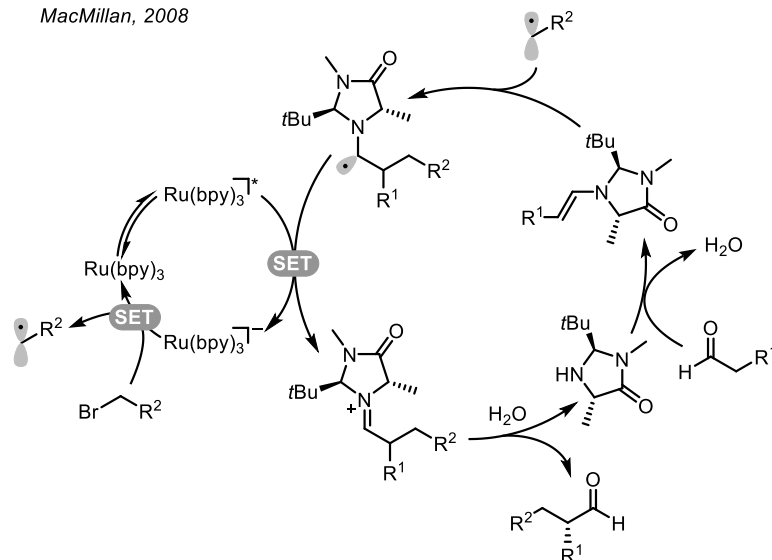
Figure 1.6. Enantioselective α-alkylation of aldehydes via photoredox/organocatalysis

In addition to radical precursors that fragment upon single electron reduction, many Giese addition methods have been developed using radical precursors that undergo single electron oxidation with an excited state photocatalyst. Among the most common of these radical precursor groups are trifluoroborates, carboxylic acids, α-silyl amines, and oxalates.

Trifluoroborates represent a highly atom economical radical precursor that can be prepared from many naturally abundant feedstocks, including alkyl halides, alkenes, and aldehydes. Akita and coworkers demonstrated the first use of organotrifluoroborates and cyclic alkyl(triol)borates as radical precursors for the hydroalkylation of electron-deficient alkenes (Figure 1.7A).[28] Later, Akita demonstrated that primary α-amino trifluoroborates underwent oxidative cleavage and Giese addition more readily than unstabilized substrates.[29] Finally, the utilization of a more strongly oxidizing organic dye (9-mesityl-10-methylacridinium perchlorate, Mes-Ac+) allowed the incorporation of primary unstabilized trifluoroborates in the hydroalkylation of activated alkenes under redox-neutral conditions.[30] Our own group has

10

demonstrated a unique defluorinative alkylation of α-trifluoromethyl alkenes using trifluoroborates as a source of radical precursors.[31] Hull and coworkers developed a broadly applicable protocol for the hydroalkylation of vinyl arenes using many different oxidatively labile radical precursors, including trifluoroborates.[32] Finally, trifluoroborates have also been incorporated into stereoselective Giese addition protocols. Meggers and coworkers developed a protocol using α,β-unsaturated acyl imidazoles in concert with trifluoroborates and a chiral Lewis acid catalyst to effect an enantioselective hydroalkylation (Figure 1.7B).[33]
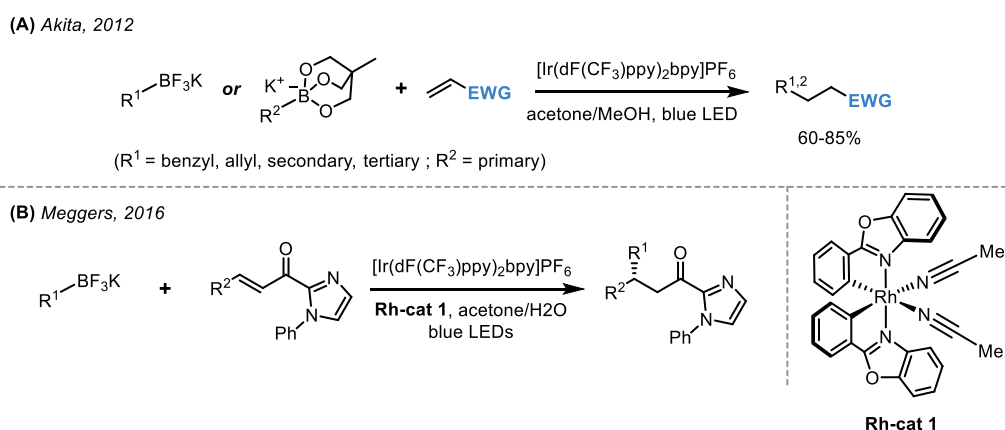
Figure 1.7. Photoredox catalyzed hydroalkylation of alkenes via borate radical precursors

Likely the most naturally abundant of all radical precursor groups are carboxylic acids, which can undergo radical decarboxylation after single electron oxidation to produce alkyl radicals. MacMillan and coworkers demonstrated that carboxylic acids could be utilized as an alkyl radical feedstock for Giese additions into activated alkenes. Though highly practical and economical, this report demonstrated that many primary and secondary alkyl carboxylates suffer from sluggish decarboxylation, and ultimately α-amino and α-alkoxy carboxylates are much more practical radical precursors. Several other unique carboxylates have been employed to incorporate "masked" groups that would be challenging if not impossible to engage with Giese acceptors. Cozzi and coworkers developed a method using 1,3-dithiane-2-carboxylate as a methyl group

11

surrogate after reductive desulfurization (Figure 1.8A),[34] while Xu and coworkers used glyoxylic

acid acetals as a formyl group equivalent after hydrolysis (Figure 1.8B).[35] Relying on the natural

abundance and excellent Giese addition reactivity of α-amino radicals, MacMillan and coworkers

extended their previous protocol for radical decarboxylation to the hydroalkylation of the C-

terminus of peptides.[36] The application of this reactivity to modification of macromolecules is a

remarkable advancement of photoredox chemistry that would have been unfeasible given the

previous Giese addition technology.
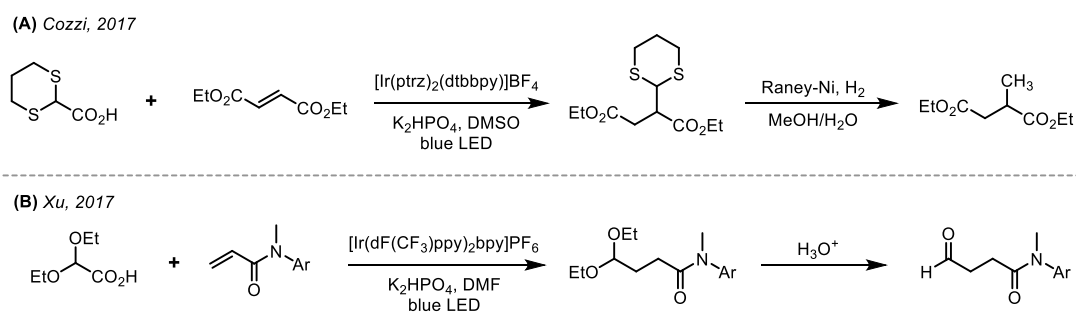
Figure 1.8. Decarboxylation of unique carboxylates serving as "masked" functional groups

Amines and alcohols may also serve as viable feedstocks for alkyl radical precursors

from α-silyl amines and oxalates, respectively. Oxidation of the nitrogen lone pair electrons in α-

silylamines results in fragmentation to generate aminomethyl radicals that efficiently undergo

Giese addition with electron-deficient alkenes (Figure 1.9A).[37] The remarkably low oxidation

potential of these α-silylamines is attributed to the hyperconjugative stabilization imparted by the

C-Si bond, offering a diverse array of amine precursors that can be incorporated into radical

hydroalkyations.[38] Similar to carboxylates, oxalates undergo single electron oxidation followed

by decarboxylation and decarbonylation to yield alkyl radicals (Figure 1.9B).[39] Given the

ubiquitous nature of alcohols, photoredox hydroalkylations using oxalate radical precursors have

been elegantly incorporated into the total synthesis of complex natural products.[40,41]

12
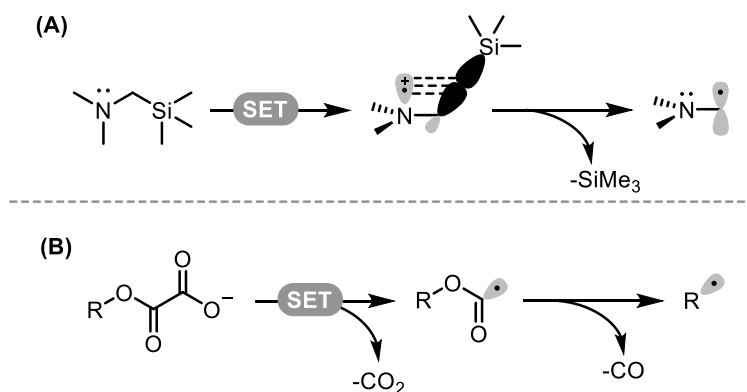
Figure 1.9. Fragmentation of α-silylamines and oxalates to product alkyl radicals

In addition to redox labile functional groups, alkyl radicals can be generated via HAT with another radical species generated via photoredox catalysis. Many different HAT catalysts have been employed with a wide range of C-H bonds that can be activated. Redox active Ni salts have been utilized to generate chloride radicals catalytically upon single electron oxidation, which in turn perform homolysis of α-alkoxy and α-amino C-H bonds for hydroalkylations.[42] Rovis and coworkers demonstrated that the radical cation of quinuclidine is an efficient HAT catalyst for the activation of α-sulfonamidyl C-H bonds in Giese reactions.[43] Decatungstate salts, which are themselves photoactive, are capable of homolyzing strong C-H bonds and have been used for hydroalkyation of unactivated radical precursors.[44] Recently, amine-boryl radicals, generated via proton-coupled electron transfer, have been demonstrated to perform selective homolysis of α-keto, -ester or -amidyl C-H bonds. These nucleophilic boryl radicals represent a unique class of HAT catalysts that can be used for hydroalkylation of electron-rich alkenes.[45] Finally, diaryl ketones represent a practical, sustainable, photoactive class of HAT catalysts that can perform hydroalkylation at activated C-H bonds in concert with catalytic metal redox catalysts such as copper(II) salts.[46]

13

In addition to the abundance of methods for radical hydroalkylations, photoredox catalysis also offers the opportunity for alkene difunctionalization reactions. Unlike classical Giese addition protocols that must undergo HAT with tin hydride reagents to sustain radical chain mechanisms, the discrete catalytic cycles employed in photoredox reactions present the opportunity to functionalize the Giese addition intermediate in either radical or polar manifolds. Ultimately, photoredox conditions leverage the most attractive aspects of both Michael and Giese additions, offering the ability to perform multicomponent 1,2-difunctionalizations with the innate chemoselectivity of radical-based mechanisms.

Among the most common homolytic functionalizations for alkyl radicals are atom transfers such as halogenations, alkene additions (radical cascades) and heteroatom functionalizations (amination, thiolation, sulfonylation, etc). Beyond these simple homolytic functionalizations, metalation of an alkyl radical can open the door to a much wider suite of possible bond-forming processes. The most popular of these metal-mediated transformations, cross coupling of an aryl electrophile with an alkyl radical, was pioneered by our group and simultaneous by others.[47,48] The hallmark of this method is the ability to utilize unstabilized C_{sp3} radicals as nucleophiles via a single-electron transmetalation with Ni, obviating the previously troublesome two-electron metalation with Pd, which often led to isomerizations and β-hydride elimination side products.

Molander, 2014
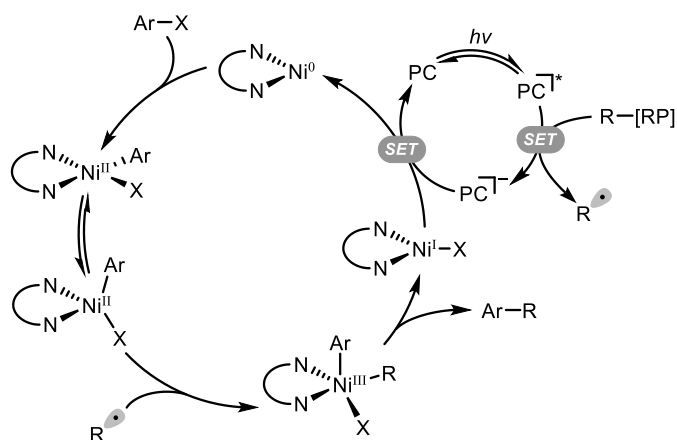
Figure 1.10. General mechanism for photoredox/nickel dual catalysis

Finally, another broad subset of functionalizations could be accessed via radical-polar crossover mechanisms (reduction of alkyl radicals to anions or oxidation to cations). From these polar intermediates, two-electron nucleophiles and electrophiles can be engaged, many of which do not pose any functional group incompatibility with radical intermediates. Indeed these strategies offer a myriad of possibilities for rapid diversification of alkene structures in a highly modular manifold. Despite these intriguing possibilities for multicomponent, vicinal alkene difunctionalization via photoredox catalysis, little had been achieved in this area prior to 2018.[49] Herein, efforts in expanding the area of photochemically-mediated, multicomponent alkene difunctionalizations are reported.

1.3. References

1. Tomioka, K. Conjugate Addition of Organometallics to Activated Olefins. *ChemInform* **2005**, *36,* 28.

2. Chapdelaine, M. J.; Hulce, M. Tandem Vicinal Difunctionalization: β-Addition to α,β-Unsaturated Carbonyl Substrates Followed by α-Functionalization. *Org. React.,* **1990**, *38*, 227-294.

3. Damon, R. E.; Schlessinger, R. H.; Blount, J. F. A short synthesis of (.+-.)-isostegane. *J. Org. Chem.,* **1976**, *41*, 3772-3773. Luo, F. T.; Negishi, E. Nickel- or palladium-catalyzed cross coupling. 28. A selective synthesis of a mixture of C-15 epimers of (.+-.)-11-deoxyprostaglandin E2 methyl ester. *J. Org. Chem.,* **1985**, *50*, 4762-4766.

4. Domingo, L. R.; Perez, P. Global and local reactivity indices for electrophilic/nucleophilic free radicals. *Org. Biomol. Chem.,* **2013**, *11*, 4350-4358.

5. Giese, B. Formation of C-C bonds by addition of free-radicals to alkenes. *Angew. Chem. Int. Ed.* **1983**, *22*, 753-764.

6. Chatgilialoglu, C.; Ingold, K. U.; Scaiano, J. C. Rate constants and Arrhenius parameters for the reactions of primary, secondary, and tertiary alkyl radicals with tri-n-butyltin hydride. *J. Am. Chem. Soc.,* **1981**, *103*, 7739-7742.

7. Zhang, W. Intramolecular free radical conjugate additions. *Tetrahedron* **2001**, *57*, 7237-7261.

8. Curran, D. P. Comprehensive Organic Synthesis, Vol. 4. Pergamon Press, 1991; pp 715-777.

9. Barton, D. H. R.; McCombie, S. W. A new method for the deoxygenation of secondary alcohols. *J. Chem. Soc., Perkin Transactions,* **975**, 1574-1585.

10. Hu, C. C.; Chen, Y. Y. Chemoselective and fast decarboxylative allylation by photoredox catalysis under mild conditions. *Org. Chem. Front.,* **2015**, *2*, 1352-1355.

11. Schwarz, J.; Konig, B. Metal-free, visible-light-mediated, decarboxylative alkylation of biomass-derived compounds. *Green Chem.,* **2016**, *18*, 4743-4749.

12. Kong, W. G.; Yu, C. J.; An, H. J.; Song, Q. L. Photoredox-Catalyzed Decarboxylative Alkylation of Silyl Enol Ethers To Synthesize Functionalized Aryl Alkyl Ketones. *Org. Lett.* **2018**, *20*, 349-352.

13. Schnermann, M. J.; Overman, L. E. A Concise Synthesis of (-)-Aplyviolene Facilitated by a Strategic Tertiary Radical Conjugate Addition. *Angew. Chem. Int. Ed.,* **2012**, *51*, 9576-9580.

14. Qin, T.; Cornella, J.; Li, C.; Malins, L. R.; Edwards, J. T.; Kawamura, S.; Maxwell, B. D.; Eastgate, M. D.; Baran, P. S. A general alkyl-alkyl cross-coupling enabled by redox-active esters and alkylzinc reagents. *Science,* **2016**, *352*, 801-805.

15. Zheng, C.; Wang, G. Z.; Shang, R. Catalyst-free Decarboxylation and Decarboxylative Giese Additions of Alkyl Carboxylates through Photoactivation of Electron Donor-Acceptor Complex. *Adv. Synth. Catal.,* **2019**, *361*, 4500-4505.

16. Elkhalifa, M.; Elbaum, M. B.; Chenoweth, D. M.; Molander, G. A. Solid-Phase Photochemical Decarboxylative Hydroalkylation of Peptides. *Org. Lett.,* **2021**, ASAP.

17. Sumino, S.; Ryu, I. Hydroalkylation of Alkenes Using Alkyl Iodides and Hantzsch Ester under Palladium/Light System. *Org. Lett.* **2016**, *18*, 52-55.

18. Nguyen, J. D.; D'Amato, E. M.; Narayanam, J. M. R.; Stephenson, C. R. J. Engaging unactivated alkyl, alkenyl and aryl iodides in visible-light-mediated free radical reactions. *Nat. Chem.,* **2012**, *4*, 854-859.

19. Giedyk, M.; Narobe, R.; Weiss, S.; Touraud, D.; Kunz, W.; Koenig, B. Photocatalytic activation of alkyl chlorides by assembly-promoted single electron transfer in microheterogeneous solutions. *Nat. Catal.,* **2020**, *3*, 40-47.

20. Andrews, R. S.; Becker, J. J.; Gagne, M. R. Intermolecular Addition of Glycosyl Halides to Alkenes Mediated by Visible Light. *Angew. Chem. Int. Ed.,* **2010**, *49*, 7274-7276.

21. Giese, B.; Dupuis, J. Diastereoselektive Synthese von C-Glycopyranosiden. *Angew. Chem. Int. Ed.* **1983**, *95*, 8.

22. Aycock, R. A.; Wang, H.; Jui, N. T. A mild catalytic system for radical conjugate addition of nitrogen heterocycles. *Chem. Sci.,* **2017**, *8*, 3121-3125. Aycock, R. A.; Vogt, D. B.; Jui, N. T. A practical and scalable system for heteroaryl amino acid synthesis. *Chem. Sci.,* **2017**, *8*, 7998-8003.

23. ElMarrouni, A.; Ritts, C. B.; Balsells, J. Silyl-mediated photoredox-catalyzed Giese reaction: addition of non-activated alkyl bromides. *Chem. Sci.,* **2018**, *9*, 6639-6646.

24. Wiles, R. J.; Phelan, J. P.; Molander, G. A. Metal-free defluorinative arylation of trifluoromethyl alkenes via photoredox catalysis. *Chem. Commun.,* **2019**, *55*, 7599-7602.

25. Diccianni, J.; Lin, Q.; Diao, T. Mechanisms of Nickel-Catalyzed Coupling Reactions and Applications in Alkene Functionalization. *Acc. Chem. Res.,* **2020**, *53*, 906-919. Green, S. A.; Huffman, T. R.; McCourt, R. O.; van der Puyl, V.; Shenvi, R. A. Hydroalkylation of Olefins To Form Quaternary Carbons. *J. Am. Chem. Soc.,* **2019**, *141*, 7709-7714.

26. Dong, J. Y.; Wang, X. C.; Wang, Z.; Song, H. J.; Liu, Y. X.; Wang, Q. M. Visible-light-initiated manganese-catalyzed Giese addition of unactivated alkyl iodides to electron-poor olefins. *Chem. Commun.,* **2019**, *55*, 11707-11710.

27. Nicewicz, D. A.; MacMillan, D. W. C. Merging photoredox catalysis with organocatalysis: The direct asymmetric alkylation of aldehydes. *Science,* **2008**, *322*, 77-80.

28. Yasu, Y.; Koike, T.; Akita, M. Visible Light-Induced Selective Generation of Radicals from Organoborates by Photoredox Catalysis. *Adv. Synth. Catal.,* **2012**, *354*, 3414-3420.

29. Miyazawa, K.; Koike, T.; Akita, M. Hydroaminomethylation of Olefins with Aminomethyltrifluoroborate by Photoredox Catalysis. *Adv. Synth. Catal.* **2014**, *356*, 2749-2755.

30. Chinzei, T.; Miyazawa, K.; Yasu, Y.; Koike, T.; Akita, M. Redox-economical radical generation from organoborates and carboxylic acids by organic photoredox catalysis. *RSC Adv.,* **2015**, *5*, 21297-21300.

31. Lang, S. B.; Wiles, R. J.; Kelly, C. B.; Molander, G. A. Photoredox Generation of Carbon-Centered Radicals Enables the Construction of 1,1-Difluoroalkene Carbonyl Mimics. *Angew. Chem. Int. Ed.,* **2017**, *56*, 15073-15077.

32. Wu, Z.; Gockel, S. N.; Hull, K. L. Anti-Markovnikov hydro(amino)alkylation of vinylarenes via photoredox catalysis. *Nat. Commun.,* **2021**, *12*, 5956-5965.

33. Huo, H.; Harms, K.; Meggers, E. Catalytic, Enantioselective Addition of Alkyl Radicals to Alkenes via Visible-Light-Activated Photoredox Catalysis with a Chiral Rhodium Complex. *J. Am. Chem. Soc.,* **2016**, *138*, 6936-6939.

34. Gualandi, A.; Matteucci, E.; Monti, F.; Baschieri, A.; Armaroli, N.; Sambri, L.; Cozzi, P. G. Photoredox radical conjugate addition of dithiane-2-carboxylate promoted by an iridium(III) phenyl-tetrazole complex: a formal radical methylation of Michael acceptors. *Chem. Sci.,* **2017**, *8*, 1613-1620.

35. Zhang, S.; Tan, Z. M.; Zhang, H. N.; Liu, J. L.; Xu, W. T.; Xu, K. An Ir-photoredox-catalyzed decarboxylative Michael addition of glyoxylic acid acetal as a formyl equivalent. *Chem. Commun.,* **2017**, *53*, 11642-11645.

36. Bloom, S.; Liu, C.; Kolmel, D. K.; Qiao, J. X.; Zhang, Y.; Poss, M. A.; Ewing, W. R.; MacMillan, D. W. C. Decarboxylative alkylation for site-selective bioconjugation of native proteins via oxidation potentials. *Nat. Chem.,* **2018**, *10*, 205-211.

37. Nakajima, K.; Kitagawa, M.; Ashida, Y.; Miyake, Y.; Nishibayashi, Y. Synthesis of nitrogen heterocycles via alpha-aminoalkyl radicals generated from alpha-silyl secondary amines under visible light irradiation. *Chem. Commun.,* **2014**, *50*, 8900-8903.

38. Remeur, C.; Kelly, C. B.; Patel, N. R.; Molander, G. A. Aminomethylation of Aryl Halides Using α-Silylamines Enabled by Ni/Photoredox Dual Catalysis. *ACS Catal.,* **2017**, *7*, 6065-6069.

39. Nawrat, C. C.; Jamison, C. R.; Slutskyy, Y.; MacMillan, D. W. C.; Overman, L. E. Oxalates as Activating Groups for Alcohols in Visible Light Photoredox Catalysis: Formation of

Quaternary Centers by Redox-Neutral Fragment Coupling. *J. Am. Chem. Soc.,* **2015**, *137*, 11270-11273.

40. Slutskyy, Y.; Jamison, C. R.; Lackner, G. L.; Müller, D. S.; Dieskau, A. P.; Untiedt, N. L.; Overman, L. E. Short Enantioselective Total Syntheses of trans-Clerodane Diterpenoids: Convergent Fragment Coupling Using a trans-Decalin Tertiary Radical Generated from a Tertiary Alcohol Precursor. *J. Org. Chem.,* **2016**, *81*, 7029-7035.

41. Abbas, S. Y.; Zhao, P.; Overman, L. E. 1,6-Addition of Tertiary Carbon Radicals Generated From Alcohols or Carboxylic Acids by Visible-Light Photoredox Catalysis. *Org. Lett.* **2018**, *20*, 868-871.

42. Deng, H.-P.; Fan, X.-Z.; Chen, Z.-H.; Xu, Q.-H.; Wu, J. Photoinduced Nickel-Catalyzed Chemo- and Regioselective Hydroalkylation of Internal Alkynes with Ether and Amide α-Hetero C(sp3)–H Bonds. *J. Am. Chem. Soc.,* **2017**, *139*, 13579-13584.

43. Ashley, M. A.; Yamauchi, C.; Chu, J. C. K.; Otsuka, S.; Yorimitsu, H.; Rovis, T. Photoredox-Catalyzed Site-Selective alpha-C(sp(3))-H Alkylation of Primary Amine Derivatives. *Angew. Chem. Int. Ed.,* **2019**, *58*, 4002-4006.

44. Laudadio, G.; Deng, Y. C.; van der Wal, K.; Ravelli, D.; Nuno, M.; Fagnoni, M.; Guthrie, D.; Sun, Y. H.; Noel, T. C(sp(3))-H functionalizations of light hydrocarbons using decatungstate photocatalysis in flow. *Science* **2020**, *369*, 92-98.

45. Lei, G.; Xu, M.; Chang, R.; Funes-Ardoiz, I.; Ye, J. Hydroalkylation of Unactivated Olefins via Visible-Light-Driven Dual Hydrogen Atom Transfer Catalysis. *J. Am. Chem. Soc.,* **2021**, *143*, 11251-11261.

46. Abadie, B.; Jardel, D.; Pozzi, G.; Toullec, P.; Vincent, J. M. Dual Benzophenone/Copper-Photocatalyzed Giese-Type Alkylation of C(sp(3))-H Bonds. *Chem. Eur. J.,* **2019**, *25*, 16120-16127.

47. Tellis, J. C.; Primer, D. N.; Molander, G. A. Single-electron transmetalation in organoboron cross-coupling by photoredox/nickel dual catalysis. *Science,* **2014**, *345*, 433-436.

48. Zuo, Z. W.; Ahneman, D. T.; Chu, L. L.; Terrett, J. A.; Doyle, A. G.; MacMillan, D. W. C. Merging photoredox with nickel catalysis: Coupling of alpha-carboxyl sp(3)-carbons with aryl halides. *Science,* **2014**, *345*, 437-440.

49. Garbarino, S.; Ravelli, D.; Protti, S.; Basso, A. Photoinduced Multicomponent Reactions. *Angew. Chem. Int. Ed.,* **2016**, *55*, 15476-15484.

Chapter 2. Synthesis of α-Fluoro-α-amino Acid Derivatives via Photoredox-Catalyzed Carbofluorination

2.1. Introduction

Amino acids are the molecular subunits that compose, arguably, the most essential biopolymer: proteins. Given their vast array of biological functions, peptides have received substantial attention as therapeutic agents. In many instances, peptides offer an advantage over conventional small molecule therapeutics as their mechanism of action more closely mimics natural biomolecular pathways. In addition to the twenty-two naturally occurring structures, many synthetic (non-natural) amino acids are often incorporated into peptide therapeutics, bolstering key pharmacological properties.

Incorporation of fluorine atoms into structure of small molecules is a critical strategy used in medicinal chemistry programs for fine-tuning the properties of a drug. The substitution of C-F bonds for C-H bonds can drastically change the lipophilicity, pharmacokinetic (PK) properties, and stability of small molecule drugs toward enzymatic degradation.[1-2] As with small molecule active pharmaceutical ingredients (APIs), fluorinated motifs have also been used to enhance the structural and pharmacological properties of therapeutic peptides. For example, Ishida and coworkers demonstrated how the replacement of a methyl group for a trifluoromethyl group in a symmetrical β-peptide helix resulted in a more rigid conformation, greatly increasing the denaturation temperature of the trifluoromethyl compared to the methyl analog (Figure 2.1). In this particular example, the incorporation of the fluorinated side chains resulted in no significant alteration of the β-helical structure but rather increased its stability for two reasons. First, the inductive effect of the fluorinated side chain increases the acidity of the N-H bond in the proximal amide bond, resulting in stronger hydrogen bonding interactions. Second, the "fluorous effect" (the tendency of polyfluorinated motifs to self-aggregate and repel other intermolecular

interactions) brings the trifluoromethyl groups into proximity and rigidifies the backbone of the peptide.
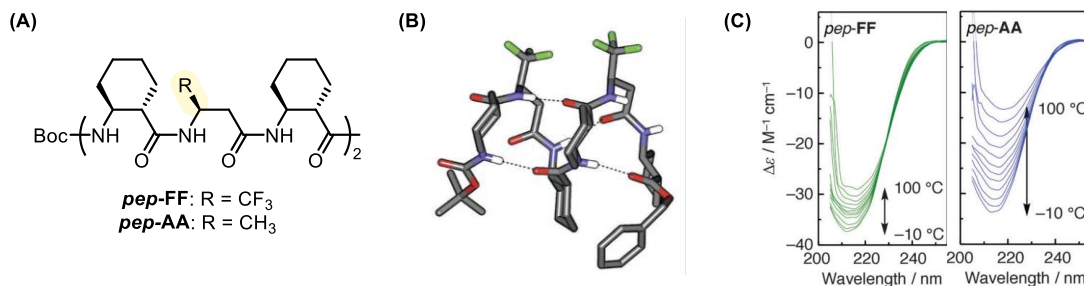
Figure 2.1. **(A)** Methyl and trifluoromethyl dimeric peptide derivatives **(B)** X-ray crystal structures of dimeric peptide derivatives **(C)** circular dichroism spectra of dimeric peptide derivatives

In addition to affecting the secondary structure of peptides, fluorinated functional groups have been demonstrated to increase the lipophilicity and potency of peptide therapeutics. In the development of a hepatitis C protease inhibitor, the C-terminus cysteine proved problematic because of its poor lipophilicity.[3] Exchanging the thiol group for a terminal methyl group resulted in improved lipophilicity but dramatically decreased potency, which was attributed to the loss of a key hydrogen bonding interaction. Incorporation of a difluoromethyl group at the C-terminus restored potency while maintaining excellent membrane permeability, demonstrating that the CF_2H group can serve as a lipophilic hydrogen bond donor.[4]

R = SH, IC_{50} = 40 nm
R = CH_3, IC_{50} = 700 nm
R = CF_2H, IC_{50} = 30 nm
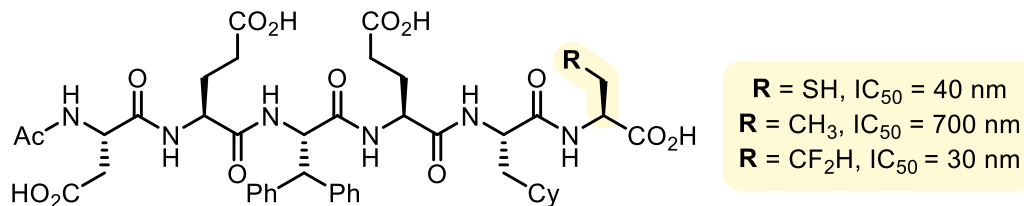
Figure 2.2. Heptatitis C protease inhibitor derivatives and measured potency values

Many more strategic examples of fluorinated amino acids have been demonstrated in peptide chemistry, with essentially all examples incorporating the fluoro group on the side chain of the amino acid.[5] In contrast, the effect of an amino acid bearing a fluorine at the α-carbon has been virtually unexplored. This disparity is mainly because of the varying difficulty in the synthesis sidechain fluorinated amino acids compared to α-fluoroamino acids. Many facile methods are available for the construction of monofluoro-, trifluoromethyl- and perfluorinated side chains in amino acids[6] while only three general strategies have been established for the preparation of α-fluoro-α-amino acids, namely: fluorination of amino acids, amination of fluoro esters, and alkylation of fluoroglycine analogs (Figure 2.3).
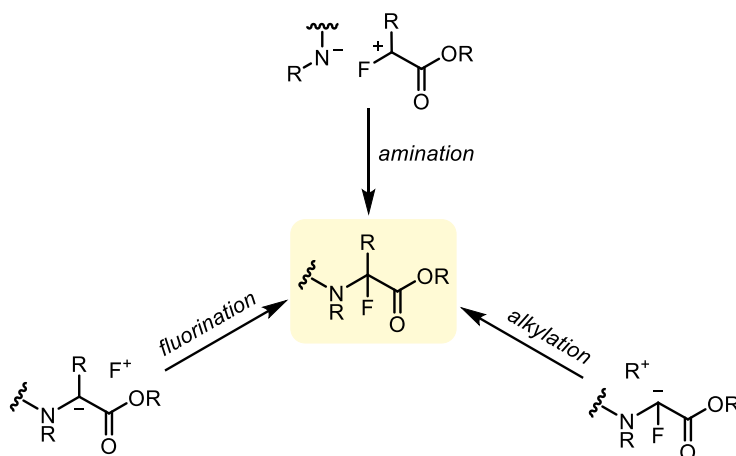
Figure 2.3. Prior retrosynthetic approaches for the preparation of α-fluoro-α-amino acids

Among the aforementioned approaches, fluorination of amino acids is the most prevalent strategy and has resulted in the largest diversity of accessible structures. Several reaction conditions have been identified for the electrophilic fluorination of the corresponding enoate anion (Figure 2.4A).[7] Though effective, the strong base required for the deprotonation necessitates the installation of protecting groups and limits the functional groups that can be included on the side chain. The umpolung approach generates an amino acid intermediate with an electrophilic α-carbon that is

trapped by fluoride anion. A rather unique, albeit low-yielding, approach to this transformation was achieved by Fuchigami using pulse electrolysis to oxidize an *N*-acyl amino acid to the corresponding iminium cation, which was then susceptible to attack by fluoride anion (Figure 2.4B).[8] The formation of the C-N bond in α-fluoro amino acids typically relies on selective nucleophilic attack of an amine nucleophile on an α,α-dihalocarbonyl adduct. Rosair and coworkers developed a highly modular protocol to generate α-fluoro-α-haloamides, which can then undergo a second amination to yield an α-fluoroamino acid with two orthogonal protecting groups at the C and N termini.[9] Nucleophilic vinylic substitution of an amine on chlorotrifluoroethene followed by acidic hydrolysis yields the α-fluoro-α-chloroamides, which can then undergo further nucleophilic amination reactions (Figure 2.4C). Finally, α-fluoro-α-nitro acetates have been demonstrated as competent nucleophiles in Michael reactions with activated alkenes. The resulting products can then be hydrogenated in the presence of *tert*-butyl pyrocarbonate to yield the protected α-fluoro-α-amino esters (Figure 2.4D).[10] This approach is particularly attractive given the excellent control of both the alpha and beta stereocenters, producing single enantio- and diastereospecific α-fluoro-α-amino acids.
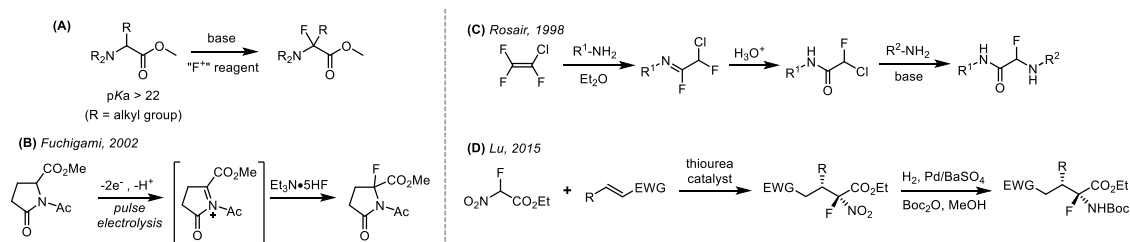
Figure 2.4. (A) Electrophlic fluorination of amino acids. **(B)** Nucleophilic fluorination via electrochemical catalysis. **(C)** Bis-amination of vinyl fluoride species. **(D)** Michael Addition of fluoro-amino acid surrogates.

2.2. Reaction Design and Optimization

Though all of these methods achieve the daunting synthetic goal of constructing α-fluoro-α-amino acids, each suffers from its own unique limitations, including the need for highly decorated starting materials, inadequate substrate specificity, harsh reaction conditions, and limited modularity. We desired to explore an entirely novel disconnection approach in the synthesis of α-fluoro-α-amino acids that would offer a more modular approach with good functional group tolerance. Photoredox chemistry has recently emerged as an exceptional, novel strategy for the generation of carbon-carbon and carbon-heteroatom bonds under extraordinarily mild conditions. Given the diversity of sensitive functional groups found in native amino acids/peptides, we deemed the mild conditions of photoredox reactions to be a prime candidate for a novel approach to the synthesis of α-fluoro-α-amino acids. Indeed, several exemplary reports provided precedent for the application of photoredox mechanisms in the modification of biomolecules. The MacMillan group demonstrated a photoredox-mediated, decarboxylative hydroalkylation at the C-terminus of complex polypeptides.[11] Furthermore, our own group successfully translated a previously developed thioarylation reaction to complex biomolecular scaffolds, including polypeptides.[12] Inspired by these two methods, we envisioned a photoredox-mediated difunctionalization reaction in which the alkyl side chain could be installed simultaneously with the fluorine atom at the alpha carbon. Given the excellent literature precedent for Giese additions mediated by photoredox chemistry, we proposed that a dehydrated amino acid could serve as a competent radical acceptor in the initial step of the anticipated carbofluorination. Indeed, two landmark reports published by the Davis[13] and Park[14] groups confirmed the viability of dehydroalanine (DHA) to act as a selective radical acceptor in polypeptides under classical Giese addition conditions. Furthermore, DHA derivatives have been demonstrated to be competent alkene acceptors for both alkyl- and aryl radicals under photoredox conditions (Figure 2.5A).[15-16] Beyond these hydroalkylation protocols there were, to our

knowledge, no examples of difunctionalizations of DHA. Despite this, we proposed that following Giese addition of an alkyl radical fragment into DHA, the resultant radical adduct could then undergo fluorination at the alpha carbon via atom transfer with a homolytically labile F-heteroatom bond. Though unprecedented in the area of photoredox chemistry, radical-based carbofluorination of alkenes had recently been accomplished via copper catalysis (Figure 2.5B).[17] In this mechanism, an excited state copper(I) complex reductively generates a trifluoromethyl radical that undergoes Giese addition with an electron-rich alkene. The resultant copper(II) species undergoes fluoride ligand exchange and subsequently fluorinates the previously generated alkyl radical adduct.
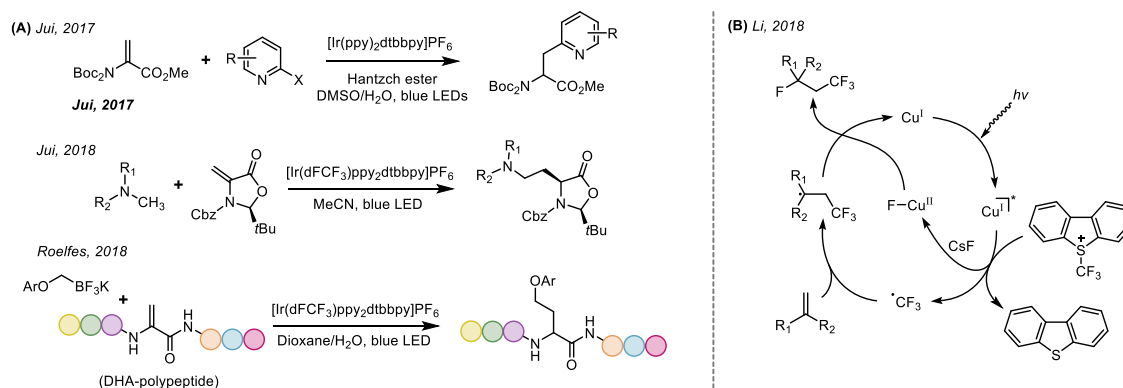
Figure 2.5. (A) Photoredox hydroarylation –alkylation of DHA derivatives. **(B)** Cu-mediated radical carbofluorinatoin of alkenes.

As we endeavored to explore this novel transformation, we proposed the following general mechanism for a photoredox-neutral carbofluorination (Figure 2.6). Reductive quenching of an excited state photocatalyst (**2.II**) via single-electron transfer with a radical precursor (**2.IV**) would generate the desired alkyl radical (**2.V**). Regioselective Giese addition of the alkyl radical at the alkene terminus would generate the key α-amino-α-ester radical **2.VII**. Fluorination of this intermediate via atom transfer with a homolytically labile F-Y bond would generate the desired α-fluoro-α-amino acid and a radical cation fragment of the fluorinating agent (**2.X**). Single-

electron transfer between the reduced photocatalyst (**2.III**) and radical cation **2.X** would complete the catalytic cycle, returning the photocatalyst to its ground state.
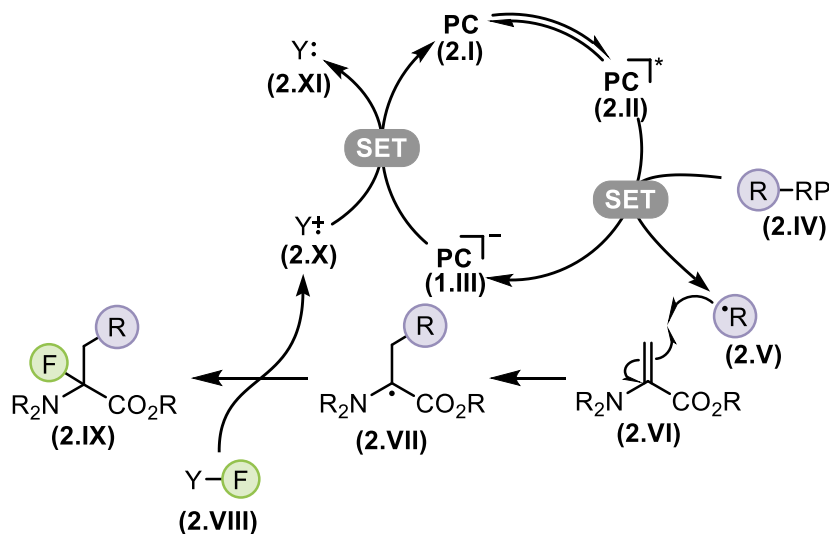
Figure 2.6. Proposed mechanism for redox-neutral carbofluorination of DHA

Careful selection of photocatalyst, radical precursor class, and fluorinating agent would be essential for the success of this reaction pathway. As outlined in Figure 2.6, the redox windows of all three reaction components must be well orchestrated so that the photocatalyst undergoes facile reductive quenching with radical precursor **2.IV** followed by oxidation via the radical cation byproduct of the fluorinating agent (**2.X**).

As we set out to explore this transformation, we focused on utilizing bis-Boc protected DHA **2.1** as our model alkene, which was prepared from commercially available Boc-Ser(Bzl)-OH via a protection/dehydration reaction (Figure 2.7). The mono-Boc DHA (**2.2**) was found to be unreactive under a variety of different conditions, and in some cases small amounts of polymerization were observed. However, the mono-Boc DHA could be used to prepare orthogonally bis-protected DHA, which gave good reactivity in the carbofluorination reaction.

Figure 2.7. Preparation of various DHA derivatives

As we began optimization of reaction conditions for the carbofluorination of **2.1**, we quickly identified alkyltrifluoroborates as the most competent class of oxidatively generated radical precursor (Table 1, entry 1). Benzyl bis(catecholato)silicate gave no conversion of starting material, while 4-benzyl-1,4-dihydropyridine resulted in a high yielding dialkylation reaction (entries 2, 3). We presume this dialkylated product arises from radical-radical coupling of the persistent pyridyl radical cation generated from oxidation of benzyl dihydropyridine and the DHA Giese addition intermediate. Solvent also proved to be critical in obtaining the desired product selectivity (entries 4-6). In solvents with activated C-H bonds, a high ratio of an α-protio side product was observed. Both 9-mesityl-10-methylacridinium (MesAcr) and Ir[dF(CF$_3$)ppy]$_2$[bpy][PF$_6$] were competent photocatalysts. However, because the iridium-based photocatalyst is more cost prohibitive and tedious to synthesize, MesAcr was selected as the model photocatalyst. Additionally, we anticipated that the higher oxidation potential of MesAcr ($*E_{red}$ = +2.06 V vs SCE)[18] as compared to Ir[dF(CF$_3$)ppy]$_2$[bpy][PF$_6$] ($*E_{red}$ = +1.32 V vs SCE)[19] would provide better yields in the case of unstabilized primary alkyltrifluoroborates, which exhibit challenging oxidation potentials (E_{red} = > +1.6 V vs SCE).[20] Photocatalysts with weaker excited state oxidation potentials, such as Ru(bpy)$_3$ and 1,2,3,5-tetrakis(carbazol-9-yl)-4,6-dicyanobenzene (4CzIPN), resulted in a mixture of the three products (**2.4** – **2.6**). Selectfluor, in

large excess, was uniquely effective for achieving fluorination at the alpha position, as other common atom transfer fluorinating agents resulted in the formation of the two non-fluorinated products (entries 10, 11). Control experiments demonstrated that in the absence of either light or photocatalyst, no conversion of starting material was achieved. The super-stoichiometric loadings of both trifluoroborate and Selectfluor were needed for complete conversion of starting material and formation of the desired product.

Table 2.1. Optimization data for the photoredox carbofluorination of DHA analog **2.1**

entry	deviation from conditions above	2.4 (%)	2.5 (%)	2.6 (%)
1	None	81	>5	8
2	benzyl bis(catecholato)silicate	0	0	0
3	4-benzyl-1,4-dihydropyridine	0	82	0
4	acetone	>5	>5	79
5	MeCN	45	>5	38
6	THF	0	87	0
7	$Ir[dF(CF_3)ppy]_2bpyPF_6$	80	>5	14
8	$Ru(bpy)_3(PF_6)_2$	21	62	15
9	4CzIPN	24	58	13
10	NSFI	0	0	87
11	*N*-fluoropyridium BF_4	0	22	47

(NSFI = *N*-Fluorobenzenesulfonimide)

2.3. Scope Exploration

With the optimized conditions in hand, we turned our attention to investigating the scope of alkyltrifluoroborates in the carbofluorination of DHA derivatives. A range of secondary (**2.7-2.13**) and tertiary (**2.26** and **2.27**) alkyltrifluoroborates gave good to excellent yields of the desired α-fluoro-α-amino acids. α-Fluoroleucine (**2.7**) was prepared in excellent yield which, to

our knowledge, is the first example of the fluorinated variant of this natural amino acid. The remaining collection of secondary alkyl examples contained fluorinated derivatives of both novel (**2.8**, **2.11**, **2.12**) and well-studied (**2.9**,[21] **2.10**,[22] **2.13**[23]) unnatural amino acid substrates. Primary unstabilized trifluoroborates, which are typically challenging to oxidize ($E_{ox} = > +1.6$ V vs SCE), were competent in the carbofluorination protocol, owing their success to the high excited state oxidation potential of MesAcr. Stabilized α-alkoxytrifluoroborates, which exhibit lower oxidation potentials, also provided good yields of the corresponding products. In addition to hydrocarbon substructures, a wide array of functionalized alkyl radicals was well tolerated under the reaction conditions, including protected amines (**2.12** and **2.16**), protected alcohols (**2.22** and **2.23**), amides (**2.19**), esters (**2.28**) and ketones (**2.29**). Products **2.28** and **2.29** demonstrate the high degree of chemoselectivity for radical addition to the DHA alkene, as no off-target reactivity was observed at the unactivated alkene or alkyne. Surprisingly, application of a primary, α-bromo radical did not generate the anticipated carbofluorination product, but rather a dimethylformamide adduct via HAT of the solvent. We believe that the highly electrophilic nature of the primary, α-bromo radical creates a polarity mismatch with the DHA alkene and thus is reluctant to undergo Giese-type addition. Rather, HAT with the dimethylformamide creates a more nucleophilic acyl radical, which readily adds to the electrophilic DHA alkene. Finally, the radical nature of the reaction was confirmed using α-cyclopropylmethyl trifluoroborate, which generated the anticipated ring-opened alkene product.

Table 2.2. Scope of trifluoroborates in the carbofluorination of DHA analog **1**

In addition to the model bis-Boc DHA substrate **2.1**, we prepared a series of unsymmetrically protected DHA derivatives for the photoredox carbofluorination. These substrates are particularly useful given that the orthogonal protecting groups can be removed sequentially. All of the bis-protected DHA substrates (**2.33**-**2.37**) were successful in providing the desired α-fluoro-α-amino acid. However, when attempting the carbofluorination of a mono-Boc DHA derivative, no consumption of starting material was observed. An *N*-Boc *N*-methyl derivative also proved unreactive, which ruled out possible incompatibility of the free carbamate N-H. An important application of this method was the translation of this reaction to a DHA-containing polypeptide for selective carbofluorination of proteins. Proof of this concept was demonstrated in model substrate **2.40**, which was formed from the DHA-Gly dipeptide. We envisioned that this product could then undergo C-terminal elongation to prepare a large polypeptide containing a single α-fluoro-α-amino acid.

Table 2.3. Scope of DHA derivatives in carbofluorination protocol
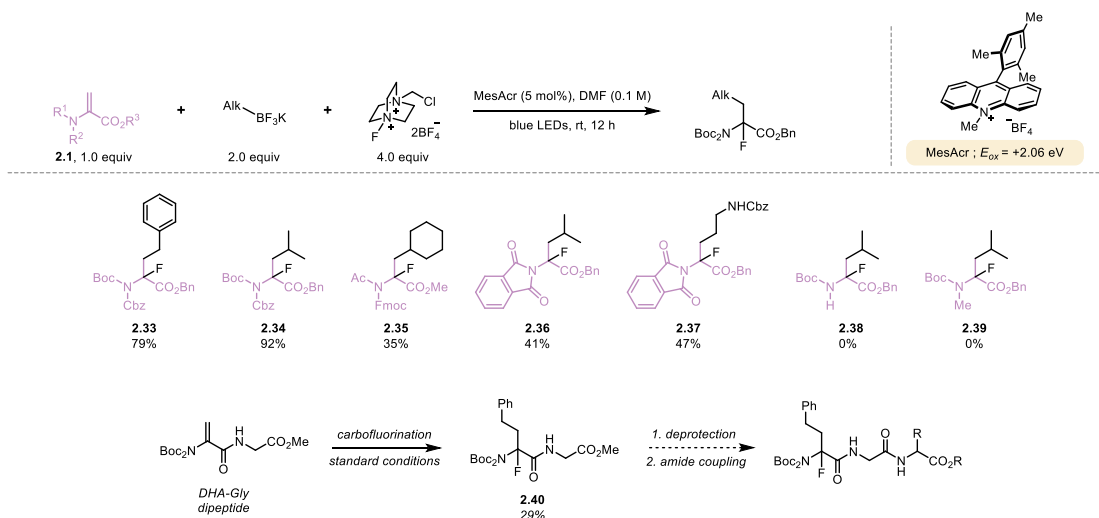
2.4. Computational and Mechanistic Studies

We then desired to provide a rationale for the atypical specificity of the DHA protecting groups in the developed carbofluorination protocol. Similar to two electron species, radicals are known to exhibit nucleophilic or electrophilic character based on electronic, structural, and conformational characteristics. Based on computational calculations, we assume that all of the alkyl radicals employed in our scope exploration were moderately to highly nucleophilic and would undergo facile Giese addition with electron deficient alkenes selectively.[24,25] When examining the alkene in the DHA substructure, it appears to display characteristics of an electron-rich enamine (conjugated to the amide/imide group) as well as an electron-deficient acrylate (conjugated to the ester). Depending on the nature of the protecting groups and molecular conformation, resonance structure **2.41** could contribute a significant amount to the overall electronic nature, making the alkene electron-rich and unsuited for Giese addition with nucleophilic radicals. Instinctively, we assumed the mono-Boc (**2.43**) and Boc-Me (**2.42**) substrates contained a more electron-rich alkene compared to the bis-Boc analog (**2.1**), therefore resulting in a polarity mismatch. Quantum mechanical calculations were employed to provide a

more quantitative metric for the electronic nature of the alkene in three DHA substrates (Figure 2.8). We immediately realized that each computed structure displayed a unique torsional angle [ω(C=C-N-C] between the plane of the olefin and the carbamate (Figure 2.8A). We proposed that this distinct change in molecular conformation was a major factor in governing the electron density of the alkene. We selected to use the Hu-Lu-Yang (HLY) method to calculate the electrostatic potential, fitting charges of each of the terminal alkene carbons. The HLY method defines the object function used for electrostatic potential in three-dimensional space.[26] The object function is therefore rotationally invariant with respect to the molecular orientation, and thus accounts for perturbations in molecular geometry. We believe that this metric gives a strong correlation to the electron density of the alkene in each derivative as it relates to each unique conformation. From the computed, energy-minimized, ground state structures, we observed the anticipated trend in electrostatic potential (ESP) value (more negative = more electron-rich) as the terminal carbon (C-3) of analog **1** was significantly more electron deficient compared to the alkene terminus of **2.42** and **2.43** (Figure 2.8D). The torsional angle correlates with the degree of conjugation of the nitrogen lone pair into the adjoining π system, impacting the electronic density at C-3 of each olefin and as expected had a strong correlation with ESP charges at the alkene terminus (C-3). In the calculated structure of adduct **2.43**, the olefin and carbamate are coplanar, resulting in a very electron-rich alkene; conversely, in substrate **2.1**, they are nearly perpendicular, resulting in minimal electronic donation from the nitrogen lone pair. The energy minimized structure of **2.1** was in strong agreement with its solid state structure determined by X-ray crystallography (Figure 2.8C). Finally, the NMR ^{13}C chemical shift at each C-3 position was used as an additional metric to support this concept.

(A)

(B)

2.1   2.42   2.43   2.44

(C)

X-Ray crystal structure

(D)

DHA	Dihedral angle ω(C=C-N-C)	ESP at C-3	Chemical shift at C-3 (ppm)
2.1 (calc.)	84.40°	-0.181	125.4
2.1 (crystal)	89.97°	—	—
2.42	54.85°	-0.355	105.7
2.43	0.00°	-0.393	116.5
2.44	89.65°	-0.150	—
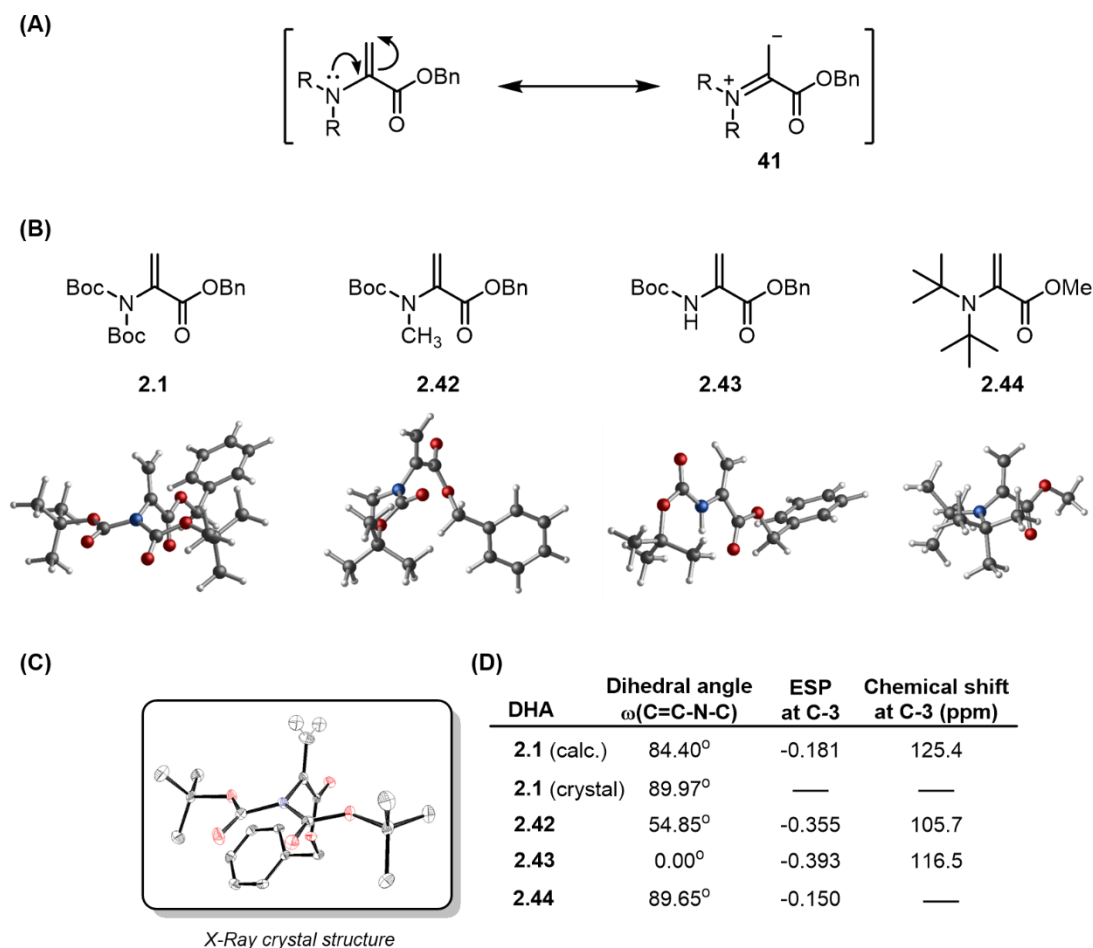
Figure 2.8. (A) Resonance forms affecting radical addition of DHA derivatives. **(B)** DHA derivatives and corresponding energy minimized conformation (B3LYP/6-31G*). **(C)** X-ray crystal structure of **1**. **(D)** Computed torsional angles, electrostatic potential values, and ^{13}C chemical shifts at C-3 of DHA derivatives.

We proposed that the electron-withdrawing nature of the carbamate protecting groups might also contribute significantly to the electron density of the adjacent alkene in DHA analog **2.1**. To probe the possibility we computed the energy minimized conformation and electrostatic potential for DHA analog **2.46**. This analog bears two bulky *tert*-butyl groups on the amine that effectively "lock" the torsional angle, making the nitrogen lone pair and π bond orthogonal while remaining electronically neutral. We found that this analog displayed a nearly identical torsional angle compared to **1** and, as expected, a similarly electron-deficient alkene. These results

35

demonstrate that the torsion angle between the amino group and alkene is the dominant factor governing the alkene electron density, and that the electronic nature of the protecting groups are essentially inconsequential.

We also reasoned that the energy minimized structure **2.1** might not be the only accessible conformation under our conditions. To explore the possibility of other rotational conformers, we performed a coordinate rotational scan about the bis-carbamate/olefin torsional angle [ω(C=C-N-C] in a simplified analog of **2.1** (Figure 2.9). We found that the barrier to rotate the bis-carbamate into a coplanar relation with the olefin was 8.6 kcal/mol, which equated to an equilibrium constant of 1.24 x 10^{-8} between **2.45** and **2.46** at 298 K. These calculations demonstrate that, under our reaction conditions, **2.1** remains almost exclusively in the energy minimized conformation displayed in Figure 2.8A, which reinforces the proposed dependence of molecular conformation on the electronic nature of the alkene.
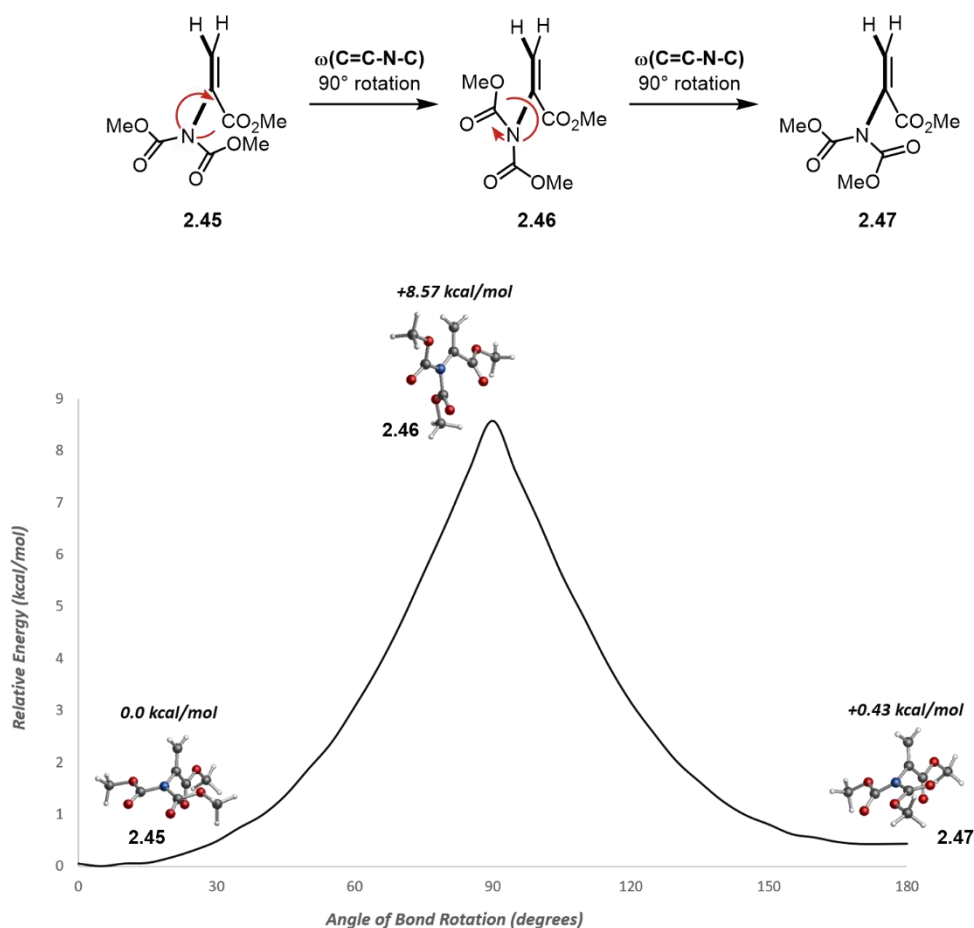
Figure 2.9. Coordinate bond rotation scan about **ω(C=C-N-C)** in DHA analog **2.45**.

We recognized that the ability to perform the carbofluorination protocol in a stereospecific manner would be highly desirable. In an effort to achieve high diastereoselectivity, we set out to prepare a DHA derivative that contained an oxazolidinone chiral auxiliary. We expected that the remote stereocenter would provide some level of facial selectivity in the fluorination step. Amide coupling between phthalimidoacrylic acid **2.48** and the oxazolidinone derived from *tert*-leucine (**2.49**) furnished the desired DHA derivative **2.50**. Unfortunately, application of this substrate under the established carbofluorination conditions failed to produce any appreciable amount of product. Given our timeline for this project we did not pursue further optimization of this protocol, however, it is very likely that under altered conditions (i.e., other

chiral auxiliaries) suitable diastereoselective reactivity could be achieved. Significant effort was devoted to optimizing conditions for the mono-Boc deprotection of the carbofluorination products derived from **2.1**. Unfortunately, under a range of different reaction conditions, significant amounts of protodefluorination were observed.
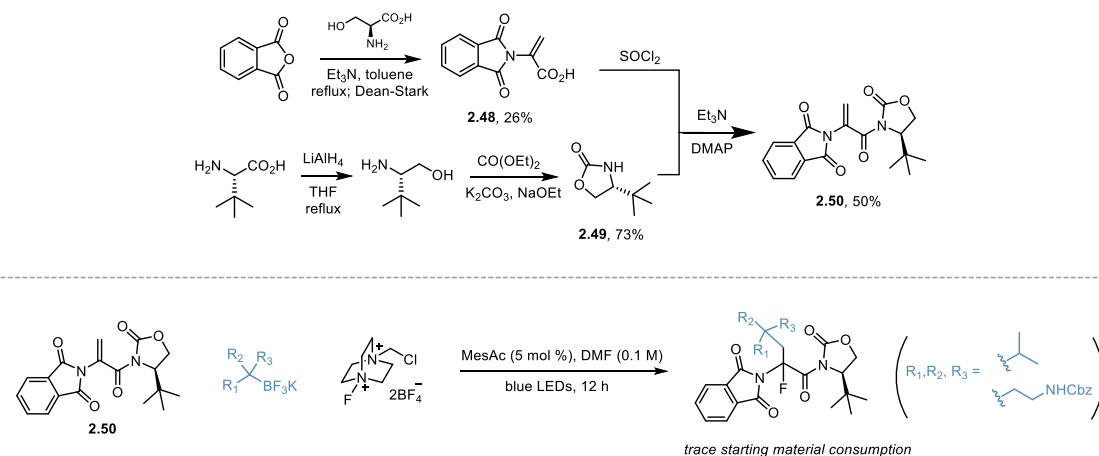
Figure 2.10. Synthesis and attempted application of chiral DHA derivative for diastereoselective carbofluorination.

In light of these observations, the following plausible mechanism for the photoredox-catalyzed carbofluorination of DHA derivatives outlined in Figure 2.11 was proposed. After absorption of light (~440 nm), excited state MesAcr (**2.II**) performs single electron reductive quenching with an alkyltrifluoroborate (**2.IV**), yielding an alkyl radical fragment (**2.V**). Stern-Volmer quenching studies support this step, as the alkyltrifluoroborate is by far the more effective quencher of the photocatalyst compared to either the DHA derivative or Selectfluor (see experimental details). This nucleophilic alkyl radical can undergo facile Giese-type addition with an electron-deficient DHA derivative (**2.VI**). As demonstrated in our quantum mechanical calculations, there appears to be a threshold value of electrostatic potential at the alkene terminus (C-3) for facile addition of the alkyl radicals. Incorporation of more electrophilic radicals resulted in a polarity mismatch, and thus alternative pathways such as hydrogen atom transfer (e.g.,

substrate **2.31**) or even direct fluorination of the alkyl radical can predominate (**2.V → 2.XIV**). After addition of the alkyl radical, intermediate **2.VII** can undergo radical fluorination via homolytic cleavage of the N⁺-F bond in Selectfluor, yielding the desired α-fluoro-α-amino acid. Alternatively, a dialkylated product may arise from radical-radical coupling of intermediate **2.VII** and a second equivalent of alkyl radical (**2.V**). The presence of an α-protio product was assumed to arise either via HAT or via single electron reduction followed by protonation. However, performing the reaction with water as a cosolvent had almost no effect on the α-fluoro/α-protio product ratio, which we believe suggests that the α-protio product is formed via HAT. Finally, the amino radical cation of Selectfluor (**2.X**) will undergo single electron transfer with the reduced photocatalyst (**2.III**), closing the catalytic cycle.
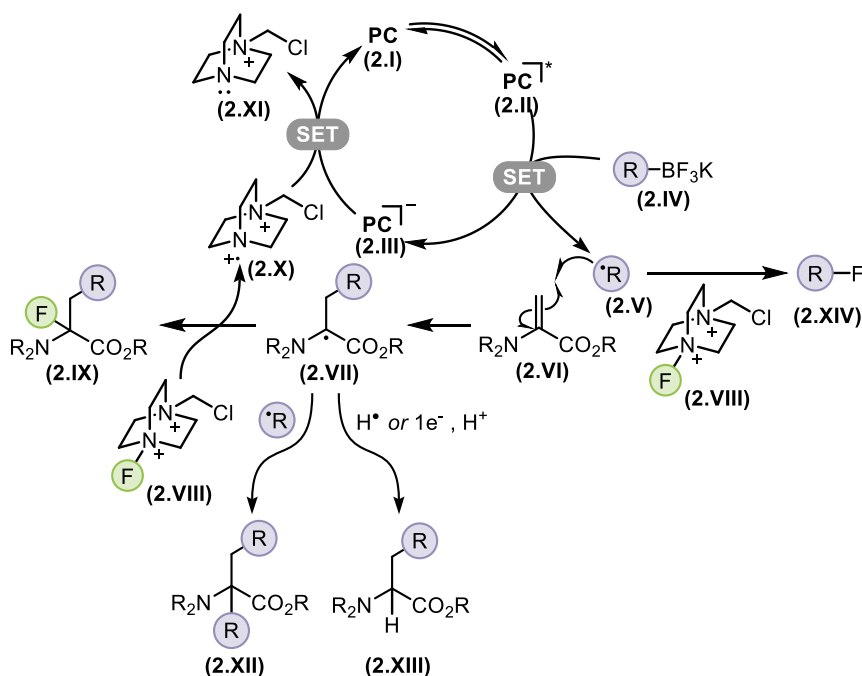
Figure 2.11. Proposed mechanism for photoredox carbofluorination of DHA derivatives

2.5. Conclusion

In conclusion, a redox neutral, metal-free, photocatalytic protocol for the preparation of α-fluoro-α-amino acids via carbofluorination has been developed. The remarkable diversity of alkyl groups and functional group tolerance was achieved via alkyltrifluoroborates serving as the choice radical precursor. Many of the substrates that were prepared represent entirely novel chemical space in the field of fluorinated amino acids, which have tremendous application to medicinal chemistry, agrochemistry, and chemical biology. Finally, a simple quantum mechanical calculation offered insight into the chemoselectivity observed in the radical addition step. We hope that such calculations will serve as a model for studying other photoredox-mediated Giese-type reactions and provide further insight into the exact nature of such reactivity.

2.6. Experimental

2.6.1 General Considerations

All chemical transformations requiring inert atmospheric conditions or vacuum distillation utilized Schlenk line techniques with a 5-port dual-bank manifold. Argon was used to provide such an atmosphere. NMR spectra (1 H, 13C, 19F) were obtained at 298 K. 1 H NMR spectra were referenced to residual, non-deuterated chloroform (δ 7.26) in CDCl3, ^{13}C NMR spectra were referenced to $CDCl_3$ (δ 77.3), and 19F NMR spectra were referenced to hexafluorobenzene (δ -161.8) as an internal standard and are run with C-F/C-H decoupling. Reactions were monitored by ^1H NMR, and/or TLC on silica gel plates (60 Å porosity, 250 µm thickness). TLC analysis was performed using hexanes/EtOAc as the eluent and visualized using Hanessian's stain and UV light. Silica plugs utilized flash silica gel (60 Å porosity, 32-63 µm). Flash chromatography was accomplished using an automated system (monitoring at 254 nm and 280 nm) with silica cartridges (60 Å porosity, 20-40 µm). Reverse phase preparative chromatography was performed by mass/UV (254 nm) directed preparatory liquid phase chromatography (Prep-LC). Solvents

were purified with drying cartridges through a solvent delivery system. Melting points (°C) are uncorrected. LED irradiation was accomplished using LED reactors described in our previous report.[27] Information for LED-based Photoreactor Components: Blue LEDs: 39.4 inch strips, 470 nm blue light, 32918 mcd ft-1 , Power Supply: 12V DC CPS series Power Supply - 15 Watt, Clip Fan: 2-Speed Clip Fan, 6-Inch, Pyrex crystallizing dishes (125 X 65 mm). Chemicals: Deuterated NMR solvents were stored over 4Å molecular sieves and/or K_2CO_3 (CDCl3). Selectfluor, MgSO4, DMF, MeCN, DMSO, CH2Cl2, CHCl3, EtOAc, pentane, hexanes, MeOH, and Et2O were used as purchased. MeCN, DMSO, and DMF (99.8%, extra dry) were stored over 4 Å molecular sieves. The photocatalyst mesityl acridinium was prepared in-house according to literature procedures.[28] The potassium alkyltrifluoroborate reagents were commercial samples or prepared via a previously published protocol.[29] Serines were purchased from commercial suppliers and used without further purification.

2.6.2 Optimization for Carbofluorination of Dehydroalanine

Procedure for optimization: To a 5 mL reaction vial equipped with stir bar were added dehydroalanine 1a (0.1 mmol, 38 mg, 1.0 equiv), radical precursor (0.2 mmol, 2.0 equiv), photocatalyst (0.05 equiv), and Selectfluor (0.4 mmol, 142 mg, 4.0 equiv). The vial was sealed with a cap containing a TFE-lined silicone septa and was evacuated and purged with argon gas three times via an inlet needle. The vial was then charged with anhydrous solvent (1 mL, 0.1 M). After this, the cap was sealed with Parafilm, and the reaction mixture was purged again with argon gas. The reaction vial was irradiated in an LED reactor. After 12 h, 4-methoxybiphenyl was added to reaction mixture, and the reaction mixture was transferred to a separatory funnel and diluted with Et2O (~5 mL) and brine (saturated aq NaCl, ~ 5 mL). The residue was extracted with Et2O (5 mL x 3) and washed with brine (10 mL x 3). The combined organic layer was dried

(MgSO4), and the solvent was removed in vacuo. The reaction mixture was analyzed by ^{1}H NMR using 4-methoxybiphenyl as an internal standard.

Table 2.4. Full Optimization Studies for Carbofluorination of DHA

entry	deviation from conditions above	2.4 (%)	2.5 (%)	2.6 (%)
1	None	81	>5	8
2	benzyl bis(catecholato)silicate	0	0	0
3	4-benzyl-1,4-dihydropyridine	0	82	0
4	acetone	>5	>5	79
5	MeCN	45	>5	38
6	THF	0	87	0
7	DMSO	0	0	0
8	DMA	21	<5	47
9	MeCN	45	<5	38
10	DMF/H_2O (2:1)	0	0	0
11	MeCN/H_2O (2:1)	44	<5	38
12	Ir[dF(CF$_3$)ppy]$_2$bpyPF$_6$	80	<5	14
13	Ir[(ppy)$_2$bpy)]PF$_6$	73	<5	17
14	Ru(bpy)$_3$(PF$_6$)$_2$	21	62	15
15	4CzIPN	24	58	13
16	NSFI	0	0	87
17	*N*-fluoropyridium BF$_4$	0	22	47
18	Cs$_2$CO$_3$ (1.0 equiv)	57	<5	32
19	In(OTf)$_3$ (1.0 equiv)	73	<5	21
20	open to air	58	<5	32
21	no light	0	0	0
22	no photocatalyst	0	0	0
23	BnBF$_3$K (1.5 equiv)	59	<5	9
24	Selectfluor (2.0 equiv)	18	21	31

(NSFI = *N*-Fluorobenzenesulfonimide)

2.6.3 General procedure for preparation of dehydroalanines

42

Dehydroalanines were prepared according to literature procedures.[30,31] To a stirred solution of serine benzyl ester in MeCN (1.0 M), DMAP (0.1 equiv) was added *tert*-butyl pyrocarbonate (2.2 equiv) at rt. After stirring for 12 h, The mixture was washed with brine and extracted with EtOAc three times. The combined organic layer was dried (MgSO4) and concentrated in vacuo. The residue was purified by column chromatography on SiO2 (gradient hexane to 50:50 hexane/EtOAc) to give the dehydroalanines.

Benzyl 2-(Bis(tert-butoxycarbonyl)amino)acrylate (2.1)
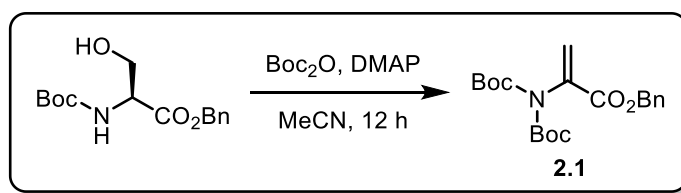
Following the general procedure for preparation of dehydroalanine using Boc-Ser-benzyl ester (8.6 g, 30.0 mmol). The title compound was isolated as white solid (7.3 g, 22.2 mmol, 78%). **¹H NMR** (500 MHz, CDCl₃) δ 7.34 (m, 5H), 6.39 (s, 1H), 5.67 (s, 1H), 5.24 (s, 2H), 1.41 (s, 18H). **¹³C NMR** (126 MHz, CDCl3) δ 163.6, 150.9, 136.5, 135.8, 128.8, 128.6, 128.5, 125.4, 83.4, 67.3, 28.1. **FT-IR** (cm⁻¹, neat, ATR) 2991, 1736, 1645, 1455, 987, 828, 615. **HRMS** (ESI⁺) calcd for $C_{20}H_{27}NNaO_6$ [M+Na]⁺: 400.1736, found: 400.1723. **MP** = 65-66 ℃

Benzyl 2-((tert-Butoxycarbonyl)amino)acrylate (2.43)
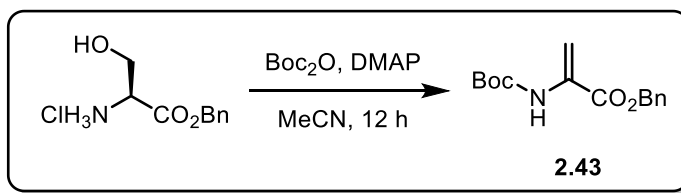
Following the general procedure for preparation of dehydroalanine using Ser-benzyl ester (2.0 g, 10.0 mmol). The title compound was isolated as a colorless oil (1.1 g, 6.5 mmol, 65%). **^{1}H NMR** (500 MHz, CDCl$_3$) δ 7.37(m, 5H), 7.04 (s, 1H), 6.18 (s, 1H), 5.79 (s, 1H), 5.26 (s, 2H), 1.48 (s, 9H). **^{13}C NMR** (126 MHz, CDCl$_3$) δ 164.2, 152.8, 135.5, 131.6, 128.9, 128.8, 128.5, 105.7, 81.0, 67.9, 28.5. **FT-IR** (cm^{-1}, neat, ATR) 3422, 2920, 1713, 1655, 1510, 1316, 1156, 1065, 772. **HRMS** (ESI$^+$) calcd for C$_{15}$H$_{19}$NNaO$_4$ [M]$^+$: 277.1314, found: 277.1314.

Benzyl 2-((tert-Butoxycarbonyl)(methyl)amino)acrylate (2.42)
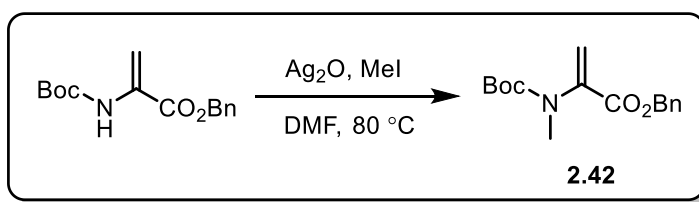
To a stirred solution of 1b (554 mg, 2.0 mmol, 1.0 equiv) in DMF (1 mL) were added Ag$_2$O (927 mg, 4.0 mmol, 2.0 equiv) and iodomethane (936 mg, 6.0 mmol, 3.0 equiv). After stirring for 4 h at 80 ºC, the mixture was diluted with Et2O (5 mL), washed with brine (5 mL) and extracted with Et$_2$O (5 mL) three times. The combined organic layer was dried (MgSO$_4$) and concentrated in S7 vacuo. The residue was purified by column chromatography on SiO$_2$ (gradient hexane to 50:50 hexane/EtOAc) to give the title compound as a colorless oil (411 mg, 1.4 mmol, 73%). **^{1}H NMR** (500 MHz, CDCl3) δ 7.35 (m, 5H), 5.87 (s, 1H), 5.37 (s, 1H), 5.22 (s, 2H), 3.12 (s, 3H), 1.38 (s, 9H). **^{13}C NMR** (126 MHz, CDCl$_3$) δ 164.9, 154.3, 141.9, 135.8, 128.8, 128.6, 128.5, 116.5, 81.4, 67.3, 37.0, 28.4. **FT-IR** (cm^{-1}, neat, ATR) 2936, 1722, 1531, 1334, 1151, 1070, 788, 690. **HRMS** (ESI$^+$) calcd for C$_{16}$H$_{21}$NNaO$_4$ [M+Na]$^+$: 314.1413, found: 314.1411.

Methyl (2-(Bis(tert-butoxycarbonyl)amino)acryloyl)glycinate (2.S1)
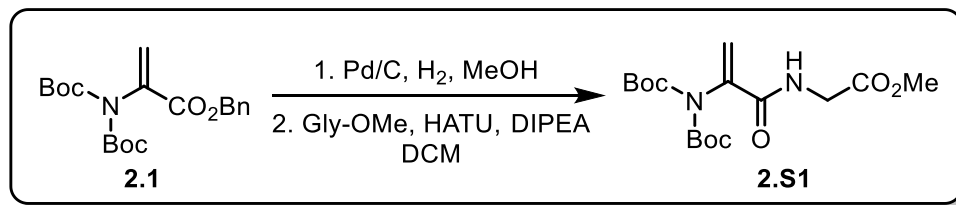
To a stirred solution of 1a (754 mg, 2.0 mmol, 1.0 equiv) in MeOH (10 mL) was added Pd/C (500 mg). After stirring for 4 h under H2, the mixture was filtered with Celite. The combined organic layers were concentrated in vacuo. The crude mixture was diluted with DCM (10 mL) and glycine methyl ester (330 mg, 2.4 mmol, 1.2 equiv), HATU (1.5 g, 4.0 mmol, 2.0 equiv), and DIPEA (0.7 mL, 4.0 mmol, 2.0 equiv) were subsequently added. After stirring for 4 h, the mixture was diluted with DCM (10 mL), and washed with brine (20 mL). The combined organic layers were dried (MgSO$_4$) and concentrated in vacuo. The residue was purified by column chromatography on SiO$_2$ (gradient hexane to 50:50 hexane/EtOAc) to give the title compound as a white solid (394 mg, 1.1 mmol, 54%). **^{1}H NMR** (500 MHz, CDCl3) δ 6.45 (m, 1H), 6.18 (s, 1H), 5.48 (s, 1H), 4.10 (d, J = 5.2 Hz, 2H), 3.75 (s, 3H), 1.46 (s, 18H). **^{13}C NMR** (126 MHz, CDCl3) δ 170.1, 164.0, 150.8, 138.8, 121.4, 84.0, 52.7, 41.7, 28.1. **FT-IR** (cm^{-1}, neat, ATR) 3411, 2920, 1751, 1713, 1655, 1510, 1333, 1170, 1051, 766. **HRMS** (ESI$^+$) calcd for C$_{16}$H$_{26}$N$_2$NaO$_7$ [M+Na]$^+$: 381.1638, found: 381.1623. **MP** = 71-72 °C

2.6.4 General Procedure A for Photoredox Carbofluorination
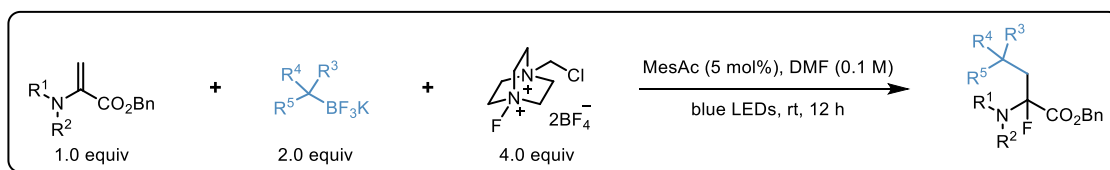
To a 5 mL reaction vial equipped with stir bar were added dehydroalanine 1 (0.5 mmol, 189 mg, 1.0 equiv), potassium alkyltrifluoroborate 2 (0.6 mmol, 2.0 equiv), 9-mesityl-10-

methylacridinium tetrafluoroborate (0.025 mmol, 10 mg, 0.05 equiv), and Selectfluor (2.0 mmol, 709 mg, 4.0 equiv). The vial was sealed with a cap containing a TFE-lined silicone septa and was evacuated and purged with argon gas three times via an inlet needle. The vial was then charged with anhyd DMF (5 mL, 0.1 M). After this, the cap was sealed with Parafilm, and the reaction mixture was purged again with argon gas. The reaction vial was irradiated in an LED reactor with a fan. After 12 h, the reaction mixture was transferred to a separatory funnel and diluted with Et2O (~10 mL) and brine (saturated aq NaCl, ~ 10 mL). The residue was extracted with Et2O (10 mL x 3) and washed with brine (10 mL x 3). The combined organic layers were dried (MgSO4), and the solvent was removed in vacuo. Further purification was accomplished by column chromatography (SiO2, EtOAc/hexane 1:20 ~ 1:5) and/or reverse phase (C18) preparative HPLC to give a fluorinated amino acid.

2.6.5 Characterization Data for Carbofluorination Products
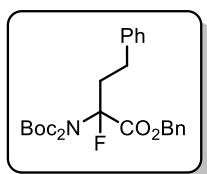
Benzyl 2-(Bis(*tert*-butoxycarbonyl)amino)-2-fluoro-4-phenylbutanoate, 2.4 (81%) was prepared according to General Procedure A. The desired compound was obtained as a colorless oil. **^{1}H NMR** (500 MHz, CDCl$_3$) δ 7.44 (d, J = 7.3 Hz, 2H), 7.37 (q, J = 7.7, 6.9 Hz, 3H), 7.25 (t, J = 7.6 Hz, 2H), 7.18 (t, J = 7.3 Hz, 1H), 7.02 (d, J = 6.9 Hz, 2H), 5.28 (s, 2H), 2.78 (td, J = 13.0, 3.2 Hz, 1H), 2.58 – 2.18 (m, 3H), 1.49 (s, 18H). **^{13}C NMR** (126 MHz, CDCl$_3$) δ 166.3 (d, J_{C-C-F} = 35 Hz), 150.9, 150.9, 139.9, 135.0, 128.6, 128.5, 128.4, 128.1, 126.1, 98.1 (d, J_{C-F} = 223 Hz), 84.2, 67.7, 36.7, 36.5, 29.6, 29.1 (d, J_{C-C-F} = 3 Hz), 27.6. **^{19}F NMR** (471 MHz, CDCl$_3$) δ -125.7 (s). **FT-IR** (cm^{-1}, neat, ATR) 2978, 1755, 1728, 1335, 1247, 1127, 847, 736, 696. **HRMS** (ESI$^+$) calcd for C$_{27}$H$_{34}$NNaFO$_6$ [M+Na]$^+$: 510.2268, found: 510.2280.
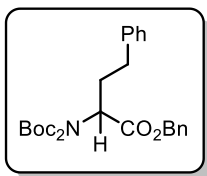
Benzyl 2-(Bis(*tert*-butoxycarbonyl)amino)-4-phenylbutanoate, 2.5 was prepared according to General Procedure A. The desired compound was obtained as a colorless oil. **^{1}H NMR** (500 MHz, CDCl$_3$) δ 7.37 (m, 7H), 7.19 (m, 3H), 5.20 (ABq, J = 12.6 Hz, 1H), 5.16 (ABq, J = 12.5 Hz, 1H), 4.96 (dd, J = 9.5, 5.2 Hz, 1H), 2.72 (t, J = 8.1 Hz, 2H), 2.52 (dtd, J = 13.6, 8.2, 5.2 Hz, 1H), 2.26 (m, 1H), 1.47 (s, 18H). **^{13}C NMR** (126 MHz, CDCl$_3$) δ 170.9, 152.5, 141.4, 135.9, 128.7, 128.7, 128.4, 128.2, 126.3, 83.3, 67.0, 58.1, 32.8, 31.6, 28.2. **FT-IR** (cm^{-1}, neat, ATR) 2979, 1699, 1741, 1366, 1136, 1114, 852, 745, 697. **HRMS** (ESI$^+$) calcd for C$_{27}$H$_{35}$NNaO$_6$ [M+Na]$^+$: 492.2362, found: 492.2316.
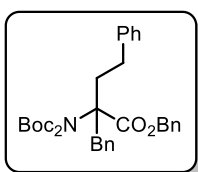
Benzyl 2-Benzyl-2-(bis(*tert*-butoxycarbonyl)amino)-4-phenylbutanoate, 2.6 was prepared according to General Procedure A. The desired compound was obtained as a colorless oil. **^{1}H NMR** (500 MHz, CDCl$_3$) δ 7.39 (m, 5H), 7.27 (m, 5H), 7.19 (m, 3H), 7.10 (d, J = 6.9 Hz, 2H), 5.20 (ABq, J = 12.5 Hz, 1H), 5.16 (ABq, J = 12.5 Hz, 1H), 3.61 (d, J = 13.6 Hz, 1H), 3.22 (d, J = 13.6 Hz, 1H), 2.83 (td, J = 13.2, 4.6 Hz, 1H), 2.61 (td, J = 13.3, 4.8 Hz, 1H), 2.29 (td, J = 13.3, 4.7 Hz, 1H), 2.13 (td, J = 13.2, 4.8 Hz, 1H), 1.45 (s, 18H). **^{13}C NMR** (126 MHz, CDCl$_3$) δ 171.9, 152.6, 141.6, 136.1, 135.9, 131.1, 128.7, 128.6, 128.6, 128.4, 128.3, 127.2, 126.2, 82.9, 67.9, 67.1, 39.1, 35.0, 30.8, 28.1. **FT-IR** (cm^{-1}, neat, ATR) 2979, 1800, 1727, 1369, 1251, 1075, 803, 736, 695. **HRMS** (ESI$^+$) calcd for C$_{34}$H$_{41}$NNaO$_6$ [M+Na]$^+$: 582.2832, found: 582.2831.
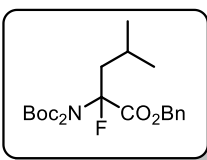
Benzyl 2-(Bis(*tert*-butoxycarbonyl)amino)-2-fluoro-4-methylpentanoate, 2.7 (87%) was prepared according to General Procedure A. The desired compound was obtained as a colorless oil. **^{1}H NMR** (500 MHz, CDCl$_3$) δ 7.36 (m, 5H) 5.29 (ABq, J = 12.5 Hz, 1H), 5.22 (ABq, J = 12.5 Hz, 1H), 2.90 (m, 2H), 1.62 (m, 1H), 1.48 (s, 18H), 0.96 (dd, J = 6.6, 1.6 Hz, 3H), 0.81 (d, J = 6.6 Hz, 3H). **^{13}C NMR** (126 MHz, CDCl$_3$) δ 166.6 (d, J_{C-C-F} = 36 Hz), 150.9(4), 150.9(3), 135.1, 128.4, 128.4, 98.8 (d, J_{C-F} = 224

Hz), 84.0, 67.6, 43.0 (d, J_{C-C-F} = 23 Hz), 27.7, 24.1, 22.8, 22.7. **^{19}F NMR** (471 MHz, CDCl$_3$) δ -

128.2 (s). **FT-IR**

(cm^{-1}, neat, ATR) 2980, 1761, 1733, 1334, 1252, 1132, 772. **HRMS** (ESI$^+$) calcd for

C$_{23}$H$_{34}$FNNaO$_6$ [M+Na]$^+$: 462.2268, found: 462.2255.
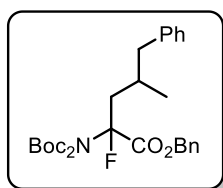
Benzyl 2-(Bis(*tert*-butoxycarbonyl)amino)-2-fluoro-4-methyl-5-phenylpentanoate, 2.8 (62%, dr 1.2:1) was prepared according to General Procedure A. The desired compound was obtained as a colorless oil. **^{1}H NMR** (500 MHz, CDCl$_3$) δ 7.34 (m, 10H), 5.26 (dd, J = 16.1, 12.4 Hz, 1H), 5.13 (dd, J = 15.9, 12.4 Hz, 1H), 2.00 (m, 1H), 1.78 (m, 1H), 1.48 (s, 9H), 1.42 (s, 9H), 1.42 (m, 2H), 1.14 (dd, J = 6.4, 1.1 Hz, 2H), 0.87 (ddd, J = 14.5, 10.6, 6.4 Hz, 2H). **^{13}C NMR** (126 MHz, CDCl$_3$) δ 172.6, 167.0, 166.8, 153.0, 152.9, 151.3, 151.3, 136.1, 135.5, 128.7, 128.7, 128.6, 128.6, 128.4, 128.3, 99.7, 84.4, 82.8, 82.8, 77.9, 67.9, 67.2, 44.0, 37.3, 37.1, 28.3, 28.2, 28.1, 28.0, 26.8, 25.8, 16.8, 16.8, 14.0, 13.8. **^{19}F NMR** (471 MHz, CDCl$_3$) δ -125.6 (s). **FT-IR** (cm^{-1}, neat, ATR) 2979, 1728, 1368, 1259, 1122, 752. **HRMS** (ESI$^+$) calcd for C$_{29}$H$_{38}$FNNaO$_6$ [M+Na]$^+$: 538.2581, found: 538.2585.

Benzyl 2-(Bis(*tert*-butoxycarbonyl)amino)-3-cyclohexyl-2-fluoropropanoate, 2.9 (72%) was prepared according to General Procedure A. The desired compound was obtained as a colorless oil. **^{1}H NMR** (500 MHz, CDCl$_3$) δ 7.36 (m, 5H), 5.28 (ABq, J = 12.1 Hz, 1H), 5.23 (ABq, J = 12.1 Hz, 1H), 2.02 (m, 1H), 1.87 (m, 2H), 1.54 (m, 2H), 1.48 (s, 18H), 1.43 (m, 1H), 1.40 (m, 2H). 1.26 (m, 3H), 0.86 (m, 2H). **^{13}C NMR** (126 MHz, CDCl$_3$) δ 166.7 (d, J_{C-C-F} = 36 Hz) 150.9, 135.2, 128.6, 128.5, 128.4 (d, J_{CF} = 225 Hz), 84.0, 67.6, 41.9, 34.3, 33.3 (d, $J_{C-C-C-F}$ = 3 Hz), 32.9, 27.7, 26.0(3), 25.9(7), 25.8. **^{19}F NMR** (471 MHz, CDCl$_3$) δ -127.2 (s). **FT-IR** (cm^{-1}, neat, ATR) 2924, 1758,

1728, 1334, 1245, 1161, 1126, 750, 696. **HRMS** (ESI$^+$) calcd for C$_{26}$H$_{38}$FNaNO$_6$ [M+Na]$^+$: 502.2581, found: 502.2568.

Benzyl 3-Bicyclo[2.2.1]heptan-2-yl-2-(bis(*tert*-butoxycarbonyl)amino)-2-fluoropropanoate, 2.10 (68%, dr 1.1:1) was prepared according to General Procedure A. The desired compound was obtained as a colorless oil. **¹H NMR** (500 MHz, CDCl$_3$) δ 7.40 (m, 2H), 7.34 (m, 3H), 5.24 (m, 2H), 2.30 – 1.90 (m, 3H), 1.78 (m, 1H), 1.48 (d, *J* = 1.9 Hz, 18H), 1.41 – 1.13 (m, 6H), 1.15 – 0.80 (m, 3H). **¹³C NMR** (126 MHz, CDCl$_3$) δ 167.3, 167.0, 167.0, 166.8, 151.2, 151.2, 151.2, 135.5, 135.4, 128.9, 128.8, 128.7, 128.7, 128.6, 128.6, 128.5, 128.3, 128.2, 99.1 (d, *J*$_{C-F}$ = 225Hz), 98.6 (d, *J*$_{C-F}$ = 224 Hz), 84.3, 67.9, 67.9, 42.8, 42.6, 42.4, 42.3, 42.1, 42.0, 41.9, 39.7, 39.4, 39.2, 39.2, 39.2, 37.0(1), 36.9(5), 36.9(2), 36.7(3), 36.7(2), 36.6, 36.0, 35.6, 35.5, 35.3, 34.6, 30.1, 30.0, 28.6, 28.5, 28.2, 28.2, 28.0. **¹⁹F NMR** (471 MHz, CDCl$_3$) δ -124.3 (s), -125.1 (s). **FT-IR** (cm^{-1}, neat, ATR) 2949, 1755, 1728, 1335, 1247, 1160, 1126, 847, 750. **HRMS** (ESI$^+$) calcd for C$_{27}$H$_{38}$FNNaO$_6$ [M+Na]$^+$: 514.2581, found: 514.2590.

Benzyl 2-(Bis(*tert*-butoxycarbonyl)amino)-2-fluoro-3-(-2-methylcyclohexyl) propanoate, 2.11 (62%, dr 5.6:1.5:1.2:1) was prepared according to General Procedure A. The desired compound was obtained as a colorless oil. **¹H NMR** (500 MHz, CDCl$_3$) δ 7.49-7.28 (m, 5H), 5.39-5.07 (m, 2H), 2.48-2.06 (m, 1H), 2.05-1.53 (m, 3H), 1.48 (m, 18H), 1.33-0.93 (m, 5H), 0.92-0.61 (m, 6H). **¹³C NMR** (126 MHz, CDCl$_3$) δ 166.5, 166.2, 150.8, 150.8, 135.0, 134.9, 128.8, 128.6, 128.5, 128.4, 128.4, 128.3, 128.3, 128.2, 100.1, 98.3, 83.9, 83.9, 67.6, 39.7, 39.1, 38.9, 38.5, 38.4, 37.5, 37.4, 36.7, 35.4, 35.2, 35.0, 34.5, 34.0, 33.8, 32.8, 32.1, 31.9, 30.1, 29.6, 28.2, 27.8, 27.6, 26.0, 25.8, 24.7, 22.6, 20.0, 19.9. **¹⁹F NMR** (471 MHz, CDCl$_3$) δ -124.3 (s), -124.9 (s), -126.6 (s), -126.9 (s). **FT-IR**

(cm^{-1}, neat, ATR) 2923, 1768, 1731, 1336, 1159, 1128, 773. **HRMS** (ESI$^+$) calcd for C$_{27}$H$_{40}$FNNaO$_6$ [M+Na]$^+$: 516.2737, found: 516.2746.
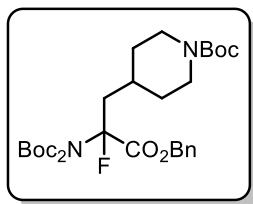
tert-Butyl 4-(3-(Benzyloxy)-2-(bis(tert-butoxycarbonyl)amino)-2-fluoro-3- oxopropyl)piperidine-1-carboxylate, 2.12 (53%) was prepared according to General Procedure A. The desired compound was obtained as a colorless oil. **¹H NMR** (500 MHz, CDCl$_3$) δ 7.42 (m, 2H),

7.36 (m, 3H), 5.28 (ABq, J = 12.3 Hz, 1H), 5.25 (ABq, J = 12.3 Hz, 1H), 3.90 (m, 2H), 2.41 (d, J = 14.2 Hz, 2H), 2.05 (dt, J = 14.1, 9.6 Hz, 1H), 1.89 (dd, J = 29.9, 13.8 Hz, 2H), 1.48 (s, 18H), 1.43 (s, 9H), 1.28 (t, J = 12.9 Hz, 2H), 1.01 (m, 2H). **¹³C NMR** (126 MHz, CDCl$_3$) δ 166.8 (d, J_{C-C-F} = 35 Hz), 155.0, 151.1(8), 151.1(6), 135.4, 129.3, 128.9, 128.8, 98.9 (d, J_{C-F} = 225 Hz), 84.6, 79.6, 68.0, 41.5, 41.3, 33.2, 32.4, 31.8, 31.2, 28.7, 28.0. **¹⁹F NMR** (471 MHz, CDCl$_3$) δ -123.8 (s). **FT-IR** (cm^{-1}, neat, ATR) 2978, 1758, 1729, 1689, 1336, 1247, 1160, 1128, 751, 698. **HRMS** (ESI$^+$) calcd for C$_{30}$H$_{45}$FN$_2$NaO$_8$ [M+Na]$^+$: 603.3058, found: 603.3052.
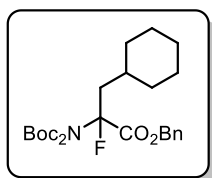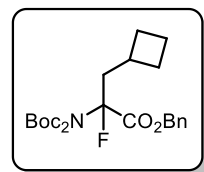

Benzyl 2-(Bis(tert-butoxycarbonyl)amino)-3-cyclobutyl-2-fluoropropanoate, 2.13 (82%) was prepared according to General Procedure A. The desired compound was obtained as a colorless oil. **¹H NMR** (500 MHz, CDCl$_3$) δ 7.36 (m, 5H), 5.30 (ABq, J = 12.3 Hz, 1H), 5.14 (ABq, J = 12.4 Hz, 1H), 2.37 (dq, J = 15.3, 7.7 Hz, 1H), 2.26 (ddd, J = 13.8, 9.5, 7.0 Hz, 1H), 2.07 (m, 2H), 1.93 (dtdd, J = 10.1, 7.6, 4.2, 2.1 Hz, 1H), 1.77 (m, 1H), 1.68 (m, 3H), 1.47 (s, 18H). **¹³C NMR** (126 MHz, CDCl$_3$) δ 166.7 (d, J_{C-C-F} = 36 Hz), 151.2, 135.4, 128.7, 128.6(2), 128.6(0), 128.5(6), 98.1 (d, J_{C-F} = 223 Hz), 84.4, 67.9, 42.0, 41.8, 30.7, 29.2, 29.1, 28.2, 28.0, 19.1. **¹⁹F NMR** (471 MHz, CDCl$_3$) δ -126.1 (s). **FT-IR** (cm^{-1}, neat, ATR) 2978, 1755, 1728, 1335, 1237, 1127, 847, 696. **HRMS** (ESI$^+$) calcd for C$_{24}$H$_{34}$FNNaO$_6$ [M+Na]+: 474.2268, found: 474.2283.
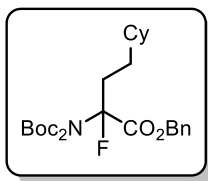
Benzyl 2-(Bis(*tert*-butoxycarbonyl)amino)-4-cyclohexyl-2-fluorobutanoate, 2.14 (58%) was prepared according to General Procedure A. The desired compound was obtained as a colorless oil. **¹H NMR** (500 MHz, CDCl₃) δ 7.36 (m, 5H), 5.25 (s, 2H), 2.13 (m, 1H), 1.96 (m, 1H), 1.48 (s, 18H), 1.26 (m, 3H), 1.11 (m, 5H), 0.91 (m, 3H), 0.74 (m, 2H). **¹³C NMR** (126 MHz, CDCl₃) δ 166.5 (d, J_{C-C-F} = 35 Hz), 151.0, 132.2, 128.6, 128.4, 128.3, 98.6 (d, J_{C-F} = 222 Hz), 84.0, 67.6, 37.3, 32.8, 32.7, 32.5, 30.0, 29.7, 27.7, 26.5, 26.1 (d, $J_{C-C-C-F}$ = 2 Hz). **¹⁹F NMR** (471 MHz, CDCl₃) δ -126.0 (s). **FT-IR** (cm⁻¹, neat, ATR) 2927, 1761, 1729, 1336, 1215, 1158, 1125, 749, 667. **HRMS** (ESI⁺) calcd for $C_{27}H_{40}FNNaO_6$ [M+Na]⁺: 516.2737, found: 516.2739.
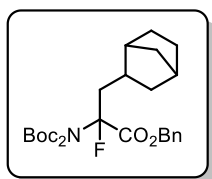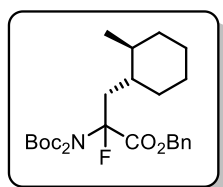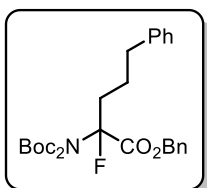

Benzyl 2-(Bis(*tert*-butoxycarbonyl)amino)-2-fluoro-5-phenylpentanoate, 2.15 (91%) was prepared according to General Procedure A. The desired compound was obtained as a colorless oil. **¹H NMR** (500 MHz, CDCl₃) δ 7.34 (m, 5H), 7.23 (m, 2H), 7.16 (m, 1H), 7.03 (d, J = 7.6 Hz, 2H), 5.26 (ABq, J = 12.3 Hz, 1H), 5.24 (ABq, J = 12.3 Hz, 1H), 2.53 (m, 2H), 2.15 (m, 1H), 2.00 (m, 1H), 1.80 (m, 1H), 1.45 (s, 18H), 1.44 (m, 1H). **¹³C NMR** (126 MHz, CDCl₃) δ 166.7 (d, J_{C-C-F} = 36 Hz), 151.2, 135.4, 128.7, 128.6, 128.6, 128.6, 98.1 (d, J_{C-F} = 223 Hz), 84.4, 67.9, 42.0, 41.8, 30.7, 29.2, 29.1, 28.2, 28.0, 19.1. **¹⁹F NMR** (471 MHz, CDCl₃) δ -128.9 (s). **FT-IR** (cm⁻¹, neat, ATR) 2980, 1758, 1727, 1337, 1248, 1161, 1127, 750, 697. **HRMS** (ESI⁺) calcd for $C_{28}H_{36}FNNaO_6$ [M+Na]⁺: 524.2424, found: 524.2432.
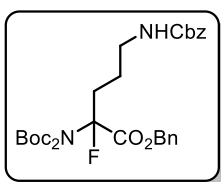
Benzyl 5-(((Benzyloxy)carbonyl)amino)-2-(bis(*tert*-butoxycarbonyl)amino)-2- fluoropentanoate, 2.16 (92%) was prepared according to General Procedure A. The desired compound was obtained as a colorless oil. **¹H NMR** (500 MHz, CDCl₃) δ 7.35 (m, 10H), 5.26 (ABq, J = 12.2 Hz, 1H), 5.23 (ABq, J = 12.4 Hz, 1H), 5.06 (s, 2H), 4.58 (s, 1H), 3.12 (q, J = 6.4 Hz, 2H), 2.18 (m, 1H), 2.03

(m, 1H), 1.58 (m, 1H), 1.47 (s, 18H), 1.36 (m, 1H). ^{13}C NMR (126 MHz, CDCl$_3$) δ 166.6 (d, $J_{C\text{-}C\text{-}F}$ = 35 Hz), 156.5, 151.2, 151.2, 136.8, 135.3, 128.9, 128.8, 128.8, 128.7, 128.4, 128.3, 98.7 (d, $J_{C\text{-}F}$ = 223 Hz), 84.6, 68.1, 66.9, 40.5, 32.5, 32.3, 28.2, 28.0, 24.0. ^{19}F NMR (471 MHz, CDCl$_3$) δ -125.1 (s). FT-IR (cm^{-1}, neat, ATR) 3321, 2981, 1758, 1725, 1339, 1249, 1128, 750, 694. HRMS (ESI$^+$) calcd for C$_{30}$H$_{39}$FN$_2$NaO$_8$ [M+Na]$^+$: 597.2588, found: 597.2590.
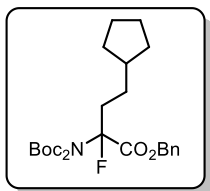
Benzyl 2-(Bis(*tert*-butoxycarbonyl)amino)-4-cyclopentyl-2-fluorobutanoate, 2.17 (82%) was prepared according to General Procedure A. The desired compound was obtained as a colorless oil. ^{1}H NMR (500 MHz, CDCl$_3$) δ 7.40 (m, 2H), 7.34 (m, 3H), 5.26 (s, 2H), 2.12 (dddd, J = 16.6, 13.5, 9.3, 4.7 Hz, 1H), 2.98 (m, 1H), 1.61 (m, 5H), 1.48 (s, 18H), 1.45 (m, 3H), 1.04 (m, 1H), 0.92 (m, 2H). ^{13}C NMR (126 MHz, CDCl$_3$) δ 166.5 (d, $J_{C\text{-}C\text{-}F}$ = 36 Hz), 151.3(4), 151.3(2), 135.6, 129.0, 128.8, 128.7, 98.4 (d, $J_{C\text{-}F}$ = 223 Hz), 84.4, 67.9, 40.0, 34.7, 34.5, 32.7, 32.6, 29.3, 28.3, 28.0(7), 28.0(5), 25.4. ^{19}F NMR (471 MHz, CDCl$_3$) δ -126.0 (s). FT-IR (cm^{-1}, neat, ATR) 2944, 1755, 1728, 1336, 1247, 1158, 1125, 848, 697. HRMS (ESI$^+$) calcd for C$_{26}$H$_{38}$FNNaO$_6$ [M+Na]$^+$: 502.2581, found: 502.2580.

Benzyl 2-(Bis(tert-butoxycarbonyl)amino)-2-fluoro-5,5-dimethylhexanoate, 2.18 (79%) was prepared according to General Procedure A. The desired compound was obtained as a white solid (mp = 87-88 ℃). ^{1}H NMR (500 MHz, CDCl$_3$) δ 7.41 (d, J = 7.1 Hz, 2H), 7.34 (q, J = 7.4 Hz, 3H), 5.26 (s, 2H), 2.09 (qd, J = 13.0, 5.4 Hz, 1H), 1.93 (dtd, J = 27.3, 13.4, 4.6 Hz, 1H), 1.49 (s, 18H), 1.33 (m, 2H), 0.75 (s, 9H). ^{13}C NMR (126 MHz, CDCl$_3$) δ 166.8 (d, $J_{C\text{-}C\text{-}F}$ = 35 Hz), 151.2(3), 151.2(2), 135.5, 129.1, 129.0, 128.7, 98.8 (d, $J_{C\text{-}F}$ = 223 Hz), 84.4, 67.9, 36.2, 30.9, 30.7, 30.0, 29.2, 28.3, 28.0(0), 27.9(7). ^{19}F NMR (471 MHz, CDCl$_3$) δ -126.5 (s). FT-IR (cm^{-1},

neat, ATR) 2957, 1756, 1730, 1368, 1335, 1246, 1161, 1125, 775, 697. **HRMS** (ESI⁺) calcd for C$_{25}$H$_{38}$FNNaO$_6$ [M+Na]⁺: 490.2581, found: 490.2598.

Benzyl 2-(Bis(*tert*-butoxycarbonyl)amino)-2-fluoro-6-oxo-6-(phenylamino) hexanoate, 2.19 (92%) was prepared according to General Procedure A. The desired compound was obtained as a colorless oil. **¹H NMR** (500 MHz, CDCl$_3$) δ 7.45 (m, 3H), 7.37 (m, 2H), 7.28 (m, 5H), 7.06 (t, J = 7.4 Hz, 1H), 7.28 (ABq, J = 12.2 Hz, 1H), 5.21 (ABq, J = 12.2 Hz, 1H), 2.29 (m, 3H), 2.13 (m, 1H), 1.73 (m, 2H), 1.44 (s, 18H). **¹³C NMR** (126 MHz, CDCl$_3$) δ 170.5, 166.7 (d, J_{C-C-F} = 35 Hz), 151.2, 151.2, 138.2, 135.2, 129.1, 128.8, 128.7, 128.7, 124.4, 120.1, 99.0 (d, J_{C-F} = 223 Hz), 84.6, 68.2, 36.7, 34.2, 34.0, 27.9, 19.7. **¹⁹F NMR** (471 MHz, CDCl$_3$) δ -124.3 (s). **FT-IR** (cm⁻¹, neat, ATR) 3321, 2981, 1758, 1726, 1339, 1249, 1150, 1128, 750, 694. **HRMS** (ESI⁺) calcd for C$_{29}$H$_{37}$FN$_2$NaO$_7$ [M+Na]⁺: 567.2482, found: 567.2497.

Benzyl 2-(Bis(*tert*-butoxycarbonyl)amino)-2-fluoro-4-(prop-2-yn-1-yloxy)butanoate, 2.20 (82%) was prepared according to General Procedure A. The desired compound was obtained as a colorless oil. **¹H NMR** (500 MHz, CDCl$_3$) δ 7.36 (m, 5H), 5.27 (ABq, J = 12.4 Hz, 1H), 5.19 (ABq, J = 12.4 Hz, 1H), 3.97 (dq, J = 18.9, 2.4 Hz, 2H), 3.67 (m, 1H), 3.50 (m, 1H), 2.50 (m, 1H), 2.38 (m 2H), 1.47 (s 18H). **¹³C NMR** (126 MHz, CDCl$_3$) δ 166.1 (d, J_{C-C-F} = 36 Hz), 150.9, 135.2, 128.4(1), 128.4(0), 128.2, 96.7 (d, J_{C-F} = 223 Hz) 84.3, 79.3, 74.6, 67.6, 64.0, 58.2, 35.3, 27.7. **¹⁹F NMR** (471 MHz, CDCl$_3$) δ -128.2 (s). **FT-IR** (cm⁻¹, neat, ATR) 3307, 2926, 1760, 1732, 1334, 1246, 1160, 1129, 774, 695. **HRMS** (ESI⁺) calcd for C$_{24}$H$_{32}$FNNaO$_7$ [M+Na]⁺: 488.2061, found: 488.2062.
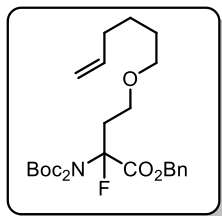
Benzyl 2-(Bis(*tert*-butoxycarbonyl)amino)-2-fluoro-4-(hex-5-en-1-yloxy)butanoate, 2.21 (63%) was prepared according to General Procedure A. The desired compound was obtained as a colorless oil. **¹H NMR** (500 MHz, CDCl₃) δ 7.36 (m, 5H), 5.77 (m, 1H), 5.27 (ABq, J = 12.4 Hz, 1H), 5.17 (ABq, J = 12.4 Hz, 1H), 4.98 (d, J = 17.4 Hz, 1H), 4.93 (d, J = 10.0 Hz, 1H), 3.47 (m, 2H), 3.28 (t, J = 6.6 Hz, 2H), 2.45 (m, 1H), 2.34 (m, 1H), 2.02 (q, J = 6.8 Hz, 2H), 1.48 (s, 2H), 1.40 (s, 18H), 1.37 (m, 2H). **¹³C NMR** (126 MHz, CDCl₃) δ 166.1 (d, JC-C-F = 35 Hz), 150.9, 138.7, 135.3, 128.4, 128.2, 128.2, 114.5, 96.8 (d, JC-F = 222 Hz), 84.2, 71.0, 67.6, 64.5, 35.4, 33.5, 29.0, 27.7, 25.3. **¹⁹F NMR** (471 MHz, CDCl₃) δ -125.1 (s). **FT-IR** (cm⁻¹, neat, ATR) 3008, 2933, 1758, 1731, 1335, 1249, 1125, 773. **HRMS** (ESI⁺) calcd for $C_{27}H_{40}FNNaO_7$ [M+Na]+: 532.2711, found: 532.2708.
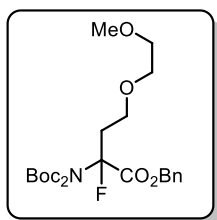
Benzyl 2-(Bis(*tert*-butoxycarbonyl)amino)-2-fluoro-4-(2-methoxyethoxy) butanoate, 2.22 (31%) was prepared according to General Procedure A. The desired compound was obtained as a colorless oil. **¹H NMR** (500 MHz, CDCl₃) δ 7.36 (m, 5H), 5.29 (ABq, J = 12.3 Hz, 1H), 5.19 (ABq, J = 12.3Hz, 1H), 3.54 (m, 6H), 3.36 (m, 3H), 2.49 (m, 1H), 2.38 (m, 1H), 1.48 (s, 18H). **¹³C NMR** (126 MHz, CDCl₃) δ 166.1 (d, JC-C-F = 36 Hz), 150.9, 135.3, 128.4, 128.3, 128.2, 96.7 (d, JC-F = 222 Hz), 84.3, 71.6, 70.2, 67.6, 65.1, 58.9, 35.3, 27.7. **¹⁹F NMR** (471 MHz, CDCl₃) δ -128.3 (s). **FT-IR** (cm⁻¹, neat, ATR) 2980, 1757, 1728, 1336, 1245, 1125, 752, 697. **HRMS** (ESI⁺) calcd for C24H36FNNaO8 [M+Na] +: 508.2323, found: 508.2310.

Benzyl 2-(Bis(*tert*-butoxycarbonyl)amino)-2-fluoro-4-((4-methoxybenzyl)oxy) butanoate, 2.23 (43%) was prepared according to General Procedure A. The desired compound was obtained as a colorless oil. **¹H NMR** (500 MHz, CDCl₃) δ 7.29 (m, 5H), 7.21 (d, *J* = 8.2 Hz, 2H), 6.84 (d, *J* = 8.4 Hz,

2H), 5.17 (ABq, J = 12.6 Hz, 1H), 5.00 (ABq, J = 12.3 Hz, 1H), 4.29 (d, J = 3.2 Hz, 2H), 3.78 (s, 3H), 3.58 (dt, J = 11.0, 5.9 Hz, 1H), 3.51 (td, J = 9.5, 6.0 Hz, 1H), 2.43 (m, 2H), 1.47 (s, 18H). ^{13}**C NMR** (126 MHz, CDCl$_3$) δ 166.4 (d, $J_{C\text{-}C\text{-}F}$ = 36 Hz), 159.5, 151.2, 151.2, 135.6, 130.3, 129.8, 128.7, 128.6, 128.5, 128.4, 128.3, 114.0, 97.1 (d, $J_{C\text{-}F}$ = 222 Hz), 84.5, 83.3, 73.1, 67.9, 64.2(8), 64.2(6), 55.6, 35.9, 35.7, 30.0, 28.0. ^{19}**F NMR** (471 MHz, CDCl$_3$) δ -125.1 (s). **FT-IR** (cm^{-1}, neat, ATR) 2980, 1757, 1728, 1336, 1245, 1125, 752, 697. **HRMS** (ESI$^+$) calcd for C$_{26}$H$_{38}$FNNaO$_7$ [M+Na]$^+$: 518.2530, found: 518.2523.

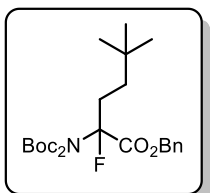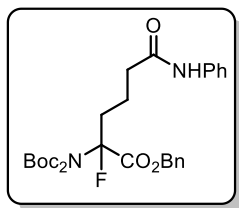**Benzyl** **2-(Bis(*tert*-butoxycarbonyl)amino)-2-fluoro-4-(2-(trimethylsilyl)ethoxy)butanoate, 2.24** (42%) was prepared according to General Procedure A. The desired compound was obtained as a colorless oil.

^{1}**H NMR** (500 MHz, CDCl$_3$) δ 7.40 (m, 2H), 7.34 (m, 3H), 5.28 (ABq, J = 12.4 Hz, 1H), 5.18 (ABq, J = 12.4 Hz, 1H), 3.49 (ddd, J = 9.7, 7.3, 5.0 Hz, 1H), 3.35 (m, 3H), 2.44 (m, 1H), 2.33 (ddt, J = 28.8, 14.4, 7.5 Hz, 1H), 1.47 (s, 18H), 0.84 (m, 2H), -0.0 (s, 9H). ^{13}**C NMR** (126 MHz, CDCl$_3$) δ 166.4 (d, $J_{C\text{-}C\text{-}F}$ = 36 Hz), 151.2, 135.5, 128.7, 128.6, 128.5, 97.1 (d, $J_{C\text{-}F}$ = 219 Hz), 84.5, 68.4, 67.9, 64.2, 64.1, 35.8, 35.6, 31.2, 28.0, 18.3, -1.2. ^{19}**F NMR** (471 MHz, CDCl$_3$) δ -125.1 (s). **FT-IR** (cm^{-1}, neat, ATR) 2980, 1761, 1732, 1370, 1249, 1129, 838, 772. **HRMS** (ESI$^+$) calcd for C$_{26}$H$_{42}$FNO$_7$Si [M+Na]$^+$: 550.2612, found: 550.2621.

Benzyl **4-(Benzyloxy)-2-(bis(*tert*-butoxycarbonyl)amino)-2-fluorobutanoate, 2.25** (41%) was prepared according to General Procedure A. The desired compound was obtained as a colorless oil. ^{1}**H NMR** (500 MHz, CDCl$_3$) δ 7.30 (m, 10H), 5.18 (ABq, J = 12.4 Hz, 1H), 5.00 (ABq, J = 12.4z Hz, 1H), 4.38 (ABq, J = 11.9z Hz, 1H), 4.35 (ABq, J = 11.9z Hz, 1H), 3.59 (m, 2H), 3.44 (m, 2H), 1.48 (s, 18H). ^{13}**C NMR** (126 MHz, CDCl$_3$) δ 166.5 (d, JC-C-F = 35 Hz), 151.2, 138.2, 135.5, 128.6, 128.5, 128.4, 128.2, 128.0, 97.1 (d, JC-F = 223 Hz), 84.6, 73.5, 67.9, 64.6, 35.90, 35.7, 31.2,

28.0. ¹⁹**F NMR** (471 MHz, CDCl$_3$) δ -125.1 (s). **FT-IR** (cm^{-1}, neat, ATR) 2980, 1767, 1729, 1336, 1249, 1127, 773, 697. **HRMS** (ESI$^+$) calcd for C$_{28}$H$_{36}$FNNaO$_7$ [M+Na]+: 540.2374, found: 540.2283.
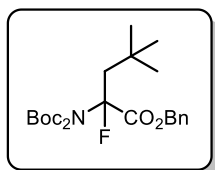
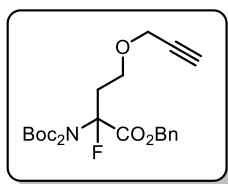**Benzyl 2-(Bis(*tert*-butoxycarbonyl)amino)-2-fluoro-4,4-dimethylpentanoate, 2.26** (61%) was prepared according to General Procedure A. The desired compound was obtained as a colorless oil. ¹**H NMR** (500 MHz, CDCl$_3$) δ 7.36 (m, 5H), 5.30 (ABq, *J* = 12.3 Hz, 1H), 5.14 (ABq, *J* = 12.3 Hz, 1H), 2.13 (dd, *J* = 14.3, 8.5 Hz, 1H), 2.00 (dd, *J* = 33.7, 14.3 Hz, 1H), 1.47 (s, 18H), 0.96 (s, 9H). ¹³**C NMR** (126 MHz, CDCl$_3$) δ 166.9 (d, $J_{C\text{-}C\text{-}F}$ = 36 Hz), 150.8, 135.0, 128.4, 128.4, 128.2, 97.7 (d, $J_{C\text{-}F}$ = 227 Hz), 84.0, 67.7, 46.6, 30.6, 30.0, 29.7, 27.7. ¹⁹**F NMR** (471 MHz, CDCl$_3$) δ -127.4 (s). **FT-IR** (cm^{-1}, neat, ATR) 2926, 1760, 1732, 1334, 1246, 1160, 1129, 774, 695. **HRMS** (ESI$^+$) calcd for C$_{24}$H$_{36}$FNNaO$_6$ [M+Na]$^+$: 476.2424, found: 476.2448.
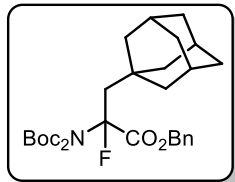
Benzyl 3-(Adamantan-1-yl)-2-(bis(*tert*-butoxycarbonyl)amino)-2-fluoropropanoate, **2.27** (67%) was prepared according to General Procedure A. The desired compound was obtained as a colorless oil. ¹**H NMR** (500 MHz, CDCl$_3$) δ 7.40 (dt, *J* = 5.5, 1.8 Hz, 2H), 7.34 (m, 3H), 5.26 (s, 2H), 2.12 (dddd, *J* = 16.6, 13.5, 9.4, 4.7 Hz, 1H), 2.98 (m, 1H), 1.61 (m, 4H), 1.48 (m, 7H), 1.47 (s, 18H), 1.25 (m, 1H), 0.97 (m, 3H). ¹³**C NMR** (126 MHz, CDCl$_3$) δ 166.8 (d, $J_{C\text{-}C\text{-}F}$ = 35.5 Hz), 151.3, 151.2, 135.5, 128.9, 128.7, 128.6, 98.8 (d, $J_{C\text{-}F}$ = 223.1 Hz), 84.4, 67.9, 39.9, 34.7, 34.5, 32.6, 32.5, 29.3, 28.2, 28.0, 25.4. ¹⁹**F NMR** (471 MHz, CDCl$_3$) δ -126.0 (s). **FT-IR** (cm^{-1}, neat, ATR) 2903, 1759, 1731, 1335, 1247, 1160, 1126, 848, 733, 695. **HRMS** (ESI$^+$) calcd for C$_{30}$H$_{42}$FNNaO$_6$ [M+Na]$^+$: 554.2894, found: 554.2905.

1-Benzyl 6-Ethyl 2-(Bis(*tert*-butoxycarbonyl)amino)-2-fluoro-4-methylhexanedioate, 2.28 (71%, dr 1.4:1) was prepared according to General Procedure A. The desired compound was obtained as a colorless oil. **^{1}H NMR** (500 MHz, CDCl$_3$) δ 7.41 (m, 3H), 7.35 (m, 2H), 5.28 (m, 2H), 4.08 (dq, J = 15.4, 7.2 Hz, 2H), 2.60 (dd, J = 15.5, 4.2 Hz, 0.4H), 2.33 (ddd, J = 14.3, 10.5, 8.4 Hz, 0.4H), 2.22 – 1.81 (m, 4.2H), 1.49 (d, J = 3.7 Hz, 18H), 1.22 (dt, J = 13.4, 7.2 Hz, 3H), 1.05 (d, J = 6.3 Hz, 1.8H), 0.90 (d, J = 6.6 Hz, 1.2H). **^{13}C NMR** (126 MHz, CDCl$_3$) δ 172.5, 172.1, 166.8, 166.6, 166.5, 151.2, 151.2, 151.1, 151.1, 135.4, 135.3, 128.8, 128.7, 128.7, 128.7, 128.6, 128.3, 128.3, 99.9 (d, J_{C-F} = 148 Hz), 98.1 (d, J_{CF} = 141 Hz), 84.5, 68.1, 68.1, 60.5, 60.4, 42.7, 40.9, 40.9, 40.8, 40.7, 40.7, 28.2, 28.2, 28.1, 28.0, 26.9, 26.3, 21.2, 20.5, 20.4, 14.5. **^{19}F NMR** (471 MHz, CDCl$_3$) δ -124.5 (s), -124.6 (s). **FT-IR** (cm^{-1}, neat, ATR) 2980, 1758, 1728, 1335, 1248, 1151, 1125, 645, 774, 697. **HRMS** (ESI$^+$) calcd for C$_{26}$H$_{38}$FNNaO$_8$ [M+Na]$^+$: 534.2479, found: 534.2490.
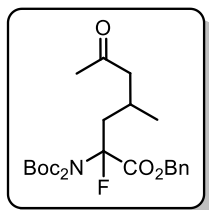
Benzyl 2-(Bis(tert-butoxycarbonyl)amino)-2-fluoro-4-methyl-6-oxooctanoate, 2.29 (51%, dr 1.9:1, major diastereomer characterized) was prepared according to General Procedure A. The desired compound was obtained as a colorless oil. **^{1}H NMR** (500 MHz, CDCl$_3$) δ 7.38 (m, 5H), 5.30 (m, 2H), 2.77 – 1.85 (m, 6H), 1.49 (d, *J* = 7.6 Hz, 18H), 1.43 (m, 3H), 1.00 (m, 4H). δ 7.42 (m, 2H), 7.34 (m, 3H), 5.34 (d, *J* = 12.2 Hz, 1H), 5.24 (d, *J* = 12.2 Hz, 1H), 2.35 (m, 5H), 2.04 (m, 4H), 1.47 (s, 18H), 1.44 (d, J = 2.7 Hz, 1H), 0.98 (t, *J* = 7.3 Hz, 3H). **^{13}C NMR** (126 MHz, CDCl$_3$) δ 209.7, 166.6 (d, J_{C-C-F} = 35 Hz), 150.9, 150.9, 135.1, 128.4, 128.3, 99.7 (d, J_{C-F} = 148 Hz), 84.1, 67.8, 50.0, 40.7, 40.6, 36.1, 28.0, 27.6, 25.4, 20.4, 20.3, 7.6. **^{19}F NMR** (471 MHz, CDCl$_3$) δ -124.5 (s). **FT-IR** (cm^{-1}, neat, ATR) 2980, 1767, 1730, 1370, 1339, 1253, 1129, 772. **HRMS** (ESI$^+$) calcd for C$_{26}$H$_{38}$FNNaO$_7$ [M+Na]$^+$: 518.2530, found: 518.2523.
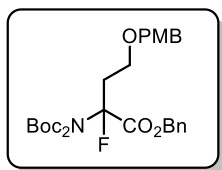
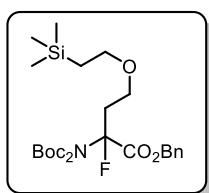**Benzyl 4-((4-Bromophenyl)sulfonamido)-2-(bis(tert-butoxycarbonyl)amino)-2- fluorobutanoate, 2.30** (32%) was prepared according to General Procedure A. The desired compound was obtained as a colorless oil. **¹H NMR** (500 MHz, CDCl₃) δ 7.63 (m, 4H), 7.35 (m, 5H), 5.24 (ABq, J = 12.4 Hz, 1H), 5.21 (ABq, J = 12.4 Hz, 1H), 4.75 (s, 1H), 3.08 (dt, J = 13.6, 6.9 Hz, 1H), 2.96 (dd, J = 13.9, 7.0 Hz, 1H), 2.43 (dq, J = 15.4, 7.5 Hz, 1H), 2.25 (ddt, J = 26.9, 13.8, 6.3 Hz, 1H), 1.46 (s, 18H). **¹³C NMR** (126 MHz, CDCl₃) δ 166.4, 150.7, 138.8, 134.5, 132.3, 128.5, 128.5, 128.5, 128.4, 127.6, 113.8, 97.4 (J_{C-F} = 128 Hz), 84.7, 68.2, 37.9, 35.1, 34.9, 30.8 (J_{C-C-F} = 38 Hz), 27.6. **¹⁹F NMR** (471 MHz, CDCl₃) δ -123.9 (s). **FT-IR** (cm⁻¹, neat, ATR) 3295, 2981, 1759, 1728, 1338, 1152, 1128, 772, 737. **HRMS** (ESI⁺) calcd for $C_{27}H_{34}FN_2NaO_8S$ [M+Na]⁺: 667.1101, found: 667.1126.
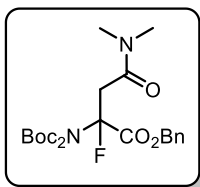
Benzyl 2-(Bis(tert-butoxycarbonyl)amino)-4-(dimethylamino)-2-fluoro-4-oxobutanoate, 2.31 (64%) was prepared according to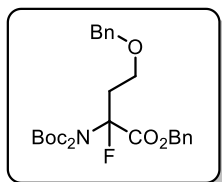 General Procedure A. The desired compound was obtained as a colorless oil. **¹H NMR** (500 MHz, CDCl₃) δ 7.43 (d, J = 7.3 Hz, 2H), 7.32 (dt, J = 12.0, 6.9 Hz, 3H), 5.30 (ABq, J = 12.3 Hz, 1H), 5.25 (ABq, J = 12.3 Hz, 1H), 3.74 (dd, J = 14.5, 9.1 Hz, 1H), 3.01 (s, 3H), 2.99 (m, 1H), 2.91 (s, 3H), 1.47 (s, 18H). **¹³C NMR** (126 MHz, CDCl₃) δ 166.1 (d, J_{C-C-F} = 32 Hz), 151.4, 135.6, 128.8, 128.6, 128.4, 97.7 (d, J_{C-F} = 226 Hz), 84.7, 68.4, 39.6, 39.4, 38.2, 35.9, 28.0. **¹⁹F NMR** (471 MHz, CDCl₃) δ -123.6 (s). **FT-IR** (cm⁻¹, neat, ATR) 2980, 1731, 1655, 1370, 1337, 1249, 1150, 1127, 773. **HRMS** (ESI⁺) calcd for $C_{23}H_{33}FN_2NaO_7$ [M+Na]⁺: 491.2169, found: 491.2177.
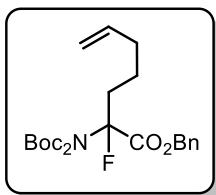
Benzyl 2-(Bis(tert-butoxycarbonyl)amino)-2-fluorohept-6-enoate, 2.32 (51%) was prepared according to General Procedure A. The desired

compound was obtained as a colorless oil. **¹H NMR** (500 MHz, CDCl₃) δ 7.39 (m, 2H), 7.34 (m, 3H), 5.63 (ddt, J = 18.4, 9.5, 6.7 Hz, 1H), 5.28 (ABq, J = 12.2 Hz, 1H), 5.24 (ABq, J = 12.3 Hz, 1H), 4.94 (m, 1H), 4.91 (t, J = 1.4 Hz, 1H), 2.13 (dddd, J = 13.9, 12.0, 9.4, 4.8 Hz, 1H), 1.99 (m, 3H), 1.48 (s, 18H), 1.21 (m, 2H). **¹³C NMR** (126 MHz, CDCl₃) δ 166.8 (d, J_{C-C-F} = 35 Hz), 151.3, 151.2, 137.7, 135.5, 128.8, 128.7, 115.7, 98.7 (d, J_{C-F} = 223 Hz), 84.4, 67.9, 34.7, 34.5, 33.4, 28.0, 22.3(7), 22.3(5). **¹⁹F NMR** (471 MHz, CDCl₃) δ -125.7 (s). **FT-IR** (cm⁻¹, neat, ATR) 3011, 2980, 1759, 1731, 1370, 1339, 1259, 1130, 772. **HRMS** (ESI⁺) calcd for C₂₄H₃₄FNNaO₆ [M+Na]+: 474.2279, found: 474.2268.
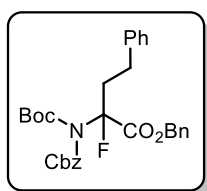
Benzyl 2-(((Benzyloxy)carbonyl)(tert-butoxycarbonyl)amino)-2-fluoro-4-phenylbutanoate, 2.33 (79%) was prepared according to General Procedure A. The desired compound was obtained as a white solid (mp = 99-100 ℃). **¹H NMR** (500 MHz, CDCl₃) δ 7.28 (m, 10H), 7.12 (m, 3H), 6.89 (m, 2H), 5.13 (m, 4H), 2.65 (m, 1H), 2.30 (m, 3H), 1.28 (s, 9H). **¹³C NMR** (126 MHz, CDCl₃) δ 166.5 (d, J_{C-C-F} = 34 Hz), 152.8(2), 152.8(1), 150.7(8), 150.7(6), 140.1, 135.3, 134.7, 129.0(1), 129.9(7), 128.9(2), 128.8(7), 128.7(3), 128.5, 126.5, 98.7 (d, J_{C-F} = 225 Hz), 85.2, 69.7, 68.2, 37.1, 36.9, 29.4(7), 29.4(5), 27.7. **¹⁹F NMR** (471 MHz, CDCl₃) δ -126.1 (s). **FT-IR** (cm⁻¹, neat, ATR) 2947, 1752, 1720, 1323, 1235, 754, 697, 621. **HRMS** (ESI⁺) calcd for C₃₀H₃₂FNNaO₆ [M+Na]⁺: 544.2111, found: 544.2111.
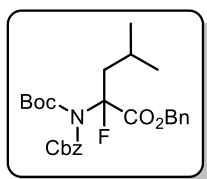
Benzyl 2-(((Benzyloxy)carbonyl)(tert-butoxycarbonyl)amino)-2-fluoro-4-methylpentanoate, 2.34 (92%) was prepared according to General Procedure A. The desired compound was obtained as a colorless oil. **¹H NMR** (500 MHz, CDCl₃) δ 7.35 (m, 10H), 5.21 (m, 4H), 1.96 (m, 2H), 1.60 (m, 1H), 1.38 (s, 9H), 0.93 (dd, J = 6.7, 1.9 Hz, 3H), 0.80 (d, J = 6.6 Hz, 3H). **¹³C NMR** (126 MHz, CDCl₃) δ 166.7 (d, J_{C-C-F} = 35 Hz), 152.7, 150.7, 135.3, 134.9, 129.0, 128.9, 128.9, 128.7(4), 128.6(8),

128.5, 128.3, 99.4 (d, J_{C-F} = 227 Hz), 85.0, 69.6, 68.0, 43.3, 43.1, 28.1, 27.7, 24.4, 24.3, 22.9(9), 22.9(6). **^{19}F NMR** (471 MHz, CDCl$_3$) δ -125.2 (s). **FT-IR** (cm^{-1}, neat, ATR) 2961, 1772, 1734, 1254, 1220, 1138, 772, 697. **HRMS** (ESI$^+$) calcd for C$_{26}$H$_{32}$FNNaO$_6$ [M+Na]$^+$: 496.2111, found: 496.2119.
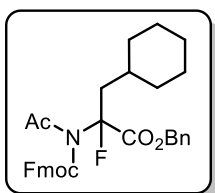
Methyl 2-(N-((((9H-Fluoren-9-yl)methoxy)carbonyl)acetamido)-3-cyclohexyl-2-fluoropropanoate, 2.35 (35%) was prepared according to General Procedure A. The desired compound was obtained as a colorless oil. **^{1}H NMR** (500 MHz, CDCl$_3$) δ 7.78 (d, J = 7.7 Hz, 2H), 7.61 (d, J = 7.5 Hz, 2H), 7.43 (t, J = 7.5 Hz, 2H), 7.34 (t, J = 7.5 Hz, 2H), 4.73 (dd, J = 10.8, 6.2 Hz, 1H), 4.65 (dd, J = 10.9, 6.2 Hz, 1H), 4.27 (t, J = 6.2 Hz, 1H), 3.79 (s, 3H), 2.10 (m, 1H), 2.02 (s, 3H), 1.89 (d, J = 13.1 Hz, 1H), 1.77 (ddd, J = 32.1, 14.3, 4.1 Hz, 1H), 1.62 (m, 3H), 1.49 (m, 1H), 1.34 (dd, J = 7.6, 3.8 Hz, 1H), 1.14 (dt, J = 45.0, 12.4 Hz, 3H), 0.87 (m, 2H). **^{13}C NMR** (126 MHz, CDCl$_3$) δ 171.11, 167.5 (d, J_{C-C-F} = 32 Hz), 153.7, 143.0(1), 142.9(9), 141.7(2), 141.6(7), 128.4(9), 128.4(6), 128.2, 127.7(0), 127.6(6), 127.4, 125.1, 120.5, 120.4, 99.2 (d, J_{C-F} = 227 Hz), 69.8, 53.2, 47.0, 46.8, 42.3, 42.1, 34.5, 33.6(9), 33.6(6), 33.6, 26.5, 26.3, 25.1. **^{19}F NMR** (471 MHz, CDCl$_3$) δ -125.7 (s). **FT-IR** (cm^{-1}, neat, ATR) 2925, 2851, 1753, 1714, 1450, 1253, 772, 741. **HRMS** (ESI$^+$) calcd for C$_{27}$H$_{30}$FNNaO$_5$ [M+Na]$^+$: 490.2006, found: 490.2024.
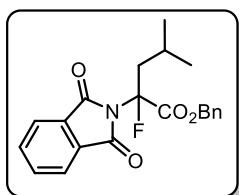
Benzyl 2-(1,3-Dioxoisoindolin-2-yl)-2-fluoro-4-methylpentanoate, 2.36 (41%) was prepared according to General Procedure A. T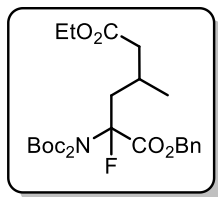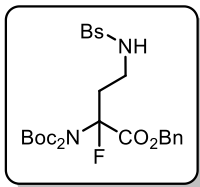he desired compound was obtained as a colorless oil. **^{1}H NMR** (500 MHz, CDCl$_3$) δ 7.87 (m, 2H), 7.78 (m, 2H), 7.36 (m, 5H), 5.37 (ABq, J = 12.1 Hz, 1H), 5.25 (ABq, J = 12.1 Hz, 1H), 3.02 (ddd, J = 14.9, 12.4, 9.1 Hz, 1H), 2.31 (dd, J = 14.9, 3.7 Hz, 1H), 1.66 (dtd, J = 12.1, 6.6, 3.3 Hz, 1H), 1.03 (dd, J = 6.6, 1.9 Hz, 3H), 0.92 (d, J = 6.7 Hz, 3H). **^{13}C NMR** (126 MHz, CDCl$_3$) δ 167.0, 166.4 (d, JC-C-F = 33 Hz), 135.1, 135.0, 131.5, 129.0, 128.9, 128.9, 124.2, 98.3

60

(d, JC-F = 222 Hz), 68.5, 42.3, 42.1, 31.2, 24.8, 24.6, 23.1, 23.0. ^{19}**F NMR** (471 MHz, CDCl$_3$) δ -122.3 (s). **FT-IR** (cm^{-1}, neat, ATR) 2960, 1790, 1735, 1366, 1220, 772, 717. **HRMS** (ESI$^+$) calcd for C$_{21}$H$_{20}$FNNaO$_4$ [M+Na]$^+$: 392.1274, found: 392.1299.
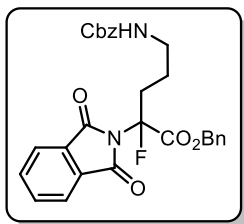
5-(((Benzyloxy)carbonyl)amino)-2-(1,3-dioxoisoindolin-2-yl)-2-fluoropentanoate, 2.37 (47%) was prepared according to General Procedure A. The desired compound was obtained as a colorless oil. ^{1}**H NMR** (500 MHz, CDCl$_3$) δ 7.88 (dd, J = 5.5, 3.0 Hz, 2H), 7.79 (dd, J = 5.6, 3.1 Hz, 2H), 7.35 (m, 10H), 5.37 (ABq, J = 12.1 Hz, 1H), 5.25 (ABq, J = 12.0 Hz, 1H), 5.11 (s, 2H), 4.73 (s, 1H), 3.23 (m, 2H), 3.00 (dd, J = 18.8, 8.4 Hz, 1H), 2.47 (m, 1H), 1.68 (dq, J = 12.2, 6.1 Hz, 1H), 1.55 (s, 18H), 1.46 (m, 1H). ^{13}**C NMR** (126 MHz, CDCl$_3$) δ 166.9, 166.2 (d, J_{C-C-F} = 32 Hz), 156.6, 135.3, 135.3, 134.9, 131.5, 129.1, 129.0, 128.9, 128.8, 128.4, 124.3, 97.3 (d, J_{C-F} = 221 Hz), 77.6, 77.3, 77.1, 68.7, 67.0, 40.6, 31.5, 31.3. ^{19}**F NMR** (471 MHz, CDCl$_3$) δ -122.5 (s). **FT-IR** (cm^{-1}, neat, ATR) 3322, 2980, 1759, 1729, 1340, 1251, 1129, 772. **HRMS** (ESI$^+$) calcd for C$_{28}$H$_{25}$FN$_2$NaO$_6$ [M+Na]$^+$: 527.1594, found: 527.1609.
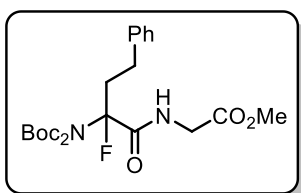
Methyl (2-(Bis(tert-butoxycarbonyl)amino)-2-fluoro-4-phenyl butanoyl) lycinate, **2.40** (29%) was prepared according to General Procedure A. The desired compound was obtained as a colorless oil. ^{1}**H NMR** (500 MHz, CDCl$_3$) δ 7.25 (d, J = 6.9 Hz, 2H), 7.18 (dd, J = 7.8, 6.0 Hz, 3H), 6.92 (s, 1H), 4.31 (dd, J = 18.3, 6.4 Hz, 1H), 3.96 (dd, J = 18.3, 4.1 Hz, 1H), 3.78 (s, 3H), 2.77 (m, 2H), 2.47 (m, 2H), 1.48 (s, 18H). ^{13}**C NMR** (126 MHz, CDCl$_3$) δ 170.0, 169.5, 167.5 (d, JC-C-F = 29 Hz), 160.3, 151.3, 150.0, 140.5, 128.8, 128.7, 126.6, 101.5 (d, JC-F = 224 Hz), 84.4, 82.3, 52.9, 41.7, 41.2, 38.7, 29.3, 28.3, 28.0. 19F NMR (CDCl3, 471 MHz) δ -126.3 (s). **FT-IR** (cm^{-1}, neat, ATR) 3411, 2971, 1754, 1722, 1655, 1515, 1334, 1173, 1054, 769. **HRMS** (ESI$^+$) calcd for C$_{23}$H$_{33}$FN$_2$NaO$_7$ [M+Na]$^+$: 491.2170, found: 491.2144.

61

2.6.6 Light/Dark studies

To a 5 mL reaction vial equipped with stir bar were added dehydroalanine 1a (0.5 mmol, 189 mg, 1.0 equiv), BnBF3K 2a (0.6 mmol, 2.0 equiv), 9-mesityl-10-methylacridinium tetrafluoroborate (0.025 mmol, 10 mg, 0.05 equiv), and Selectfluor (2.0 mmol, 709 mg, 4.0 equiv). The vial was sealed with a cap containing a TFE-lined silicone septa and was evacuated and purged with argon three times via an inlet needle. The vial was then charged with degassed anhyd DMF (5 mL) followed by 1-trifluoromethyl-naphthalene (98 mg, 0.5 mmol, 1 equiv) as an internal standard. The vial was sealed with Parafilm® and stirred in darkness for 20 min. At this point an aliquot (~0.1 mL) was taken for a t0 time point. The reaction was alternatively irradiated in the aforementioned LED reactor and kept in the dark in 20 minute intervals. Aliquots were removed at the start and after each interval and diluted with DMSO. Yield was determined by ^{19}F NMR.
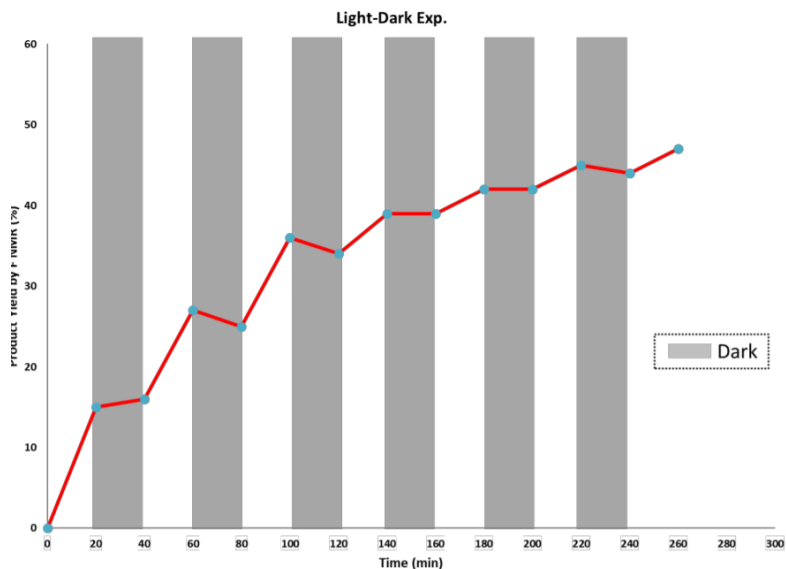
Figure 2.12. Effect of light exposure on DHA yield over time.

2.6.7. Stern-Volmer Emission Quenching Studies

Stern Volmer fluorescence quenching experiments were performed using the following parameters: emission was scanned from 500 nm to 600 nm in 1 nm increments with an integration time of 0.2 seconds and an excitation wavelength of 510 nm. Each experiment is an average of three scans.

Fluorescence emission of mesityl acridinium: To a quartz cuvette with a rubber stopper was added 500 µL of a $2.5 \times 10\text{-}4$ M solution of mesityl acridinium in anhyd MeCN. To the solution was added 500 µL anhyd MeCN to achieve a final concentration of $1.25 \times 10\text{-}4$ M. The solution was degassed with Ar for 30 seconds, capped with the rubber stopper, and then the emission of the sample without quencher was measured
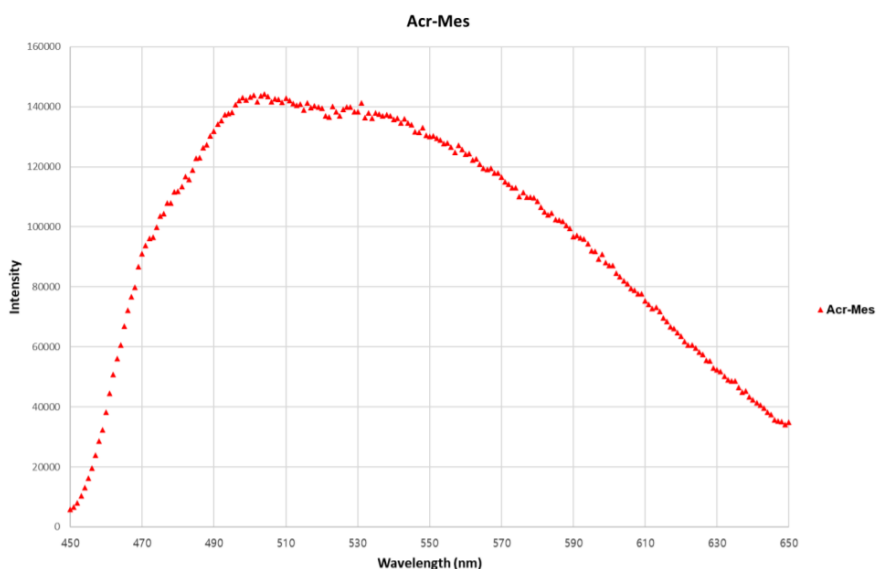
Figure 2.13. Plot of fluorescence emission of mesityl acridinium *vs* wavelength.

Fluorescence quenching ability of dehydroalanine 1a, potassium benzyltrifluoroborate 2a, and Selectfluor: To a quartz cuvette with a rubber stopper was added 500 µL of a $2.5 \times 10\text{-}4$ M solution of mesityl acridinium in anhyd MeCN. and **2.1** or potassium benzyltrifluoroborate or

Selectfluor of appropriate concentration in anhyd MeCN ([mesityl acridinium] = 1.25 x 10-4 M, [quencher] = 0.001 M, 0.002 M, 0.004 M, 0.008 M, 0.016 M, 0.032 M). Each solution was degassed with Ar for 30 seconds, capped with the rubber stopper, and then the emission of the sample was measured. Intensity was plotted against wavelength at each concentration.
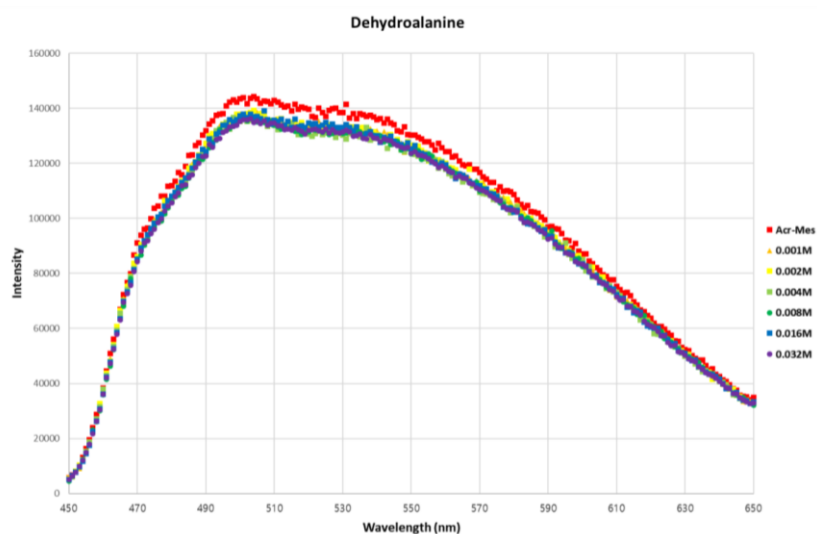
Figure 2.14. Plot of fluorescence quenching quenching of Mes-Acr$^+$ with **2.1**.
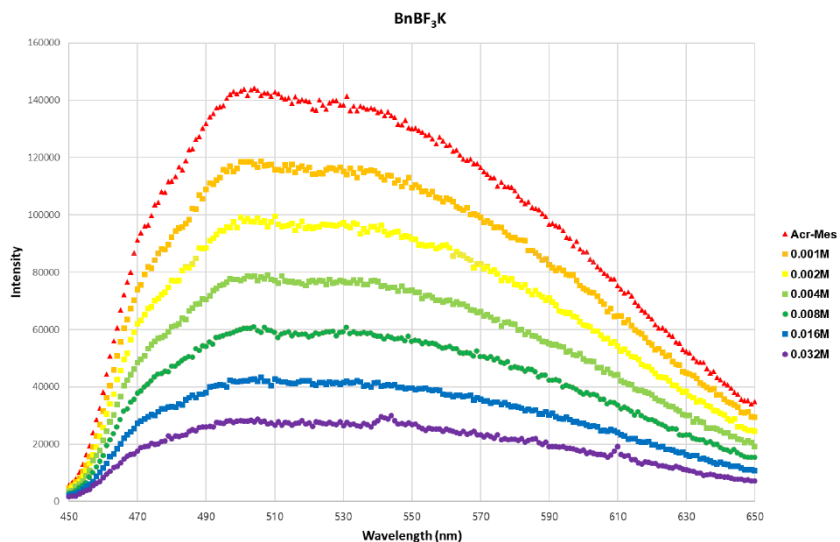
Figure 2.15. Plot of fluorescence quenching of Mes-Acr$^+$ with benzyl-BF$_3$K.
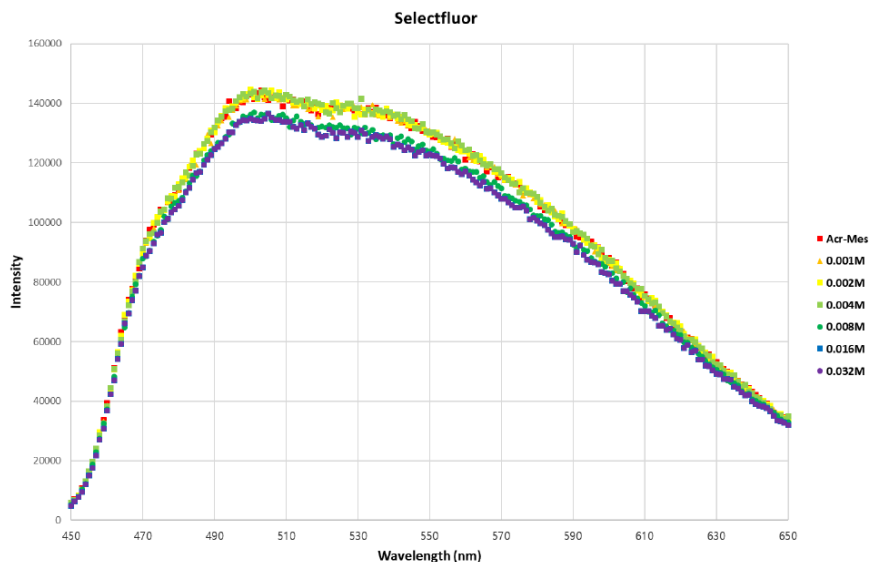
Figure 2.16. Plot of fluorescence quenching of Mes-Acr$^+$ with Selectfluor.

Calculation of the quencher rate coefficient: I^0/I at the wavelength of maximum emission (510 nm) was also plotted versus concentration of quencher according to the Stern Volmer relationship

$$\frac{I^0}{I} = 1 + k_q \tau_0 \cdot [Q]$$

where I^0 = Intensity of fluorescence without a quencher

I = intensity of fluorescence with a quencher

k$_q$ = quencher rate coefficient

τ_0 = excited state lifetime of the photocatalyst (4.2 ps)[18]

[Q] = concentration of the quencher.

Based on the data obtained via this equation, the quencher rate coefficient is 2.5 x 10^{7}M^{-1}s^{-1} for benzyl-BF$_3$K

65
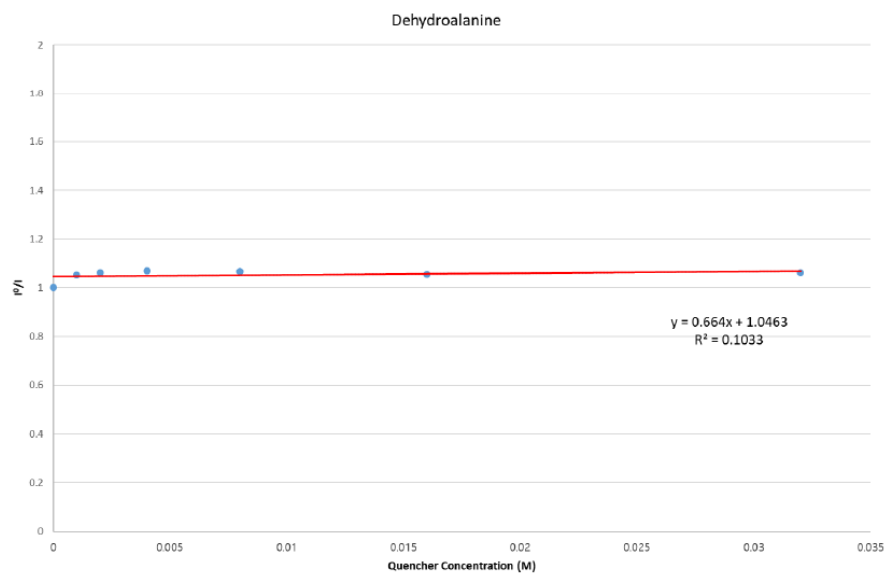
Figure 2.17. Stern-Volmer plot for **2.1**.
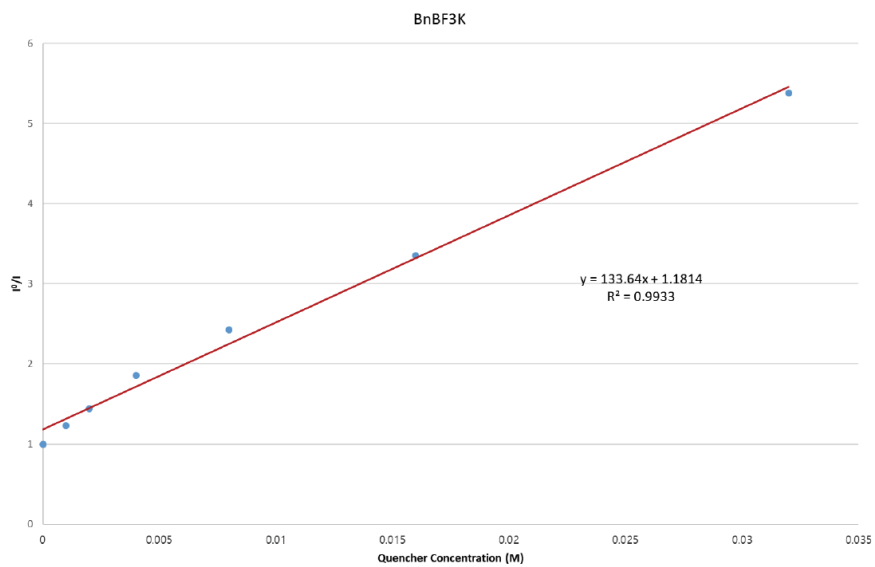
Figure 2.18. Stern-Volmer plot for benzyl-BF$_3$K.
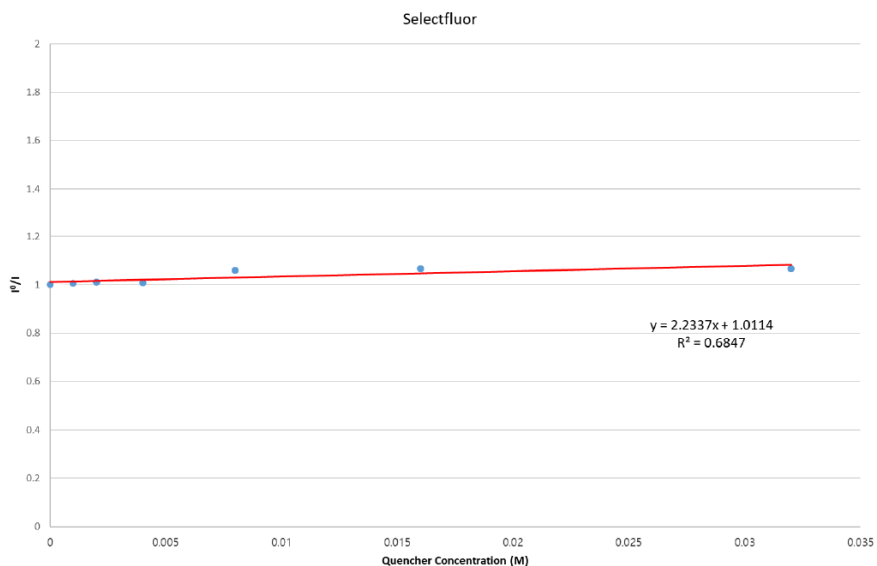
Figure 2.19. Stern-Volmer plot for selectfluor.

2.6.8. Computational Studies

All computational calculations were performed at the B3LYP/6-31G(d) level of theory using Gaussian 09 visualized via WebMO with implicit solvent model (PCM; DMF).[32,33] The energy minimized conformations of Dha analogs **1a, 1b** and **1c** were determined and visualized using CYL View, and the torsional angle was measured between the atoms indicated in **Figure 2.20**.
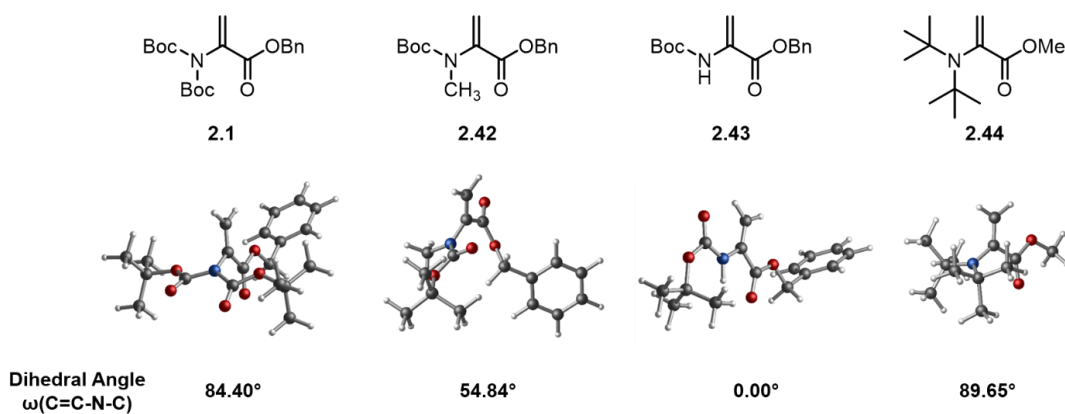
Figure 2.20. Energy-minimized structures of DHA derivatives and dihedral angles

To evaluate the propensity of **2.1** to exist as other rotational conformers, a coordinate scan of the N-C(olefin) bond was examined. A simplified model of **2.1** was utilized to minimize calculation time. The energies of different geometric conformations of the carbamate and ester groups were first calculated (**Figure 2.21**).

| Total energy (Hartrees) : | -512946.48725 | -512946.218048 | -512945.65078 |
| Energy difference : | 0 | +0.27 | +0.84 |

| Total energy (Hartrees) : | -512946.48725 | -512945.236623 |
| Energy difference : | 0 | +1.25 |
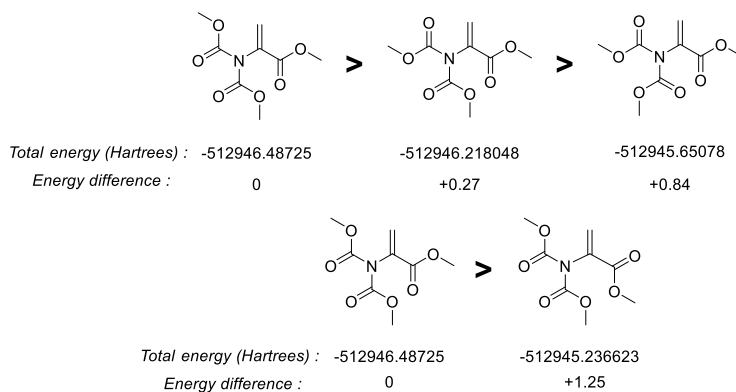
Figure 2.21. Computed energetics for ground state structure of different conformers of DHA

analog

After determining the lowest energy conformer the coordinate scan was performed along the dihedral angle between a carbamate and the olefin. The coordinate scan was performed over 180° at 5°/step (36 steps total). The absolute, uncorrected energies of each step are summarized in Table 2.5. The energies were then plotted against the degree of rotation (Figure 2.22) with structures of the rotational conformers at steps 0, 18 and 36. Zero-point energies were then calculated for the lowest energy (step 1: -512946.48725 kcal/mol) and highest energy (step 18: -512935.7041249 kcal/mol) structures to determine the total energetic barrier (10.78 kcal/mol). The zero-point energy for step 18 structure resulted in a single negative vibrational frequency which indicated that this is a transition state for the bond rotation. From the Gibbs energy the equilibrium constant between step 1 and step 18 was determined to be 1.24 x 10^{-8}. This value demonstrates that **2.1** exists almost exclusively in this confirmation under our reaction conditions.
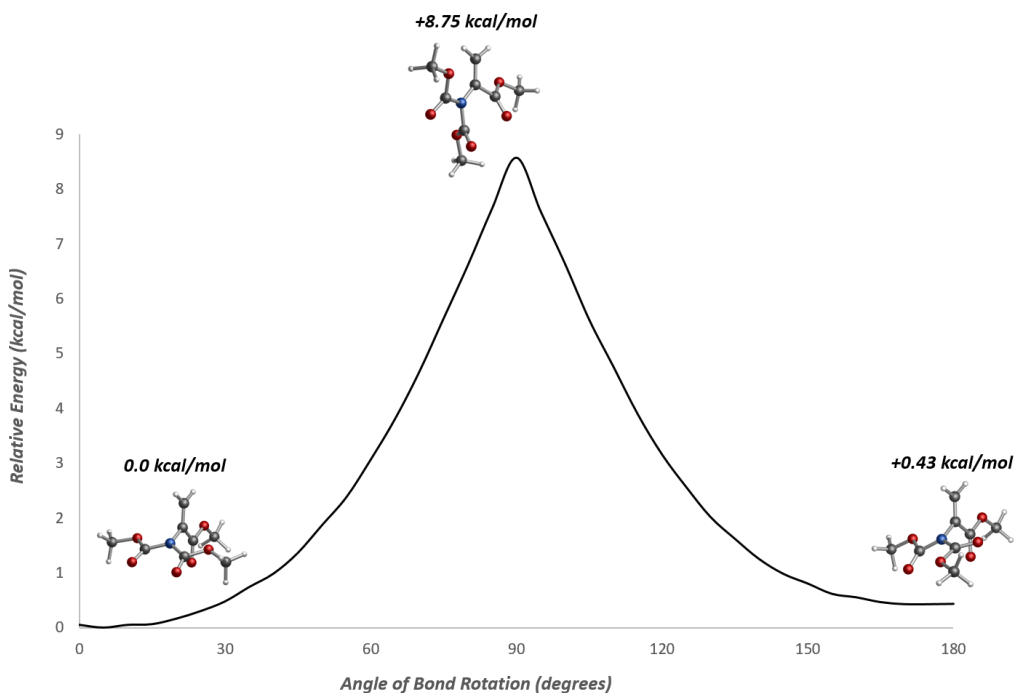
Figure 2.22: Plot of uncorrected energies (relative to minimum energy structure) vs angle of

rotation

Table 2.5: Energetic data for the coordinate scan of DHA analog

Step	Angle of Rotation	Uncorrected Energy (kcal/mol)	Energy difference (kcal/mol)
0	0	-513041.3183	0.050201
1	5	-513041.3685	0
2	10	-513041.3183	0.050201
3	15	-513041.3057	0.062751
4	20	-513041.2053	0.163152
5	25	-513041.0673	0.301204
6	30	-513040.8915	0.476907
7	35	-513040.628	0.740461
8	40	-513040.3833	0.985189

9	45	-513040.0068	1.361695
10	50	-513039.4985	1.869977
11	55	-513038.9902	2.378259
12	60	-513038.3062	3.062244
13	65	-513037.5658	3.802705
14	70	-513036.7061	4.662392
15	75	-513035.7334	5.635031
16	80	-513034.7608	6.60767
17	85	-513033.7254	7.64306
18	90	-513032.7967	8.571773
19	95	-513033.7756	7.592859
20	100	-513034.7294	6.639045
21	105	-513035.7523	5.616206
22	110	-513036.6119	4.756518
23	115	-513037.4779	3.890556
24	120	-513038.2121	3.15637
25	125	-513038.8082	2.560237
26	130	-513039.3542	2.014304
27	135	-513039.7495	1.618973
28	140	-513040.1197	1.248743
29	145	-513040.3895	0.978914
30	150	-513040.5652	0.803212
31	155	-513040.7535	0.614959
32	160	-513040.8162	0.552208
33	165	-513040.9041	0.464357
34	170	-513040.9418	0.426706
35	175	-513040.9418	0.426706

| 36 | 180 | -513040.9355 | 0.432981 |

The electrostatic potential for adducts **1a**, **1b** and **1c** were calculated using the HLY method from the energy minimized structures which were previously generated. The values for electrostatic potential at each atomic center are summarized below with labeled structures.
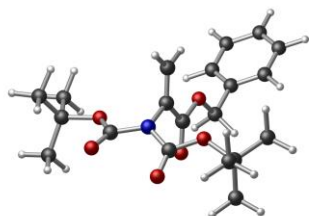
Center Number	Atomic Number	Atomic Type	Coordinates (Angstroms) X	Y	Z
1	6	C	-1.787775	3.714770	0.074066
2	8	O	-1.481784	2.320717	0.230971
3	6	C	-2.421847	1.354710	0.089577
4	7	N	-1.866140	0.081225	0.248865
5	6	C	-0.479509	-0.001706	0.620871
6	6	C	-0.133764	0.119388	1.914444
7	1	H	0.903701	0.075393	2.251390
8	1	H	-0.892513	0.267531	2.687732
9	6	H	0.496046	-0.188247	-0.396816
10	8	H	0.161877	-0.301735	-1.568601
11	8	H	1.803974	-0.229415	-0.027770
12	6	H	2.760163	-0.394441	-1.071500
13	6	H	4.149273	-0.246064	-0.489065
14	6	H	4.967897	0.798180	-0.859458
15	6	H	6.227794	0.927665	-0.324155

16	6	H	6.683039	0.011621	0.594263
17	6	H	5.873660	-1.034501	0.971686
18	6	H	4.616585	-1.160167	0.431268
19	1	H	3.977265	-1.995522	0.739127
20	1	H	6.229307	-1.766989	1.704553
21	1	H	7.685115	0.115601	1.024838
22	1	H	6.867452	1.763454	-0.628157
23	1	H	4.615841	1.537590	-1.587557
24	1	H	2.638850	-1.400416	-1.516481
25	1	H	2.579851	0.357453	-1.860613
26	6	C	-2.533876	-1.119759	-0.004613
27	8	O	-3.680861	-1.187412	-0.389751
28	8	O	-1.729856	-2.180794	0.246400
29	6	C	-2.154672	-3.533057	0.017492
30	6	C	-0.929233	-4.388749	0.378940
31	1	C	-0.062065	-4.129405	-0.254245
32	1	C	-0.633159	-4.234855	1.431886
33	1	C	-1.145042	-5.460950	0.239314
34	6	C	-3.323965	-3.909590	0.942422
35	1	H	-3.082672	-3.678174	1.995202
36	1	H	-4.254010	-3.380619	0.681322
37	1	H	-3.534023	-4.991003	0.872694
38	6	C	-2.509740	-3.766076	-1.461050
39	1	H	-1.701823	-3.402473	-2.120773
40	1	H	-2.645537	-4.844181	-1.655653
41	1	H	-3.445159	-3.265985	-1.756538
42	8	O	-3.594474	1.552463	-0.144918
43	6	C	-0.447845	4.433466	0.304364
44	1	H	0.313624	4.097733	-0.422061
45	1	H	-0.564263	5.524628	0.195933

72

46	1	H	-0.056792	4.231107	1.317451
47	6	C	-2.282370	4.018115	-1.350326
48	1	H	-1.580219	3.617640	-2.103128
49	1	H	-3.278154	3.592881	-1.550774
50	1	H	-2.358129	5.108398	-1.505140
51	6	C	-2.799173	4.187796	1.131873
52	1	H	-2.470461	3.900172	2.146479
53	1	H	-2.892624	5.287425	1.106539
54	1	H	-3.806504	3.774263	0.968243
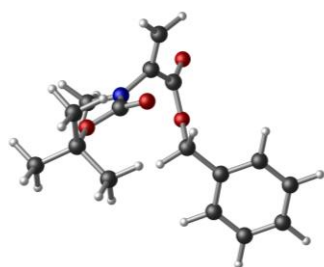
Center Number	Atomic Number	Atomic Type	Coordinates (Angstroms) X	Y	Z
1	6	C	1.990464	2.448702	-0.310435
2	7	N	1.645718	0.980172	-0.123439
3	6	C	0.191292	0.541909	-0.068942
4	6	C	-0.105598	-0.722766	0.092096
5	1	H	-1.148575	-1.037046	0.131176
6	1	H	0.690160	-1.461577	0.187112
7	6	H	-0.932990	1.585734	-0.203185
8	8	O	-2.368279	1.153238	-0.149406
9	6	H	-2.708489	-0.295970	0.035130
10	6	H	-4.239004	-0.465434	0.055264
11	6	H	-5.016245	0.199471	1.046727
12	6	H	-6.431972	0.042717	1.065351

13	6	H	-7.070457	-0.778942	0.092512
14	6	H	-6.293215	-1.443846	-0.898950
15	6	H	-4.877489	-1.287092	-0.917574
16	1	H	-4.282758	-1.795865	-1.676222
17	1	H	-6.781772	-2.072564	-1.643347
18	1	H	-8.153744	-0.898887	0.106763
19	1	H	-7.026702	0.551489	1.823998
20	1	H	-4.527689	0.828188	1.791124
21	1	H	-2.289599	-0.875159	-0.787774
22	1	H	-2.291310	-0.649927	0.977880
23	8	O	-0.643811	2.817561	-0.360041
24	6	C	2.755399	-0.050097	0.009061
25	8	O	4.190688	0.382399	-0.044719
26	6	C	5.285768	-0.634313	0.086037
27	6	C	6.652760	0.069329	-0.002397
28	1	H	6.739509	0.575134	-0.964028
29	1	H	6.737798	0.800367	0.801626
30	1	H	7.448517	-0.669482	0.092620
31	6	C	5.163204	-1.348937	1.444673
32	1	H	4.195657	-1.846970	1.507266
33	1	H	5.958961	-2.087748	1.539689
34	1	H	5.248242	-0.617900	2.248695
35	6	C	5.165621	-1.667156	-1.049921
36	1	H	4.198075	-2.165188	-0.987328
37	1	H	5.252371	-1.161350	-2.011552
38	1	H	5.961379	-2.405967	-0.954905
39	8	O	2.466221	-1.281924	0.165916
40	1	H	3.073751	2.568648	-0.324686
41	1	H	1.573286	2.802659	-1.253185
42	1	H	1.571575	3.027892	0.512469
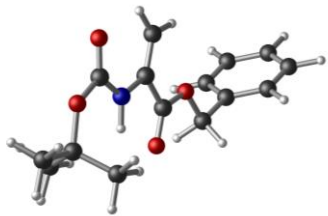
74

Center Number	Atomic Number	Atomic Type	Coordinates (Angstroms)		
			X	Y	Z
1	6	C	0.000000	0.000000	0.000000
2	6	C	0.000000	0.000000	1.536535
3	1	H	0.999571	0.000000	1.980559
4	1	H	-0.540632	0.875406	1.910106
5	1	H	-0.511997	-0.898210	1.898421
6	6	C	-1.443180	-0.098230	-0.511239
7	1	H	-1.462190	-0.053995	-1.604237
8	1	H	-1.900498	-1.039441	-0.188696
9	1	H	-2.039790	0.733555	-0.125036
10	6	C	0.835658	-1.139465	-0.603525
11	1	H	0.866577	-1.043252	-1.693460
12	1	H	1.864413	-1.179353	-0.234240
13	1	H	0.369061	-2.099636	-0.358092
14	8	O	0.410561	1.304247	-0.534110
15	6	C	1.597056	1.955255	-0.417414
16	7	N	2.589044	1.330025	0.302718
17	6	C	3.880531	1.820177	0.546057
18	6	C	4.412043	2.982258	0.134946
19	1	H	5.432434	3.217072	0.408371
20	1	H	3.839508	3.679380	-0.459731
21	6	C	4.640932	0.829049	1.370613
22	8	O	5.891690	1.209497	1.656467

75

23	6	C	6.668514	0.272856	2.458395
24	6	C	8.031997	0.867230	2.674212
25	6	C	9.066519	0.619687	1.763904
26	6	C	10.326803	1.186880	1.951624
27	6	C	10.564763	2.008607	3.055246
28	6	C	9.539442	2.260582	3.969061
29	6	C	8.280389	1.691708	3.778160
30	1	H	7.482328	1.888078	4.490423
31	1	H	9.721077	2.897038	4.830795
32	1	H	11.547162	2.448448	3.204564
33	1	H	11.122624	0.985798	1.239664
34	1	H	8.881917	-0.020499	0.904332
35	1	H	6.137037	0.106514	3.399640
36	1	H	6.713483	-0.679696	1.922955
37	8	O	4.148343	-0.227397	1.740676
38	1	H	2.429738	0.425769	0.721891
39	8	O	1.724828	3.040935	-0.945462

Zero-point correction = 0.198480 (Hartree/Particle)
Thermal correction to Energy = 0.215119
Thermal correction to Enthalpy = 0.216063
Thermal correction to Gibbs Free Energy = 0.151745
Sum of electronic and zero-point Energies = -817.384921
Sum of electronic and thermal Energies = -817.368282
Sum of electronic and thermal Enthalpies = -817.367338
Sum of electronic and thermal Free Energies = -817.431656

Center	Atomic	Atomic	Coordinates (Angstroms)		
Number	Number	Type	X	Y	Z

```
-----------------------------------------------------------------------
  1       6       C      -1.462852    2.947569   -0.620678

  2       8       O      -0.717617    1.726024   -0.819197

  3       6       C       0.114254    1.396991    0.170580

  4       7       N       0.662408    0.081528   -0.079343

  5       6       C      -0.211702   -1.043075   -0.171692

  6       6       C       0.128985   -2.330403   -0.342870

  7       1       H      -0.660054   -3.070629   -0.338100

  8       1       H       1.141190   -2.665100   -0.504533

  9       6       C      -1.634072   -0.758493    0.235299

 10       8       O      -2.504451   -1.566810   -0.377050

 11       6       C      -3.878424   -1.453962    0.055548

 12       1       H      -4.427127   -2.179853   -0.542550

 13       1       H      -3.960845   -1.688807    1.118989

 14       1       H      -4.248619   -0.443260   -0.128258

 15       8       O      -1.947200    0.076392    1.065552

 16       6       C       2.067898    0.067437   -0.073146

 17       8       O       2.579591   -1.155596    0.088982

 18       6       C       4.022257   -1.230687    0.046677

 19       1       H       4.253476   -2.288753    0.159963

 20       1       H       4.392344   -0.853812   -0.908676

 21       1       H       4.452296   -0.651461    0.865860

 22       8       O       2.727499    1.078487   -0.214965

 23       8       O       0.422954    2.090692    1.105661

 24       1       H      -2.066464    3.065344   -1.519343

 25       1       H      -2.098427    2.850261    0.262143

 26       1       H      -0.778907    3.789611   -0.500261
```

Zero-point correction = 0.198480 (Hartree/Particle)
Thermal correction to Energy = 0.215119
Thermal correction to Enthalpy = 0.216063
Thermal correction to Gibbs Free Energy = 0.151745
Sum of electronic and zero-point Energies = -817.384921
Sum of electronic and thermal Energies = -817.368282
Sum of electronic and thermal Enthalpies = -817.367338
Sum of electronic and thermal Free Energies = -817.431656

Center Number	Atomic Number	Atomic Type	Coordinates (Angstroms) X	Y	Z
1	6	C	0.000000	0.000000	0.000000
2	8	O	0.000000	0.000000	1.444486
3	6	C	1.206586	0.000000	2.005588
4	7	N	1.176960	0.001225	3.414564
5	6	C	2.479213	0.024667	4.037071
6	6	C	3.030616	1.167054	4.445699
7	1	H	4.009519	1.175980	4.909975
8	1	H	2.512014	2.112387	4.325051
9	6	C	3.118645	-1.321396	4.163987
10	8	O	4.343399	-1.256122	4.704678
11	6	C	5.028505	-2.515102	4.867090
12	1	H	5.989094	-2.265434	5.315639
13	1	H	4.457593	-3.175505	5.523759
14	1	H	5.170758	-2.996580	3.896928
15	8	O	2.576170	-2.353204	3.813995

16	6	C	0.042902	-0.289209	4.199811
17	8	O	0.415208	-0.408327	5.485802
18	6	C	-0.652688	-0.703306	6.409272
19	1	H	-0.176054	-0.755228	7.387248
20	1	H	-1.402130	0.090679	6.388549
21	1	H	-1.119537	-1.658050	6.158035
22	8	O	-1.093431	-0.409015	3.799815
23	8	O	2.260340	0.020037	1.397916
24	1	H	-1.052180	-0.007293	-0.281236
25	1	H	0.493925	0.896832	-0.379532
26	1	H	0.506280	-0.889567	-0.380269
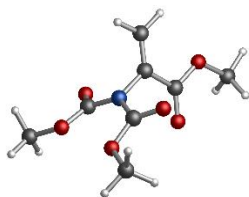
Zero-point correction = 0.198454 (Hartree/Particle)
Thermal correction to Energy = 0.215128
Thermal correction to Enthalpy = 0.216072
Thermal correction to Gibbs Free Energy = 0.151453
Sum of electronic and zero-point Energies = -817.383751
Sum of electronic and thermal Energies = -817.367077
Sum of electronic and thermal Enthalpies = -817.366133
Sum of electronic and thermal Free Energies = -817.430752

Center Number	Atomic Number	Atomic Type	Coordinates (Angstroms) X	Y	Z
1	6	C	2.477295	2.772238	-0.422610
2	8	O	2.038697	1.408400	-0.240393
3	6	C	0.832762	1.273700	0.306937
4	7	N	0.424141	-0.064488	0.474445

5	6	C	-0.960898	-0.217931	0.849263
6	6	C	-1.309163	-0.513700	2.100958
7	1	H	-2.350188	-0.642146	2.372208
8	1	H	-0.559108	-0.637521	2.875138
9	6	C	-1.924596	-0.032414	-0.279156
10	8	O	-3.200417	-0.161457	0.112324
11	6	C	-4.194454	-0.002884	-0.920628
12	1	H	-5.153357	-0.138931	-0.422318
13	1	H	-4.127765	0.994742	-1.360601
14	1	H	-4.055547	-0.756424	-1.699259
15	8	O	-1.578568	0.208964	-1.420739
16	6	C	1.060651	-1.253087	0.056937
17	8	O	2.377229	-1.125259	-0.093283
18	6	C	3.063430	-2.320091	-0.525185
19	1	H	4.107962	-2.026664	-0.620272
20	1	H	2.951905	-3.110870	0.219628
21	1	H	2.669676	-2.659028	-1.485596
22	8	O	0.438256	-2.286721	-0.093876
23	8	O	0.110456	2.194930	0.638440
24	1	H	3.467294	2.692344	-0.869505
25	1	H	1.795327	3.304291	-1.088997
26	1	H	2.529421	3.285780	0.539583
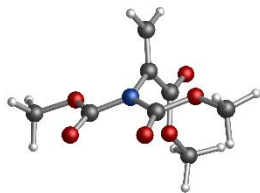
Zero-point correction = 0.198348 (Hartree/Particle)
Thermal correction to Energy = 0.214105
Thermal correction to Enthalpy = 0.215049
Thermal correction to Gibbs Free Energy = 0.153934
Sum of electronic and zero-point Energies = -817.385678
Sum of electronic and thermal Energies = -817.369921
Sum of electronic and thermal Enthalpies = -817.368977
Sum of electronic and thermal Free Energies = -817.430092

Center Number	Atomic Number	Atomic Type	Coordinates (Angstroms) X	Y	Z
1	6	C	-3.574509	-0.789904	-0.118404
2	8	O	-2.244335	-0.379661	0.258920
3	6	C	-1.261695	-1.221358	-0.105010
4	7	N	-0.024343	-0.709496	0.334139
5	6	C	0.007262	0.535757	1.063927
6	6	C	-0.007360	0.561843	2.396569
7	1	H	0.014713	1.511208	2.919535
8	1	H	-0.041548	-0.351944	2.979465
9	6	C	0.054774	1.807820	0.276001
10	8	O	0.083828	2.915807	0.777914
11	8	O	0.061483	1.577211	-1.045839
12	6	C	0.106056	2.748651	-1.886350
13	1	H	1.012908	3.323412	-1.685289
14	1	H	0.107968	2.372000	-2.908234
15	1	H	-0.770975	3.374846	-1.707745
16	6	C	1.185212	-1.281860	-0.108240
17	8	O	1.297550	-2.302628	-0.748544
18	8	O	2.211089	-0.512567	0.294735
19	6	C	3.519459	-0.982934	-0.088116
20	1	H	4.215152	-0.251984	0.321805
21	1	H	3.706445	-1.971548	0.336390
22	1	H	3.604246	-1.026390	-1.176022
23	8	O	-1.428262	-2.255107	-0.711493

24	1	H	-4.231151	-0.007806	0.260253
25	1	H	-3.654480	-0.866394	-1.204860
26	1	H	-3.818900	-1.751456	0.337928
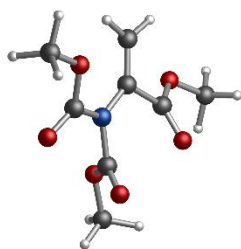
Zero-point correction =   0.198622 (Hartree/Particle)
Thermal correction to Energy =   0.214085
Thermal correction to Enthalpy =   0.215029
Thermal correction to Gibbs Free Energy = 0.155508
Sum of electronic and zero-point Energies = -817.371787
Sum of electronic and thermal Energies =   -817.356324
Sum of electronic and thermal Enthalpies = -817.355380
Sum of electronic and thermal Free Energies = -817.414901

| Center Number	Atomic Number	Atomic Type	Coordinates (Angstroms)		
			X	Y	Z
1	6	C	-1.462852	2.947569	-0.620678
2	8	O	-0.717617	1.726024	-0.819197
3	6	O	0.114254	1.396991	0.170580
4	7	N	0.662408	0.081528	-0.079343
5	6	O	-0.211702	-1.043075	-0.171692
6	6	O	0.128985	-2.330403	-0.342870
7	1	H	-0.660054	-3.070629	-0.338100
8	1	H	1.141190	-2.665100	-0.504533
9	6	O	-1.634072	-0.758493	0.235299
10	8	O	-2.504451	-1.566810	-0.377050

11	6	C	-3.878424	-1.453962	0.055548
12	1	H	-4.427127	-2.179853	-0.542550
13	1	H	-3.960845	-1.688807	1.118989
14	1	H	-4.248619	-0.443260	-0.128258
15	8	O	-1.947200	0.076392	1.065552
16	6	C	2.067898	0.067437	-0.073146
17	8	O	2.579591	-1.155596	0.088982
18	6	C	4.022257	-1.230687	0.046677
19	1	H	4.253476	-2.288753	0.159963
20	1	H	4.392344	-0.853812	-0.908676
21	1	H	4.452296	-0.651461	0.865860
22	8	O	2.727499	1.078487	-0.214965
23	8	O	0.422954	2.090692	1.105661
24	1	H	-2.066464	3.065344	-1.519343
25	1	H	-2.098427	2.850261	0.262143
26	1	H	-0.778907	3.789611	-0.500261

2.6.9. X-ray crystallographic data for 2.1
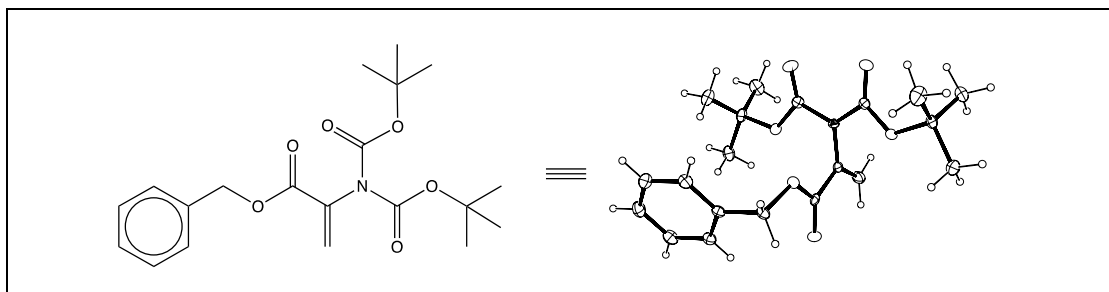
Compound **2.1**, $C_{20}H_{27}NO_6$, crystallizes in the monoclinic space group $P2_1$ (systematic absences

0k0: k=odd) with a=6.0300(2)Å, b=19.3547(8)Å, c=9.0029(3)Å, β=102.4530(10)°,

V=1026.00(6)Å^3, Z=2, and d$_{calc}$=1.222 g/cm$_3$. X-ray intensity data were collected on a Bruker

D8QUEST [1] CMOS area detector employing graphite-monochromated Mo-Kα radiation (λ=0.71073Å) at a temperature of 100K. Preliminary indexing was performed from a series of twenty-four 0.5° rotation frames with exposures of 10 seconds. A total of 9129 frames were collected with a crystal to detector distance of 33.0 mm, rotation widths of 0.5° and exposures of 10 seconds:

scan type	2θ	ω	φ	χ	Frames
ω	3.18	196.87	72.00	54.72	304
ω	3.18	196.87	0.00	54.72	304
ω	3.18	196.87	288.00	54.72	304

Rotation frames were integrated using SAINT [2], producing a listing of unaveraged F^2 and $\sigma(F^2)$ values. A total of 16695 reflections were measured over the ranges $6.262 \leq 2\theta \leq 50.784°$, $-7 \leq h \leq 7$, $-23 \leq k \leq 22$, $-10 \leq l \leq 10$ yielding 3746 unique reflections ($R_{int} = 0.0254$). The intensity data were corrected for Lorentz and polarization effects and for absorption using SADABS [3] (minimum and maximum transmission 0.7155, 0.7452). The structure was solved by direct methods - ShelXT [4]. Refinement was by full-matrix least squares based on F^2 using SHELXL-2017 [5]. All reflections were used during refinement. The weighting scheme used was $w=1/[\sigma^2(F_o^2)+ (0.0367P)^2 + 0.0896P]$ where $P = (F_o^2 + 2F_c^2)/3$. Non-hydrogen atoms were refined anisotropically and hydrogen atoms were refined using a riding model. Refinement converged to R1=0.0279 and wR2=0.0653 for 3630 observed reflections for which $F > 4\sigma(F)$ and R1=0.0296 and wR2=0.0664 and GOF =1.162 for all 3746 unique, non-zero reflections and 250 variables. The maximum Δ/σ in the final cycle of least squares was 0.000 and the two most prominent peaks in the final difference Fourier were +0.18 and -0.28 e/Å^3.

Table 1. lists cell information, data collection parameters, and refinement data. Final positional and equivalent isotropic thermal parameters are given in Tables 2. and 3. Anisotropic thermal parameters are in Table 4. Tables 5. and 6. list bond distances and bond angles. Figure 1 is an ORTEP representation of the molecule with 50% probability thermal ellipsoids displayed.
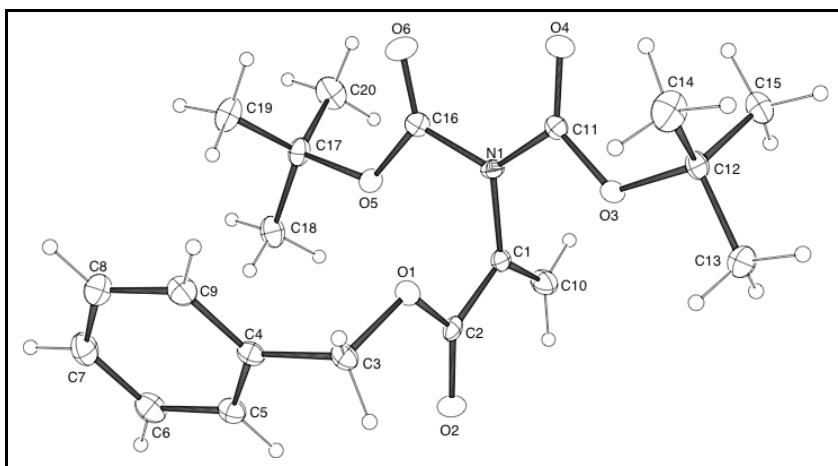
ORTEP drawing of the title compound with 50% thermal ellipsoids.

Table 2.6. Summary of Structure Determination of Compound **2.1**

Empirical formula	$C_{20}H_{27}NO_6$
Formula weight	377.42
Temperature/K	100
Crystal system	monoclinic
Space group	$P2_1$
a	6.0300(2)Å
b	19.3547(8)Å
c	9.0029(3)Å
β	102.4530(10)°
Volume	1026.00(6)Å^3

85

Z	2
d_{calc}	1.222 g/cm^3
μ	0.090 mm^{-1}
F(000)	404.0
Crystal size, mm	0.49 × 0.11 × 0.07
2θ range for data collection	6.262 - 50.784°
Index ranges	-7 ≤ h ≤ 7, -23 ≤ k ≤ 22, -10 ≤ l ≤ 10
Reflections collected	16695
Independent reflections	3746[R(int) = 0.0254]
Data/restraints/parameters	3746/1/250
Goodness-of-fit on F^2	1.162
Final R indexes [I>=2σ (I)]	R$_1$ = 0.0279, wR$_2$ = 0.0653
Final R indexes [all data]	R$_1$ = 0.0296, wR$_2$ = 0.0664
Largest diff. peak/hole	0.18/-0.28 eÅ^{-3}
Flack parameter	0.2(2)

Table 2.7. Refined positional parameters for **2.1**

Atom x	y	z	U(eq)
O1	0.7324(2)	0.53533(7)	0.80231(14)	0.0137(3)
O2	0.4108(2)	0.56611(7)	0.87585(15)	0.0166(3)
O3	0.6732(2)	0.36786(7)	0.87304(14)	0.0145(3)
O4	0.7877(2)	0.32694(7)	0.66566(15)	0.0165(3)
O5	0.4487(2)	0.50125(7)	0.47330(15)	0.0157(3)

O6	0.6875(2)	0.41631(8)	0.43064(16)	0.0233(3)
N1	0.5543(3)	0.42246(8)	0.65288(18)	0.0120(3)
C1	0.4152(3)	0.46270(9)	0.7329(2)	0.0125(4)
C2	0.5153(3)	0.52662(10)	0.81228(19)	0.0118(4)
C3	0.8405(3)	0.60054(10)	0.8619(2)	0.0145(4)
C4	0.8082(3)	0.65452(10)	0.7389(2)	0.0137(4)
C5	0.6196(3)	0.69820(10)	0.7128(2)	0.0158(4)
C6	0.5929(3)	0.74878(11)	0.6008(2)	0.0201(4)
C7	0.7553(3)	0.75572(11)	0.5134(2)	0.0213(4)
C8	0.9435(3)	0.71254(11)	0.5380(2)	0.0211(4)
C9	0.9699(3)	0.66200(11)	0.6498(2)	0.0175(4)
C10	0.2023(3)	0.44507(11)	0.7297(2)	0.0192(4)
C11	0.6852(3)	0.36721(10)	0.7269(2)	0.0119(4)
C12	0.7865(3)	0.31235(10)	0.9768(2)	0.0156(4)
C13	0.7404(4)	0.33458(11)	1.1287(2)	0.0218(5)
C14	1.0404(3)	0.31180(13)	0.9810(3)	0.0256(5)
C15	0.6730(4)	0.24388(11)	0.9257(2)	0.0231(5)
C16	0.5754(3)	0.44438(10)	0.5072(2)	0.0142(4)
C17	0.4064(3)	0.53124(11)	0.3183(2)	0.0160(4)
C18	0.2545(4)	0.59217(11)	0.3344(2)	0.0215(4)
C19	0.6263(4)	0.55569(12)	0.2803(2)	0.0249(5)
C20	0.2811(4)	0.47832(12)	0.2058(2)	0.0251(5)

Table 2.8. Positional parameters for hydrogens in **2.1**

Atom	x	y	z	U(eq)
H3a	1.00475	0.59284	0.902149	0.017
H3b	0.773184	0.616975	0.946587	0.017
H5	0.508175	0.6933	0.772254	0.019
H6	0.464298	0.778422	0.584065	0.024
H7	0.737578	0.790135	0.436453	0.026
H8	1.054448	0.717587	0.478247	0.025
H9	1.098433	0.632376	0.665876	0.021
H10a	0.138654	0.40544	0.674272	0.023
H10b	0.113076	0.472045	0.782921	0.023
H13a	0.803274	0.380838	1.154171	0.033
H13b	0.811868	0.301848	1.207654	0.033
H13c	0.576119	0.335441	1.122529	0.033
H14a	1.066786	0.292944	0.885312	0.038
H14b	1.118219	0.283031	1.065981	0.038
H14c	1.099505	0.359076	0.994569	0.038
H15a	0.509468	0.247601	0.920805	0.035
H15b	0.737526	0.207719	0.998453	0.035
H15c	0.698582	0.232084	0.824884	0.035
H18a	0.124338	0.576015	0.373841	0.032
H18b	0.200395	0.613841	0.234791	0.032
H18c	0.340901	0.625976	0.404993	0.032
H19a	0.708224	0.585097	0.362751	0.037

88

H19b	0.592687	0.58214	0.185293	0.037
H19c	0.720419	0.515641	0.2684	0.037
H20a	0.379306	0.438174	0.203337	0.038
H20b	0.240635	0.499038	0.104243	0.038
H20c	0.142743	0.463645	0.237445	0.038

Table 2.9. Refined thermal parameters (U's) for **2.1**

Atom	U_{11}	U_{22}	U_{33}	U_{23}	U_{13}	U_{12}
O1	0.0116(6)	0.0124(7)	0.0176(6)	-0.0003(5)	0.0041(5)	0.0003(5)
O2	0.0160(7)	0.0173(7)	0.0177(7)	-0.0028(6)	0.0068(5)	0.0031(6)
O3	0.0203(7)	0.0116(7)	0.0117(6)	0.0007(5)	0.0036(5)	0.0046(6)
O4	0.0182(7)	0.0148(8)	0.0166(7)	-0.0013(6)	0.0040(5)	0.0047(6)
O5	0.0191(7)	0.0157(7)	0.0128(7)	0.0038(5)	0.0047(5)	0.0051(6)
O6	0.0292(8)	0.0266(8)	0.0166(7)	0.0025(6)	0.0103(6)	0.0113(7)
N1	0.0127(7)	0.0125(8)	0.0117(8)	-0.0010(6)	0.0048(6)	0.0022(6)
C1	0.0154(9)	0.0113(10)	0.0113(9)	0.0037(7)	0.0041(7)	0.0041(8)
C2	0.0121(9)	0.0142(9)	0.0092(8)	0.0049(7)	0.0026(7)	0.0024(8)
C3	0.0128(9)	0.0127(9)	0.0171(9)	-0.0017(8)	0.0011(7)	-0.0008(7)
C4	0.0130(9)	0.0129(10)	0.0137(9)	-0.0040(8)	-0.0003(7)	-0.0023(7)
C5	0.0135(9)	0.0151(10)	0.0184(9)	-0.0025(8)	0.0024(7)	-0.0005(8)
C6	0.0178(9)	0.0167(10)	0.0237(10)	0.0000(9)	-0.0004(8)	0.0033(8)
C7	0.0254(11)	0.0169(10)	0.0203(10)	0.0041(9)	0.0016(8)	-0.0006(9)
C8	0.0203(10)	0.0215(11)	0.0230(10)	0.0005(9)	0.0079(8)	-0.0025(9)

89

C9	0.0124(9)	0.0166(11)	0.0234(11)	-0.0004(9)	0.0034(8)	0.0010(8)
C10	0.0171(10)	0.0155(10)	0.0270(11)	-0.0014(9)	0.0090(8)	0.0003(8)
C11	0.0105(8)	0.0111(9)	0.0135(9)	-0.0008(7)	0.0014(7)	-0.0018(7)
C12	0.0177(9)	0.0132(10)	0.0153(9)	0.0047(8)	0.0023(7)	0.0044(8)
C13	0.0293(11)	0.0213(11)	0.0153(10)	0.0030(8)	0.0055(8)	0.0026(9)
C14	0.0175(10)	0.0338(13)	0.0234(11)	0.0082(10)	0.0000(8)	0.0060(9)
C15	0.0313(11)	0.0142(10)	0.0248(11)	0.0021(8)	0.0080(9)	0.0006(9)
C16	0.0139(9)	0.0147(10)	0.0131(9)	-0.0006(8)	0.0011(7)	0.0002(8)
C17	0.0178(10)	0.0190(10)	0.0098(8)	0.0044(8)	0.0003(7)	-0.0009(8)
C18	0.0230(10)	0.0183(11)	0.0215(10)	0.0067(8)	0.0014(8)	0.0020(9)
C19	0.0237(11)	0.0300(13)	0.0229(11)	0.0053(9)	0.0091(9)	-0.0032(9)
C20	0.0267(11)	0.0228(12)	0.0217(11)	-0.0006(9)	-0.0038(9)	-0.0017(9)

Table 2.10. Bond distances in **2.1**, (Å)

O1-C2	1.342(2)	O1-C3	1.468(2)	O2-C2	1.210(2)
O3-C11	1.333(2)	O3-C12	1.489(2)	O4-C11	1.201(2)
O5-C16	1.337(2)	O5-C17	1.482(2)	O6-C16	1.195(2)
N1-C1	1.446(2)	N1-C11	1.409(2)	N1-C16	1.410(2)
C1-C2	1.490(3)	C1-C10	1.322(3)	C3-C4	1.504(3)
C4-C5	1.396(3)	C4-C9	1.397(3)	C5-C6	1.390(3)
C6-C7	1.389(3)	C7-C8	1.388(3)	C8-C9	1.388(3)
C12-C13	1.516(3)	C12-C14	1.523(3)	C12-C15	1.517(3)
C17-C18	1.519(3)	C17-C19	1.515(3)	C17-C20	1.521(3)

90

Table 2.11. Bond Angles in **2.1**, (°)

C2-O1-C3	116.49(14)	C11-O3-C12	119.80(14)	C16-O5-C17	120.74(15)
C11-N1-C1	119.95(15)	C11-N1-C16	120.99(15)	C16-N1-C1	118.68(15)
N1-C1-C2	117.90(16)	C10-C1-N1	121.00(17)	C10-C1-C2	121.03(17)
O1-C2-C1	111.87(15)	O2-C2-O1	124.55(18)	O2-C2-C1	123.58(17)
O1-C3-C4	110.55(15)	C5-C4-C3	121.07(17)	C5-C4-C9	118.99(18)
C9-C4-C3	119.93(17)	C6-C5-C4	120.78(18)	C7-C6-C5	119.58(19)
C8-C7-C6	120.20(19)	C9-C8-C7	120.16(18)	C8-C9-C4	120.28(18)
O3-C11-N1	108.41(15)	O4-C11-O3	127.04(17)	O4-C11-N1	124.54(17)
O3-C12-C13	102.27(15)	O3-C12-C14	110.08(16)	O3-C12-C15	108.94(15)
C13-C12-C14	110.98(17)	C13-C12-C15	111.28(17)	C15-C12-C14	112.77(18)
O5-C16-N1	107.36(15)	O6-C16-O5	127.52(18)	O6-C16-N1	125.12(18)
O5-C17-C18	101.47(15)	O5-C17-C19	110.69(16)	O5-C17-C20	108.83(16)
C18-C17-C20	111.31(17)	C19-C17-C18	110.74(17)	C19-C17-C20	113.17(17)

2.7. References

1. Bohm, H. J.; Banner, D.; Bendels, S.; Kansy, M.; Kuhn, B.; Muller, K.; Obst-Sander, U.; Stahl, M. Fluorine in medicinal chemistry. *Chembiochem* **2004**, *5* (5), 637-643.

2. Meanwell, N. A. Fluorine and Fluorinated Motifs in the Design and Application of Bioisosteres for Drug Design. *J. Med. Chem.,* **2018**, *61*, 5822-5880.

3. Narjes, F.; Koehler, K. F.; Koch, U.; Gerlach, B.; Colarusso, S.; Steinkuhler, C.; Brunetti, M.; Altamura, S.; De Francesco, R.; Matassa, V. G. A designed P-1 cysteine mimetic for covalent and non-covalent inhibitors of HCVNS3 protease. *Bioorg. Med. Chem. Lett.,* **2002**, *12*, 701-704.

4. Zafrani, Y.; Yeffet, D.; Sod-Moriah, G.; Berliner, A.; Amir, D.; Marciano, D.; Gershonov, E.; Saphier, S. Difluoromethyl Bioisostere: Examining the "Lipophilic Hydrogen Bond Donor" Concept. *J. Med. Chem.,* **2017**, *60*, 797-804.

5. Mei, H. B.; Han, J. L.; Klika, K. D.; Izawa, K.; Sato, T.; Meanwell, N. A.; Soloshonok, V. A. Applications of fluorine-containing amino acids for drug design. *Eur. J. Med. Chem.,* **2020**, *186,* 111826.

6. Moschner, J.; Stulberg, V.; Fernandes, R.; Huhmann, S.; Leppkes, J.; Koksch, B. Approaches to Obtaining Fluorinated alpha-Amino Acids. *Chem. Rev.,* **2019**, *119*, 10718-10801.

7. Ulbrich, D.; Daniliuc, C. G.; Haufe, G. Synthesis of alpha,omega-polyfluorinated alpha-amino acid derivatives and delta,delta-difluoronorvaline. *Org. Biomol. Chem.,* **2016**, *14*, 2755-2767.

8. Baba, D.; Fuchigami, T. Electrolytic partial fluorination of organic compounds. Part 61: The first example of direct alpha-fluorination of protected alpha-amino acids. *Tet. Lett.,* **2002**, *43*, 4805-4808.

9. Bailey, P. D.; Baker, S. R.; Boa, A. N.; Clayson, J.; Rosair, G. M. Synthesis of alpha-heterosubstituted glycine derivatives from dihaloethanamides. *Tet. Lett.,* **1998**, *39*, 7755-7758.

10. Kwiatkowski, J.; Lu, Y. X. Asymmetric Michael addition of alpha-fluoro-alpha-nitro esters to nitroolefins: towards synthesis of alpha-fluoro-alpha-substituted amino acids. *Org. Biomol. Chem.,* **2015**, *13*, 2350-2359.

11. Bloom, S.; Liu, C.; Kolmel, D. K.; Qiao, J. X.; Zhang, Y.; Poss, M. A.; Ewing, W. R.; MacMillan, D. W. C. Decarboxylative alkylation for site-selective bioconjugation of native proteins via oxidation potentials. *Nat. Chem.,* **2018**, *10*, 205-211.

12. Vara, B. A.; Li, X. P.; Berritt, S.; Walters, C. R.; Petersson, E. J.; Molander, G. A. Scalable thioarylation of unprotected peptides and biomolecules under Ni/photoredox catalysis. *Chem. Sci.,* **2018**, *9*, 336-344.

13. Wright, T. H.; Bower, B. J.; Chalker, J. M.; Bernardes, G. J. L.; Wiewiora, R.; Ng, W. L.; Raj, R.; Faulkner, S.; Vallee, M. R. J.; Phanumartwiwath, A.; et al. Posttranslational mutagenesis: A chemical strategy for exploring protein side-chain diversity. *Science* **2016**, *354*, 6312.

14. Yang, A.; Ha, S.; Ahn, J.; Kim, R.; Kim, S.; Lee, Y.; Kim, J.; Soll, D.; Lee, H. Y.; Park, H. S. A chemical biology route to site-specific authentic protein modifications. *Science* **2016**, *354*, 623-626.

15. Aycock, R. A.; Vogt, D. B.; Jui, N. T. A practical and scalable system for heteroaryl amino acid synthesis. *Chem. Sci.,* **2017**, *8*, 7998-8003.

16. de Bruijn, A. D.; Roelfes, G. Chemical Modification of Dehydrated Amino Acids in Natural Antimicrobial Peptides by Photoredox Catalysis. *Chem. Eur. J.,* **2018**, *24*, 11314-11318.

17. Liu, Z. L.; Chen, H.; Lv, Y.; Tan, X. Q.; Shen, H. G.; Yu, H. Z.; Li, C. Z. Radical Carbofluorination of Unactivated Alkenes with Fluoride Ions. *J. Am. Chem. Soc.,* **2018**, *140*, 6169-6175.

18. Fukuzumi, S.; Kotani, H.; Ohkubo, K.; Ogo, S.; Tkachenko, N. V.; Lemmetyinen, H. Electron-transfer state of 9-mesityl-10-methylacridinium ion with a much longer lifetime and

higher energy than that of the natural photosynthetic reaction center. *J. Am. Chem. Soc.,* **2004**, *126*, 1600-1601.

19. Tellis, J. C.; Primer, D. N.; Molander, G. A. Single-electron transmetalation in organoboron cross-coupling by photoredox/nickel dual catalysis. *Science* **2014**, *345*, 433-436.

20. Matsui, J. K.; Primer, D. N.; Molander, G. A. Metal-free C-H alkylation of heteroarenes with alkyltrifluoroborates: a general protocol for 1 degrees, 2 degrees and 3 degrees alkylation. *Chem. Sci.,* **2017**, *8*, 3512-3522.

21. Fleeman, R.; LaVoi, T. M.; Santos, R. G.; Morales, A.; Nefzi, A.; Wemaker, G. S.; Medina-Franco, J. L.; Giulianotti, M. A.; Houghten, R. A.; Shaw, L. N. Combinatorial Libraries As a Tool for the Discovery of Novel, Broad-Spectrum Antibacterial Agents Targeting the ESKAPE Pathogens. *J. Med. Chem.,* **2015**, *58*, 3340-3355.

22. Xin, B. T.; Huber, E. M.; de Bruin, G.; Heinemeyer, W.; Maurits, E.; Espinal, C.; Du, Y. M.; Janssens, M.; Weyburne, E. S.; Kisselev, A. F.; et al. Structure-Based Design of Inhibitors Selective for Human Proteasome beta 2c or beta 2i Subunits. *J. Med. Chem.,* **2019**, *62*, 1626-1642.

23. Venkatraman, S.; Bogen, S. L.; Arasappan, A.; Bennett, F.; Chen, K.; Jao, E.; Liu, Y. T.; Lovey, R.; Hendrata, S.; Huang, Y. H.; et al. Discovery of (1R, 5S)-N- 3-amino-1-(cyclobutylmethyl)-2,3-dioxopropyl -3- 2(S)- (1,1-dim ethylethyl)amino carbonyl amino -3,3-dimethyl-1-oxobutyl -6,6-dimethyl-3 -azabicyclo 3.1.0 hexan-2(S)-carboxamide (SCH 503034), a selective, potent, orally bioavailable hepatitis C virus NS3 protease inhibitor: A potential therapeutic agent for the treatment of hepatitis C infection. *J. Med. Chem.,* **2006**, *49*, 6074-6086.

24. De Vleeschouwer, F.; Van Speybroeck, V.; Waroquier, M.; Geerlings, P.; De Proft, F. Electrophilicity and nucleophilicity index for radicals. *Org. Lett.,* **2007**, *9*, 2721-2724.

25. Parsaee, F.; Senarathna, M. C.; Kannangara, P. B.; Alexander, S. N.; Arche, P. D. E.; Welin, E. R. Radical philicity and its role in selective organic transformations. *Nat. Rev. Chem.,* **2021**, *5*, 486-499.

26. Hu, H.; Lu, Z. Y.; Yang, W. T. Fitting molecular electrostatic potentials from quantum mechanical calculations. *J. Chem. Theo. Comput.,* **2007**, *3*, 1004-1013.

27. Patel, N. R.; Kelly, C. B.; Jouffroy, M.; Molander, G. A. Engaging Alkenyl Halides with Alkylsilicates via Photoredox Dual Catalysis. *Org. Lett.,* **2016**, *18*, 764-767.

28. Wilger, D. J.; Grandjean, J. M. M.; Lammert, T. R.; Nicewicz, D. A. The direct anti-Markovnikov addition of mineral acids to styrenes. *Nat. Chem.,* **2014**, *6*, 720-726.

29. Molander, G. A.; McKee, S. A. Copper-Catalyzed beta-Boration of alpha,beta-Unsaturated Carbonyl Compounds with Tetrahydroxydiborane. *Org. Lett.,* **2011**, *13*, 4684-4687.

30. M. T. Ferreira, P.; L. S. Maia, H.; S. Monteiro, L.; Sacramento, J. High yielding synthesis of dehydroamino acid and dehydropeptide derivatives. *J. Chem. Soc. Per. Trans.,* **1999**, *24*, 3697-3703.

31. Ulbrich, D.; Daniliuc, C. G.; Haufe, G. Halofluorination of N-protected alpha,beta-dehydro-alpha-amino acid esters-A convenient synthesis of alpha-fluoro-alpha-amino acid derivatives. *J. Fluor. Chem.,* **2016**, *188*, 65-75.

32. Devlin, F. J.; Finley, J. W.; Stephens, P. J.; Frisch, M. J. Ab Initio Calculation of Vibrational Absorption and Circular Dichroism Spectra Using Density Functional Force Fields: A Comparison of Local, Nonlocal, and Hybrid Density Functionals. *J. Phys. Chem.,* **1995**, *99*, 16883-16902. =

33. Petersson, G. A.; Allaham, M. A. A complete basis set model chemistry II. open-shell systems and the total energies of the 1st-row atoms. *J. Chem. Phys.,* **1991**, *94*, 6081-6090.

Chapter 3. Three-Component Olefin Dicarbofunctionalization (DCF) Enabled by Nickel/Photoredox Dual Catalysis

3.1. Introduction

The formation of C-C bonds is arguably the most critical transformation in the construction of organic molecules. Since the inception of organic synthesis, these C-C bond-forming reactions were almost exclusively accomplished using strongly nucleophilic or electrophilic reagents that are "poised-to-react". Among the most common strategies for C_{sp3}-C_{sp3} bond formation are additions of organometallic carbon nucleophiles onto a polarized alkene, known as Michael additions. Initially employed in hydroalkylation reactions, it was soon realized that the anionic 1,4 addition intermediate could be trapped with an electrophile other than a proton. Many carbon-based electrophiles, including alkyl substituted leaving groups (acetates, tosylates, triflates, mesylates, etc.), acyl chlorides, anhydrides, and aldehydes could be utilized to achieve three-component 1,2-vicinal dicarbofunctionalization (DCF) of alkenes.[1] These strategies were employed in many total syntheses, among the most notable of which are Negishi's total synthesis of 11-deoxyprostaglandin-E2[2] and the synthesis of isostegane by scientists at Hoffman-La Roche.[3] In the synthesis of 11-deoxyprostaglandin-E2 (Figure 3.1A), lithium divnyl cuprate underwent a conjugate addition onto cyclopentenone, followed by trapping of the resulting enolate with trimethylsilyl chloride. The silyl enol ether was then coupled with an allylic acetate under Tsjui-Trost conditions yielding the difunctionalized cyclopentanone. Vicinal DCF also provided an exceptionally efficient synthesis of (±)-isostegane (Figure 3.1B) in which a two-step, one-pot procedure was used to dialkylate the central butyrolactone ring. Though effective under select instances, these strategies innately restrict compatibility to a meager range of unreactive functional groups, necessitating the tedious installation and cleavage of protecting groups. Furthermore, many of the more common C_{sp3}-centered nucleophiles (e.g., alkyllithium and alkyl

Grignard reagents) are not amenable to these reactions, as hard nucleophiles offer poor 1,2- vs 1,4

addition selectivity. To effect greater 1,4-selectivity, various soft carbon nucleophilic group must

be implemented. However, many such species, including organocuprates, are not particularly

stable and must be made "on-demand", and even then they are often generated with variable

quality. Though a conceptually intriguing transformation, vicinal difunctionalization lacked the

versatility and practicality required for broad application in the synthesis of complex molecular

architecture.
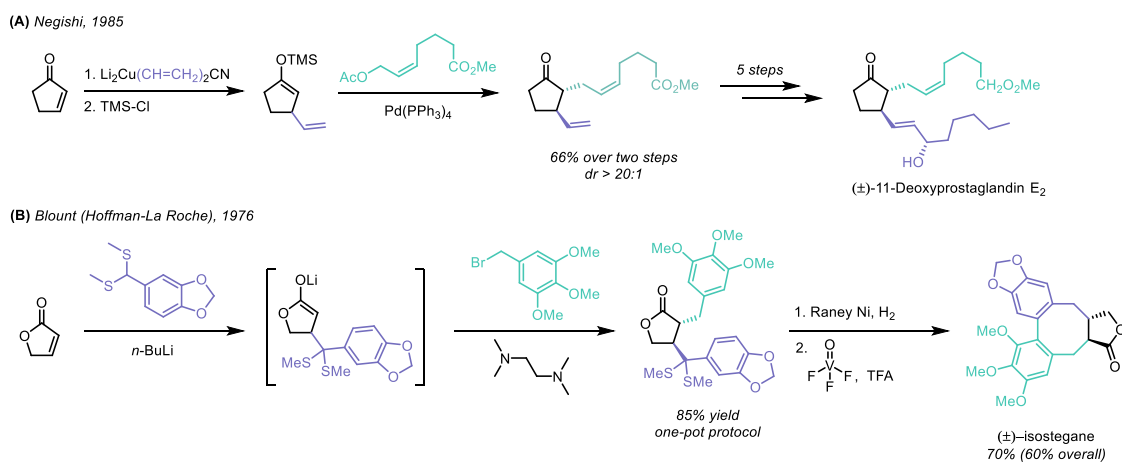
Figure 3.1. Vicinal dicarbofunctionalization (DCF) via organometallic nucleophiles in the synthesis of **(A)** 11-deoxyprostaglandin-E$_2$ and **(B)** (±)-isostegane.

The advent of transition metal-catalyzed cross-coupling completely revolutionized the

manner in which chemists accomplished C-C bond formation. Although the first explorations of

transition metal cross couplings focused on two component reactivity, it was not long until these

strategies were extended to include a third (alkene) component. Some of the earliest examples of

transition metal-mediated DCF, developed by Chiusoli[4] and Migita,[5] were accomplished using

norbornene as the alkene lynchpin (Figure 3.2A,B). The mechanisms were similar (Figure 3.2C):

a Heck-type cross coupling occurred between an aryl electrophile and norbornene. Reductive

carbopalladation of the aryl norbornene intermediate via palladium hydride produced a key

alkylpalladium(II) complex. Finally, transmetalation of a carbon nucleophile (alkyne or C_{sp2}-organostannane) and followed by reductive elimination yielded the DCF product. Though remarkably pioneering on a conceptual basis, these protocols were severely limited in the substructures that could be constructed. Because of palladium's strong tendency to undergo β-hydride elimination, only C_{sp2} and C_{sp} coupling partners can be incorporated into these protocols.[6] Additionally, norbornene was uniquely effective at producing a single 1,2 DCF regioisomer. The bicyclic structure of norbornene ensured that only one methylene position offered the appropriate *syn*-coplanar alignment from the alkyl Pd(II) intermediates for β-hydride elimination. Further studies of Pd-mediated DCF of acyclic alkenes resulted in either a 1,1-DCF product or a mixture of regioisomers because of β-hydride elimination/isomerization steps.[7]
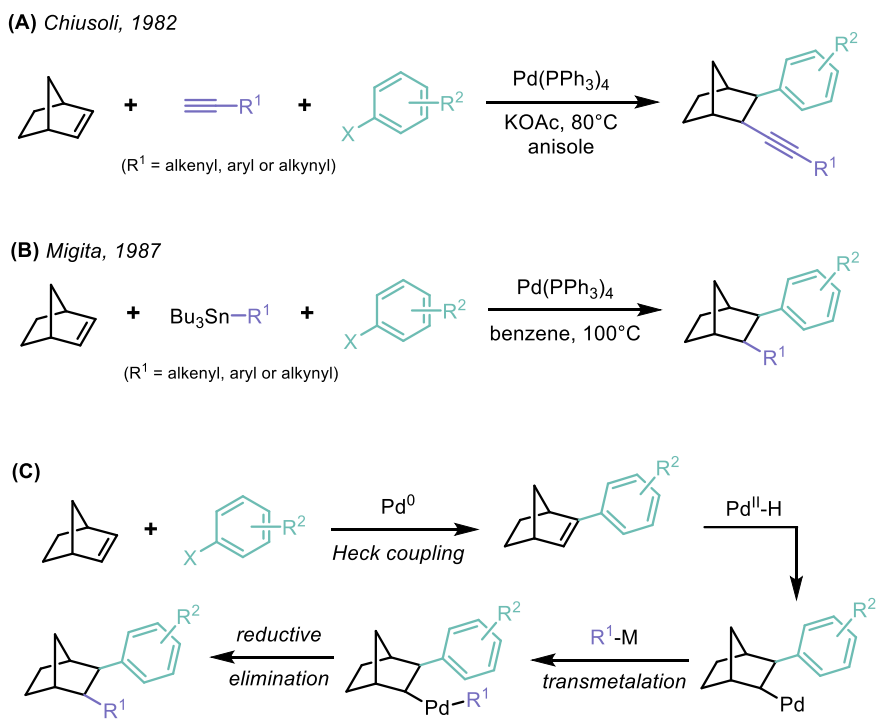
Figure 3.2. Early DCF strategies using **(A)** alkynyl or **(B)** organostannyl nucleophiles. **(C)** General mechanism for Pd-catalyzed DCF of norborene.

The development of a functionally tolerant, regiospecific 1,2 alkylation/arylation DCF protocol seemed intangible until significant advances in Ni-catalyzed cross couplings were made in the late 1990s and early 2000s. At its inception, Ni catalysis was often viewed as an inexpensive replacement for Pd in typical Heck, Suzuki, Stille, Negishi, and Kumada couplings. However, detailed studies revealed more subtle distinctions between Ni and Pd that had significant implications for cross-coupling mechanisms.[8] In particular, Ni-alkyl complexes are, in general, much more resistant to β-hydride elimination compared to their Pd counterparts.[9] Computational studies revealed that the dissimilar rate of β-hydride elimination stems from the energetics of the β-agostic complex, which is significantly higher in energy for the less flexible Ni-alkyl intermediate compared to analogous Pd-alkyl intermediate (Figure 3.3).[10]
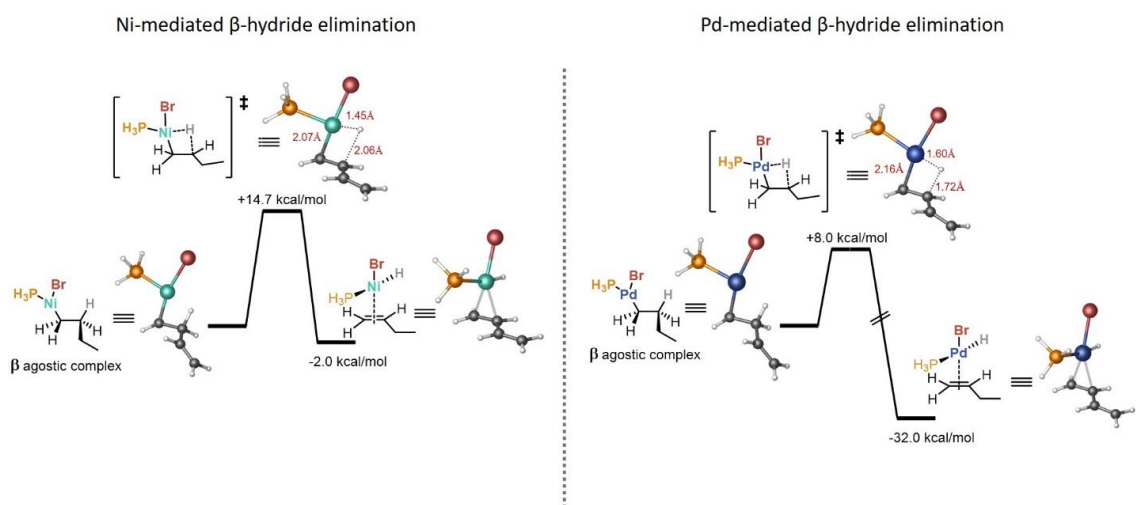
Figure 3.3. Comparing Ni- and Pd-promoted β-hydride elimination from 1-bromobutane (computed by Lin and coworkers)[10]

Armed with this knowledge, chemists were able to develop a tremendous breadth of Ni-mediated C_{sp3}-C_{sp3} bond-forming processes, because these protocols were much more resilient in their ability to minimize β-hydride elimination byproducts.[8] These Ni-mediated coupling mechanisms thus emerged as a prime candidate for enabling highly functional group tolerant

three-component 1,2-DCF reactions of alkenes. Many protocols for two-component (intramolecular) DCF exist, but will not be discussed here. Instead, this chapter will focus solely on three-component (intermolecular) DCF reactions.[11] Three-component Ni-catalyzed DCF reactions can be grouped into two broad categories: catalytic cycles involving only two-electron fundamental steps (typically Ni^0/Ni^{II} cycles) and catalytic cycles involving both single and two-electron fundamental steps (typically $Ni^0/Ni^{II}/Ni^{III}/Ni^{I}$ cycles).

The most common protocol for the "two-electron only" Ni-catalyzed DCF reactions involves an C_{sp3} or C_{sp2} organometallic nucleophile and an C_{sp2} electrophile, which are installed in a regioselective manner across an alkene (or alkyne). The most common mechanism invoked for these protocols is outlined in Figure 3.4.[12] The low-valent Ni species (typically Ni^0) undergoes oxidative addition with the C_{sp2} electrophile which, in turn, undergoes migratory insertion into the alkene, generating the key Ni^{II} intermediate. Transmetalation of the organometallic nucleophile to the Ni^{II} complex followed by reductive elimination generates the DCF product. Even though Ni-mediated β-hydride elimination is much slower than the Pd-mediated process, it still poses a major challenge to overcome in DCF reactions. Under typical Ni-catalysis conditions, unactivated alkenes often produced a mixture of DCF regioisomers (predominantly the 1,1 isomer for terminal alkenes) similar to the results observed with Pd-catalysis.[13] In an effort to suppress this undesired β-hydride elimination/isomerization, designer ligand scaffolds and intramolecular Lewis basic coordinating groups have been employed (Figure 3.4B). Alkenes that are tethered to Lewis basic groups can form five- or six-membered nickelacycles that are conformationally locked such that the Ni-C bond cannot rotate to access the β-agostic transition state required for hydride elimination. Thus, these unique alkenes effect highly regioselective 1,2-DCF via Ni^0/Ni^{II} cycles. The groups of Giri[13, 14] and Engle[15] have performed extensive investigation into these protocols, focusing mainly on imine and aminoquinolone coordinating groups, respectively.
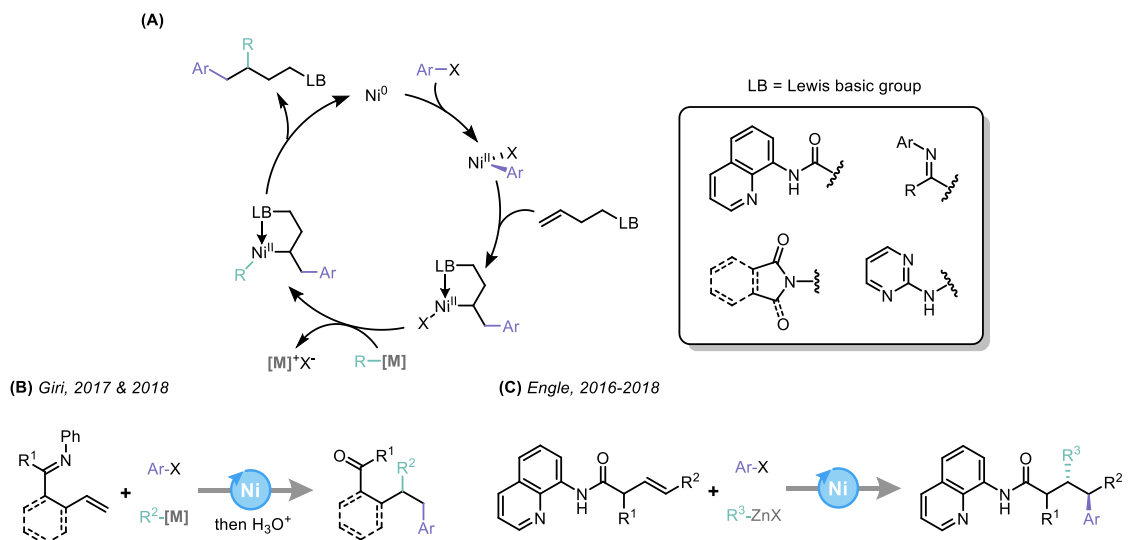
Figure 3.4. (A) General mechanism for three-component DCF via two electron, Ni^0/Ni^{II} cycles and exemplary Lewis basic coordinating groups. **(B)** General reaction using imine coordinating group developed by Giri and coworkers. **(C)** General reaction using aminoquinoline coordinating group developed by Engle and coworkers.

In the case of three-component DCF protocols that access single-electron species, one C_{sp3}-hybridized nucleophile and one C_{sp2}-hybridized electrophile are typically utilized. These reactions proceed via the following mechanism, although the exact order of the steps can vary depending on the substrates and reaction conditions.[9] Single-electron reduction of an alkyl halide via low valent nickel (typically Ni^0 or Ni^I) produces an alkyl radical that undergoes regioselective Giese addition into an alkene. A sacrificial reductant engages in single-electron transfer with nickel, returning it to its original oxidation state, then undergoing oxidative addition to a C_{sp2}-hybridized (most typically aryl) electrophile. Radical metalation produces a Ni^{III} intermediate, which rapidly undergoes reductive elimination to yield the three-component coupled product. Given that these radical mechanisms proceed through a Ni^{III}-alkyl complex rather than the Ni^{II}-alkyl complexes accessed in the aforementioned two-electron mechanisms, β-hydride elimination is much less problematic. Presumably, the barrier for Ni-C rotation to access the β-agostic transition state in Ni^{III} complexes becomes significantly high because of constraints in the trigonal

101

bipyramidal geometry.[9] Additionally, reductive elimination from Ni^{III} complexes, in most instances, is appreciably faster than from the Ni^{II} complexes accessed in two-electron pathways.[16] Overall, these radical-mediated pathways are liberated from the constraints of specialized coordinating groups and complex ligand scaffolds that are required to suppress the β-hydride elimination byproducts that plague two-electron mechanisms. Many examples using alkyl iodides and a wide range of C_{sp2} coupling partners have been developed for the effective 1,2-DCF of terminal alkenes (Figure 3.5B).[17,18,19] The remaining limitation in radical-mediated DCF reactions is their net reductive mechanism, requiring stoichiometric reductants to sustain the Ni cycle. In addition to being inefficient and uneconomical, these reductants can often limit the functional groups that can be incorporated into these protocols.
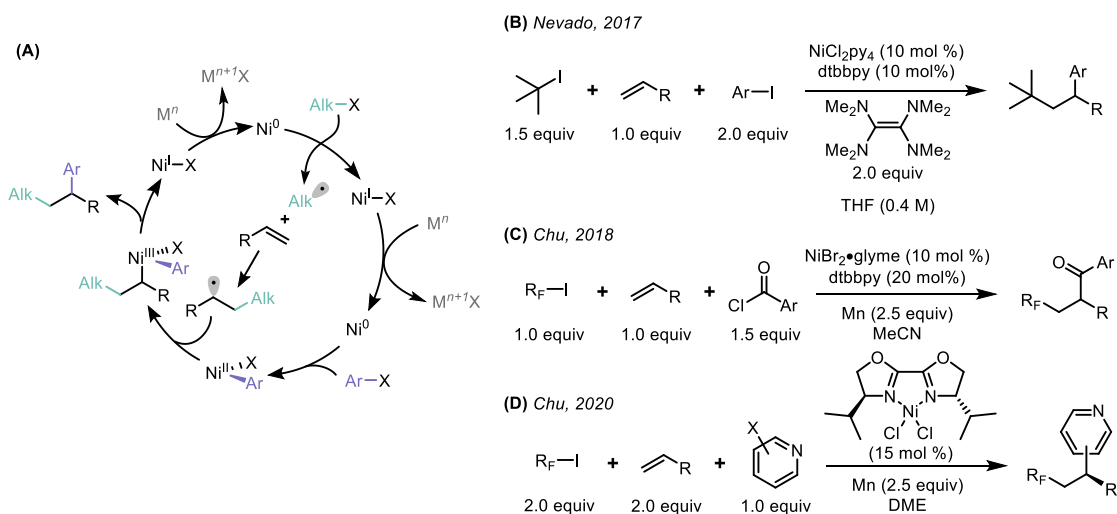
Figure 3.5. (A) General mechanism for three-component DCF involving single electron species (Ni^0/Ni^{II}/Ni^{III}/Ni^I cycle). **(B-D)** Exemplary three-component DCF reaction via radical mechanisms.

3.2. Reaction Design and Optimization

The ideal Ni-catalyzed 1,2-alkyl/arylation DCF would involve the generation of alkyl radicals via catalytic, single electron *oxidation*. Thus, the oxidized Ni^I species that forms after

reductive elimination could then engage in single electron transfer with a catalytic redox additive to close both catalytic cycles in a net neutral manifold. Fortunately, photoredox catalysis offers a precise solution to this mechanistic proposal (Figure 3.6). An excited state photocatalyst (**3.II**) can undergo reductive quenching with a radical precursor (**3.IV**) to generate the desired alkyl radical (**3.V**) and reduced photocatalyst (**3.III**). This nucleophilic alkyl radical can then engage in regioselective Giese addition with an electron-deficient alkene to produce radical adduct **3.VII**. After oxidative addition, Ni complex **3.X** could undergo a critical singlet-square planar to triplet-tetrahedral isomerization (elucidated by later computational studies).[20] The tetrahedral oxidative addition complex (**3.XI**) could metalate radical **3.VII**, which would approach from a *pseudo*-equatorial position. The trigonal bipyramidal Ni^{III} complex (**3.XII**) maintains an ~90° angle between the axial aryl group and equatorial alkyl group, which would enable facile reductive elimination to form the desired DCF product **3.XIII** along with the concomitant Ni^{I} species (**3.XIV**). Finally, the reduced state photocatalyst (**3.III**) and oxidized Ni^{I} species (**3.XIV**) could engage in single electron transfer, closing the catalytic cycle, obviating the need for any stoichiometric redox additives.
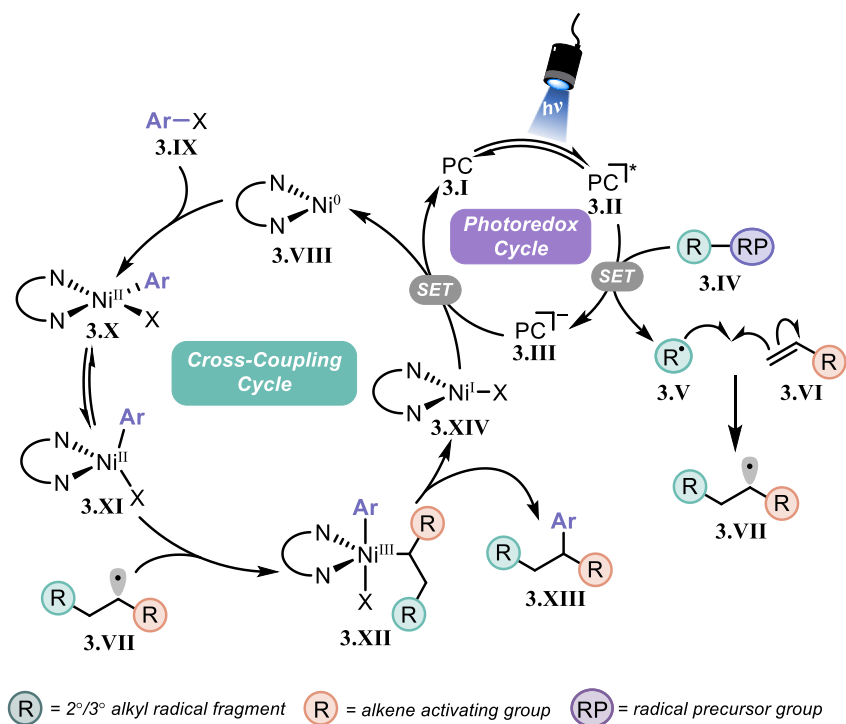
Figure 3.6. Proposed mechanism for photoredox/nickel dicarbofunctionalization

We immediately realized that the success of such a DCF reaction would depend upon a series of well-orchestrated steps. It would be critical that the rate of Giese addition of **3.V** onto **3.VI** be significantly faster than the rate of metalation of **3.V** with Ni complexes **3.VIII** or **3.XI** to suppress undesired two-component cross coupling of **3.V**. Relying on principles derived from previous research in our group, we elected to focus on acyclic, tertiary alkyl radicals, which are particularly reluctant to undergo metalation and have only been successfully cross coupled under specific reaction conditions.[21] Because of this structural limitation, we began our optimization studies with organotrifluoroborates as our model class of radical precursor given the vast array of feedstocks and strategies for rapidly accessing tertiary alkyl boronates.[22-24] We deemed vinylboronic acid pinacol ester (vinyl Bpin) to be a highly desirable alkene lynchpin. Alkenyl boronates had been previously demonstrated as competent acceptors in Giese additions with alkyl radicals under photoredox conditions.[25] Most importantly, this alkene retains the boronate group,

a functional handle capable of a remarkably diverse array of transformations, rendering the DCF

products as excellent synthetic intermediates.

Table 3.1. Optimization studies in photoredox/nickel DCF reaction

entry	deviation from conditions above	^{1}H NMR yield (%)
1	None	70%
2	{Ir[dF(CF$_3$)$_2$ppy]$_2$dtbbpy}PF$_6$ in place of Ir photocat	65%
3	[Ru(bpy)$_3$]PF$_6$ in place of Ir photocat	0%
4	4-Cl-CzIPN in place of Ir photocat	61%
5	Ni(dtbbpy)Br$_2$ in place of Ni(bpy)Br$_2$	59%
6	Ni(phen)Br$_2$ in place of Ni(bpy)Br$_2$	55%
7	Ni(DME)Br$_2$ in place of Ni(bpy)Br$_2$	16%
8	K$_3$PO$_4$ in place of K$_2$HPO$_4$	7%
9	K$_2$CO$_3$ in place of K$_2$HPO$_4$	64%
10	KOAc in place of K$_2$HPO$_4$	0%
11	EtOAc in place of THF	69%
12	acetone in place of THF	39%
13	MeCN in place of THF	4%
14	30W 440 nm Kessil lamp in place of blue LEDs	60%
15	"zero precautions"	44%

4-Cl-CzIPN = 2,4,5,6-tetrakis(3,6-dichloro-9H-carbazol-9-yl)isophthalonitrile ; dtbbpy = 4,4'-di-*tert*-butyl-2,2'-bipyridyl
bpy = 2,2'-bipyridyl ; phen = 1,10-phenanthroline ; DME = dimethoxyethane

Evident from the results in Table 3.1, each reaction component was critical to the success

of the anticipated DCF reaction. A select range of photocatalysts with strong excited state

oxidation potentials (E^*_{ox} = +1.21 – +1.71 V vs SCE) were able to effect the desired reactivity

(entries **1**, **2** and **4**), while weaker single electron oxidants such as Ru(bpy)$_3$PF$_6$ (E^*_{ox} = +0.77 V

vs SCE) were unable to induce fragmentation of *tert*-butyltrifluoroborate (*t*-BuBF$_3$K, E_{ox} = +1.26

V vs SCE). Several bipyridyl-type ligands complexed to nickel(II) bromide were competent

cross-coupling catalysts (entries **5-7**), however, in the absence of a strong σ-donor ligand, the

yield dropped significantly. Other bases with similar pKas could be utilized, but the reaction

suffered when using less than 2 equivalents. THF and EtOAc served as superlative solvents; THF was selected as the standard solvent because of the simplified procedure for obtaining it in anhydrous form. Interestingly, more intense irradiation (compare entries 14 and 1) resulted in the formation of multiple side products and erosion of desired product yield. A "zero-precautions" experiment (non-rigorously dried solvent, reaction performed under an air atmosphere) showed a rather significant decrease in yield compared to standard conditions (compare entries 1 and 15), emphasizing the need for conducting the reaction free of moisture and air. Control studies confirmed that this DCF process was indeed dual catalytic in nature and that all the components of the reaction were necessary to ensure a successful DCF reaction (see 3.6 Experimental Section).

3.3. Scope Exploration and Application to Medicinal Chemistry

With suitable conditions established, we then set out to explore the scope of the aryl electrophile coupling partner. We focused on utilizing aryl bromides, given the diverse array of commercially available structures. A wide range of sensitive functional groups including acidic (**3.14**), nucleophilic (**3.12**), electrophilic (**3.17** and **3.19**), homolytically labile C−H bonds (**3.16** and **3.26**), and strained rings (**3.24**) were all tolerated under the developed reaction conditions. The efficacy of the reaction was not significantly impacted by sterically demanding *ortho*-substituted aryl bromides (**3.20** and **3.21**), although these did require extended reaction times for full conversion. Overall, aryl bromides substituted with electron-withdrawing groups fared best, which suggests that a high population of the Ni^{II} oxidative addition complex (Figure 3.6, **X** or **XI**) is beneficial. Electron-neutral and electron-donating aryl bromides were also amenable, although some substrates required extended reaction times for full conversion. A critical goal we set in developing this protocol was to include complex, functionally dense architectures such as would be found in pharmaceutically relevant moieties. Two aryl bromides derived from FDA-approved

drug structures, each displaying a diverse suite of multifaceted scaffolds, could be incorporated in the DCF protocol with excellent yields (**3.29** and **3.30**). These substrates set this DCF protocol apart from previous net-reductive processes, whose reaction conditions would not be tolerant of such sensitive functional groups. Heterocyclic bromides were also compatible with the DCF process. Two of these substrates yielded a product without the boronate functional group, exposing one potential limitation of the method (**3.32** and **3.33**). Reaction monitoring revealed that protodeborylation occurred during the progress of the reaction, likely because of the presence of a Lewis basic nitrogen in these systems combined with the electron-withdrawing nature of α-pyridyl groups. Such boronates are particularly electrophilic, and the corresponding borate complexes particularly prone to protodeborylation.[26] We also demonstrated that this photochemical reaction could be carried out on larger scale, and substrate **3.28** was prepared on a 5.0 mmol scale with an excellent isolated yield. Finally, a series of bifunctional reagents could be prepared by selective functionalization of arenes bearing multiple cross-coupling handles. Substrates **3.35** and **3.36** were derived from aryl bromides bearing C_{sp2} nucleophiles without exhibiting any byproducts stemming from transmetalation of these nucleophilic groups to Ni. Substrate **3.37** demonstrates the excellent chemoselectivity for oxidative addition into aryl bromides over aryl triflates. Finally, controlled reactivity was demonstrated when using 1,4-diiodobenzene, which displayed selective mono reactivity, producing **3.38** in good yield. These polyfunctionalized arenes would likely be problematic in the aforementioned "two-electron only" DCF protocols, which are designed to functionalize all of the arene handles in starting aryl bromides of substrates **3.35-3.38**.

**Table 3.2.** Scope of Aryl Bromides in Photoredox/Ni DCF

Reaction conditions:
tBu–BF$_3$K (1.5 equiv, **3.1**) + CH$_2$=CH–Bpin (1.2 equiv, **3.2**) + Ar–Br (1 equiv)
5 mol % Ni(bpy)Br$_2$, 2 mol % [Ir{dF(CF$_3$)$_2$ppy}$_2$(bpy)]PF$_6$, 2 equiv K$_2$HPO$_4$, THF (0.1 M), 16 h, blue LEDs

Arene Scope

	R	yield
3.3:	Cl	69%
3.4:	H	62%
3.5:	Me	66%
3.6:	CN	86%[a]
3.7:	CO$_2$Me	66%
3.8:	CF$_3$	81%[b]
3.9:	OMe	53%[c]
3.10:	Ph	91%
3.11:	SO$_2$Me	80%
3.12:	CH$_2$OH	58%

3.13 98% | **3.14** 86% | **3.15** 70% | **3.16** 59% | **3.17** 81% | **3.18** 74% | **3.19** 85%[d] (98%)[e]

	R	yield
3.20:	CN	63%[a]
3.21:	Cl	43%[a]

	R	yield
3.22:	tBu	55%[a]
3.23:	OMe	81%

Polycycles
3.24 46% | **3.25** 76% | **3.26** 59% | **3.27** 52%

Scale Up
3.28 86%, 5.0 mmol scale

Pharmacophores
3.29 76% — Phenazapam® (benzodiazepine) derivative, psychiatric therapeutic
3.30 88% — Romazicon® (flumazenil) derivative, GABA receptor antagonist

Heterocycles
3.31 73% | **3.32** 42% | **3.33** 79% | **3.34** 61%

Bifunctional Reagents
3.35 90% | **3.36** 70% | **3.37** 64% | **3.38** 64%

[a]Reaction time extended to 48 h. [b]Ni(dtbbpy)Br2 used in place of Ni(bpy)Br$_2$. [c]Ni(phen)Br$_2$ used in place of Ni(bpy)Br$_2$. [d]Isolated as the corresponding trifluoroborate. [e]H NMR yield.

As we continued the evaluation of the developed DCF reaction, a range of other alkene lynchpins was examined. Other electron deficient alkenes such as acrylates and acrylonitrile provided excellent yields of the desired product (**3.39-3.42**). In addition to 4-bromobenzonitrile, 5-bromo-2-pyridinecarbonitrile was utilized (which previously exhibited a protodeborylation product), along with *tert*-butyl acrylate to demonstrate that these heteroaryl bromides are still viable arene structures for desired DCF reactivity (**3.40**). Based on previous experience in controlling Giese addition selectivity based on radical/alkene philicities, the applicability of electron neutral alkenes in this protocol was examined. When the DCF reaction using an unactivated alkene (allyl acetate) was attempted, none of the desired DCF product (**3.43**) was isolated. This result was entirely logical, as computational studies have revealed that tertiary

acyclic radicals such as *tert*-butyl are nucleophilic[27] and exhibit very slow addition into electron neutral alkenes.[28] Rather than interpreting this result as a limitation, we instead demonstrated how the DCF protocol could demonstrate chemoselectivity for various alkenes. We prepared a diene via acryloylation of 4-penten-1-ol, and under the standard DCF conditions complete regioselectivity for Giese addition into the electron deficient alkene was observed (**3.44**). Inspired by this result, a suite of polyenes was prepared by performing acryloylation of complex, alkene-containing natural product alcohols. When employing these substrates in the DCF reaction, only radical addition into the acrylate was observed, and the electron neutral alkenes provided no off-target reactivity. These results are very unique in the context of DCF reactions, as many protocols demonstrate more indiscriminate reactivity in regard to the electronic nature of the alkene component.

Table 3.3. Scope of alkenes in Photoredox/Ni DCF
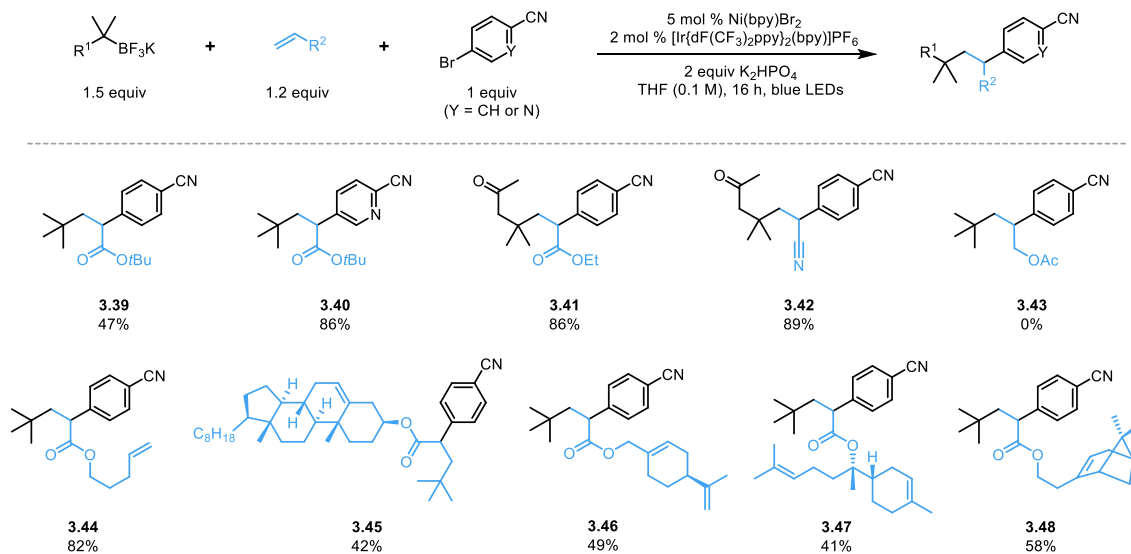
The final exploration of the scope was the trifluoroborate radical precursor component. In addition to *t*-BuBF$_3$K, a range of other acyclic- and cyclic alkyltrifluoroborates were prepared

using various protocols. β-Boryl carbonyls are among the most common substructures and can be easily prepared in a single, high-yielding step by performing a Cu-mediated conjugate borylation of an α,β-unsaturated carbonyl derivative. A two-step, one pot approach developed previously by the group was utilized, relying on tetrahydroxydiboron to serve as the boryl nucleophile, which was immediately quenched with potassium bifluoride following conjugate addition.[23] Implementation of these cyclic- and acylic β-trifluoroborato ketones and esters in the developed protocol yielded the desired DCF products in good to excellent yields (**3.49**-**3.55**). Even sterically demanding alkyl radicals, such as the cyclopentylcyclopentanone used in the preparation of **3.52**, underwent addition to vinyl Bpin, and the highly congested Giese adduct was able to metalate to Ni and produce the arylated product.

Tertiary alkyltrifluoroborates bearing hydrocarbon fragments were prepared via a radical borylation procedure from carboxylic acid feedstocks.[22] These commercially available carboxylic acids were first converted to the corresponding *N*-hydroxyphthalimide esters via a Steglich esterification protocol. These so-called redox active esters were irradiated in the presence of bis(catecholato)diboron (B_2cat_2), which triggered radical fragmentation of both species. The resulting alkyl radical then underwent borylation with a second equivalent of B_2cat_2. This protocol offered the preparation of several unique tertiary alkyltrifluoroborates that would have otherwise been impossible through traditional borylation techniques.[24] Cyclohexylmethyl- and cyclopentylmethyl radicals gave the desired DCF products **3.56** and **3.57** in excellent yields. Interestingly, bridgehead bicyclic radicals (adamantyl and bicyclo[2.2.2]octyl), which have been demonstrated to undergo two-component cross coupling under standard conditions,[21] preferentially underwent Giese addition, leading to the desired three-component DCF product. A trifluoroborate derived from the HDL regulator gemfibrizol gave an excellent yield of the desired product, again, demonstrating the applicability of this method to medicinal chemistry.

Unfortunately, a tertiary benzylic radical was unable to afford any of the DCF product (**3.62**). A large amount of the protodeborylated byproduct (cumene) was observed, suggesting that after fragmentation of the trifluoroborate, the benzylic radical participates in a HAT process rather than undergoing Giese addition. This result is not particularly surprising as benzylic radicals are known to undergo slower Giese addition compared to non-functionalized alkyl radicals because of their conjugation with the aromatic system.[29] These conjugated radicals are more electrophilic[27] and more reluctant to undergo the trigonal planar to *pseudo*-tetrahedral isomerization required for the Giese addition transition state compared to normal alkyl radicals.[30]

Table 3.4. Scope of alkyltrifluoroborate radicals in photoredox/Ni DCF
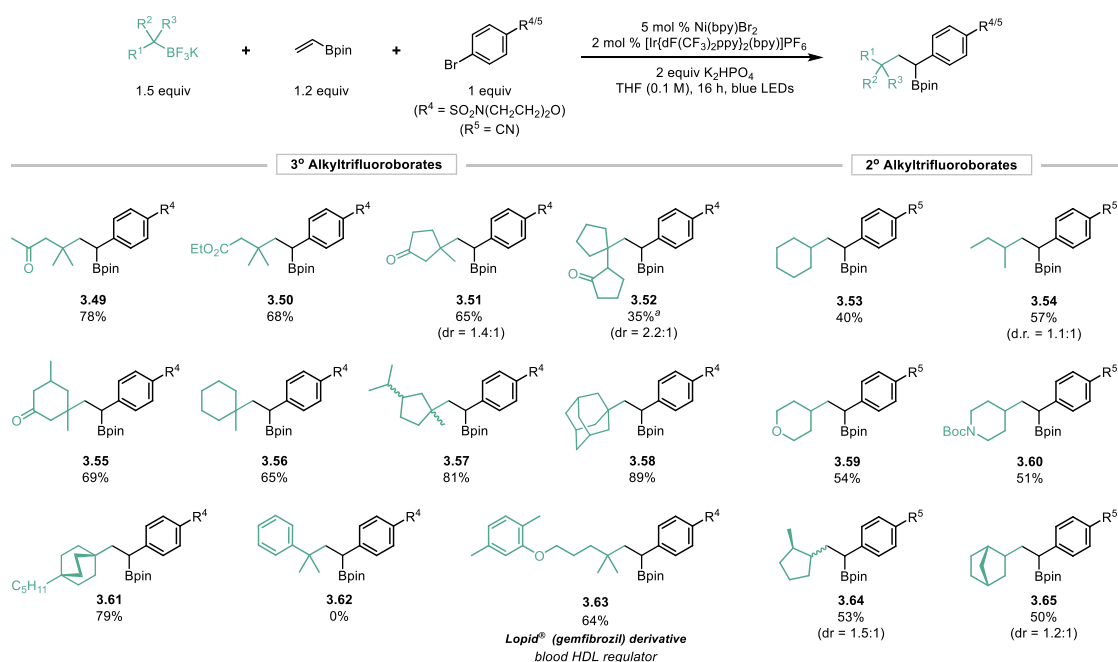
Though we initially focused solely on the implementation of tertiary alkyl radicals, we desired to expand the modularity of the DCF process by including secondary alkyltrifluoroborates. As anticipated, under the standard conditions, use of cyclohexyltrifluoroborate yielded a majority of the two-component, direct cross-coupling product

and only a small amount of the desired three-component DCF product. As optimization of the DCF:CC selectivity was sought, we assumed that the only factor influencing the rate of Giese addition that could be easily manipulated was the concentration of the alkene. We found a relatively linear relationship between the loading of the alkene and selectivity for the three-component DCF product, and ultimately decided that increasing the loading of the alkene to three equivalents provided a respectable yield while still maintaining reasonable stoichiometry (Figure 3.7). Based on the proposed mechanism, it also seemed logical that decreasing the rate of radical metalation would also increase the selectivity for the DCF product. A suite of various bipyridine- and phenanthroline-based ligands for the Ni catalyst was examined, and several scaffolds were found to increase the selectivity for the DCF product significantly. In general, the data suggests that increasing the steric environment distal to the Ni center improved the DCF product formation by decreasing the rate of direct metalation of the alkyl radical generated from oxidative cleavage of the trifluoroborate. Ligands that had substitution *ortho* to the nitrogen atoms resulted in a poor yield of either the DCF or cross-coupling product, and high amounts of hydroalkylation were observed. 1,10-Phenanthroline was selected as a suitable optimal ligand scaffold as it presumably provides an increased steric environment to retard the rate of cyclohexyl radical metalation while not inhibiting metalation of the Giese addition adduct.
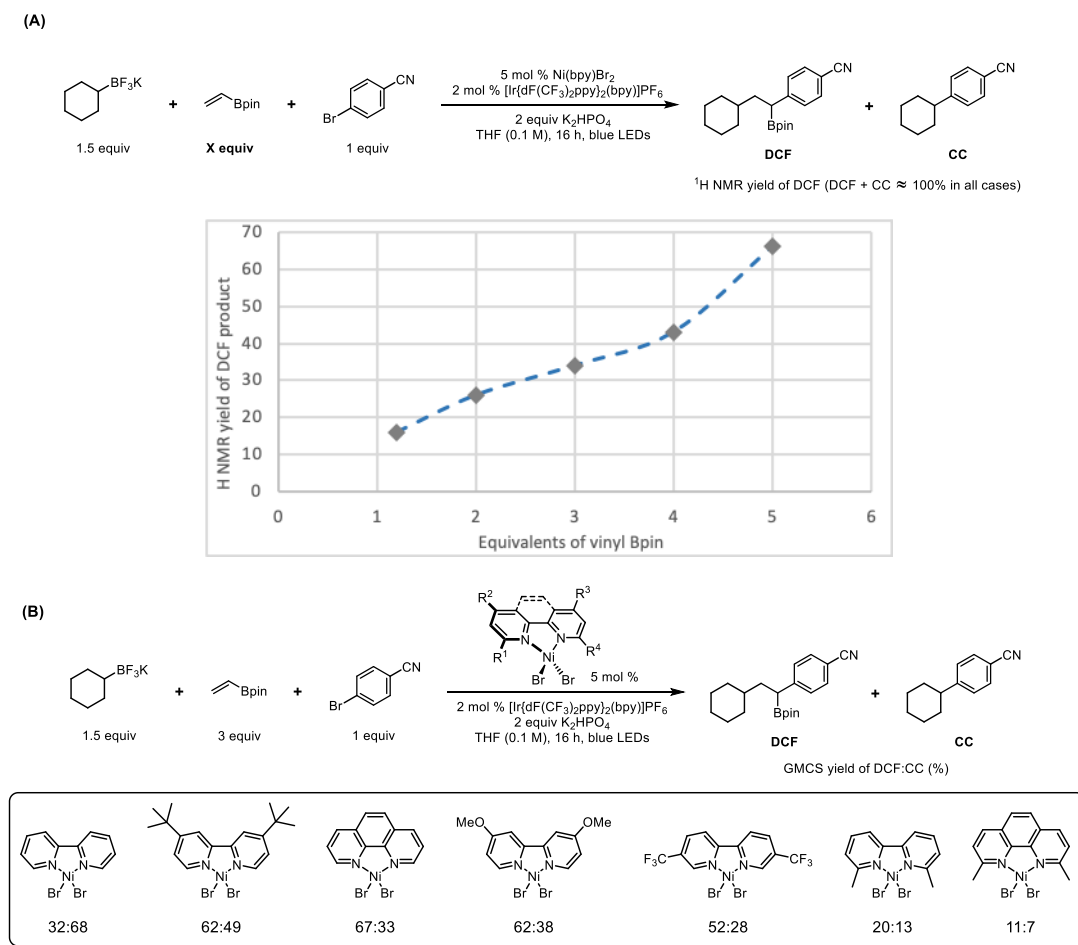
Figure 3.7. (A) Yield of DCF product as a function of vinyl Bpin loading. (B) GCMS yields of DCF/CC across a range of Ni^{II} ligand scaffolds.

With these new optimized conditions in hand, a small range of secondary alkyltrifluoroborates was surveyed (Table 3.4). Cyclic- as well as acyclic radicals all produced synthetically useful yields of the desired DCF product, with the two-component direct cross coupling accounting for the remainder of the mass balance.

We also desired to showcase the applicability of this method toward the synthesis of medicinally relevant molecular architecture. A key intermediate (**3.67**) in the literature synthesis of a thymidylate kinase inhibitor (TK-666) developed by AstraZeneca,[31] whose substructure would be amenable to a DCF reaction, was identified. The literature synthesis of the benzylic

alcohol *en route* to TK-666 begins with formation of an arylzinc species, which undergoes a Pd-mediated acylation to yield the corresponding ketone. Benzylic alcohol **3.67** is then furnished via a particularly low-yielding borohydride reduction. An analogous intermediate (**3.69**) was preparted via a two-step, one-pot approach. First, the developed DCF reaction produced benzylic boronate **3.68**, which was immediately submitted to oxidation without any purification. This protocol furnished the benzylic alcohol (**3.69**) in significantly higher yield and greater efficiency compared to the synthesis previously reported in the literature.
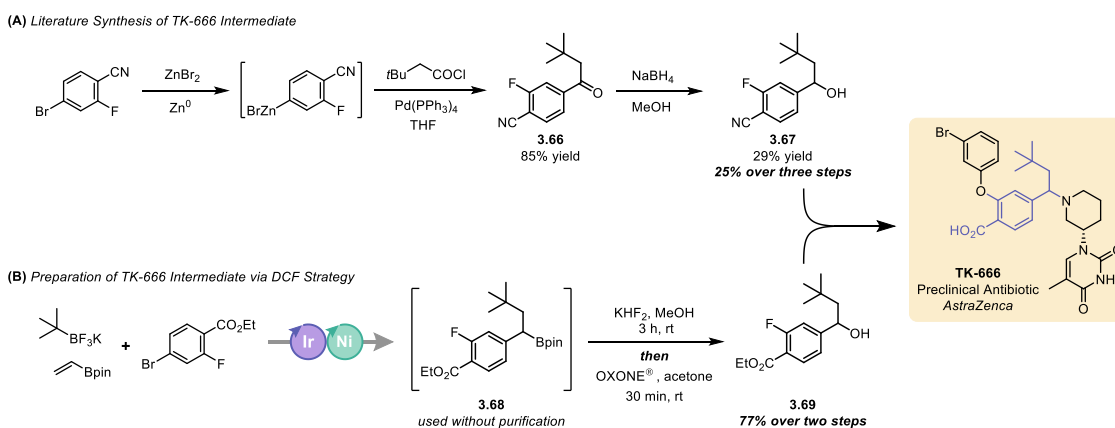

Figure 3.8. Strategies to access a synthetic intermediate en route to preclinical antibiotic TK-666

In addition to an improved yield and synthetic efficiency, the incorporation of the DCF protocol in the synthesis of TK-666 offered greater modularity to access a library of related derivatives rapidly. In the initial report of TK-666, the researchers examined a variety of analogs, each bearing a unique tertiary or secondary alkyl group at the homobenzylic carbon. These were incorporated into the structure of TK-666 in the first step of the synthesis via the acetyl chloride derivative, many of which were not commercially available. We demonstrated how our library of alkyltrifluoroborate radical precursors offered a more diverse set of alkyl groups that could be easily incorporated in a highly modular fashion. We engaged an advanced aryl bromide in the DCF protocol with various alkyltrifluoroborates to prepare novel TK-666 derivative analogues

3.70-3.72. Further oxidation of these boronates yielded the corresponding benzylic alcohols that would serve as intermediates toward unique variants of TK-666. In addition to the oxidation protocol described here, these DCF-derived alkylboronates open up exploration into the role of the benzylic functional group (given the vast array of functional group transformations available from the boronate ester) to enable rapid diversification for SAR studies.
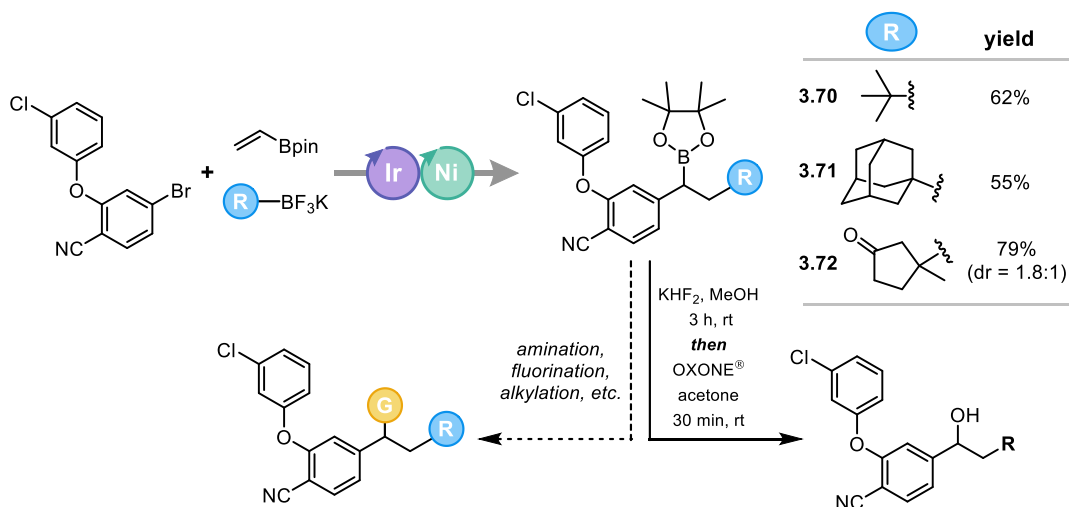

Figure 3.9. Preparation of novel TK-666 analogous via photoredox/Ni DCF strategies

3.4. Mechanistic Experiments

To help gauge the relative rates of the fundamental steps in the proposed mechanism, two alkyltrifluoroborate radical precursors containing radical trap functional groups were prepared. Alkyltrifluoroborate **3.73** contained an alkene, which would offer the possibility for various intramolecular radical cyclization events. The product isolated from the DCF reaction with **3.73** contained a cyclopentyl ring, which presumably forms via a 5-*exo*-trig cyclization of the Giese addition intermediate. The formation of this cyclopentyl product and the absence of any arylation of the intermediate α-boryl radical indicates that vinyl Bpin is not precomplexed to the Ni catalyst and/or that the rate of this 5-*exo*-trig radical cyclization ($\sim 2 \times 10^5$ s^{-1})[32] outcompetes the rate of metalation.
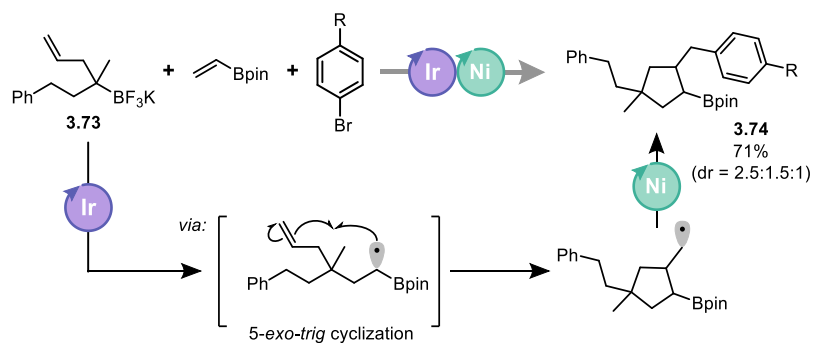
115

Figure 3.10. Photoredox/Ni DCF reaction of trifluoroborate **3.73** demonstrating 5-*exo*-trig

cyclization

We also employed a trifluoroborate derived from beta-borylation of (-)-verbenone. Oxidative fragmentation of this trifluoroborate would generate an α-cyclobutyl, tertiary radical which might undergo ring-opening, depending on the rate of Giese addition. As anticipated, radical ring opening outcompeted Giese addition of the initially generated tertiary radical as a [4+2] cycloaddition product (**3.76**) was isolated from the reaction. The formation of this bicyclononane ring system reveals two kinetic aspects of this mechanism. First, the rate of cyclobutane fragmentation in this pinene ring system ($\sim$1.1 x 10^7 s^{-1})[33] outcompetes Giese addition of the tertiary radical into vinyl Bpin. Second, the rate of 6-*exo*-trig cyclization of the intermediate α-boryl radical ($\sim$5 x 10^3 s^{-1})[32] outcompetes its metalation and arylation.
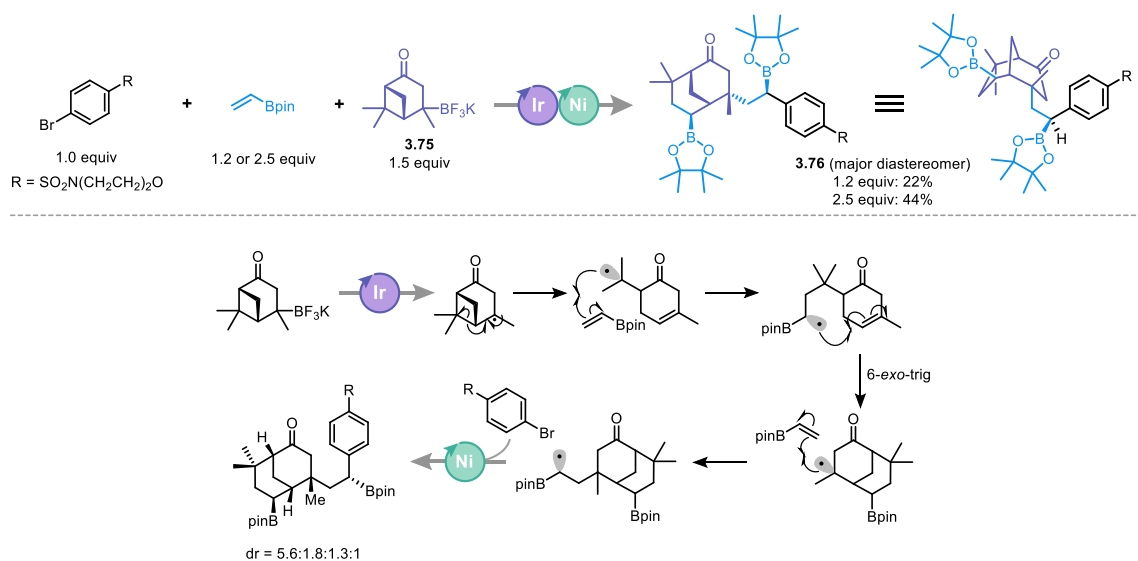
Figure 3.11. Photoredox/Ni DCF reaction of trifluoroborate **3.75** derived from (-)-verbenone

Finally we performed additional experiments to provide evidence for the mechanism proposed in Figure 3.6. An alternative mechanism, outlined in Figure 3.12A, could be envisioned. A Ni-mediated Heck reaction between vinyl Bpin and the aryl bromide could produce the branched styrene intermediate. Addition of the alkyl radical into the styrene followed by radical/polar crossover to access the α-boryl, benzylic anion would close the photoredox cycle. To rule out the possibility of this mechanism, we attempted to produce the α-boryl styrene intermediate under the standard conditions (without the trifluoroborate radical precursor) and typical Ni-mediated Heck coupling conditions (Figure 3.12B). No formation of either branched or linear Heck products under any conditions was observed, providing support for the previously proposed mechanism.

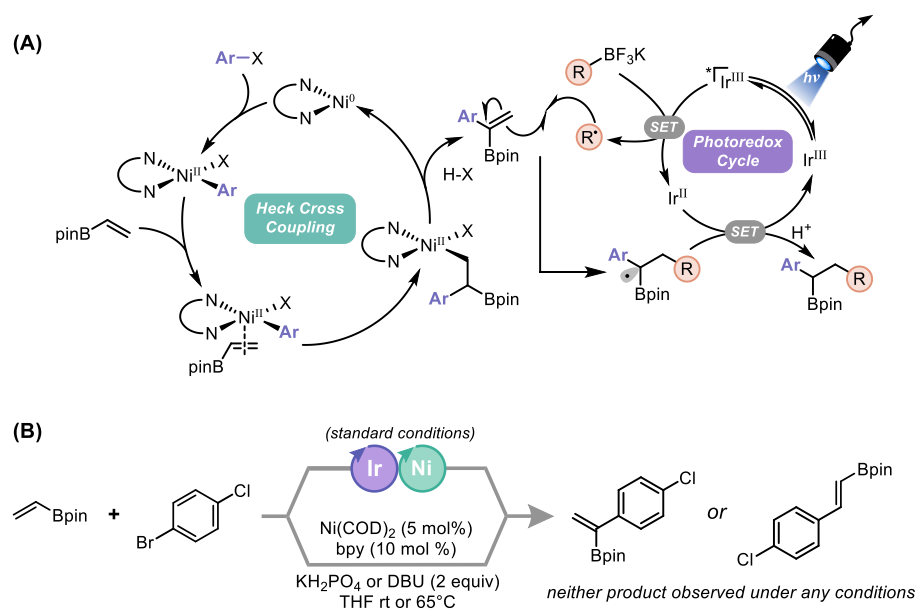**Figure 3.12.** (A) Possible alternative mechanism for photoredox/Ni DCF involving Heck coupling intermediate. (B) Attempts to form Heck coupling intermediate under various conditions

3.5. Conclusion

In summary, the developed protocol allowed the incorporation of a broad palette of aryl halides, olefins, and radical architectures, highlighting the advancements in DCF technology achieved by a novel, photoredox/Ni mechanism. This three-component process enables two C−C bonds to be formed in a single step (C_{sp3}−C_{sp3} and C_{sp3}−C_{sp2}) and sets both quaternary and tertiary centers, all while retaining the mild, functional group tolerant nature characteristic of Ni/photoredox dual catalysis. The inherent mechanistic underpinnings enable selective olefin functionalization in polyolefinic systems based on olefin electronics. The focus on the utilization of vinyl boronates is particularly attractive from the standpoint of late-stage functionalization and enabled the preparation of an intermediate to a preclinical antibiotic. The implications of the developed process sparked additional mechanistic investigations, leading to the discovery of

several fundamental aspects of radical reactivity. These results sparked further questions and motivated continued exploration in radical/Ni DCF reactions.

3.6. Experimental

3.6.1 General Considerations

All chemical transformations requiring inert atmospheric conditions or vacuum distillation utilized Schlenk line techniques with a 4- or 5-port dual-bank manifold. LED irradiation was accomplished using the LED reactor described in our previous report.[34] Tetrahydrofuran was dried using a solvent delivery system. All reagents were purchased and used as received from suppliers unless otherwise noted. Nickel pre-complexes were prepared as described here. The transition metal photocatalysts ($Ru(bpy)_3(PF_6)_2$ and $[Ir\{dFCF_3ppy\}_2(bpy)]PF_6$) were prepared in-house by the procedure outlined in our previous publications;[35] others were purchased from commercial sources. The organic photocatalysts 4CzIPN and Cl-4CzIPN were prepared in-house by the procedure outlined in our previous publication.[36] Aryl- and heteroaryl bromides were either purchased from commercial sources, prepared as previously reported,[37] or prepared as outlined here. Potassium alkyltrifluoroborates were either purchased from commercial sources or prepared by the methods outlined here. Solvents were purified with drying cartridges through a solvent delivery system. Reactions were monitored by GC/MS or TLC using silica gel F_{254} plates (60 Å porosity, 250 μm thickness). TLC analysis was performed using EtOAc/hexanes, CH_2Cl_2/hexanes, or EtOAc with 1% MeOH/hexanes and visualized using permanganate stain, Seebach's stain,[38] CAM (Hanessian's) stain, and/or UV light. Silica plugs utilized flash silica gel (60 Å porosity, 32-63 μm). Flash chromatography was accomplished using an automated system (monitoring at 254 nm and 280 nm) with silica cartridges (60 Å porosity, 20-40 μm). Accurate

mass measurement analyses were conducted using electron ionization (EI) or electrospray ionization (ESI). The signals were mass measured against an internal lock mass reference of perfluorotributylamine (PFTBA) for EI-GCMS, and leucine enkephalin for ESI-LCMS. The utilized software calibrates the instruments and reports measurements by use of neutral atomic masses. The mass of the electron is not included. IR spectra were recorded using either neat oil or solid products. Melting points (°C) are uncorrected. NMR spectra [^{1}H, ^{13}C {^{1}H}, ^{11}B, ^{19}F {^{1}H}] were obtained at 298 K. ^{1}H NMR (500.4 MHz) chemical shifts are referenced to residual, non-deuterated CHCl$_3$ (δ 7.26) in CDCl$_3$ and acetone-d_5 (δ 2.09) in acetone-d_6. ^{13}C{^{1}H} NMR (125.8 MHz) chemical shifts are reported relative to CDCl$_3$ (δ 77.3) and the carbonyl carbon of acetone (δ 205.9). ^{11}B NMR (128.4 MHz) chemical shifts are uncorrected. ^{19}F NMR spectra were referenced to hexafluorobenzene (δ –161.64 in CDCl$_3$ or –164.67 in acetone-d_6).[37] Data are presented as follows: chemical shift (ppm), multiplicity (s = singlet, d = doublet, t = triplet, q = quartet, m = multiplet, br = broad), coupling constant J (Hz) and integration.

3.6.1 Preparation of (2,2-Bipyridine)nickel(II) dibromide
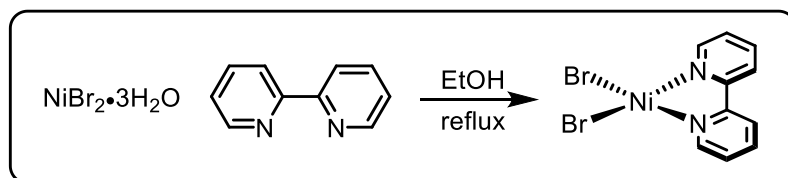
A flask was charged with NiBr$_2$•3H$_2$O (5.45 g, 20.0 mmol, 1.00 equiv) and 2,2′-bipyridine (3.28 g, 21.0 mmol, 1.05 equiv) and evacuated and purged with argon three times. Absolute EtOH (75 mL) was added, and the suspension was heated to a vigorous reflux for 24 h. During the refluxing period the color of the suspension changed from light brown to yellow/green. The resulting suspension was cooled to rt and filtered through a medium porosity fritted glass funnel and washed with Et$_2$O (3 × 150 mL). The resulting powder was dried under high vacuum at 50 °C for

24 h and stored in a desiccator. This complex is hygroscopic, and absorption of H_2O from the atmosphere is accompanied by a change in color (dull yellow/green to bright blue). We observed that the efficacy of the dicarbofunctionalization reaction was dependent upon the anhydrous nature of the nickel catalysts.[39]
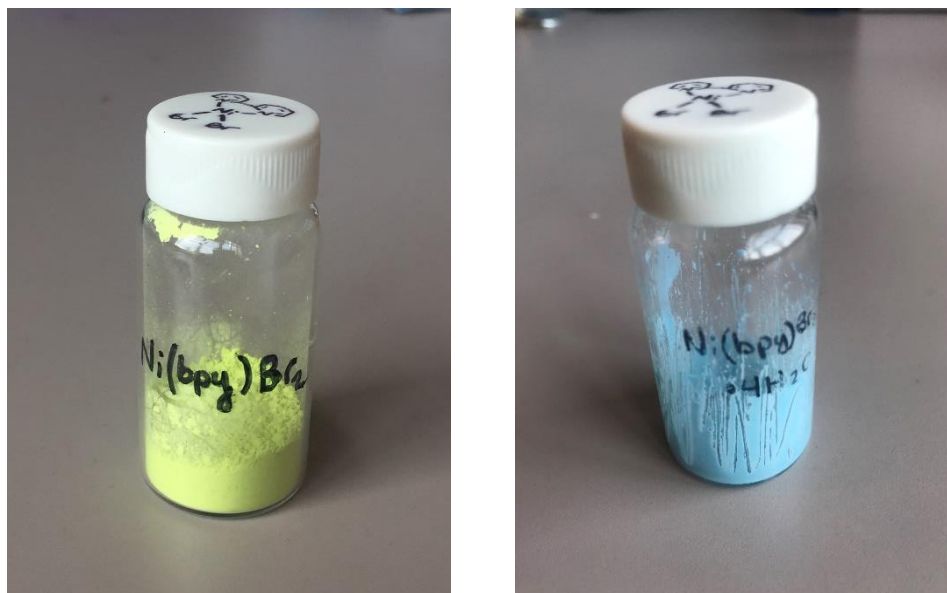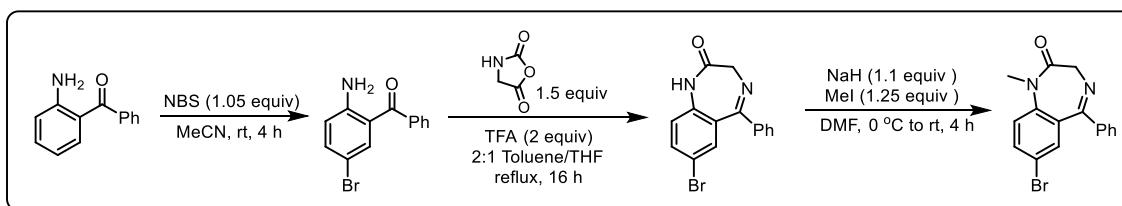

Figure 3.13. (Left) A sample of anhydrous Ni(bpy)Br$_2$ (Right) A sample of hydrated Ni(bpy)Br$_2$

3.6.2 Preparation of Non-Commerical Aryl Halides

7-Bromo-1-methyl-5-phenyl-1H-benzo[e][1,4]diazepin-2(3H)-one

Bromination

To a 100 mL flask equipped with a stirrer bar was added 2-aminobenzophenone (0.510 g, 2.60 mmol, 1 equiv) followed by MeCN (30 mL). The flask was then cooled to 0 °C via an ice/water bath. After 10 min, NBS (0.483 g, 2.71 mmol, 1.05 equiv) was added to the reaction in five portions over the course of 50 min. The mixture was stirred at rt for 3 h. The solvent was then removed *in vacuo* by rotary evaporation. The resulting crude solid was taken up in a 1:1 Et_2O/EtOAc soln (30 mL). This soln was then washed with deionized H_2O (30 mL) followed by brine (30 mL). The organic layer was dried (Na_2SO_4), and the solvent was removed *in vacuo* by rotary evaporation. The crude solid was recrystallized from hexanes/Et_2O (2:1) to yield (2-amino-5-bromophenyl)(phenyl)methanone as yellow needles (0.509 g, 71%). All data matched that reported in the literature.[40]

Condensation/Annulation

To a 100 mL flask equipped with a stirrer bar was added (2-amino-5-bromophenyl)(phenyl)methanone (1.11 g, 4.00 mmol, 1 equiv) dissolved in a 2:1 mixture of toluene and THF (60 mL). Oxazolidine-2,5-dione (0.505 g, 5.00 mmol, 1.25 equiv) was added in one portion followed by CF_3CO_2H (0.91 g, 0.61 mL, 8.0 mmol, 2 equiv). The reaction mixture was heated at reflux overnight. The reaction mixture was concentrated *in vacuo* by rotary evaporation. The resulting crude solid was taken up in EtOAc (30 mL) and washed with satd aq $NaHCO_3$ (30 mL). The layers were separated, and the aq layer was extracted with EtOAc (2×30 mL). The organic layer was washed with brine (100 mL) and dried (Na_2SO_4). The solvent was removed *in vacuo* by rotary evaporation to give the crude annulation product. The crude solid was purified *via* SiO_2 column chromatography to yield 7-bromo-5-phenyl-1H-

benzo[*e*][1,4]diazepin-2(3*H*)-one as a crystalline, yellow solid (0.44 g, 35%). All data matched that reported in the literature.[41]

Methylation

To a slurry of NaH (35 mg, 1.47 mmol, 1.1 equiv) in anhyd DMF (10 mL) cooled to 0 °C in an ice-water bath was added 7-bromo-5-phenyl-1H-benzo[e][1,4]diazepin-2(3H)-one (0.420 g, 1.33 mmol, 1 equiv) dissolved in 5 mL of anhyd DMF, which resulted in vigorous bubbling. The reaction mixture was stirred for 30 min, after which MeI was added dropwise, neat. The reaction was allowed to stir for 4 h while coming to rt. The reaction mixture was diluted with H$_2$O and EtOAc, and the layers were separated. The aq layer was extracted with EtOAc (3 × 15 mL). The organic layer was washed with brine, dried (Na$_2$SO$_4$), and concentrated *via* rotary evaporation. The crude solid was purified *via* silica gel chromatography to afford 7-bromo-1-methyl-5-phenyl-1H-benzo[e][1,4]diazepin-2(3H)-one as a powdery yellow solid (0.282 mg, 64%). All data matched that reported in the literature.[42]

2-(4-Bromophenyl)-1,3-dioxolane
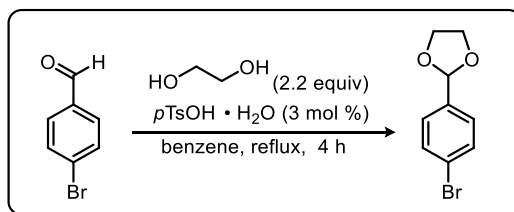
2-(4-Bromophenyl)-1,3-dioxolane was prepared *via* a modified literature procedure.[11] To a 50 mL round bottom flask equipped with a stirrer bar was added *p*-bromobenzaldehyde (0.485 g, 2.62 mmol, 1 equiv) followed by benzene (10 mL). The contents of the flask were stirred and, after 2 min, *p*-TsOH•H$_2$O (15.0 mg, 0.0789 mmol, 0.03 equiv) and ethylene glycol (0.358 g, 0.322 mL, 5.77 mmol, 2.2 equiv) were added. The flask was equipped with a Dean-Stark trap and heated at

reflux for 4 h. After cooling to rt, the reaction mixture was diluted with EtOAc (20 mL) and transferred to a separatory funnel. The organic layer was washed with cold, deionized H_2O (30 mL). The organic layer was then washed with brine (30 mL) and dried (Na_2SO_4). The solvent was removed *in vacuo* by rotary evaporation to yield 2-(4-bromophenyl)-1,3-dioxolane as a colorless oil (0.585 g, 97%). All data matched that reported in the literature.[43]

1-Bromo-3-(methoxymethoxy)benzene
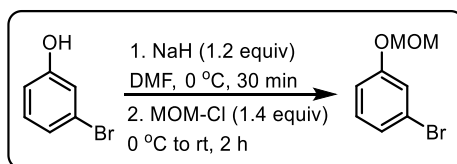
1-Bromo-3-(methoxymethoxy)benzene was prepared via a modified literature procedure.[44] To a 100 mL round bottom flask equipped with a stirrer bar was added NaH (0.230 g, 9.60 mmol, 1.2 equiv). The flask was sealed with a rubber septum and placed under an Ar atmosphere via an inlet needle. The flask was charged with anhyd DMF (24 mL) and then cooled to 0 °C in an ice-water bath. After 5 min, a soln of 3-bromophenol (1.38 g, 8.00 mmol, 1 equiv) in anhyd DMF (5 mL) was added to the flask. **CAUTION:** *Evolves H_2 gas*! The mixture was stirred for 30 min at 0 °C. After this time, a soln of MOM-Cl (0.902 g, 0.85 mL, 11.2 mmol, 1.4 equiv) in anhyd DMF (5 mL) was added dropwise. After complete addition, the ice bath was removed, and the reaction mixture was stirred at rt for 2 h. After this time, the reaction was carefully quenched with cold, deionized H_2O (20 mL). The contents of the flask were transferred to a separatory funnel and diluted with EtOAc (30 mL). The layers were separated, and the aq layer was extracted with EtOAc (2×20 mL). The combined organic layers were washed with deionized H_2O (60 mL), brine (100 mL), and dried (Na_2SO_4). The solvent was removed *in vacuo* by rotary evaporation to

afford 1-bromo-3-(methoxymethoxy)benzene as a clear, colorless oil (1.51g, 87%). All data matched that reported in the literature.[45]

N,N-Dibenzyl-4-bromobenzamide
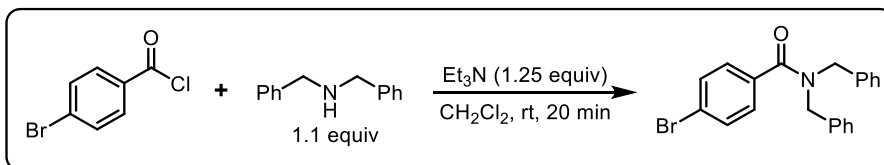
To a 150 mL round bottom flask equipped with a stirrer bar was added 4-bromobenzoyl chloride (2.20 g, 10.0 mmol, 1.00 equiv) followed by CH_2Cl_2 (30 mL). The flask was sealed with a rubber septum and placed under an Ar atmosphere *via* an inlet needle. The flask was charged with Et_3N (1.77 g, 2.44 mL, 17.5 mmol, 1.75 equiv) and was then cooled to 0 °C in an ice-water bath. After 5 min, Bn_2NH (2.96 g, 15.0 mmol, 1.50 equiv) was added dropwise to the flask. The mixture was stirred for 20 min at 0 °C. After this time, 2 M aq HCl (50 mL) was added to the flask. The contents of the flask were transferred to a separatory funnel and diluted with CH_2Cl_2 (30 mL). The layers were separated, and the aq layer was extracted with CH_2Cl_2 (2 × 30 mL). The combined organic layers were washed with 2 M HCl (2 × 50 mL), brine (100 mL), and dried (Na_2SO_4). The solvent w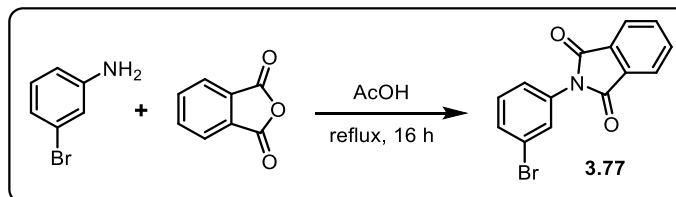as removed *in vacuo* by rotary evaporation to afford *N,N*-dibenzyl-4-bromobenzamide as an off-white solid (2.315 g, 91%). All data matched that reported in the literature.[46]

N-(3-Bromophenyl)phthalimide), 3.77

N-(3-Bromophenyl)phthalimide), **S1** was prepared *via* a modified literature procedure.[47] To a 100 mL round bottom flask equipped with a stirrer bar was added 3-bromoaniline (1.72 g, 10.0 mmol, 1 equiv) followed by AcOH (50 mL). The mixture was stirred for 2 min, and then phthalic anhydride (1.48 g, 10.0 mmol, 1 equiv) was added. The flask was equipped with a reflux condenser, and the reaction mixture was heated to reflux for 16 h. After this time, the reaction mixture was cooled to rt, and ice was added to the mixture, which caused the precipitation of a white powder. This solid was collected by vacuum filtration through a medium porosity fritted funnel and dried to yield *N*-(3-bromophenyl)phthalimide) as a white powder (2.65 g, 88 %) (mp = 162 – 163 °C).

¹H NMR (CDCl₃, 500 MHz) δ ppm 7.97 (dd, *J* = 5.3, 3.1 Hz, 2H), 7.81 (dd, *J* = 5.3, 3.1 Hz, 2H), 7.66 (s, 1H), 7.54 (d, *J* = 7.8 Hz, 1H), 7.36 - 7.45 (m, 2H). **¹³C NMR** (CDCl₃, 125 MHz) δ ppm 167.0, 134.8, 133.1, 131.7, 131.3, 130.4, 129.7, 125.2, 124.1, 122.6. **FT-IR** (cm⁻¹, neat, ATR) 3012 (w), 1711 (vs), 1477 (m), 1376 (s), 1078 (m), 862 (m). **HRMS** (EI) calcd for C₁₄H₈BrNO₂ [M]⁺: 300.9738, found: 300.9741.

**tert-Butyl Acetyl(4-bromophenyl)carbamate, 3.78**
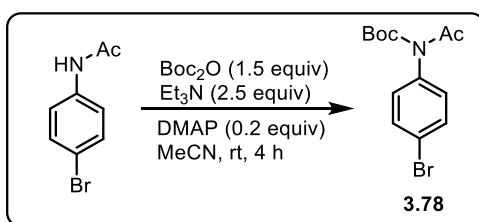
To a 150 mL round bottom flask equipped with a stirrer bar was added 4-bromoacetanilide (2.14 g, 10.0 mmol, 1.00 equiv) and DMAP (0.244 g, 2.00 mmol, 0.2 equiv). The flask was sealed with a rubber septum and placed under an Ar atmosphere *via* an inlet needle. The flask was charged

with MeCN (35 mL) and Et$_3$N (3.5 mL, 25 mmol, 2.5 equiv). After stirring for 2 min, Boc$_2$O (3.27 g, 15.0 mmol, 1.5 equiv) was added *via* a syringe. The mixture was stirred for 4 h at rt. After this time, 1 M aq HCl (50 mL) was added to the flask. The contents of the flask were transferred to a separatory funnel and diluted with EtOAc (60 mL). The layers were separated, and the aq layer was extracted with EtOAc (2 × 30 mL). The combined organic layers were washed with 2 M HCl (2 × 50 mL), brine (100 mL), and dried (Na$_2$SO$_4$). The solvent was removed *in vacuo* by rotary evaporation to afford the crude Boc aniline. Further purification was accomplished by recrystallization from MeOH to afford *tert*-butyl acetyl(4-bromophenyl)carbamate, **S2,** as a white solid (2.307 g, 73%) (mp = 122-123 ºC).

^{1}H NMR (CDCl$_3$, 500 MHz) δ ppm 7.52 (d, *J* = 8.4 Hz, 2H), 6.96 (d, *J* = 8.4 Hz, 2H), 2.59 (s, 3H), 1.39 (s, 9H). **^{13}C NMR** (CDCl$_3$, 125 MHz) δ ppm 173.0, 152.5, 138.1, 132.3, 130.1, 121.8, 83.8, 278.0, 26.6. **FT-IR** (cm^{-1}, neat, ATR) 2985 (vw), 1737 (s), 1704 (vs), 1367 (m), 1271 (s), 1257 (s), 845 (m). **HRMS** (EI) calcd for C$_8$H$_7$BrNO [M-Boc]$^+$: 212.9789, found: 212.9769.
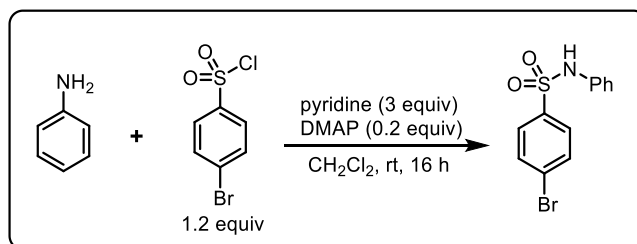
4-((4-Bromophenyl)sulfonyl)morpholine)
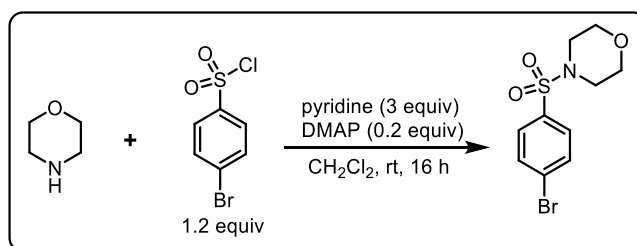
To a 150 mL round bottom flask equipped with a stirrer bar was added 4-bromobenzenesulfonyl chloride (6.13 g, 24.0 mmol, 1.2 equiv) and DMAP (0.489 g, 4.80 mmol, 0.2 equiv). The flask was sealed with a rubber septum and placed under an Ar atmosphere *via* an inlet needle. The flask

was charged with CH$_2$Cl$_2$ (67 mL) and pyridine (4.83 mL, 60.0 mmol, 3 equiv) followed by morpholine (1.73 mL, 20.0 mmol, 1 equiv). The mixture was stirred overnight at rt. After this time, 1 M aq HCl (50 mL) was added to the flask. The contents of the flask were transferred to a separatory funnel and diluted with CH$_2$Cl$_2$ (25 mL). The layers were separated, and the aq layer was extracted with CH$_2$Cl$_2$ (2 × 30 mL). The combined organic layers were washed with 1 M HCl (2 × 50 mL), deionized H$_2$O (100 mL), brine (100 mL), and dried (Na$_2$SO$_4$). The solvent was removed *in vacuo* by rotary evaporation to afford the sulfonamide. Further purification was accomplished by recrystallization from CH$_2$Cl$_2$ at -20 ℃ to afford 4-((4-bromophenyl)sulfonyl)morpholine) as a white crystalline solid (4.96 g, 81%) (mp = 149-150 ℃). All data matched that reported in the literature. [48]

4-Bromo-*N*-phenylbenzenesulfonamide

To a 150 mL round bottom flask equipped with a stirrer bar was added 4-bromobenzenesulfonyl chloride (1.66 g, 6.50 mmol, 1.3 equiv) and DMAP (0.122 g, 1.00 mmol, 0.2 equiv). The flask was sealed with a rubber septum and placed under an Ar atmosphere *via* an inlet needle. The flask was charged with CH$_2$Cl$_2$ (17 mL) and pyridine (1.21 mL, 15.0 mmol, 3 equiv) followed by aniline (0.456 mL, 5.00 mmol, 1 equiv). The mixture was stirred overnight at rt. After this time, 1 M aq HCl (50 mL) was added to the flask. The contents of the flask were transferred to a separatory funnel and diluted with CH$_2$Cl$_2$ (25 mL). The layers were separated, and the aq layer was extracted with CH$_2$Cl$_2$ (2 × 30 mL). The combined organic layers were washed with 1 M HCl

(2 × 50 mL), deionized H₂O (100 mL), brine (100 mL), and dried (Na₂SO₄). The solvent was removed *in vacuo* by rotary evaporation to afford the sulfonamide. Further purification was accomplished by recrystallization from MeOH to afford 4-bromo-*N*-phenylbenzenesulfonamide as a white crystalline solid (1.34 g, 86%) (mp = 114-115 °C). All data matched that reported in the literature.[49]
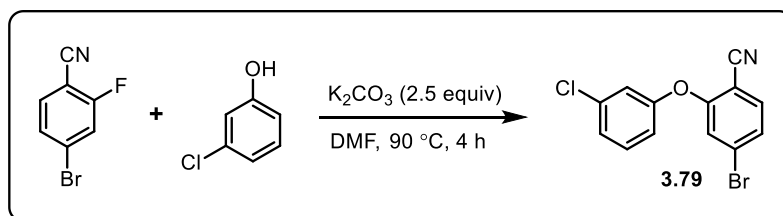
4-Bromo-2-(3-chlorophenoxy)benzonitrile, 3.79

To a 100 mL round bottom flask equipped with a stir bar was added 4-bromo-2-fluorobenzonitrile (0.643 g, 3.21 mmol, 1.0 equiv) and potassium carbonate (1.11 g, 8.03 mmol, 2.5 equiv). The flask was capped with a septum and placed under an Ar atmosphere via an inlet needle. Anhydrous DMF (15 mL) was added to the flask via syringe followed by 3-chlorophenol (0.475 g, 3.69 mmol, 1.15 equiv). The reaction was then heated to 90 °C for 4 hours. After cooling to room temperature the reaction was quenched with saturated aq NH₄Cl (30 mL) and the mixture was extracted with diethyl ether (3 X 25 mL). The combined organic extracts were washed with 2 M aq NaOH (2 × 25 mL). The organic layer was dried (Na₂SO₄), filtered, and concentrated via rotary evaporation. Further purification was accomplished by SiO₂ column chromatography (hexanes to 93:7 hexanes/EtOAc) to yield the desired compound **S3** as a white solid (0.960 g, 97%) (mp = 88-90 °C)

¹H NMR (CDCl₃, 500 MHz) δ ppm 7.53 (d, *J* = 8.2 Hz, 1H), 7.37 (t, *J* = 8.2 Hz, 1H), 7.33 (dd, *J* = 8.3, 1.5 Hz, 1H), 7.28 - 7.23 (m, 1H), 7.11 (t, *J* = 2.0 Hz, 1H), 7.02 (d, *J* = 1.4 Hz, 1H), 7.00 (dd, *J* = 8.2, 2.2 Hz, 1H). **¹³C NMR** (CDCl₃, 125 MHz) δ ppm 159.7,

155.4, 136.0, 135.0, 131.4, 129.0, 127.2, 126.2, 120.9, 120.9, 118.5, 115.3, 103.3. **FT-IR**

(cm^{-1}, neat, ATR) 3092 (vw), 2232 (w), 1584 (m), 1471 (s), 1400 (m), 1234 (s), 923 (m),

853 (m). **HRMS** (EI) calcd for $C_{13}H_7BrClNO$ [M$^+$]: 306.9400, found: 306.9396.

3.6.3 Preparation of Bis(catecholato)diboron
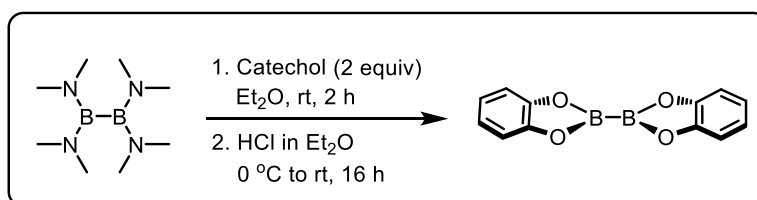
Bis(catecholato)diboron was prepared according to a modified literature procedure.[50] A 500 mL,

three-necked round bottom flask was equipped with large stirrer bar, two rubber septa, and an

addition funnel capped with a rubber septum. The flask was equipped with an inlet needle, and

the flask was evacuated and backfilled with Ar three times. The addition funnel was sealed off

from the flask, equipped with an inlet needle, and backfilled with Ar. The funnel was charged

with 200 mL of Et$_2$O. The Et$_2$O was degassed for 5 min, then added to the flask.

Tetrakis(dimethylamido)diboron (6.00 g, 6.48 mL, 30.3 mmol, 1 equiv) was added *via* a syringe.

The boron soln was allowed to drain into the flask, and then the addition funnel was sealed off

from the flask. The funnel was then charged with a degassed soln of catechol (6.67 g, 60.6 mmol,

2.0 equiv) in anhyd Et$_2$O (50 mL). This soln was then added to the flask dropwise over 15 min.

The soln became a thick, white slurry. After stirring for 2 h at rt, the reaction mixture was cooled

to 0 °C in an ice-water bath, and the septum was removed from the addition funnel. To the

addition funnel was added a degassed 1 M solution of HCl in Et$_2$O (150 mL, 151.5 mmol, 5

equiv), and this was added to the chilled flask, dropwise, over 20 min. The reaction mixture was

allowed to warm to rt overnight. The reaction mixture was concentrated *in vacuo via* rotary

evaporation to yield a crude, white solid. The solid was taken up in boiling toluene and filtered through a coarse fritted glass funnel to remove the diethylammonium chloride by-product. This was repeated two times. The filtrate was concentrated *via* rotary evaporation, and the crude solid was washed with cold MeCN (2 × 20 mL) to afford a fluffy white solid (5.1 g, 71%). All data matched that reported in the literature.[51]

3.6.4. Preparation of organotrifluoroborates

Conversion of carboxylic acids to NHPI esters
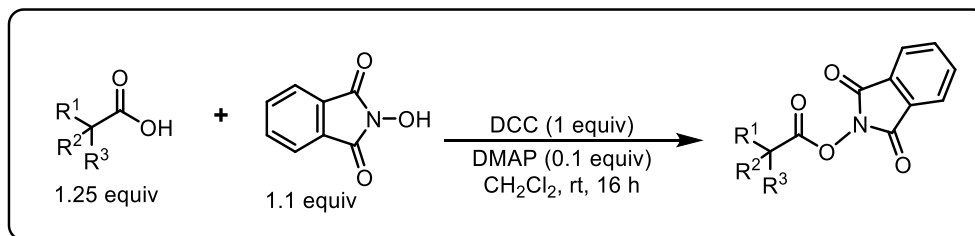
General Procedure A1: To an appropriately-sized round bottom flask equipped with a stirrer bar was added *N*-hydroxyphthalimide (1.1 equiv), DMAP (0.1 equiv), and the requisite carboxylic acid (1.25 equiv). The flask was sealed with a rubber septum and placed under an Ar atmosphere *via* an inlet needle. The flask was charged with CH_2Cl_2 (0.3 M), and the flask was cooled to 0 °C via an ice water bath. After 5 min, a soln of DCC (1 equiv) in CH_2Cl_2 (2 M) was added to the flask over 2 min. After complete addition, the ice-bath was removed, and the mixture was stirred overnight at rt. A voluminous precipitate was observed. After this time, the reaction mixture was filtered through a medium porosity fritted funnel (to remove the urea by-product). The filtrate was transferred to a separatory funnel and washed with satd aq Na_2CO_3, and the aq layer was extracted twice with CH_2Cl_2. The organic layer was washed with deionized H_2O, brine, and dried (Na_2SO_4). The solvent was removed *in vacuo* by rotary evaporation. Further purification was

131

accomplished by passing the crude material over a pad of silica, eluting with a proper ratio of hexane/EtOAc.
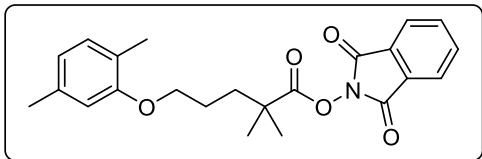
1,3-Dioxoisoindolin-2-yl 5-(2,5-Dimethylphenoxy)-2,2-dimethylpentanoate, 3.80 (2.168 g, 47%) was prepared from 5-(2,5-dimethylphenoxy)-2,2-dimethyl pentanoic acid (3.476 g, 13.89 mmol) according to **General Procedure A1.** The desired compound was obtained as a powdery white solid (mp = 74-75 °C). **^{1}H NMR** (CDCl$_3$, 500 MHz) δ ppm 7.89 (dd, J = 5.4, 3.1 Hz, 2H), 7.79 (dd, J = 5.5, 3.2 Hz, 2H), 7.00 (d, J = 7.3 Hz, 1H), 6.69 - 6.63 (m, 2H), 4.01 (t, J = 4.7 Hz, 2H), 2.33 - 2.29 (m, 3H), 2.21 - 2.17 (m, 3H), 1.98 - 1.92 (m, 4H), 1.45 (s, 6H). **^{13}C NMR** (CDCl$_3$, 125 MHz) δ ppm 157.3, 136.5, 130.4, 123.8, 120.6, 112.2, 83.1, 68.8, 37.4, 26.6, 25.0, 24.8, 21.5, 15.9. **FT-IR** (cm^{-1}, neat, ATR) 3001 (vw), 2950 (w), 1742 (vs), 1146 (s), 696 (m). **HRMS** (ESI) calcd for C$_{23}$H$_{25}$NO$_5$ [M]$^+$: 395.1733, found: 395.1740.
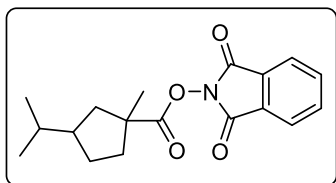
1,3-Dioxoisoindolin-2-yl 3-Isopropyl-1-methylcyclopentane Carboxylate, 3.81 (3.004 g, 97%) was prepared from 3-isopropyl-1-methylcyclopentane-1-carboxylic acid (2.063 g, 10.00 mmol) according to **General Procedure A1.** The desired compound was obtained as a powdery white solid (mp = 74-75 °C). **^{1}H NMR** (CDCl$_3$, 500 MHz) δ ppm 7.88 (dd, J = 5.5, 3.1 Hz, 2 H), 7.78 (dd, J = 5.3, 3.2 Hz, 2 H), 2.45 (ddd, J = 13.0, 9.1, 3.5 Hz, 1 H), 2.05 - 1.96 (m, 1 H), 1.96 - 1.85 (m, 2 H), 1.81 - 1.70 (m, 1 H), 1.69 - 1.60 (m, 1 H), 1.51 - 1.41 (m, 5 H), 0.94 - 0.86 (m, 6 H). **^{13}C NMR** (CDCl$_3$, 125 MHz) δ 174.8, 162.3, 134.8, 129.2, 124.0, 48.0, 47.1, 42.8, 38.1, 33.4, 30.7, 25.5, 21.7, 21.6 ppm. **FT-IR** (cm^{-1}, neat, ATR) 2958 (w), 1741 (vs), 696 (m). **HRMS** (EI) calcd for C$_9$H$_{17}$ [M – CO$_2$phthalimide]: 125.1325, found: 125.1243 and C$_8$H$_5$NO$_2$ [phthalimide]: 147.0320, found: 147.0320.

Synthesis of 3º Bpins via Decarboxylative Borylation of NHPI Esters
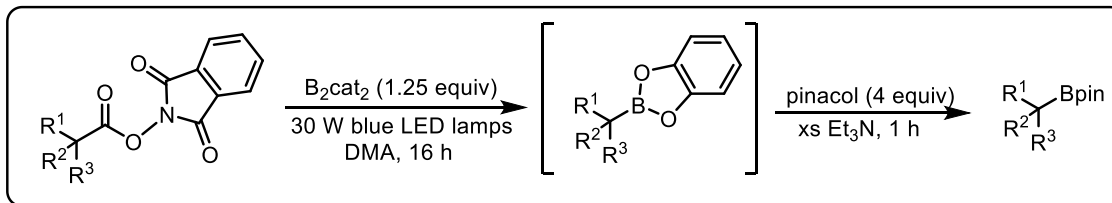
General Procedure A2: Pinacolboronate esters were prepared from NHPI redox-active esters *via* a modified literature procedure.[52] To an appropriately sized reaction vial equipped with a stirrer bar was added the NHPI ester (1 equiv) and B_2cat_2 (1.25 equiv). The reaction vessel was sealed with a cap containing a TFE-lined silicone septum and placed under an inert atmosphere of argon. Thoroughly degassed DMA (0.1 M) was added, and the headspace of the vial was purged with Ar for 30 sec. The vial was sealed with Parafilm® and irradiated overnight with Kessil H150-Blue lamps using a previously described photoreactor.[52] After this time, the vial was removed from the reactor and was charged with a soln of pinacol (4 equiv) in Et_3N (25 equiv) and then stirred for 1 h. The contents of the vial were transferred to a separatory funnel and diluted with EtOAc and a 1:1 H_2O/satd NH_4Cl soln. The layers were separated, and the aq layer was extracted twice with EtOAc. The organic layer was washed with H_2O, brine, and dried (Na_2SO_4). The solvent was removed *in vacuo* by rotary evaporation to give the crude ester. Further purification was accomplished by rapid silica gel column chromatography to yield the desired boronic ester.
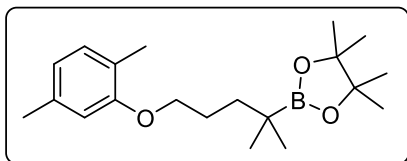
2-(5-(2,5-Dimethylphenoxy)-2-methylpentan-2-yl)-4,4,5,5-tetramethyl-1,3,2-dioxaborolane, 3.82 (combined yield: 0.822 g, 50%) was prepared from **3.80** (0.198 g, 0.500

133

mmol) according to **General Procedure A2**. The reaction was carried out 10 times in parallel (5.00 mmol total). After 24 h of irradiation, the reactions were combined and converted into the corresponding pinacol boronate ester and purified together. The desired compound was obtained as a light, salmon-colored solid (mp = 57-59 °C). **^{1}H NMR** (CDCl$_3$, 500 MHz) δ ppm 6.99 (d, J = 7.3 Hz, 1H), 6.64 (d, J = 7.5 Hz, 1H), 6.62 (s, 1H), 3.91 (t, J = 6.6 Hz, 2H), 2.30 (s, 3H), 2.18 (s, 3H), 1.74 (br s, 2H), 1.46 - 1.40 (m, 2H), 1.23 (s, 12H), 0.96 (s, 6H). **^{13}C NMR** (CDCl$_3$, 125 MHz) δ ppm 157.3, 136.5, 130.4, 123.8, 120.6, 112.2, 83.1, 68.8, 37.4, 26.6, 25.0, 24.8, 21.5, 15.9. **^{11}B NMR** (CDCl$_3$, 128.4 MHz) δ 34.3. **FT-IR** (cm^{-1}, neat, ATR) 2937 (w), 2863 (w), 1308 (m), 1265 (m), 1140 (s). **HRMS** (EI) calcd for C$_{20}$H$_{33}$BO$_3$ [M]$^+$: 332.2523, found: 332.2535.

2-(-3-Isopropyl-1-methylcyclopentyl)-4,4,5,5-tetramethyl-1,3,2-
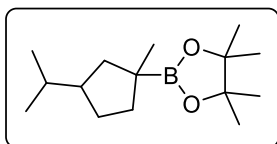
dioxaborolane, 3.83 (0.290 g, 23%) was prepared from **3.81** (1.577 g, 5.00 mmol) according to **General Procedure A2**. The desired compound was obtained as a pink-tinted oil. **^{1}H NMR** (CDCl$_3$, 500 MHz) δ ppm 2.05 - 1.75 (m, 2H), 1.75 - 1.60 (m, 1H), 1.58 - 1.29 (m, 3H), 1.28 - 1.13 (m, 14H), 0.99 (d, J = 14.0 Hz, 3H), 0.87 (dd, J = 6.0, 4.6 Hz, 6H). **^{13}C NMR** (CDCl$_3$, 125 MHz) δ ppm 83.0, 82.9, 48.7, 46.9, 43.0, 41.6, 36.9, 36.8, 34.3, 33.9, 31.3, 30.2, 24.8, 24.8, 24.3, 22.0, 21.9, 21.8, 21.7. **^{11}B NMR** (CDCl$_3$, 128.4 MHz) δ 34.7. **FT-IR** (cm^{-1}, neat, ATR) 2973 (m), 2945 (m), 1433 (w), 1364 (m), 1318 (m), 1204 (m). **HRMS** (EI) calcd for C$_9$H$_{17}$ [M – Bpin; C$_9$H$_{17}$]: 125.1325, found: 125.1337.

Conversion of Pinacolboronate Esters to Organotrifluoroborates
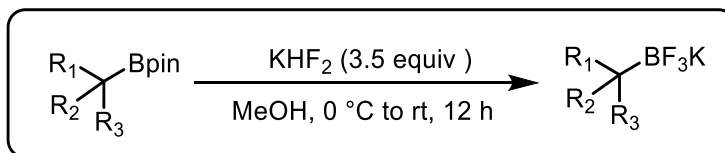
General Procedure A3: To an appropriately sized round bottom flask equipped with a stirrer bar was added the pinacolboronate ester (1 equiv). MeOH was added to the flask, and the soln was cooled to 0 °C in an ice-water bath. After cooling for 5 min, aq KHF$_2$ (3.5 equiv, 4.5 M) was added dropwise *via* an addition funnel. After complete addition, the ice-water bath was removed, and the reaction was allowed to stir at rt overnight. After this time, the solvent was removed *in vacuo via* rotary evaporation. The resulting crude solid was taken up in boiling acetone (three to five portions) and filtered through a fritted glass funnel to remove inorganic salts. The filtrate was concentrated *via* rotary evaporation, and the crude solid was washed with a 1:1 mixture of pentane/CH$_2$Cl$_2$ then CH$_2$Cl$_2$ to afford the pure organotrifluoroborate.

Potassium   (5-(2,5-Dimethylphenoxy)-2-methylpentan-2-yl)trifluoroborate, 3.84 (0.951 g, 93%) was prepared from **3.82** according to **General Procedure A3**. The desired compound was obtained as a crystalline, white solid (mp = 82-83 °C). **¹H NMR** (CDCl$_3$, 500 MHz) δ ppm 6.94 (d, *J* = 7.5 Hz, 1H), 6.70 (s, 1H), 6.58 (d, *J* = 7.5 Hz, 1H), 3.86 (t, *J* = 7.1 Hz, 2H), 2.26 (s, 3H), 2.12 (s, 3H), 1.88 - 1.78 (m, 2H), 1.30 - 1.23 (m, 2H), 0.73 (s, 6H). **¹³C NMR** (CDCl$_3$, 125 MHz) δ ppm 157.3, 136.5, 130.4, 123.8, 120.6, 112.2, 83.1, 68.8, 37.4, 26.6, 25.0, 24.8, 21.5, 15.9. **¹⁹F NMR** (CDCl$_3$, 471 MHz) δ - 151.00 (s, 3F).**¹¹B NMR** (CDCl$_3$, 128.4 MHz) δ 6.9. **FT-IR** (cm^{-1}, neat, ATR) 2948 (w), 2861 (vw), 1509 (m), 1263 (m), 1025 (s), 948 (m). **HRMS** (ESI) calcd for C$_{14}$H$_{21}$BF$_3$O [M-K$^+$]$^+$: 277.1630, found: 273.1657.

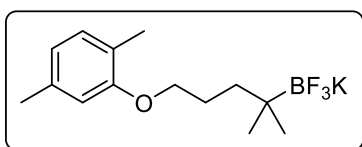**Potassium (3-Isopropyl-1-methylcyclopentyl)trifluoroborate, 3.85** (0.290 g, 66%) was prepared from **3.83** (0.480 g, 1.90 mmol) according to **General Procedure A3**. The desired compound was obtained as a powdery white solid (mp = 234-235 ℃). **^{1}H NMR** (CDCl$_3$, 500 MHz) δ) δ ppm 1.94 (dd, J = 11.9, 7.9 Hz) and 0.54 (t, J = 10.8 Hz, 1H total), 1.69 (m, 2H), 1.53 (dt, J = 17.0, 8.2 Hz, 1H), 1.24 (m, 2H), 1.12 (m, 1H), 0.97 (m, 1H), 0.85 (m, 6H), 0.78 (d, J = 7.6 Hz, 3H) ppm. **^{13}C NMR** (CDCl$_3$, 125 MHz) δ ppm 50.3, 48.2, 43.9, 42.6, 37.4, 37.2, 35.7, 35.0, 32.4, 31.9, 27.4, 26.0, 22.5, 22.4. **^{19}F NMR** (CDCl$_3$, 471 MHz) δ - 151.93 (s, 3F). **^{11}B NMR** (CDCl$_3$, 128.4 MHz) δ 5.6. **FT-IR** (cm^{-1}, neat, ATR) 2951 (m), 1465 (w), 1049 (w), 938 (s). **HRMS** (ESI) calcd for C$_9$H$_{17}$BF$_3$ [M-K$^+$]$^-$: 193.1375, found: 193.1369.
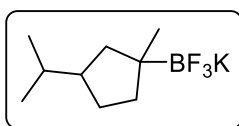
Potassium (4-Pentylbicyclo[2.2.2]octan-1-yl)trifluoroborate, 3.86 (0.730 g, 88%) was prepared from the corresponding NHPI ester (0.890 g, 2.91 mmol) according to **General Procedure A3**. The desired compound was obtained as a powdery white solid (mp = 255-257 ℃). **^{1}H NMR** (acetone-d$_6$, 500 MHz) δ ppm 1.48 - 1.40 (m, 6H), 1.28 - 1.37 (m, 2H), 1.26 - 1.15 (m, 10H), 1.03 - 0.96 (m, 2H), 0.90 (t, J = 7.2 Hz, 3H). **^{13}C NMR** (acetone-d$_6$, 125 MHz) δ ppm 43.9, 33.9, 32.9, 31.2, 28.4, 24.0, 23.4, 14.4, 0.5. **^{19}F NMR** (CDCl$_3$, 471 MHz) δ - 152.67 (s, 3F). **^{11}B NMR** (CDCl$_3$, 128.4 MHz) δ 4.6. **FT-IR** (cm^{-1}, neat, ATR) 2923 (m), 2854 (m), 1202 (m), 908 (s). **HRMS** (ESI) calcd for C$_{13}$H$_{23}$BF$_3$ [M-K$^+$]$^-$: 247.1845, found: 247.1866.
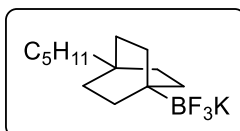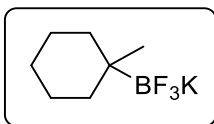
Potassium (1-Methylcyclohexyl)trifluoroborate, 3.87 (0.330 g, 39%) was prepared from the corresponding NHPI ester (0.935 g, 4.17 mmol) according to **General Procedure A2**. The desired compound was obtained as a powdery white solid (mp = 195-197 °C). **^{1}H NMR** (acetone-d_6, 500 MHz) δ ppm 1.58 - 1.50 (m, 2H), 1.49 - 1.37 (m, 5H), 1.32 - 1.23 (m, 1H), 1.09 – 1.02 (m, 2H), 0.76 (s, 3H). **^{13}C NMR** (acetone-d_6, 125 MHz) δ ppm 35.6, 28.6, 23.3, 22.9, 22.8, 22.7. **^{19}F NMR** (CDCl$_3$, 471 MHz) δ -151.80 (s, 3F). **^{11}B NMR** (CDCl$_3$, 128.4 MHz) δ 6.4. **FT-IR** (cm^{-1}, neat, ATR) 3657 (m), 3541 (w), 2919 (m), 949 (s), 921 (s), 871 (m). **HRMS** (ESI) calcd for C$_7$H$_{13}$BF$_3$ [M-K$^+$]$^+$: 165.1062, found: 165.1078.

Synthesis of Pinacolboronate Esters from α,β-Unsaturated Carbonyl Compounds
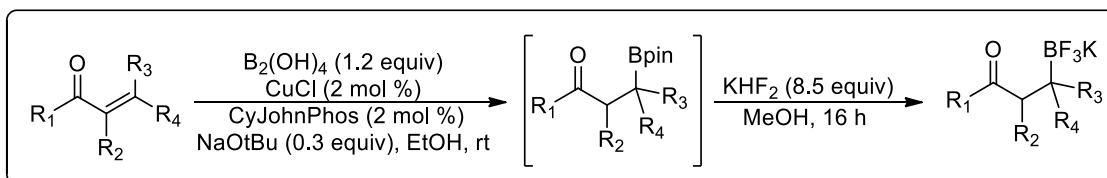
General Procedure B: The following protocol is a modified literature procedure.[53] In an argon filled glovebox, CuCl (2 mol %), NaOt-Bu (30 mol %), CyJohnPhos (2 mol %), and B$_2$(OH)$_4$ (1.2 equiv) were added to the flask. The flask was sealed with a rubber septum and removed from the glovebox. Absolute EtOH (0.1 M) and the enone (1 equiv) were then added via a syringe. The reaction was allowed to stir at rt under Ar until the solution turned colorless (1–24 h), at which point the borylation was judged to be complete. The reaction mixture was filtered through a pad of Celite, and the pad was washed with EtOAc. The filtrate was concentrated *via* rotary evaporation, and the resultant crude Bpin was taken up in MeOH (0.1 M) and cooled to 0 °C in an ice-water bath. After 5 min, aqueous KHF$_2$ (8.5 equiv, 4.5 M) was added dropwise *via* an

addition funnel. After complete addition, the ice bath was removed, and the reaction was allowed to stir overnight. After this time, the crude reaction mixture was concentrated *via* rotary evaporation. The crude solid was taken up in portions of boiling acetone and filtered through a coarse fritted glass funnel to remove inorganic byproducts. The filtrate was concentrated via rotary evaporation, and the crude solid was washed with a 1:1 mixture of pentane/CH_2Cl_2 then CH_2Cl_2 to afford pure organotrifluoroborate.

Potassium (1-methyl-3-oxocyclopentyl)trifluoroborate,[54] **3.88** (0.717 g, 70%) was prepared according to **General Procedure B**. All data matched that recorded in the literature.

Potassium (2-methyl-4-oxopentan-2-yl) trifluoroborate,[53] **3.89** (5.99 g, 83%) was prepared according to **General Procedure B**. All data matched that recorded in the literature.
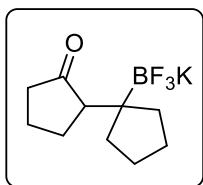
Potassium (2'-Oxo-[1,1'-bi(cyclopentan)]-1-yl)trifluoroborate, **3.90** (0.690 g, 54%) was prepared according to **General Procedure B**. The desired compound was obtained as a crystalline, white solid (mp = 170-171 ºC). **^{1}H NMR** (acetone-d_6, 500 MHz) δ ppm 2.18 - 2.07 (m, 2H), 2.01 - 1.91 (m, 2H), 1.91 - 1.83 (m, 1H), 1.80 - 1.65 (m, 3H), 1.59 - 1.39 (m, 6H), 1.35 (dd, *J* = 11.5, 6.8 Hz, 1H). **^{13}C NMR** (CDCl$_3$, 125 MHz) δ 223.8, 56.8, 40.7, 35.9, 34.3, 29.3, 26.8, 26.1, 21.6 ppm. **^{19}F NMR** (CDCl$_3$, 471 MHz) δ - 143.10 (s, 3F). **^{11}B NMR** (CDCl$_3$, 128.4 MHz) δ 4.9, 4.4. **FT-IR** (cm^{-1}, neat, ATR) 2951 (w), 1593 (m), 1364 (m), 1318 (m), 1204 (m), 1140 (vs) **HRMS** (ESI) calcd for C$_{10}$H$_{15}$BF$_3$O [M-K$^+$]$^-$: 21s9.1168, found: 219.1169.
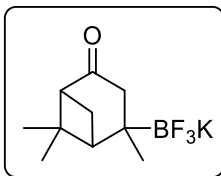
Potassium (2,6,6-Trimethyl-4-oxobicyclo[3.1.1]heptan-2-yl)trifluoroborate, 3.75 (1.340 g, 80%) was prepared according to **General Procedure B**. The desired compound was obtained as a crystalline, white

solid (mp = 115-117 °C). **^{1}H NMR** (acetone-d6, 500 MHz) δ ppm 2.75 and 2.71 (s, total 1H),

2.24 - 2.17 (m, 2H), 2.13 (d, J = 8.8 Hz, 1H), 2.09 – 2.05 (m, 1H), 1.81 and 1.77 (s, total 1H),

1.26 (s, 3H), 0.99 (s, 3H), 0.95 (s, 3H). **^{13}C NMR** (CDCl$_3$, 125 MHz) δ 216.9, 58.9, 51.0, 45.0,

42.4, 27.6, 26.3, 25.6, 23.5 ppm **^{19}F NMR** (CDCl$_3$, 471 MHz) δ - 150.75 (s, 3F). **^{11}B NMR**

(CDCl$_3$, 128.4 MHz) δ 4.8. **FT-IR** (cm^{-1}, neat, ATR) 2937 (w), 1690 (m), 1025 (m), 982 (s), 950

(m). **HRMS** (ESI) calcd for C$_{10}$H$_{15}$BF$_3$O [M-K$^+$]$^+$: 219.1168, found: 219.1178.

Alternative Procedure for Borylation of Enones

Potassium (1,3-Dimethyl-5-oxocyclohexyl)trifluoroborate, 3.91
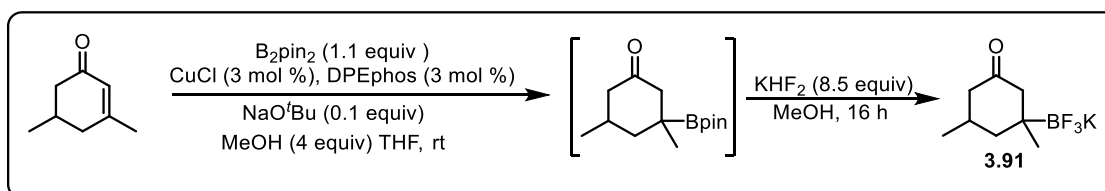
The following protocol is modified from a literature procedure.[55] To a 100 mL round bottom flask

was added the enone (*if solid*) (1 equiv). The flask was carefully brought into the glovebox. CuCl

(0.018 g, 0.18 mmol 0.03 equiv), DPEphos (0.097 g, 0.18 mmol, 0.03 equiv), and NaO*t*-Bu

(0.058 g, 0.60 mmol, 0.01 equiv) were added to the flask. The flask was sealed with a rubber

septum and removed from the glovebox. Anhyd THF (12 mL) was added to the flask, and the

contents of the flask were stirred for ~30 min. After this time, the flask was charged with a soln

of B$_2$pin$_2$ in THF (4 mL). After 10 min, the flask was charged with the enone (0.745 g, 6.00

mmol, 1 equiv) followed by MeOH (0.769 g, 0.97 mL, 24.0 mmol, 4 equiv) added via syringe.

The reaction was allowed to stir at rt under Ar until TLC analysis confirmed reaction completion.

The reaction mixture was filtered through a pad of Celite, and the pad was washed Et$_2$O (2 x 15

mL). The filtrate was concentrated via rotary evaporation, and the resultant crude Bpin was taken

up in MeOH (0.1 M) and cooled to 0 ºC in an ice-water bath. After 5 min, 4.5 M aq KHF$_2$ (11.3 mL, 0.051 mmol, 8.5 equiv) was added dropwise via an addition funnel. After complete addition, the ice bath was removed, and the reaction was allowed to stir overnight. After this time, the crude reaction mixture was concentrated via rotary evaporation. The crude solid was taken up in portions of boiling acetone (5 x 15 mL), and filtered through a coarse fritted glass funnel to remove inorganic byproducts. The filtrate was concentrated via rotary evaporation, and the crude solid was washed with a 1:1 mixture of pentane/CH$_2$Cl$_2$ (50 mL) then CH$_2$Cl$_2$ (20 mL) to afford pure organotrifluoroborate **3.92** (0.141 g, 10% over two steps) as a crystalline, white solid (mp = 180-181 ºC).

¹H NMR (acetone-d_6, 500 MHz) δ ppm 2.36 - 2.23 (m, 1H), 2.18 (d, J = 13.0 Hz, 1H), 1.86 (d, J = 12.2 Hz, 1H), 1.72 (t, J = 12.9 Hz, 1H), 1.56 (d, J = 13.0 Hz, 1H), 1.17 (s, 2H), 0.88 (d, J = 6.4 Hz, 3H), 0.78 (s, 3H). **¹³C NMR** (acetone-d_6, 125 MHz) δ ppm 52.8, 50.2, 46.9, 31.4, 28.1, 25.3, 25.2, 23.7. **¹⁹F NMR** (acetone-d_6, 471 MHz) δ -147.46 (s, 3F). **¹¹B NMR** (acetone-d_6, 128.4 MHz) δ 9.8, 9.4. **FT-IR** (cm⁻¹, neat, ATR) 2954 (w), 2922 (vw), 2866 (vw), 2820 (vw), 1701 9s), 1016 (s), 958 (s). **HRMS** (ESI) calcd for C$_8$H$_{13}$BF$_3$O [M-K⁺]⁺: 193.1012, found: 193.0993.

Preparation of Alkene-containing Organotrifluoroborate, 3.73
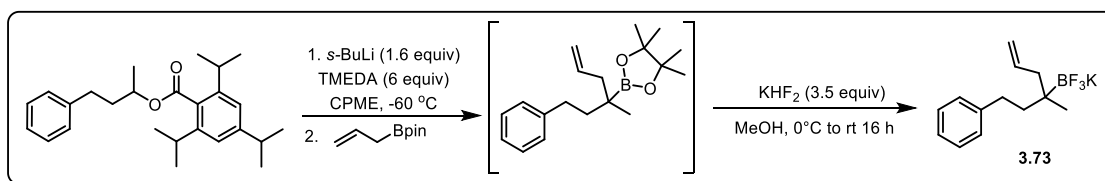
4,4,5,5-Tetramethyl-2-(3-methyl-1-phenylhex-5-en-3-yl)-1,3,2-dioxaborolane (**3.73**) was prepared via known literature procedure.[56] After the lithiation/borylation reaction, the product was passed through a silica plug, eluting with Et$_2$O. After removal of the solvent, the crude

product was converted to the corresponding organotrifluoroborate using **General Procedure A3**. The desired compound was obtained as a white crystalline solid (mp = 156-158 °C) (0.401 g, 36% yield).

¹H NMR (acetone-d_6, 500 MHz) δ ppm 7.21 - 7.16 (m, 2H), 7.16 - 7.11 (m, 2H), 7.08 - 7.03 (m, 1H), 6.14 - 6.03 (m, 1H), 4.85 (dt, *J* = 17.1, 1.4 Hz, 1H), 4.79 (dd, *J* = 10.1, 2.9 Hz, 1H), 2.68 - 2.56 (m, 2H), 2.14 - 2.07 (m, 1H), 1.99 (dd, *J* = 13.4, 7.7 Hz, 1H), 1.42 (t, *J* = 8.7 Hz, 2H), 0.79 - 0.72 (m, 3H). **¹³C NMR** (acetone-d_6, 125 MHz) δ ppm 147.2, 141.6, 129.2, 128.7, 125.4, 113.1, 43.8, 42.3, 32.6, 23.3. **¹⁹F NMR** (acetone-d_6, 471 MHz) δ -148.42 (s, 3F).**¹¹B NMR** (acetone-d_6, 128.4 MHz) δ 9.8. **FT-IR** 3063 (w), 2944 (m), 1495 (w), 937 (vs) (cm⁻¹, neat, ATR). **HRMS** (ESI) calcd for $C_{13}H_{17}BF_3$ [M-K⁺]⁺: 241.1375, found: 241.1377.

3.6.5. Preparation of Non-commerical Alkenes
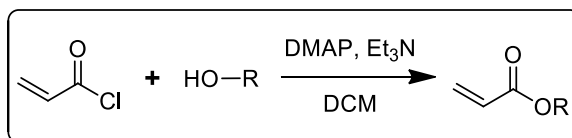
General Procedure C: An appropriately sized flask equipped with a stir bar was charged with the desired alcohol (1 equiv), sealed with a rubber septum with inlet needle, and purged with Ar. The flask was then charged with anhydrous dichloromethane (0.3 M) and the flask was placed in an ice/water bath and allowed to cool to 0 °C. Acryloyl chloride (1.5 equiv) was added followed by DMAP (0.1 equiv). Triethylamine (2.5 equiv) was added dropwise and the solution darkened. The flask was stirred at 0 °C for five minutes after this addition and then the ice bath was removed. The contents of the flask were stirred at rt for two h. The reaction was then quenched with saturated aqueous NH₄Cl and the layers were separated. The aqueous layer was extracted with dichloromethane and the combined organic layers were washed with brine, dried (Na₂SO₄),

and concentrated *via* rotary evaporation. The resulting crude acylated product was purified via passage of the crude material over a pad of silica and/or vacuum distillation.
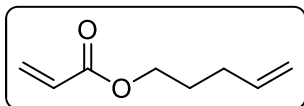
Pent-4-en-1-yl acrylate, 3.92 (1.12 g, 81%) was prepared from 4-penten-1-ol (850 mg, 9.87 mmol) using **General Procedure C**. The desired compound was isolated as colorless liquid. [1]**H NMR** (CDCl$_3$, 500 MHz) δ ppm 6.40 (dd, *J*=17.4, 1.4 Hz, 1 H), 6.12 (dd, *J* = 17.3, 10.5 Hz, 1H), 5.75 - 5.89 (m, 2H), 5.04 (dq, *J* = 17.2, 1.6 Hz, 1H), 4.99 (dq, *J* = 10.1, 1.1 Hz, 1H), 4.17 (t, *J* = 6.6 Hz, 2H), 2.15 (q, *J* = 7.3 Hz, 2H), 1.78 (dt, *J* = 13.6, 6.9 Hz, 2H). [13]**C NMR** (CDCl$_3$, 125 MHz) δ ppm 166.5, 137.7, 130.8, 128.9, 115.6, 64.2, 30.3, 28.1. **FT-IR** (cm^{-1}, neat, ATR) 2956 (w), 1723 (vs), 1407 (m), 1270 (s), 1184 (vs), 809 (s). **HRMS** (ESI) calcd for C$_8$H$_{12}$O$_2$ [M]$^+$: 140.0837, found: 140.0835.
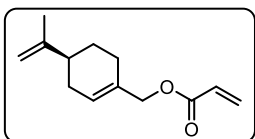
(*S*)-(4-(Prop-1-en-2-yl)cyclohex-1-en-1-yl)methyl acrylate, 3.93 (1.54 g, 75%) was prepared from (*S*)-perillyl alcohol (1.52 g, 10.0 mmol) using **General Procedure C**. The desired compound was isolated as a colorless liquid. [1]**H NMR** (CDCl$_3$, 500 MHz) δ ppm 6.42 (d, *J* = 17.2 Hz, 1H), 6.14 (dd, *J* = 17.3, 10.5 Hz, 1H), 5.83 (d, *J* = 10.5 Hz, 1H), 5.78 (br. s, 1H), 4.72 (d, *J* = 8.4 Hz, 2H), 4.55 (s, 2H), 2.22 - 2.05 (m, 4H), 2.03 - 1.92 (m, 1H), 1.91 - 1.81 (m, 1H), 1.74 (s, 3H), 1.50 (tt, *J* = 12.0, 8.5 Hz, 1H). [13]**C NMR** (CDCl$_3$, 125 MHz) δ ppm 166.4 (s), 149.9 (s), 132.8 (s), 131.0 (s), 128.8 (s), 126.1 (s), 109.1 (s), 68.8 (s), 41.1 (s), 30.7 (s), 27.6 (s), 26.7 (s), 21.0 (s). **FT-IR** (cm^{-1}, neat, ATR) 2920 (w), 1724 (vs), 1405 (m), 1180 (vs), 808 (m). **HRMS** (ESI) calcd for C$_{13}$H$_{18}$O$_2$ [M]$^+$: 206.1307, found: 206.1321.
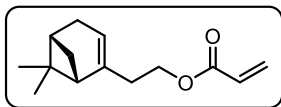
2-((1*S*,5*R*)-6,6-dimethylbicyclo[3.1.1]hept-2-en-2-yl)ethyl acrylate, 3.94 (1.15 g, 87%) was prepared from 1-(S)-nopol (998 mg, 6.00

mmol) using **General Procedure C**. The compound was isolated as colorless oil. [1]**H NMR** (CDCl$_3$, 500 MHz) δ ppm 6.38 (d, *J* = 17.2 Hz, 1H), 6.10 (dd, *J* = 17.3, 10.5 Hz, 1H), 5.80 (d, *J* = 10.5 Hz, 1H), 5.31 (s, 1H), 4.10 - 4.24 (m, 2H), 2.30 - 2.41 (m, 3H), 2.22 (q, *J* = 17.2 Hz, 2H), 2.00 - 2.11 (m, 2H), 1.27 (s, 3H), 1.15 (d, *J* = 8.5 Hz, 1H), 0.82 (s, 3H). [13]**C NMR** (CDCl$_3$, 125 MHz) δ ppm 166.5, 144.4, 130.7, 128.9, 119.2, 63.2, 46.0, 41.0, 38.3, 36.2, 31.9, 31.7, 26.6, 21.4. **FT-IR** (cm^{-1}, neat, ATR) 2915 (m), 1725 (vs), 1406 (m), 1183 (vs), 984 (m), 808 (m). **HRMS** (ESI) calcd for C$_{14}$H$_{20}$O$_2$ [M]$^+$: 220.1463 found: 220.1456.

Cholesteryl acrylate, 3.95 (1.83 g, 69%) was prepared from cholesterol (2.32 g, 6.00 mmol)
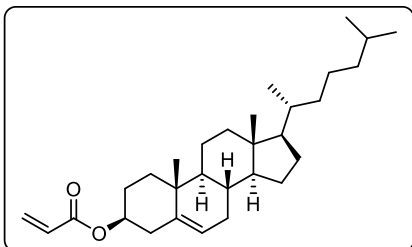
using **General Procedure C**. The desired compound was isolated as white powdery solid (mp = 119-121 ºC). [1]**H NMR** (CDCl$_3$, 500 MHz) δ ppm 6.38 (dd, *J* = 17.4, 1.4 Hz, 1H), 6.10 (dd, *J* = 17.4, 10.4 Hz, 1H), 5.79 (dd, *J* = 10.5, 1.4 Hz, 1H), 5.39 (d, *J* = 4.7 Hz, 1H), 4.62 - 4.75 (m, 1H), 2.36 (d, *J* = 7.5 Hz, 2H), 1.78 - 2.08 (m, 5H), 1.41 - 1.69 (m, 7H), 1.21 - 1.40 (m, 4H), 1.05 - 1.21 (m, 7H), 1.03 (s, 3H), 0.90 - 1.02 (m, 6H), 0.87 (dd, *J* = 6.6, 2.1 Hz, 6H), 0.68 (s, 3H). [13]**C NMR** (CDCl$_3$, 125 MHz) δ ppm 165.9, 139.9, 130.5, 129.4, 123.0, 74.4, 57.0, 56.5, 50.3, 42.6, 40.0, 39.8, 38.4, 37.3, 36.9, 36.5, 36.1, 32.2, 32.2 , 28.5, 28.3, 28.1, 24.6, 24.1, 23.1, 22.9, 21.3, 19.6, 19.0, 12.2. **FT-IR** (cm^{-1}, neat, ATR) 2934 (w), 1719 (s), 1409 (m), 1203 (vs), 984 (m), 804 (m). **HRMS** (ESI) calcd for C$_{30}$H$_{48}$O$_2$ [M]$^+$: 440.3654, found: 440.3650.
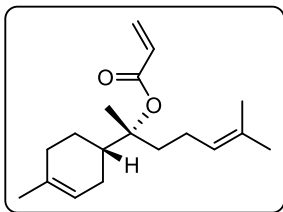
(*R*)-6-Methyl-2-((*S*)-4-methylcyclohex-3-en-1-yl)hept-5-en-2-yl acrylate, 3.96 (890 mg, 32%) was prepared from (-)-α-Bisabolol (2.250 g, 10.12 mmol) using **General Procedure C** with the following

modifications: 1) CHCl$_3$ was used in place of dichloromethane as the solvent; 2) The reaction was heated to 55 °C for 16 hrs. The desired compound was isolated as a yellow-tinted, viscous oil. **¹H NMR** (CDCl$_3$, 500 MHz) δ ppm 6.29 (dd, J = 17.4, 1.5 Hz, 1H), 6.05 (dd, J = 17.3, 10.3 Hz, 1H), 5.73 (dd, J = 10.4, 1.5 Hz, 1H), 5.32 - 5.40 (m, 1H), 5.04 - 5.14 (m, 1H), 2.25 (tdd, J = 11.7, 11.7, 5.0, 2.0 Hz, 1H), 1.76 - 2.10 (m, 9H), 1.66 (s, 3H), 1.64 (s, 3H), 1.58 (s, 3H), 1.44 (s, 3H), 1.34 (qd, J = 11.9, 5.3 Hz, 1H). **¹³C NMR** (CDCl$_3$, 125 MHz) δ ppm 165.6, 134.4, 131.9, 130.6, 129.6, 124.3, 120.5, 87.6, 40.8, 35.8, 31.2, 26.6, 26.0, 23.9, 23.6, 22.3, 20.8, 17.8. **FT-IR** (cm^{-1}, neat, ATR) 2926 (w), 1719 (vs), 1401 (m), 1203 (vs), 1046 (m), 809 (m). **HRMS** (ESI) calcd for C$_{15}$H$_{24}$ [M − CH$_2$=CHCO$_2$H]$^+$: 204.1878, found: 204.1866.

3.6.7. Optimization of Ni/Photoredox DCF reaction

General Optimization Procedure A: To a 4 mL reaction vial equipped with a stirrer bar was added 1-bromo-4-chlorobenzene (19.1 mg, 0.1 mmol, 1 equiv), ^{t}BuBF$_3$K (24.6 mg, 0.15 mmol, 1.5 equiv), the appropriate amount of K$_2$HPO$_4$ (1 or 2 equiv), the appropriate photocatalyst (0.002 mmol, 0.02 equiv for organometallic complexes or 0.005 mmol, 0.05 equiv for organic dyes), and anhyd Ni(bpy)Br$_2$ (0.005 mmol, 0.05 equiv). The vial was sealed with a cap containing a TFE-lined silicone septa and was evacuated and purged with argon three times via an inlet needle. The vial was then charged with the vinyl boronate (20.6 mg, 0.12 mmol, 1.2 equiv) in anhyd, degassed THF (1 mL). After this, the cap was sealed with Parafilm®, and the vial was irradiated with blue LEDs for 16 h (470 nm, ~10 W, at a distance of ~4.5 cm). The temperature of the reaction was maintained at approximately 27 °C via a fan. After 16 h, an aliquot of a solution of 4,4′-di-*tert*-butylbiphenyl in MeCN with a known concentration (20 mol % relative to the aryl halide) was added to each vial. Reaction progress was evaluated by GCMS to determine product-to-internal standard ratio (P/IS). These ratios were determined by comparing the values of the corrected peak areas of the desired product against 4,4′-di-*tert*-butylbiphenyl or 2,6-dimethylnaphthalene.

General Optimization Procedure B: To a 4 mL reaction vial equipped with a stirrer bar was added the appropriate aryl halide (0.1 mmol, 1 equiv), ^{t}BuBF$_3$K (24.6 mg, 0.15 mmol, 1.5 equiv), the appropriate base (0.1 mmol, 1 equiv), the appropriate Ni source (0.005 mmol, 0.05 equiv), and [Ir{dF(CF$_3$)$_2$ppy}$_2$(bpy)]PF$_6$ (2.0 mg, 0.002 mmol, 0.02 equiv). The reaction vessel was sealed with a cap containing a TFE-lined silicone septum, evacuated, and filled with argon three times. The vinyl boronate and aryl bromides (if liquid) were dissolved in degassed THF and added to the reaction mixture. The vial was further sealed with Parafilm® and irradiated with

blue LEDs (470 nm, ~10 W, at a distance of ~4.5 cm) for 16 h. Upon reaction completion, a 250 µL aliquot of the reaction mixture concentrated via rotary evaporation then re-dissolved in 250 µL of CDCl3. The resulting soln was passed through a hydrophobic PTFE 0.2 µm syringe-driven filter unit and dispensed into an NMR tube. To the NMR tube was also added 250 µL of a stock soln of dimethyl fumarate (0.1 M in CDCl3). NMR yields were calculated based on relative integrations of the alkenyl peak of dimethyl fumarate and the benzylic proton in the dicarbofunctionalized products.

Table 3.5: Solvent Screen for Ni/Photoredox Dicarbofunctionalization

solvent	P/IS
NMP	2.04
1,4-dioxane	3.31
THF	4.15
MeCN	0.19
DMA	3.30
DMSO	0.04
acetone	2.16
EtOAc	4.10

a
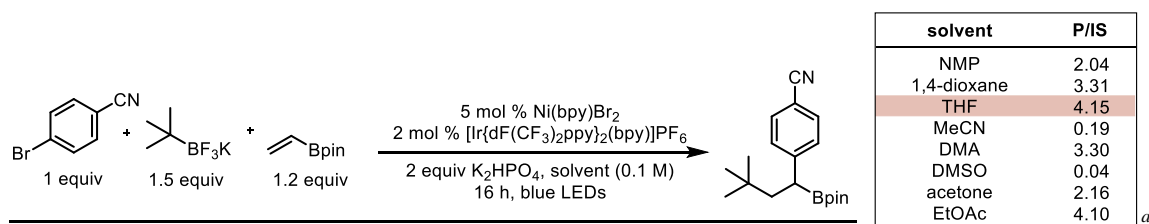
Performed according to **General Optimization Procedure A**

Table 3.6: Photocatalyst Screen for Ni/Photoredox Dicarbofunctionalization

photocatalyst	P/IS
[Ir{dF(CF3)2ppy}2(bpy)]PF6	2.00
[Ir{dF(CF3)2ppy}2(dtbpy)]PF6	1.88
[Ir{ppy}2(dtbpy)]PF6	0.11
[Ru(bpy)3](PF6)2	-
[Ru(bpz)3](PF6)2	-
4-CzIPN	0.24
4-Cl-CzIPN	1.78

Performed according to **General Optimization Procedure A**

146
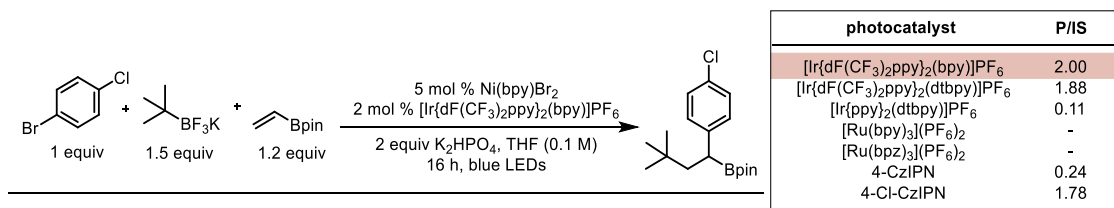
Table 3.7: Nickel/Ligand Screen for Ni/Photoredox Dicarbofunctionalization
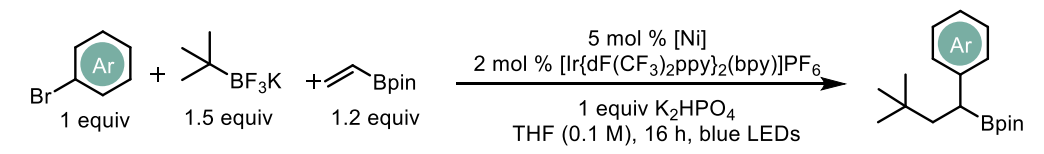
[Ni]	NMR yield (%)	[Ni]	NMR yield (%)	[Ni]	NMR yield (%)
Ni(dme)Br$_2$	15	Ni(dme)Br$_2$	0	Ni(dme)Br$_2$	0
Ni(dtbbpy)Br$_2$	45	Ni(dtbbpy)Br$_2$	34	Ni(dtbbpy)Br$_2$	31
Ni(Me-pyr)Br$_2$	9	Ni(Me-pyr)Br$_2$	4	Ni(Me-pyr)Br$_2$	0
Ni(acac)$_2$	0	Ni(acac)$_2$	0	Ni(acac)$_2$	0
Ni(TMHD)$_2$	0	Ni(TMHD)$_2$	0	Ni(TMHD)$_2$	0
Ni(phthaloCN)	0	Ni(phthaloCN)	0	Ni(phthaloCN)	0
Ni(phen)Br$_2$	31	Ni(phen)Br$_2$	41	Ni(phen)Br$_2$	6
Ni(imine)Br$_2$	0	Ni(imine)Br$_2$	0	Ni(imine)Br$_2$	0
Ni(bpy)Br$_2$	55	Ni(bpy)Br$_2$	29	Ni(bpy)Br$_2$	19

Performed according to **General Optimization Procedure B**

Table 3.8: Base Screen for Ni/Photoredox Dicarbofunctionalization

base	NMR yield (%)
K$_2$HPO$_4$	63
KOAc	0
Cs$_2$CO$_3$	0
K$_3$PO$_4$	7
K$_2$CO$_3$	64[b]
NaHCO$_3$	75[b]
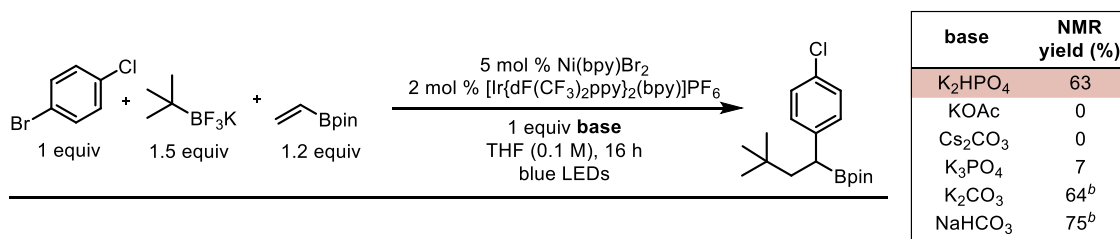
Performed according to **General Optimization Procedure B.** [b]Although slightly higher NMR yields were achieved for these entries, the formation of inseparable, undesired products were observed.

Table 3.9: Stoichiometry Variation for Ni/Photoredox Dicarbofunctionalization

equiv vinyl Bpin	equiv ^{t}BuBF$_3$K	equiv K$_2$HPO$_4$	NMR yield (%)
1.2	1.5	1	63
1.5	1.5	1	58
1.2	2	1	56
1.2	1.5	2	70
1.5	1.1	1	41
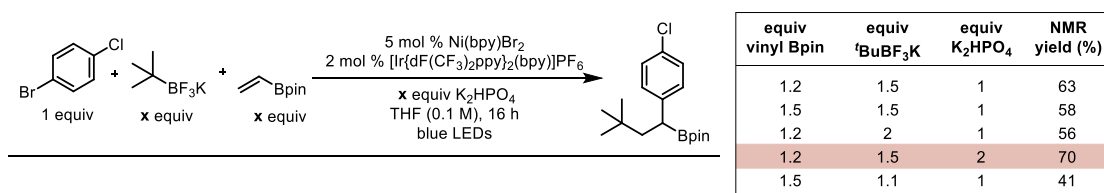
Performed according to **General Optimization Procedure A**

Table 3.10: Catalyst Loading Analysis for Ni/Photoredox Dicarbofunctionalization

mol % Ir	mol % Ni	NMR yield (%)
2	5	63
5	10	66
3	3	58
5	3	59

Performed according to **General Optimization Procedure A**

148

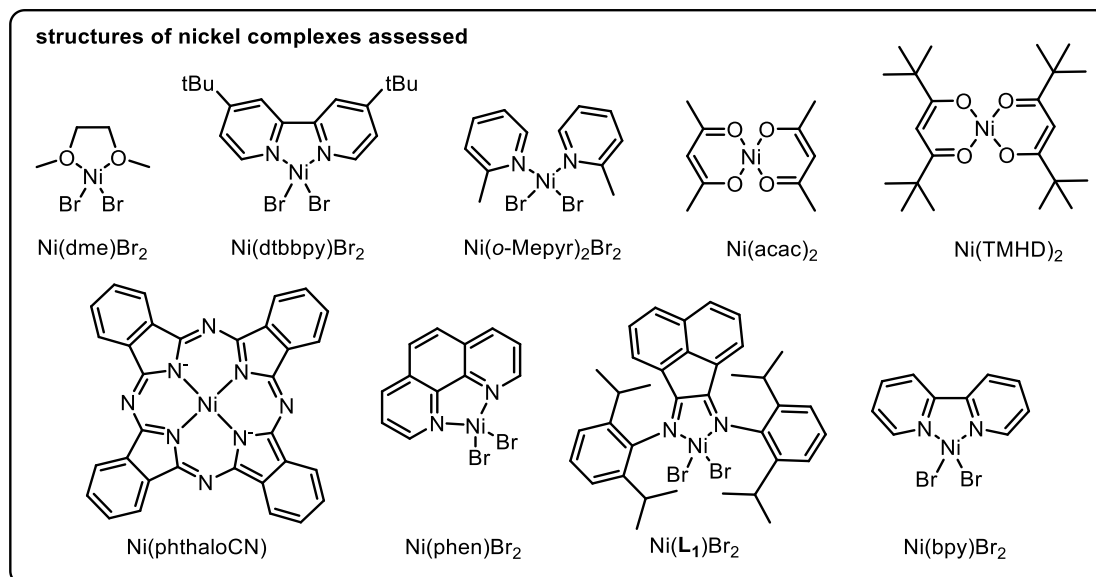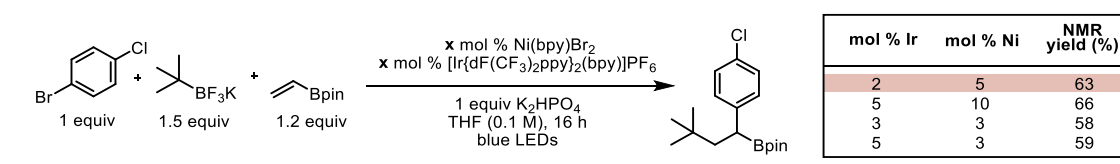**Table 3.11:** Concentration Screen for Ni/Photoredox Dicarbofunctionalization

conc. (M)	NMR yield (%)
0.05	67
0.075	61
0.1	70
0.175	63
0.25	39
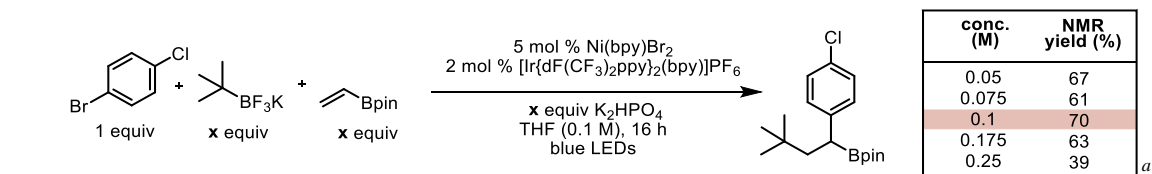
Performed according to **General Optimization Procedure A**

3.6.8. General Procedure and Characterization Data for Ni/Photoredox DCF Reaction
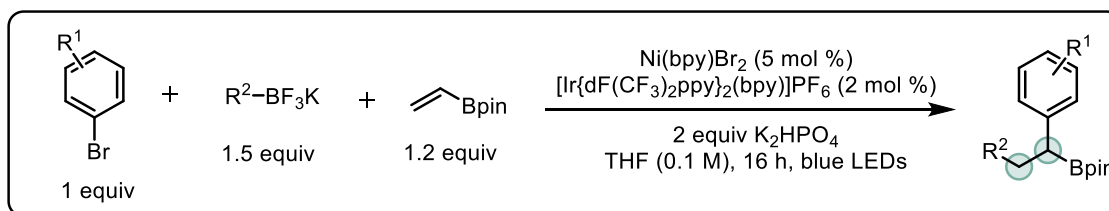
To an 8 mL reaction vial equipped with a stirrer bar was added organotrifluoroborate (0.75 mmol, 1.5 equiv), aryl halide (*if solid*) (0.5 mmol, 1 equiv), K_2HPO_4 (0.173 g, 1.0 mmol, 2 equiv), anhyd $NiBr_2(bpy)$ (9.5 mg, 5 mol %), and $[Ir\{dF(CF_3)_2ppy\}_2(bpy)]PF_6$ (10 mg, 2 mol %). The reaction vessel was sealed with a cap containing a TFE-lined silicone septum, evacuated, and backfilled with argon three times. VinylBpin (0.093 g, 0.6 mmol, 1.2 equiv) and aryl bromides (*if liquid*) were dissolved in degassed THF (5 mL) and added to the reaction mixture. The vial was further sealed with Parafilm® and irradiated with blue LEDs (470 nm, ~10 W, at a distance of ~4.5 cm). The reaction was monitored by TLC. When the reaction was judged complete (typically 16-48 h), the crude reaction mixture was transferred to a round bottom flask and concentrated via rotary evaporation. Further purification was accomplished by passing the crude material through a pad of Celite®, eluting with either CH_2Cl_2 or EtOAc followed by SiO_2 column chromatography (hexanes/EtOAc or hexanes/CH_2Cl_2). In select cases, the crude product was passed through a small pad of SiO_2, eluting with either (hexanes/EtOAc or hexanes/CH_2Cl_2). In event that these methods did not provide the pure DCF prduct, further purification was accomplished by recrystallization from MeOH.
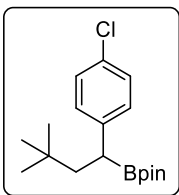
2-(1-(4-Chlorophenyl)-3,3-dimethylbutyl)-4,4,5,5-tetramethyl-1,3,2-dioxaborolane, 3.3 (0.111 g, 69%) was prepared according to the general DCF procedure. The desired compound was obtained as a crystalline, white solid (mp = 97-99 °C). **^{1}H NMR** (CDCl$_3$, 500 MHz) δ 7.20 (d, J = 8.4 Hz, 2H), 7.15 (d, J = 8.4 Hz, 2H), 2.36 (dd, J = 9.7, 3.9 Hz, 1H), 1.98 (dd, J = 13.3, 9.7 Hz, 1H), 1.46 (dd, J = 13.3, 3.9z Hz, 1H), 1.14 (s, 12H), 0.89 (s, 9H) δ ppm. **^{13}C NMR** (CDCl$_3$, 125 MHz) δ 143.7, 130.9, 129.8, 128.6, 83.6, 46.7, 31.7, 29.9, 24.9 (2C), 24.7 (2C) ppm. **^{11}B NMR** (CDCl$_3$, 128.4 MHz) δ 32.7. **FT-IR** (cm^{-1}, neat, ATR) 2953 (w), 1489 (w), 1365 (s), 1327 (s), 1140 (vs), 841 (w) **HRMS** (EI) calcd for C$_{18}$H$_{28}$BClO$_2$ [M]$^+$: 322.1871, found: 322.1862.
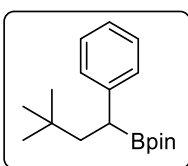
2-(3,3-Dimethyl-1-phenylbutyl)-4,4,5,5-tetramethyl-1,3,2-dioxaborolane, 3.4 (0.090 g, 62%) was prepared according to the general DCF procedure. The desired compound was obtained as a crystalline, white solid (mp = 80-82 °C). **^{1}H NMR** (CDCl$_3$, 500 MHz) δ ppm 7.23 (d, J = 4.1 Hz, 4H), 7.13 - 7.08 (m, 1H), 2.39 (dd, J = 9.9, 3.5 Hz, 3H), 2.02 (dd, J = 13.1, 10.1 Hz, 3H), 1.50 (dd, J = 13.3, 3.5 Hz, 3H), 1.14 (d, J = 2.7 Hz, 12H), 0.90 (s, 9H). **^{13}C NMR** (CDCl$_3$, 125 MHz) δ ppm 1445.1, 128.5, 128.4, 125.2, 83.5, 46.8, 31.6, 29.9, 24.8, 24.7. **^{11}B NMR** (CDCl$_3$, 128.4 MHz) δ 32.8. **FT-IR** (cm^{-1}, neat, ATR) 2954 (w), 1365 (vs), 1349 (s), 1327 (s), 1143 (s), 702 (m). **HRMS** (EI) calcd for C$_{18}$H$_{29}$BO$_2$ [M]$^+$: 288.2261, found: 288.2253.
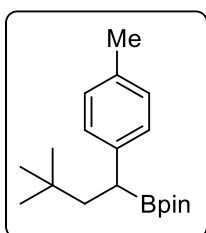
2-(3,3-Dimethyl-1-(*p*-tolyl)butyl)-4,4,5,5-tetramethyl-1,3,2-dioxaborolane, 3.5 (0.099 g, 66%) was prepared according to the general DCF procedure. The desired compound was obtained as a crystalline, white solid (mp = 93-94 °C). **^{1}H NMR** (CDCl$_3$, 500 MHz) δ ppm 7.12 (d, J = 7.8 Hz, 2H), 7.07 - 7.02 (m, 2H), 2.35 (dd, J = 10.1, 3.2 Hz, 1H), 2.29 (s, 3H), 2.01 (dd, J = 13.1, 10.2 Hz, 1H), 1.46 (dd, J = 13.3, 3.4 Hz, 1H), 1.15 (d, J = 3.1 Hz, 12H), 0.90 (s, 9H) . **^{13}C NMR**

(CDCl$_3$, 125 MHz) δ ppm 142.0, 134.6, 129.3, 128.3, 83.4, 47.1, 31.6, 30.0, 24.9, 24.7, 21.3. **[11]B**

NMR (CDCl$_3$, 128.4 MHz) δ 32.8. **FT-IR** (cm^{-1}, neat, ATR) 2951 (w), 1364 (s), 1346 (s), 1323

(s), 1142 (vs). **HRMS** (EI) calcd for C$_{19}$H$_{31}$BO$_2$ [M]$^+$: 302.2417, found: 302.2410.

4-(3,3-Dimethyl-1-(4,4,5,5-tetramethyl-1,3,2-dioxaborolan-2-yl)butyl)benzonitrile, 3.6 (0.134 g, 86%) was prepared according to the general DCF procedure. The desired compound was obtained as a crystalline, white solid (mp = 106-108 ºC).**^{1}H NMR** (CDCl$_3$, 500 MHz) δ

^{1}H NMR (500 MHz, CDCl$_3$) δ 7.52 (d, *J* = 8.2 Hz, 2H), 7.32 (d, *J* = 8.2 Hz, 2H), 2.47 (dd, *J* =

9.3, 4.3 Hz, 1H), 2.01 (dd, *J* = 13.4, 9.3 Hz, 1H), 1.49 (dd, *J* = 13.4, 4.3 Hz, 1H), 1.13 (s, 12H),

0.88 (s, 9H) ppm **^{13}C NMR** (CDCl$_3$, 125 MHz) δ 151.4, 132.3, 129.2, 119.6, 109.0, 83.9 (2C),

46.2, 31.8, 29.9 (3C), 24.8 (2C), 24.7 (2C) ppm.**^{11}B NMR** (CDCl$_3$, 128.4 MHz) δ 32.7. **FT-IR**

(cm^{-1}, neat, ATR) 2957 (w), 2225 (m), 1603 (w), 1365 (s), 1329 (s), 1138 (vs), 840 (m), 559 (w).

HRMS (EI) calcd for C$_{19}$H$_{28}$BNO$_2$ [M]$^+$: 313.2213, found: 313.2225.

Methyl 4-(3,3-Dimethyl-1-(4,4,5,5-tetramethyl-1,3,2-dioxaborolan-2-yl)butyl)benzoate, 3.7 (0.114 g, 66%) was prepared according to the general DCF procedure *with the following modification:* The reaction was run for 48 h. The desired compound was obtained as a crystalline, white

solid (mp = 100-102 ºC). **^{1}H NMR** (CDCl$_3$, 500 MHz) δ 7.91 (d, *J* = 8.1 Hz, 2H), 7.29 (d, *J* = 8.1

Hz, 2H), 3.88 (s, 3H), 2.48 (dd, *J* = 9.4, 4.1 Hz, 1H), 2.03 (dd, *J* = 13.3, 9.4 Hz, 1H), 1.52 (dd, *J* =

13.4, 4.1 Hz, 1H), 1.13 (s, 12H), 0.89 (s, 9H) ppm **^{13}C NMR** (CDCl$_3$, 125 MHz) δ 167.6, 151.1,

129.9 (2C), 128.4 (2C), 127.2, 83.7 (2C), 52.2, 46.3, 31.8, 30.0 (3C), 24.8 (2C), 24.7 (2C)

ppm**^{11}B NMR** (CDCl$_3$, 128.4 MHz) δ 32.5. **FT-IR** (cm

$^{-1}$, neat, ATR) 2952 (w), 1718 (vs), 1365 (m), 1327 (m), 1282 (vs), 1140 (m), 1107 (w). **HRMS**

(EI) calcd for C$_{20}$H$_{31}$BO$_4$ [M]$^+$: 346.2315, found: 346.2319.
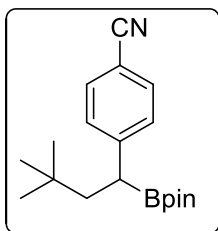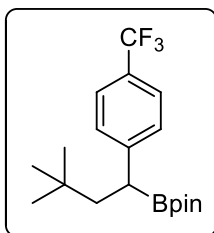
2-(3,3-Dimethyl-1-(4-(trifluoromethyl)phenyl)butyl)-4,4,5,5-tetramethyl-1,3,2-dioxaborolane, 3.8 (0.144 g, 81%) was prepared according to the general DCF procedure. The desired compound was obtained as a crystalline, white solid (mp = 94-96 °C). **^{1}H NMR** (CDCl$_3$, 500 MHz) δ 7.53 – 7.43 (d, *J* = 8.0 Hz, 2H), 7.33 (d, *J* = 8.0 Hz, 2H), 2.47 (dd, *J* = 9.6, 4.0 Hz, 1H), 2.03 (dd, *J* = 13.3, 9.6 Hz, 1H), 1.50 (dd, *J* = 13.3, 4.0 Hz, 1H), 1.14 (s, 12H), 0.90 (s, 9H) ppm **^{13}C NMR** (CDCl$_3$, 125 MHz) δ ppm 149.6, 128.7, 127.4 (q, $_{C-C-F}$ *J* = 31.9 Hz), 125.3 (q, *J*$_{C-C-C-F}$ =3.6 Hz), 124.7 (q, *J* $_{C-F}$ = 272.5 Hz), 83.8, 46.6, 31.8, 29.9, 24.9, 24.7 **^{11}B NMR** (CDCl$_3$, 128.4 MHz) δ 32.6. **^{19}F NMR** (CDCl$_3$, 471 MHz) δ -115.17 (s, 1 F). **FT-IR** (cm^{-1}, neat, ATR) 2958 (vw), 1324 (s), 1123 (m), 906 (s), 729 (vs). **HRMS** (EI) calcd for C$_{19}$H$_{28}$BF$_3$O$_2$ [M]$^+$: 356.2134, found: 356.2143.
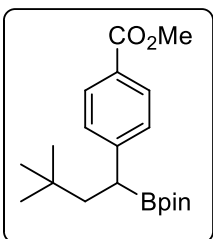
2-(1-(4-Methoxyphenyl)-3,3-dimethylbutyl)-4,4,5,5-tetramethyl-1,3,2-dioxaborolane, 3.9 (0.085 g, 53%) was prepared according to the general DCF procedure *with the following modification:* NiBr$_2$(dtbbpy) was used as the Ni catalyst. The desired compound was obtained as a crystalline, white solid (mp = 106-108 °C). **^{1}H NMR** (CDCl$_3$, 500 MHz) δ 7.14 (d, *J* = 8.2 Hz, 2H), 6.79 (d, *J* = 8.2 Hz, 2H), 3.77 (s, 3H), 2.33 (d, *J* = 9.6 Hz, 1H), 1.98 (t, *J* = 13.1 Hz, 1H), 1.45 (d, *J* = 13.1 Hz, 1H), 1.14 (s, 12H), 0.89 (s, 9H) ppm. **^{13}C NMR** (CDCl$_3$, 125 MHz) δ 157.5, 137.1, 129.3 (2C), 114.0 (2C), 83.4 (2C), 55.5, 47.1, 31.6, 30.0 (3C), 24.9 (2C), 24.7 (2C) ppm **^{11}B NMR** (CDCl$_3$, 128.4 MHz) δ 32.8. **FT-IR** (cm^{-1}, neat, ATR) 2951 (m), 1508 (vs), 1366 (s), 1322 (s), 1246 (s), 1143 (vs). **HRMS** (EI) calcd for C$_{19}$H$_{31}$BO$_3$ [M]$^+$: 318.2366, found: 318.2352.

2-(1-([1,1'-Biphenyl]-4-yl)-3,3-dimethylbutyl)-4,4,5,5-tetramethyl-1,3,2-dioxaborolane, 3.10 (0.165 g, 91%) was prepared according to the general DCF procedure *with the following modification:* NiBr$_2$(phen) used as the Ni catalyst. The desired compound was obtained as a crystalline, white solid (mp = 101-103 ºC). **^{1}H NMR** (CDCl$_3$, 500 MHz) δ ppm 7.57 - 7.61 (m, 2H), 7.49 (d, *J* = 8.1 Hz, 2H), 7.41 (t, *J* = 7.5 Hz, 2H), 7.28 - 7.33 (m, 3H), 2.44 (dd, *J* = 9.9, 3.7 Hz, 1H), 2.06 (dd, *J* = 13.3, 10.1 Hz, 1H), 1.53 (dd, *J* = 13.3, 3.7 Hz, 1H), 1.16 (d, *J* = 2.1 Hz, 12H), 0.92 (s, 9H). **^{13}C NMR** (CDCl$_3$, 125 MHz) δ ppm 144.3, 141.4, 138.0, 128.9, 128.8, 127.2, 127.1(4), 127.1(0), 83.6, 46.9, 31.7, 30.0, 24.9, 24.7. **^{11}B NMR** (CDCl$_3$, 128.4 MHz) δ 33.1. **FT-IR** (cm^{-1}, neat, ATR) 2951 (w), 1365 (s), 1322 (s), 1141 (vs), 697 (m). **HRMS** (EI) calcd for C$_{24}$H$_{33}$BO$_2$ [M]$^+$: 364.2574, found: 364.2598.
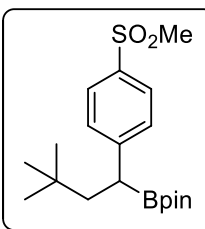
2-(3,3-Dimethyl-1-(4-(methylsulfonyl)phenyl)butyl)-4,4,5,5-tetramethyl-1,3,2-dioxaborolane, 3.11 (0.146 g, 80%) was prepared according to the general DCF procedure. The desired compound was obtained as a crystalline, white solid (mp = 143-145 ºC). **^{1}H NMR** (CDCl$_3$, 500 MHz) δ ppm 7.80 (d, *J* = 7.3 Hz, 2H), 7.42 (d, *J* = 7.6 Hz, 2H), 3.03 (s, 3H), 2.51 (d, *J* = 9.0 Hz, 1H), 2.01 - 2.08 (m, 1H), 1.50 (d, *J* = 13.4 Hz, 1H), 1.14 (s, 12H), 0.90 (s, 9H). **^{13}C NMR** (CDCl$_3$, 125 MHz) δ ppm 152.4, 137.4, 129.3, 127.6, 84.0, 46.5, 44.9, 31.8, 29.9, 24.9, 24.7. **^{11}B NMR** (CDCl$_3$, 128.4 MHz) δ 32.6. **FT-IR** (cm^{-1}, neat, ATR) 2952 (w), 1366 (w), 1318 (m), 1305 (s), 1139 (vs). **HRMS** (EI) calcd for C$_{19}$H$_{31}$BO$_4$S [M]$^+$: 366.2036, found: 366.2032.
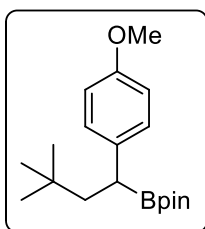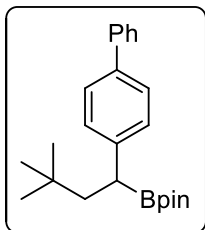
(4-(3,3-Dimethyl-1-(4,4,5,5-tetramethyl-1,3,2-dioxaborolan-2-yl)butyl)phenyl)methanol, 3.12 (0.073 g, 58%) was prepared according to the general DCF procedure *with the following modification*: upon reaction completion, AcOH (3 equiv, 86 µL, 1.5 mmol) was added to the
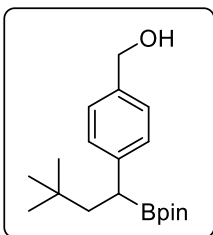
reaction, and the reaction was stirred for 5 minutes prior to chromatographic purification. The desired compound was obtained as a dense, colorless oil.

¹H NMR (CDCl₃, 500 MHz) δ ppm 7.25 - 7.21 (m, 4H), 4.63 (s, 2H), 2.39 (dd, J = 9.9, 3.8 Hz, 1H), 2.01 (dd, J = 13.3, 9.9 Hz, 1H), 1.60 (br. s, 1H), 1.47 (dd, J = 13.4, 3.7 Hz, 1H), 1.14 (d, J = 3.1 Hz, 12H), 0.90 (s, 9H) **¹³C NMR** (CDCl₃, 125 MHz) δ ppm 144.8, 137.8, 128.7, 127.5, 83.5, 65.6, 46.9, 31.7, 29.9, 24.9, 24.7. **¹¹B NMR** (CDCl₃, 128.4 MHz) δ 33.4. **FT-IR** (cm⁻¹, neat, ATR) 3320 (br), 2951 (m), 1385 (m), 1293 (m), 1122 (s). **HRMS** (EI) calcd for C₁₈H₃₁BO₃ [M]⁺: 318.2366, found: 318.2358.
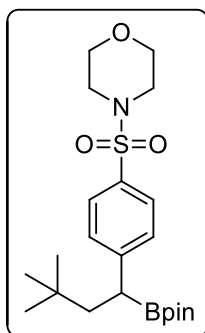
4-((4-(3,3-Dimethyl-1-(4,4,5,5-tetramethyl-1,3,2-dioxaborolan-2-yl)butyl)phenyl)sulfonyl) Morpholine, 3.13 (0.210 g, 98%) was prepared according to the general DCF procedure. The desired compound was obtained as a crystalline, white solid (mp = 219-221 °C). **¹H NMR** (CDCl₃, 500 MHz) δ ppm 7.61 (d, J = 7.5 Hz, 2H), 7.40 (d, J = 7.6 Hz, 2H), 3.73 (br s, 4H), 2.97 (br s, 4H), 2.51 (d, J = 9.0 Hz, 1H), 2.04 (dd, J = 12.7, 10.2 Hz, 1H), 1.49 - 1.54 (m, 1H), 1.13 (s, 12H), 0.90 (s, 9H). **¹³C NMR** (CDCl₃, 125 MHz) δ ppm 151.6, 131.7, 129.0, 128.2, 83.9, 66.4, 46.3, 46.2, 31.8, 29.9, 24.8, 24.7. **¹¹B NMR** (CDCl₃, 128.4 MHz) δ 33.2. **FT-IR** (cm⁻¹, neat, ATR) 2978 (w), 2950 (w), 2862 (w), 1345 (s), 1165 (vs), 1140 (m), 1115 (m), 947 (m). **HRMS** (ESI) calcd for C₂₂H₃₇BNO₅S [M+H]⁺: 438.2469, found: 438.2486.
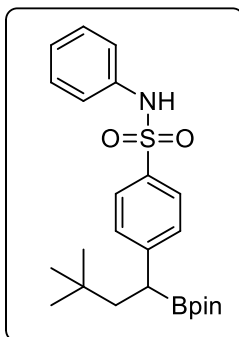
4-(3,3-Dimethyl-1-(4,4,5,5-tetramethyl-1,3,2-dioxaborolan-2-yl)butyl)-*N*-phenylbenzenesulfonamide, 3.14 (0.190 g, 86%) was prepared according to the general DCF procedure. The desired compound was obtained as a crystalline, white solid (mp = 149-151 °C). **¹H NMR** (CDCl₃, 500 MHz) δ ppm 7.61 (d, J = 7.9 Hz, 2H), 7.26 - 7.29 (m, 2H), 7.16 - 7.23 (m, 2H), 7.09 (d, J = 6.9 Hz, 1H), 7.02 (d, J = 7.8 Hz, 2H),

6.45 (s, 1H), 2.48 – 2.41 (m, 1H), 2.02 - 1.92 (m, 1H), 1.52 - 1.44 (m, 1H), 1.09 (s, 12H), 0.86 (s, 9H) ^{13}C NMR (CDCl$_3$, 125 MHz) δ ppm 151.4, 136.8, 135.5, 129.5, 128.9, 127.6, 125.7, 122.2, 83.8, 45.9, 31.7, 29.9, 24.7, 24.6. ^{11}B NMR (CDCl$_3$, 128.4 MHz) δ 32.7. FT-IR (cm^{-1}, neat, ATR) 3256 (w), 2954 (w), 1330 (m), 1157 (vs), 1140 (vs). HRMS (EI) calcd for C$_{24}$H$_{34}$BNO$_4$S [M]$^+$: 443.2302, found: 443.2309.
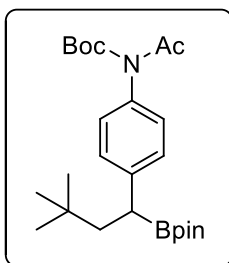
tert-Butyl **Acetyl(4-(3,3-dimethyl-1-(4,4,5,5-tetramethyl-1,3,2-dioxaborolan-2-yl)butyl)phenyl) carbamate, 3.15** (0.156 g, 70%) was prepared according to the general DCF procedure. The desired compound was obtained as a crystalline, white solid (mp = 99-101 °C). ^{1}H NMR (CDCl$_3$, 500 MHz) δ ppm 7.24 (d, J = 8.4 Hz, 2H), 6.93 (d, J = 8.2 Hz, 2 H), 2.52 (s, 3H), 2.43 (dd, J =9.8, 3.8 Hz, 1H), 2.00 (dd, J = 13.3, 9.9 Hz, 1 H), 1.54 (dd, J = 13.4, 4.0 Hz, 1H), 1.34 (s, 9H), 1.12 (s, 12H), 0.89 (s, 9H). ^{13}C NMR (CDCl$_3$, 125 MHz) δ ppm 173.3, 153.2, 144.7, 136.2, 128.9, 128.0, 83.5, 83.0, 46.3, 31.7, 30.0, 28.1, 26.7, 24.8, 24.7. ^{11}B NMR (CDCl$_3$, 128.4 MHz) δ 32.3. FT-IR (cm^{-1}, neat, ATR) 2978 (w), 2951 (w), 1735 (s), 1709 (s), 1367 (s), 1270 (vs), 1254 (s), 1154 (vs), 1142 (vs), 1095 (s). HRMS (ESI) calcd for C$_{25}$H$_{40}$BNO$_5$ [M+ Na]$^+$: 268.2897, found: 268.2898.
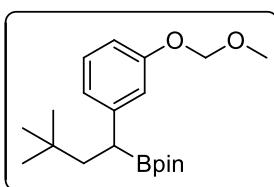
2-(1-(3-(Methoxymethoxy)phenyl)-3,3-dimethylbutyl)-4,4,5,5-tetramethyl-1,3,2-dioxaborolane, 3.16 (0.098 g, 59%) was prepared according to the general DCF procedure. The desired compound was obtained as a colorless, dense oil. ^{1}H NMR (CDCl$_3$, 500 MHz) δ ppm 7.14 (t, J = 7.9 Hz, 1H), 6.92 (t, J = 1.8 Hz, 1H), 6.88 (d, J = 7.6 Hz, 1H), 6.77 - 6.81 (m, 1H), 5.15 (q, J = 6.2 Hz, 2H), 3.47 (s, 3H), 2.36 (dd, J = 10.0, 3.6 Hz, 1H), 2.00 (dd, J = 13.4, 10.0 Hz, 1H), 1.48 (dd, J = 13.4, 3.7 Hz, 1H), 1.15 (d, J = 3.1 Hz, 12H), 0.90 (s, 9H). ^{13}C NMR (CDCl$_3$, 125 MHz) δ ppm 157.5, 146.9, 129.4, 122.3, 116.6, 113.1, 94.8, 83.5, 56.2, 46.8, 31.6, 29.9, 24.9, 24.7. ^{11}B NMR

(CDCl$_3$, 128.4 MHz) δ 32.3. **FT-IR** (cm^{-1}, neat, ATR) 2952 (m), 1366 (m), 1321 (m), 1147 (vs), 1020 (m). **HRMS** (EI) calcd for C$_{20}$H$_{33}$BO$_4$ [M]$^+$: 348.2472, found: 348.2482.
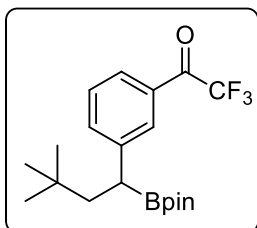
1-(3-(3,3-Dimethyl-1-(4,4,5,5-tetramethyl-1,3,2-dioxaborolan-2-yl)butyl)phenyl)-2,2,2-trifluoroethanone, 3.17 (0.184 g, 99%) was prepared according to the general DCF procedure. The desired compound was obtained as a clear, colorless oil. **¹H NMR** (CDCl$_3$, 500 MHz) δ 7.95 (s, 1H), 7.83 (d, *J* = 7.7 Hz, 1H), 7.58 (dt, *J* = 7.7, 1.3 Hz, 1H), 7.41 (t, *J* = 7.7 Hz, 1H), 2.49 (dd, *J* = 9.4, 3.9 Hz, 1H), 2.04 (dd, *J* = 13.4, 9.5 Hz, 1H), 1.49 (dd, *J* = 13.4, 4.0 Hz, 1H), 1.14 (s, 12H), 0.90 (s, 9H). **¹³C NMR** (CDCl$_3$, 125 MHz) δ 181.0 (q, $_{C\text{-}C\text{-}F}$ *J* = 35.4 Hz, C), 146.7, 136.0, 130.2, 130.0, 129.3, 127.3 (q, $_{C\text{-}C\text{-}C\text{-}F}$ *J* = 2.2 Hz, C), 117.0 (q, $_{C\text{-}F}$ *J* = 291.9 Hz, CF$_3$), 83.8, 46.8, 31.7, 29.9, 24.8, 24.7. **¹⁹F NMR** (CDCl3, 471 MHz) -71.14 (s, 3F). **¹¹B NMR** (CDCl$_3$, 128.4 MHz) δ 32.6. **FT-IR** (cm^{-1}, neat, ATR) 2959 (w), 1716 (m), 1365 (m), 1325 (m), 1199 (s), 1143 (vs), 966 (w), 734 (m). **HRMS** (EI) calcd for C$_{20}$H$_{29}$BF$_3$O$_3$ [M+H]$^+$: 385.2162, found: 385.2148.
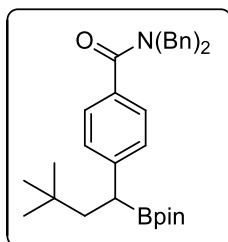
N,N-Dibenzyl-4-(3,3-dimethyl-1-(4,4,5,5-tetramethyl-1,3,2-dioxaborolan-2-yl)butyl)benzamide, 3.18 (0.191 g, 75%) was prepared according to the general DCF procedure. The desired compound was obtained as a crystalline, white solid (mp = 115-116 °C). **¹H NMR** (CDCl$_3$, 500 MHz) δ ppm 7.39 (d, *J* = 7.9 Hz, 2H), 7.26 - 7.37 (m, 8H), 7.23 (d, *J* = 7.9 Hz, 2H), 7.13 (br s, 2H), 4.69 (br s, 2H), 4.41 (br s, 2H), 2.40 (dd, *J* = 9.7, 3.6 Hz, 1H), 1.99 (dd, *J* = 13.2, 9.8 Hz, 1H), 1.46 (dd, *J* = 13.4, 3.7 Hz, 1H), 1.12 (s, 12H), 0.88 (s, 9H). **¹³C NMR** (CDCl$_3$, 125 MHz) δ ppm 172.7, 147.2, 132.8, 128.9, 128.5, 128.4, 127.7, 127.2, 127.1, 83.5, 51.8, 47.1, 46.4, 31.5, 29.8, 24.7, 24.6. **¹¹B NMR** (CDCl$_3$, 128.4 MHz) δ 33.3. **FT-IR** (cm^{-1}, neat, ATR) 2951 (w), 1635

(s), 1364 (s), 1324 (s), 1140 (vs), 699 (s). **HRMS** (EI) calcd for $C_{33}H_{42}BNO_3$ [M]$^+$: 511.3258, found: 511.3258.
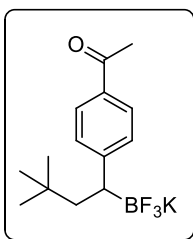
Potassium (1-(4-Acetylphenyl)-3,3-dimethylbutyl)trifluoroborate, 3.19 (0.133 g, 88%) was prepared according to the general DCF procedure *with the following modification*: After filtration of the crude reaction through Celite, the solvent was removed, and the crude material was converted to the trifluoroborate following **GPA2**. The desired compound was obtained as a crystalline yellow solid (mp = 152-153 ºC). **^{1}H NMR** (CDCl$_3$, 500 MHz) δ ppm 7.69 (d, *J*=8.2 Hz, 2 H), 7.26 (d, *J*=8.1 Hz, 2 H), 2.46 (s, 3 H), 1.99 - 1.90 (m, 1 H), 1.84 - 1.71 (m, 2 H), 0.71 (s, 9 H). **^{13}C NMR** (CDCl$_3$, 125 MHz) δ ppm 205.9, 197.1, 161.1 , 132.6 , 129.0 , 127.7 , 45.8 , 32.8 , 30.5 , 26.1. **^{11}B NMR** (CDCl$_3$, 128.4 MHz) δ 4.13. **^{19}F NMR** (CDCl$_3$, 471 MHz) -146.0 (s, 3F). **FT-IR** (cm^{-1}, neat, ATR) 2950 (w), 1669 (m), 1600 (m), 1361 (m), 1277 (m), 955 (s). **HRMS** (ESI) calcd for $C_{14}H_{19}BF_3O$ [M-K$^+$]$^-$: 271.1481, found: 271.1494.
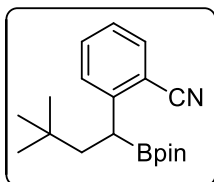
2-(3,3-Dimethyl-1-(4,4,5,5-tetramethyl-1,3,2-dioxaborolan-2-yl)butyl)benzonitrile, 3.20 (0.099 g, 63%) was prepared according to the general DCF procedure *with the following modification:* The reaction was run for 48 h. The desired compound was obtained as a crystalline, white solid (mp = 78-80 ºC). **^{1}H NMR** (CDCl$_3$, 500 MHz) δ ppm 7.56 (d, *J* = 7.8 Hz, 1H), 7.39 - 7.48 (m, 2H), 7.19 (t, *J* = 7.4 Hz, 1H), 2.87 (dd, *J* = 7.5, 5.5 Hz, 1H), 2.02 (dd, *J* = 13.5, 8.2 Hz, 1H), 1.54 (dd, *J* = 13.7, 5.3 Hz, 1H), 1.17 (d, *J* = 9.8 Hz, 12H), 0.90 (s, 9H). **^{13}C NMR** (CDCl$_3$, 125 MHz) δ ppm 149.8, 133.3, 132.6, 129.3, 125.7, 118.9, 112.7, 83.9, 46.8, 31.9, 29.2 - 30.2 (m), 24.9, 24.8. **^{11}B NMR** (CDCl$_3$, 128.4 MHz) δ 32.4. **FT-IR** (cm^{-1}, neat, ATR) 2955 (m), 2224 (w), 1356 (s), 1325 (s), 1319 (m), 1141 (vs). **HRMS** (EI) calcd for $C_{19}H_{28}BNO_2$[M]$^+$: 313.2213, found: 313.2217.
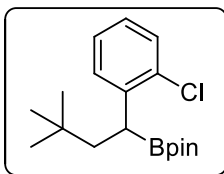
2-(1-(2-Chlorophenyl)-3,3-dimethylbutyl)-4,4,5,5-tetramethyl-1,3,2-

dioxaborolane, 3.21 (0.069 g, 43%) was prepared according to the general

DCF procedure *with the following modification:* The reaction was run for

48 h. The desired compound was obtained as a crystalline, white solid (mp

= 68-70 ºC). **^{1}H NMR** (CDCl$_3$, 500 MHz) δ ppm 7.32 (dd, *J* = 15.0, 7.8 Hz, 2H), 7.15 (t, *J* = 7.2

Hz, 1H), 7.04 (t, *J* = 7.5 Hz, 1H), 2.92 (dd, *J* = 7.3, 4.7 Hz, 1H), 1.97 (dd, *J* = 13.4, 8.5 Hz, 1H),

1.49 (dd, *J* = 13.4, 4.3 Hz, 1H), 1.18 (d, *J* = 8.4 Hz, 12H), 0.90 (s, 9H). **^{13}C NMR** (CDCl$_3$, 125

MHz) δ ppm 143.1, 133.9, 130.2, 129.7, 126.8, 126.4, 83.6, 46.4, 31.6 - 32.1 (m), 29.9, 24.9,

24.8. **^{11}B NMR** (CDCl$_3$, 128.4 MHz) δ 32.7. **FT-IR** (cm^{-1}, neat, ATR) 2952 (w), 1365 (s), 1321

(s), 1141 (vs). **HRMS** (EI) calcd for C$_{18}$H$_{28}$BClO$_2$ [M]$^+$: 322.1871, found: 322.1866.
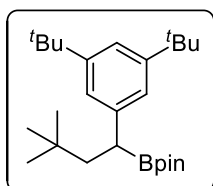
2-(1-(3,5-di-*tert*-Butylphenyl)-3,3-dimethylbutyl)-4,4,5,5-tetramethyl-

1,3,2-dioxaborolane, 3.22 (0.110 g, 55%) was prepared according to the

general DCF procedure *with the following modification:* The reaction was

run for 48 h. The desired compound was obtained as a crystalline, white

solid (mp = 111-112 ºC). **^{1}H NMR** (CDCl$_3$, 500 MHz) δ ppm 7.14 - 7.17 (m, 1H), 7.07 (d, *J* =

1.5 Hz, 2H), 2.38 (dd, *J* = 11.0, 2.4 Hz, 1H), 2.04 (dd, *J* = 13.0, 11.1 Hz, 1H), 1.49 (dd, *J* = 13.1,

2.6 Hz, 1H), 1.30 (s, 18H), 1.14 (d, *J* = 3.8 Hz, 12H), 0.92 (s, 9H). **^{13}C NMR** (CDCl$_3$, 125 MHz)

δ ppm 150.5, 143.7, 122.9, 119.1, 83.3, 47.1, 35.1, 31.8, 31.6, 30.0, 25.0, 24.6. **^{11}B NMR** (CDCl$_3$,

128.4 MHz) δ 32.8. **FT-IR** (cm^{-1}, neat, ATR) 2953 (m), 2865 (s), 1362 (m), 11433 (s), 870 (w).

HRMS (EI) calcd for C$_{26}$H$_{45}$BO$_2$ [M]$^+$: 400.3513, found: 400.3515.
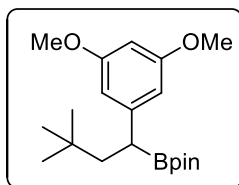
2-(1-(3,5-Dimethoxyphenyl)-3,3-dimethylbutyl)-4,4,5,5-tetramethyl-

1,3,2-dioxaborolane, 3.23 (0.141 g, 81%) was prepared according to the

general DCF procedure. The desired compound was obtained as a

crystalline, white solid (mp = 74-75 ºC). **^{1}H NMR** (CDCl$_3$, 500

159

MHz) δ ppm 6.41 (s, 2H), 6.24 (s, 1H), 3.76 (s, 6H), 2.32 (dd, J = 9.8, 2.5 Hz, 1H), 1.98 (dd, J = 13.0, 10.3 Hz, 1H), 1.47 (dd, J = 13.3, 2.9 Hz, 1H), 1.16 (s, 12H), 0.90 (s, 9H). **^{13}C NMR** (CDCl$_3$, 125 MHz) δ ppm 160.9, 147.6, 106.4, 97.8, 83.6, 55.5, 46.9, 31.6, 29.9, 25.0, 24.7**. ^{11}B NMR** (CDCl$_3$, 128.4 MHz) δ 32.7. **FT-IR** (cm^{-1}, neat, ATR) 2951 (w), 1593 (m), 1364 (m), 1318 (m), 1204 (m), 1140 (vs) **HRMS** (EI) calcd for C$_{20}$H$_{33}$BO$_4$ [M]$^+$: 348.2472, found: 348.2471.

2-(3,3-Dimethyl-1-(4-(1-(trifluoromethyl)cyclopropyl)phenyl)butyl)-
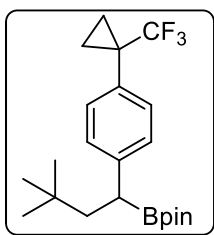
4,4,5,5-tetramethyl-1,3,2-dioxaborolane, 3.24 (0.091 g, 46%) was prepared according to the general DCF procedure. The desired compound was obtained as clear, colorless oil. **^{1}H NMR** (CDCl$_3$, 500 MHz) δ 7.30 (d, J = 7.7 Hz, 2H), 7.18 (d, J = 7.7 Hz, 2H), 2.38 (dd, J = 10.1, 2.6 Hz, 1H), 2.02 (dd, J = 12.7, 11.0 Hz, 1H), 1.45 (dd, J = 13.4, 2.9 Hz, 1H), 1.28 - 1.31 (m, 2H), 1.14 (s, 12H), 0.99 (br s, 2H), 0.90 (s, 9H). **^{13}C NMR** (CDCl$_3$, 125 MHz) δ 145.3, 132.9, 131.3, 128.3, 126.8 (q, J_{C-F} = 273.1 Hz, CF$_3$), 83.6, 46.9, 31.6, 29.9, 28.0 (q, J_{C-C-F} = 33.2 Hz, C), 24.9 , 24.7, 9.9. **^{19}F NMR** (CDCl$_3$, 471 MHz) -70.11 (s, 3F).**^{11}B NMR** (CDCl$_3$, 128.4 MHz) δ 33.0. **FT-IR** (cm^{-1}, neat, ATR) 2954 (w), 1360 (m), 1324 (m), 1136 (vs), 1087 (m), 839 (w), 735 (w), 573 (m). **HRMS** (EI) calcd for C$_{22}$H$_{32}$BF$_3$O$_2$ [M]$^+$: 396.2447, found: 396.2446.

5-(3,3-Dimethyl-1-(4,4,5,5-tetramethyl-1,3,2-dioxaborolan-2-

yl)butyl)isobenzo furan-1(3H)-one, 3.25 (0.130 g, 76%) was prepared according to the general DCF procedure. The desired compound was obtained as a crystalline, white solid (mp = 111-113 ºC). **^{1}H NMR** (CDCl$_3$, 500 MHz) δ ppm 7.78 (d, J = 7.9 Hz, 1H), 7.40 (d, J = 7.9 Hz, 1H), 7.33 (s, 1H), 5.26 (s, 2H), 2.55 (dd, J = 9.3, 4.1 Hz, 1H), 2.06 (dd, J = 13.3, 9.3 Hz, 1H), 1.53 (dd, J = 13.4, 4.1 Hz, 1H), 1.14 (s, 12H), 0.90 (s, 9H). **^{13}C NMR** (CDCl$_3$, 125 MHz) δ ppm 171.6, 153.1, 147.4, 129.7, 125.7, 123.0, 121.6, 84.0, 69.8, 46.6, 31.8, 29.9, 24.8, 24.7. **^{11}B NMR** (CDCl$_3$, 128.4 MHz) δ 32.7. **FT-IR** (cm^{-}

[1], neat, ATR) 2954 (w), 1768 (vs) 1352 (m) 1136 (m), 1035 (m). **HRMS** (EI) calcd for $C_{20}H_{29}BO_4$ [M]$^+$: 344.2159, found: 344.2168.

2-(1-(4-(1,3-Dioxolan-2-yl)phenyl)-3,3-dimethylbutyl)-4,4,5,5-tetramethyl-1,3,2-dioxaborolane, 3.26 (0.106 g, 59%) was prepared according to the general DCF procedure. The desired compound was obtained as a crystalline, white solid (mp = 88-90 °C). **^{1}H NMR** (CDCl$_3$, 500 MHz) δ ppm 7.34 (d, J = 7.9 Hz, 2H), 7.24 (d, J = 8.1 Hz, 2H), 5.75 (s, 1H), 4.11 - 4.16 (m, 2H), 4.00 - 4.04 (m, 2H), 2.40 (dd, J = 9.8, 3.7 Hz, 1H), 2.00 (dd, J = 13.4, 9.8 Hz, 1H), 1.48 (dd, J = 13.4, 3.7 Hz, 1H), 1.14 (d, J = 2.3 Hz, 12H), 0.89 (s, 9H). **^{13}C NMR** (CDCl$_3$, 125 MHz) δ ppm 146.5, 134.6, 128.5, 126.7, 104.3, 83.6, 65.5(7), 65.5(5), 46.9, 31.7, 29.9, 24.9, 24.7. **^{11}B NMR** (CDCl$_3$, 128.4 MHz) δ 32.9. **FT-IR** (cm^{-1}, neat, ATR) 2952 (w), 1365 (s), 1322 (s), 1141 (vs) 1080 (s), 967 (m). **HRMS** (EI) calcd for $C_{21}H_{33}BO_4$ [M]$^+$: 360.2472, found: 360.2484.

2-(3-(3,3-Dimethyl-1-(4,4,5,5-tetramethyl-1,3,2-dioxaborolan-2-yl)butyl)phenyl)isoindoline-1,3-dione, 3.27 (0.112 g, 52%) was prepared according to the general DCF procedure. The desired compound was obtained as a crystalline, white solid (mp = 118-119 °C). **^{1}H NMR** (CDCl$_3$, 500 MHz) δ ppm 7.94 (dd, J = 5.3, 3.1 Hz, 2H), 7.78 (dd, J = 5.5, 3.1 Hz, 2H), 7.37 (t, J = 7.8 Hz, 1H), 7.26 - 7.30 (m, 2H), 7.17 (d, J = 7.9 Hz, 1H), 2.47 (dd, J = 10.0, 3.7 Hz, 1H), 2.02 (dd, J = 13.3, 10.1 Hz, 1H), 1.55 (dd, J = 13.3, 3.8 Hz, 1H), 1.17 (d, J = 3.7 Hz, 12H), 0.91 (s, 9H) . **^{13}C NMR** (CDCl$_3$, 125 MHz) δ ppm 167.6, 146.3, 134.5, 132.2, 131.8, 129.2, 128.4, 126.9, 123.9, 123.7, 83.7, 46.6, 31.7, 30.0, 24.8, 24.7. **^{11}B NMR** (CDCl$_3$, 128.4 MHz) δ 33.6. **FT-IR** (cm^{-1}, neat, ATR) 2951 (w), 1721 (vs), 1371 (s), 1322 (m), 1141 (m), 717 (m). **HRMS** (EI) calcd for $C_{26}H_{32}BNO_4$ [M]$^+$: 433.2424, found: 433.2430.
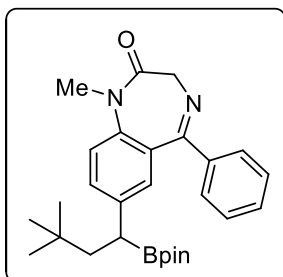
7-(3,3-Dimethyl-1-(4,4,5,5-tetramethyl-1,3,2-dioxaborolan-2-yl)butyl)-1-methyl-5-phenyl-1H-benzo[e][1,4]diazepin-2(3H)-one, 3.29 (0.175 g, 76%) was prepared according to the general DCF procedure. The desired compound **30** was obtained as a dense, yellow oil. Compound rapidly decomposed upon standing neat but is stable in solution; ^{1}H NMR was therefore taken with residual chromatography solvent. **^{1}H NMR** (CDCl$_3$, 500 MHz) δ ppm 7.61 (dd, J = 6.9, 4.8 Hz, 2H), 7.34 - 7.47 (m, 4H), 7.22 (dd, J = 8.5, 3.8 Hz, 1H), 7.14 (d, J = 1.8 Hz, 1H), 4.77 (dd, J = 10.6, 2.1 Hz, 1H), 3.76 (d, J = 10.7 Hz, 1H), 3.35 - 3.40 (m, 3H), 2.33 - 2.41 (m, 1H), 1.88 - 1.98 (m, 1H), 1.44 (ddd, J = 18.3, 13.5, 4.3 Hz, 1H), 1.09 - 1.16 (m, 12H), 0.86 (d, J = 10.7 Hz, 9H). **^{13}C NMR** (CDCl$_3$, 125 MHz) δ ppm 143.4, 142.6, 136.3, 135.9, 134.9, 134.8, 132.6, 131.9, 129.5, 122.2, 84.1, 46.8, 45.8, 36.0, 31.9, 31.7, 30.4, 29.9, 29.8, 24.9, 24.8(4), 24.7(6). **^{11}B NMR** (CDCl$_3$, 128.4 MHz) δ 33.3. **FT-IR** (cm^{-1}, neat, ATR) 2951 (w), 1680 (vs), 1321 (m), 1140 (m) 699 (w). **HRMS** (EI) calcd for C$_{28}$H$_{37}$BN$_2$O$_3$ [M]$^+$: 460.2897, found: 460.2884.

Ethyl 8-(3,3-Dimethyl-1-(4,4,5,5-tetramethyl-1,3,2-dioxaborolan-2-yl)butyl)-5-methyl-6-oxo-5,6-dihydro-4H-benzo[f]imidazo[1,5-a][1,4]diazepine-3-carboxylate, 3.30 (0.219 g, 88%) was prepared according to the general DCF procedure. The desired compound was obtained as a cr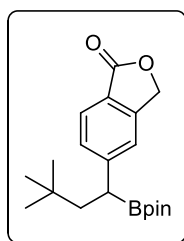ystalline, white solid (mp = 132-133 ºC). **^{1}H NMR** (CDCl$_3$, 500 MHz) δ ppm 7.91 (br s, 1H), 7.85 (s, 1H), 7.50 (d, J = 7.8 Hz, 1H), 7.28 (d, J = 8.2 Hz, 1H), 5.23 – 5.03 (br s, 1H), 4.96 – 4.24 (m, 3H), 3.22 (s, 3H), 2.55 - 2.45 (m, 1H), 2.06 – 1.99 (m, 1H), 1.57 - 1.47 (m, 1H), 1.43 (t, J = 7.1 Hz, 3H), 1.16 (s, 12H), 0.90 (s, 9H). **^{13}C NMR** (CDCl$_3$, 125 MHz) δ ppm 167.0, 163.5, 146.5, 135.9, 135.2, 132.8, 132.3, 129.6, 129.1, 128.7, 128.6, 121.9, 83.9, 61.2, 42.7, 36.0, 31.8, 29.9, 24.9, 24.7, 14.7. **^{11}B NMR**
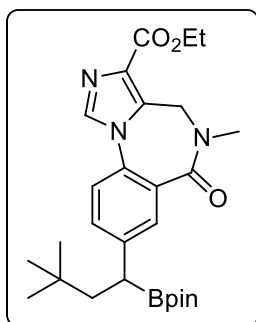
(CDCl$_3$, 128.4 MHz) δ 33.3. **FT-IR** (cm^{-1}, neat, ATR) 2952 (m), 1366 (m), 1321 (m), 1147 (vs),

1020 (m). **HRMS** (ESI) calcd for C$_{27}$H$_{39}$BN$_3$O$_5$ [M+H]$^+$: 496.2983, found: 496.2960.
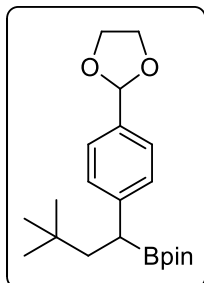
2-Chloro-5-(3,3-dimethyl-1-(4,4,5,5-tetramethyl-1,3,2-dioxaborolan-2-
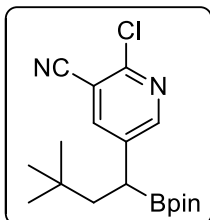
yl)butyl)nicotinonitrile, 3.31 (0.127g, 73%) was prepared according to the

general DCF procedure. The desired compound was obtained as a crystalline,

white solid (mp = 76-78 °C). **^{1}H NMR** (CDCl$_3$, 500 MHz) δ 8.42 (d, *J* = 2.3

Hz, 1H), 7.85 (d, *J* = 2.4 Hz, 1H), 2.44 (dd, *J* = 8.5, 4.7 Hz, 1H), 1.99 (dd, *J*

= 13.5, 8.9 Hz, 1H), 1.43 (dd, *J* = 13.5, 4.8 Hz, 1H), 1.16 (d, *J* = 4.6 Hz, 12H), 0.89 (s, 9H). **^{13}C**

NMR (CDCl$_3$, 125 MHz) δ ppm 153.0, 149.4, 142.0, 140.7, 115.3, 110.4, 84.4, 46.4, 312.0, 29.9,

24.9, 24.8. **^{11}B NMR** (CDCl$_3$, 128.4 MHz) δ 32.5. **FT-IR** (cm^{-1}, neat, ATR) 2950 (m), 12234 (w).

1355(s), 1352 (s), 1326 (s), 1139 (vs). **HRMS** (EI) calcd for C$_{18}$H$_{26}$BClN$_2$O$_2$ [M]$^+$: 348.1776,

found: 348.1788.

Methyl 5-(3,3-Dimethylbutyl)picolinate, **3.32** (0.046 g, 42%) was prepared
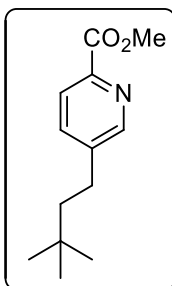
according to the general DCF procedure. The desired compound was obtained as

a colorless oil. **^{1}H NMR** (CDCl$_3$, 500 MHz) δ ppm 8.54 (s, 1H), 8.04 (d, *J* = 7.9

Hz, 1H), 7.63 (dd, *J* = 8.0, 1.9 Hz, 1H), 3.98 (s, 3H), 2.59 - 2.67 (m, 2H), 1.45 -

1.53 (m, 2H), 0.96 (s, 9H). **^{13}C NMR** (CDCl$_3$, 125 MHz) δ ppm 166.1, 150.3,

145.8, 143.2, 136.8, 125.2, 53.0, 45.9, 30.9, 29.5, 28.8. **FT-IR** (cm^{-1}, neat, ATR) 2987 (m), 1721

(vs) 1378 (m) 1256 (m), 936 (w). **HRMS** (ESI) calcd for C$_{13}$H$_{20}$NO$_2$ [M+H]$^+$: 222.1494, found:

222.1497.
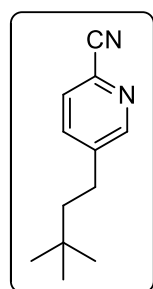
5-(3,3-Dimethylbutyl)picolinonitrile, 3.33 (0.074 g, 79%) was prepared

according to the general DCF procedure. The desired compound was obtained as a

crystalline, white solid (mp = 65-67 °C). **^{1}H NMR** (CDCl$_3$, 500 MHz) δ ppm 8.54

(s, 1H), 7.59 - 7.65 (m, 2H), 2.61 - 2.69 (m, 2H), 1.45 - 1.53 (m, 2H), 0.98 (s, 9H).

163

^{13}**C NMR** (CDCl$_3$, 125 MHz) δ ppm 151.7, 143.4, 136.7, 131.5, 128.4, 117.7, 45.8, 31.0, 29.5, 29.0. **FT-IR** (cm^{-1}, neat, ATR) 2955 (s), 2235 (w), 1470 (s) 1366 (m). **HRMS** (ESI) calcd for C$_{12}$H$_{16}$N$_2$ [M]$^+$: 188.1313, found: 188.1301.
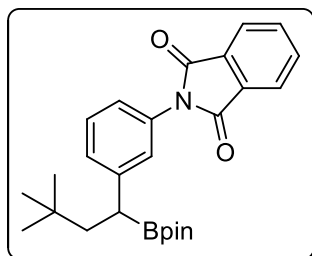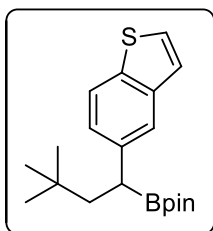
2-(1-(Benzo[b]thiophen-5-yl)-3,3-dimethylbutyl)-4,4,5,5-tetramethyl-1,3,2-dioxaborolane, 3.34 (0.105 g, 61%) was prepared according to the general DCF procedure. The desired compound was obtained as a powdery, white solid (mp = 143–144 °C). ^{1}**H NMR** (CDCl$_3$, 500 MHz) δ ppm7.74 (d, *J* = 8.4 Hz, 1H), 7.67 (s, 1H), 7.37 (d, *J* = 5.5 Hz, 1H), 7.24 (m, 2H), 2.50 (dd, *J* = 9.7, 3.3 Hz, 1H), 2.08 (dd, *J* = 12.5, 9.9 Hz, 1H), 1.55 (dd, *J* = 13.0, 3.1 Hz, 1H), 1.14 (d, *J* = 5.7 Hz, 12H), 0.92 (s, 9H). ^{13}**C NMR** (CDCl$_3$, 125 MHz) δ ppm 141.3, 140.3, 136.9, 126.3, 125.6, 124.1, 123.0, 122.4, 83.5, 47.3, 31.7, 30.0, 24.9, 24.7. ^{11}**B NMR** (CDCl$_3$, 128.4 MHz) δ ppm 33.0. **FT-IR** (cm^{-1}, neat, ATR) 2954 (w), 1361 (s), 1330 (s), 1137 (vs), 967 (m), 837 (m), 702 (s). **HRMS** (EI) calcd for C$_{20}$H$_{30}$BO$_2$S [M+H]$^+$: 345.2060 found: 345.2066.
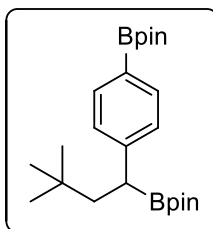
(4-(3,3-Dimethyl-1-(4,4,5,5-tetramethyl-1,3,2-dioxaborolan-2-yl)butyl)phenyl)trimethylsilane, 3.35 (0.162 g, 90%) was prepared according to the general DCF procedure. The desired compound was obtained as a crystalline, white solid (mp = 89-90 °C). ^{1}**H NMR** (CDCl$_3$, 500 MHz) δ ppm 7.38 (d, *J* = 7.8 Hz, 2H), 7.21 (d, *J* = 7.8 Hz, 2H), 2.37 (dd, *J* = 10.2, 3.1 Hz, 1H), 2.03 (dd, *J* = 13.3, 10.4 Hz, 1H), 1.47 (dd, *J* = 13.3, 3.2 Hz, 1H), 1.15 (d, *J* = 1.5 Hz, 12H), 0.90 (s, 9H), 0.23 (s, 9H). ^{13}**C NMR** (CDCl$_3$, 125 MHz) δ ppm 145.8, 136.5, 133.6, 127.9, 83.5, 47.0, 31.6, 29.9, 24.9, 24.7, -0.7. ^{11}**B NMR** (CDCl$_3$, 128.4 MHz) δ 21.2. **FT-IR** (cm^{-1}, neat, ATR) 2953 (w), 1364 (m), 1315 (m), 1247 (m), 1142 (s), 1107 (m), 835 (vs). **HRMS** (EI) calcd for C$_{21}$H$_{37}$BO$_2$Si [M]$^+$: 360.2656, found: 360.2659.
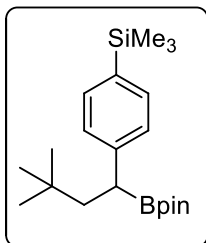
2-(4-(3,3-Dimethyl-1-(4,4,5,5-tetramethyl-1,3,2-dioxaborolan-2-yl)butyl)phenyl)-4,4,5,5-tetramethyl-1,3,2-dioxaborolane, 3.36 (0.144 g, 70%) was prepared according to the general DCF procedure. The desired compound was obtained as a crystalline, white solid (mp = 137-139 ºC). **^{1}H NMR** (CDCl$_3$, 500 MHz) δ ppm 7.68 (d, *J* = 7.6 Hz, 2H), 7.24 (d, *J* = 7.8 Hz, 2H), 2.37 - 2.44 (m, 1H), 1.96 - 2.05 (m, 1H), 1.50 (dd, *J* = 13.3, 3.5 Hz, 1H), 1.33 (s, 12H), 1.13 (s, 12H), 0.89 (s, 9H). **^{13}C NMR** (CDCl$_3$, 125 MHz) δ ppm 148.8, 135.1, 128.0, 83.8, 83.6, 46.6, 31.7, 30.0, 25.2, 25.1, 24.9, 24.7. **^{11}B NMR** (CDCl$_3$, 128.4 MHz) δ 31.4 (2 × B). **FT-IR** (cm^{-1}, neat, ATR) 2978 (x), 2952 (vw), 1607 (w), 1358 (vs), 1319 (m), 1142 (s). **HRMS** (EI) calcd for C$_{24}$H$_{40}$B$_2$O$_4$ [M]$^+$: 414.3113, found: 414.3102.
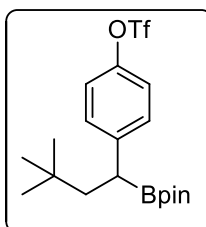
4-(3,3-Dimethyl-1-(4,4,5,5-tetramethyl-1,3,2-dioxaborolan-2-yl)butyl)phenyl trifluoromethanesulfonate, 3.37 (0.140 g, 64%) was prepared according to the general DCF procedure. The desired compound was obtained as a powdery, white solid (mp = 74–75 ºC). **^{1}H NMR** (CDCl$_3$, 500 MHz) δ 7.28 (d, *J* = 7.9 Hz, 2H), 7.13 (d, *J* = 8.1 Hz, 2H), 2.43 (dd, *J* = 13.2, 3.5 Hz, 1H), 2.00 (dd, *J* = 13.0, 12.3 Hz, 1H), 1.47 (dd, *J* = 13.3, 3.4 Hz, 1H), 1.13 (s, 12H), 0.89 (s, 9H). **^{13}C NMR** (CDCl$_3$, 125 MHz) δ 147.5, 145.9, 130.0, 121.2, 119.0 (q, C-F *J* = 319.5 Hz, CF$_3$), 83.8, 46.6, 31.7, 29.9, 24.8, 24.7. **^{19}F NMR** (CDCl$_3$, 471 MHz) -72.80 (s, 3F). **^{11}B NMR** (CDCl$_3$, 128.4 MHz) δ 33.3. **FT-IR** (cm^{-1}, neat, ATR) 2977 (w), 1426 (m), 1202 (vs), 1134 (vs), 883 (s), 610 (s). **HRMS** (ESI) calcd for C$_{19}$H$_{28}$BF$_3$O$_5$S [M]$^+$: 436.1703, found: 436.1711.
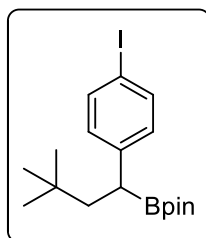
2-(1-(4-Iodophenyl)-3,3-dimethylbutyl)-4,4,5,5-tetramethyl-1,3,2-dioxaborolane, 3.38 (0.132 g, 64%) was prepared according to the general DCF procedure *with the following modifications:* 1,4-diiodobenze (0.165 g, 0.500 mmol) was used. The desired compound was obtained as a white

crystalline solid (mp = 120-121 °C). **¹H NMR** (CDCl₃, 500 MHz) δ ppm 7.54 (d, *J* = 8.1 Hz, 2H),

6.98 (d, *J* = 8.2 Hz, 2H), 2.33 (dd, *J* = 9.5, 3.7 Hz, 1H), 1.97 (dd, *J* = 13.2, 9.8 Hz, 1H), 1.45 (dd,

J = 13.3, 3.8 Hz, 1H), 1.14 (s, 12 H), 0.88 (s, 9 H). **¹³C NMR** (CDCl₃, 125 MHz) 145.0, 137.5,

130.6, 90.2, 83.7, 46.6, 31.7, 29.9, 24.9, 24.7. **¹¹B NMR** (CDCl₃, 128.4 MHz) 32.5. **FT-IR** (cm⁻¹,

neat, ATR) 2955 (m), 1462 (m), 1380 (s), 1210 (s), 810 (m). **HRMS** (EI) calcd for C₁₈H₂₈BIO₂

[M⁺]: 414.1227, found: 414.1216.
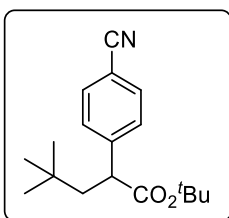
***tert*-Butyl 2-(4-Cyanophenyl)-4,4-dimethylpentanoate, 3.39** (0.068 g,

47%) was prepared according to the general DCF procedure *with the*

following modification: tert-Butyl acrylate (0.077 g, 0.60 mmol, 1.2 equiv)

was used in place of vinylBpin. The desired compound was obtained as a

crystalline, white solid (mp = 84-85 °C). **¹H NMR** (CDCl₃, 500 MHz) δ ppm 7.59 (d, *J* = 7.5 Hz,

2H), 7.41 (d, *J* = 7.9 Hz, 2H), 3.57 (dd, *J* = 8.9, 3.4 Hz, 1H), 2.26 (dd, *J* = 14.1, 9.0 Hz, 1H),

1.47 (dd, *J* = 13.9, 3.3 Hz, 1H), 1.37 (s, 9H), 0.90 (s, 9H). **¹³C NMR** (CDCl₃, 125 MHz) δ ppm

172.9, 147.2, 132.6, 128.8, 119.1, 111.0, 81.4, 49.8, 47.2, 31.4, 29.7, 28.0. **FT-IR** (cm⁻¹, neat,

ATR) 2954 (w), 2228 (w), 1722 (m), 1365 (m), 1141 (s), 839 (m), 564 (m). **HRMS** (EI) calcd for

C₁₄H₂₅NO₂ [M-C₄H₈]⁺: 231.1259, found: 231.1265.
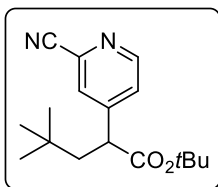
***tert*-Butyl 2-(2-Cyanopyridin-4-yl)-4,4-dimethylpentanoate**, **3.40** (0.82

g, 57%) was prepared according to the general DCF procedure *with the*

following modification: *tert*-butyl acrylate (0.077 g, 0.60 mmol, 1.2 equiv)

was used in place of vinylBpin. The desired compound was obtained as a

white solid (mp = 77 – 79 °C). **¹H NMR** (CDCl₃, 500 MHz) δ ppm 8.64 (d, *J* = 1.7 Hz, 1H), 7.80

(dd, *J* = 8.0, 2.2 Hz, 1H), 7.64 (d, *J* = 8.1 Hz, 1H), 3.62 (dd, *J* = 8.9, 4.0 Hz, 1H), 2.28 (dd, *J* =

14.0, 8.8 Hz, 1H), 1.48 (dd, *J* = 14.0, 4.0 Hz, 1H) 1.38 (s, 9H), 0.91 (s, 9H). **¹³C NMR** (CDCl₃,

125 MHz) δ 172.3, 151.2, 141.5, 136.1, 132.6, 128.6, 117.5, 82.1, 47.3, 31.5, 29.7, 28.1. **FT-IR**

(cm^{-1}, neat, ATR) 2958 (m), 2236 (w), 1727 (s) 1368 (m), 1144 (vs), 857 (w). **HRMS** (EI) calcd

for C$_{13}$H$_{15}$N$_2$O$_2$ [M-tBu]$^+$: 232.1221, found: 232.1222.

Ethyl 2-(4-Cyanophenyl)-4,4-dimethyl-6-oxoheptanoate, 3.41 (0.133

g, 88%) was prepared according to the general DCF procedure *with the*

following modification. Ethyl acrylate (0.060 g, 0.60 mmol, 1.2 equiv)

was used in place of vinylBpin. The desired compound was obtained as a

colorless oil. **^{1}H NMR** (CDCl$_3$, 500 MHz) δ ppm 7.59 (d, J = 8.2 Hz, 2H), 7.44 (d, J = 8.1 Hz,

2H), 4.17 - 4.02 (m, 2H), 3.69 (dd, J = 8.9, 4.0 Hz, 1H), 2.39 - 2.28 (m, 3H), 2.07 (s, 3H), 1.81

(dd, J = 14.1, 4.0 Hz, 1H), 1.20 (t, J = 7.1 Hz, 3H), 1.00 (s, 3H), 0.98 (s, 3H). **^{13}C NMR** (CDCl$_3$,

125 MHz) δ ppm 208.2, 173.7, 146.1, 132.7, 129.0, 119.0, 111.4, 61.6, 53.9, 48.4, 45.0, 34.2,

32.6, 27.7, 27.5, 14.3. **FT-IR** (cm^{-1}, neat, ATR) 2960 (m), 1728 (vs), 1366 (m), 1152 (vs), 1020

(m). **HRMS** (EI) calcd for C$_{18}$H$_{23}$NO$_3$ [M]$^+$: 301.1678, found: 301.1687.
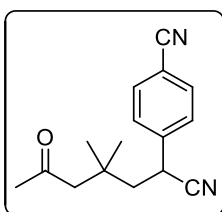
4-(1-Cyano-3,3-dimethyl-5-oxohexyl)benzonitrile 3.42 (0.113 g, 89%)

was prepared according to the general DCF procedure *with the following*

modification: Acrylonitrile (0.039 g, 0.60 mmol, 1.2 equiv) was used in

place of vinylBpin. The desired compound was obtained as an off-white

wax. **^{1}H NMR** (CDCl$_3$, 500 MHz) δ ppm 7.68 (d, J = 8.1 Hz, 2H), 7.51 (d, J = 8.1 Hz, 2H), 3.92

(dd, J = 11.1, 3.4 Hz, 1H), 2.66 - 2.59 (m, 1H), 2.47 (d, J = 16.5 Hz, 1H), 2.22 - 2.12 (m, 4H),

1.89 (dd, J = 14.2, 3.4 Hz, 1H), 1.19 (s, 3H), 1.12 (s, 3H). **^{13}C NMR** (CDCl$_3$, 125 MHz) δ ppm

208.6, 151.0, 132.0, 129.1, 128.2, 84.1, 66.4, 54.4, 46.3, 44.3, 34.8, 32.8, 27.7, 27.4, 24.8, 24.7.

FT-IR (cm^{-1}, neat, ATR) 2959 (m), 2230 (m), 1711 (s), 1325 (vs),

835 (s), 576 (s). **HRMS** (EI) calcd for C$_{16}$H$_{18}$N$_2$O [M]$^+$: 254.1419,

found: 254.1427.

Pent-4-en-1-yl-2-(4-cyanophenyl)-4,4-dimethylpentanoate, 3.44

167

(0.122 g, 82%) was prepared according to the general DCF procedure *with the following modifications:* Pent-4-en-1-yl acrylate (0.084 g, 0.600 mmol) was used in place of vinylBpin. The desired compound was obtained as a colorless oil. [1]**H NMR** (CDCl$_3$, 500 MHz) δ ppm 7.59 (d, *J* = 8.2 Hz, 2H), 7.44 (d, *J* = 8.2 Hz, 2H), 5.77 - 5.66 (m, 1H), 4.95 (s, 1H), 4.93 (d, *J* = 4.7 Hz, 1H), 4.11 – 3.97 (m, 2H), 3.69 (dd, *J* = 8.9, 4.0 Hz, 1H), 2.29 (dd, *J* = 14.0, 9.0 Hz, 1H), 2.01 (q, *J* = 7.1 Hz, 2H), 1.70 - 1.62 (m, 2H), 1.54 (dd, *J* = 14.0, 4.0 Hz, 1H), 0.89 (s, 9H). [13]**C NMR** (CDCl$_3$, 125 MHz) 173.9, 146.6, 137.4, 132.7, 129.0, 119.0, 115.7, 111.3, 64.9, 48.8, 47.4, 31.4, 30.2, 29.7, 27.9. **FT-IR** (cm^{-1}, neat, ATR) 2969 (m), 1486 (s), 1010 (s), 807 (s). **HRMS** (EI) calcd for C$_{19}$H$_{25}$NO$_2$ [M$^+$]: 299.1885, found: 299.1897.
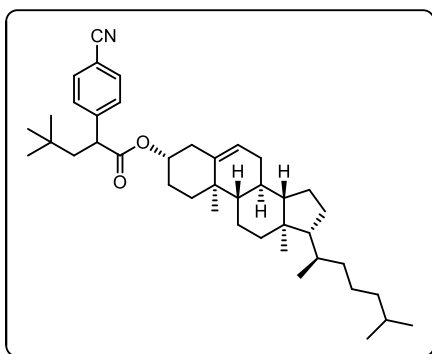
(3*S*,8*S*,9*S*,10*R*,13*R*,14*S*,17*R*)-10,13-Dimethyl-17-((*R*)-6-methylheptan-2-yl)-2,3,4,7,8,9,10,11, 12,13,14,15,16,17-tetradecahydro-1H-cyclopenta [a] phenan thren-3-yl2-(4-Cyanophenyl)-4,4-dimethyl pentanoate, 3.45 (0.125 g, 42%) was prepared according to the general DCF procedure *with the following modifications:* cholesteryl acrylate (0.265 g, 0.600 mmol) was used in place of vinylBpin. The desired compound was obtained as a white powdery solid (mp = 136-138 ºC). [1]**H NMR** (CDCl$_3$, 500 MHz) δ ppm 7.59 (dd, *J*=8.3, 1.8 Hz, 2H), 7.43 (d, *J*=7.9 Hz, 2H), 5.38 – 5.28 (m, 1H), 4.60 – 4.52 (m, 1H), 3.65 (dd, *J*=9.1, 3.6 Hz, 1H), 2.33 - 2.26 (m, 2H), 2.24 - 2.10 (m, 1H), 2.02 – 1.91 (m, 2H), 1.87 - 1.64 (m, 3H), 1.60 - 1.40 (m, 8H), 1.39 - 1.06 (m, 11H), 1.03 - 0.95 (m, 5H), 0.93 - 0.88 (m, 13H), 0.86 (dd, *J*=6.6, 2.1 Hz, 6H), 0.66 (s, 3H). [13]**C NMR** (CDCl$_3$, 125 MHz) δ ppm 173.3, 146.8, 139.6, 139.6, 132.6, 128.9, 123.2, 123.1, 119.0, 111.2, 75.0, 56.9, 56.4, 50.3, 49.0, 47.5, 42.6, 40.0, 39.8, 38.1, 38.0, 37.2, 37.1, 36.8, 36.5, 36.0, 32.2, 32.1, 32.1, 32.1, 31.4, 29.7, 28.5, 28.3, 27.8, 27.7, 24.5, 24.1, 23.1, 22.8, 21.3, 19.6, 19.0, 12.1.

FT-IR (cm^{-1}, neat, ATR) 2948 (s), 2229 (w), 1732 (s), 1467 (w), 1154 (m), 839 (vw). **HRMS** (EI) calcd for C$_{27}$H$_{44}$ [M - C$_{14}$H$_{17}$NO$_2$$^+$]: 368.3443, found: 368.3429.
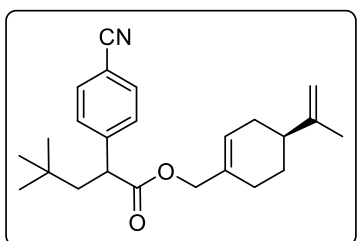
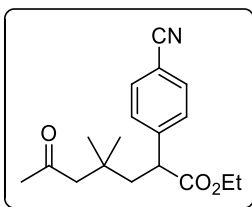**((S)-4-(Prop-1-en-2-yl)cyclohex-1-en-1-yl)methyl-2-(4-cyanophenyl)-4,4-dimethylpentanoate, 3.46** (0.089 g, 41%) was prepared according to the general DCF procedure *with the following modifications:* (S)-(4-(prop-1-en-2-yl)cyclohex-1-en-1-yl)methyl acrylate (0.124 g, 0.600 mmol) was used in place of vinylBpin. The desired compound **66** was obtained as colorless oil. ^{1}**H NMR** (CDCl$_3$, 500 MHz) δ ppm 7.59 (d, *J* = 8.2 Hz, 2H), 7.44 (dd, *J* = 8.2, 1.4 Hz, 2H), 5.67 (br. s, 1H), 4.70 (d, *J* = 16.5 Hz, 2H), 4.49 - 4.36 (m, 2H), 3.71 (dd, *J* = 8.9, 4.0 Hz, 1H), 2.30 (dd, *J* = 14.0, 8.9 Hz, 1H), 2.16 – 2.05 (br. s, 2H), 1.97 – 1.88 (m, 3H), 1.83 - 1.75 (m, 1H), 1.72 (s, 3H), 1.55 (dd, *J* = 14.0, 4.0 Hz, 1H), 1.46 - 1.35 (m, 1H), 0.89 (s, 9H). ^{13}**C NMR** (CDCl$_3$, 125 MHz) δ ppm 173.8, 173.8, 149.6, 146.5, 132.7, 132.4, 129.0, 126.7, 126.7, 119.0, 111.3, 109.1, 69.5, 48.8, 48.8, 47.4, 47.4, 40.9, 31.4, 30.7, 29.6, 27.4, 27.4, 26.6, 26.6, 21.0. **FT-IR** (cm^{-1}, neat, ATR) 2954 (m), 2229 (w), 1733 (s), 1147 (vs), 837 (m), 737 (vs). **HRMS** (EI) calcd for C$_{24}$H$_{31}$NO$_2$ [M$^+$]: 365.2355, found: 365.2363.
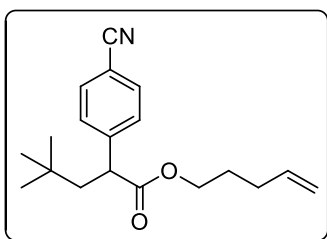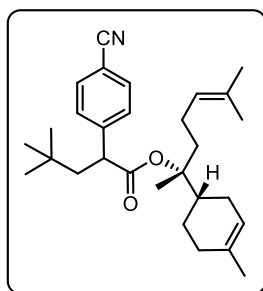

(R)-6-Methyl-2-((S)-4-methylcyclohex-3-en-1-yl)hept-5-en-2-yl-2-(4-cyanophenyl)-4,4-dimethyl pentanoate, 3.47 (0.089 g, 41%) was prepared according to the general DCF procedure *with the following modifications:* (S)-6-methyl-2-((S)-4-methylcyclohex-3-en-1-yl)hept-5-en-2-ol (0.123 g, 0.600 mmol) was used in place of vinylBpin. The desired compound **65** was obtained as colorless oil. ^{1}**H NMR** (CDCl$_3$, 500 MHz) δ ppm 7.59 (d, *J* = 7.8 Hz, 2H), 7.42 (d, *J* = 7.9 Hz, 2H), 5.33 - 5.23 (m, 1H), 4.99 – 4.89 (m, 1H), 3.60 (dd, *J* = 7.1, 4.0 Hz, 2H), 2.28 (dd, *J* = 13.9, 8.2 Hz, 1H), 2.08 - 1.86 (m, 4H), 1.80 - 1.71 (m, 4H), 1.67 - 1.61 (m, 8H), 1.57 - 1.51 (m, 2H),

1.50 - 1.41 (m, 3 H), 1.30 (d, J=19.5 Hz, 3 H), 0.89 (s, 9 H). ^{13}C NMR (CDCl$_3$, 125 MHz) δ ppm 172.8, 172.6, 147.4, 147.4, 134.5, 134.3, 132.6, 132.0, 129.1, 124.1, 124.0, 120.4, 119.1, 111.1, 88.3, 50.0, 50.0, 46.8, 46.7, 40.8, 40.6, 35.8, 35.7, 31.4, 31.1, 29.8, 26.5, 26.4, 25.9, 25.9, 24.0, 23.8, 23.6, 22.1, 22.0, 20.6, 20.5, 17.8, 17.7. FT-IR (cm^{-1}, neat, ATR) 2958 (m), 2229 (w), 1726 (vs), 1210 (m), 1151 (vs), 835 (m). HRMS (EI) calcd for C$_{15}$H$_{24}$ [M$^+$ - C$_{14}$H$_{17}$NO$_2^+$]: 204.1878, found: 204.1883.
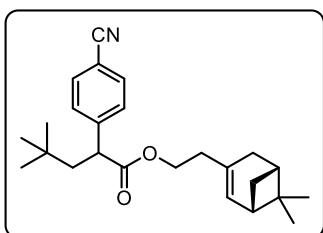
2-((1S,5R)-6,6-dimethylbicyclo[3.1.1]hept-2-en-3-yl)ethyl-2-(4-cyanophenyl)-4,4-dimethyl pentanoate, 3.48 (0.110 g, 58%) was prepared according to the general DCF procedure *with the following modifications:* 2-((1S)-6,6-dimethylbicyclo[3.1.1]hept-2-en-2-yl)ethyl acrylate (0.132 g, 0.600 mmol) was used in place of vinylBpin. The desired compound was obtained as a colorless oil. ^{1}H NMR (CDCl$_3$, 500 MHz) δ ppm 7.59 (dd, J = 8.3, 1.4 Hz, 2H), 7.43 (d, J = 7.9 Hz, 2H), 5.15 (dd, J = 19.0, 1.3 Hz, 1H), 4.12 – 4.05 (m, 1H), 4.05 – 3.98 (m, 1H), 3.67 (dd, J = 8.6, 4.2 Hz, 1H), 2.34 - 2.25 (m, 2H), 2.24 - 2.11 (m, 4H), 2.05 (br. s, 1H), 1.99 - 1.94 (m, 1H), 1.57 - 1.52 (m, 1H), 1.23 (s, 3H), 1.04 (dd, J = 17.2, 8.5 Hz, 1H), 0.88 (d, J = 0.9 Hz, 9H), 0.74 (d, J = 16.8 Hz, 3H). ^{13}C NMR (CDCl$_3$, 125 MHz) 173.9, 173.8, 146.6, 144.0, 132.7, 129.1, 119.2, 119.1, 119.0, 111.3, 63.6, 48.8, 47.4, 47.3, 45.9, 45.9, 40.9, 38.2, 38.2, 36.0, 31.9, 31.6, 31.4, 29.7, 26.5, 21.4, 21.3 FT-IR (cm^{-1}, neat, ATR) 2952 (w), 2914 (w), 2229 (w), 1732 (s), 1149 (vs), 837 (m). HRMS (EI) calcd for C$_{24}$H$_{31}$NO$_2$ [M$^+$]: 365.2355, found: 365.2363.
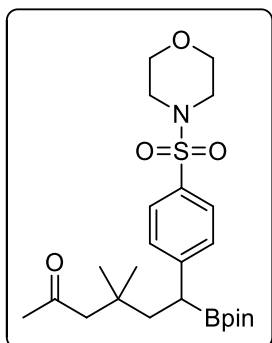
4,4-Dimethyl-6-(4-(morpholinosulfonyl)phenyl)-6-(4,4,5,5-tetramethyl-1,3,2-dioxaborolan-2-yl)hexan-2-one, 3.49 (0.186 g, 78%) was prepared according to the general DCF procedure. The

desired compound was obtained as a crystalline, white solid (mp = 133-135 ℃). **^{1}H NMR** (CDCl$_3$, 500 MHz) δ ppm 7.62 (d, *J* = 8.4 Hz, 2H), 7.39 (d, *J* = 8.2 Hz, 2H), 3.76 - 3.70 (m, 4H), 3.01 - 2.93 (m, 4H), 2.49 (dd, *J* = 8.9, 4.7 Hz, 1H), 2.33 (d, *J* = 4.7 Hz, 2H), 2.11 – 2.05 (m, 4H), 1.75 (dd, *J* = 13.5, 4.7 Hz, 1H), 1.13 (s, 12H), 1.02 (s, 3H), 0.99 (s, 3H). **^{13}C NMR** (CDCl$_3$, 125 MHz) δ ppm 208.6, 151.0, 132.0, 129.1, 128.2, 84.1, 66.4, 54.4, 46.3, 44.3, 34.8, 32.8, 27.7, 27.4, 24.8, 24.7. **^{11}B NMR** (CDCl$_3$, 128.4 MHz) δ 33.3. **FT-IR** (cm^{-1}, neat, ATR) 2975 (m), 1342 (s), 1152 (vs), 944 (s), 571 (m). **HRMS** (ESI) calcd for C$_{24}$H$_{39}$BNO$_6$S [M+H]$^+$: 480.2591, found: 480.2583.
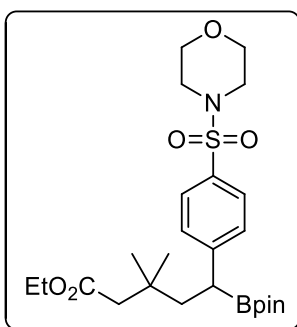
Ethyl 3,3-Dimethyl-5-(4-(morpholinosulfonyl)phenyl)-5-(4,4,5,5-tetramethyl-1,3,2-dioxaborolan-2-yl)pentanoate, 3.50 (0.172 g, 68%) was prepared according to the general DCF procedure. The desired compound was obtained as a crystalline, white solid (mp = 92-94 ℃). **^{1}H NMR** (CDCl$_3$, 500 MHz) δ ppm 7.62 (d, *J* = 8.2 Hz, 2H), 7.40 (d, *J* = 8.4 Hz, 2H), 4.08 (q, *J* = 7.1 Hz, 2H), 3.73 (t, *J* = 4.7 Hz, 4H), 2.97 (t, *J* = 4.4 Hz, 4H), 2.53 (dd, *J* = 9.2, 4.1 Hz, 1H), 2.21 (d, *J* = 2.1 Hz, 2H), 2.12 (dd, *J* = 13.6, 9.3 Hz, 1H), 1.69 (dd, *J* = 13.6, 4.3 Hz, 1H), 1.20 (t, *J* = 7.1 Hz, 3H), 1.13 (s, 12H), 1.01 (d, *J* = 8.2 Hz, 6H). **^{13}C NMR** (CDCl$_3$, 125 MHz) δ ppm 172.2, 151.0, 131.9, 129.1, 128.2, 84.0, 66.4, 60.2, 46.6, 46.3, 44.4, 34.6, 27.8, 27.4, 24.8, 24.7, 14.6. **^{11}B NMR** (CDCl$_3$, 128.4 MHz) δ 32.7. **FT-IR** (cm^{-1}, neat, ATR) 2986 (m), 1732 (s) 1360 (m) 1218 (vs) 903 (m). **HRMS** (ESI) calcd for C$_{25}$H$_{40}$BNO$_7$S [M+Na]$^+$: 532.2521, found: 532.2548.
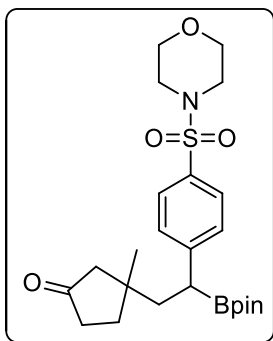
3-Methyl-3-(2-(4-(morpholinosulfonyl)phenyl)-2-(4,4,5,5-tetramethyl-1,3,2-dioxaborolan-2-yl)ethyl)cyclopentanone, 3.51 (0.155 g, 65%) was prepared according to the general DCF procedure.

The desired compound was obtained as a crystalline, white solid (mp = 215-217 °C). The diastereomeric ratio was 1.4:1 as determined by ^{1}H NMR analysis of the crude reaction. **^{1}H NMR** (CDCl$_3$, 500 MHz) δ ppm 7.63 (d, *J* = 7.8 Hz, 2H), 7.39 (d, *J* = 8.9 Hz, 2H), 3.78 - 3.68 (m, 4H), 3.00 – 2.95 (m, 4H), 2.58 - 2.47 (m, 1H), 2.34 - 2.20 (m, 3H), 2.15 - 1.67 (m, 5H), 1.14 (d, *J* = 1.7 Hz, 12H), 1.06 (s, 3H). **^{13}C NMR** (CDCl$_3$, 125 MHz) δ ppm 219.4, 219.3, 150.5, 150.4, 132.3, 132.2, 129.0, 128.4, 84.3, 84.2, 66.4, 52.8, 52.8, 46.3, 44.0, 43.9, 40.7, 36.9, 36.8, 35.7, 35.7, 30.0, 25.4, 25.3, 24.9, 24.8, 24.7. **^{11}B NMR** (CDCl$_3$, 128.4 MHz) δ 32.3. **FT-IR** (cm^{-1}, neat, ATR) 2976 (w), 2915 (w), 2855 (w), 1741 (s), 1344 (s), 1164 (vs). **HRMS** (ESI) calcd for C$_{24}$H$_{37}$BNO$_6$S [M+H]$^+$: 478.2435, found: 478.2422.
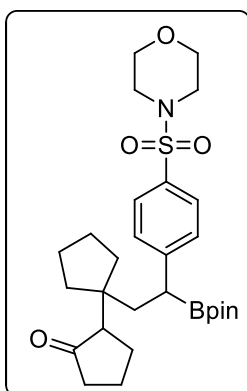
1'-(2-(4-(Morpholinosulfonyl)phenyl)-2-(4,4,5,5-tetramethyl-1,3,2-dioxaborolan-2-yl)ethyl)-[1,1'-bi(cyclopentan)]-2-one, 3.52 (0.092 g, 35%) was prepared according to the general DCF procedure *with the following modification*: The reaction was run for 48 h. The desired compound was obtained as a crystalline, white solid (mp = 141-143 °C). The diastereomeric ratio was 2.2:1 as determined by ^{1}H NMR analysis of the crude reaction. **^{1}H NMR** (CDCl$_3$, 500 MHz) δ ppm 7.61 (d, *J* = 8.1 Hz, 2H), 7.39 (d, *J* = 8.7 Hz, 2H), 3.77 - 3.69 (m, 4H), 3.01 - 2.93 (m, 4H), 2.49 – 2.41 (m, 1H), 2.36 - 2.12 (m, 3H), 2.12 - 1.88 (m, 4H), 1.81 - 1.31 (m, 10H), 1.14 (d, *J* = 2.0 Hz, 12H). **^{13}C NMR** (CDCl$_3$, 125 MHz) δ ppm 220.8, 220.6, 151.2, 131.9, 129.2, 129.1, 128.2, 128.2, 84.0, 66.4, 54.4, 54.2, 48.2, 48.2, 46.3, 41.0, 40.8, 39.1, 36.0, 35.5, 35.4, 34.7, 27.6, 27.0, 25.2, 25.1, 25.1, 25.0, 24.9, 24.8, 24.6, 20.5. **^{11}B NMR** (CDCl$_3$, 128.4 MHz) δ 33.2. **FT-IR** (cm^{-1}, neat, ATR) 2952 (m), 2870 (w), 1719 (s), 979 (m). **HRMS** (ESI) calcd for C$_{28}$H$_{43}$BNO$_6$S [M+H]$^+$: 532.2904, found: 532.2888.
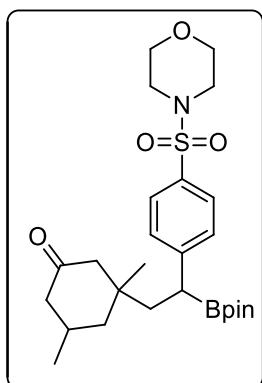
3,5-Dimethyl-3-(2-(4-(morpholinosulfonyl)phenyl)-2-(4,4,5,5-tetramethyl-1,3,2-dioxaborolan-2-yl)ethyl)cyclohexanone, **3.55**

172

(0.174 g, 69%) was prepared according to the general DCF procedure. The desired compound was obtained as a crystalline, white solid (mp = 208-209 °C). The diastereomeric ratio was 5:3:1 determined by ^{1}H NMR analysis of the crude reaction. **^{1}H NMR** (CDCl$_3$, 500 MHz) δ ppm 7.61 (d, J = 8.6 Hz, 2H), 7.37 (dd, J = 13.9, 8.2 Hz, 2H), 3.73 (t, J = 3.9 Hz, 4H), 3.00 - 2.94 (m, 4H), 2.72 - 2.40 (m, 1H), 2.37 - 2.26 (m, 1H), 2.21 - 1.82 (m, 5H), 1.79 - 1.55 (m, 2H), 1.55 - 1.31 (m, 1H), 1.13 (d, J = 7.2 Hz, 12H), 1.01 (t, J = 6.3 Hz, 3H), 0.96 - 0.87 (m, 3H). **^{13}C NMR** (CDCl$_3$, 125 MHz) δ ppm 211.5, 211.4, 150.7, 150.6, 132.1, 129.3, 129.2, 129.1, 129.0, 128.4, 128.3, 128.3, 84.2, 84.1, 66.4, 66.4, 53.3, 53.0, 49.7, 49.4, 47.2, 46.4, 46.3, 46.3, 45.5, 40.2, 39.3, 39.2, 29.7, 29.1, 29.0, 24.9, 24.8, 24.8, 24.7, 24.6, 23.8, 22.8. **^{11}B NMR** (CDCl$_3$, 128.4 MHz) δ 33.0. **FT-IR** (cm^{-1}, neat, ATR) 2958 (m), 1710 (m), 1348 (s), 1153 (vs) **HRMS** (EI) calcd for C$_{26}$H$_{40}$BNO$_6$S [M]$^+$: 505.2669, found: 505.2667.
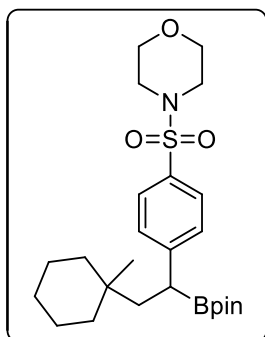
4-((4-(2-(1-Methylcyclohexyl)-1-(4,4,5,5-tetramethyl-1,3,2-dioxaborolan-2-yl)ethyl)phenyl)sulfonyl)morpholine, 3.56 (0.155g, 65%) was prepared according to the general DCF procedure. The desired compound was obtained as a crystalline, white solid (mp = 185-187 °C). **^{1}H NMR** (CDCl$_3$, 500 MHz) δ ppm 7.61 (d, J = 8.2 Hz, 2H), 7.41 (d, J = 8.2 Hz, 2H), 3.77 -3.69 (m, 4H), 3.03 - 2.92 (m, 4H), 2.52 (dd, J = 9.5, 3.7 Hz, 1H), 2.03 (dd, J = 13.4, 9.6 Hz, 1H), 1.55 (dd, J = 13.5, 3.9 Hz, 1H), 1.52 - 1.35 (m, 5H), 1.31 - 1.19 (m, 5H), 1.13 (d, J = 4.6 Hz, 12H), 0.88 (s, 3H). **^{13}C NMR** (CDCl$_3$, 125 MHz) δ ppm 151.9, 131.6, 129.1, 128.2, 83.9, 66.4, 46.3, 38.3, 38.2, 34.1, 26.7, 24.8, 24.6, 22.4, 22.3. **^{11}B NMR** (CDCl$_3$, 128.4 MHz) δ 33.8. **FT-IR** (cm^{-1}, neat, ATR) 2945 (m), 1455 (w), 1346 (s), 1169 (vs), 710 (vs). **HRMS** (ESI) calcd for C$_{25}$H$_{41}$BNO$_5$S [M+H]$^+$: 478.2799, found: 478.2808.

173
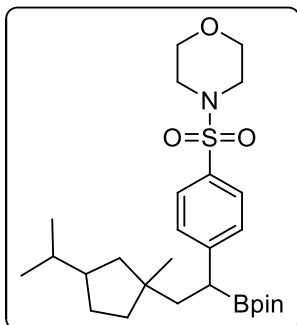
4-((4-(2-(3-Isopropyl-1-methylcyclopentyl)-1-(4,4,5,5-tetramethyl-1,3,2-dioxaborolan-2-yl)ethyl) phenyl)sulfonyl) Morpholine, 3.57 (0.205 g, 81%) was prepared according to the general DCF procedure. The desired compound was obtained as a crystalline, white solid (mp = 127-128 ℃). The diastereomeric ratio was 1.2:1.1:1.1:1 as determined by ^{1}H NMR analysis of the crude reaction. **^{1}H NMR** (CDCl$_3$, 500 MHz) δ ppm 7.61 (d, J = 7.9 Hz, 2H), 7.40 (d, J = 8.7 Hz, 2H), 3.73 (t, J = 4.5 Hz, 4H), 3.02 - 2.91 (m, 4H), 2.54 - 2.46 (m, 1H), 2.18 – 2.06 (m, 1H), 1.82 - 1.18 (m, 9H), 1.14 (s, 12H), 0.98 - 0.92 (m, 3H), 0.87 – 0.78 (m, 6H). **^{13}C NMR** (CDCl$_3$, 125 MHz) δ ppm 151.8, 151.7, 151.6, 131.7, 129.1, 128.2, 128.1, 83.9, 66.4, 47.5, 47.5, 46.7, 46.4, 46.3, 45.9, 45.9, 45.6, 45.4, 45.2, 45.0, 44.7, 44.4, 43.4, 43.4, 43.0, 40.6, 39.8, 39.7, 39.2, 34.4, 34.4, 34.3, 34.2, 30.4, 30.1, 30.0, 29.8, 29.6, 28.3, 28.1, 26.8. **^{11}B NMR** (CDCl$_3$, 128.4 MHz) δ 34.0. **FT-IR** (cm^{-1}, neat, ATR) 2952 (m), 1366 (m), 1321 (m), 1147 (vs), 1020 (m). **HRMS** (EI) calcd for C$_{27}$H$_{44}$BNO$_5$S [M]$^+$: 505.3033, found: 505.3027.
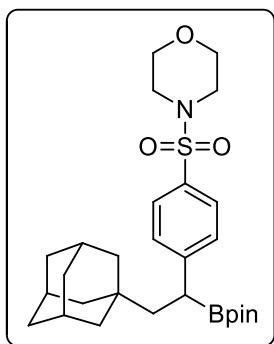
4-(Adamantan-1-yl)-1-(4,4,5,5-tetramethyl-1,3,2-dioxaborolan-2-yl)ethyl)phenyl)sulfonyl) morpholine, 3.58 (0.230 g, 89%) was prepared according to the general DCF procedure. The desired compound was obtained as a crystalline, white solid (mp = 219-220 ℃). **^{1}H NMR** (CDCl$_3$, 500 MHz) δ ppm 7.61 (d, J = 8.2 Hz, 2H), 7.39 (d, J = 8.2 Hz, 2H), 3.73 (t, J = 4.6 Hz, 4H), 2.97 (t, J = 4.3 Hz, 4H), 2.55 (dd, J = 9.6, 3.8 Hz, 1H), 1.97 - 1.85 (m, 4H), 1.72 – 1.58 (m, 6H), 1.55 – 1.40 (m, 6H), 1.38 (dd, J = 13.4, 3.8 Hz, 1H), 1.13 (d, J = 1.8 Hz, 12H) **^{13}C NMR** (CDCl$_3$, 125 MHz) δ ppm 151.8, 131.6, 129.1, 128.1, 83.9, 66.4, 46.9, 46.3, 42.9, 37.4, 33.6, 29.0, 24.8, 24.7. **^{11}B NMR** (CDCl$_3$,

128.4 MHz) δ 32.8. **FT-IR** (cm⁻¹, neat, ATR) 2900 (m), 2847 (w), 1344 (m), 1163 (s), 1114 (m), 945 (m). **HRMS** (ESI) calcd for $C_{28}H_{43}BNO_5S$ [M+H]⁺: 516.2955, found: 516.2964.
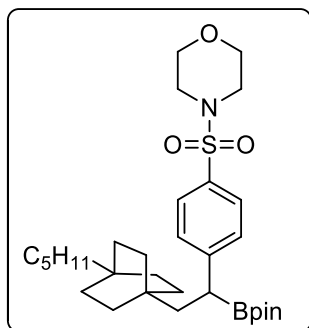
4-((4-(2-(4-Pentylbicyclo[2.2.2]octan-1-yl)-1-(4,4,5,5-tetramethyl-1,3,2-dioxaborolan-2-yl)ethyl)phenyl)sulfonyl)morpholine, **3.61** (0.220 g, 79%) was prepared according to the general DCF procedure *with the following modification:* The reaction was run for 48 h. The desired compound was obtained as a crystalline, white solid (mp = 199-200 ºC). **¹H NMR** (CDCl₃, 500 MHz) δ 7.60 (d, *J* = 8.2 Hz, 2H), 7.37 (d, *J* = 8.2 Hz, 2H), 3.73 (t, *J* = 4.3 Hz, 4H), 3.00 - 2.92 (m, 4H), 2.49 (dd, *J* = 9.5, 3.7 Hz, 1H), 1.91 (dd, *J* = 13.4, 9.8 Hz, 1H), 1.43 - 1.35 (m, 4H), 1.35 - 1.24 (m, 12H), 1.20 - 1.15 (m, 3H), 1.13 (s, 12H), 1.04 - 0.99 (m, 2H), 0.86 (t, *J* = 7.2 Hz, 3H). **¹³C NMR** (CDCl₃, 125 MHz) δ ppm 151.7, 131.6, 129.0, 128.1, 83.9, 66.4, 46.3, 44.1, 42.0, 33.2, 32.1, 31.8, 31.5, 30.8, 24.8, 24.7, 23.6, 23.0, 14.4. **¹¹B NMR** (CDCl₃, 128.4 MHz) δ 33.6. **FT-IR** (cm⁻¹, neat, ATR) 2926 (m), 1454 (w), 1352 (s), 1165 (vs), 945 (m). **HRMS** (ESI) calcd for $C_{31}H_{51}BNO_5S$ [M+H]⁺: 560.3581, found: 560.3568.
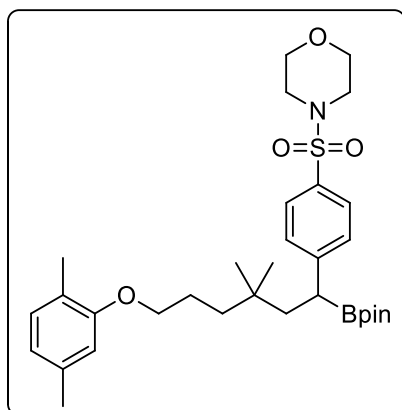
4-((4-(6-(2,5-Dimethylphenoxy)-3,3-dimethyl-1-(4,4,5,5-tetramethyl-1,3,2-dioxaborolan-2-yl)hexyl)phenyl)sulfonyl)morpholine, 3.63 (0.186 g, 64%) was prepared according to the general DCF procedure. The desired compound was obtained as a crystalline, white solid (mp = 99-100 ºC). **¹H NMR** (CDCl₃, 500 MHz) δ ppm 7.61 (d, *J* = 8.2 Hz, 2H), 7.40 (d, *J* = 8.2 Hz, 2H), 7.00 (d, *J* = 7.3 Hz, 1H), 6.65 (d, *J* = 7.5 Hz, 1H),

6.60 (s, 1H), 3.89 (t, J = 6.4 Hz, 2H), 3.73 (t, J = 4.6 Hz, 4H), 2.97 (t, J = 4.6 Hz, 4H), 2.51 (dd,

J = 9.4, 3.7 Hz, 1H), 2.30 (s, 3H), 2.18 (s, 3H), 2.07 (dd, J = 13.4, 9.5 Hz, 1H), 1.72 (dd, J =

14.2, 7.6 Hz, 2H), 1.57 (dd, J = 13.5, 3.9 Hz, 1H), 1.40 (t, J = 8.5 Hz, 2H), 1.13 (s, 12H), 0.91 (s,

6H). ^{13}C NMR (CDCl$_3$, 125 MHz) δ ppm 157.3, 151.6, 136.8, 131.8, 130.6, 129.1, 128.2, 123.8,

120.9, 84.0, 68.8, 66.4, 46.3, 44.4, 38.8, 34.0, 27.5, 27.4, 24.8, 24.7, 24.6, 21.7, 16.1. ^{11}B NMR

(CDCl$_3$, 128.4 MHz) δ 33.0. FT-IR (cm^{-1}, neat, ATR) 2956 (w), 2924 (w), 1351 (m), 1262 (m),

1165 (s), 945 (m). HRMS (EI) calcd for C$_{32}$H$_{48}$BNO$_6$S [M]$^+$: 608.3295, found: 608.3204.
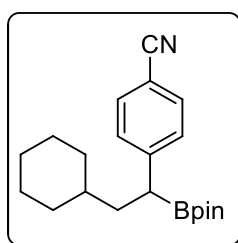
4-(2-Cyclohexyl-1-(4,4,5,5-tetramethyl-1,3,2-dioxaborolan-2-yl)ethyl)benzonitrile, 3.53 (0.068 g, 40%) was prepared according to the general DCF procedure *with the following modifications:* NiBr$_2$(phen) (10 mg, 0.05 mmol, 5 mol%) was used in place of NiBr$_2$(bpy). An excess of

vinylBpin was used (0.231 g, 1.50 mmol, 3.0 equiv). The desired compound **55** was obtained as a

crystalline, white solid (mp = 96-98 ºC). ^{1}H NMR (CDCl$_3$, 500 MHz) δ 7.53 (d, J = 8.1 Hz, 2H),

7.29 (d, J = 8.2 Hz, 2H), 2.52 (t, J = 8.1 Hz, 1H), 1.77 - 1.55 (m, 7H), 1.27 - 1.03 (m, 16H), 0.93

- 0.80 (m, 2H) ppm. ^{13}C NMR (CDCl$_3$, 125 MHz) δ 150.1, 132.3, 129.3, 119.7, 109.1, 83.9, 39.6,

36.8, 33.9, 33.1, 26.8, 26.5, 26.5, 24.8, 24.8 ppm. ^{11}B NMR (CDCl$_3$, 128.4 MHz) δ 32.1 FT-IR

(cm^{-1}, neat, ATR) 2921 (s), 2226 (m), 1606 (m), 1380 (vs), 1140 (s), 851 (m) HRMS (EI) calcd

for C$_{21}$H$_{30}$BNO$_2$ [M$^+$]: 339.2370, found: 339.2370.
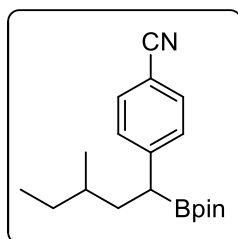
4-(3-Methyl-1-(4,4,5,5-tetramethyl-1,3,2-dioxaborolan-2-yl)pentyl)benzonitrile, 3.54 (0.089 g, 57%) was prepared according to the General Procedure *with the following modifications:* NiBr$_2$(phen) (10 mg, 0.05 mmol, 5 mol %) was used in place of NiBr$_2$(bpy). An excess of

vinylBpin was used (0.231 g, 1.50 mmol, 3.0 equiv). The desired compound was obtained as a

dense oil that solidified after standing overnight in a refrigerator (mp = 44-45 ºC). The diastereomeric ratio was 1.1:1 as determined by ^{1}H NMR analysis of the crude reaction. **^{1}H NMR** (CDCl$_3$, 500 MHz) δ 7.53 (d, J = 8.1 Hz, 2H), 7.30 (d, J = 8.5 Hz, 2H), 2.52 -2.48 (m, 1H), 1.91 - 1.69 (m, 1H), 1.62 – 1.42 (m, 1H), 1.41 - 1.23 (m, 2H), 1.20 - 1.13 (m, 13H), 0.87 - 0.79 (m, 6H). **^{13}C NMR** (CDCl$_3$, 125 MHz) δ 150.3, 150.0, 132.3, 129.3, 129.3, 119.6, 109.1, 83.9, 39.3, 38.6, 33.9, 33.3, 29.9, 29.3, 24.9, 24.8, 24.8, 19.7, 18.9, 11.5, 11.5 ppm. **^{11}B NMR** (CDCl$_3$, 128.4 MHz) δ 31.5 **FT-IR** (cm^{-1}, neat, ATR) 2961 (w), 2226 (w), 1462 (w), 1370 (s), 1326 (vs), 852 (m). **HRMS** (EI) calcd for C$_{19}$H$_{28}$BNO$_2$ [M$^+$] : 313.2213, found : 313.2220.
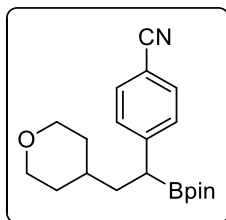
4-(2-(Tetrahydro-2H-pyran-4-yl)-1-(4,4,5,5-tetramethyl-1,3,2-dioxaborolan-2-yl)ethyl)benzonitrile, 3.59 (0.092 g, 54%) was prepared according to the general DCF procedure *with the following modifications:* Ni(phen)Br$_2$ (10 mg, 0.05 mmol, 5 mol %) was used in place of Ni(bpy)Br$_2$. An excess of vinylBpin was used (0.231 g, 1.50 mmol, 3.0 equiv). The desired compound was obtained as a colorless oil. **^{1}H NMR** (CDCl$_3$, 500 MHz) δ ppm 7.54 (d, J=8.2 Hz, 2H), 7.30 (d, J = 8.2 Hz, 2H), 3.92 (td, J = 11.2, 2.6 Hz, 2H), 3.27 (tt, J = 11.9, 2.6 Hz, 2H), 2.52 (t, J = 8.1 Hz, 1H), 1.80-1.74 (m, 1H), 1.69 (dd, J = 8.5, 5.6 Hz, 1H), 1.62 (d, J = 13.0 Hz, 1H), 1.52 (d, J = 12.4 Hz, 1H), 1.39-1.32 (m, 1H), 1.30-1.23 (m, 2H), 1.18 (d, J = 4.7 Hz, 12H) **^{13}C NMR** (CDCl$_3$, 125 MHz) 149.5, 132.5, 129.3, 119.5, 109.4, 84.1, 68.2, 39.0, 34.2, 33.7, 32.8, 24.8. **^{11}B NMR** (CDCl$_3$, 128.4 MHz) δ 32.5. **FT-IR** (cm^{-1}, neat, ATR) 2977 (m), 2926 (m), 2226 (w), 1371 (m), 1324 (m), 1140 (s). **HRMS** (EI) calcd for C$_{20}$H$_{28}$BNO$_3$ [M$^+$]: 341.2162, found: 341.2172.

177
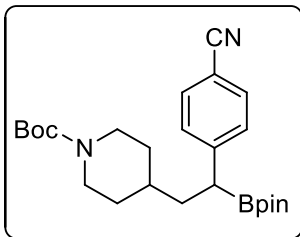
***tert*-Butyl-4-(2-(4-cyanophenyl)-2-(4,4,5,5-tetramethyl-1,3,2-dioxaborolan-2-yl)ethyl)piperidine-1-carboxylate, 3.60** (0.112 g, 51%) was prepared according to the general DCF procedure *with the following modifications:* Ni(phen)Br$_2$ (10 mg, 0.05 mmol, 5 mol %) was used in place of Ni(bpy)Br$_2$. An excess of vinylBpin was used (0.231 g, 1.50 mmol, 3.0 equiv). The desired compound was obtained as a colorless oil. **^{1}H NMR** (CDCl$_3$, 500 MHz) δ ppm 7.54 (d, *J* = 8.2 Hz, 2H), 7.29 (d, *J* = 8.2 Hz, 2H), 4.02 (br. s, 2H), 2.58 (br. s, 2H), 2.52 (t, *J* = 8.1 Hz, 1H), 1.79-1.72 (m, 1H), 1.71-1.62 (m, 2H), 1.58 (s, 1H), 1.44 (s, 9H), 1.17 (d, *J* = 4.9 Hz, 12H), 1.07 (t, *J* = 13.6 Hz, 2H). **^{13}C NMR** (CDCl$_3$, 125 MHz) 155.1, 149.5, 132.5, 129.2, 119.5, 109.4, 84.1, 79.5, 38.6, 35.2, 28.7, 24.9. **^{11}B NMR** (CDCl$_3$, 128.4 MHz) δ 32.8. **FT-IR** (cm^{-1}, neat, ATR) 2977 (m), 2926 (m), 2226 (w), 1689 (vs), 1365 (s), 1165 (m), 1142 (m). **HRMS** (EI) calcd for C$_{20}$H$_{28}$BN$_2$O$_2$ [M$^+$ - Boc]: 339.2244, found: 339.2231.
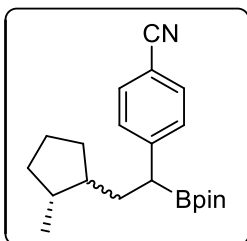
4-(2-(2-Methylcyclopentyl)-1-(4,4,5,5-tetramethyl-1,3,2-dioxaborolan-2-yl)ethyl)benzonitrile, 3.64 (0.090 g, 53%) was prepared according to the general DCF procedure *with the following modifications:* Ni(phen)Br$_2$ (10 mg, 0.05 mmol, 5 mol %) was used in place of Ni(bpy)Br$_2$. An excess of vinylBpin was used (0.231 g, 1.50 mmol, 3.0 equiv). The desired compound was obtained as a colorless oil. The diastereomeric ratio was 1.5:1 as determined by ^{1}H NMR analysis of the crude reaction. **^{1}H NMR** (CDCl$_3$, 500 MHz) δ ppm 7.53 (d, *J* = 8.1 Hz, 2H), 7.29 (d, *J* = 8.1 Hz, 2H), 2.44 (dd, *J* = 9.9, 5.8 Hz, 1H), 1.98 - 1.90 (m, 1H), 1.79 - 1.73 (m, 2H), 1.61 – 1.55 (m, 1H), 1.52 - 1.48 (m, 2H), 1.39 (pent, *J* = 7.5 Hz, 1H), 1.29 - 1.24 (m, 2H), 1.18 (m, 13H), 0.87 (d, *J* = 6.6 Hz, 3H). **^{13}C NMR** (CDCl$_3$, 125 MHz). 149.8, 132.4, 129.3, 119.6, 109.1, 83.9, 46.3, 40.8, 36.6, 35.0, 32.1, 24.9, 24.8, 23.6, 19.4. **^{11}B NMR** (CDCl$_3$, 128.4 MHz) δ 33.2. **FT-IR** (cm^{-1}, neat,

ATR). 2987 (m), 2221 (w), 1390 (m), 1120 (m), 871 (m). **HRMS** (EI) calcd for $C_{24}H_{31}NO_2$ [M$^+$]: 365.2355, found: 365.2363.
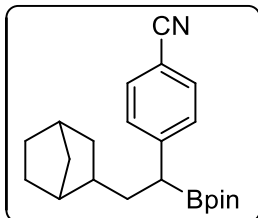
4-(2-(Bicyclo[2.2.1]heptan-2-yl)-1-(4,4,5,5-tetramethyl-1,3,2-dioxaborolan-2-yl)ethyl)benzonitrile, 3.65 (0.087 g, 50%) was prepared according to the general DCF procedure *with the following modifications:* Ni(phen)Br$_2$ (10 mg, 0.05 mmol, 5 mol %) was used in place of Ni(bpy)Br$_2$. An excess of vinylBpin was used (0.231 g, 1.50 mmol, 3.0 equiv). The desired compound was obtained as crystalline solid (mp = 69-71 °C). The diastereomeric ratio was 1.2:1 as determined by ^{1}H NMR analysis of the crude reaction. **^{1}H NMR** (CDCl$_3$, 500 MHz) δ ppm 7.53 (dd, J = 8.4, 1.8 Hz, 2H), 7.29 (dd, J = 8.2, 1.6 Hz, 2H), 2.43 (q, J = 7.3 Hz, 1H), 2.19 – 2.13 (m, 1H), 2.03 - 1.86 (m, 1H), 1.85 – 1.62 (m, 1H) 1.45 - 1.40 (m, 2H), 1.36 - 1.22 (m, 4H), 1.20 - 1.15 (m, 12H), 1.10 - 1.00 (m, 4H). **^{13}C NMR** (CDCl$_3$, 125 MHz) δ ppm 150.1, 149.9, 132.3, 129.5, 129.4, 119.7, 109.1, 83.9, 41.5, 41.4, 41.3, 40.9, 39.3, 39.0, 38.6, 38.0, 36.8, 35.6, 35.5, 30.3, 30.3, 29.0, 24.8. **^{11}B NMR** (CDCl$_3$, 128.4 MHz) δ 32.4. **FT-IR** (cm^{-1}, neat, ATR) 2947 (m), 2227 (w), 1353 (m), 1327 (m), 1142 (s), 850 (m). **HRMS** (EI) calcd for $C_{22}H_{30}BNO_2$ [M$^+$]: 351.2370, found: 351.2398.
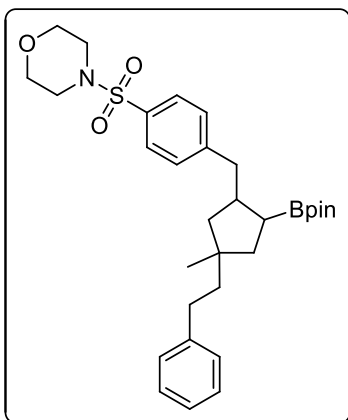
4-((4-((4-Methyl-4-phenethyl-2-(4,4,5,5-tetramethyl-1,3,2-dioxaborolan-2-yl)cyclopentyl)methyl) phenyl)sulfonyl) morpholine, 3.74 (0.197 g, 71%) was prepared according to the general DCF procedure. The desired compound **62** was obtained as a crystalline, white solid (mp = 101-103 °C). The diastereomeric ratio was 2.5:1.5:1 as determined by ^{1}H NMR

179

analysis of the crude reaction. ^{1}H NMR (CDCl$_3$, 500 MHz) δ ppm 7.64 (d, J = 8.2 Hz, 2H), 7.34 (d, J = 7.9 Hz, 2H), 7.29 - 7.22 (m, 2H), 7.20 - 7.12 (m, 3H), 3.77- 3.70 (m, 4H), 3.07 - 2.94 (m, 4H), 2.64 - 2.46 (m, 4H), 1.81 - 1.73 (m, 1H), 1.72 - 1.63 (m, 2H), 1.59 (dd, J = 11.9, 8.4 Hz, 1H), 1.55 (s, 2H), 1.53 - 1.47 (m, 1H), 1.29 - 1.23 (m, 13H), 1.14 and 0.98 (s, 3H total). ^{13}C NMR (CDCl$_3$, 125 MHz) δ ppm 148.8, 148.7, 143.8, 132.5, 129.8, 128.6, 128.6, 128.2, 125.8, 125.8, 83.4, 66.4, 46.6, 46.4, 46.3, 46.2, 44.0, 43.0, 42.8, 42.5, 42.1, 41.7, 41.3, 40.9, 40.6, 32.5, 31.8, 27.6, 26.0, 25.9, 25.3, 25.2. ^{11}B NMR (CDCl$_3$, 128.4 MHz) δ 34.1. FT-IR (cm^{-1}, neat, ATR) 2927 (w), 1371 (m), 1349 (s), 1165 (vs), 1113 (s), 942 (m). HRMS (EI) calcd for C$_{31}$H$_{44}$BNO$_5$SNa [M+Na]$^+$: 576.2931, found: 576.2958.
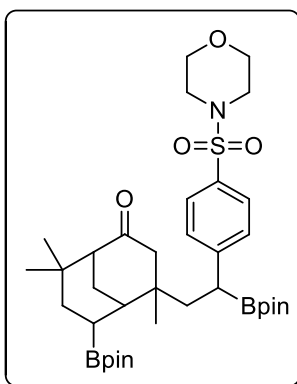
4,8,8-Trimethyl-4-(2-(4-(morpholinosulfonyl)phenyl)-2-(4,4,5,5-tetramethyl-1,3,2-dioxaborolan-2-yl)ethyl)-6-(4,4,5,5-tetramethyl-1,3,2-dioxaborolan-2-yl)bicyclo[3.3.1] Nonan-2-one,

3.76 (0.137 g, 40%) was prepared according to the general DCF procedure *with the following modification*: 2.5 equiv of vinylboronic acid pinacol ester were used. The desired compound **61** was obtained as a crystalline, white solid (mp = 120-121 ºC). The diastereomeric ratio was 5.8:1.8:1.3:1 as determined by HPLC analysis of the isolated material. ^{1}H NMR (CDCl$_3$, 500 MHz) δ ppm 7.60 (d, J = 8.2 Hz, 2H), 7.37 (d, J = 8.2 Hz, 2H), 3.76 - 3.71 (m, 4H), 3.00 - 2.94 (m, 4H), 2.48 (dd, J = 7.9, 4.7 Hz, 1H), 2.35 - 2.15 (m, 2H), 2.07 - 1.64 (m, 7H), 1.51 - 1.40 (m, 2H), 1.25 (d, J = 6.6 Hz, 12H), 1.13 (d, J = 4.3 Hz, 12H), 1.07 (s, 3H), 1.03 (s, 3H), 0.81 (s, 3H). ^{13}C NMR (CDCl$_3$, 125 MHz) δ ppm 214.1, 150.9, 131.9, 129.2, 128.3, 84.1, 83.5, 66.4, 57.4, 55.0, 46.4, 44.6, 42.6, 35.6, 35.4, 31.6, 29.7, 29.6, 27.8, 27.0, 25.3, 25.2, 24.9, 24.7. ^{11}B NMR (CDCl$_3$, 128.4 MHz) δ 34.9. FT-IR (cm^{-1}, neat, ATR) 2978 (w), 1793 (s), 1361 (vs),

1143 (vs), 1138 (vs), 935 (m). **HRMS** (EI) calcd for $C_{36}H_{58}B_2NO_8S$ $[M+H]^+$: 686.4069, found: 686.3861.

Peak#	Ret. Time	Area	Height	Mark	Conc.	Unit	ID#	Name	Area%
2	13.552	401080	29136	V	2.713				2.713
3	13.840	1176227	105082	V	7.956				7.956
4	14.081	564560	41450	V	3.819				3.819
5	15.916	415508	28669	V	2.811				2.811
6	16.534	2068995	160416	SV	13.995				13.995
7	17.803	364459	38251	V	2.465				2.465
8	18.719	1580914	157856	SV	10.694				10.694
9	20.769	6650686	697487	V	44.987				44.987
10	21.844	252139	30016	V	1.706				1.706
11	24.575	553006	49738	V	3.741				3.741
Total		14783592	1370494		100.000				100.000

3.6.9. Procedure for Large Scale Ni/Photoredox DCF Reaction
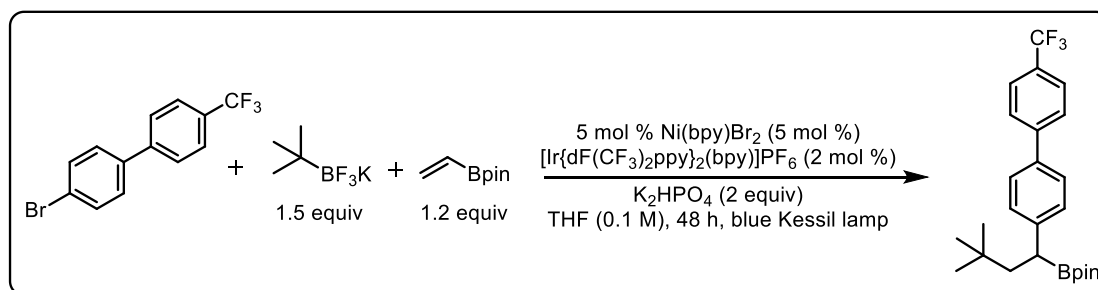
To a 100 mL Schlenk tube (dimensions: height = 15 cm, diameter = 4 cm) equipped with a stirrer bar was added ^{t}BuBF$_3$K (1.230 g, 7.50 mmol, 1.5 equiv), 4-bromo-4′-(trifluoromethyl)-1,1′-biphenyl (1.506 g, 5.00 mmol, 1 equiv), K$_2$HPO$_4$ (1.742 g, 10.0 mmol, 2 equiv), anhyd

NiBr$_2$(bpy) (0.094 g, 0.25 mmol, 5 mol %), and [Ir{dF(CF$_3$)$_2$ppy}$_2$(bpy)]PF$_6$ (0.101 g, 0.1 mmol, 2 mol %). The top of the vessel was sealed with a rubber septum, and the reaction was evacuated and backfilled with argon three times. The tube was charged with vinylboronic acid pinacol ester (0.924 g, 6.00 mmol, 1.2 equiv) dissolved in degassed THF (50 mL) via a syringe. The side-arm was closed, and the septum was sealed with Parafilm®. The tube was placed in front of two Kessil® H150 Blue lamps (24VDC, 1.5A, 30W) approximately 6 in away from the tube and irradiated for 48 h. The reaction was maintained at rt via air cooling by a clip fan. Below are pictures of the reaction set-up.

After confirmation that the reaction was complete by TLC, the crude reaction was filtered through a pad of Celite®, eluting with CH$_2$Cl$_2$. The filtrate was concentrated by rotary evaporation. The resulting light orange solid was recrystallized from MeOH to yield the desired cross-coupled product, **3.28** (1.863 g, 86%) as a white crystalline solid (mp = 118-120 ºC).

^{1}H NMR (CDCl$_3$, 500 MHz) δ ppm 7.67 (ABq, J_{AB} = 8.8 Hz, 4H), 7.49 (d, J = 8.1 Hz, 2H), 7.33 (d, J = 8.2 Hz, 2H), 2.45 (dd, J = 9.8, 3.6 Hz, 1H), 2.06 (dd, J = 13.3, 9.9 Hz, 1H), 1.50 - 1.56

(m, 1H), 1.16 (d, J = 1.7 Hz, 12H), 0.92 (s, 9H). ^{13}C NMR (CDCl$_3$, 125 MHz) δ ppm 145.6, 145.0, 136.6, 129.1, 127.4, 125.9 (q, $J_{C\text{-}C\text{-}F}$ = 3.6 Hz, C), 124.7 (q, $J_{C\text{-}F}$ = 271.6 Hz, CF$_3$), 83.6, 46.9, 31.7, 30.0, 24.9, 24.8. ^{11}B NMR (CDCl$_3$, 128.4 MHz) δ 33.1. ^{19}F NMR (CDCl$_3$, 471 MHz) δ ppm -62.3 (3F). FT-IR (cm^{-1}, neat, ATR) 2950 (m) 1573 (w), 1310 (vs), 1132 (m) 1087 (m). HRMS (EI) calcd for C$_{25}$H$_{32}$BF$_3$O$_2$ [M]$^+$: 432.2447, found: 432.2455.

3.6.10. Synthesis of a TK-666 Intermediate via Ni/Photoredox DCF/Oxidation Protocol
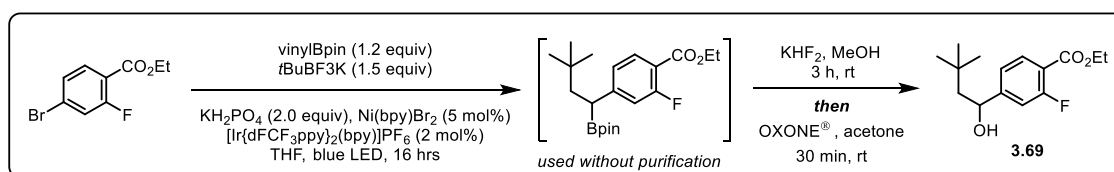
Ethyl 2-fluoro-4-(1-hydroxy-3,3-dimethylbutyl)benzoate, 3.69 (0.102 g, 77%) was prepared via a three-step reaction sequence.[31] Ethyl 4-bromo-2-fluorobenzoate (0.124 g, 0.500 mmol) was subjected to standard conditions used in General DCF procedure *with the following modification*. After 16 hours of irradiation the crude material was passed through a fritted disk filter and washed with THF (5 mL). The crude solution was concentrated to ~5 mL total volume. The reaction flask was placed in an ice/water bath and saturated aqueous KHF$_2$ (0.44 mL, 2.0 mmol, 4.5 M) was added dropwise. After stirring for 3 hours, the reaction was evaporated to dryness and the crude material was extracted with three portions of boiling acetone (~5 mL each). The solution was concentrated to ~3 mL total volume. Oxone$^®$ (0.308 g, 0.500 mmol, 1.0 equiv) in water (2.5 mL) was added in one portion. After stirring at room temperature for 30 min, saturated aqueous NH$_4$Cl (5 mL) was added and the mixture was extracted twice with ethyl acetate (5 mL each). The combined organic extracts were dried over sodium sulfate,

filtered and concentrated via rotary evaporation. The crude oil was purified via flash silica column chromatography (hexanes to 8:2 hexanes/EtOAc) to yield the desired compound, **69**, as a clear, colorless oil.

¹H NMR (CDCl₃, 500 MHz) δ ppm 7.86 (t, J = 8.1 Hz, 1H), 7.14 – 7.09 (m, 2H), 4.84 (d, J = 8.6 Hz, 1H), 4.37 (q, J = 7.2 Hz, 2H), 2.04 (br. s, 1H), 1.68 (dd, J = 14.6, 8.7 Hz, 1H), 1.53 (dd, J = 14.6, 3.0 Hz, 1H), 1.38 (t, J = 7.2 Hz, 3H), 1.00 (s, 9H).**¹³C NMR** (CDCl₃, 125 MHz) δ ppm 164.6 (d, J = 3.7 Hz), 162.4 (d, J = 261 Hz), 154.4 (d, J = 8.2 Hz), 132.5, 121.3 (d, J = 3.6 Hz), 117.8 (d, J = 10.0 Hz), 114.3 (d, J = 23 Hz), 71.8, 61.5, 52.3, 30.9, 30.4, 14.5. **¹⁹F NMR** (CDCl₃, 471 MHz) δ ppm -112.0. **FT-IR** (cm⁻¹, neat, ATR) 3456 (br), 2953 (m), 1711 (s), 1278 (vs), 1084 (vs), 775 (m). **HRMS** (EI) calcd for $C_{15}H_{21}FO_3$ [M⁺]: 268.1465, found: 268.1475.
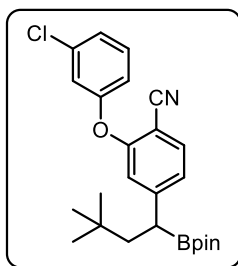
2-(3-Chlorophenoxy)-4-(3,3-dimethyl-1-(4,4,5,5-tetramethyl-1,3,2-dioxaborolan-2-yl)butyl) benzonitrile, 3.70 (0.136 g, 62%) was prepared according to the general DCF procedure. The desired compound was obtained as a colorless viscous oil. **¹H NMR** (CDCl₃, 500 MHz) δ ppm 7.53 (d, J = 8.1 Hz, 1H), 7.30 (t, J = 8.1 Hz, 1H), 7.16 (ddd, J = 7.0, 4.0, 2.6 Hz, 1H), 7.06 (dd, J = 8.1, 1.4 Hz, 1H), 7.00 (t, J=2.1 Hz, 1 H), 6.94 (ddd, J = 8.2, 2.3, 0.8 Hz, 1H), 6.84 (d, J = 1.2 Hz, 1H), 2.40 (dd, J = 9.0, 4.6 Hz, 1H), 1.90 (dd, J = 13.4, 9.0 Hz, 1 H), 1.43 (dd, J=13.4, 4.6 Hz, 1H), 1.12 (d, J=5.5 Hz, 12H), 0.85 (s, 9H).**¹³C NMR** (CDCl₃, 125 MHz) δ ppm 158.6, 156.9, 153.9, 135.6, 133.9, 131.0, 124.9, 124.4, 119.7, 118.4, 117.7, 116.4, 101.6, 84.0, 46.0, 31.8,

29.9, 24.8, 24.7. ¹¹**B NMR** (CDCl₃, 128.4 MHz) 32.3. **FT-IR** (cm⁻¹, neat, ATR) 2891 (w), 2229 (w), 1239 (vs), 1138 (s), 1110 (m), 848 (m). **HRMS** (EI) calcd for $C_{25}H_{31}BClNO_3$ [M⁺]: 439.2086, found: 439.2087.
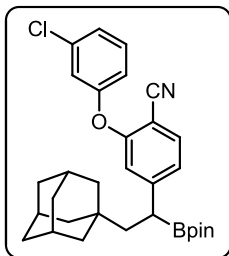
4-(2-(Adamantan-1-yl)-1-(4,4,5,5-tetramethyl-1,3,2-dioxaborolan-2-yl)ethyl)-2-(3-chloro phenoxy)benzonitrile, 3.71 (0.142 g, 55%) was prepared according to the general DCF procedure. The desired compound was obtained as a white foam. ¹**H NMR** (CDCl₃, 500 MHz) δ ppm 7.53 (d, J = 8.1 Hz, 1H), 7.30 (t, J = 8.1 Hz, 1H), 7.16 (ddd, J = 7.0, 4.0, 2.6 Hz, 1H), 7.06 (dd, J = 8.1, 1.4 Hz, 1H), 7.00 (t, J=2.1 Hz, 1 H), 6.94 (ddd, J = 8.2, 2.3, 0.8 Hz, 1H), 6.84 (d, J = 1.2 Hz, 1H), 2.40 (dd, J = 9.0, 4.6 Hz, 1H), 1.90 (dd, J = 13.4, 9.0 Hz, 1 H), 1.43 (dd, J=13.4, 4.6 Hz, 1H), 1.12 (d, J=5.5 Hz, 12H), 0.85 (s, 9H). ¹³**C NMR** (CDCl₃, 125 MHz) δ ppm 158.5, 157.0, 154.1, 135.6, 133.9, 131.0, 124.9, 124.5, 119.7, 118.6, 117.7, 116.4, 101.5, 84.0, 46.6, 42.9, 37.3, 33.7, 28.9, 24.8, 24.7. ¹¹**B NMR** (CDCl₃, 128.4 MHz) 33.2. **FT-IR** (cm⁻¹, neat, ATR) 2901 (m), 2846 (w), 2229 (w), 1358 (m), 1239 (vs), 1140 (s), 840 (m), 778 (w). **HRMS** (EI) calcd for $C_{31}H_{37}BClNO_3$ [M⁺]: 517.2555, found: 517.2540.
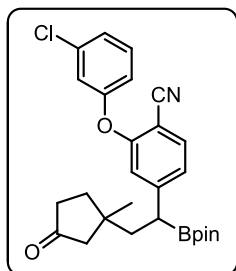
2-(3-Chlorophenoxy)-4-(2-(1-methyl-3-oxocyclopentyl)-1-(4,4,5,5-tetramethyl-1,3,2-dioxaborolan-2-yl)ethyl)benzonitrile, 3.72 (0.190 g, 79%) was prepared according to the general DCF procedure. The desired compound, **72**, was obtained as a yellow-tinted oil. ¹**H NMR**

(CDCl$_3$, 500 MHz) δ ppm 7.55 (dd, J = 8.1, 3.2 Hz, 1H), 7.31 (t, J = 8.2 Hz, 1H), 7.17 (ddd, J = 7.9, 1.8, 0.8 Hz, 1H), 7.07 - 7.02 (m, 1H), 7.02 - 6.98 (m, 1H), 6.97 - 6.93 (m, 1H), 6.81 (dd, J = 12.2, 1.4 Hz, 1H), 2.40 (dd, J = 8.2, 5.6 Hz, 1H), 2.28 - 2.21 (m, 2 H), 2.14 – 2.09 (m, 1H), 2.08 - 2.00 (m, 1 H), 1.89 (d, J = 6.1 Hz, 1H), 1.79 - 1.73 (m, 1H), 1.69 - 1.64 (m, 2H), 1.13 (d, J = 3.2 Hz, 12 H), 1.00 (s, 3 H). ^{13}C NMR (CDCl$_3$, 125 MHz) δ ppm 219.3, 158.8, 158.8, 156.7, 156.7, 152.8, 152.6, 135.6, 134.2, 131.1, 125.1, 124.2, 119.9, 119.8, 118.2, 118.1, 117.9, 117.8, 116.1, 101.9, 84.3, 84.3, 52.8, 52.7, 43.7, 40.7, 40.6, 36.9, 36.7, 35.7, 25.2, 24.9, 24.8, 24.7. ^{11}B NMR (CDCl$_3$, 128.4 MHz) 33.4. FT-IR (cm^{-1}, neat, ATR) 2977 (w), 2229 (w), 1738 (m), 1371 (m), 1138 (vs), 849 (m). HRMS (EI) calcd for C$_{27}$H$_{31}$BClNO$_4$ [M$^+$]: 479.2035, found: 479.2041.

3.6.11. Synthesis of a TK-666 Derivative via Oxidation
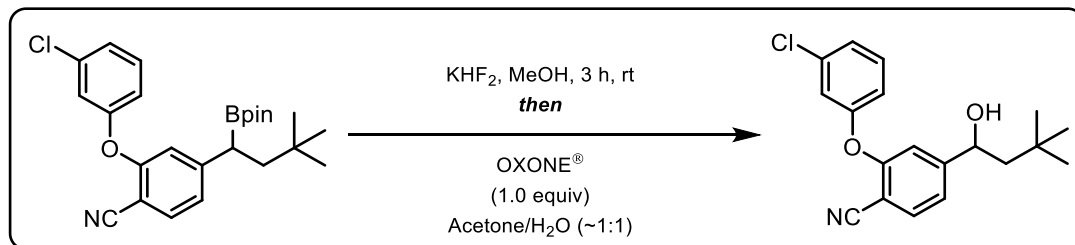
2-(3-Chlorophenoxy)-4-(1-hydroxy-3,3-dimethylbutyl)benzonitrile, 3.70a (0.143 g, 71%) was prepared from 2-(3-chlorophenoxy)-4-(3,3-dimethyl-1-(4,4,5,5-tetramethyl-1,3,2-dioxaborolan-2-yl)butyl)benzonitrile **68** (0.269 g, 0.611 mmol) in a two-step reaction sequence. Intermediate **3.70** was converted to the corresponding organotrifluoroborate using GPA3 (*see page S13*). The resulting solid (0.190 g, 0.453 mmol) was then dissolved in acetone (3 mL) and a solution Oxone® (0.278 g, 0.453

mmol, 1.0 equiv) in water (2.5 mL) was added in one portion. After stirring at room temperature for 30 min, saturated aqueous NH₄Cl (5 mL) was added and the mixture was extracted twice with ethyl acetate (5 mL each). The combined organic extracts were dried over sodium sulfate, filtered and concentrated via rotary evaporation. The crude oil was purified via flash silica column chromatography to yield the desired compound, **68a**, as a clear, colorless oil.

^{1}H NMR (CDCl₃, 500 MHz) δ ppm 7.63 (d, J = 7.9 Hz, 1H), 7.32 (t, J = 8.1 Hz, 1H), 7.19 (dd, J = 8.1, 0.9 Hz, 1H), 7.14 (d, J = 7.9, 0.9 Hz, 1H), 7.06 (m, 1H), 6.96 (m, 2H), 4.86 - 4.77 (m, 1H), 1.80 (d, J = 3.4 Hz, 1H), 1.63 (dd, J = 14.6, 8.9 Hz, 1H), 1.48 (dd, J = 14.6, 2.4 Hz, 1H), 0.99 (s, 9H). **^{13}C NMR** (CDCl₃, 125 MHz) δ ppm 159.2, 156.5, 154.5, 135.7, 134.3, 131.2, 125.3, 121.4, 120.1, 117.9, 115.9, 115.4, 103.3, 72.0, 53.4, 31.0, 30.4. **FT-IR** (cm⁻¹, neat, ATR) 3436 (br w) 2952 (m), 2237 (w), 1566 (m), 1243 (vs), 1243 (s), 1109 (m), 871 (m), 678 (m). **HRMS** (EI) calcd for C₁₉H₂₀ClNO₂ [M⁺]: 329.1183, found: 329.1190.

3.6.12. Crystallographic Data

X-ray Structure Determination of Compound 3.3
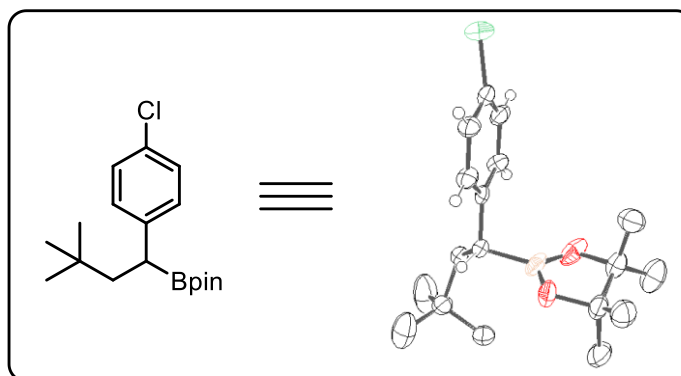
Compound **3.3**, $C_{18}H_{28}O_2BCl$, crystallizes in the triclinic space group $P\bar{1}$ with a=9.2264(4)Å, b=9.8051(4)Å, c=12.0617(6)Å, α=112.120(2)°, β=103.086(2)°, γ=101.278(2)°, V=935.71(7)Å^3, Z=2, and d$_{calc}$=1.145 g/cm$_3$. X-ray intensity data were collected on a Bruker APEXII [1] CCD area detector employing graphite-monochromated Mo-Kα radiation (λ=0.71073Å) at a temperature of 173K. Preliminary indexing was performed from a series of thirty-six 0.5° rotation frames with exposures of 10 seconds. A total of 2724 frames were collected with a crystal to detector distance of 37.5 mm, rotation widths of 0.5° and exposures of 15 seconds:

scan type	2θ	ω	φ	χ	Frames
φ	-23.00	315.83	12.48	28.88	739
ω	-5.50	321.59	133.99	70.63	69

scan type	2θ	ω	φ	χ	Frames
φ	-23.00	334.21	38.95	73.66	739
φ	24.50	7.41	12.48	28.88	739
φ	-25.50	323.22	190.42	83.36	438

Rotation frames were integrated using SAINT [2], producing a listing of unaveraged F^2 and $\sigma(F^2)$ values. A total of 22602 reflections were measured over the ranges $3.862 \leq 2\theta \leq 55.014°$, $-11 \leq h \leq 11$, $-12 \leq k \leq 12$, $-15 \leq l \leq 15$ yielding 4181 unique reflections (R_{int} = 0.0306). The intensity data were corrected for Lorentz and polarization effects and for absorption using SADABS [3] (minimum and maximum transmission 0.6228, 0.7456). The structure was solved by direct methods – ShelXS-97 [4]. The CH_2-CH-PhCl substituent is disordered in two different orientations in a ratio of 55:45. Refinement was by full-matrix least squares based on F^2 using SHELXL-2017 [5]. All reflections were used during refinement. The weighting scheme used was $w=1/[\sigma^2(F_o^2) + (0.0869P)^2 + 0.6032P]$ where $P = (F_o^2 + 2F_c^2)/3$. Non-hydrogen atoms were refined anisotropically and hydrogen atoms were refined using a riding model. Refinement converged to R1=0.0613 and wR2=0.1682 for 3338 observed reflections for which $F > 4\sigma(F)$ and R1=0.0751 and wR2=0.1802 and GOF =1.030 for all 4181 unique, non-zero reflections and 263 variables. The maximum Δ/σ in the final cycle of least squares was 0.000 and the two most prominent peaks in the final difference Fourier were +0.69 and -0.40 e/$Å^3$.
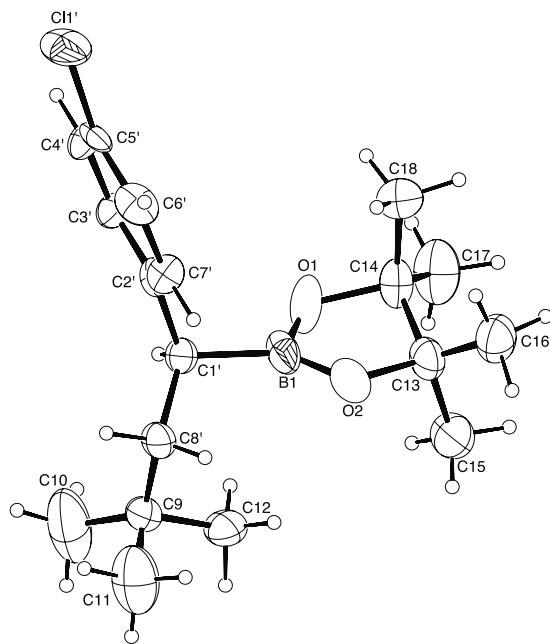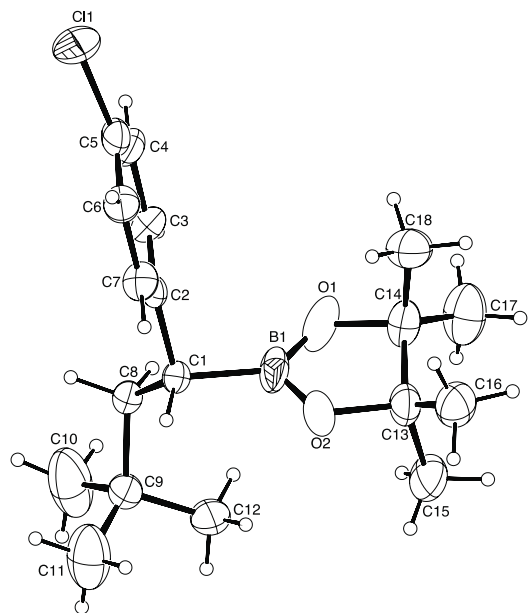
ORTEP drawing of the two disorder models with 50% thermal ellipsoids.

Table 3.12. Summary of Structure Determination of Compound **3.3**

Empirical formula $C_{18}H_{28}O_2BCl$

Formula weight 322.66

Temperature/K	173
Crystal system	triclinic
Space group	P$\overline{1}$
a	9.2264(4)Å
b	9.8051(4)Å
c	12.0617(6)Å
α	112.120(2)°
β	103.086(2)°
γ	101.278(2)°
Volume	935.71(7)Å^3
Z	2
d$_{calc}$	1.145 g/cm^3
μ	0.208 mm^{-1}
F(000)	348.0
Crystal size, mm	0.17 × 0.16 × 0.04
2θ range for data collection	3.862 - 55.014°
Index ranges	-11 ≤ h ≤ 11, -12 ≤ k ≤ 12, -15 ≤ l ≤ 15
Reflections collected	22602
Independent reflections	4181[R(int) = 0.0306]
Data/restraints/parameters	4181/108/263
Goodness-of-fit on F^2	1.030
Final R indexes [I>=2σ (I)]	R$_1$ = 0.0613, wR$_2$ = 0.1682
Final R indexes [all data]	R$_1$ = 0.0751, wR$_2$ = 0.1802

Largest diff. peak/hole   0.69/-0.40 eÅ^{-3}

Table 3.13. Refined Positional Parameters for Compound **3.3**

Atom	x	y	z	U(eq)
O1	0.79119(18)	0.9307(2)	0.33128(17)	0.0600(5)
O2	0.71082(19)	0.7671(2)	0.12189(19)	0.0563(5)
C1	0.9897(4)	0.7974(4)	0.2176(4)	0.0292(7)
C2	1.0967(7)	0.9542(6)	0.2380(4)	0.0254(11)
C3	1.1666(8)	1.0760(8)	0.3596(4)	0.0319(13)
C4	1.2613(11)	1.2174(8)	0.3777(7)	0.0387(15)
C5	1.2861(13)	1.2370(9)	0.2740(9)	0.041(2)
C6	1.2163(13)	1.1152(10)	0.1524(8)	0.0387(14)
C7	1.1216(10)	0.9738(8)	0.1343(4)	0.0340(11)
Cl1	1.4271(10)	1.4016(9)	0.2938(10)	0.0634(13)
C1'	1.0071(5)	0.8428(5)	0.2925(5)	0.0318(8)
C2'	1.1068(9)	0.9804(7)	0.2849(5)	0.0263(14)
C3'	1.1976(10)	1.1138(9)	0.3957(5)	0.0345(15)
C4'	1.2956(13)	1.2364(9)	0.3892(9)	0.039(2)
C5'	1.3027(16)	1.2256(11)	0.2720(11)	0.0308(17)
C6'	1.2119(15)	1.0922(12)	0.1613(8)	0.0416(19)
C7'	1.1139(11)	0.9696(9)	0.1677(5)	0.0321(16)
Cl1'	1.4132(10)	1.3842(10)	0.2694(12)	0.0627(16)

C8	1.0633(4)	0.7438(4)	0.3151(3)	0.0325(7)
C8'	1.0202(5)	0.6855(5)	0.2088(4)	0.0355(9)
C9	0.9905(2)	0.5664(2)	0.2721(2)	0.0461(5)
C10	1.0982(5)	0.5654(5)	0.3863(3)	0.1075(16)
C11	0.9945(4)	0.4367(5)	0.1561(3)	0.0801(10)
C12	0.8250(3)	0.5380(3)	0.2786(2)	0.0482(5)
C13	0.5719(2)	0.8042(3)	0.1468(2)	0.0442(5)
C14	0.6455(2)	0.9539(3)	0.2724(2)	0.0468(5)
C15	0.4752(3)	0.6702(3)	0.1613(4)	0.0716(9)
C16	0.4786(3)	0.8205(3)	0.0361(2)	0.0554(6)
C17	0.5543(3)	0.9833(4)	0.3620(3)	0.0700(8)
C18	0.6939(3)	1.0981(3)	0.2492(3)	0.0603(7)
B1	0.8288(3)	0.8350(3)	0.2337(4)	0.0557(8)

Table 3.14. Positional Parameters for Hydrogens in Compound **3.3**

Atom	x	y	z	U(eq)
H1	0.967821	0.716581	0.129717	0.035
H3	1.149623	1.062598	0.430209	0.038
H4	1.308807	1.300308	0.460528	0.046
H6	1.233199	1.12858	0.081771	0.046
H7	1.074053	0.890856	0.051446	0.041
H1'	1.030414	0.859065	0.382485	0.038

H3'	1.192784	1.121139	0.475489	0.041
H4'	1.357413	1.327282	0.4646	0.046
H6'	1.2167	1.084867	0.081452	0.05
H7'	1.05205	0.878706	0.092322	0.039
H8a	1.049085	0.802795	0.396687	0.039
H8b	1.177214	0.767554	0.329376	0.039
H8a'	1.125611	0.700025	0.200201	0.043
H8b'	0.941861	0.641493	0.123176	0.043
H10a	1.206662	0.595731	0.388054	0.161
H10b	1.070081	0.461088	0.381404	0.161
H10c	1.087674	0.638769	0.463718	0.161
H11a	0.918986	0.428162	0.080263	0.12
H11b	0.967126	0.339044	0.162883	0.12
H11c	1.099843	0.458633	0.149962	0.12
H12a	0.823641	0.621755	0.354759	0.072
H12b	0.791068	0.438868	0.281902	0.072
H12c	0.753916	0.535057	0.203214	0.072
H15a	0.462067	0.571887	0.090439	0.107
H15b	0.372267	0.68217	0.161281	0.107
H15c	0.529435	0.67057	0.241324	0.107
H16a	0.54651	0.893714	0.017973	0.083
H16b	0.392941	0.859039	0.056193	0.083
H16c	0.43521	0.719383	-0.038304	0.083
H17a	0.53561	0.897626	0.385484	0.105

H17b	0.453753	0.991159	0.32089	0.105		
H17c	0.613573	1.080307	0.438253	0.105		
H18a	0.76453	1.185663	0.328747	0.09		
H18b	0.600291	1.12393	0.218088	0.09		
H18c	0.747399	1.076229	0.185963	0.09		

Table 3.15. Refined Thermal Parameters (U's) for Compound **3.3**

Atom	U_{11}	U_{22}	U_{33}	U_{23}	U_{13}	U_{12}
O1	0.0271(7)	0.0923(14)	0.0692(11)	0.0524(11)	0.0069(7)	0.0127(8)
O2	0.0417(9)	0.0551(10)	0.0920(13)	0.0368(9)	0.0388(9)	0.0283(7)
C1	0.0232(15)	0.0297(18)	0.0357(19)	0.0128(15)	0.0142(15)	0.0085(12)
C2	0.0238(16)	0.0295(19)	0.029(3)	0.013(2)	0.017(3)	0.0118(14)
C3	0.027(3)	0.038(4)	0.026(3)	0.013(2)	0.008(3)	0.003(2)
C4	0.023(4)	0.042(3)	0.043(3)	0.013(2)	0.012(2)	0.0060(19)
C5	0.029(3)	0.039(4)	0.066(4)	0.028(3)	0.026(3)	0.016(3)
C6	0.039(3)	0.039(3)	0.056(3)	0.033(2)	0.023(2)	0.014(2)
C7	0.036(2)	0.043(2)	0.035(3)	0.024(2)	0.019(2)	0.0125(17)
Cl1	0.0530(13)	0.0424(14)	0.094(2)	0.0328(13)	0.0308(11)	0.0004(9)
C1'	0.0253(19)	0.033(2)	0.040(2)	0.016(2)	0.0157(19)	0.0103(16)
C2'	0.022(2)	0.040(4)	0.028(4)	0.020(3)	0.016(3)	0.015(3)
C3'	0.029(4)	0.032(4)	0.038(4)	0.013(3)	0.009(3)	0.005(3)
C4'	0.022(5)	0.037(3)	0.054(3)	0.019(3)	0.014(3)	0.002(2)

C5'	0.028(3)	0.028(3)	0.059(4)	0.029(3)	0.028(3)	0.020(3)
C6'	0.053(4)	0.050(4)	0.045(3)	0.033(3)	0.029(3)	0.025(4)
C7'	0.033(3)	0.039(3)	0.026(3)	0.014(3)	0.016(3)	0.010(2)
Cl1'	0.057(3)	0.043(2)	0.118(5)	0.049(3)	0.054(3)	0.019(2)
C8	0.0251(15)	0.0318(17)	0.0410(19)	0.0164(14)	0.0105(13)	0.0090(12)
C8'	0.030(2)	0.035(2)	0.047(3)	0.0180(19)	0.0191(18)	0.0145(16)
C9	0.0342(10)	0.0346(11)	0.0728(15)	0.0273(10)	0.0160(10)	0.0123(8)
C10	0.083(2)	0.133(4)	0.0635(19)	-0.0003(19)	-0.0058(16)	0.068(2)
C11	0.0671(18)	0.120(3)	0.0595(16)	0.0324(17)	0.0301(14)	0.0461(19)
C12	0.0435(12)	0.0365(11)	0.0699(15)	0.0269(10)	0.0245(11)	0.0095(9)
C13	0.0326(10)	0.0506(12)	0.0611(13)	0.0295(10)	0.0224(9)	0.0191(9)
C14	0.0320(10)	0.0632(14)	0.0462(12)	0.0242(10)	0.0116(9)	0.0182(9)
C15	0.0425(13)	0.0619(17)	0.133(3)	0.0590(18)	0.0405(16)	0.0183(11)
C16	0.0454(13)	0.0596(15)	0.0482(13)	0.0149(11)	0.0077(10)	0.0167(11)
C17	0.0581(16)	0.109(3)	0.0523(14)	0.0350(15)	0.0295(12)	0.0338(16)
C18	0.0568(15)	0.0439(14)	0.0719(17)	0.0244(12)	0.0122(13)	0.0114(11)
B1	0.0276(11)	0.0587(16)	0.115(2)	0.0650(18)	0.0319(14)	0.0193(11)

Table 3.16. Bond Distances in Compound 3.3, **Å**

O1-C14	1.473(3)	O1-B1	1.366(4)	O2-C13	1.463(2)
O2-B1	1.350(4)	C1-C2	1.553(6)	C1-C8	1.538(5)
C1-B1	1.633(4)	C2-C3	1.3950	C2-C7	1.3950

196

C3-C4	1.3950	C4-C5	1.3952	C5-C6	1.3949
C5-Cl1	1.761(10)	C6-C7	1.3950	C1'-C2'	1.523(7)
C1'-C8'	1.539(6)	C1'-B1	1.611(5)	C2'-C3'	1.3950
C2'-C7'	1.3951	C3'-C4'	1.3950	C4'-C5'	1.3948
C5'-C6'	1.3950	C5'-Cl1'	1.700(11)	C6'-C7'	1.3951
C8-C9	1.566(4)	C8'-C9	1.632(5)	C9-C10	1.510(4)
C9-C11	1.509(4)	C9-C12	1.522(3)	C13-C14	1.543(3)
C13-C15	1.528(3)	C13-C16	1.498(3)	C14-C17	1.493(3)
C14-C18	1.544(4)				

Table 3.17. Bond Angles in Compound 3.3, °

B1-O1-C14	106.11(18)	B1-O2-C13	107.7(2)	C2-C1-B1	103.3(3)
C8-C1-C2	111.7(3)	C8-C1-B1	111.9(3)	C3-C2-C1	120.0(3)
C3-C2-C7	120.0	C7-C2-C1	120.0(3)	C2-C3-C4	120.0
C3-C4-C5	120.0	C4-C5-Cl1	121.6(6)	C6-C5-C4	120.0
C6-C5-Cl1	117.7(6)	C5-C6-C7	120.0	C6-C7-C2	120.0
C2'-C1'-C8'	114.1(4)	C2'-C1'-B1	104.9(4)	C8'-C1'-B1	105.4(4)
C3'-C2'-C1'	120.0(4)	C3'-C2'-C7'	120.0	C7'-C2'-C1'	119.9(4)
C2'-C3'-C4'	120.0	C5'-C4'-C3'	120.0	C4'-C5'-C6'	120.0
C4'-C5'-Cl1'	117.7(7)	C6'-C5'-Cl1'	122.1(7)	C5'-C6'-C7'	120.0
C2'-C7'-C6'	120.0	C1-C8-C9	112.9(3)	C1'-C8'-C9	110.0(3)
C10-C9-C8	94.8(3)	C10-C9-C8'	128.7(3)	C10-C9-C12	109.1(3)
C11-C9-C8	125.9(3)	C11-C9-C8'	90.1(3)	C11-C9-C10	107.2(2)
C11-C9-C12	109.9(2)	C12-C9-C8	108.2(2)	C12-C9-C8'	109.3(2)
O2-C13-C14	101.70(17)	O2-C13-C15	107.94(19)	O2-C13-C16	108.56(19)
C15-C13-C14	112.6(2)	C16-C13-C14	115.6(2)	C16-C13-C15	109.8(2)
O1-C14-C13	101.83(18)	O1-C14-C17	109.14(19)	O1-C14-C18	106.91(19)
C17-C14-C13	117.2(2)	C17-C14-C18	109.5(2)	C18-C14-C13	111.58(19)
O1-B1-C1	134.6(3)	O1-B1-C1'	106.6(3)	O2-B1-O1	113.10(19)
O2-B1-C1	112.0(3)	O2-B1-C1'	140.3(3)		

This report has been created with Olex2, compiled on 2018.05.29 svn.r3508 for OlexSys.

X-ray Structure Determination of Compound 3.76
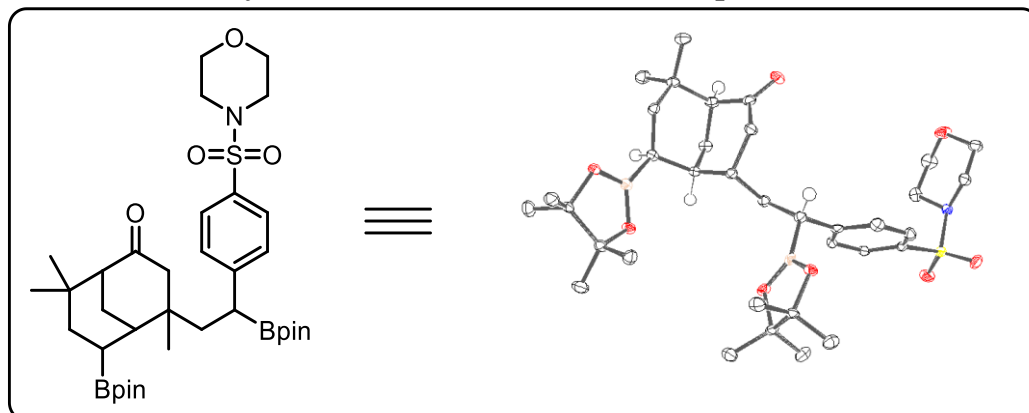
Compound **3.76**, $C_{37}H_{59}B_2Cl_2NO_8S$, crystallizes in the triclinic space group $P\bar{1}$ with a=11.9599(6)Å, b=13.0727(6)Å, c=14.6426(7)Å, α=106.075(2)°, β=108.081(2)°, γ=102.136(2)°, V=1978.23(17)Å^3, Z=2, and d_{calc}=1.293 g/cm$_3$. X-ray intensity data were collected on a [1] CMOS area detector employing graphite-monochromated Mo-Kα radiation (λ=0.71073Å) at a temperature of 100K. Preliminary indexing was performed from a series of twenty-four 0.5° rotation frames with exposures of 10 seconds. A total of 2460 frames were collected with a crystal to detector distance of 33.0 mm, rotation widths of 0.5° and exposures of 5 seconds:

scan type	2θ	ω	φ	χ	Frames
ω	3.18	196.87	216.00	54.72	304
ω	-46.78	146.91	259.43	54.72	304
ω	3.18	196.87	288.00	54.72	304
φ	3.18	349.56	0.00	54.72	720
ω	3.18	196.87	0.00	54.72	304
ω	3.18	196.87	144.00	54.72	304
ω	3.18	196.87	72.00	54.72	220

Rotation frames were integrated using SAINT, producing a listing of unaveraged F^2 and $\sigma(F^2)$ values. A total of 81673 reflections were measured over the ranges $5.798 \le 2\theta \le 50.866°$, $-14 \le h \le 14$, $-15 \le k \le 15$, $-17 \le l \le 17$ yielding 7288 unique reflections (R_{int} = 0.0625). The intensity

199

data were corrected for Lorentz and polarization effects and for absorption using SADABS (minimum and maximum transmission 0.7205, 0.7452). The structure was solved by direct methods - ShelXT. Refinement was by full-matrix least squares based on F^2 using SHELXL-2018. All reflections were used during refinement. The weighting scheme used was $w=1/[\sigma^2(F_o^2) + (0.0294P)^2 + 1.6812P]$ where $P = (F_o^2 + 2F_c^2)/3$. Non-hydrogen atoms were refined anisotropically and hydrogen atoms were refined using a riding model. Refinement converged to R1=0.0374 and wR2=0.0799 for 6117 observed reflections for which $F > 4\sigma(F)$ and R1=0.0489 and wR2=0.0856 and GOF =1.037 for all 7288 unique, non-zero reflections and 471 variables. The maximum Δ/σ in the final cycle of least squares was 0.001 and the two most prominent peaks in the final difference Fourier were +0.39 and -0.34 e/$\mathring{A}^3$.
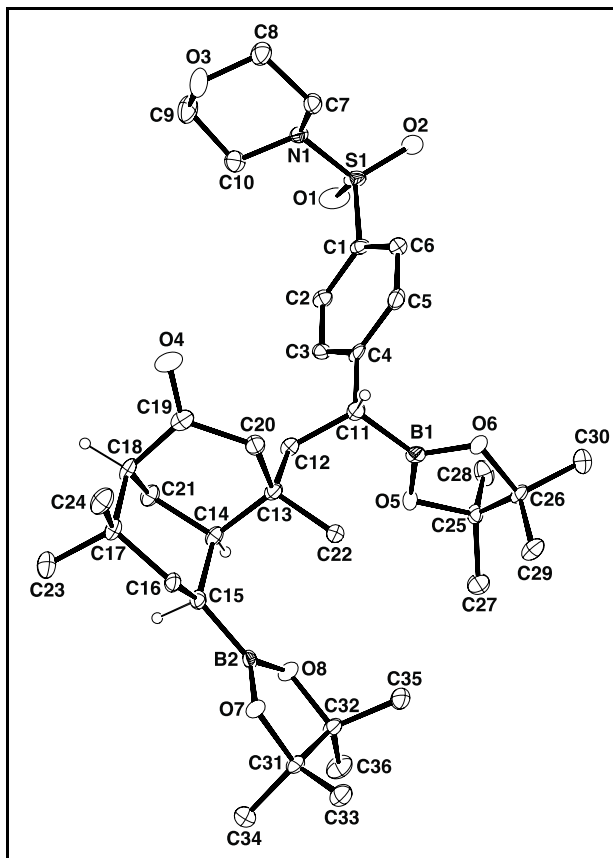
ORTEP drawing of Compound **3.76** with 50% thermal ellipsoids.

Table 3.18. Summary of Structure Determination of Compound **3.76**

Empirical formula	$C_{37}H_{59}B_2Cl_2NO_8S$
Formula weight	770.43
Temperature/K	100
Crystal system	triclinic
Space group	$P\bar{1}$
a	11.9599(6)Å
b	13.0727(6)Å
c	14.6426(7)Å
α	106.075(2)°
β	108.081(2)°
γ	102.136(2)°
Volume	1978.23(17)Å^3
Z	2
d_{calc}	1.293 g/cm^3
μ	0.267 mm^{-1}
F(000)	824.0
Crystal size, mm	$0.25 \times 0.12 \times 0.1$
2θ range for data collection	5.798 - 50.866°
Index ranges	$-14 \le h \le 14, -15 \le k \le 15, -17 \le l \le 17$
Reflections collected	81673
Independent reflections	7288[R(int) = 0.0625]
Data/restraints/parameters	7288/0/471
Goodness-of-fit on F^2	1.037
Final R indexes [I>=2σ (I)]	$R_1 = 0.0374$, $wR_2 = 0.0799$
Final R indexes [all data]	$R_1 = 0.0489$, $wR_2 = 0.0856$
Largest diff. peak/hole	0.39/-0.34 eÅ^{-3}

Table 3.19. Refined Positional Parameters for Compound **3.76**

Atom	x	y	z	U(eq)
Cl1	0.94031(5)	0.81099(5)	0.32619(4)	0.03656(14)
Cl2	0.68381(4)	0.66348(4)	0.21230(4)	0.02620(12)
S1	0.41138(4)	0.87086(4)	0.07484(4)	0.01827(11)
O1	0.38549(13)	0.95070(11)	0.14791(12)	0.0278(3)
O2	0.34689(12)	0.84223(12)	-0.03382(11)	0.0258(3)
O3	0.81562(12)	0.94695(12)	0.15394(10)	0.0265(3)
O4	0.80335(12)	0.46697(11)	0.29010(11)	0.0253(3)
O5	0.17240(11)	0.39448(10)	0.19654(9)	0.0160(3)
O6	0.15777(11)	0.30999(10)	0.03214(9)	0.0152(3)
O7	0.43926(10)	0.09969(10)	0.43196(9)	0.0155(3)
O8	0.33107(11)	0.22382(10)	0.42726(9)	0.0162(3)
N1	0.56015(13)	0.91989(12)	0.10064(11)	0.0154(3)
C1	0.38864(15)	0.74484(15)	0.09907(14)	0.0150(4)
C2	0.40063(16)	0.74860(15)	0.19751(14)	0.0157(4)
C3	0.39434(16)	0.65121(15)	0.21907(14)	0.0164(4)
C4	0.37941(15)	0.55034(14)	0.14392(14)	0.0147(4)
C5	0.36460(16)	0.54883(15)	0.04539(14)	0.0182(4)
C6	0.36832(16)	0.64428(15)	0.02211(14)	0.0179(4)
C7	0.60402(16)	0.85434(15)	0.02822(14)	0.0181(4)
C8	0.73515(17)	0.92033(17)	0.05001(15)	0.0222(4)
C9	0.77454(19)	1.01564(17)	0.22136(16)	0.0276(5)
C10	0.64530(17)	0.95443(15)	0.20923(14)	0.0199(4)
C11	0.37627(16)	0.44256(14)	0.16563(14)	0.0153(4)
C12	0.45688(16)	0.46474(14)	0.27807(13)	0.0148(4)
C13	0.49866(15)	0.36513(14)	0.29737(14)	0.0141(4)
C14	0.54755(15)	0.39454(14)	0.41600(13)	0.0135(4)
C15	0.56325(15)	0.29844(14)	0.45573(13)	0.0136(4)
C16	0.66347(15)	0.25329(14)	0.43241(14)	0.0145(4)
C17	0.78885(15)	0.34564(14)	0.46783(14)	0.0149(4)
C18	0.77081(15)	0.44890(14)	0.43874(14)	0.0159(4)
C19	0.73226(16)	0.42661(15)	0.32480(15)	0.0172(4)
C20	0.60074(16)	0.35258(15)	0.25463(14)	0.0170(4)
C21	0.67286(16)	0.49039(14)	0.47152(14)	0.0164(4)
C22	0.38814(16)	0.25571(14)	0.23958(13)	0.0148(4)
C23	0.85718(17)	0.38588(17)	0.58548(15)	0.0231(4)
C24	0.87000(17)	0.29592(16)	0.41816(15)	0.0215(4)
C25	0.03859(15)	0.34959(15)	0.13160(13)	0.0151(4)
C26	0.03326(15)	0.26468(15)	0.03007(14)	0.0150(4)

C27	-0.02948(17)	0.29815(17)	0.18810(15)	0.0225(4)
C28	0.00109(18)	0.45001(16)	0.11746(15)	0.0219(4)
C29	0.01794(17)	0.14607(15)	0.02942(15)	0.0206(4)
C30	-0.06064(17)	0.26030(16)	-0.06956(14)	0.0211(4)
C31	0.32204(15)	0.04560(15)	0.43703(14)	0.0152(4)
C32	0.23873(16)	0.11535(15)	0.40015(14)	0.0160(4)
C33	0.27799(17)	-0.07765(15)	0.36878(15)	0.0194(4)
C34	0.35093(18)	0.05836(17)	0.54898(14)	0.0223(4)
C35	0.16604(17)	0.06829(16)	0.28360(15)	0.0216(4)
C36	0.15272(18)	0.13660(17)	0.45496(16)	0.0245(4)
C37	0.83790(18)	0.68845(18)	0.22022(17)	0.0289(5)
B1	0.23299(18)	0.37867(16)	0.13167(16)	0.0149(4)
B2	0.44155(18)	0.20522(17)	0.43478(15)	0.0137(4)

Table 3.20. Positional Parameters for Hydrogens in Compound **3.76**

Atom	x	y	z	U(eq)
H2	0.413016	0.817206	0.249541	0.019
H3	0.400256	0.653026	0.285751	0.02
H5	0.351629	0.480325	-0.007048	0.022
H6	0.357112	0.641432	-0.045789	0.022
H7a	0.549075	0.838966	-0.043746	0.022
H7b	0.601831	0.781417	0.036544	0.022
H8a	0.765857	0.875709	0.002659	0.027
H8b	0.735685	0.990746	0.036918	0.027
H9a	0.774246	1.084902	0.206295	0.033
H9b	0.83313	1.038049	0.293709	0.033
H10a	0.645682	0.887436	0.228228	0.024
H10b	0.617558	1.004565	0.255293	0.024
H11	0.408013	0.396037	0.119457	0.018
H12a	0.409853	0.485714	0.321213	0.018
H12b	0.532107	0.530222	0.301859	0.018
H14	0.486593	0.423641	0.439904	0.016
H15	0.600591	0.337206	0.532593	0.016
H16a	0.632819	0.211887	0.357033	0.017
H16b	0.677309	0.199113	0.466932	0.017
H18	0.851938	0.511551	0.476404	0.019
H20a	0.598707	0.273224	0.236408	0.02
H20b	0.57869	0.3679	0.189902	0.02
H21a	0.698839	0.513207	0.547288	0.02

H21b	0.664624	0.556498	0.452924	0.02
H22a	0.414322	0.19352	0.253569	0.022
H22b	0.358457	0.240036	0.165183	0.022
H22c	0.320969	0.263607	0.26303	0.022
H23a	0.867406	0.321437	0.604932	0.035
H23b	0.808679	0.42113	0.619423	0.035
H23c	0.939093	0.44077	0.6072	0.035
H24a	0.949962	0.354028	0.440685	0.032
H24b	0.827953	0.268624	0.342781	0.032
H24c	0.884131	0.233227	0.439163	0.032
H27a	0.005126	0.241538	0.206386	0.034
H27b	-0.118002	0.262468	0.143341	0.034
H27c	-0.019581	0.357172	0.251121	0.034
H28a	0.019197	0.505739	0.185141	0.033
H28b	-0.088118	0.425168	0.075097	0.033
H28c	0.047989	0.483919	0.08301	0.033
H29a	0.025816	0.099847	-0.032098	0.031
H29b	-0.064257	0.113279	0.028379	0.031
H29c	0.082395	0.148581	0.091545	0.031
H30a	-0.043479	0.33541	-0.073214	0.032
H30b	-0.144661	0.235126	-0.071174	0.032
H30c	-0.054444	0.207523	-0.128623	0.032
H33a	0.27253	-0.084229	0.299093	0.029
H33b	0.195893	-0.114918	0.365497	0.029
H33c	0.337061	-0.113487	0.397599	0.029
H34a	0.415962	0.025452	0.571758	0.033
H34b	0.275688	0.019466	0.555174	0.033
H34c	0.37978	0.138392	0.592229	0.033
H35a	0.131419	0.123883	0.263046	0.032
H35b	0.098277	-0.000863	0.264007	0.032
H35c	0.221649	0.051586	0.248756	0.032
H36a	0.201903	0.177715	0.529069	0.037
H36b	0.095488	0.064549	0.444207	0.037
H36c	0.105066	0.181291	0.427095	0.037
H37A	0.86455	0.623249	0.227099	0.035
H37B	0.841362	0.696306	0.155729	0.035

Table 3.21. Refined Thermal Parameters (U's) for Compound **3.76**

Atom	U_{11}	U_{22}	U_{33}	U_{23}	U_{13}	U_{12}
Cl1	0.0188(3)	0.0411(3)	0.0360(3)	0.0077(3)	0.0057(2)	-0.0006(2)
Cl2	0.0139(2)	0.0289(3)	0.0354(3)	0.0130(2)	0.0098(2)	0.00451(19)
S1	0.0154(2)	0.0204(2)	0.0276(3)	0.0166(2)	0.0107(2)	0.00872(18)
O1	0.0315(8)	0.0249(7)	0.0468(9)	0.0218(7)	0.0265(7)	0.0193(6)
O2	0.0157(7)	0.0349(8)	0.0309(8)	0.0242(7)	0.0046(6)	0.0066(6)
O3	0.0140(7)	0.0306(8)	0.0241(7)	0.0025(6)	0.0013(6)	0.0055(6)
O4	0.0188(7)	0.0303(8)	0.0355(8)	0.0182(7)	0.0170(6)	0.0074(6)
O5	0.0104(6)	0.0179(6)	0.0151(6)	0.0055(5)	0.0006(5)	0.0026(5)
O6	0.0100(6)	0.0151(6)	0.0182(7)	0.0053(5)	0.0052(5)	0.0014(5)
O7	0.0096(6)	0.0172(6)	0.0209(7)	0.0096(5)	0.0061(5)	0.0027(5)
O8	0.0129(6)	0.0129(6)	0.0222(7)	0.0060(5)	0.0078(5)	0.0023(5)
N1	0.0143(7)	0.0158(8)	0.0171(8)	0.0080(6)	0.0065(6)	0.0040(6)
C1	0.0110(8)	0.0170(9)	0.0220(10)	0.0126(8)	0.0074(7)	0.0058(7)
C2	0.0131(9)	0.0164(9)	0.0201(10)	0.0072(8)	0.0085(8)	0.0058(7)
C3	0.0125(8)	0.0226(10)	0.0171(9)	0.0113(8)	0.0068(7)	0.0051(7)
C4	0.0047(8)	0.0154(9)	0.0221(10)	0.0079(8)	0.0035(7)	0.0012(7)
C5	0.0139(9)	0.0160(9)	0.0177(9)	0.0031(8)	0.0030(8)	0.0003(7)
C6	0.0146(9)	0.0215(10)	0.0161(9)	0.0084(8)	0.0051(8)	0.0022(7)
C7	0.0161(9)	0.0205(9)	0.0144(9)	0.0036(8)	0.0056(8)	0.0039(8)
C8	0.0157(9)	0.0269(10)	0.0225(10)	0.0070(8)	0.0080(8)	0.0061(8)
C9	0.0237(11)	0.0223(10)	0.0223(11)	-0.0018(9)	0.0038(9)	0.0005(8)
C10	0.0241(10)	0.0155(9)	0.0163(9)	0.0025(8)	0.0073(8)	0.0043(8)
C11	0.0136(9)	0.0140(9)	0.0171(9)	0.0057(7)	0.0052(7)	0.0036(7)
C12	0.0127(8)	0.0133(9)	0.0171(9)	0.0050(7)	0.0058(7)	0.0030(7)
C13	0.0102(8)	0.0134(9)	0.0190(9)	0.0078(7)	0.0051(7)	0.0030(7)
C14	0.0102(8)	0.0115(8)	0.0175(9)	0.0029(7)	0.0061(7)	0.0033(7)
C15	0.0122(8)	0.0153(9)	0.0107(8)	0.0027(7)	0.0039(7)	0.0027(7)
C16	0.0104(8)	0.0140(9)	0.0162(9)	0.0066(7)	0.0016(7)	0.0025(7)
C17	0.0091(8)	0.0146(9)	0.0176(9)	0.0040(7)	0.0037(7)	0.0021(7)
C18	0.0086(8)	0.0124(9)	0.0205(10)	0.0021(7)	0.0035(7)	-0.0001(7)
C19	0.0146(9)	0.0144(9)	0.0268(10)	0.0097(8)	0.0100(8)	0.0075(7)
C20	0.0134(9)	0.0226(10)	0.0156(9)	0.0072(8)	0.0068(7)	0.0053(7)
C21	0.0145(9)	0.0117(9)	0.0192(9)	0.0024(7)	0.0056(8)	0.0028(7)
C22	0.0132(9)	0.0151(9)	0.0145(9)	0.0062(7)	0.0040(7)	0.0028(7)
C23	0.0139(9)	0.0268(11)	0.0219(10)	0.0068(8)	0.0018(8)	0.0046(8)
C24	0.0134(9)	0.0194(10)	0.0303(11)	0.0069(8)	0.0084(8)	0.0057(8)
C25	0.0093(8)	0.0176(9)	0.0162(9)	0.0065(7)	0.0019(7)	0.0047(7)
C26	0.0076(8)	0.0156(9)	0.0203(9)	0.0066(7)	0.0051(7)	0.0016(7)

C27	0.0174(10)	0.0276(11)	0.0242(10)	0.0106(9)	0.0105(8)	0.0057(8)
C28	0.0238(10)	0.0225(10)	0.0178(10)	0.0056(8)	0.0039(8)	0.0128(8)
C29	0.0163(9)	0.0145(9)	0.0293(11)	0.0078(8)	0.0087(8)	0.0029(7)
C30	0.0168(9)	0.0233(10)	0.0181(10)	0.0052(8)	0.0027(8)	0.0064(8)
C31	0.0091(8)	0.0188(9)	0.0185(9)	0.0085(8)	0.0063(7)	0.0024(7)
C32	0.0115(8)	0.0145(9)	0.0211(10)	0.0071(8)	0.0064(7)	0.0017(7)
C33	0.0153(9)	0.0180(9)	0.0244(10)	0.0082(8)	0.0077(8)	0.0040(7)
C34	0.0209(10)	0.0261(10)	0.0184(10)	0.0110(8)	0.0060(8)	0.0036(8)
C35	0.0138(9)	0.0231(10)	0.0241(10)	0.0123(8)	0.0019(8)	0.0023(8)
C36	0.0176(10)	0.0255(11)	0.0349(12)	0.0117(9)	0.0151(9)	0.0077(8)
C37	0.0165(10)	0.0339(12)	0.0322(12)	0.0064(10)	0.0124(9)	0.0039(9)
B1	0.0149(10)	0.0118(9)	0.0213(11)	0.0111(8)	0.0056(9)	0.0062(8)
B2	0.0114(9)	0.0184(10)	0.0075(9)	0.0033(8)	0.0021(8)	0.0023(8)

Table 3.22. Bond Distances in Compound 3.76, **Å**

Cl1-C37	1.759(2)	Cl2-C37	1.7635(19)	S1-O1	1.4328(14)
S1-O2	1.4330(14)	S1-N1	1.6397(15)	S1-C1	1.7632(17)
O3-C8	1.421(2)	O3-C9	1.421(2)	O4-C19	1.220(2)
O5-C25	1.470(2)	O5-B1	1.361(2)	O6-C26	1.470(2)
O6-B1	1.364(2)	O7-C31	1.465(2)	O7-B2	1.363(2)
O8-C32	1.465(2)	O8-B2	1.370(2)	N1-C7	1.472(2)
N1-C10	1.474(2)	C1-C2	1.389(2)	C1-C6	1.390(3)
C2-C3	1.387(2)	C3-C4	1.399(3)	C4-C5	1.392(3)
C4-C11	1.523(2)	C5-C6	1.377(3)	C7-C8	1.508(2)
C9-C10	1.514(3)	C11-C12	1.535(2)	C11-B1	1.588(3)
C12-C13	1.554(2)	C13-C14	1.553(2)	C13-C20	1.553(2)
C13-C22	1.533(2)	C14-C15	1.545(2)	C14-C21	1.539(2)
C15-C16	1.530(2)	C15-B2	1.571(2)	C16-C17	1.544(2)
C17-C18	1.560(2)	C17-C23	1.535(3)	C17-C24	1.528(2)
C18-C19	1.509(3)	C18-C21	1.539(2)	C19-C20	1.508(2)
C25-C26	1.563(2)	C25-C27	1.515(2)	C25-C28	1.519(2)
C26-C29	1.520(2)	C26-C30	1.517(2)	C31-C32	1.561(2)
C31-C33	1.516(2)	C31-C34	1.519(2)	C32-C35	1.523(3)
C32-C36	1.513(2)				

Table 3.23. Bond Angles in Compound **3.76,** °

O1-S1-O2	120.28(9)	O1-S1-N1	106.83(8)	O1-S1-C1	108.30(8)
O2-S1-N1	106.79(8)	O2-S1-C1	107.63(8)	N1-S1-C1	106.22(8)
C9-O3-C8	109.07(14)	B1-O5-C25	106.91(13)	B1-O6-C26	107.23(13)
B2-O7-C31	107.57(13)	B2-O8-C32	107.51(13)	C7-N1-S1	115.41(12)
C7-N1-C10	112.18(14)	C10-N1-S1	116.25(12)	C2-C1-S1	119.40(14)
C2-C1-C6	120.58(16)	C6-C1-S1	119.84(13)	C3-C2-C1	119.35(17)
C2-C3-C4	120.87(16)	C3-C4-C11	122.43(16)	C5-C4-C3	118.27(16)
C5-C4-C11	119.29(16)	C6-C5-C4	121.58(17)	C5-C6-C1	119.26(17)
N1-C7-C8	109.10(15)	O3-C8-C7	111.21(15)	O3-C9-C10	111.39(15)
N1-C10-C9	108.45(15)	C4-C11-C12	112.83(14)	C4-C11-B1	104.65(13)
C12-C11-B1	114.08(14)	C11-C12-C13	115.69(14)	C14-C13-C12	106.31(14)
C20-C13-C12	108.75(14)	C20-C13-C14	112.27(14)	C22-C13-C12	109.76(14)
C22-C13-C14	111.33(14)	C22-C13-C20	108.38(14)	C15-C14-C13	117.60(14)
C21-C14-C13	110.85(14)	C21-C14-C15	107.39(14)	C14-C15-B2	117.29(14)
C16-C15-C14	112.05(14)	C16-C15-B2	114.57(14)	C15-C16-C17	113.82(14)
C16-C17-C18	111.83(14)	C23-C17-C16	109.63(14)	C23-C17-C18	108.67(14)
C24-C17-C16	109.07(14)	C24-C17-C18	109.79(14)	C24-C17-C23	107.77(15)
C19-C18-C17	113.82(14)	C19-C18-C21	107.20(14)	C21-C18-C17	111.99(14)
O4-C19-C18	122.00(16)	O4-C19-C20	120.80(17)	C20-C19-C18	117.19(15)
C19-C20-C13	116.80(15)	C14-C21-C18	108.83(14)	O5-C25-C26	102.43(13)
O5-C25-C27	108.64(14)	O5-C25-C28	105.78(14)	C27-C25-C26	115.31(15)
C27-C25-C28	110.45(15)	C28-C25-C26	113.37(14)	O6-C26-C25	102.54(13)
O6-C26-C29	107.25(13)	O6-C26-C30	107.44(14)	C29-C26-C25	113.77(15)
C30-C26-C25	115.53(14)	C30-C26-C29	109.58(15)	O7-C31-C32	102.53(13)
O7-C31-C33	107.42(14)	O7-C31-C34	106.78(14)	C33-C31-C32	115.73(15)
C33-C31-C34	110.36(15)	C34-C31-C32	113.17(15)	O8-C32-C31	102.20(13)
O8-C32-C35	107.69(14)	O8-C32-C36	107.74(14)	C35-C32-C31	113.04(15)
C36-C32-C31	115.46(15)	C36-C32-C35	110.02(15)	Cl1-C37-Cl2	111.41(11)
O5-B1-O6	114.12(16)	O5-B1-C11	123.28(17)	O6-B1-C11	122.39(16)
O7-B2-O8	113.14(15)	O7-B2-C15	122.56(16)	O8-B2-C15	124.04(16)

X-ray Structure Determination of Compound 3.97
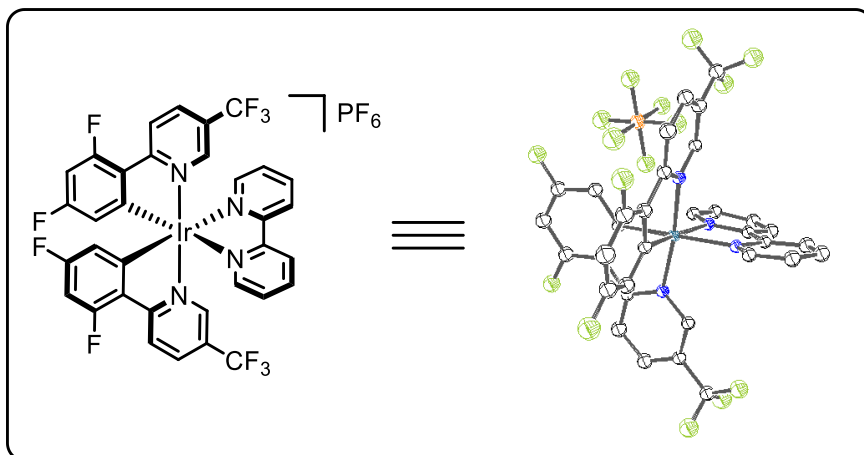
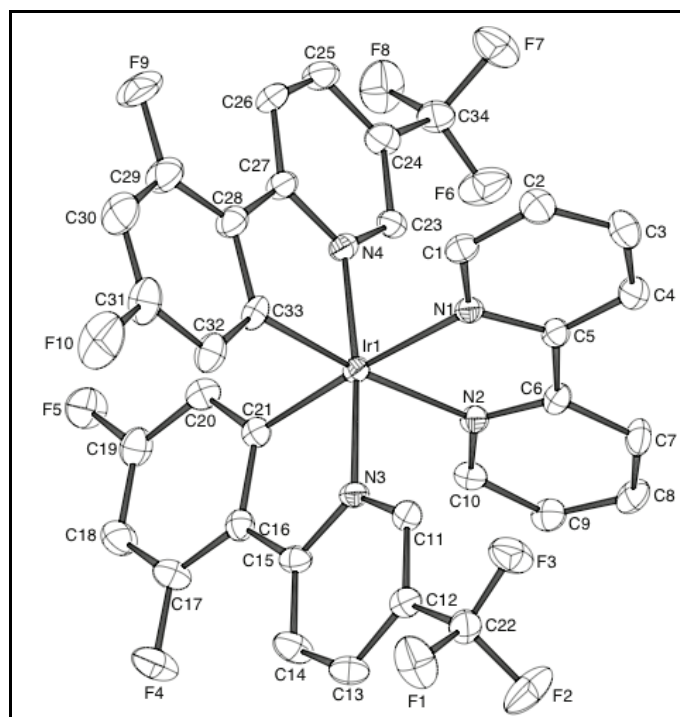
Compound 3.97, $C_{77}H_{54}F_{32}Ir_2N_8O_3P_2$, crystallizes in the triclinic space group $P\bar{1}$ with a=11.4834(8)Å, b=13.1501(9)Å, c=14.4544(10)Å, α=72.640(2)°, β=89.929(2)°, γ=77.252(2)°, V=2027.1(2)Å^3, Z=1, and d_{calc}=1.797 g/cm$_3$. X-ray intensity data were collected on a Bruker D8QUEST [1] CMOS area detector employing graphite-monochromated Mo-Kα radiation (λ=0.71073Å) at a temperature of 100K. Preliminary indexing was performed from a series of twenty-four 0.5° rotation frames with exposures of 10 seconds. A total of 2448 frames were collected with a crystal to detector distance of 60.0 mm, rotation widths of 0.5° and exposures of 4 seconds:

scan type	2θ	ω	φ	χ	Frames
ω	22.35	190.09	255.00	54.72	408
ω	22.35	190.09	0.00	54.72	408
ω	22.35	190.09	153.00	54.72	408
ω	22.35	190.09	51.00	54.72	408
ω	22.35	190.09	306.00	54.72	408

scan type	2θ	ω	φ	χ	Frames
ω	22.35	190.09	204.00	54.72	408

Rotation frames were integrated using SAINT [2], producing a listing of unaveraged F^2 and $\sigma(F^2)$ values. A total of 51347 reflections were measured over the ranges $5.84 \leq 2\theta \leq 55.174°$, $-14 \leq h \leq 14$, $-17 \leq k \leq 17$, $-18 \leq l \leq 18$ yielding 9324 unique reflections ($R_{int} = 0.0356$). The intensity data were corrected for Lorentz and polarization effects and for absorption using SADABS [3] (minimum and maximum transmission 0.7456, 0.6399). The structure was solved by direct methods - ShelXT [4]. Refinement was by full-matrix least squares based on F^2 using SHELXL-2017 [5]. All reflections were used during refinement. The weighting scheme used was $w=1/[\sigma^2(F_o^2) + (0.0001P)^2 + 28.5043P]$ where $P = (F_o^2 + 2F_c^2)/3$. Non-hydrogen atoms were refined anisotropically and hydrogen atoms were refined using a riding model. Refinement converged to R1=0.0478 and wR2=0.1216 for 8590 observed reflections for which $F > 4\sigma(F)$ and R1=0.0532 and wR2=0.1246 and GOF =1.275 for all 9324 unique, non-zero reflections and 565 variables. The maximum Δ/σ in the final cycle of least squares was 0.001 and the two most prominent peaks in the final difference Fourier were +3.98 and -2.21 e/Å^3.

Table 1. lists cell information, data collection parameters, and refinement data. Final positional and equivalent isotropic thermal parameters are given in Tables 2. and 3. Anisotropic thermal parameters are in Table 4. Tables 5. and 6. list bond distances and bond angles. Figure 1. is an ORTEP representation of the molecule with 50% probability thermal ellipsoids displayed.

ORTEP drawing of Compound 3.97 with 50% thermal ellipsoids.

Table 3.24. Summary of Structure Determination of Compound **3.97**

Empirical formula	$C_{77}H_{54}F_{32}Ir_2N_8O_3P_2$
Formula weight	2193.62
Temperature/K	100
Crystal system	triclinic
Space group	$P\bar{1}$
a	11.4834(8)Å
b	13.1501(9)Å
c	14.4544(10)Å
α	72.640(2)°
β	89.929(2)°
γ	77.252(2)°
Volume	2027.1(2)Å^3
Z	1
d_{calc}	1.797 g/cm^3
μ	3.445 mm^{-1}
F(000)	1068.0
Crystal size, mm	$0.3 \times 0.25 \times 0.2$
2θ range for data collection	5.84 - 55.174°
Index ranges	$-14 \le h \le 14$, $-17 \le k \le 17$, $-18 \le l \le 18$
Reflections collected	51347
Independent reflections	9324[R(int) = 0.0356]
Data/restraints/parameters	9324/0/565

211

Goodness-of-fit on F^2 1.275

Final R indexes [I>=2σ (I)]   R$_1$ = 0.0478, wR$_2$ = 0.1216

Final R indexes [all data]   R$_1$ = 0.0532, wR$_2$ = 0.1246

Largest diff. peak/hole   3.98/-2.21 eÅ^{-3}

Table 3.25. Refined Positional Parameters for Compound **3.97**

Atom	x	y	z	U(eq)
Ir1	0.26250(2)	0.31756(2)	0.29199(2)	0.01566(8)
N1	0.1275(5)	0.4409(4)	0.3219(4)	0.0171(11)
N2	0.3475(5)	0.3593(4)	0.4025(4)	0.0172(11)
N3	0.2339(5)	0.1857(4)	0.4001(4)	0.0174(11)
N4	0.2969(5)	0.4376(5)	0.1760(4)	0.0183(11)
C1	0.0207(6)	0.4856(6)	0.2725(5)	0.0206(13)
C2	-0.0598(7)	0.5714(6)	0.2898(6)	0.0263(15)
C3	-0.0299(7)	0.6121(6)	0.3621(6)	0.0275(15)
C4	0.0793(7)	0.5670(6)	0.4142(5)	0.0261(15)
C5	0.1571(6)	0.4812(5)	0.3936(5)	0.0178(12)
C6	0.2774(6)	0.4297(6)	0.4420(5)	0.0188(13)
C7	0.3174(7)	0.4518(6)	0.5234(5)	0.0247(15)
C8	0.4344(7)	0.4019(6)	0.5617(5)	0.0254(15)
C9	0.5076(6)	0.3331(6)	0.5193(5)	0.0233(14)
C10	0.4611(6)	0.3130(5)	0.4399(5)	0.0199(13)

C11	0.1421(6)	0.1901(6)	0.4582(5)	0.0189(13)
C12	0.1313(6)	0.0996(6)	0.5328(5)	0.0205(13)
C13	0.2147(7)	0.0011(6)	0.5493(5)	0.0267(15)
C14	0.3058(7)	-0.0038(6)	0.4877(6)	0.0280(16)
C15	0.3161(6)	0.0888(5)	0.4126(5)	0.0197(13)
C16	0.4063(6)	0.0956(6)	0.3416(5)	0.0198(13)
C17	0.4972(7)	0.0088(6)	0.3344(6)	0.0262(15)
C18	0.5776(7)	0.0189(6)	0.2636(6)	0.0296(16)
C19	0.5643(7)	0.1217(6)	0.1971(5)	0.0269(15)
C20	0.4772(6)	0.2117(6)	0.2005(5)	0.0229(14)
C21	0.3961(6)	0.2003(5)	0.2728(5)	0.0179(13)
C22	0.0304(7)	0.1043(6)	0.5984(5)	0.0247(15)
C23	0.3708(6)	0.5035(5)	0.1808(5)	0.0185(13)
C24	0.3892(6)	0.5856(6)	0.1008(5)	0.0240(14)
C25	0.3301(7)	0.6002(6)	0.0119(5)	0.0276(16)
C26	0.2560(7)	0.5347(6)	0.0060(5)	0.0281(16)
C27	0.2395(6)	0.4507(6)	0.0884(5)	0.0218(14)
C28	0.1688(6)	0.3705(6)	0.0935(5)	0.0236(14)
C29	0.1037(7)	0.3632(7)	0.0160(6)	0.0317(17)
C30	0.0374(8)	0.2854(7)	0.0262(6)	0.0363(19)
C31	0.0379(7)	0.2135(7)	0.1169(6)	0.0321(17)
C32	0.1024(6)	0.2142(7)	0.1975(5)	0.0259(15)
C33	0.1675(6)	0.2936(6)	0.1866(5)	0.0198(13)
C34	0.4720(7)	0.6556(6)	0.1088(5)	0.0283(16)

F1	-0.0292(5)	0.0269(4)	0.6026(4)	0.0431(13)
F2	0.0701(5)	0.0883(5)	0.6898(3)	0.0496(14)
F3	-0.0489(4)	0.1993(4)	0.5720(4)	0.0368(11)
F4	0.5108(4)	-0.0922(4)	0.3994(4)	0.0371(11)
F5	0.6415(4)	0.1359(4)	0.1265(3)	0.0364(11)
F6	0.5293(5)	0.6254(4)	0.1952(4)	0.0460(14)
F7	0.4118(5)	0.7609(4)	0.0914(4)	0.0426(12)
F8	0.5538(5)	0.6580(5)	0.0429(4)	0.0461(13)
F9	0.1034(5)	0.4333(4)	-0.0737(3)	0.0469(14)
F10	-0.0253(5)	0.1358(5)	0.1278(4)	0.0518(15)
P1	0.77550(19)	0.31570(17)	0.32440(16)	0.0305(4)
F11	0.8192(5)	0.3849(5)	0.2261(3)	0.0437(13)
F12	0.7328(5)	0.2459(4)	0.4247(4)	0.0456(14)
F13	0.6987(6)	0.2663(6)	0.2669(5)	0.069(2)
F14	0.6653(5)	0.4150(4)	0.3203(4)	0.0479(13)
F15	0.8536(5)	0.3643(4)	0.3859(3)	0.0381(11)
F16	0.8895(5)	0.2168(4)	0.3348(5)	0.0487(14)
O1	0.7801(13)	0.8238(9)	0.1611(8)	0.069(5)
C35	0.7656(8)	0.8889(7)	0.0805(8)	0.033(4)
C36	0.6670(15)	0.8953(16)	0.0086(12)	0.071(7)
C37	0.8450(13)	0.9682(11)	0.0463(10)	0.039(4)
O2	0.2962(6)	0.6794(5)	0.3083(4)	0.0505(17)
C38	0.2373(4)	0.7644(4)	0.2545(3)	0.043(2)
C39	0.2561(9)	0.8740(5)	0.2555(7)	0.056(3)

| C40 | 0.1410(7) | 0.7666(7) | 0.1826(6) | 0.055(3) |

Table 3.26. Positional Parameters for Hydrogens in Compound **3.97**

Atom	*x*	*y*	*z*	U(eq)
H1	-0.00046	0.456881	0.223479	0.027
H2	-0.134372	0.602102	0.252718	0.035
H3	-0.084309	0.670751	0.375803	0.037
H4	0.100973	0.594508	0.463765	0.035
H7	0.266238	0.499603	0.55189	0.033
H8	0.463816	0.415333	0.617337	0.034
H9	0.58824	0.300296	0.543839	0.031
H10	0.510828	0.264816	0.410873	0.026
H11	0.083844	0.256949	0.447473	0.025
H13	0.209031	-0.061318	0.601553	0.036
H14	0.362533	-0.071133	0.496444	0.037
H18	0.638926	-0.041478	0.260573	0.039
H20	0.472641	0.281081	0.153687	0.03
H23	0.41132	0.492819	0.241415	0.025
H25	0.341628	0.65592	-0.044317	0.037
H26	0.214822	0.545663	-0.054348	0.037
H30	-0.007001	0.28184	-0.027782	0.048
H32	0.102	0.161544	0.258954	0.034
H36a	0.670089	0.952804	-0.052137	0.106
H36b	0.6776	0.824803	-0.004163	0.106

H36c	0.589307	0.912393	0.035518	0.106
H37a	0.818984	1.013759	-0.020671	0.058
H37b	0.839731	1.014914	0.088438	0.058
H37c	0.928017	0.927322	0.048756	0.058
H39a	0.200064	0.932546	0.206857	0.084
H39b	0.242181	0.882361	0.32	0.084
H39c	0.338412	0.878434	0.240213	0.084
H40a	0.103733	0.842706	0.145891	0.083
H40b	0.176385	0.727324	0.137668	0.083
H40c	0.080158	0.731254	0.217457	0.083

Table 3.27. Refined Thermal Parameters (U's) for Compound **3.97**

Atom	U_{11}	U_{22}	U_{33}	U_{23}	U_{13}	U_{12}
Ir1	0.01686(12)	0.01657(12)	0.01365(12)	-0.00384(9)	0.00014(8)	-0.00511(9)
N1	0.020(3)	0.016(3)	0.015(3)	-0.003(2)	0.000(2)	-0.005(2)
N2	0.019(3)	0.017(3)	0.017(3)	-0.005(2)	-0.002(2)	-0.007(2)
N3	0.021(3)	0.016(3)	0.015(3)	-0.002(2)	-0.001(2)	-0.006(2)
N4	0.018(3)	0.020(3)	0.015(3)	-0.004(2)	0.001(2)	-0.002(2)
C1	0.019(3)	0.024(3)	0.018(3)	-0.003(3)	0.001(2)	-0.007(3)
C2	0.021(3)	0.027(4)	0.030(4)	-0.009(3)	-0.002(3)	-0.004(3)
C3	0.024(4)	0.024(4)	0.035(4)	-0.013(3)	0.003(3)	-0.002(3)
C4	0.031(4)	0.023(3)	0.024(4)	-0.009(3)	-0.005(3)	-0.004(3)

C5	0.019(3)	0.018(3)	0.018(3)	-0.006(2)	0.001(2)	-0.006(2)
C6	0.020(3)	0.023(3)	0.016(3)	-0.007(3)	0.003(2)	-0.009(3)
C7	0.027(4)	0.028(4)	0.024(3)	-0.016(3)	-0.001(3)	-0.006(3)
C8	0.026(4)	0.033(4)	0.019(3)	-0.009(3)	-0.005(3)	-0.010(3)
C9	0.022(3)	0.025(3)	0.024(3)	-0.006(3)	-0.004(3)	-0.009(3)
C10	0.018(3)	0.018(3)	0.022(3)	-0.003(3)	-0.001(3)	-0.004(2)
C11	0.019(3)	0.020(3)	0.019(3)	-0.006(3)	0.003(2)	-0.008(3)
C12	0.021(3)	0.022(3)	0.019(3)	-0.005(3)	0.000(3)	-0.008(3)
C13	0.030(4)	0.021(3)	0.025(4)	0.002(3)	0.003(3)	-0.009(3)
C14	0.027(4)	0.018(3)	0.034(4)	-0.001(3)	0.006(3)	-0.005(3)
C15	0.019(3)	0.019(3)	0.019(3)	-0.002(3)	-0.002(3)	-0.005(3)
C16	0.018(3)	0.022(3)	0.020(3)	-0.008(3)	0.000(3)	-0.004(3)
C17	0.026(4)	0.019(3)	0.030(4)	-0.002(3)	0.002(3)	-0.006(3)
C18	0.028(4)	0.024(4)	0.032(4)	-0.008(3)	0.003(3)	0.002(3)
C19	0.025(4)	0.034(4)	0.025(4)	-0.013(3)	0.009(3)	-0.009(3)
C20	0.021(3)	0.026(4)	0.021(3)	-0.005(3)	0.001(3)	-0.007(3)
C21	0.017(3)	0.020(3)	0.020(3)	-0.007(3)	0.000(2)	-0.008(2)
C22	0.030(4)	0.024(3)	0.022(3)	-0.007(3)	0.009(3)	-0.012(3)
C23	0.019(3)	0.016(3)	0.020(3)	-0.004(2)	0.004(2)	-0.003(2)
C24	0.023(3)	0.023(3)	0.024(3)	-0.004(3)	0.009(3)	-0.007(3)
C25	0.033(4)	0.025(4)	0.019(3)	0.000(3)	0.005(3)	-0.005(3)
C26	0.040(4)	0.028(4)	0.013(3)	-0.004(3)	0.000(3)	-0.003(3)
C27	0.025(3)	0.023(3)	0.015(3)	-0.004(3)	0.001(3)	-0.004(3)
C28	0.022(3)	0.027(4)	0.019(3)	-0.007(3)	-0.002(3)	-0.002(3)

218

C29	0.032(4)	0.037(4)	0.023(4)	-0.008(3)	-0.007(3)	-0.005(3)
C30	0.036(4)	0.044(5)	0.033(4)	-0.017(4)	-0.011(3)	-0.009(4)
C31	0.027(4)	0.045(5)	0.036(4)	-0.023(4)	0.002(3)	-0.018(3)
C32	0.021(3)	0.036(4)	0.024(4)	-0.015(3)	0.002(3)	-0.009(3)
C33	0.016(3)	0.030(4)	0.016(3)	-0.011(3)	0.002(2)	-0.005(3)
C34	0.037(4)	0.023(4)	0.024(4)	-0.001(3)	0.010(3)	-0.013(3)
F1	0.041(3)	0.038(3)	0.063(3)	-0.022(3)	0.027(3)	-0.025(2)
F2	0.042(3)	0.083(4)	0.020(2)	-0.013(3)	0.007(2)	-0.009(3)
F3	0.038(3)	0.026(2)	0.040(3)	-0.002(2)	0.014(2)	-0.003(2)
F4	0.036(3)	0.021(2)	0.044(3)	0.001(2)	0.010(2)	-0.0005(19)
F5	0.032(2)	0.039(3)	0.034(3)	-0.009(2)	0.017(2)	-0.003(2)
F6	0.059(3)	0.046(3)	0.033(3)	0.003(2)	-0.007(2)	-0.033(3)
F7	0.048(3)	0.024(2)	0.054(3)	-0.007(2)	0.008(3)	-0.012(2)
F8	0.044(3)	0.056(3)	0.049(3)	-0.022(3)	0.025(3)	-0.026(3)
F9	0.068(4)	0.049(3)	0.020(2)	-0.002(2)	-0.017(2)	-0.018(3)
F10	0.054(3)	0.073(4)	0.049(3)	-0.029(3)	0.000(3)	-0.044(3)
P1	0.0302(10)	0.030(1)	0.0373(11)	-0.0130(9)	0.0097(9)	-0.0157(8)
F11	0.047(3)	0.067(4)	0.024(2)	-0.010(2)	0.001(2)	-0.033(3)
F12	0.042(3)	0.029(3)	0.059(3)	-0.003(2)	0.028(3)	-0.008(2)
F13	0.058(4)	0.096(5)	0.089(5)	-0.059(4)	0.012(4)	-0.049(4)
F14	0.046(3)	0.037(3)	0.049(3)	-0.003(2)	0.001(3)	0.000(2)
F15	0.052(3)	0.040(3)	0.025(2)	-0.008(2)	0.000(2)	-0.020(2)
F16	0.039(3)	0.043(3)	0.070(4)	-0.024(3)	0.023(3)	-0.014(2)
O1	0.097(13)	0.028(7)	0.072(11)	-0.007(7)	0.034(10)	-0.005(8)

C35	0.027(8)	0.025(8)	0.047(10)	-0.022(7)	0.010(7)	0.008(6)
C36	0.048(13)	0.055(14)	0.12(2)	-0.027(14)	0.011(14)	-0.029(11)
C37	0.043(10)	0.036(9)	0.043(10)	-0.018(8)	0.017(8)	-0.014(8)
O2	0.054(4)	0.058(4)	0.041(4)	-0.010(3)	-0.002(3)	-0.020(4)
C38	0.035(5)	0.057(6)	0.040(5)	-0.018(5)	0.002(4)	-0.010(4)
C39	0.064(7)	0.055(6)	0.058(7)	-0.028(5)	0.005(5)	-0.018(5)
C40	0.043(6)	0.072(8)	0.050(6)	-0.020(5)	-0.002(5)	-0.010(5)

Table 3.28. Bond Distances in Compound 3.97**, (Å)**

Ir1-N1	2.127(6)	Ir1-N2	2.138(5)	Ir1-N3	2.047(5)
Ir1-N4	2.038(6)	Ir1-C21	2.005(7)	Ir1-C33	2.013(7)
N1-C1	1.339(8)	N1-C5	1.371(8)	N2-C6	1.347(9)
N2-C10	1.349(8)	N3-C11	1.349(9)	N3-C15	1.371(9)
N4-C23	1.356(9)	N4-C27	1.374(8)	C1-C2	1.378(10)
C2-C3	1.383(10)	C3-C4	1.378(10)	C4-C5	1.383(10)
C5-C6	1.471(9)	C6-C7	1.394(9)	C7-C8	1.392(10)
C8-C9	1.377(11)	C9-C10	1.384(9)	C11-C12	1.376(9)
C12-C13	1.386(10)	C12-C22	1.499(10)	C13-C14	1.376(10)
C14-C15	1.396(9)	C15-C16	1.456(9)	C16-C17	1.395(10)
C16-C21	1.418(9)	C17-C18	1.374(11)	C17-F4	1.355(8)
C18-C19	1.381(11)	C19-C20	1.384(10)	C19-F5	1.349(8)
C20-C21	1.396(9)	C22-F1	1.333(8)	C22-F2	1.338(9)

C22-F3	1.323(9)	C23-C24	1.379(9)	C24-C25	1.394(10)
C24-C34	1.489(10)	C25-C26	1.356(11)	C26-C27	1.407(10)
C27-C28	1.451(10)	C28-C29	1.386(10)	C28-C33	1.424(10)
C29-C30	1.380(12)	C29-F9	1.348(9)	C30-C31	1.367(12)
C31-C32	1.386(10)	C31-F10	1.352(9)	C32-C33	1.385(10)
C34-F6	1.319(9)	C34-F7	1.353(9)	C34-F8	1.335(9)
P1-F11	1.589(5)	P1-F12	1.609(5)	P1-F13	1.571(6)
P1-F14	1.592(6)	P1-F15	1.612(5)	P1-F16	1.600(6)
O1-C35	1.2079	C35-C36	1.5088	C35-C37	1.5087
O2-C38	1.2078	C38-C39	1.5088	C38-C40	1.5088

Table 3.29. Bond Angles in Compound 3.97, (°)

N1-Ir1-N2	76.4(2)	N3-Ir1-N1	98.2(2)	N3-Ir1-N2	86.8(2)
N4-Ir1-N1	87.1(2)	N4-Ir1-N2	97.4(2)	N4-Ir1-N3	173.9(2)
C21-Ir1-N1	175.9(2)	C21-Ir1-N2	99.6(2)	C21-Ir1-N3	80.4(2)
C21-Ir1-N4	94.6(2)	C21-Ir1-C33	86.8(3)	C33-Ir1-N1	97.2(2)
C33-Ir1-N2	173.4(3)	C33-Ir1-N3	95.5(3)	C33-Ir1-N4	80.7(3)
C1-N1-Ir1	125.1(5)	C1-N1-C5	118.5(6)	C5-N1-Ir1	116.3(4)
C6-N2-Ir1	116.1(4)	C6-N2-C10	119.2(6)	C10-N2-Ir1	124.4(5)
C11-N3-Ir1	124.1(5)	C11-N3-C15	120.0(6)	C15-N3-Ir1	115.9(4)
C23-N4-Ir1	124.2(4)	C23-N4-C27	119.5(6)	C27-N4-Ir1	116.3(5)
N1-C1-C2	122.7(7)	C1-C2-C3	118.7(7)	C4-C3-C2	119.5(7)

C3-C4-C5	119.4(7)	N1-C5-C4	121.1(6)	N1-C5-C6	114.9(6)
C4-C5-C6	124.0(6)	N2-C6-C5	115.7(6)	N2-C6-C7	121.6(6)
C7-C6-C5	122.7(6)	C8-C7-C6	118.3(7)	C9-C8-C7	120.1(6)
C8-C9-C10	118.5(7)	N2-C10-C9	122.2(7)	N3-C11-C12	121.2(6)
C11-C12-C13	120.3(7)	C11-C12-C22	121.5(6)	C13-C12-C22	118.2(6)
C14-C13-C12	118.2(7)	C13-C14-C15	120.9(7)	N3-C15-C14	119.4(6)
N3-C15-C16	113.6(6)	C14-C15-C16	127.0(6)	C17-C16-C15	125.9(6)
C17-C16-C21	118.7(6)	C21-C16-C15	115.5(6)	C18-C17-C16	123.5(7)
F4-C17-C16	120.5(7)	F4-C17-C18	115.9(7)	C17-C18-C19	116.3(7)
C18-C19-C20	123.3(7)	F5-C19-C18	118.5(7)	F5-C19-C20	118.2(7)
C19-C20-C21	119.8(7)	C16-C21-Ir1	114.5(5)	C20-C21-Ir1	127.1(5)
C20-C21-C16	118.4(6)	F1-C22-C12	112.1(6)	F1-C22-F2	106.1(6)
F2-C22-C12	111.4(6)	F3-C22-C12	113.3(6)	F3-C22-F1	107.1(6)
F3-C22-F2	106.4(6)	N4-C23-C24	122.3(6)	C23-C24-C25	118.5(7)
C23-C24-C34	120.7(7)	C25-C24-C34	120.8(6)	C26-C25-C24	119.8(7)
C25-C26-C27	120.7(7)	N4-C27-C26	119.1(7)	N4-C27-C28	113.2(6)
C26-C27-C28	127.7(7)	C29-C28-C27	125.5(7)	C29-C28-C33	118.2(7)
C33-C28-C27	116.3(6)	C30-C29-C28	122.5(8)	F9-C29-C28	120.4(7)
F9-C29-C30	117.1(7)	C31-C30-C29	117.4(7)	C30-C31-C32	123.5(7)
F10-C31-C30	118.2(7)	F10-C31-C32	118.3(8)	C33-C32-C31	118.5(7)
C28-C33-Ir1	113.4(5)	C32-C33-Ir1	126.7(5)	C32-C33-C28	119.9(6)
F6-C34-C24	113.6(6)	F6-C34-F7	106.7(7)	F6-C34-F8	107.8(7)
F7-C34-C24	110.9(7)	F8-C34-C24	112.0(6)	F8-C34-F7	105.4(6)
F11-P1-F12	179.2(3)	F11-P1-F14	90.9(3)	F11-P1-F15	90.2(3)

F11-P1-F16	90.7(3)	F12-P1-F15	89.0(3)	F13-P1-F11	91.2(3)
F13-P1-F12	89.6(4)	F13-P1-F14	91.5(4)	F13-P1-F15	178.5(4)
F13-P1-F16	91.7(4)	F14-P1-F12	89.3(3)	F14-P1-F15	88.7(3)
F14-P1-F16	176.3(3)	F16-P1-F12	89.0(3)	F16-P1-F15	88.0(3)
O1-C35-C36	121.8	O1-C35-C37	121.8	C37-C35-C36	116.3
O2-C38-C39	121.8	O2-C38-C40	121.8	C40-C38-C39	116.3

3.7. References

1. Chapdelaine, M. J.; Hulce, M. Tandem Vicinal Difunctionalization: β-Addition to α,β-Unsaturated Carbonyl Substrates Followed by α-Functionalization. *Org. React.,* **1990**, *38*, 227-294.

2. Luo, F. T.; Negishi, E. Nickel- or palladium-catalyzed cross coupling. 28. A selective synthesis of a mixture of C-15 epimers of (.+-.)-11-deoxyprostaglandin E2 methyl ester. *J. Org. Chem.,* **1985**, *50*, 4762-4766.

3. Damon, R. E.; Schlessinger, R. H.; Blount, J. F. A short synthesis of (.+-.)-isostegane. *J. Org. Chem.,* **1976**, *41*, 3772-3773.

4. Catellani, M.; Chiusoli, G. P. One-pot palladium-catalyzed synthesis of 2,3-disubstituted bicyclo 2.2.1 heptanes and bicyclo 2.2.1 hept-5-enes. *Tet. Lett.,* **1982**, *23*, 4517-4520.

5. Kosugi, M.; Tamura, H.; Sano, H.; Migita, T. Palladium-catalyzed reaction of organic halides with organotin compounds involving olefin insertion - synthesis of 2,3-di-substituted norboranes. *Tetrahedron,* **1989**, *45*, 961-967.

6. Wu, X.; Lin, H.-C.; Li, M.-L.; Li, L.-L.; Han, Z.-Y.; Gong, L.-Z. Enantioselective 1,2-Difunctionalization of Dienes Enabled by Chiral Palladium Complex-Catalyzed Cascade Arylation/Allylic Alkylation Reaction. *Journal of the American Chemical Society* **2015**, *137* (42), 13476-13479. DOI: 10.1021/jacs.5b08734.

7. Saini, V.; Liao, L. Y.; Wang, Q. F.; Jana, R.; Sigman, M. S. Pd(0)-Catalyzed 1,1-Diarylation of Ethylene and Allylic Carbonates. *Org. Lett.,* **2013**, *15*, 5008-5011.

8. Tasker, S. Z.; Standley, E. A.; Jamison, T. F. Recent advances in homogeneous nickel catalysis. *Nature,* **2014**, *509*, 299-309.

9. Diccianni, J.; Lin, Q.; Diao, T. Mechanisms of Nickel-Catalyzed Coupling Reactions and Applications in Alkene Functionalization. *Acc. Chem. Res.,* **2020**, *53*, 906-919.

10. Lin, B. L.; Liu, L.; Fu, Y.; Luo, S. W.; Chen, Q.; Guo, Q. X. Comparing nickel- and palladium-catalyzed Heck reactions. *Organometal.,* **2004**, *23*, 2114-2123.

11. Qi, X. X.; Diao, T. N. Nickel-Catalyzed Dicarbofunctionalization of Alkenes. *ACS Catal.,* **2020**, *10*, 8542-8556.

12. Derosa, J.; Apolinar, O.; Kang, T.; Tran, V. T.; Engle, K. M. Recent developments in nickel-catalyzed intermolecular dicarbofunctionalization of alkenes. *Chem. Sci.,* **2020**, *11*, 4287-4296.

13. Shrestha, B.; Basnet, P.; Dhungana, R. K.; Shekhar, K. C.; Thapa, S.; Sears, J. M.; Giri, R. Ni-Catalyzed Regioselective 1,2-Dicarbofunctionalization of Olefins by Intercepting Heck Intermediates as Imine-Stabilized Transient Metallacycles. *J. Am. Chem. Soc.,* **2017**, *139*, 10653-10656.

14. Basnet, P.; Dhungana, R. K.; Thapa, S.; Shrestha, B.; Shekhar, K. C.; Sears, J. M.; Giri, R. Ni-Catalyzed Regioselective beta,delta-Diarylation of Unactivated Olefins in Ketimines via Ligand-Enabled Contraction of Transient Nickellacycles: Rapid Access to Remotely Diarylated Ketones. *J. Am. Chem. Soc.,* **2018**, *140*, 7782-7786.

15. Derosa, J.; Tran, V. T.; Boulous, M. N.; Chen, J. S.; Engle, K. M. Nickel-Catalyzed beta,gamma-Dicarbofunctionalization of Alkenyl Carbonyl Compounds via Conjunctive Cross-Coupling. *J. Am. Chem. Soc.,* **2017**, *139*, 10657-10660.

16. Bour, J. R.; Camasso, N. M.; Meucci, E. A.; Kampf, J. W.; Canty, A. J.; Sanford, M. S. Carbon-Carbon Bond-Forming Reductive Elimination from Isolated Nickel(III) Complexes. *J. Am. Chem. Soc.,* **2016**, *138*, 16105-16111.

17. Garcia-Dominguez, A.; Li, Z. D.; Nevado, C. Nickel-Catalyzed Reductive Dicarbofunctionalization of Alkenes. *J. Am. Chem. Soc.,* **2017**, *139*, 6835-6838.

18. Zhao, X.; Tu, H. Y.; Guo, L.; Zhu, S. Q.; Qing, F. L.; Chu, L. L. Intermolecular selective carboacylation of alkenes via nickel-catalyzed reductive radical relay. *Nat. Commun.,* **2018**, *9.*

19. Tu, H. Y.; Wang, F.; Huo, L. P.; Li, Y. B.; Zhu, S. Q.; Zhao, X.; Li, H.; Qing, F. L.; Chu, L. L. Enantioselective Three-Component Fluoroalkylarylation of Unactivated Olefins through Nickel-Catalyzed Cross-Electrophile Coupling. *J. Am. Chem. Soc.,* **2020**, *142*, 9604-9611.

20. Yuan, M. B.; Song, Z. H.; Badir, S. O.; Molander, G. A.; Gutierrez, O. On the Nature of C(sp(3))-C(sp(2)) Bond Formation in Nickel-Catalyzed Tertiary Radical Cross-Couplings: A Case Study of Ni/Photoredox Catalytic Cross-Coupling of Alkyl Radicals and Aryl Halides. *J. Am. Chem. Soc.,* **2020**, *142*, 7225-7234.

21. Primer, D. N.; Molander, G. A. Enabling the Cross-Coupling of Tertiary Organoboron Nucleophiles through Radical-Mediated Alkyl Transfer. *J. Am. Chem. Soc.,* **2017**, *139*, 9847-9850.

22. Fawcett, A.; Pradeilles, J.; Wang, Y.; Mutsuga, T.; Myers, E. L.; Aggarwal, V. K. Photoinduced decarboxylative borylation of carboxylic acids. *Science,* **2017**, *357*, 283-286.

23. Molander, G. A.; McKee, S. A. Copper-Catalyzed beta-Boration of alpha,beta-Unsaturated Carbonyl Compounds with Tetrahydroxydiborane. *Org. Lett.,* **2011**, *13*, 4684-4687.

24. Bose, S. K.; Brand, S.; Omoregie, H. O.; Haehnel, M.; Maier, J.; Bringmann, G.; Marder, T. B. Highly Efficient Synthesis of Alkylboronate Esters via Cu(II)-Catalyzed Borylation of Unactivated Alkyl Bromides and Chlorides in Air. *ACS Catal.,* **2016**, *6*, 8332-8335.

25. Noble, A.; Mega, R. S.; Pflasterer, D.; Myers, E. L.; Aggarwal, V. K. Visible-Light-Mediated Decarboxylative Radical Additions to Vinyl Boronic Esters: Rapid Access to gamma-Amino Boronic Esters. *Angew. Chem. Int. Ed.,* **2018**, *57*, 2155-2159.

26. Dick, G. R.; Woerly, E. M.; Burke, M. D. A General Solution for the 2-Pyridyl Problem. *Angew. Chem. Int. Ed.,* **2012**, *51*, 2667-2672.

27. De Vleeschouwer, F.; Van Speybroeck, V.; Waroquier, M.; Geerlings, P.; De Proft, F. Electrophilicity and nucleophilicity index for radicals. *Org. Lett.,* **2007**, *9*, 2721-2724.

28. Parsaee, F.; Senarathna, M. C.; Kannangara, P. B.; Alexander, S. N.; Arche, P. D. E.; Welin, E. R. Radical philicity and its role in selective organic transformations. *Nat. Rev. Chem.,* **2021**, *5*, 486-499.

29. Studer, A. The persistent radical effect in organic synthesis. *Chem. Eur. J.,* **2001**, *7*, 1159-1164.

30. Tutkowski, B.; Meggers, E.; Wiest, O. Understanding Rate Acceleration and Stereoinduction of an Asymmetric Giese Reaction Mediated by a Chiral Rhodium Catalyst. *J. Am. Chem. Soc.,* **2017**, *139*, 8062-8065.

31. Martinez-Botella, G.; Breen, J. N.; Duffy, J. E. S.; Dumas, J.; Geng, B. L.; Gowers, I. K.; Green, O. M.; Guler, S.; Hentemann, M. F.; Hernandez-Juan, F. A.; et al. Discovery of Selective and Potent Inhibitors of Gram-Positive Bacterial Thymidylate Kinase (TMK). *J. Med. Chem.,* **2012**, *55*, 10010-10021.

32. Beckwith, A. L. J.; Schiesser, C. H. Regio-selectivity and stereo-selectivity of alkenyl radical ring-closure - a theoretical-study. *Tetrahedron,* **1985**, *41*, 3925-3941.

33. Fernandez-Mateos, A.; Teijon, P. H.; Clemente, R. R.; Gonzalez, R. R. A Radical Clock for Reactions of Epoxy Derivatives Induced by Titanocene Chloride. *Synlett,* **2008**, (20), 3208-3212.

34. For information on this reactor and its construction see the Photochemical Reactor Design of the Supporting Information of: Remeur, C.; Kelly, C. B.; Patel, N. R.; Molander, G. A. Aminomethylation of Aryl Halides Using α-Silylamines Enabled by Ni/Photoredox Dual Catalysis. *ACS Catal.* **2017**, *7*,6065.

35. Kelly, C. B.; Patel, N. R.; Primer, D. N.; Jouffroy, M.; Tellis, J. C.; Molander, G. Preparation of visible-light-activated metal complexes and their use in photoredox/nickel dual catalysis. *Nat. Prot.* **2017**, *12*, 472.

36. Patel, N. P.; Kelly, C. B.; Siegenfeld, A. P.; Molander, G. A. Mild, Redox-Neutral Alkylation of Imines Enabled by an Organic Photocatalyst. *ACS Catal.* **2017**, *7*, 1766.

37. Phelan, J. P.; Wiles, R. W.; Lang, S. B.; Kelly, C. B.; Molander, G. A. Rapid access to diverse, trifluoromethyl-substituted alkenes using complementary strategies. *Chem. Sci.* **2018**, *9*, 3215.

38. Seebach, D.; Imwinkelried, R; Stucky, G. Optisch aktive Alkohole aus 1,3-Dioxan-4-onen: eine praktikable Variante der enantioselektiven Synthese unter nucleophiler Substitution an Acetal-Zentren. *Helv. Chim. Acta* **1987**, *70*, 448.

39. Rosenau, C. P.; Jelier, B. J.; Gossert, A. D.; Togni, A. Exposing the Origins of Irreproducibility in Fluorine NMR Spectroscopy. *Angew. Chem., Int. Ed.* **2018**, *57*, 9528.

40. Durandetti, M., Maddaluno, J. *Nickel Bromide Bipyridine* in Encyclopedia of Reagents for Organic

Synthesis; **2014.**

41. Patterson, S.; Alphey, M. S.; Jones, D. C.; Shanks, E. J.; Street, I. P.; Frearson, J. A.; Wyatt, P. G.;

Gilbert, I. H.; Fairlamb, A. H. Dihydroquinazolines as a Novel Class of *Trypanosoma brucei* Trypanothione Reductase Inhibitors: Discovery, Synthesis, and Characterization of their Binding Mode by Protein Crystallography. *J. Med. Chem.* **2011**, *54*, 6514.

42. Abdelkafi, H.; Michau, A.; Clerget, A.; Buisson, D.-A.; Johannes, L.; Gillet, D.; Barbier, J.; Cintrat, J.-

C. Synthesis, Chiral Separation, Absolute Configuration Assignment, and Biological Activity of Enantiomers of Retro-1 as Potent Inhibitors of Shiga Toxin. *ChemMedChem*, **2015**, *10*, 1153.

43. Linstad, E. J.; Vāvere, A. L.; Hu B.; Kempinger J. J.; Snyder S. E.; DiMagno, S.G. Thermolysis and radiofluorination of diaryliodonium salts derived from anilines. *Org. Biomol. Chem.* **2017**, *15*, 2246.

44. Lee, Y.; Silverman, R. B. Catalysis by Amino Acid-Derived Tetracoordinate Complexes: Enantioselective Addition of Dialkylzincs to Aliphatic and Aromatic Aldehydes. *Org. Lett.* **2000**, *2*, 3003.

45. Stone, I. B.; Jermaks, J.; MacMillan, S. N.; Lambert, T. H. The Hydrazine–O$_2$ Redox Couple as a Platform for Organocatalytic Oxidation: Benzo[*c*]cinnoline-Catalyzed Oxidation of Alkyl Halides to Aldehydes. *Angew. Chem. Int. Ed.* **2018**, *57*, 12494.

46. Choshi, T.; Yamada, S.; Sugino, E.; Kuwada, T.; Hibino, S. Total synthesis of grossularines-1 and -2. *J. Org. Chem.* **1995**, *60*, 5899.

47. Doering, N. A.; Kou, K. G. M.; Norseeda, K.; Lee, J. C.; Marth, C. J.; Gallego, G. M.; Sarpong, R. A Copper-Mediated Conjugate Addition Approach to Analogues of Aconitine-Type Diterpenoid Alkaloids. *J. Org. Chem.* **2018**, *83*, 12911.

48. Barbe, G.; Charette, A. B. Highly Chemoselective Metal-Free Reduction of Tertiary Amides. *J. Am. Chem. Soc.* **2008**, *130*, 18.

49. Yuan, Y.-C.; Kamaraj, R.; Bruneau, C.; Labasque, T.; Roisnel, T.; Gramage-Doria, R. Unmasking Amides: Ruthenium-Catalyzed Protodecarbonylation of N-Substituted Phthalimide Derivatives. *Org. Lett.*
2017, *19*, 6404.

50. Devine, W.; Woodring, J. L.; Swaminathan, U.; Amata, E.; Patel, G.; Erath, J.; Roncal, N. E.; Lee, P.
J.; Leed, S. E.; Rodriguez, A.; Mensa-Wilmot, K.; Sciotti, R. J.; Pollastri, M. P. Protozoan Parasite Growth Inhibitors Discovered by Cross-Screening Yield Potent Scaffolds for Lead Discovery. *J. Med. Chem.* **2015**, *58*, 5522.

51. Goodwin, N. C.; Cianchetta, G.; Burgoon, H. A.; Healy, J.; Mabon, R.; Strobel, E. D.; Allen, J.;

Wang, S.; Hamman, B. D.; Rawlins, D. B. Discovery of a Type III Inhibitor of LIM Kinase 2 That Binds in a DFG-Out Conformation. *ACS Med. Chem. Lett.* **2015**, *6*, 53.

52. Fawcett, J. P.; Wang, Y.; Mutsuga, T.; Myers, E. L.; Aggarwal, V. K. Photoinduced decarboxylative borylation of carboxylic acids. *Science* **2017**, *357*, 283.

53. Molander, G. A.; McKee, S. A. Copper-Catalyzed β-Boration of α,β-Unsaturated Carbonyl Compounds with Tetrahydroxydiborane *Org. Lett.* **2011**, *13*, 4684.

54. Dai, J.-J.; Zhang, W.-M.; Shu, Y.-J.; Sun, Y.-Y.; Xu, J.; Feng, Y.-S.; Xu, H.-J. Deboronative cyanation of potassium alkyltrifluoroborates via photoredox catalysis. *Chem. Commun.* **2016**, *52*, 6793.

55. Mun, S.; Lee, J.-E.; Yun, J. Copper-Catalyzed β-Boration of α,β-Unsaturated Carbonyl Compounds: Rate Acceleration by Alcohol Additives. *Org. Lett.* **2006**, *8*, 4887.

56. Pulis, A. P.; Blair, D. J.; Torres, E.; Aggarwal, V. K. Synthesis of Enantioenriched Tertiary Boronic Esters by the Lithiation/Borylation of Secondary Alkyl Benzoates. *J. Am. Chem. Soc.* **2013**, *135*, 16054.

Chapter 4. Photochemical C–H Activation Enables Nickel-Catalyzed Olefin Dicarbofunctionalization

4.1. Introduction

Our previous exploration of photoredox/Ni-mediated dicarbofunctionalization (DCF) made significant advancements in the field, as the developed protocol was able to include a significantly wider suite of functional groups and more diverse alkyl radicals than any previous literature example. Several subsequent reports reiterated this net-neutral photoredox mechanistic paradigm, each focusing on a different class of radical precursor (Figure 4.1). Complex alkyl radicals were accessed from trifluoroborates,[1, 2] oxalates,[3] bis(catecholato)silicates,[4] and alkyl halides (in a net-reductive mechanism),[5] while α-amino- and α-alkoxy radicals were derived from oxidation of α-silylamines[6] and α-amino/ α-alkoxy acids.[7]

Cesium Oxalate	Trifluoroborates	Bis(catecholato)silicates	α-silyl amines	α-amino acids	alkyl halides
Chu, 2018 & 2019	Molander, 2019	Nevado, 2019	Yuan, 2020	Reuping, 2019	Nevado, 2017
Overman 2019	Chu, 2020			Aggarwal, 2020	Martin, 2020
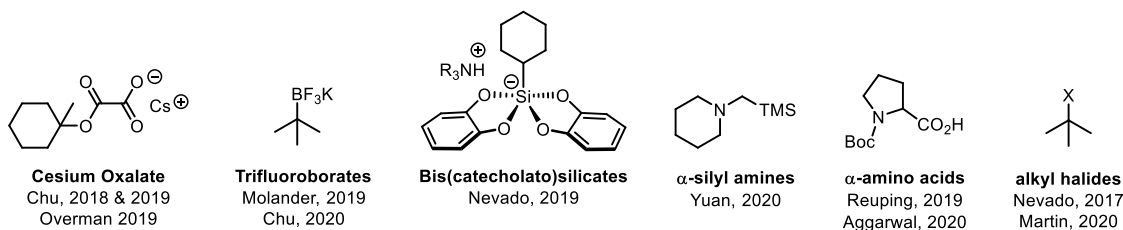
Figure 4.1. Various radical precursor groups used in Ni-catalyzed radical DCF reactions

Although these reports serve as prodigious examples of modern DCF reactions, each relied on the use of prefunctionalized radical precursors. With the exception of the naturally occurring α-amino acids utilized in Aggarwal's report, all other classes of radical precursors required preparative steps. The synthesis of each radical precursor group presents its own unique challenges and limitations: oxalates are hydrolytically sensitive; trifluoroborates are prone to protodeborylation; silicates are prepared via highly reactive precursors (i.e., SiCl₄), and α-aminosilanes are unstable to air over prolonged periods of time. In addition to the synthetic challenges, all of the aforementioned radical precursor groups are limited to a select few classes

of feedstocks. Because of this restriction, no radical DCF protocol was able to examine a diverse suite of electronically and sterically unique radicals under a single set of reaction conditions. Each focused on a different class of alkene, alkyl radical substructure, stoichiometry, catalyst etc., thus resulting in a wide range of three-component DCF to two-component cross-coupled (CC) product selectivities. As eluded to in the previous chapter, the mechanistic nature of radical DCF reactions make them a prime candidate for studying several fundamental aspects of both Giese additions and Ni-mediated radical cross-coupling. However, none of the current examples in the literature offered a set of standard conditions that can easily access a wide range of sterically and electronically unique radicals, and the significant variability among these protocols makes it essentially impossible to compare the observed selectivities with each other.
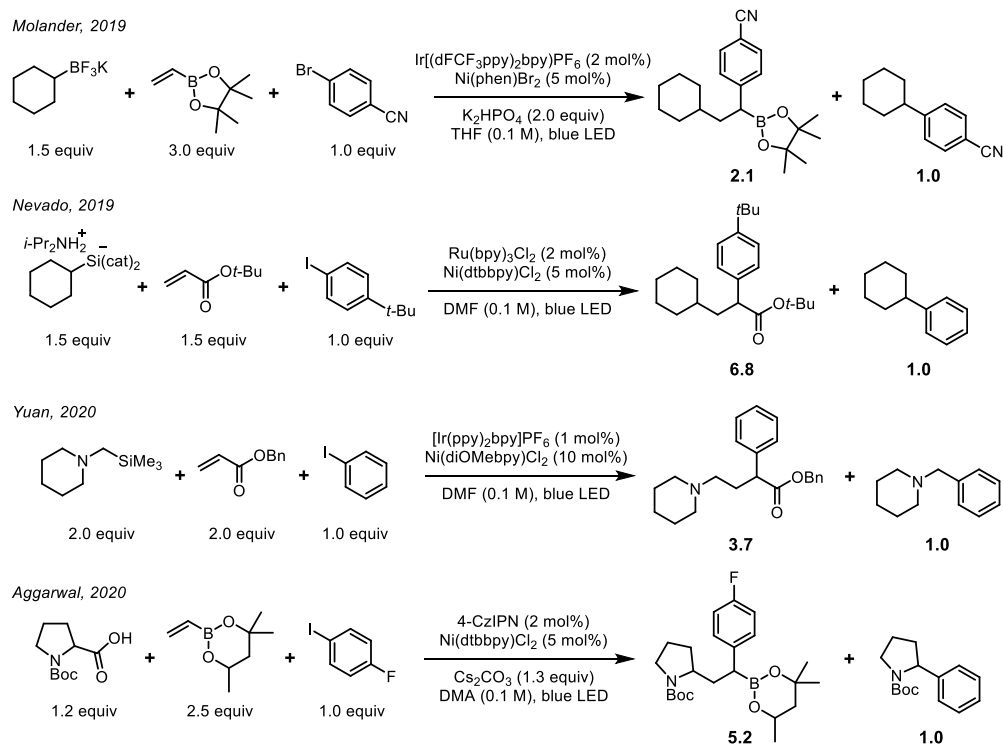
Figure 4.2. DCF vs CC product selectivities from various photoredox DCF reports

As we considered what paradigm could be leveraged to access the exceptionally broad scope of alkyl radicals that would be required to study the factors governing DCF vs CC

selectivity, hydrogen atom transfer (HAT) emerged as a prime candidate. HAT is the homolysis of a Y-H bond (typically C-H) in which an odd electron species induces the concerted movement of a proton and an electron. HAT is one of the most common mechanistic steps for oxidation of C-H bonds in both synthetic and biological systems.[8] The majority of these oxidation mechanisms rely on metal-oxo species that perform HAT followed by single-electron oxidation. Because most HAT events occur on C-H bonds, a wide variety of subsequent mechanistic steps can be used in a reaction to accomplish a variety of alkyl C-H functionalizations.[9] Indeed, HAT is a fundamental step in classical Giese addition reactions in which a radical initiator and tin hydride species perform sequential HATs to sustain a radical chain mechanism.[10] Though synthetically useful, these classical Giese reactions rely on stoichiometric HAT agents that have very poor atom economy and often complicated purification protocols.

In contrast, several photochemical reactions enable C-H activation via catalytic HAT agents. In the context of photoredox catalysis, amine radical cations were among the first species identified as catalytic HAT agents. Azabicyclo[2.2.2]octanes (e.g., quinuclidine and aceclidine) are easily oxidized (E_{ox} = +1.1-1.5 V vs SCE) by typical photoredox catalysts, and their resulting amine radical cations can abstract several types of activated C-H bonds (BDE < 85 kcal/mol), including those at α-amino-, α-amido-, α-alkoxy-, and benzylic positions.[11-12] In addition to tertiary amines, some Ni complexes have been demonstrated to be effective HAT catalysts that operate via an energy transfer mechanism, which ultimately liberates chlorine- or bromine radicals that perform HAT with activated C-H bonds in a catalytic manifold.[13,14] Though effective in many scenarios, these HAT catalysts must undergo some type of initial activation from an exogenous photocatalyst (performing either electron transfer or energy transfer), and these dual catalytic systems often exhibit challenging kinetic profiles.

However, several HAT agents exist that are both catalytic and photoactive, circumventing the need for an exogenous activating catalyst.[15] Eosin Y is a well-studied organic dye that upon photoexcitation can perform sequential HAT events. Eosin Y is particularly effective for the hydroalkylation of activated C-H bonds. However, it exhibits weak redox potentials, making it essentially impossible to induce any electron transfer steps, thus restricting its synthetic applicability.[16] In contrast, tetrabutylammonium decatungstate (TBADT) has been demonstrated to be a potent HAT agent with the capability of performing single electron reduction following HAT. With these dual HAT and redox capabilities, TBADT has been utilized to accomplish a diverse suite of radical C-H activations, including hydroalkylation, fluorination, Ni-mediated arylation, and Cu-mediated trifluoromethylation.[17-18] Although remarkably effective at facilitating the aforementioned transformations, the major limitations associated with TBADT are its high cost, massive molecular weight and, most importantly, poor HAT chemoselectivity. Several methods using TBADT for C-H functionalization report poor regioselectivity observed in the HAT step, even with substrates that contained a single, highly activated C-H bond.

Finally, diaryl ketones are the oldest and likely most well-developed of all photoactive HAT agents. Photoexcitation of a diaryl ketone at wavelengths >350 nm results in an n→π* transition to the S_1 state with a simultaneous reorganization of the non-bonding (NBE) and π electrons (Figure 4.3).[19] This reorganization is best understood as a reforming of a lone pair in the NBE orbital and the formation of a singly-occupied molecular orbital (SOMO) localized at oxygen that has significant π character. This hypothesis is based on computational studies of the photoexcitation of formaldehyde (model system for diaryl ketones) in which an increase in the atomic distance between oxygen and carbon nuclei is observed with a slight pyramidalization of the carbon geometry.[20] Subsequently, intersystem crossing ($S_1 \rightarrow T_1$) accesses a long-lived triplet state that can best be described as a diradical species in which two SOMOs are centered on the

carbon and oxygen, respectively, of the carbonyl group. This hypothesis is supported by computing electron localization function (ELF) isosurfaces that are used to analyze the distribution of non-bonding electrons.[20] The ELF isosurface in Figure 4.3 depicts the coplanar electron densities localized on oxygen and carbon in the T_1 state, which is indicative of a diradical species. In this diradical state the oxygen SOMO is an efficient hydrogen atom abstractor, with the resulting newly formed O-H exhibiting a bond dissociation enthalpy of ~100-105 kcal/mol (depending on the aryl groups).[21]
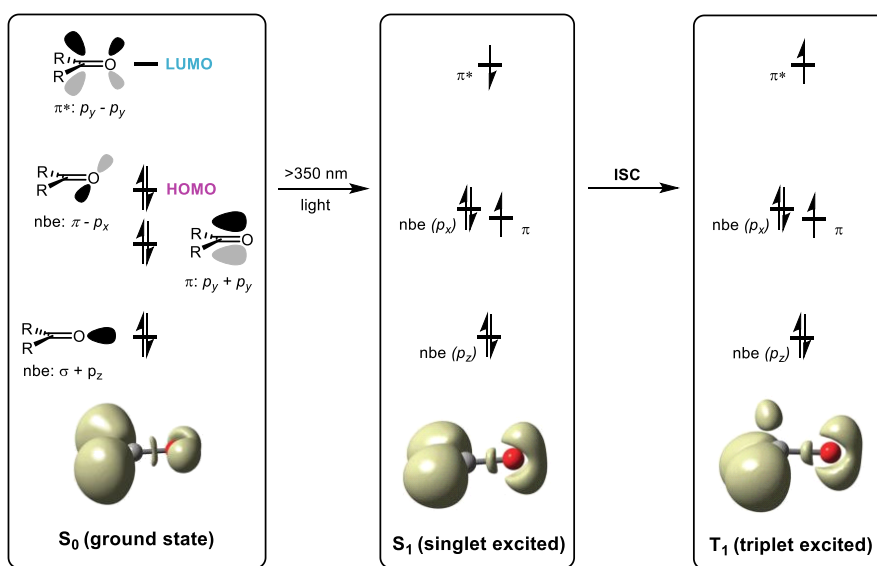
Figure 4.3. Molecular orbital description of the photoexcitation of the carbonyl group with ELF isosurfaces for S_0, S_1 and T_1 states calculated for formaldehyde.[20]

Following HAT the bis-benzylic carbon radical can undergo single electron oxidation (followed by deprotonation) to return to the original ground state diaryl ketone (Figure 4.4). Similar to TBADT, the dual HAT/redox capabilities of diaryl ketones open the door to a diverse range of possible mechanisms to leverage C-H functionalization.[9] Diaryl ketones also offer excellent modularity in their structure (changing the substitution of aryl or heteroaryl groups), allowing the user to "dial in" optimal photophysical and redox properties.
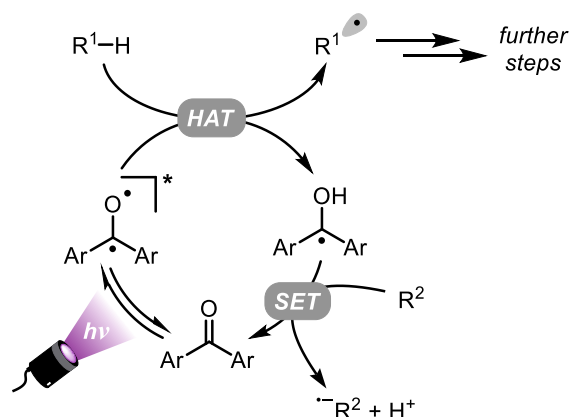
Figure 4.4. Typical mechanism for a redox-neutral catalytic cycle of diaryl ketone C-H activation

The first examples of photo-sensitized C-H hydroalkylation catalyzed by diaryl ketones were reported in the 1950s, using benzophenone and sunlight.[22] For decades, diaryl ketones were used extensively in photochemical C-H activation reactions. However, it was not until very recently that this mode of HAT was merged with Ni-catalyzed cross coupling to achieve arylation of activated C-H bonds.[23] Considering the superior chemoselectivity of diaryl ketone catalysts as compared to TBADT and the diverse range of C-H bonds that can be activated, this mode of catalysis emerged as a prime candidate to study the factors governing DCF vs CC selectivity in Ni-catalyzed, radical DCF reactions. The following mechanism for a DCF reaction catalyzed by synergistic diaryl ketone-HAT and Ni-mediated cross coupling was proposed (**Figure 4.5**). Photoexcitation of a benzophenone derivative (**4.I**) would access the previously described triplet diradical species (**4.II**), which could engage in regioselective HAT with a substrate bearing an activated C-H bond. The newly formed alkyl radical (**4.IV**) could then undergo a Giese addition with an activated alkene to produce radical adduct **4.VI**. Two plausible pathways emerged in regard to the order of steps in the Ni-mediated cross-coupling cycle. Metalation of adduct **4.VI** with a ligated Ni[0] species (**4.VII**) followed by oxidative addition into an aryl halide would produce the key Ni[III] intermediate, **4.IX** (blue pathway). Alternatively, oxidative addition of the

aryl halide with the ligated Ni⁰ complex might occur prior to metalation of the radical adduct (green pathway), leading to the same Ni^{III} intermediate. Finally, reductive elimination from this Ni^{III} complex would furnish the desired DCF product (**4.XII**). The exact order of these fundamental steps might have significant impacts on the DCF vs CC selectivity, and therefore it was deemed critical that these mechanistic details be thoroughly investigated.
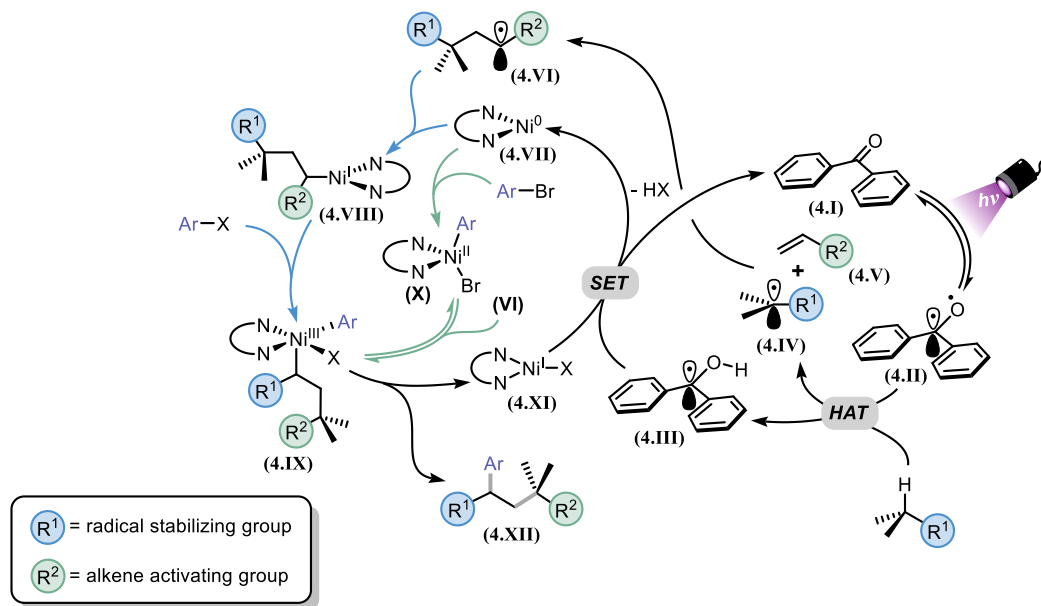
Figure 4.5. Proposed mechanism for HAT-mediated DCF reaction.
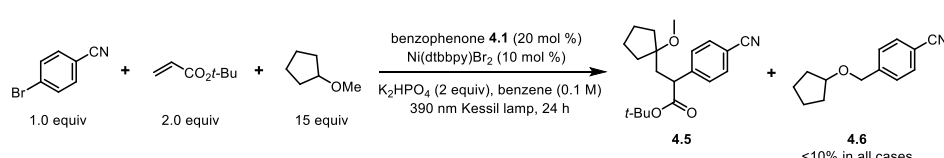
4.2. Reaction Design and Optimization
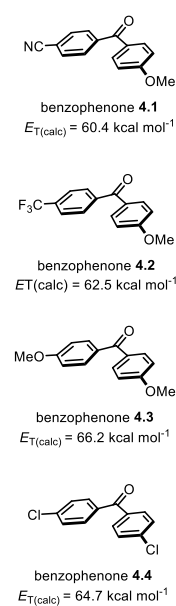
Based on the recent reports of Martin[24] and Rueping,[25] diaryl ketones bearing one electron rich and one electron deficient aryl group were first examined in the optimization of the catalyst for the proposed HAT-mediated DCF protocol. It was suggested that such diaryl ketones experience captodative stabilization[26] (stabilization of a radical via synergistic effect of conjugated electron-withdrawing and electron-donating groups), leading to longer lived triplet diradical species. Indeed, computational studies on the triplet state energy of a series of diaryl ketones revealed that those structures that experience captodative stabilization tended to have

lower triplet state energies and thus longer excited state lifetimes (see 4.6 Experimental Section for full details). Optimization studies on the proposed HAT-mediated DCF began using 4-(4-methoxybenzoyl)benzonitrile (benzophenone **4.1**) as the HAT catalyst because of its low triplet state energy and the bathochromic shift (λ_{max} = 325 nm) observed compared to many other benzophenone derivatives. In most previous reports of diaryl ketone HAT catalysis, the C-H precursor is typically used in large excess compared to the other coupling partners (limiting reagents). Therefore, we elected to focus on small organic structures that are typically used as commodity solvents. In this vein, we identified a diverse array of structures bearing C-H bonds alpha to alcohols, ethers, amides, sulfides, and borates, all of which were commercially available at minimal cost. Cyclopentyl methyl ether was selected as a model C-H radical precursor as it possess two different C-H bonds alpha to the oxygen. Using a standard bipyridyl nickel(II) dibromide catalyst in concert with *tert*-butyl acrylate and 4-bromobenzonitrile, the major product observed was the DCF product that stemmed from C-H activation at the tertiary α-oxy C-H bond (**4.5**, **Table 4.1,** entry 1). Only trace amounts of a two-component cross coupling product (**4.6**), which was formed via activation at the primary site, were detected, demonstrating the excellent regiochemical selectivity of the designed diaryl ketone HAT catalyst **4.4**. Other benzophenone derivatives demonstrated equivalent regiochemical selectivity. However, the overall yield of the desired product appeared to be inversely correlated with the calculated triplet state energy (entries 2-4). Other bipyridine-ligated nickel(II) salts were competent catalysts, but the sterically demanding 4,4'-di-*tert*-butyl derivative was the most effective (entries 5-7). Trifluorotoluene as a solvent showed improvement over benzene, likely because of its greater dielectric constant, resulting in better solubility of all species (entry 8). However, more polar solvents such as ethyl acetate and acetone yielded hydroalkylation of the acrylate and protodebromination of the aryl halide and only poor yields of the DCF product. Irradiation with a lower intensity 370 nm LED chip (10 W) produced a similar yield compared to the higher output 390 nm Kessil lamp (52 W).

238

Using lower wavelength light sources (300 nm Rayonet lamp) resulted in a dramatic decrease in the product yield, indicating that the appropriate excitation to affect the n → π* transition is >360 nm as previously calculated.[19] A household CFL was completely ineffective at converting any of the starting materials, demonstrating the need for more intense irradiation at the appropriate wavelengths.

Table 4.1. Optimization data for HAT-mediated DCF

entry	deviation from conditions above	^{1}H NMR yield of 4.5
1	None	73%
2	benzophenone **4.2** in place of benzophenone **4.1**	50%
3	benzophenone **4.3** in place of benzophenone **4.1**	47%
4	benzophenone **4.4** in place of benzophenone **4.1**	40%
5	Ni(bpy)Br$_2$ in place of Ni(dtbbpy)Br$_2$	30%
6	Ni(dmbpy)Br$_2$ in place of Ni(dtbbpy)Br$_2$	67%
7	Ni(d(OMe)bpy)Br$_2$ in place of Ni(dtbbpy)Br$_2$	42%
8	TFT in place of benzene	86%
9	EtOAc in place of benzene	39%
10	acetone in place of benzene	26%
11	370 nm LED chip in place of 390 nm Kessil lamp	70%
12	300 nm Rayonet lamp in place of 390 nm Kessil lamp	37%
13	Household CFL	0%

bpy = 2,2'-bipyridyl ; dmbpy = 4,4'-dimethyl-2,2'-bipyridyl ; d(OMe)bpy = 4,4'-dimethoxy-2,2'-bipyridyl ; TFT = α,α,α-trifluorotoluene

4.3. Scope Exploration

With these optimized conditions in hand, the scope of the (hetero)aryl halide coupling partner was then explored (**Table 4.2**). An excellent range of aryl halides containing complex functional groups was well tolerated under the reaction conditions. Generally speaking, aryl bromides bearing electron-withdrawing groups produced good to excellent yields of the desired product under standard conditions. However, electron-neutral and electron-rich aryl bromides gave incomplete conversion and a majority of hydroalkylation and protodebromination byproducts. To resolve this sluggish reactivity, the corresponding aryl iodides were employed,

which resulted in a dramatic improvement of yield for the DCF product. In instances where the aryl halide contained activated C-H bonds, increasing the loading of the C-H radical precursor to a cosolvent (1:1 v/v ratio with TFT) provided better yields of the DCF product as this suppressed any undesired additional reactivity. A series of DCF structures prepared from bifunctional arenes bearing multiple nucleophilic and/or electrophilic handles for further elaboration of the arene core were isolated with no undesired secondary reactivity at these sites (**4.20-4.22**). A suite of heteroaryl bromides was also included in the scope of electrophiles.

Table 4.2. Scope of aryl halides in HAT-mediated DCF
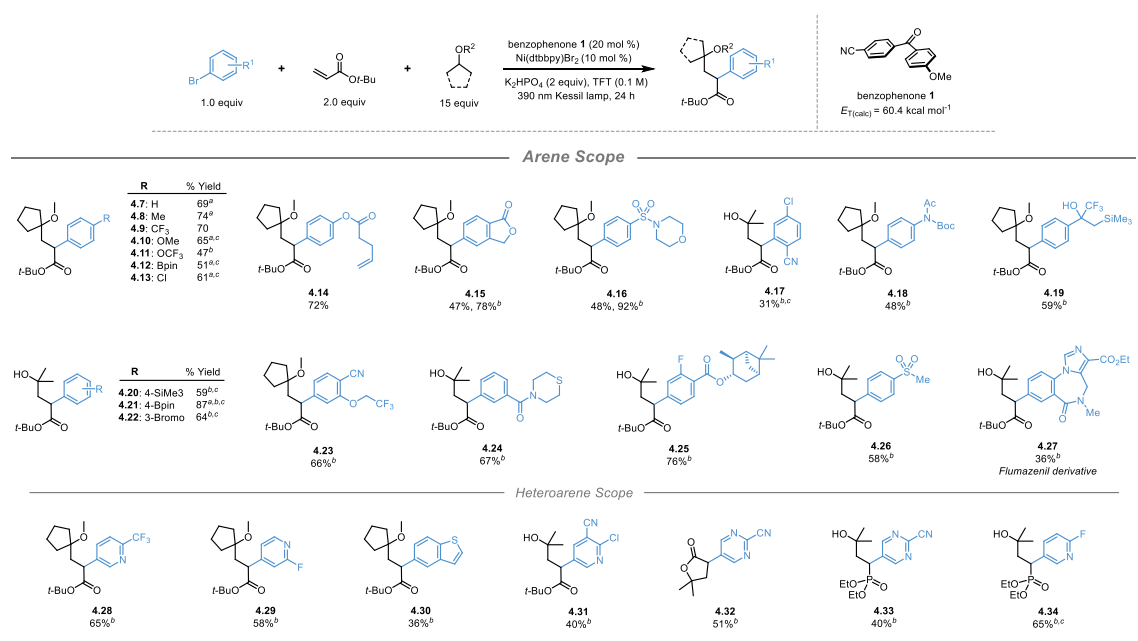
The DCF product furnished from reaction with 5-bromopyrimidine-2-carbonitrile was isolated as the corresponding lactone (**4.32**). The lactonization occurred prior to exposure to SiO_2 chromatography and it is plausible that the highly electrophilic nature of the pyrimidine facilitated a nucleophilic acyl substitution at the benzylic ester via an intramolecular S_NAr-type intermediate as proposed in **Figure 4.6**.
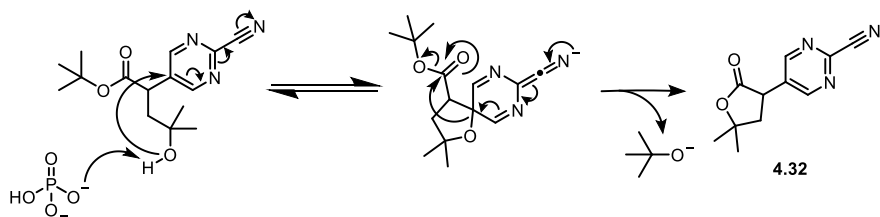
Figure 4.6. Plausible mechanism for the formation of the pyrimidinyl lactone DCF product, **4.32**.

In addition to acrylates, a range of other alkenes were competent coupling partners for the developed DCF reaction. The α-alkoxy/ α-hydroxyl radicals generated via HAT are strongly nucleophilic in electronic nature, and thus electron deficient alkenes provided an appropriate "polarity-match" for efficient reactivity.[27] A variety of vinyl electron-withdrawing groups including a nitrile, boronate, phosphonate, and amide produced the desired products in good yields (**Table 4.3, 4.35-4.38**). Internal alkenes, including both cyclic and acyclic structures, yielded the anticipated DCF products, all with excellent levels of diastereoselectivity (**4.39-4.42**). Surprisingly, the reaction with dimethyl fumarate as a radical acceptor produced two stereoisomers; the *syn* diastereomer was obtained as the anticipated hydroxyl succinate (**4.43**), while the *anti* diastereomer underwent spontaneous lactonization to provide **4.44**. We assume that selective lactonization occurs only with the *anti* diastereomer because of the less sterically demanding conformation of the nucleophilic acyl substitution intermediate that orients the methyl ester and arene groups on opposing faces of the lactone ring.

241

Table 4.3. Scope of alkenes in HAT-mediated DCF

— *Alkene Scope* —

4.35
80%

4.36
34%[a,b]

4.37
79%[b]

4.38
48%[b]

(±)
4.39
53%[a]
dr = >20:1

(±)
4.40
70%[a]
dr = >20:1

(±)
4.41
74%[a]
dr = >20:1

(±)
4.42
58%[b], 90%[a,b]
dr = >20:1

(±)
4.43 + 4.44
72[a,c]
1.4:1 ratio
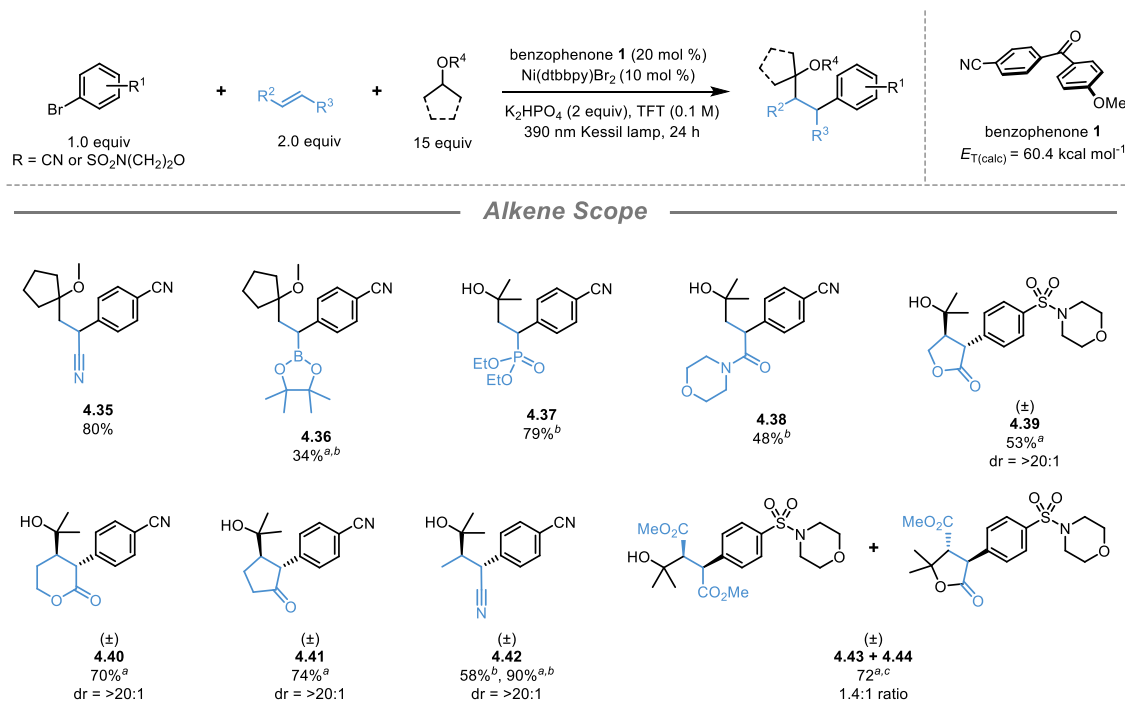
[a]Using a 1:1 v/v ratio of C-H precursor/TFT. [b]Using 4.0 equiv of alkene. [c]Using the corresponding aryl iodide

Finally, the scope of the C-H precursor was examined (**Table 4.4**). In this scope, a systematic exploration of C-H precursors bearing many different α-heteroatom groups and substitution patterns was examined to understand the electronic and steric factors governing DCF vs CC selectivity. As anticipated, a variety of cyclic and acyclic tertiary α-alkoxy- and α-hydroxy precursors produced the desired DCF product with *tert*-butyl acrylate and 4-bromobenzonitrile with no two-component CC product detected (**4.45**, **4.53-4.56**). As demonstrated by previous research in our group,[28] these tertiary radicals are very reluctant to undergo direct inner-sphere metalation to Ni complexes, and thus under the optimized conditions the rate of Giese addition leading to three-component DCF coupling entirely outcompetes direct metalation and two-component cross coupling. However, all secondary radicals exhibited competitive three-component DCF vs two-component CC reactivity. To increase the formation of the DCF product

and ease of purification the loading of alkene was increased to 4 equivalents. A range of secondary cyclic- and acyclic α-alkoxy and α-hydroxy C-H precursors underwent the desired reaction with DCF/CC selectivities ranging from 2.7:1 – 1:1 (**4.46-4.50**, **4.57**). When employing 1,3-dioxolane as C-H precursor, HAT occurred selectively at the bis-α-oxy position, providing a surrogate for a formyl radical that then underwent the DCF transformation (**4.51**). Surprisingly, tetrahydrothiophene gave very poor DCF/CC selectivity compared to tetrahydrofuran, indicative of the very dissimilar natures of α-alkoxy- and α-thio radicals. Secondary amides and -carbamates were also amenable to this mode of HAT and gave excellent DCF/CC ratios (**4.58-4.60**). Finally, a tertiary α-boryl radical was generated via diaryl ketone-mediated HAT and was amenable to the desired transformation (**4.61**). Unfortunately, primary radicals were unable to undergo the desired transformation under the optimized conditions, and only trace consumption of the starting material was observed with a variety of primary C-H precursors.

Table 4.4. Scope of C-H precursors in HAT-mediated DCF
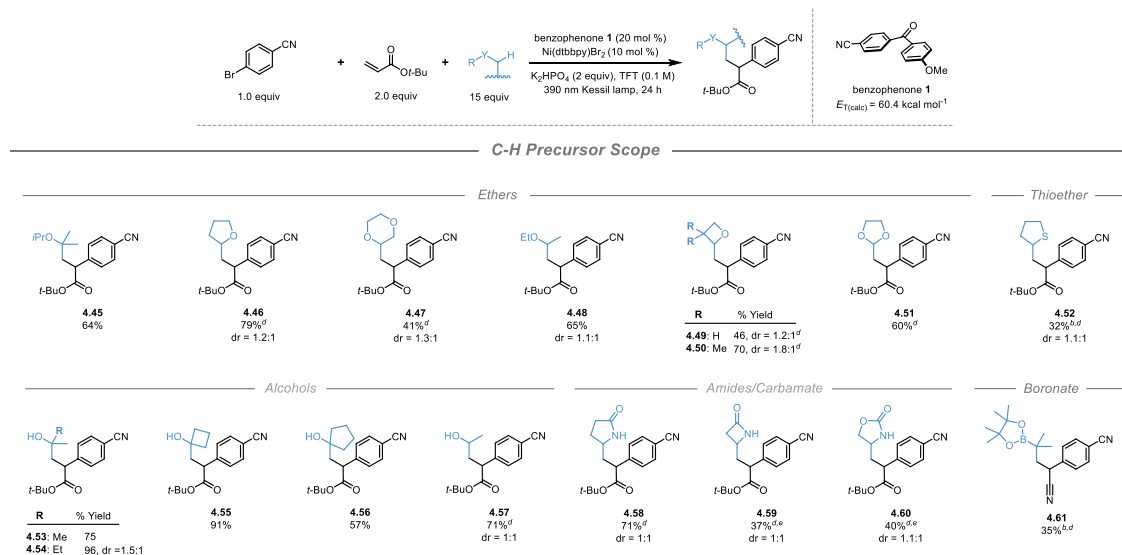
The DCF/CC ratios for a range of secondary radicals generated from HAT are listed in **Figure 4.6**. Generally speaking, two clear trends arise from these observations. First, the more

243

sterically demanding the radical (based on the substitution of radical center and steric nature of the overall structure), the higher the DCF/CC selectivity. Tertiary radicals produced no direct two-component cross coupling product. This result is entirely logical, as previous research has demonstrated that Ni complexes are particularly reluctant to metalate tertiary C_{sp3} radicals, while secondary C_{sp3} radicals rapidly undergo metalation, ultimately leading to arylation. However, even among various secondary C_{sp3} radicals, more sterically demanding structures resulted in an increase in the formation of the DCF product. This concept is well illustrated when comparing the DCF/CC selectivities observed with the *gem*-dimethyl oxetane and the unsubstituted oxetane. The more sterically congested α-*gem*-dimethyl radical was 1.5 times more selective for the DCF pathway compared to its unsubstituted counterpart. The second trend that can be inferred from these results is that the more nucleophilic the alkyl radical, the greater its selectivity for the DCF pathway. Alpha-amido radicals were more selective than α-hydroxy/ α-alkoxy radicals, which in turn were more selective than α-thio radicals. The nucleophilicity of each radical is governed by the amount of electron donation experienced by the various α-heteroatom groups. Computed nucleophilicity indices for radical species analogous to those used in this series are in good agreement with the observed DCF/CC trend.[29] Overall, it can be concluded that both steric and electronic factors are critical in determining the DCF/CC selectivity for various alkyl radicals.

DCF/CC selectivity	4.4:1	2.3:1	1.3:1	1.1:1	1:1	0.75:1	0.16:1
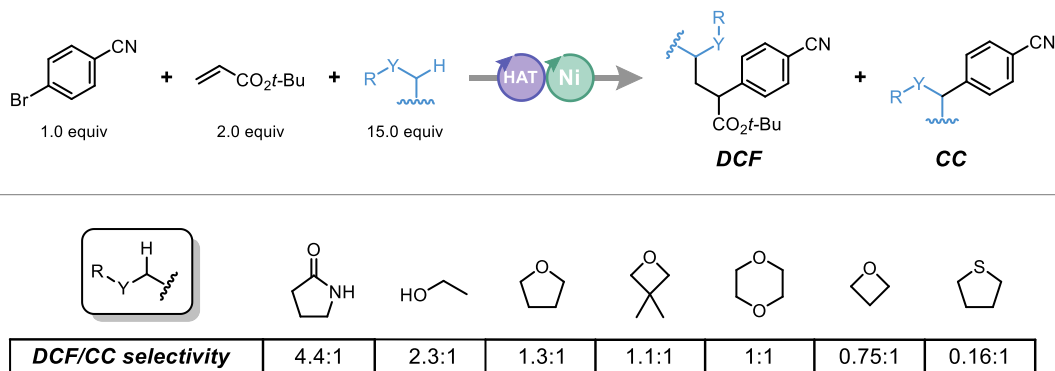
Figure 4.6. Experimentally measured DCF/CC ratios for a suite of secondary alkyl radicals.

244

4.3. Computational and Mechanistic Studies

To fully comprehend the entire mechanism for both DCF and CC pathways and the nature of the product-determining steps in each pathway, computational studies were undertaken (**Figure 4.7**) by Mingbin Yuan and Prof. Osvaldo Gutierrez. DLPNO−CCSD(T) and dispersion-corrected DFT calculations were utilized to explore both two-component CC and three-component DCF pathways for 2-propanol, methacrylate, and 4-bromobenzonitrile under standard conditions.[30] Two plausible mechanisms for the formation of the two component coupling products were examined that differ in the geometry of the Ni^{II} oxidative addition complex. After formation of the singlet, square planar Ni^{II} complex (**4.C$_1$**), this species is expected to equilibrate rapidly under photocatalytic conditions to the triplet, tetrahedral geometry (**4.C$_3$**).[31] The α-hydroxy radical (**A**) is expected to add to either the "axial" position of **4.C$_1$** (blue pathway, via **4.A-TS-B**) or the "equatorial" position of **4.C$_3$** (green pathway, via **4.A-TS-B'**), the latter being more energetically favorable. On the basis of these calculations, at low concentration of alkene, α-hydroxy radical **A** is expected to produce the two component CC product (**4.P^{cc}**) via the green pathway. However, at high concentrations of alkene, α-hydroxy radical **4.A** is expected to undergo irreversible Giese addition to methyl acrylate via **4.A-TS-D**, which is isoenergetic to the barrier for metalation of **4.A** (**4.A-TS-B'**). We also considered radical addition of **4.A** to Ni^0-bound alkene (η^2 complex formation), but found this pathway less likely because of the inherent higher concentration of alkene in the system with respect to nickel, as well as the low barrier for the oxidative addition of aryl bromide to the Ni^0 center (see 4.6 Experimental S). Finally, subsequent metalation of Giese adduct **4.D** to **C$_3$** affords the key Ni^{III} intermediate **4.E**, which will quickly undergo reductive elimination (via **4.E-TS-F**) to form the desired, three-component product (**4.P^{DCF}**) and Ni^I bromide species **4.F**. Notably, both metalation (via **4.A-TS-B**) and Giese addition (via **4.A-TSD**) of radical **4.A** were found to be irreversible, and their transition states

higher in energy than the subsequent reductive eliminations (**4.B'-TS-F** and **4.E-TS-F**, respectively). Thus, these calculations demonstrate that the kinetic product selectivity for the competing pathways (DCF vs CC) is determined by the relative energy difference between the metalation (**4.A-TS-B'**) versus Giese addition (**4.A-TS-D**) transition states and, given the small energetic difference between these, is highly dependent on the relative concentration of nickel to alkene.
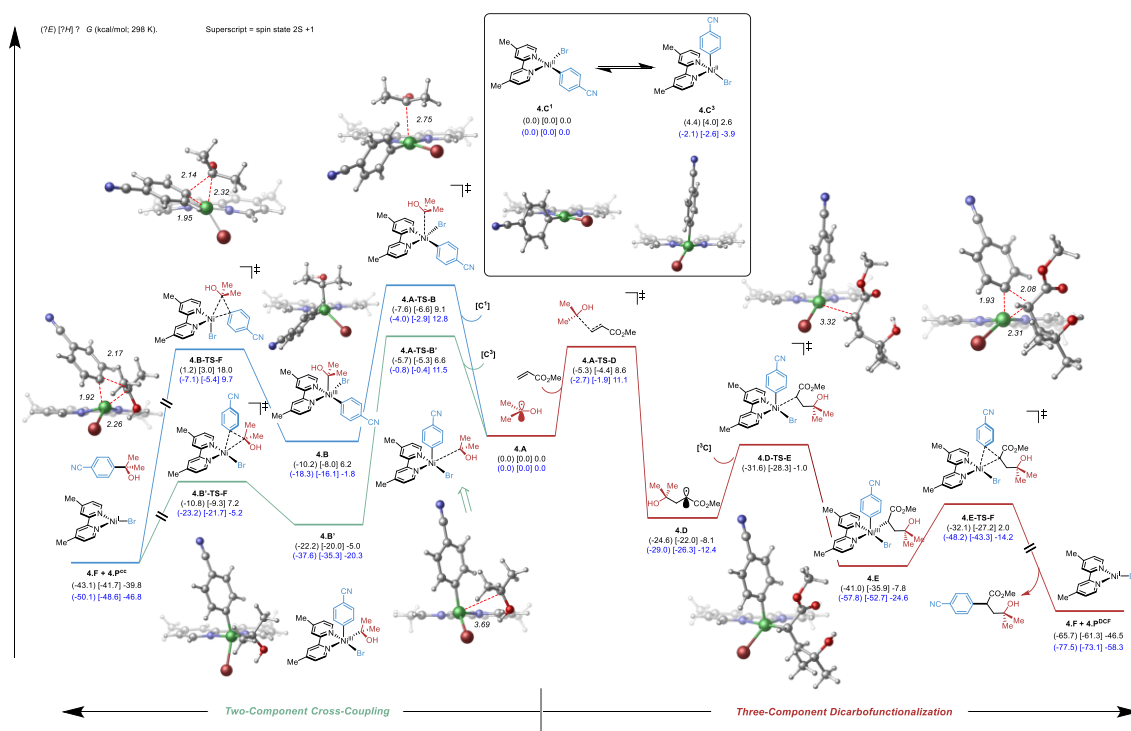
Figure 4.7. Computational analysis of the divergent reactivity of alkyl radical in the isopropyl alcohol system. Electronic (in parentheses), enthalpy (in bracket), and free energies (kcal/mol; 298 K) given were calculated at the (U)B3LYP-D3/def2-TZVPP-CPCM (benzene)//(U)B3LYP-D3/def2-SVP-PCM (benzene) (black) and DLPNO−CCSD(T)/def2-TZVPP//(U)B3LYP-D3/def2-SVP-CPCM (benzene) (blue) levels of theory.

The same computational investigation was performed by Prof. Osvaldo Gutierrez and Mingbin Yuan for the reaction of THF in place of 2-propanol. In the case of this secondary α-alkoxy radical, a dramatic change in the relative energetic barriers for the product determining steps was observed. The metalation of the α-alkoxy THF radical was appreciably lower than its

246

Giese addition into methacrylate. **Figure 4.8** contrasts the computational results for transition state barriers that determine the product selectivity for both 2-propanol and THF. These calculated kinetics are in good agreement with our experimental results in which no two-component CC product was observed for reaction with 2-propanol, but in which the two-component CC product was formed in significant amounts in the reaction with THF. It is logical to assume that the dissimilar DCF/CC selectivities for 2-propanol and THF stem from the difference in their steric nature. The barriers for Giese addition of either radical are quite similar, however, the barriers for the metalation are vastly different. THF exhibits a markedly lower barrier for metalation, leading to competitive two-component CC product formation.
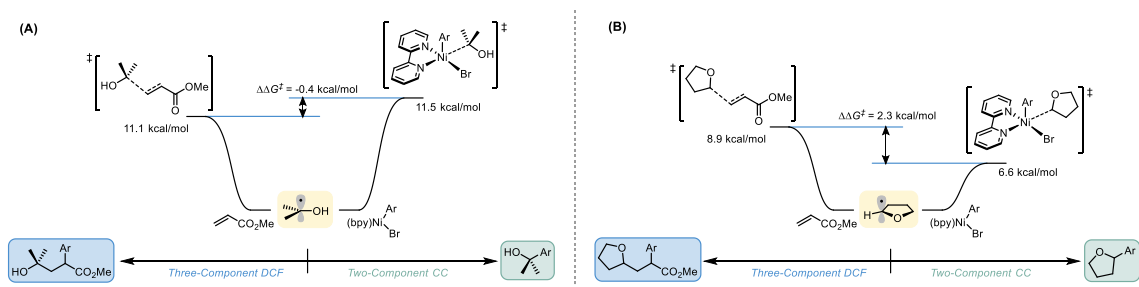
Figure 4.8. (A) Transition state barriers for product determining steps in the reaction of 2-propanol. **(B)** Transition state barriers for product determining steps in the reaction of 2-propanol.

The steric and electronic effects governing the DCF vs CC selectivity for the suite of examined radicals was accounted for in our computational studies. However, one surprising result was the high DCF/CC selectivity observed with secondary α-hydroxy radicals compared to secondary α-alkoxy. At a first approximation it appeared that the only key difference between these α-hydroxy- and α-alkoxy radicals was the presence of the hydroxyl proton, which has the propensity to engage in hydrogen bonding. Prior studies revealed that the presence of hydrogen bonding significantly accelerates the rate of HAT on such substrates, presumably by weakening the α-hydroxy C−H bond in the presence of exogenous hydrogen bond acceptors.[12 32 33] However, there are very few computational studies that examine the role of hydrogen bonding between the

radical component and Giese acceptor.[29] We hypothesized that this type of hydrogen bonding interaction could play a paramount role in controlling selectivity for this DCF protocol. To probe for the presence of this effect, the DCF/CC selectivity was measured when using acrylonitrile in place of *tert*-butyl acrylate, which resulted in a dramatic inversion of the selectivity (Figure 4.9). These dissimilar selectivities were attributed to the difference in hydrogen bonding capabilities of the two alkenes: the acrylate serves as an excellent H-bond acceptor that accelerates the Giese addition, whereas no such interaction is possible with acrylonitrile, resulting in a more two-component CC product formation.
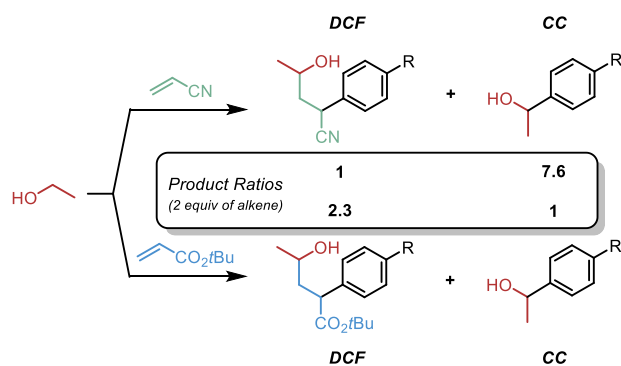
Figure 4.9. DCF vs CC selectivities for standard reactions using α-hydroxy C-H precursor with *tert*-butyl acrylate and acrylonitrile.

Computational studies were then performed using the addition of the α-hydroxy radicals into methacrylate as a model system. The lowest energy conformation for the Giese addition transition state with ethanol (**TS-4.62**) revealed that the hydroxyl group was oriented at an appropriate angle/distance to engage in intermolecular hydrogen bonding with the carbonyl oxygen of the acrylate. Non-covalent interaction (NCI) plots revealed an attractive interaction occurring between the hydroxyl and carbonyl groups, confirming the presence of a hydrogen bonding event in this Giese addition step (**TS-4.63**). To approximate the energetic benefit of this hydrogen bonding interaction, the same computation was performed with a restricted approach

248

angle of the α-hydroxy radical such that the hydrogen and carbon groups were orthogonal to each other and would not engage in any hydrogen bonding (**TS-4.64**). This restricted conformation increased the transition state energy by 1.2 kcal/mol, and the corresponding NCI plot strongly suggests that this is mainly because of the loss of the hydrogen bond interaction. Finally, the corresponding ether (*i*-PrOMe) was subjected to the same analysis, which resulted in a 1.9 kcal/mol increase in the transition state energy barrier (**TS-4.65**). The NCI plot reveals only minimal steric repulsion from the methyl group, and therefore the increase in the transition state barrier is again attributed mainly to the loss of hydrogen bonding.
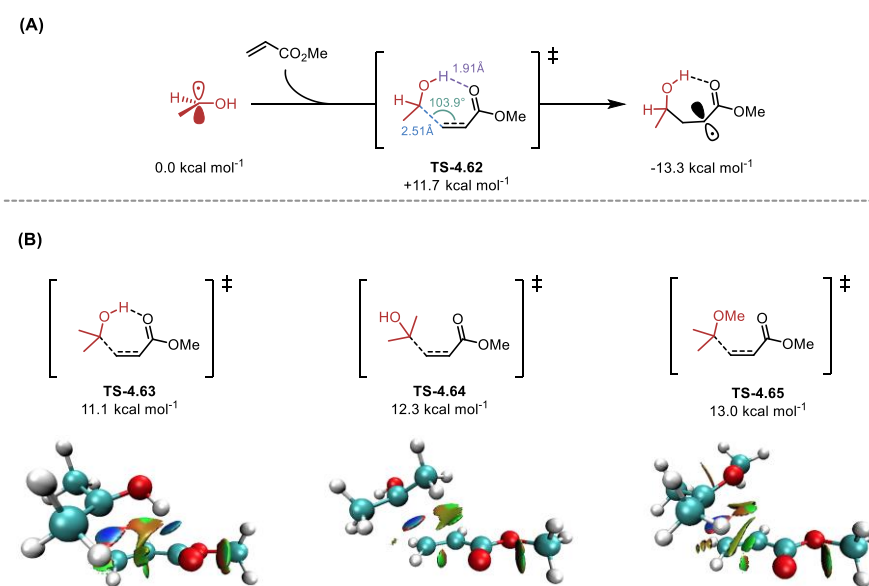
Figure 4.10. (A) Computed transition state for the Giese addition of secondary ethanol radical into methacrylate displaying hydrogen bonding. **(B)** Computed transition states and NCI plots for the Giese addition of various α-oxy radicals into methacrylate.

To understand more fully how the hydrogen bonding capability and electronic nature of each alkene influences the rate of Giese addition with various α-oxy radicals, hydroalkylation competition reactions were performed (**Figure 4.11A**). From entries 1-3, a qualitative ranking of the most reactive alkenes toward Giese addition of α-hydroxy radicals (i.e., 2-propanol) can be

established: acrylonitrile > acrylate >> acrylamide. Though lacking the ability to engage in hydrogen bonding, acrylonitrile was the most reactive alkene, indicating that the strong electron-withdrawing nature of the nitrile group results in a very electrophilic π-bond which, we conclude, is the dominant factor in determining the rate of the Giese addition step in these DCF reactions. When comparing the selectivities for the same competition reactions using diisopropyl ether (entry 3), the effect of hydrogen bonding becomes evident. Diisopropyl ether was ~7 times more selective for addition into acrylonitrile over an acrylate as compared to 2-propanol. This result demonstrates that in the case the α-alkoxy radicals, which lack any hydrogen bond donor group, complete selectivity for the most electrophilic alkene (acrylonitrile) is observed. However, selectivity for the less electrophilic acrylate is dramatically increased in the case of α-hydroxy radicals, which can engage in hydrogen bonding, accelerating the rate of Giese addition into the acrylate. The use of phenyl vinyl sulfone in analogous competition reactions (entries 4 and 5) gave similar results to *tert*-butyl acrylate, indicating that sulfones function as competent hydrogen bond acceptors in these Giese additions. Finally, the addition of $MgCl_2$ (a chaotropic reagent that disrupts hydrogen bonding with hydroxyl groups) in entry 6, resulted in 6.5:1 ratio of acrylonitrile- to acrylate-based products. This result emphasizes that any inhibition of the hydrogen bonding interaction between the α-hydroxy radical and acrylate has a significant impact on the rate of Giese addition.
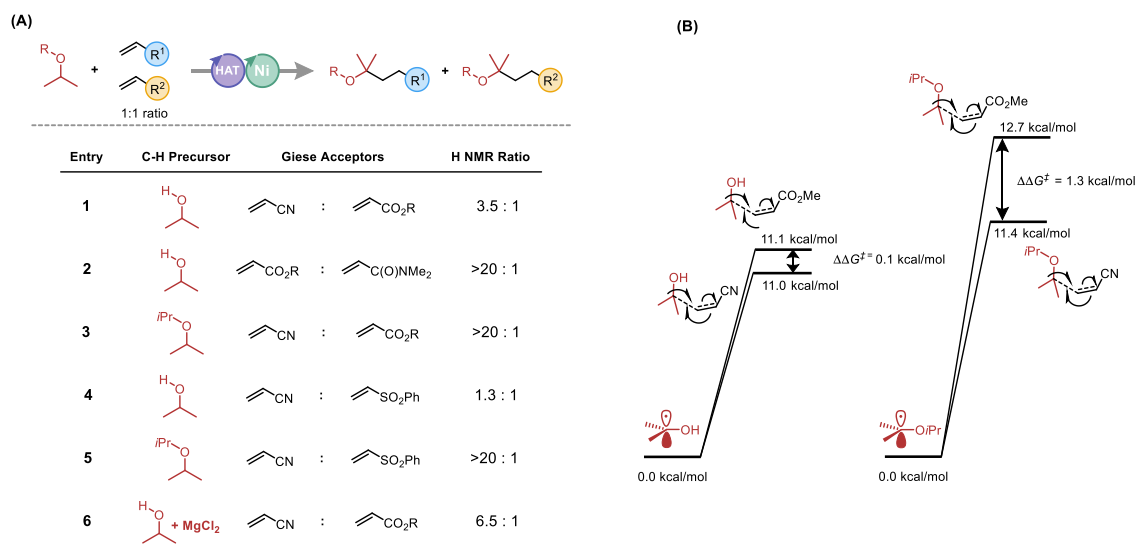
Figure 4.11. (A) Hydroalkylation competition reactions. **(B)** Computational studies on hydroalkylation competition reactions.

Computational analysis of the competition reactions in entries 1 and 3 was in good agreement with the experimental results (**Figure 4.11B**). The difference in the transition state energy barrier for addition into either acrylonitrile or methacrylate ($\Delta\Delta G^{\ddagger}$) corresponded to the calculated selectivity in the hydroalkylation competition reactions. The small $\Delta\Delta G^{\ddagger}$ calculated for the Giese additions of 2-propanol reflected the close product ratio observed in the hydroalkylation competition reaction (**Figure 4.11A**, entry 1), which was influenced by the hydrogen bonding. In contrast, the computed barrier for addition of diisopropyl ether into acrylonitrile was much lower than the barrier for addition into methacrylate. This significantly larger $\Delta\Delta G^{\ddagger}$ is also in agreement with the results of the hydroalkylation competition reaction in which complete selectivity for addition into acrylonitrile was observed when employing diisopropyl ether as C-H precursor. From the these experimental and computational results we conclude that the selectivity for Giese additions of α-oxy radicals is mainly governed by the electrophilic nature of the alkene but is also strongly influenced by the potential formation of hydrogen bonding events between α-hydroxy radicals and Giese acceptors that can function as hydrogen bond acceptors.

251

To understand more fully the effect of hydrogen bonding motifs in both the Giese addition and arylation steps of the mechanism, DCF competition reactions were conducted (**Figure 4.12**). When using an α-hydroxy radical (2-propanol) with equimolar ratios of acrylonitrile and *tert*-butyl acrylate, the DCF product distribution greatly favored the ester product over the nitrile. However, CPME exhibited an equivalent ratio of nitrile- and ester-based DCF products. Furthermore, a significant amount of the acrylonitrile-based hydroalkylation product was again detected in the competition reaction with 2-propanol. From these results we hypothesize that the hydrogen bonding capabilities of the C-H precursor and alkene also have a significant impact on the arylation step.
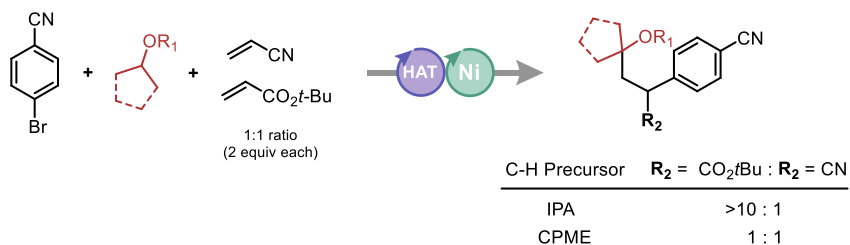
Figure 4.12. DCF competition reactions for α-hydroxy and α-alkoxy radicals with various alkenes.

Recalling the results of the hydroalkylation competition reactions, we hypothesized that 2-propanol should also exhibit greater selectivity for addition into acrylonitrile in the DCF competition reactions. However, the distribution of the DCF products in the competition reaction with 2-propanol did not agree with the previously observed Giese addition selectivity. Upon a closer examination, a significant amount of acrylonitrile hydroalkylation occurred in the DCF competition reaction with 2-propanol. Considering the results from both the hydroalkylation and DCF competition reactions, we conclude that in the reaction of α-hydroxy radicals and acrylonitrile, the Giese addition step is very favorable, however, the arylation step is inhibited to some extent, leading to the formation of the hydroalkylation byproduct. With these assumptions

252

in mind, the result of the DCF competition with 2-propanol could be rationalized (**Figure 4.13**). Though *tert*-butyl acrylate was less reactive than acrylonitrile in the Giese addition step, the resulting ester-based radical adduct, **4.67**, was able to undergo facile arylation, leading to the DCF product (**4.69**), whereas the nitrile-based radical adduct, **4.66**, favored the hydroalkylation pathway (**4.68**). The observed product distribution was entirely logical as the major product stemmed from acrylonitrile hydroalkylation (**4.68**), the secondary product was the acrylate-based DCF adduct (**4.69**), and finally the acrylonitrile DCF product (**4.70**) and acrylate hydroalkylation (**4.71**) were much more minor contributors. Comparing Giese adducts **4.66** and **4.67**, the most apparent difference is again the ability/inability of the two functional groups to engage in hydrogen bonding with each other. We then turned to computational analysis to understand how the difference in hydrogen bonding capabilities was impacting the arylation step.
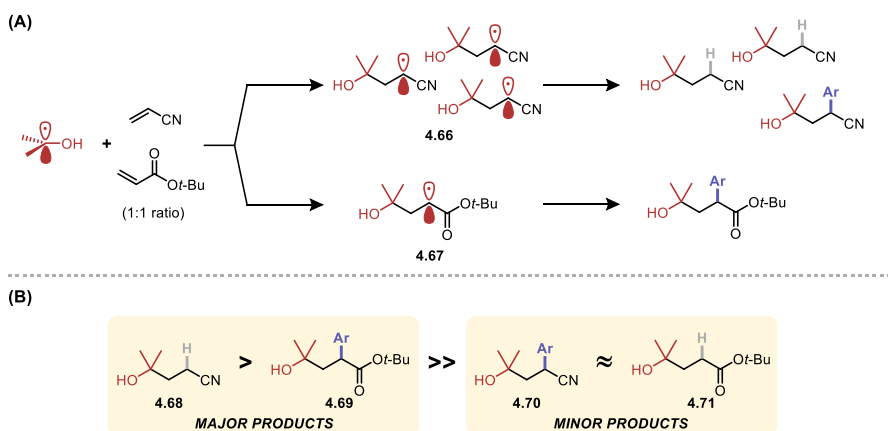
Figure 4.13. Mechanistic rationale for the observed selectivity in DCF competition reactions.

Computational analysis of the mechanism for the formation of DCF products **4.69** and **4.70** revealed a significant difference in the structure of the Ni^{III} complex formed after radical metalation (**Figure 4.14**). Following Giese addition of the α-hydroxy radical into methacrylate, adduct **4.67** maintains an intramolecular hydrogen bonded complex. After metalation of **4.67** via the Ni^{II} oxidative addition complex, the hydroxyl group remains engaged in hydrogen bonding

253

with the ester group, and facile reductive elimination from Ni^{III} complex **4.72** yields the three-component DCF product (**4.69**). In contrast, Giese addition of the α-hydroxy radical of 2-propanol into acrylonitrile yields adduct **4.66**, which does not have the ability to engage in any intramolecular hydrogen bonding. After radical metalation, the conformation of the radical adduct in the trigonal bipyramidal Ni^{III} complex **4.73** is quite dissimilar to **4.72**. In the absence of any intramolecular hydrogen bonding, the free hydroxyl group is oriented toward the axial bromide ligand and this interaction, presumably, negatively impacts the arylation step, ultimately leading to hydroalkylation. The precise mechanistic details regarding the formation of the hydroalkylation product have yet to be fully elucidated, but it appears that a significant change in the Ni^{III} complex conformation (perhaps even a ligand exchange/cyclization) is detrimental to the arylation step. Finally, the good yield of the acrylonitrile-based DCF product using an ether as C-H precursor (e.g., **4.35**, **Table 4.3**) can be rationalized as the arylation step is no longer negatively impacted in the absence of any hydroxyl group.
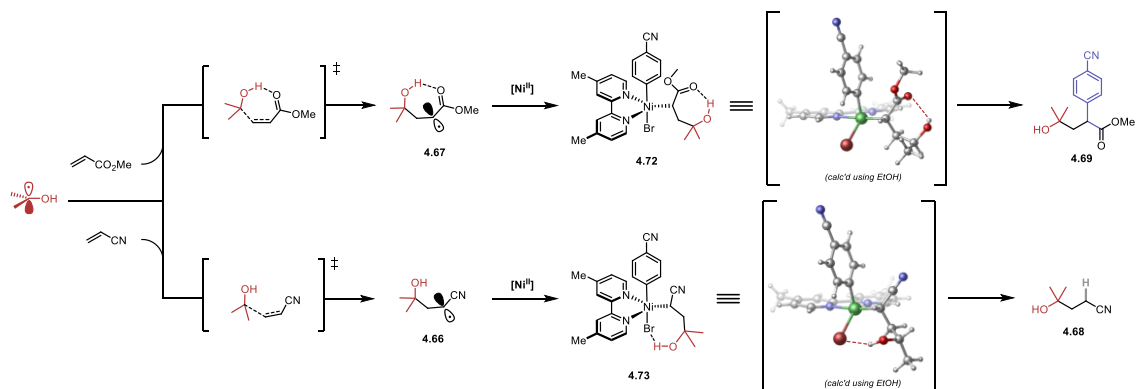
Figure 4.14. Computational analysis of the mechanism for the formation of **4.69** and **4.68**.

Finally, radical-clock experiments were performed using 1-cyclopropylethanol as C-H precursor. It was assumed that following HAT, the newly generated α-cyclopropyl radical would trigger ring-opening followed by arylation of the resultant primary radical to generate a two-component cross coupling product (**4.74**) along with various other ring-opened products. To our

astonishment, when employing 1-cyclopropylethanol in a standard DCF reaction with *tert*-butyl acrylate, no two-component cross coupling product (**4.74**) was formed. Rather, a significant amount of the standard three-component DCF product was formed with the cyclopropyl ring still intact (**4.75**). The other major product isolated from this reaction was a cyclopentyl adduct (**4.76**), which presumably forms via a ring-opening/[3+2] cycloaddition mechanism outlined in **Figure 4.16**. Similar reactivity was observed in our previous DCF report when employing an organotrifluoroborate derived from (*S*)-verbenone, which produced a [4+2] cycloaddition adduct.[1] Under identical reaction conditions, using acrylonitrile in place of *tert*-butyl acrylate produced some cyclopropane-containing DCF product (**4.77**). However, the major product obtained in this system was the anticipated ring-opened, cross-coupled product **4.78**.
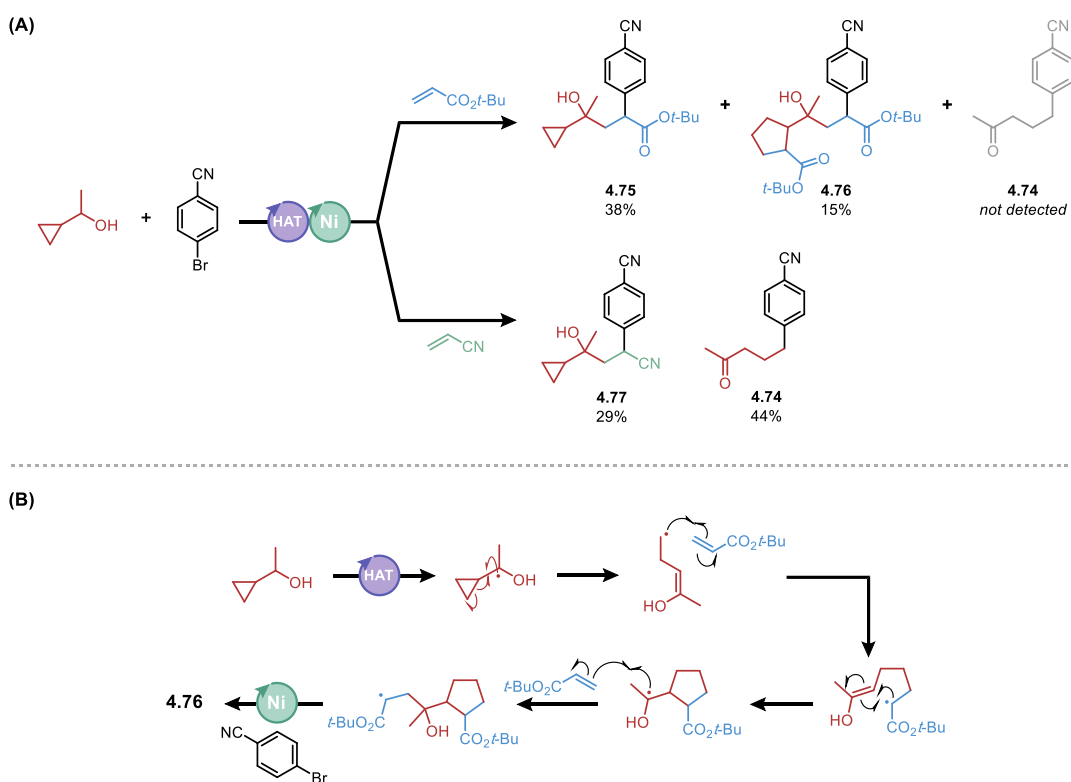
Figure 4.15. (A) DCF reactions with 1-cyclopropylethanol as C-H precursor. **(B)** Proposed mechanism for the formation of cycloadduct **4.76**.

255

Computed energetics for these systems show that ring opening of the α-cyclopropyl radical (**4.79**) is competitive with Giese addition to either acrylate or acrylonitrile and thus account for the mixture of both cyclopropyl DCF products **4.75** and **4.77** as well as various ring-opened products (**4.74** and **4.77, Figure 4.16**). The higher yield of ester-based cyclopropyl DCF product **4.75** compared to nitrile-based product, **4.77**, is likely because of a hydrogen bond-accelerated Giese addition of radical **4.78** with *tert*-butyl acrylate. We propose that **4.74** and **4.76** are formed via primary radical **4.81** (generated from reversible cyclopropane ring opening), which could undergo either Giese addition to the corresponding alkene or metalation to the Ni center (not calculated). The formation of **4.74** as the major product in the reaction with acrylonitrile suggests that the Giese addition barrier of **4.81** into acrylonitrile (**TS-4.82**) is appreciably higher than the barrier for its metalation. Conversely, the absence of **4.74** and the formation of **4.76** in the reaction with *tert*-butyl acrylate is rationalized by the significantly lower barrier of Giese addition of primary radical **4.81** to the acrylate. As demonstrated by the transition state structure (**TS-4.83**), hydrogen bonding between **4.81** and the acrylate is responsible for the accelerated Giese addition leading to the [3+2] cycloadduct (**4.76**). We therefore conclude that hydrogen bonding is again a prevailing factor in determining product selectivity in this DCF protocol.
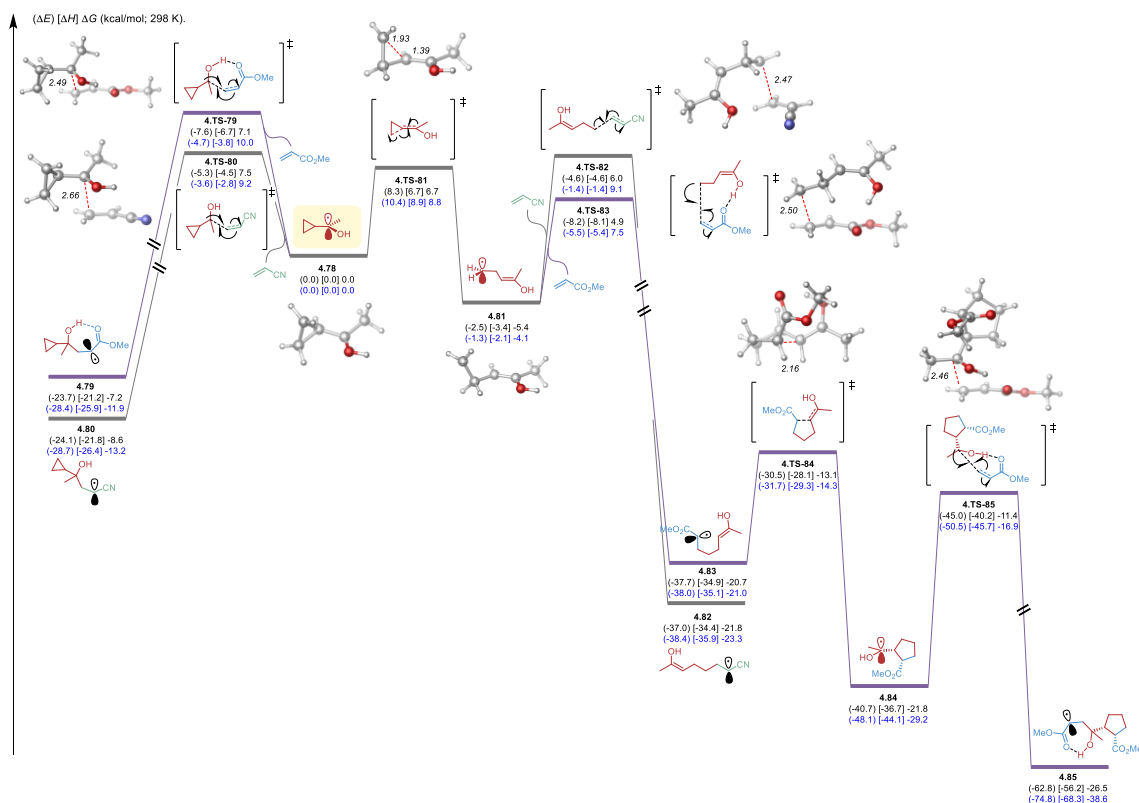
Figure 4.16. Computational analysis of the competing ring opening and Giese addition of tertiary radical in acrylate and acrylonitrile systems. Electronic (in parentheses), enthalpy (in bracket), and free energies (kcal/mol; 298 K) given were calculated at the (U)B3LYP-D3/def2-TZVPP-CPCM (benzene)// (U)B3LYP-D3/def2-SVP-CPCM-(benzene) (black) and DLPNO−CCSD(T)/def2-TZVPP//(U)B3LYP-D3/def2-SVP-CPCM (benzene) (blue) levels of method.

4.5. Conclusion

The developed HAT-mediated DCF protocol made significant advancements in radical DCF reactions by accessing a previously unfeasible suite of radical structures. The utilization of diaryl ketones as HAT agents enabled highly regioselective HAT via a modular, inexpensive, and sustainable mode of catalysis in sharp contrast to other HAT catalysts that are more predominant in photocatalysis. Through detailed computational studies, the mechanistic details of this transformation were thoroughly investigated. New insights into the nature and effect of hydrogen bonding in radical/alkene reactivity as well as metallaphotoredox cross-coupling were discovered.

257

These findings not only provide a new and efficient strategy for small molecule synthesis but also afford mechanistic insights that will prompt further discovery in the area of radical reactivity mediated by hydrogen bonding.

4.6. Experimental

4.6.1. General Considerations

All chemical transformations requiring inert atmospheric conditions or vacuum distillation utilized Schlenk line techniques with a 4- or 5-port dual-bank manifold. α,α,α-Trifluorotoluene (TFT) was distilled from anhyd CaH_2 and stored over 5Å molecular sieves, i-PrOH was stored over 5Å molecular sieves, and cyclopentyl methyl ether (CPME) was dried using a solvent delivery system. 1,1,1,3,3,3-Hexafluoro-2-propanol (HFIP) was stored over 5Å molecular sieves. All reagents were purchased and used as received from suppliers unless otherwise noted. Nickel pre-complexes were prepared as outlined here. 4-(4-Methoxybenzoyl)benzonitrile was prepared as outlined here. Aryl- and heteroaryl bromides were either purchased from commercial sources or prepared as outlined here. Reactions were monitored by ^{1}H NMR or TLC using silica gel F254 plates (60 Å porosity, 250 μm thickness). TLC analysis was performed using EtOAc/hexanes and visualized using permanganate stain, CAM (Hanessian's) stain, and/or UV light. Silica plugs utilized flash silica gel (60 Å porosity, 32-63 μm). Flash chromatography was accomplished using an automated system (monitoring at 254 nm and 280 nm in conjunction with an evaporative light scattering detector) with silica cartridges (60 Å porosity, 20-40 μm). Accurate mass measurement analyses were conducted using electron ionization (EI) or electrospray ionization (ESI). The signals were mass measured against an internal lock mass reference of perfluorotributylamine (PFTBA) for EI-GCMS, and leucine enkephalin for ESI-LCMS. The utilized software calibrates the instruments and reports measurements by use of neutral atomic masses. The mass of the electron is not included. IR spectra were recorded using either neat oil or

solid products. Melting points (°C) are uncorrected. NMR spectra [^{1}H, ^{13}C ^{1}H, ^{11}B, ^{19}F ^{1}H] were obtained at 298 K. ^{1}H NMR (500.4 MHz) chemical shifts are referenced to residual, non-deuterated CHCl$_3$ (δ 7.26) in CDCl$_3$. ^{13}C^{1}H NMR (125.8 MHz) chemical shifts are reported relative to CDCl$_3$ (δ 77.3) and the carbonyl carbon of acetone (δ 205.9). ^{11}B NMR (128.4 MHz) chemical shifts are uncorrected. ^{19}F NMR spectra were referenced to hexafluorobenzene (δ – 161.64 in CDCl$_3$). Data are presented as follows: chemical shift (ppm), multiplicity (s = singlet, d = doublet, t = triplet, q = quartet, m = multiplet, br = broad), coupling constant J (Hz) and integration.

4.6.2. Preparation of Catalysts

Preparation of 4,4'-di-*tert*-butyl-2,2'-bipyridine nickel(II) bromide [Ni(dtbppy)Br$_2$]
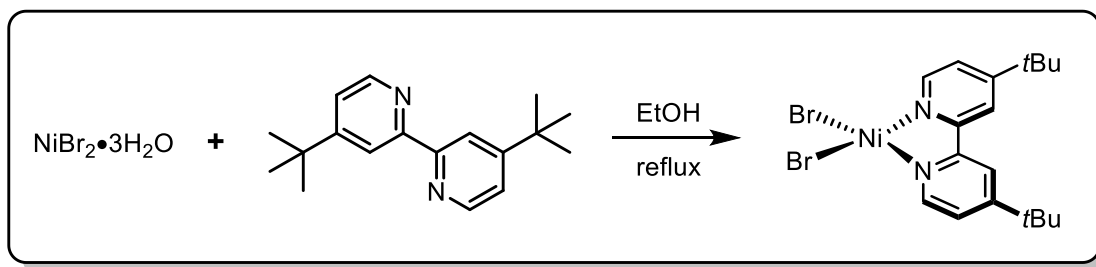
A flask was charged with NiBr$_2$•3H$_2$O (2.563 g, 10.00 mmol, 1.0 equiv) and 4,4'-di-*tert*-butyl-2,2'-bipyridine (3.000 g, 11.00 mmol, 1.1 equiv) and equipped with a reflux condenser. The system was vacuum filled under argon (x3). Absolute EtOH (50 mL) was added to the reaction flask via syringe, and the reaction was heated to a vigorous reflux for 24 h. During the refluxing period the color of the suspension changed from light brown to green/blue. After the reflux period, the reaction was cooled to rt, and the solvent was removed via rotary evaporation. The resulting sticky solid was then washed with three portions of boiling Et$_2$O followed by pentane.

The resulting solid was dried under high vacuum at 50 ºC for 24 h and stored in a vacuum desiccator.

Preparation of Benzophenone Catalyst (1)
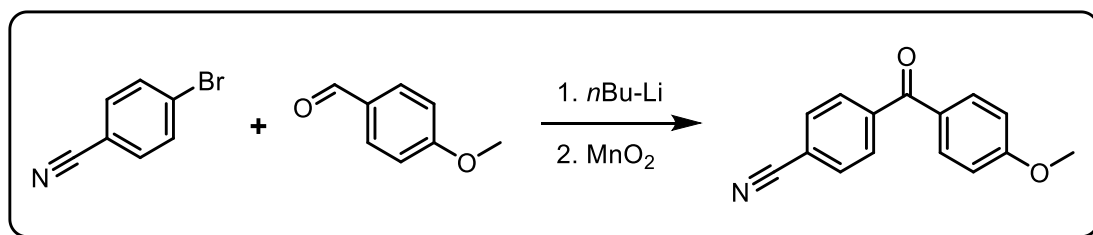
A flask was charged with 4-bromobenzonitrile (1.820 g, 10.00 mmol, 1.0 equiv) and vacuum filled with argon (x3). THF (30 mL) was added via syringe, and the reaction flask was placed in an acetone/dry ice bath to cool. *n*-BuLi was added slowly in a dropwise manner over 30 min, which caused a dramatic color change to dark red. After stirring in the cold bath for 30 min, freshly distilled anisaldehyde (1.633 g, 12.00 mmol, 1.2 equiv) was added dropwise, which caused no noticeable change in color. The reaction was left to stir in the bath overnight as the system slowly returned to rt. The reaction was then quenched with H_2O (20 mL) and sat aq NH_4Cl (20 mL) and extracted with two portions of 1:1 Et_2O/EtOAc (20 mL). The combined organic extracts were washed with brine, dried (anhyd Na_2SO_4), and the solvent was removed via rotary evaporation. The resulting crude oil was passed through a silica plug to remove any excess anisaldehyde, and the alcohol product was obtained as a yellow tinted oil. The oil was dissolved in CH_2Cl_2 (35 mL) and MnO_2 (8.69 g, 100 mmol, 10.0 equiv) was added in a single portion. The reaction was then stoppered and stirred at rt overnight. Celite (~10 g) was added to the reaction, and the resulting black slurry was then filtered through a pad of silica and then washed with additional CH_2Cl_2 (100 mL). The resulting soln was concentrated via rotary evaporation, and the

impure oil was recrystallized from MeOH to yield 4-(4-methoxybenzoyl)benzonitrile (1.905 g, 80%) as colorless needles. All data matched that which was reported in the literature.[34]

4.6.3. UV-Vis Spectra of Catalysts 1 and Ni(dtbbpy)Br₂
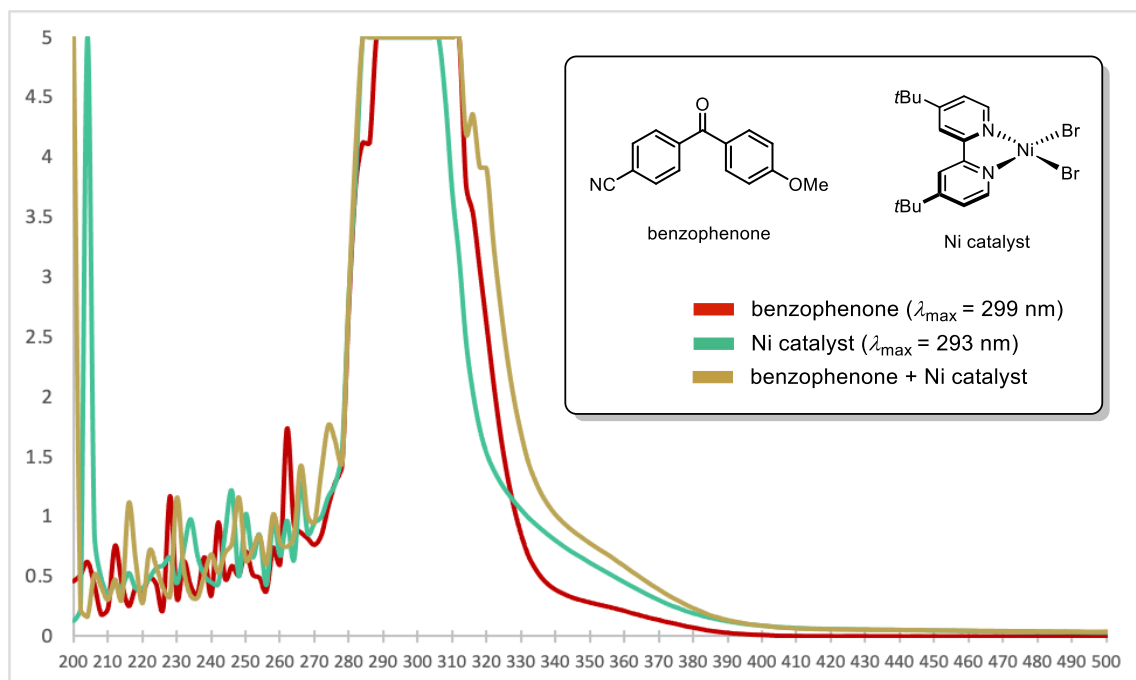
Figure 4.17. UV-Vis spectra of benzophenone catalyst, nickel catalyst and mixture (0.005 M) in TFT.

4.6.4 Preparation of Non-Commercial Aryl Halides

4-Bromophenyl pent-4-enoate, 86
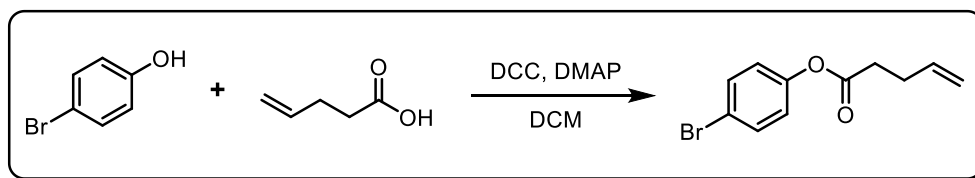
A flask was charged with 4-bromophenol (2.600 g, 15.00 mmol, 1.0 equiv) and 4-dimethylaminopyridine (0.275 g, 15 mol%) and then vacuum filled under argon (x3). CH_2Cl_2 (25 mL) was added via syringe followed by 4-pentenoic acid (1.652 g, 16.50 mmol, 1.1 equiv). The reaction flask was placed in an ice/water bath and a soln of *N,N*-dicyclohexylcarbodiimide (3.404 g, 16.50 mmol, 1.1 equiv) in CH_2Cl_2 (25 mL) was added dropwise. After the addition, the cold bath was removed, and a voluminous white precipitate formed. After stirring for 4 h, the reaction slurry was filtered through a pad of Celite that was washed with additional CH_2Cl_2 (20 mL). The resulting soln was washed with satd aq Na_2CO_3 (30 mL) followed by brine (20 mL). The organic extract was then dried (anhyd Na_2SO_4), and the solvent was removed via rotary evaporation. The crude material was then purified via short-path, high vacuum distillation (135-140 °C, 9.50 mmHg) to yield 4-bromophenyl pent-4-enoate as a colorless liquid (3.290 g, 86%).

¹H NMR (CDCl$_3$, 500 MHz) δ ppm 7.48 (d, *J* = 8.9 Hz, 2H), 6.97 (d, *J* = 8.7 Hz, 2H), 5.89 (ddt, *J* = 17.0, 10.4, 6.5 Hz, 1H), 5.14 (dq, *J* = 17.1, 1.6 Hz, 1H), 5.08 (dq, *J* = 10.2, 1.3 Hz, 1H), 2.66 (t, *J* = 7.3 Hz, 2H), 2.52-2.47 (m, 2H).

¹³C NMR (CDCl$_3$, 125 MHz) δ ppm 171.4, 149.9, 136.4, 132.7, 123.6, 119.1, 116.3, 33.8, 29.0.

FT-IR (cm⁻¹, neat, ATR) 2979 (w), 1756 (s), 1483 (s), 1197 (vs), 1129 (s).

HRMS (EI) calcd for $C_{11}H_{11}BrO_2$ [M⁺]: 253.9942, found: 253.9955.

4-((4-Bromo/iodophenyl)sulfonyl)morpholine
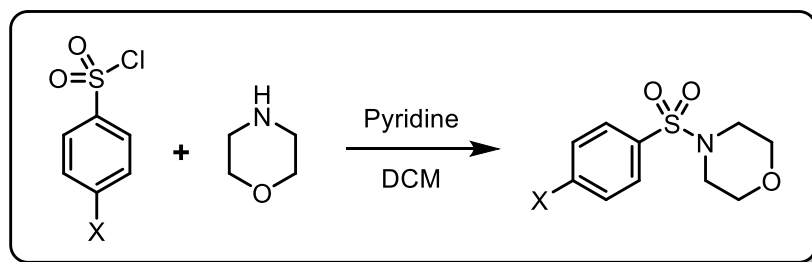
A flask was charged with 4-bromobenzenesulfonyl chloride or 4-iodobenzenesulfonyl chloride (1.10 equiv) which was then dissolved in CH_2Cl_2 (0.3 M). Pyridine (2.50 equiv) was added, and the reaction flask was placed in an ice/water bath. Morpholine (1.00 equiv) was then added dropwise, which caused the immediate evolution of a yellow precipitate. After stirring for 4 h, the reaction was quenched by the addition of satd aq NH_4Cl (~30 mL). The layers were separated, and the aq layer was extracted with an additional portion of CH_2Cl_2 (~20 mL). The combined organic extracts were washed with brine, dried (anhyd Na_2SO_4), and the solvent was removed via rotary evaporation. The resulting crude solids were recrystallized from hexanes, and a minimal amount CH_2Cl_2 to yield the respective desired products. All data matched that which was reported in the literature for the bromo[1] and iodo[35] compounds.

tert-Butyl Acetyl(4-bromophenyl)carbamate
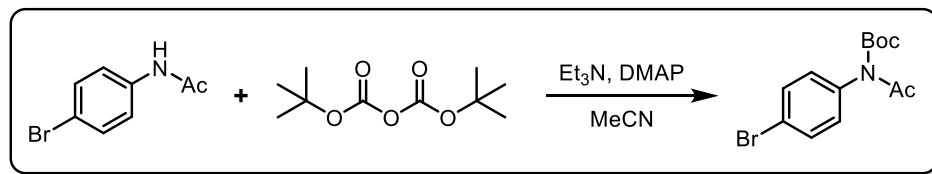
A flask was charged with 4-bromoacetanilide (2.14 g, 10.0 mmol, 1.00 equiv) and DMAP (0.244 g, 2.00 mmol, 0.2 equiv) and then vacuum filled under argon (x3). MeCN (35 mL) was added to

the flask via syringe followed by Et₃N (3.5 mL, 25 mmol, 2.5 equiv). After stirring for 2 min,

Boc-anhydride (3.27 g, 15.0 mmol, 1.5 equiv) was added *via* a syringe. The mixture was stirred

for 4 h at rt. The reaction was then quenched by the addition of aq HCl (50 mL, 1 M) to the flask.

The contents of the flask were transferred to a separatory funnel and diluted with EtOAc (60 mL).

The layers were separated, and the aq layer was extracted with additional EtOAc (2 × 30 mL).

The combined organic extracts were washed with brine (100 mL) and dried (anhyd Na₂SO₄), and

the solvent was removed via rotary evaporation. The crude solid was then purified by

recrystallization from MeOH to afford *tert*-butyl acetyl(4-bromophenyl)carbamate (2.307 g, 73%)

as a white solid. All data matched that which was reported in the literature.[1]

2-(4-Bromophenyl)-1,1,1-trifluoro-3-(trimethylsilyl)propan-2-ol
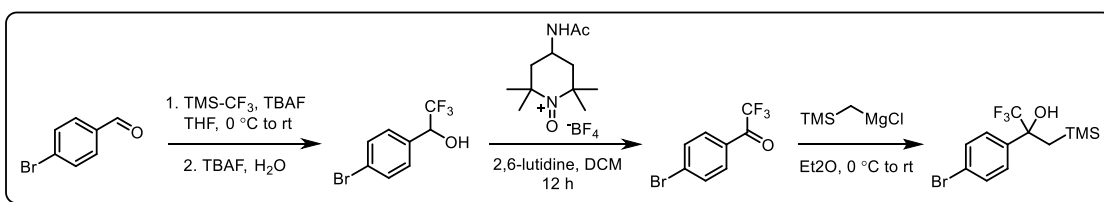
The synthesis of 2-(4-bromophenyl)-1,1,1-trifluoro-3-(trimethylsilyl)propan-2-ol was carried out

as reported in the literature. All data matched that which was reported in the literature.[36]

4-Bromo-2-(2,2,2-trifluoroethoxy)benzonitrile, 87

264
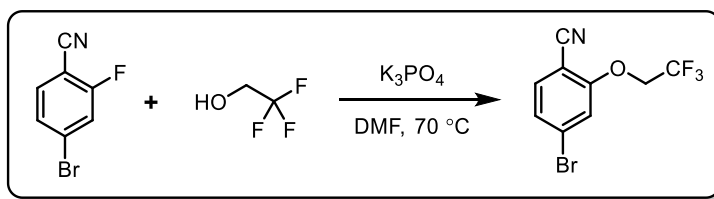
A flask was charged with 4-bromo-2-fluorobenzonitrile (0.600 g, 3.00 mmol, 1.0 equiv) and K$_3$PO$_4$ (1.592 g, 7.50 mmol, 2.50 equiv) and then vacuum filled under argon (x3). DMF (15 mL) and 2,2,2-trifluoroethanol (0.350 mg, 3.50 mmol, 1.2 equiv) were added via syringe, and the reaction was heated to 70 ºC for 4 h. The reaction was then quenched with H$_2$O (30 mL) and extracted with Et$_2$O (3 x 20 mL). The combined organic extracts were then washed with H$_2$O (2 x 30 mL) followed by brine (10 mL), dried (anhyd Na$_2$SO$_4$), and the solvent was removed via rotary evaporation. The crude solid was purified via silica gel chromatography to yield the desired product as a white powdered solid (0.670 g, 80%) (mp = 77-79 °C).

^{1}H NMR (CDCl$_3$, 500 MHz) δ ppm 7.49 (d, J = 8.2 Hz, 1 H), 7.31 (dd, J = 8.2, 1.5 Hz, 1 H), 7.17 (d, J = 1.1 Hz, 1 H), 4.49 (q, J = 7.8 Hz, 2 H).

^{13}C NMR (CDCl$_3$, 125 MHz) δ ppm 159.1, 135.2, 129.1, 126.7, 122.8 (q, J = 278 Hz), 117.2, 114.9, 102.5, 66.9 (q, J = 36 Hz).

^{19}F NMR (CDCl$_3$, 471 MHz) δ ppm -73.41.

FT-IR (cm^{-1}, neat, ATR) 3091 (w), 2228 (m), 1590 (s), 1279 (s), 1252 (vs), 1163 (vs).

HRMS (EI) calcd for C$_9$H$_5$BrF$_3$NO [M$^+$]: 278.9507, found: 278.9517.

4-Bromophenyl (*S*)-2-((*tert*-butoxycarbonyl)amino)-4-phenylbutanoate, 88
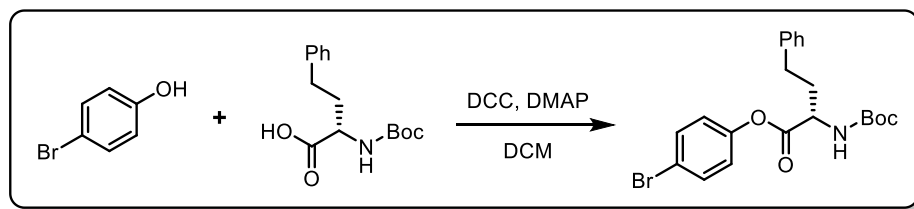
A flask was charged with 4-bromophenol (1.838 g, 10.63 mmol, 1.25 equiv), L-homophenylalanine (2.968 g, 10.63 mmol, 1.25 equiv) and 4-dimethylaminopyridine (1.038 g,

8.50 mmol, 1.0 equiv) and then vacuum filled under argon (x3). The solids were then suspended in CH$_2$Cl$_2$ (15 mL), and the reaction flask was placed in an ice/water bath. *N,N*-Dicyclohexylcarbodiimide (1.754 g, 8.50 mmol, 1.0 equiv) in CH$_2$Cl$_2$ (15 mL) was then added dropwise to the reaction flask. After the addition the bath was removed, a voluminous white precipitate formed. After stirring for 4 h, the reaction was filtered through a pad of Celite, which was washed with additional CH$_2$Cl$_2$ (20 mL). The organic solution was then washed with satd aq Na$_2$CO$_3$ (30 mL) followed by brine. The organic extracts were dried (Na$_2$SO$_4$), and the solvent was removed via rotary evaporation. The crude material was purified via silica gel chromatography using a gradient of hexanes/EtOAc to yield 4-bromophenyl (*S*)-2-((*tert*-butoxycarbonyl)amino)-4-phenylbutanoate as a white, powdered solid (3.430 g, 93%) (mp =102-104 ºC).

¹H NMR (CDCl$_3$, 500 MHz) δ ppm 7.49 (d, *J* = 8.7 Hz, 2H), 7.34-7.28 (m, 2H), 7.25-7.20 (m, 3H), 6.95 (d, *J* = 8.9 Hz, 2H), 5.16-4.99 (m, 1H), 4.62-4.47 (m, 1H), 2.79 (t, *J* = 8.0 Hz, 2H), 2.37-2.25 (m, 1H), 2.17-2.06 (m, 1H), 1.47 (s, 9H)

¹³C NMR (CDCl$_3$, 125 MHz) δ ppm 171.4, 155.6, 149.7, 140.6, 132.8, 128.9, 128.7, 126.7, 123.4, 119.5, 80.6, 53.8, 34.5, 32.0, 28.6

FT-IR (cm^{-1}, neat, ATR) 3356 (br), 2977 (w), 1763 (m), 1709 (m), 1483 (m), 1163 (vs).

HRMS (ESI) calcd for C$_9$H$_5$BrF$_3$NO [M$^+$]: 434.0967, found: 434.0940.

(1*S*,2*S*,3*S*,5*R*)-2,6,6-Trimethylbicyclo[3.1.1]heptan-3-yl 4-bromo-2-fluorobenzoate, 89
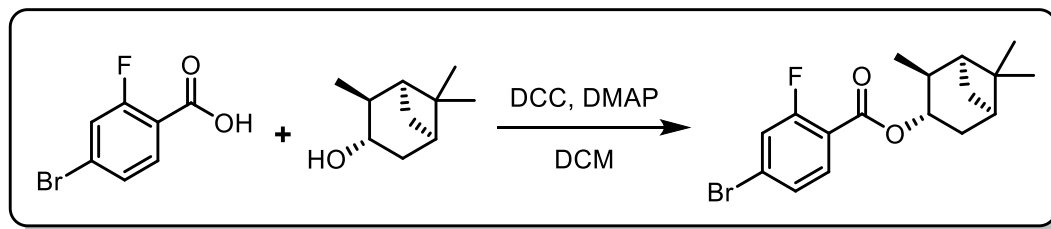
A flask was charged with 4-bromo-2-fluorobenzoic acid (2.327 g, 10.63, 1.25 equiv), isopinocampheol (1.639 g, 10.63 mmol, 1.25 equiv) and 4-dimethylaminopyridine (1.038 g, 8.50 mmol, 1.0 equiv) and then vacuum filled under argon (x3). The solids were then suspended in CH$_2$Cl$_2$ (15 mL), and the reaction flask was placed in an ice/water bath. *N,N*-Dicyclohexylcarbodiimide (1.754 g, 8.50 mmol, 1.0 equiv) in CH$_2$Cl$_2$ (15 mL) was then added dropwise to the reaction flask. After the addition the bath was removed a voluminous white precipitate formed. After stirring for 4 h, the reaction was filtered through a pad of Celite, which was washed with additional CH$_2$Cl$_2$ (20 mL). The organic soln was then washed with satd aq Na$_2$CO$_3$ (30 mL) followed by brine. The organic extracts were dried (Na$_2$SO$_4$), and the solvent was removed via rotary evaporation. The crude material was purified via silica chromatography using a gradient of hexanes/EtOAc to yield 4-bromophenyl (1*S*,2*S*,3*S*,5*R*)-2,6,6-trimethylbicyclo[3.1.1]heptan-3-yl 4-bromo-2-fluorobenzoate as a dense, colorless oil (2.580 g, 85%)

¹**H NMR** (CDCl$_3$, 500 MHz) δ ppm 7.81 (t, *J* = 8.0 Hz, 1H), 7.37-7.30 (m, 2H), 5.28 (dt, *J* = 9.3, 4.6 Hz, 1H), 2.71-2.66 (m, 1H), 2.44-2.38 (m, 1H), 2.32-2.25 (m, 1H), 1.99-1.95 (m, 1H), 1.87 (td, *J* = 5.8, 2.2 Hz, 1H), 1.83 (dt, *J* = 14.5, 3.4 Hz, 1H), 1.25 (s, 3H), 1.18-1.15 (m, 4H), 1.00 (s, 3H)

¹³C NMR (CDCl₃, 125 MHz) δ ppm 164.0 (d, J = 4.4 Hz), 162.8, 161.1, 133.3, 127.8, 127.7 (d, J = 4.4 Hz), 120.9 (d, J = 25 Hz), 118.9 (d, J = 9.8 Hz), 76.0, 47.8, 44.0, 41.5, 38.5, 36.2, 33.6, 27.7, 24.1, 20.8.

¹⁹F NMR (CDCl₃, 471 MHz) δ ppm -106.52.

FT-IR (cm⁻¹, neat, ATR) 2910 (m), 1711 (s), 1601 (s), 1220 (s), 1134 (s).

HRMS (EI) calcd for C₁₇H₂₀BrFO₂ [M⁺]: 354.0631, found: 217.9386 and 136.1234.

(3a*R*,5*R*,6*S*,6a*R*)-6-((4-Bromobenzyl)oxy)-5-((*R*)-2,2-dimethyl-1,3-dioxolan-4-yl)-2,2-dimethyltetrahydrofuro[2,3-d][1,3]dioxole
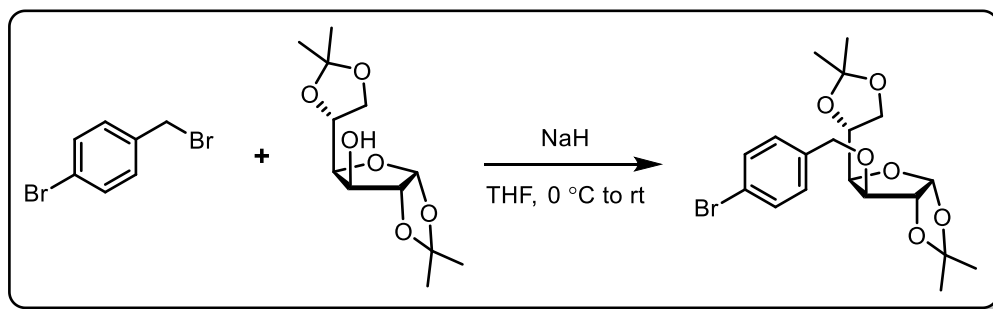
A flask was charged with D-glucose diacetonide (1.691 g, 6.50 mmol, 1.0 equiv), which was then dissolved in THF (25 mL). The reaction flask was placed in an ice/water bath, and NaH (0.234 g, 9.75 mmol, 1.5 equiv) was added in one portion (*caution gas evolution*). After stirring in the cold bath for 30 min, 4-bromobenzyl bromide (2.437 g, 9.75 mmol, 1.5 equiv) was added in one portion, causing the soln to turn a dark red/brown color. After stirring for 4 h, the reaction was quenched by the addition of satd aq NH₄Cl (20 mL) and diluted with Et₂O (30 mL). The layers were separated, and the aq layer was extracted with an additional portion of Et₂O (20 mL). The combined organic extracts were washed with brine, dried (anhyd Na₂SO₄), and the solvent was removed via rotary evaporation. The crude material was purified via a short silica plug, eluting

268

with hexanes/EtOAc to yield (3a*R*,5*R*,6*S*,6a*R*)-6-((4-bromobenzyl)oxy)-5-((*R*)-2,2-dimethyl-1,3-dioxolan-4-yl)-2,2-dimethyltetrahydrofuro[2,3-d][1,3]dioxole as a dense, colorless oil. All data matched that which was reported in the literature.[37]

4.6.5. HAT DCF Reaction Optimization Data

General Optimization Procedure: To a 4 mL reaction vial with a stir bar was added aryl bromide (if solid, 0.10 mmol, 1.0 equiv), K_2HPO_4 (35 mg, 0.20 mmol, 2 equiv), nickel catalyst (0.01 mmol, 10 mol %), and benzophenone catalyst (0.02 mmol, 20 mol %). The vial was capped and vacuum filled under argon (x3). A soln of C-H radical precursor (1.50 mmol, 15 equiv) in the reaction solvent (1.0 mL) was sparged with argon for 5 min and then added via syringe to the reaction tube. Finally, the alkene (0.20 mmol, 2 equiv) and aryl bromide (if liquid, 0.10 mmol, 1.0 equiv) were added via syringe. Irradiation was performed with a Kessil® PR160 390nm lamp at 1.0" from the surface of the reaction vial. The vial was cooled with two fans (Delta compact brushless DC12V fan and household clip fan, see image below) to maintain the temperature on the surface of the vial between 25-34 ⁰C (measured using Fisherbrand® traceable type-K thermometer). After 24 h of irradiation, the reaction soln was passed through a pipette plug of Celite/silica gel and the eluted with CH_2Cl_2 (5 mL). The solvent was removed, and the reaction analyzed via ^{1}H NMR using trimethoxybenzene as an internal standard or via GC/MS.

Table 4.5: Optimization of Nickel Catalyst

Bipyridine Ligand	H NMR Yield
R_1 = H	30%
R_1 = 4,4'-*t*Bu	73%
R_1 = 4,4'-OMe	42%
R_1 = 4,4'-Me	67%
R_1 = 5,5'-CF_3	11%
R_1 = 6,6'-Me	0%
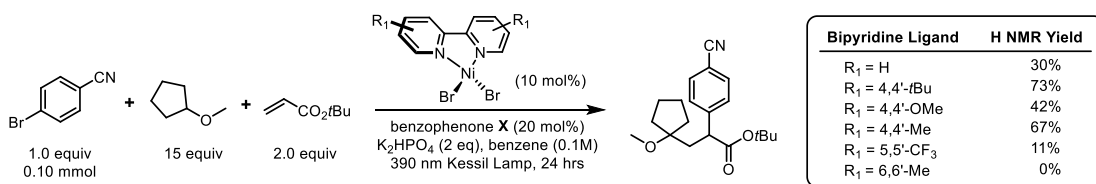
Table 4.6: Optimization of Solvent

Solvent	H NMR Yield
TFT	86%
3:1 Benzene/*t*BuOH	30%
3:1 Benzene/CF_3CH_2OH	0%
3:1 Benzene/Acetone	74%
3:1 Benzene/HFIP	0%
MeCN	0%
EtOAc	39%
Acetone	26%
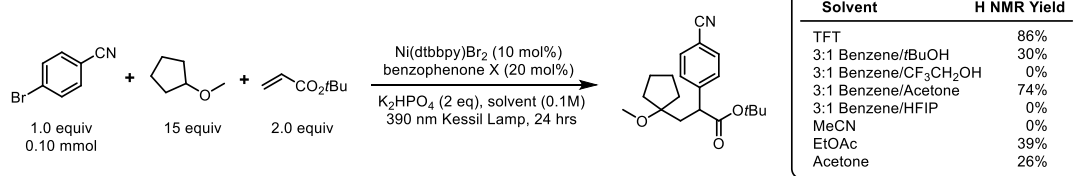
Table 4.7: Optimization of Light Source

Light Source	H NMR Yield
390 nm Kessil lamp	86%
370 nm LED chip	70%
300 nm Rayonet lamp	37%
440 nm Kessil lamp	0%
Household CFL	0%

T
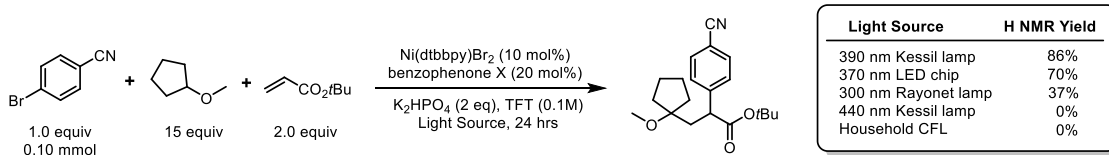
Table 4.8: Optimization of HAT Catalyst

H NMR Yields

R_2=R_3=H	11%
R_2=R_3=Cl	40%
R_2=R_3=OMe	47%
R_2=CF_3 R_3=OMe	50%
R_2=CN R_3=OMe	73%

>5% 0% >5%

0% >5% 10%

270
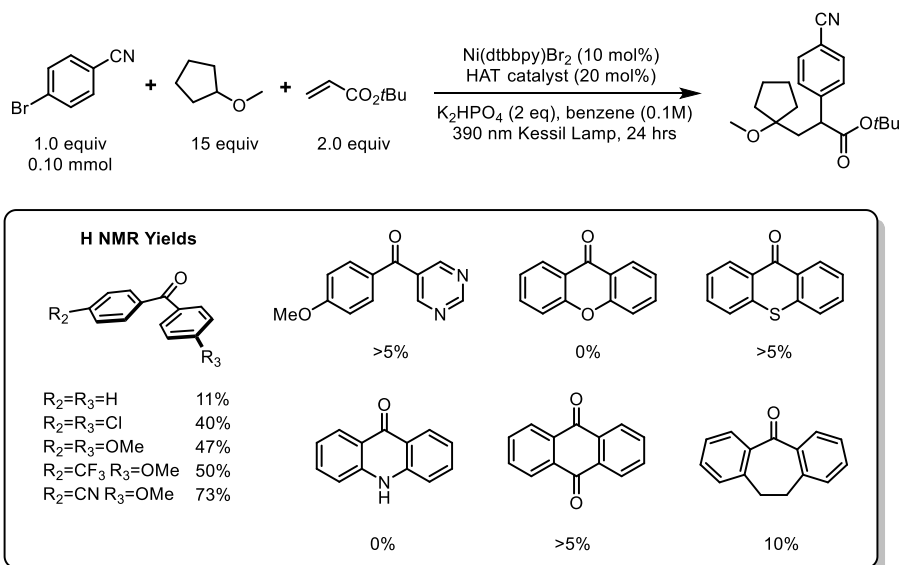
Table 4.9: Optimization of Electronically Rich Aryl Halides
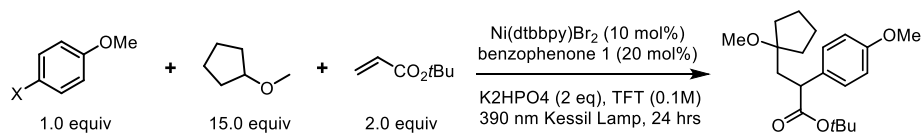
Halide	Deviation from above conditions	^{1}H NMR Yield
bromo	standard, 24hrs / 0.1 mmol	22%, ~40% SM remaining
iodo	standard, 24hrs / 0.1 mmol	36%, ~20% SM remaining
bromo	1:1 CPME/TFT, 24hrs / 0.1 mmol	58%, ~15% SM remaining
iodo	1:1 CPME/TFT, 24hrs / 0.1 mmol	74%, no SM remaining
iodo	1:1 CPME/TFT, 24hrs / 0.5 mmol	65%, isolated yield

4.6.6. General Procedure A for HAT-Mediated Dicarbofunctionalization
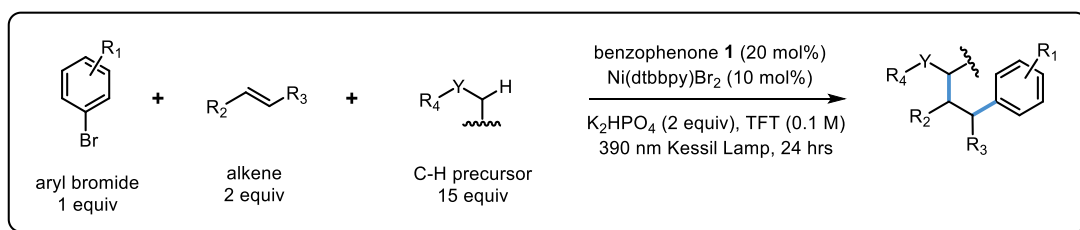
To an 8 mL fused quartz reaction tube, equipped with a 12 mm magnetic stir bar, was added aryl bromide (if solid, 0.50 mmol, 1.0 equiv), K$_2$HPO$_4$ (174 mg, 1.0 mmol, 2 equiv), 4,4'-di-*tert*-butyl-2,2'-bipyridine nickel(II) bromide (24 mg, 0.05 mmol, 10 mol %), and 4-(4-methoxybenzoyl)benzonitrile (24 mg, 0.10 mmol, 20 mol %). The vial was capped with a 19/22 rubber septum and vacuum filled under argon (x3). A soln of C-H radical precursor (7.50 mmol, 15 equiv) in trifluorotoluene (TFT) (5.0 mL) was sparged with argon for 10 min and then added via syringe to the reaction tube. Finally, the alkene (1.00 mmol, 2 equiv) and aryl bromide (if liquid, 0.50 mmol, 1.0 equiv) were added via syringe. The septa was secured with Parafilm, and the reaction was irradiated for 24 h. Irradiation was performed with a Kessil® PR160 390 nm lamp at 1.0" from the surface of the reaction vial. The vial was cooled with two fans (Delta

271

compact brushless DC12V fan and household clip fan, see image below) to maintain the temperature on the surface of the vial between 25-34 ºC (measured using Fisherbrand® traceable type-K thermometer). After 24 h of irradiation, the reaction soln was passed through a plug of 5 cc of Celite atop 10 cc of silica gel. The plug was then washed with CH_2Cl_2 (30 mL), and the solvent was removed via rotary evaporation. The resulting crude material was purified via silica gel chromatography, eluting with a gradient of hexanes/EtOAc.
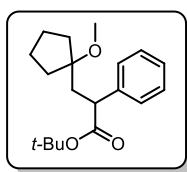
tert-Butyl 3-(1-methoxycyclopentyl)-2-phenylpropanoate, 4.7 (0.105 g, 69%) was prepared according to General Procedure A using the corresponding aryl iodide. The desired compound was obtained as a dense, colorless oil. **^{1}H NMR** (CDCl$_3$, 500 MHz) δ ppm 7.34-7.26 (m, 4H), 7.25-7.19 (m, 1H), 3.67 (dd, _J_ = 8.8, 3.5 Hz, 1H), 3.07 (s, 3H), 2.57 (dd, _J_ = 14.7, 8.7 Hz, 1H), 1.85 (dd, _J_ = 14.8, 3.8 Hz, 1H), 1.82-1.51 (m, 6H), 1.46-1.40 (m, 1H), 1.37 (s, 9H), 1.33-1.24 (m, 1H). **^{13}C NMR** (CDCl$_3$, 125 MHz) δ ppm 173.9, 141.6, 128.6 - 128.9 (m), 128.0, 127.0, 86.7, 80.6, 49.6, 48.6, 39.1, 36.0, 35.8, 28.1, 23.7, 23.6. **FT-IR** (cm^{-1}, neat, ATR) 2963 (w), 1725 (m), 1142 (vs), 1075, 726 (m). **HRMS** (EI) calcd for C$_{15}$H$_{19}$O$_3$ [M$^+$-_t_-Bu]: 247.1334, found: 247.1340.
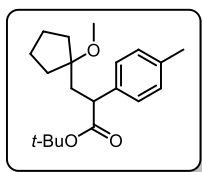
tert-Butyl 3-(1-methoxycyclopentyl)-2-(_p_-tolyl)propanoate, 4.8 (0.118 g, 74%) was prepared according to General Procedure A using the corresponding aryl iodide. The desired compound was obtained as a white, amorphous solid (mp = 66-68 °C). **^{1}H NMR** (CDCl$_3$, 500 MHz) δ ppm 7.20 (d, _J_ = 8.0 Hz, 2H), 7.10 (d, _J_ = 7.8 Hz, 2H), 3.63 (dd, _J_ = 8.7, 3.6 Hz, 1H), 3.07 (s, 3H), 2.55 (dd, _J_ = 14.8, 8.8 Hz, 1H), 2.32 (s, 3H), 1.85-1.72 (m, 3H), 1.71-1.64 (m, 2H), 1.63-1.51 (m, 2H), 1.45-1.39 (m, 1H), 1.37 (s, 9 H), 1.31-1.24 (m, 1H). **^{13}C NMR** (CDCl$_3$, 125 MHz) δ ppm 174.1, 138.6, 136.6, 129.4,

127.9, 86.7, 80.5, 49.7, 48.2, 39.2, 36.1, 35.9, 28.2, 23.7, 23.6, 21.3. **FT-IR** (cm^{-1}, neat, ATR) 2963 (m), 1726, 1366 (w), 1143 (vs), 1078 (m). **HRMS** (EI) calcd for C$_{20}$H$_{30}$O$_3$ [M$^+$]: 318.2195, found: 318.2193.
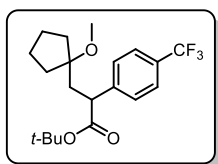
***tert*-Butyl 3-(1-methoxycyclopentyl)-2-(4-(trifluoromethyl)phenyl) propanoate, 4.9** (0.131 g, 70%) was prepared according to General Procedure A. The desired compound was obtained as a white, amorphous solid (mp = 50-52 °C). **^{1}H NMR** (CDCl$_3$, 500 MHz) δ ppm 7.55 (d, *J* = 8.1 Hz, 2H), 7.44 (d, *J* = 8.1 Hz, 2H), 3.74 (dd, *J* = 8.2, 3.8 Hz, 1H), 3.05 (s, 3H), 2.57 (dd, *J* = 14.7, 8.3 Hz, 1H), 1.84 (dd, *J* = 14.7, 3.9 Hz, 2H), 1.78-1.64 (m, 3H), 1.62-1.53 (m, 2H), 1.44-1.39 (m, 1H), 1.37 (s, 9H), 1.30-1.22 (m, 1H). **^{13}C NMR** (CDCl$_3$, 125 MHz) δ ppm 173.2, 145.5, 129.4 (q, *J* = 32.2 Hz), 128.5, 125.7 (q, *J* = 3.7 Hz), 124.5 (q, *J* = 271 Hz), 86.6, 81.1, 49.6, 48.7, 39.1, 36.01, 35.96, 28.1, 23.7, 23.6. **^{19}F NMR** (CDCl$_3$, 471 MHz) δ ppm −62.35. **FT-IR** (cm^{-1}, neat, ATR) 2966 (w), 1727, 1323 (vs), 1123 (vs), 1018 (m). **HRMS** (EI) calcd for C$_{16}$H$_{19}$F$_3$O$_3$ [M$^+$- *t*Bu+H]: 316.1286, found: 316.1300.
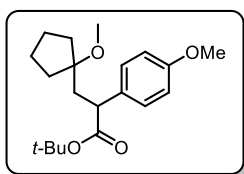
***tert*-Butyl 3-(1-methoxycyclopentyl)-2-(4-methoxyphenyl)propanoate, 4.10** (0.108 g, 65%) was prepared according to General Procedure A using the corresponding aryl iodide and was irradiated for 48 h. The desired compound was obtained as a dense, colorless oil. **^{1}H NMR** (CDCl$_3$, 500 MHz) δ ppm 7.24 (d, *J* = 8.4 Hz, 2H), 6.83 (d, *J* = 8.4 Hz, 2H), 3.79 (s, 3H), 3.61 (dd, *J* = 8.5, 3.7 Hz, 1H), 3.06 (s, 3H), 2.53 (dd, *J* = 14.6, 8.5 Hz, 1H), 1.85-1.72 (m, 3 H), 1.70-1.63 (m, 2H), 1.62-1.51 (m, 2H), 1.44-1.38 (m, 1H), 1.37 (s, 9H), 1.30-1.23 (m, 1H). **^{13}C NMR** (CDCl$_3$, 125 MHz) δ ppm 174.2, 158.7, 133.7, 129.0, 114.1, 86.7, 80.5, 55.5, 49.7, 47.8, 39.1, 36.0, 35.9, 28.2, 23.7, 23.6. **FT-IR** (cm^{-1},

neat, ATR) 2959 (w), 1725, 1510, 1249, 1143 (vs), 1077 (m). **HRMS** (EI) calcd for $C_{20}H_{30}O_4$ [M⁺]: 334.2144, found: 334.2148.
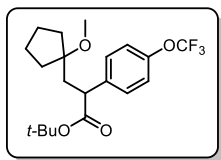
tert-**Butyl 3-(1-methoxycyclopentyl)-2-(4-(trifluoromethoxy)phenyl) propanoate, 4.11** (0.092 g, 47%) was prepared according to General Procedure A using a 1:1 CPME/TFT solvent mixture. The desired compound was obtained as a colorless oil. **¹H NMR** (500 MHz, CDCl₃) δ ppm 7.34 (d, J = 8.6 Hz, 2H), 7.14 (d, J = 8.1 Hz, 2H), 3.68 (dd, J = 8.6, 3.9 Hz, 1H), 3.05 (s, 3H), 2.54 (dd, J = 1.7, 8.6 Hz, 1H), 1.82 (dd, J = 14.7, 3.9 Hz, 3H), 1.73-1.64 (m, 2H), 1.62-1.56 (m, 2H), 1.46-1.39 (m, 1H), 1.37 (s, 9H), 1.30-1.23 (m, 1H). **¹³C NMR** (126 MHz, CDCl₃) δ ppm 173.50, 148.4, 140.2, 129.4, 121.2, 120.8 (q, $J_{C\text{-}F}$ = 256.1 Hz) 86.6, 81.0, 49.6, 48.1, 39.2, 36.0, 35.9, 23.6, 23.5. **¹⁹F NMR** (471 MHz, CDCl₃) δ ppm -58.03. **FT-IR** (cm⁻¹, neat, ATR) 2966 (w), 1727, 1255(s), 1210(s), 1142(vs). **HRMS** (EI) calcd for $C_{16}H_{19}F_3O_4$ [M⁺- *t*Bu+H]: 332.1233, found: 332.1247.
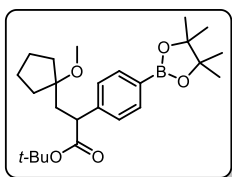
tert-**Butyl 3-(1-methoxycyclopentyl)-2-(4-(4,4,5,5-tetramethyl-1,3,2-dioxaborolan-2-yl)phenyl) propanoate, 4.12** (0.110 g, 65%) was prepared according to General Procedure A using the corresponding aryl iodide and was irradiated for 48 h. The desired compound was obtained as a white, amorphous solid (mp = 77-79 °C). **¹H NMR** (CDCl₃, 500 MHz) δ ppm 7.74 (d, J = 8.1 Hz, 2H), 7.32 (d, J = 8.1 Hz, 2H), 3.67 (dd, J = 8.6, 3.7 Hz, 1H), 3.06 (s, 3 H), 2.56 (dd, J = 14.7, 8.5 Hz, 1 H), 1.85-1.73 (m, 3 H), 1.71-1.63 (m, 2H), 1.59-1.50 (m, 2H), 1.44-1.38 (m, 1H), 1.35 (s, 9H), 1.33 (s, 12H), 1.29-1.24 (m, 1H). **¹³C NMR** (CDCl₃, 125 MHz) δ ppm 173.6, 144.8, 135.3, 127.5, 86.7, 84.0, 80.7, 49.7, 48.9, 38.9, 36.0, 35.9, 28.1, 25.2, 23.7, 23.6. **¹¹B NMR** (CDCl₃, 128.4 MHz) δ ppm 31.0. **FT-IR**

(cm^{-1}, neat, ATR) 2975 (w), 1727 (m), 1610 (m), 1358, 1141 (vs), 1089 (m). **HRMS** (EI) calcd for C$_{25}$H$_{40}$BO$_5$ [M + H$^+$]: 431.2969, found: 431.2968.
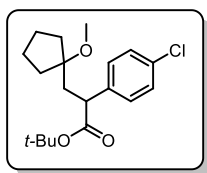
***tert*-Butyl 2-(4-chlorophenyl)-3-(1-methoxycyclopentyl)propanoate, 4.13** (0.103 g, 61%) was prepared according to General Procedure A. The desired compound was obtained as a dense, colorless oil. **^{1}H NMR** (CDCl$_3$, 500 MHz) δ ppm 7.26 (s, 4H), 3.64 (dd, *J* = 8.3, 4.0 Hz, 1H), 3.04 (s, 3H), 2.53 (apt. dd, *J* = 14.7, 8.3 Hz, 1H), 1.80 (dd, *J* = 14.7, 4.0 Hz, 2H), 1.77-1.71 (m, 1H), 1.70-1.64 (m, 2H), 1.61-1.52 (m, 2H), 1.42-1.37 (m, 1H), 1.36 (s, 9H), 1.28-1.28 (m, 1H). **^{13}C NMR** (CDCl$_3$, 125 MHz) δ ppm 173.5, 140.0, 132.9, 129.4, 128.9, 86.5, 80.9, 49.6, 48.1, 39.0, 36.0, 28.1, 23.6, 23.6. **FT-IR** (cm^{-1}, neat, ATR) 2964 (w), 1726 (s), 1144 (vs), 1092 (m), 1077 (m). **HRMS** (EI) calcd for C$_{19}$H$_{28}$ClO$_3$ [M+H$^+$]: 339.1727, found: 339.1713.
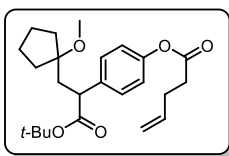
4-(1-(*tert*-Butoxy)-3-(1-methoxycyclopentyl)-1-oxopropan-2-yl)phenyl pent-4-enoate, 4.14 (0.145 g, 72%) was prepared according to General Procedure A. The desired compound was obtained as a dense, colorless oil. **^{1}H NMR** (CDCl$_3$, 500 MHz) δ ppm 7.32 (d, *J* = 8.5 Hz, 2H), 7.00 (d, *J* = 8.6 Hz, 2H), 5.94-5.84 (m, 1H), 5.14 (dd, *J* = 17.1, 1.5 Hz, 1H), 5.07 (dd, *J* = 10.2, 1.4 Hz, 1H), 3.66 (dd, *J* = 8.8, 3.4 Hz, 1H), 3.06 (s, 3H), 2.65 (t, *J* = 7.3 Hz, 2H), 2.58-2.45 (m, 3H), 1.85-1.75 (m, 3H), 1.72-1.64 (m, 2H), 1.61-1.54 (m, 2H), 1.46-1.40 (m, 1H), 1.37 (s, 9H), 1.32-1.24 (m, 1H). **^{13}C NMR** (CDCl$_3$, 125 MHz) δ ppm 173.7, 171.8, 149.8, 139.0, 136.6, 129.0, 121.8, 116.2, 86.6, 80.8, 49.7, 48.1, 39.2, 36.1, 35.9, 33.9, 29.2, 28.1, 23.7, 23.6. **FT-IR** (cm^{-1}, neat, ATR) 2964 (m), 1759, 1725, 1202 (m), 1140 (vs) 1076, 914 (m). **HRMS** (EI) calcd for C$_{20}$H$_{26}$O$_5$ [M$^+$ - *t*-Bu+H]: 346.1780, found: 346.1777.
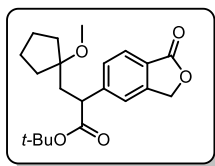
***tert*-Butyl 3-(1-methoxycyclopentyl)-2-(1-oxo-1,3-dihydroisobenzofuran-5-yl)propanoate, 4.15** (0.087 g, 48%) was prepared according to General Procedure A using a 1:1 solvent mixture of CPME/TFT (0.140 g, 78%). The desired compound was obtained as a white amorphous solid (mp = 99-101 °C). **^{1}H NMR** (CDCl$_3$, 500 MHz) δ ppm 7.85 (d, *J* = 7.9 Hz, 1H), 7.50 (d, *J* = 8.1 Hz, 1H), 7.47 (s, 1H), 5.30 (s, 2H), 3.81 (dd, *J* = 8.1, 4.1 Hz, 1H), 3.04 (s, 3H), 2.60 (dd, *J* = 14.6, 8.2 Hz, 1H), 1.86 (dd, *J* = 14.6, 4.1 Hz, 2H), 1.78 - 1.65 (m, 3H), 1.61 - 1.55 (m, 2H), 1.45-1.42 (m, 1H), 1.38 (s, 9H), 1.27-1.24 (m, 1H). **^{13}C NMR** (CDCl$_3$, 125 MHz) δ ppm 172.9, 171.1, 148.4, 147.3, 129.4, 126.1, 124.8, 121.7, 86.5, 81.5, 69.8, 49.7, 49.2, 39.4, 36.0, 36.0, 28.1, 23.6, 23.6. **FT-IR** (cm^{-1}, neat, ATR) 2964 (w), 1761 (vs), 1724, 1367 (m), 1148, 1075 (m) 1043 (m). **HRMS** (EI) calcd for C$_{17}$H$_{20}$O$_5$ [M$^+$ - *t*-Bu+H]: 304.1311, found: 304.1314.
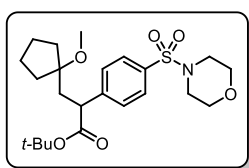
***tert*-Butyl 3-(1-methoxycyclopentyl)-2-(4-(morpholinosulfonyl) phenyl) propanoate, 4.16** (0.110 g, 48%) was prepared according to General Procedure A using a 1:1 CPME/TFT solvent mixture (0.208 g, 92%). The desired compound was obtained as a white amorphous solid (mp = 107-109 °C). **^{1}H NMR** (CDCl$_3$, 500 MHz) δ ppm 7.68 (d, *J* = 8.2 Hz, 2H), 7.51 (d, *J* = 8.4 Hz, 2H), 3.78 - 3.72 (m, 5H), 3.04 (s, 3H), 2.99 (t, *J* = 4.6 Hz, 4H), 2.57 (dd, *J* = 14.6, 8.2 Hz, 1H), 1.84 (dd, *J* = 14.7, 4.0 Hz, 2H), 1.79-1.66 (m, 3H), 1.63-1.57 (m, 2H), 1.45-1.42 (m, 1 H), 1.38 (s, 9H), 1.28-1.23 (m, 1H). **^{13}C NMR** (CDCl$_3$, 125 MHz) δ ppm 172.8, 147.1, 133.8, 128.9, 128.4, 86.5, 81.4, 66.4, 49.7, 48.8, 46.3, 39.3, 36.0, 28.1, 23.7, 23.6. **FT-IR** (cm^{-1}, neat, ATR) 2967 (w), 1726, 1352 (m), 1167 (vs), 1145 (vs), 944 (m). **HRMS** (EI) calcd for C$_{23}$H$_{35}$O$_6$S [M$^+$]: 453.2083, found: 453.2085.
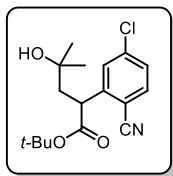
tert-Butyl 2-(5-chloro-2-cyanophenyl)-4-hydroxy-4-methylpentanoate, 4.17

(0.050 g, 31%) was prepared according to General Procedure A using a 1:1 *i*-PrOH/TFT solvent mixture. The desired compound was obtained as a dense, colorless oil. **^{1}H NMR** (CDCl$_3$, 500 MHz) δ ppm 7.58 (d, J = 8.4 Hz, 1H), 7.48 (d, J = 2.0 Hz, 1H), 7.33 (dd, J = 8.4, 2.0 Hz, 1H), 4.18 (dd, J = 9.6, 3.3 Hz, 1H), 2.51 (dd, J = 14.4, 9.6 Hz, 1H), 1.70 (dd, J = 14.3, 3.4 Hz, 1H), 1.53 (br s, 1H), 1.41 (s, 9H), 1.29 (d, J = 3.3 Hz, 6H). **^{13}C NMR** (CDCl$_3$, 125 MHz) δ ppm 172.3, 146.7, 140.0, 134.4, 128.6, 128.1, 117.3, 111.2, 82.4, 70.6, 46.8, 46.6, 30.8, 29.1, 28.1. **FT-IR** (cm^{-1}, neat, ATR) 3528 (br), 2975 (w), 2232 (w), 1728 (s), 1369 (m), 1149 (vs). **HRMS** (EI) calcd for C$_{17}$H$_{23}$ClNO$_3$ [M + H$^+$]: 324.1366, found: 324.1370.
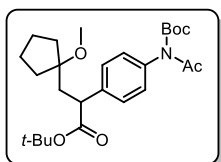
tert-Butyl 2-(4-(*N*-(*tert*-butoxycarbonyl)acetamido)phenyl)-3-(1-methoxycyclopentyl)propanoate, 4.18 (0.110 g, 48%) was prepared according to General Procedure A using a 1:1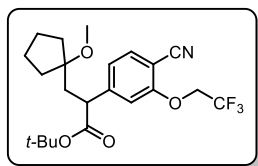 CPME/TFT solvent mixture. The desired compound was obtained as a dense, colorless oil. **^{1}H NMR** (CDCl$_3$, 500 MHz) δ ppm 7.34 (d, J = 8.0 Hz, 2H), 7.00 (d, J = 8.0 Hz, 2H), 3.68 (dd, J = 8.4, 3.6 Hz, 1H), 3.06 (s, 3H), 2.62-2.53 (m, 4H), 1.90-1.74 (m, 3H), 1.71-1.63 (m, 2H), 1.55-1.50 (m, 1H), 1.47-1.40 (m, 2H), 1.35 (s, 9H), 1.34 (s, 9H), 1.29-1.24 (m, 1H). **^{13}C NMR** (CDCl$_3$, 125 MHz) δ ppm 173.7, 173.2, 153.0, 141.1, 137.9, 128.7, 128.4, 86.6, 83.3, 80.7, 49.7, 48.4, 38.8, 36.0, 36.0, 28.1, 28.0, 26.7, 23.6, 23.6. **FT-IR** (cm^{-1}, neat, ATR) 2974 (w), 1729 (s), 1711 (s), 1368 (m), 1271 (s), 1254 (s), 1146 (vs). **HRMS** (EI) calcd for C$_{26}$H$_{39}$NO$_6$Na [M + Na$^+$]: 484.2686, found: 484.2675.
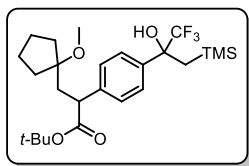
tert-Butyl 3-(1-methoxycyclopentyl)-2-(4-(1,1,1-trifluoro-2-hydroxy-3-(trimethylsilyl)propan-2-yl)phenyl)propanoate, 4.19 (0.145 g, 59%) was prepared according to General Procedure A using a 1:1 CPME/TFT

solvent mixture. The desired compound was obtained as a white, amorphous solid (mp = 78-80 °C). **¹H NMR** (500 MHz, CDCl₃) δ ppm 7.46 (d, *J* = 8.4 Hz, 2H), 7.33 (d, *J* = 8.4 Hz, 2H), 3.68 (dd, *J* = 8.5, 3.7 Hz, 1H), 3.06 and 3.05 (s, 3H), 2.59 (dd, *J* = 14.7, 8.5 Hz, 1H), 2.27 (s, 1H), 1.89-1.73 (m, 3H), 1.72-1.55 (m, 5H), 1.47-1.42 (m, 3H), 1.34 (s, 9H), -0.23 and -0.24 (s, 9 H). **¹³C NMR** (126 MHz, CDCl₃) δ ppm 173.7, 141.5, 141.5, 136.9, 127.7, 126.5, 126.0 (q, J_{C-F} = 286.1 Hz), 86.5, 80.5, 77.2 (q, J_{C-F} = 28.2 Hz), 49.5, 48.2, 48.1, 38.5, 38.4, 35.9, 35.8, 35.7, 27.9, 25.1, 25.0, 23.5, 23.4, -0.16. **¹⁹F NMR** (471 MHz, CDCl₃) δ ppm -81.9. **FT-IR** (cm⁻¹, neat, ATR) 3457 (w, br), 2957 (w), 1712, 1147 (vs), 909, 839 (s), 731 (vs). **HRMS** (EI) calcd for C₂₀H₃₀F₃O₂Si [M⁺ - CO₂*t*Bu]: 387.1967, found: 387.1950.
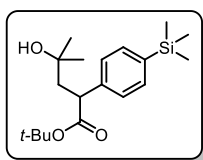
***tert*-Butyl 4-hydroxy-4-methyl-2-(4-(trimethylsilyl)phenyl)pentanoate, 4.20** (0.099 g, 59%) was prepared according to General Procedure A using a 1:1 *i*-PrOH/TFT solvent mixture and was irradiated for 48 h. The desired compound was obtained as a dense, colorless oil. **¹H NMR** (CDCl₃, 500 MHz) δ ppm 7.45 (d, *J* = 8.0 Hz, 2H), 7.27 (d, *J* = 8.0 Hz, 2H), 3.71 (dd, *J* = 10.2, 3.2 Hz, 1H), 2.50 (dd, *J* = 14.3, 10.4 Hz, 1H), 1.73 (dd, *J* = 14.4, 3.1 Hz, 1H), 1.53 (s, 1H), 1.39 (s, 9H), 1.25 (d, *J* = 4.9 Hz, 6H), 0.25 (s, 9H). **¹³C NMR** (CDCl₃, 125 MHz) δ ppm 174.4, 141.5, 139.1, 133.9, 127.3, 81.1, 70.9, 48.7, 47.2, 30.7, 29.1, 28.2, -0.8. **FT-IR** (cm⁻¹, neat, ATR) 3440 (br), 2969 (w), 1726 (s), 1367 (s), 1143 (vs), 837 (vs), 755 (s). **HRMS** (EI) calcd for C₁₉H₃₂O₃Si [M⁺]: 337.2199, found: 337.2186.
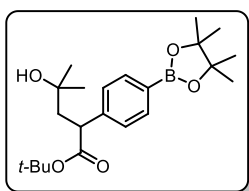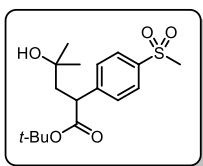

***tert*-Butyl 4-hydroxy-4-methyl-2-(4-(4,4,5,5-tetramethyl-1,3,2-dioxaborolan-2-yl)phenyl)pentanoate, 4.21** (0.170 g, 87%) was prepared according to General Procedure A using the corresponding aryl iodide and a 1:1 *i*-PrOH/TFT solvent mixture and was irradiated for 48 h. The desired compound

was obtained as a dense, colorless oil. **^{1}H NMR** (CDCl$_3$, 500 MHz) δ ppm 7.74 (d, *J* = 8.0 Hz, 2H), 7.29 (d, *J* = 8.0 Hz, 2H), 3.73 (dd, *J* = 10.0 3.3 Hz, 1H), 2.50 (dd, *J* = 14.4, 10.0 1H), 1.72 (dd, *J* = 14.4, 3.3 Hz, 1H), 1.56 (s, 1H), 1.35 (s, 9H), 1.34 (s, 12H), 1.23 (d, *J* = 8.5 Hz, 6H). **^{13}C NMR** (CDCl$_3$, 125 MHz) δ ppm 174.2, 144.3, 135.4, 127.4, 84.1, 81.1, 70.8, 48.9, 46.9, 30.8, 29.1, 28.1, 25.2, 25.1. **^{11}B NMR** (CDCl$_3$, 128.4 MHz) δ ppm 30.6. **FT-IR** (cm^{-1}, neat, ATR) 3420 (br), 2977 (w), 1726 (m), 1359 (vs), 1320 (m), 1140 (vs), 1090 (s). **HRMS** (EI) calcd for C$_{21}$H$_{32}$BO$_5$ [M$^+$ - Me]: 374.2379, found: 374.2380.
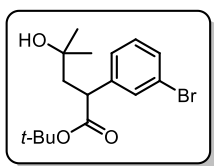
***tert*-Butyl 2-(3-bromophenyl)-4-hydroxy-4-methylpentanoate, 4.22** (0.110 g, 64%) was prepared according to General Procedure A using a 1:1 *i*-PrOH/TFT solvent mixture and was irradiated for 48 h. The desired compound was obtained as a dense, colorless oil. **^{1}H NMR** (CDCl$_3$, 500 MHz) δ ppm 7.45 (t, *J* = 1.83, 1H), 7.38-7.35 (m, 1H), 7.24-7.22 (m, 1H), 7.17 (t, *J* = 7.9 Hz, 1H), 3.68 (dd, *J* = 10.1, 3.2 Hz, 1H), 2.48 (dd, *J* = 14.3, 10.1 Hz, 1H), 1.70 (dd, *J* = 14.3, 3.2 Hz, 1H), 1.47 (br s, 1H), 1.38 (s, 9H), 1.24 (d, *J* = 8.8 Hz, 6H). **^{13}C NMR** (CDCl$_3$, 125 MHz) δ ppm 173.8, 143.4, 131.1, 130.4, 130.3, 126.6, 122.8, 81.4, 70.8, 48.4, 46.9, 30.7, 29.2, 28.1. **FT-IR** (cm^{-1}, neat, ATR) 3418 (br), 2973 (w), 1726 (m), 1368 (m), 1144 (vs), 765 (m). **HRMS** (EI) calcd for C$_{16}$H$_{23}$BrO$_3$ [M$^+$]: 342.0831, found: 342.0836.

***tert*-Butyl 2-(4-cyano-3-(2,2,2-trifluoroethoxy)phenyl)-3-(1-methoxy cyclopentyl)propanoate, 4.23** (0.142 g, 66%) was prepared according to General Procedure A using a 1:1 CPME/TFT solvent mixture. The desired compound was obtained as a dense, colorless oil. **^{1}H NMR** (CDCl$_3$, 500 MHz) δ ppm 7.55 (d, *J* = 8.0 Hz, 1H), 7.09 (dd, *J* = 8.0, 1.3 Hz, 1H), 6.98 (s, 1H), 4.49 (q, *J* = 7.9 Hz, 2H),

3.71 (dd, J = 8.2, 4.1 Hz, 1H), 3.04 (s, 3 H), 2.54 (dd, J = 14.7, 8.2 Hz, 1H), 1.85-1.75 (m, 2H), 1.74-1.63 (m, 3H), 1.62-1.58 (m, 1H), 1.48-1.41 (m, 2H), 1.38 (s, 9H) 1.26-1.21 (m, 1H). **^{13}C NMR** (CDCl$_3$, 125 MHz) δ ppm 172.5, 171.4, 158.9, 149.0, 134.4, 123.0 (q, J = 279 Hz) 122.9, 115.6, 112.7, 101.9, 86.4, 81.7, 68.2, 66.4 (t, J = 36 Hz), 60.6, 49.6, 49.2, 39.3, 36.0, 35.9, 28.1, 25.9, 23.6, 23.6, 21.3, 14.4. **^{19}F NMR** (CDCl$_3$, 471 MHz) δ ppm −73.44. **FT-IR** (cm^{-1}, neat, ATR) 2962 (w), 2233 (w), 1725 (m), 1430 (m), 1368 (m), 1162 1144. **HRMS** (EI) calcd for C$_{18}$H$_{20}$NO$_4$F$_3$ [M$^+$ - t-Bu+H]: 371.1344, found: 371.1348.
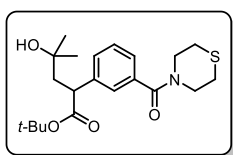
***tert*-Butyl 4-hydroxy-4-methyl-2-(3-(thiomorpholine-4-carbonyl) phenyl)pentanoate, 4.24** (0.101 g, 59%) was prepared according to General Procedure A using a 1:1 i-PrOH/TFT solvent mixture. The desired compound was obtained as a dense, colorless oil. **^{1}H NMR** (CDCl$_3$, 500 MHz) δ ppm 7.37-7.30 (m, 3H), 7.26-7.24 (m, 1H), 4.01 (br s, 2H), 3.74 (dd, J = 10.0, 3.2 Hz, 1H), 3.62 (br s, 2H), 2.80-2.46 (m, 5H), 1.71 (dd, J = 14.3, 3.2 Hz, 1H), 1.63 (br s, 1H), 1.36 (s, 9H), 1.25 (s, 3H), 1.23 (s, 3H). **^{13}C NMR** (CDCl$_3$, 125 MHz) δ ppm 174.0, 170.8, 141.7, 136.3, 129.3, 129.3, 126.3, 125.7, 81.3, 70.8, 48.5, 47.0, 30.7, 29.2, 28.1. **FT-IR** (cm^{-1}, neat, ATR) 3427 (br), 2971 (w), 1723 (m), 1624 (m), 1144 (vs). **HRMS** (ESI) calcd for C$_{21}$H$_{32}$NO$_4$S [M + H$^+$]: 394.2052, found: 394.2043.
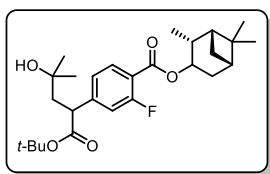
(1R,2R,3R,5S)-2,6,6-Trimethylbicyclo[3.1.1]heptan-3-yl 4-(1-($tert$-butoxy)-4-hydroxy-4-methyl-1-oxopentan-2-yl)-2-fluorobenzoate, 4.25 (0.176 g, 76%) was prepared according to General Procedure A using a 1:1 i-PrOH/TFT solvent mixture. The diastereomeric ratio was determined to be 1:1 via crude H NMR. The desired compound was obtained as a dense, colorless oil. **^{1}H NMR** (CDCl$_3$,

500 MHz) δ ppm 7.86 (t, J = 7.8 Hz, 1H), 7.13 (dd, J = 8.0, 1.6 Hz, 1H), 7.08 (dd, J = 11.6, 1.6 Hz, 1H), 5.28 (m, 1H), 3.76 (dd, J = 9.9, 3.2 Hz, 1H), 2.72-2.64 (m, 1H), 2.49 (dd, J = 14.3, 9.9 Hz, 1H), 2.43-2.37 (m, 1H), 2.33-2.26 (m, 1H), 1.97 (m, 1H), 1.87 (td, J = 6.0, 2.2 Hz, 1H), 1.83 (dt, J = 14.5, 3.7 Hz, 1H), 1.69 (dd, J = 14.4, 3.3 Hz, 1H), 1.48 (s, 1H), 1.37 (s, 9H), 1.25 (d, J = 4.0 Hz, 6H), 1.23 (s, 3H), 1.18-1.14 (m, 4H), 1.00 (s, 3H). **13C NMR** (CDCl$_3$, 125 MHz) δ ppm 173.2, 164.5 (d, J = 3.3 Hz), 163.1, 161.4, 148.3 (d, J = 7.6 Hz), 132.5, 123.5 (d, J = 3.3 Hz), 118.3 (d, J = 9.8 Hz), 116.4 (d, J = 23 Hz), 81.7, 75.6, 70.7, 48.5, 47.8, 46.6, 44.0, 41.5, 38.5, 36.2, 33.6, 30.6, 29.3, 28.1, 27.7, 24.1, 20.8. **19F NMR** (CDCl$_3$, 471 MHz) δ ppm -108.9. **FT-IR** (cm^{-1}, neat, ATR) 3510 (br), 2932 (w), 1709 (m), 1259 (m), 1139 (vs). **HRMS** (ESI) calcd for C$_{27}$H$_{40}$O$_5$F [M + H$^+$]: 463.2860, found: 463.2866.

tert-Butyl 4-hydroxy-4-methyl-2-(4-(methylsulfonyl)phenyl) pentanoate, 4.26 (0.101 g, 59%) was prepared according to General Procedure A using a 1:1 *i*-PrOH/TFT solvent mixture. The desired compound was obtained as a white, amorphous solid (mp = 92-94 °C). **1H NMR** (CDCl$_3$, 500 MHz) δ ppm 7.88 (d, J = 8.4 Hz, 2H), 7.51 (d, J = 8.2 Hz, 2H), 3.84 (dd, J = 9.9, 3.0 Hz, 1H), 3.05 (s, 3H), 2.53 (dd, J = 14.2, 10.0 Hz, 1H), 1.70 (dd, J = 14.4, 3.1 Hz, 1H), 1.44 (br s, 1H), 1.38 (s, 9H), 1.27 (s, 3H), 1.24 (s, 3H). **13C NMR** (CDCl$_3$, 125 MHz) δ ppm 173.3, 147.5, 139.4, 129.0, 128.0, 81.8, 70.8, 48.7, 46.9, 44.8, 30.6, 29.3, 28.1. **FT-IR** (cm^{-1}, neat, ATR) 3023 (br), 2989 (w), 1785 (m), 1633 (m), 1411 (s), 1089 (m). **HRMS** (EI) calcd for C$_{11}$H$_{14}$O$_3$S [M − CO$_2$$t$Bu − Me$^+$]: 226.0664, found: 226.0883.
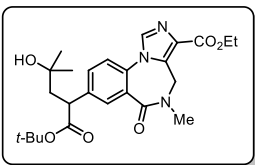
Ethyl 8-(1-(*tert*-butoxy)-4-hydroxy-4-methyl-1-oxopentan-2-yl)-5-methyl-6-oxo-5,6-dihydro-4H-benzo[f]imidazo[1,5-*a*][1,4]diazepine-

3-carboxylate, 4.27 (0.085 g, 36%) prepared according to General Procedure A using a 1:1 *i*-PrOH/TFT solvent mixture. The desired compound was obtained as a dense, colorless oil. **¹H NMR** (CDCl₃, 500 MHz) δ ppm 7.99 (d, *J* = 1.2 Hz, 1H), 7.87 (s, 1H), 7.61 (dd, *J* = 8.3, 2.1 Hz, 1H), 7.37 (d, *J* = 8.2 Hz, 1H), 5.20 (br s, 1H), 4.49-4.31 (m, 3 H), 3.87 (dd, *J* = 10.1, 2.5 Hz, 1H), 3.25 (s, 3H), 2.53 (dd, *J* = 14.2, 10.2 Hz, 1H), 1.76 (dd, *J* = 14.2, 2.8 Hz, 1H), 1.63 (s, 1H), 1.45 (t, *J* = 7.1 Hz, 3H), 1.40 (s, 9H), 1.27 (d, *J* = 6.3 Hz, 6H). **¹³C NMR** (CDCl₃, 125 MHz) δ ppm 166.6, 163.4, 142.0, 135.8, 135.2, 132.4, 132.1, 131.1, 129.4, 129.0, 122.4, 81.8, 70.8, 61.3, 46.9, 42.7, 36.2, 30.7, 29.2, 28.1, 14.7. **FT-IR** (cm⁻¹, neat, ATR) 3440 (br), 2975 (w), 1725 (m), 1640 (m), 1499 (m), 1145 (s), 1117 (s). **HRMS** (EI) calcd for $C_{25}H_{34}N_3O_6$ [M + H⁺]: 472.2448, found: 472.2454.
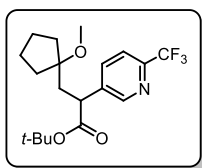
***tert*-Butyl 3-(1-methoxycyclopentyl)-2-(6-(trifluoromethyl)pyridin-3-yl)propanoate, 4.28** (0.121 g, 65%) was prepared according to General Procedure A using a 1:1 CPME/TFT solvent mixture. The desired compound was obtained as a dense, colorless oil. **¹H NMR** (CDCl₃, 500 MHz) δ ppm 8.67 (s, 1H), 7.86 (d, *J* = 8.0 Hz, 1H), 7.63 (d, *J* = 8.0 Hz, 1H), 3.80 (dd, *J* = 8.0, 4.5 Hz, 1H), 3.03 (s, 3H), 2.59 (dd, *J* = 14.7, 8.2 Hz, 1H), 1.89-1.80 (m, 2H), 1.80-1.64 (m, 3H), 1.62-1.55 (m, 2H), 1.46-1.41 (m, 1H), 1.39 (s, 9H), 1.28-1.22 (m, 1H). **¹³C NMR** (CDCl₃, 125 MHz) δ ppm 172.4, 150.1, 147.1 (q, *J* = 35 Hz), 140.3, 136.7, 121.9 (q, *J* = 274 Hz), 120.5 (q, *J* = 2.4 Hz), 86.4, 81.9, 49.6, 46.4, 39.3, 36.1, 35.9, 28.1, 23.7. **¹⁹F NMR** (CDCl₃, 471 MHz) δ ppm -67.69. **FT-IR** (cm⁻¹, neat, ATR) 2965 (w), 1727 (s), 1369 (m), 1336 (s), 1138 (vs), 1086 (vs). **HRMS** (EI) calcd for $C_{15}H_{18}F_3NO_3$ [M⁺ - *t*-Bu+H]: 317.1239, found: 317.1244.
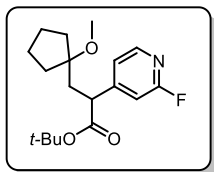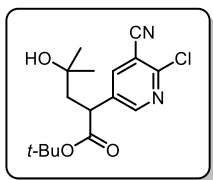
***tert*-Butyl 2-(6-fluoropyridin-3-yl)-3-(1-methoxycyclopentyl)propanoate, 26** (0.090 g, 56%) was prepared according to General Procedure A using a 1:1 CPME/TFT solvent mixture. The desired compound was obtained as a dense, colorless oil. **¹H NMR** (CDCl₃, 500 MHz) δ ppm 8.13 (d, *J* = 5.3 Hz, 1H), 7.14 (d, *J* = 5.0 Hz, 1H), 6.90 (s, 1H), 3.71 (dd, *J* = 8.0, 4.0 Hz, 1H), 3.04 (s, 3H), 2.54 (dd, *J* = 14.6, 8.3 Hz, 1H), 1.76 (m, 6H), 1.44 (m, 2H), 1.39 (s, 9H), 1.29-1.23 (m, 1H). **¹³C NMR** (CDCl₃, 125 MHz) δ ppm 172.0, 164.3 (d, *J* = 240 Hz), 156.1 (d, *J* = 8.1 Hz), 147.9 (d, *J* = 15 Hz), 121.2 (d, *J*=3.7 Hz), 109.0 (d, *J* = 38 Hz), 86.4, 81.8, 49.6, 48.4, 48.4, 38.8, 36.0, 35.9, 28.1, 23.7, 23.6. **¹⁹F NMR** (CDCl₃, 471 MHz) δ ppm -69.97. **FT-IR** (cm⁻¹, neat, ATR) 2966 (w), 1727 (s), 1608 (m), 1412 (m), 1142 (s). **HRMS** (EI) calcd for $C_{18}H_{27}FNO_3$ [M+H⁺]: 324.1975, found: 324.1948.
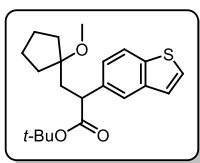
***tert*-Butyl 2-(benzo[b]thiophen-5-yl)-3-(1-methoxycyclopentyl)propanoate, 4.30** (0.065 g, 36%) was prepared according to General Procedure A using a 1:1 CPME/TFT solvent mixture. The desired compound was obtained as a white amorphous solid (mp = 85-87 °C). **¹H NMR** (CDCl₃, 500 MHz) δ ppm 7.80 (d, *J* = 8.4 Hz, 1H), 7.78 (d, *J* = 1.3 Hz, 1H), 7.42 (d, *J* = 5.4 Hz, 1H), 7.33 (dd, *J* = 8.4, 1.5 Hz, 1H), 7.30 (d, *J* = 5.4 Hz, 1H), 3.79 (dd, *J* = 8.7, 3.6 Hz, 1H), 3.08 (s, 3H), 2.64 (dd, *J* = 14.7, 8.5 Hz, 1H), 1.90 (dd, *J* = 14.7, 3.8 Hz, 1H), 1.86-1.80 (m, 1H), 1.80-1.75 (m, 1H), 1.72-1.64 (m, 2H), 1.63-1.52 (m, 2H) 1.45-1.41 (m, 1H), 1.37 (s, 9H), 1.30-1.25 (m, 1H). **¹³C NMR** (CDCl₃, 125 MHz) δ ppm 174.1, 140.2, 138.5, 137.8, 126.9, 124.7, 124.2, 122.9, 122.7, 86.7, 80.7, 49.7, 48.5, 39.5, 36.1, 35.9, 28.2, 23.7, 23.6. **FT-IR** (cm⁻¹, neat, ATR) 2965 (m), 1725 (vs), 1367 (m), 1141 (vs). **HRMS** (EI) calcd for $C_{21}H_{28}O_3S$ [M⁺]: 360.1759, found: 360.1750.

***tert*-Butyl** **2-(6-chloro-5-cyanopyridin-3-yl)-4-hydroxy-4-methylpentanoate, 4.31** (0.065 g, 40%) was prepared according to General Procedure A using a 1:1 *i*-PrOH/TFT solvent mixture. The desired compound was obtained as a dense, colorless oil. **¹H NMR** (CDCl₃, 500 MHz) δ ppm 8.52 (d, *J* = 2.2 Hz, 1H), 7.98 (d, *J* = 2.4 Hz, 1H), 3.82 (dd, *J* = 9.3, 3.7 Hz, 1H), 2.47 (dd, *J* = 14.1, 9.4 Hz, 1H), 1.69 (dd, *J* = 14.2, 3.7 Hz, 1H), 1.48 (br s, 1H), 1.40 (s, 9H), 1.28 (s, 3H), 1.25 (s, 3H). **¹³C NMR** (CDCl₃, 125 MHz) δ ppm 172.2, 152.7, 151.4, 141.9, 136.4, 114.8, 110.9, 82.7, 70.7, 46.6, 45.3, 30.4, 29.8, 28.1. **FT-IR** (cm⁻¹, neat, ATR) 3480 (br), 2232 (w), 1724 (m), 1145 (vs). **HRMS** (ESI⁺) calcd for C₁₆H₂₁ClN₂O₃ [M+H⁺]: 325.1319, found: 325.1295.
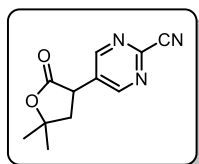

5-(5,5-Dimethyl-2-oxotetrahydrofuran-3-yl)pyrimidine-2-carbonitrile, 4.32 (0.055 g, 51%) was prepared according to General Procedure A us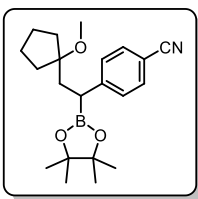ing a 1:1 *i*-PrOH/TFT solvent mixture. The desired compound immediately lactonized upon exposure to silica and was obtained as a white amorphous solid (mp = 117-119 °C). **¹H NMR** (CDCl₃, 500 MHz) δ ppm 8.86 (s, 2 H), 4.15 (dd, *J* = 12.5, 9.0 Hz, 1 H), 2.70 (dd, *J* = 12.7, 9.0 Hz, 1H), 2.28 (t, *J* = 12.6 Hz, 1H), 1.61 (s, 3H), 1.56 (s, 3H). **¹³C NMR** (CDCl₃, 125 MHz) δ ppm 172.8, 157.8, 144.3, 133.3, 115.7, 83.5, 42.5, 42.4, 29.1, 26.9. **FT-IR** (cm⁻¹, neat, ATR) 2981 (w), 1766 (vs), 1421 (s), 1274 (s), 1142 (s). **HRMS** (EI) calcd for C₁₁H₉N₃O₂ [M⁺ - 2H]: 215.0695, found: 215.0682.
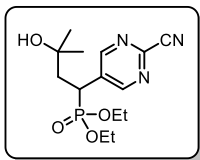
Diethyl (1-(2-cyanopyrimidin-5-yl)-3-hydroxy-3-methylbutyl)phosphonate, 4.33 (0.066 g, 40%) was prepared according to General Procedure A using a 1:1 *i*-PrOH/TFT solvent mixture. The desired compound was isolated as a viscous, clear, colorless oil. **^{1}H NMR** (CDCl$_3$, 500 MHz) δ ppm 8.77 (d, *J* = 2.3 Hz, 2 H), 4.03 - 4.16 (m, 4 H), 3.44 (ddd, *J* = 24.4, 8.9, 3.8 Hz, 1 H), 2.37 (td, *J* = 14.9, 3.8 Hz, 1 H), 2.10 (dt, *J* = 14.7, 9.3 Hz, 1 H), 2.07 (br s, 1H) 1.28 (t, *J* = 7.1 Hz, 3 H), 1.26 (s, 3 H), 1.25 (t, *J* = 7.1 Hz, 3 H), 1.12 (s, 3 H). **^{13}C NMR** (CDCl$_3$, 151 MHz) δ ppm 158.2 (d, *J*=6.5 Hz), 143.2 (d, *J*=4.4 Hz), 136.0 (d, *J*=7.6 Hz), 115.7 (d, *J*=2.2 Hz), 70.4 (d, *J*=10.9 Hz), 63.2 (d, *J*=6.5 Hz), 63.0 (d, *J*=7.6 Hz), 42.0 (d, *J*=3.3 Hz), 37.1 (s), 36.2 (s), 30.1 (d, *J*=7.6 Hz), 16.4 (d, *J*=2.2 Hz), 16.4 (s). **^{31}P NMR** (162 MHz, CDCl$_3$) δ ppm 25.9 (s). **FT-IR** (cm^{-1}, neat, ATR) 3397 (w), 2964 (w), 2923 (m), 2852 (w), 1727 (w), 1549 (w), 1417 (m), 1231 (m), 1050 (s), 1018 (vs), 964 (s), 792 (m), 587 (m). **HRMS** (EI) calcd for C$_{14}$H$_{22}$N$_3$O$_4$P [M$^+$]: 328.1426, found: 328.1401.
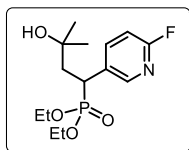
Diethyl (1-(6-fluoropyridin-3-yl)-3-hydroxy-3-methylbutyl)phosphonate, 4.34 (0.104 g, 65%) prepared according to General Procedure A using a 1:1 *i*-PrOH/TFT solvent mixture and a 48 h reaction time. The desired compound was obtained as a viscous, clear, colorless oil. **^{1}H NMR** (CDCl$_3$, 500 MHz) δ ppm 8.11 (br s, 1 H), 7.83 - 7.75 (m, 1 H), 6.89 (dd, *J* = 8.4, 2.7 Hz, 1 H), 4.12 – 3.89 (m, 4 H), 3.41 (ddd, *J* = 23.8, 7.9, 4.4 Hz, 1 H), 2.74 - 2.54 (m, 1 H), 2.36 (td, *J* = 15.1, 4.2 Hz, 1 H), 2.02 (ddd, *J* = 14.6, 11.6, 8.2 Hz, 1 H), 1.26 (t, *J* = 7.1 Hz, 3 H), 1.21 (s, 3 H), 1.18 (t, *J* = 7.1 Hz, 3 H), 1.07 (s, 3 H). **^{13}C NMR** (CDCl3, 151 MHz) δ ppm 162.9 (dd, *J* = 238.7, 2.2 Hz), 148.3 (dd, *J* = 14.7, 8.2 Hz), 141.8 (dd, *J* = 7.6, 5.5 Hz), 132.2 (dd, *J* = 8.2, 4.9 Hz), 109.5 (dd, *J* = 37.1, 2.2 Hz), 70.5 (d, *J* = 12.0 Hz), 63.1 (d, *J* = 6.5 Hz), 62.7 (d, *J* = 6.5 Hz), 43.4 (d, *J* = 2.2 Hz), 37.2 (d, *J* = 138.4 Hz), 31.2, 29.2, 16.6 (t, *J* = 5.4 Hz). **^{19}F NMR** (CDCl$_3$, 471 MHz) δ ppm -70.4 (d, *J$_{F-P}$* = 4.6 Hz). **^{31}P**

NMR (CDCl$_3$, 162 MHz) δ ppm 28.4 (d, $J_{P\text{-}F}$ = 3.9 Hz). **FT-IR** (cm^{-1}, neat, ATR) 3397 (br), 2975 (w), 2930 (w), 1596 (w), 1484 (m), 1396 (w) 1230 (m), 1048 (s), 1021 (vs), 963 (s), 592 (w). **HRMS** (EI) calcd for C$_{13}$H$_{20}$FNO$_4$P [M$^+$- CH$_3$]: 304.114, found: 304.1107.
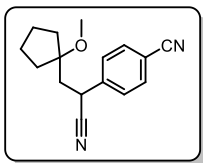

4-(1-Cyano-2-(1-methoxycyclopentyl)ethyl)benzonitrile, 4.35 (0.102 g, 80%) was prepared according to General Procedure A. The desired compound was obtained as a colorless oil. **^{1}H NMR** (500 MHz, CDCl$_3$) δ ppm 7.68 (d, J = 8.5 Hz, 2H), 7.49 (d, J = 8.2 Hz, 2H), 4.01 (dd, J = 8.9, 4.2 Hz, 1H), 3.14 (s, 3H), 2.33 (dd, J = 14.6, 9.0 Hz, 1H), 2.03 (dd, J = 14.6, 4.3 Hz, 1H), 2.03-1.97 (m, 1H), 1.87-1.80 (m, 1H), 1.79-1.55 (m, 5H), 1.30-1.22 (m, 1H). **^{13}C NMR** (151 MHz, CDCl$_3$) δ ppm 142.8, 133.2, 128.6, 120.9, 118.4, 112.5, 85.7, 49.8, 42.4, 36.0, 36.0, 33.2, 23.9, 23.6. **FT-IR** (cm^{-1}, neat, ATR) 2953(m), 2230, 1073 (vs), 835, 577. **HRMS** (EI) calcd for C$_{16}$H$_{18}$N$_2$O [M$^+$]: 254.1410, found: 254.1419.

4-(2-(1-Methoxycyclopentyl)-1-(4,4,5,5-tetramethyl-1,3,2-dioxaborolan-2-yl)ethyl)benzonitrile, 4.36 (0.060 g, 34%) was prepared according to General Procedure A using 4 equiv of vinyl boronic acid pinacol ester and a 1:1 CPME/TFT solvent mixture. The desired compound was obtained as a colorless crystalline solid (mp = 105-108 °C). **^{1}H NMR** (CDCl$_3$, 500 MHz) δ ppm 7.52 (d, J = 8.4 Hz, 2H), 7.35 (d, J = 8.4 Hz, 2H), 3.05 (s, 3H), 2.59 (dd, J = 9.1, 4.7 Hz, 1H), 2.32 (dd, J = 14.2, 9.1 Hz, 1H), 1.88-1.83 (m, 1H), 1.77 (dd, J = 14.1, 4.8 Hz, 1H), 1.75-1.70 (m, 1H), 1.69-1.62 (m, 2H), 1.59- 1.54 (m, 1H), 1.42-1.36 (m, 1H), 1.33-1.22 (m, 2H), 1.16 (s, 6H), 1.13 (s, 6H). **^{13}C NMR** (CDCl$_3$, 125 MHz) δ ppm 151.0, 132.3, 129.3, 119.7 (m), 109.1, 87.2, 83.8, 49.6, 38.8, 36.1, 35.8, 25.1, 24.6, 24.0, 23.9. **^{11}B NMR** (CDCl$_3$, 128.4 MHz) δ ppm 32.4. **FT-IR** (cm^{-1}, neat, ATR) 2973 (m), 2227

(w), 1361 (m), 1329 (m), 1141 (vs). **HRMS** (EI) calcd for $C_{20}H_{27}BNO_2$ [M − OCH_3^+]: 323.2057, found: 323.2088.
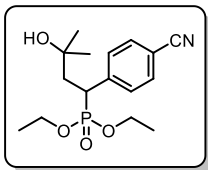
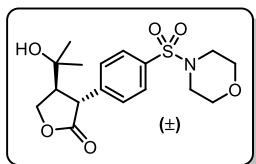**Diethyl (1-(4-cyanophenyl)-3-hydroxy-3-methylbutyl)phosphonate, 4.37** (0.128 g, 79%) was prepared according to General Procedure A using a 1:1 *i*-PrOH/TFT solvent mixture. The desired compound was obtained as a dense, colorless oil. **¹H NMR** (CDCl₃, 500 MHz) δ ppm 7.60 (d, J = 8.0 Hz, 2H), 7.45 (dd, J = 8.4, 2.3 Hz, 2H), 4.10-4.02 (m, 2H), 4.00-3.93 (m, 1H), 3.93-3.85 (m, 1H), 3.45 (ddd, J = 24.1, 8.2, 4.2 Hz, 1H), 2.37 (td, J = 15.3, 4.2 Hz, 1H), 2.23 (br s, 1H), 2.09 (ddd, J = 14.7, 11.5, 8.2 Hz, 1H), 1.27 (t, J = 7.1 Hz, 3H), 1.22 (s, 3H), 1.17 (t, J = 7.1 Hz, 3H), 1.06 (s, 3H). **¹³C NMR** (CDCl₃, 125 MHz) δ ppm 144.4 (d, J = 7.6 Hz), 132.5 (d, J = 2.2 Hz), 130.4 (d, J = 6.5 Hz), 119.0 (d, J = 2.2 Hz), 111.2 (d, J = 3.3 Hz), 70.7 (d, J = 10.9 Hz), 63.2 (d, J = 6.5 Hz), 62.7 (d, J = 7.6 Hz), 43.5 (d, J = 3.3 Hz), 41.1 (d, J = 136 Hz), 31.2, 29.1, 16.6 (d, J = 6.5 Hz), 16.6 (d, J = 5.4 Hz). **³¹P NMR** (CDCl₃, 202 MHz) δ ppm 28.1. **FT-IR** (cm⁻¹, neat, ATR) 3391 (br, s), 2976 (w), 2229 (w), 1607 (br), 1019 (vs). **HRMS** (EI) calcd for $C_{14}H_{18}NO_3P$ [M⁺ - EtOH]: 279.1024, found: 279.1030.
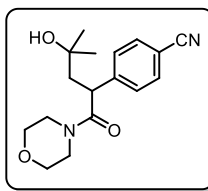
4-(4-Hydroxy-4-methyl-1-morpholino-1-oxopentan-2-yl)benzonitrile, 4.38 (0.073 g, 48%) was prepared according to General Procedure A using a 1:1 *i*-PrOH/TFT solvent mixture. The desired compound was obtained as a dense, yellow oil. **¹H NMR** (500 MHz, CDCl₃) δ ppm 7.62 (d, J = 8.4 Hz, 2 H), 7.38 (d, J = 8.4 Hz, 2H), 4.08 (dd, J = 10.0, 2.5 Hz, 1H), 3.73-3.64 (m, 2H), 3.62-3.49 (m, 4H), 3.35 (ddd, J = 13.2, 5.8, 2.8 Hz, 1H), 3.26-3.20 (m, 1H), 2.74 (dd, J = 14.4, 10.0 Hz, 1H), 2.10 (s, 1H), 1.61 (dd, J = 14.3, 2.6 Hz, 1H), 1.24 (s, 3H), 1.22 (s, 3H). **¹³C NMR** (151 MHz, CDCl₃) δ ppm 171.8,

146.7, 133.2, 128.6, 118.8, 111.4, 70.3, 66.9, 66.5, 47.8, 46.5, 44.5, 43.1, 31.2, 29.0. **FT-IR** (cm⁻¹, neat, ATR) 3435 (br, w), 2968 (w), 2926 (w), 2856 (w), 2229, 1628 (s), 1435, 1226, 1027 (s), 1027, 912, 841, 728 (vs), 647, 573. **HRMS** (ESI+) calcd for $C_{17}H_{22}N_2O_3$ [M+H]: 303.1705, found: 303.1697.

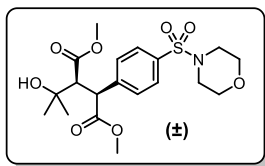*trans*-**4-(2-hydroxypropan-2-yl)-3-(4-(morpholinosulfonyl)phenyl) dihydrofuran-2(3H)-one, 4.39** (0.098 g, 53%) was prepared according to General Procedure A using a 1:1 *i*-PrOH/TFT solvent mixture. The diastereomeric ratio was determined to be >20:1 via crude ¹H NMR analysis. The desired compound was obtained as a white solid (mp = 165-166 °C). **¹H NMR** (500 MHz, CDCl₃) δ ppm 7.76 (d, *J* = 8.4 Hz, 2H), 7.46 (d, *J* = 8.4 Hz, 2H), 4.52 (dd, *J* = 9.1, 8.4 Hz, 1H), 4.38 (dd, *J* = 9.1, 8.6 Hz, 1H), 4.02 (d, *J* = 9.5 Hz, 1H), 3.77-3.73 (m, 4H), 3.05-2.99 (m, 4H), 2.82 (q, *J* = 8.5 Hz) 1.48 (s, 1H), 1.24 (s, 3H), 1.08 (s, 3H). **¹³C NMR** (151 MHz, CDCl₃) δ ppm 176.9, 143.9, 135.0, 129.7, 128.8, 70.4, 67.9, 66.4, 54.1, 48.1, 46.2, 29.3, 28.5. **FT-IR** (cm⁻¹, neat, ATR) 3516 (br, w), 2979 (w), 2922 (w), 2864 (w), 2256 (w), 1767, 1165, 945, 906 (s), 724 (vs), 536. **HRMS** (ESI+) calcd for $C_{17}H_{23}NO_6S$ [M+H]: 369.1246, found: 369.1242.
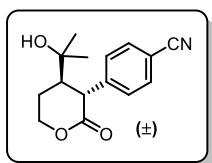
trans-**4-(4-(2-Hydroxypropan-2-yl)-2-oxotetrahydro-2H-pyran-3-yl) benzonitrile, 4.40** (0.091 g, 70%) was prepared according to General Procedure A using a 1:1 *i*-PrOH/TFT solvent mixture. The diastereomeric ratio was determined to be >20:1 via crude ¹H NMR analysis. The desired compound was obtained as a dense, colorless oil. **¹H NMR** (CDCl₃, 500 MHz) δ ppm 7.67 (d, *J* = 8.4 Hz, 2H), 7.37 (d, *J* = 8.4 Hz, 2H), 3.63 (d, *J* = 12.5 Hz, 1H), 3.52-3.47 (m, 1H), 3.38 (m, 1H), 2.64 (dt, *J* = 12.6, 6.9 Hz, 1H), 1.85-1.79 (m, 1H), 1.74-1.68 (m, 1H), 1.59 (s, 3H), 1.58 (s, 1H), 1.41 (s, 3H).

288

^{13}**C NMR** (CDCl$_3$, 125 MHz) δ ppm 174.8, 142.1, 133.0, 129.9, 118.7, 112.2, 85.5, 60.3, 53.8, 50.5, 32.3, 28.2, 22.4. **FT-IR** (cm^{-1}, neat, ATR) 3483 (br), 2978 (w), 2229 (w), 1755 (vs), 1264 (m). **HRMS** (EI) calcd for C$_{15}$H$_{17}$NO$_3$ [M$^+$]: 259.1208, found: 259.1195.
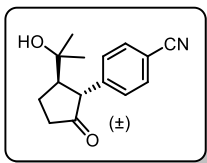
***trans*-4-(2-(2-Hydroxypropan-2-yl)-5-oxocyclopentyl)benzonitrile, 4.41** (0.090 g, 74%) was prepared according to General Procedure A using a 1:1 *i*-PrOH/TFT solvent mixture. The diastereomeric ratio was determined to be >20:1 via crude ^{1}H NMR analysis. The desired compound was obtained as a dense, pink oil. ^{1}**H NMR** (CDCl$_3$, 500 MHz) δ ppm 7.62 (d, *J* = 8.4 Hz, 2H), 7.26 (d, *J* = 8.2 Hz, 2H), 3.48 (d, *J* = 12.0 Hz, 1H), 2.60-2.54 (m, 2H), 2.38 (ddd, *J* = 18.8, 11.9, 9.3 Hz, 1H), 2.26-2.20 (m, 1H), 1.94-1.86 (m, 1H), 1.25 (s, 1H), 1.24 (s, 3H), 1.02 (s, 3H). ^{13}**C NMR** (CDCl$_3$, 125 MHz) δ ppm 216.6, 146.1, 132.8, 129.9, 119.0, 111.1, 71.8, 58.1, 54.3, 38.6, 29.8, 28.5, 22.6. **FT-IR** (cm^{-1}, neat, ATR) 3404 (br s), 2975 (w), 2228 (w), 1735 (vs), 1160 (m), 1113 (m). **HRMS** (EI) calcd for C$_{15}$H$_{17}$NO$_2$ [M$^+$]: 243.1259, found: 243.1259.
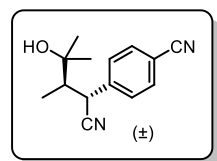
4-(1-Cyano-3-hydroxy-2,3-dimethylbutyl)benzonitrile, 4.42 was prepared either according to General Procedure A using a 1:1 *i*-PrOH/TFT solvent mixture (0.103 g, 58%) or accor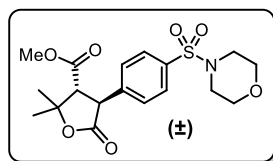ding to General Procedure A using a 1:1 *i*-PrOH/TFT solvent mixture and 4 equiv of crotonitrile (0.160 g, 90%). The diastereomeric ratio was determined to be >20:1 via crude ^{1}H NMR analysis. The desired compound was obtained as a dense, colorless oil. ^{1}**H NMR** (CDCl$_3$, 500 MHz) δ ppm 7.69 (d, *J* = 8.4 Hz, 2H), 7.52 (d, *J* = 8.4 Hz, 2H), 4.65 (d, *J* = 1.3 Hz, 1H), 1.82 (qd, *J* = 7.1, 1.6 Hz, 1H), 1.55 (s, 1H), 1.38 (s, 3H), 1.33 (s, 3H), 1.03 (d, *J* = 7.1 Hz, 3H). ^{13}**C NMR** (CDCl$_3$, 125 MHz) δ ppm 142.5, 133.0, 128.7,

119.2, 118.5, 112.1, 73.1, 50.8, 37.8, 30.3, 25.0, 11.4. **FT-IR** (cm^{-1}, neat, ATR) 3401 (br, s), 2976 (w), 2231 (m), 1609 (w). **HRMS** (EI) calcd for C$_{14}$H$_{16}$N$_2$O [M$^+$]: 228.1263, found: 228.1253.


Dimethyl 2-(2-hydroxypropan-2-yl)-3-(4-(morpholinosulfonyl) phenyl)succinate, 4.43 (0.077 g, 36%) was prepared according to General Procedure A using the corresponding aryl iodide and a 1:1 *i*-PrOH/TFT solvent mixture. The desired compound was obtained a white, powdered solid (mp = 187 ºC, decomp). **^{1}H NMR** (CDCl$_3$, 500 MHz) δ ppm 7.71 (d, *J* = 8.4 Hz, 2H), 7.60 (d, *J* = 8.4 Hz, 2H), 4.38 (d, *J* = 9.9 Hz, 1H), 3.76 (s, 3H), 3.74 (t, *J* = 4.7 Hz, 4H), 3.62 (s, 3H), 3.25 (d, *J* = 10.0 Hz, 1H), 2.99 (t, *J* = 4.5 Hz, 4H), 2.22 (s, 1H), 1.14 (s, 3H), 0.95 (s, 3H). **^{13}C NMR** (CDCl$_3$, 125 MHz) δ ppm 174.5, 173.0, 143.7, 134.9, 129.8, 128.7, 71.7, 66.4, 58.6, 53.0, 52.4, 51.0, 46.3, 30.0, 28.5. **FT-IR** (cm^{-1}, neat, ATR) 3529 (br), 2898 (w), 1732 (s), 1164 (vs), 1112 (s). **HRMS** (ESI) calcd for C$_{19}$H$_{28}$NO$_8$S [M+H$^+$]: 430.1536, found: 430.1525

***trans*-Methyl 2,2-dimethyl-4-(4-(morpholinosulfonyl)phenyl)-5-oxotetrahydrofuran-3-carboxylate, 4.44** (0.052 g, 26%) was prepared according to General Procedure A using the corresponding aryl iodide and a 1:1 *i*-PrOH/TFT solvent mixture. The desired compound was obtained a white, powdered solid (mp = 189-191 ºC). **^{1}H NMR** (CDCl$_3$, 500 MHz) δ ppm 7.75 (d, *J* = 8.4 Hz, 2H), 7.48 (d, *J* = 8.2 Hz, 2H), 4.55 (d, *J* = 12.2 Hz, 1H), 3.77 (s, 3H), 3.74 (t, *J* = 4.7 Hz, 4H), 3.30 (d, *J* = 12.0 Hz, 1H), 3.02 (t, *J* = 4.7 Hz, 4H), 1.73 (s, 3H), 1.56 (s, 1H), 1.40 (s, 3H). **^{13}C NMR** (CDCl$_3$, 125 MHz) δ ppm 173.5, 169.4, 141.1, 135.3, 129.8, 128.8, 82.7, 66.4, 59.9, 53.2, 49.1, 46.2, 28.8, 23.7. **FT-IR** (cm^{-1}, neat, ATR) 2931 (w), 1770 (s), 1737 (s), 1249 (m), 1166 (vs), 1112 (vs). **HRMS** (ESI) calcd for C$_{18}$H$_{24}$NO$_7$S [M+H$^+$]: 398.1273, found: 398.1265
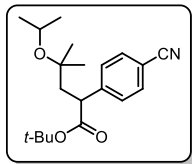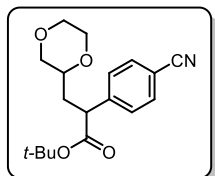
***tert*-Butyl 2-(4-cyanophenyl)-4-isopropoxy-4-methylpentanoate, 4.45** (0.106 g, 64%) was prepared according to General Procedure A. The desired compound was obtained as a dense colorless, oil. **^{1}H NMR** (CDCl$_3$, 500 MHz) δ ppm 7.58 (d, *J* = 8.4 Hz, 2H), 7.41 (d, *J* = 8.4 Hz, 2H), 3.78 (dd, *J* = 8.5, 3.5 Hz, 1H), 3.72 (m, 1H), 2.45 (dd, *J* = 14.2, 8.7 Hz, 1H), 1.72 (dd, *J* = 14.2, 3.5 Hz, 1H), 1.35 (s, 9H), 1.14 (s, 3H), 1.11 (s, 3H), 1.08 (d, *J* = 6.2 Hz, 3H), 1.05 (d, *J* = 6.2 Hz, 3H). **^{13}C NMR** (CDCl$_3$, 125 MHz) δ ppm 173.0, 147.2, 132.6, 129.0, 119.1, 110.9, 81.3, 74.7, 63.6, 48.7, 44.8, 28.1, 26.6, 26.4, 25.3, 25.2. **FT-IR** (cm^{-1}, neat, ATR) 2974, 2932 (w), 2229 (w), 1727(s), 1367 (s), 1142 (vs), 1114, 1006. **HRMS** (EI) calcd for C$_{16}$H$_{21}$NO$_3$ [M$^+$-*t*Bu+H]: 275.1521, found: 275.1525.
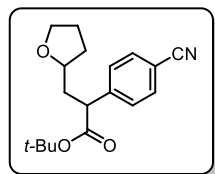
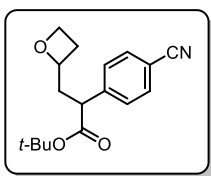***tert*-Butyl 2-(4-cyanophenyl)-3-(tetrahydrofuran-2-yl)propanoate, 33** (0.119 g, 79%) was prepared according to General Procedure A using 4 equiv of *tert*-butyl acrylate. The diastereomeric ratio was determined to be 1.2:1 via crude ^{1}H NMR analysis. The desired compound was obtained as a dense, colorless oil. **^{1}H NMR** (CDCl$_3$, 500 MHz) δ ppm 7.61 (d, *J* = 8.4 Hz, 2H), 7.43 (d, *J* = 8.2 Hz, 2H), 3.83 (m, 1H), 3.76 (dd, *J* = 9.2, 6.0 Hz, 1H), 3.67 (m, 1H), 3.54 (m, 1H), 2.18 (m, 1H), 1.89 (m, 3H), 1.81 (m, 1H), 1.45 (m, 1H), 1.37 (s, 9H). **^{13}C NMR** (CDCl$_3$, 125 MHz) δ ppm 172.4, 145.1, 132.6, 129.3, 119.1, 111.2, 81.5, 76.3, 67.9, 50.3, 39.3, 31.8, 28.1, 25.9. **FT-IR** (cm^{-1}, neat, ATR) 2977 (w), 2229 (w), 1724 (s), 1368 (m), 1145 (vs), 1068 (m). **HRMS** (EI) calcd for C$_{14}$H$_{14}$NO$_3$ [M$^+$ -*t*-Bu]: 244.0974, found: 244.0984.

***tert*-Butyl 2-(4-cyanophenyl)-3-(1,4-dioxan-2-yl)propanoate, 4.47** (0.065 g, 41%) was prepared according to General Procedure A using 4 equiv of

tert-butyl acrylate. The diastereomeric ratio was determined to be 1.3:1 via crude ^{1}H NMR analysis. The desired compound was obtained as a dense, colorless oil. **^{1}H NMR** (CDCl$_3$, 500 MHz) δ ppm 7.63 and 7.60 (d, *J* = 8.3 Hz, 2H), 7.41 and 7.39 (d, *J* = 5.6 Hz, 2H), 3.84-3.78 (m, 1H), 3.77-3.73 (m, 1H), 3.72-3.68 (m, 1H), 3.66-3.54 and 3.20-3.16 (m, 3H), 3.31-3.24 (m, 1H), 2.14-2.08 (m, 1H), 1.73 and 1.61 (ddd, *J* = 12.8, 9.6, 3.0 Hz, 1H), 1.46-1.43 (m, 1H), 1.40 and 1.37 (s, 9H). **^{13}C NMR** (CDCl$_3$, 125 MHz) δ ppm 172.2, 171.8, 145.6, 144.6, 132.7, 129.2, 128.8, 118.9, 111.5, 111.4, 82.0, 81.7, 73.6, 72.7, 71.3, 71.3, 67.1, 66.9, 66.8, 66.7, 48.4, 48.3, 35.5, 34.8, 28.2, 28.1. **FT-IR** (cm^{-1}, neat, ATR) 2975 (w), 2229 (w), 1725 (m), 1149 (vs), 1123 (s). **HRMS** (EI) calcd for C$_{14}$H$_{14}$NO$_4$ [M$^+$ -*t*Bu]: 260.0923, found: 260.0922.
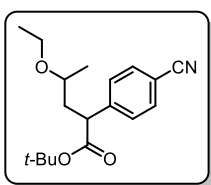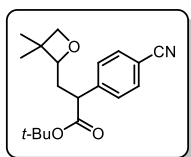

***tert*-Butyl 2-(4-cyanophenyl)-4-ethoxypentanoate, 4.48** (0.099 g, 65%) was prepared according to General Procedure A. The diastereomeric ratio was determined to be 1.1:1 via crude ^{1}H NMR analysis. The desired compound was obtained as a dense, colorless oil. **^{1}H NMR** (CDCl$_3$, 500 MHz) δ ppm 7.60 (t, *J* = 7.4 Hz, 2H), 7.41 (t, *J* = 6.8 Hz, 2H), 3.81 (td, *J* = 10.2, 5.3 Hz, 1H), 3.60-3.30 (m, 2H), 3.18-3.01 (m, 1H), 2.25-2.13 (m, 1H), 1.83 and 1.73 (ddd, *J* = 13.3, 9.4, 3.5, 1H), 1.39 and 1.37 (s, 9H), 1.15 (m, 6H). **^{13}C NMR** (CDCl$_3$, 125 MHz) δ ppm 172.5, 172.4, 145.8, 145.3, 132.6, 132.6, 129.3, 128.9, 119.1, 111.2, 111.1, 81.6, 81.4, 73.2, 72.3, 66.1, 64.3, 63.9, 49.4, 49.3, 41.2, 40.4, 28.2, 28.1, 20.2, 19.9, 15.9, 15.8. **FT-IR** (cm^{-1}, neat, ATR) 2974 (w), 2229 (w), 1725 (s), 1368 (m), 1143 (vs), 1093 (m). **HRMS** (EI) calcd for C$_{14}$H$_{16}$NO$_3$ [M$^+$ -*t*Bu]: 246.1130, found: 246.1122.
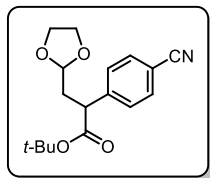

***tert*-Butyl 2-(4-cyanophenyl)-3-(oxetan-2-yl)propanoate, 4.49** (0.066 g, 46%) was prepared according to General Procedure A using 4 equiv of *tert*-

butyl acrylate. The diastereomeric ratio was determined to be 1.2:1 via crude ^{1}H NMR analysis. The desired compound was obtained as a dense, colorless oil. **^{1}H NMR** (CDCl$_3$, 500 MHz) δ ppm 7.61 (d, J = 8.3 Hz, 2H), 7.41 and 7.39 (d, J = 8.4 Hz, 2H), 4.83-4.77 and 4.55-4.46 (m, 2H), 4.67-4.59 (m, 1H), 3.68 (dd, J = 9.5, 5.9 Hz, 1H), 2.72-2.42 (m, 2H), 2.37-2.33 (m, 1H), 2.11 and 2.05 (ddd, J = 14.0, 9.7, 4.4 Hz, 1H), 1.38 and 1.37 (s, 9H). **^{13}C NMR** (CDCl$_3$, 125 MHz) δ ppm 172.0, 171.8, 145.2, 144.5, 132.7, 132.7, 129.3, 128.8, 119.0, 111.5, 111.4, 81.9, 81.8, 80.6, 79.7, 68.5, 48.3, 48.2, 41.7, 41.2, 28.4, 28.1, 27.7, 27.7. **FT-IR** (cm^{-1}, neat, ATR) 2977 (w), 2228 (w), 1724 (s), 1392 (m), 1144 (vs). **HRMS** (EI) calcd for C$_{178}$H$_{21}$NO$_3$ [M$^+$]: 287.1521, found: 287.1526.
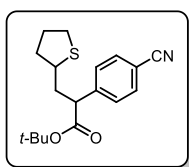

tert-Butyl 2-(4-cyanophenyl)-3-(3,3-dimethyloxetan-2-yl)propanoate, 4.50 (0.110 g, 70%) was prepared according to General Procedure A using 4 equiv of tert-butyl acrylate. The diastereomeric ratio was determined to be 1.8:1 via crude ^{1}H NMR analysis. The desired compound was obtained as a dense, colorless oil. **^{1}H NMR** (CDCl$_3$, 500 MHz) δ ppm 7.63-7.60 (m, 2H), 7.40 (t, J = 8.2 Hz, 2H), 4.38 and 4.05 (dd, J = 10.0, 3.2 Hz, 1H), 4.29 and 4.25 (d, J = 5.5 Hz, 1H), 4.13 and 4.11 (d, J = 5.5 Hz, 1H), 3.65 and 3.62 (dd, J = 10.3, 4.6 Hz, 1H), 2.29 and 1.90 (ddd, J = 13.6, 10.4, 3.3 Hz, 1H), 2.47 and 2.00 (ddd, J = 14.0, 10.1, 5.5 Hz, 1H), 1.37 (s, 9H), 1.25 and 1.13 (s, 3H), 1.17 (s, 3H). **^{13}C NMR** (CDCl$_3$, 125 MHz) δ ppm 172.2, 171.8, 145.4, 144.5, 132.7, 129.3, 128.9, 119.0, 111.5, 111.4, 88.7, 87.7, 81.9, 81.8, 81.5, 81.3, 48.3, 48.2, 38.4, 38.1, 36.3, 35.5, 28.4, 26.9, 26.8, 21.4, 21.2. **FT-IR** (cm^{-1}, neat, ATR) 2968 (w), 2228 (w), 1724 (s), 1368 (m), 1146 (vs), 967 (w). **HRMS** (EI) calcd for C$_{19}$H$_{26}$NO$_3$ [M + H$^+$]: 316.1913, found: 316.1909.

tert-Butyl 2-(4-cyanophenyl)-3-(1,3-dioxolan-2-yl)propanoate, 4.51 (0.090 g, 60%) was prepared according to General Procedure A using 4 equiv of _tert_-butyl acrylate. The desired compound was obtained as a dense, colorless oil. **^{1}H NMR** (CDCl$_3$, 500 MHz) δ ppm 7.61 (d, J = 8.4 Hz, 2H), 7.43 (d, J = 8.4 Hz, 2H), 4.83 (dd, J = 4.7, 4.2 Hz, 1H), 3.97-3.93 (m, 2H), 3.85-3.82 (m, 2H), 3.77 (dd, J = 8.7, 6.2 Hz, 1H), 2.51 (ddd, J = 13.9, 8.7, 4.9 Hz, 1H), 2.01 (ddd, J = 9.0, 6.0, 3.9 Hz, 1H), 1.38 (s, 9H). **^{13}C NMR** (CDCl$_3$, 125 MHz) δ ppm 171.8, 145.0, 132.7, 129.0, 119.0, 111.4, 102.5, 81.7, 65.4, 65.2, 48.0, 37.2, 28.1. **FT-IR** (cm^{-1}, neat, ATR) 2977 (w), 2229 (w), 1725 (s), 1392 (w), 1367 (m), 1144 (vs), 1021 (m). **HRMS** (EI) calcd for C$_{17}$H$_{21}$NO$_4$ [M$^+$]: 303.1471, found: 303.1465.

**_tert_-Butyl 2-(4-Cyanophenyl)-3-(tetrahydrothiophen-2-yl)propanoate, 4.52** (0.050 g, 32%) was prepared according to General Procedure A using 4 equiv of _tert_-butyl acrylate and a 1:1 tetrahydrothiophene/TFT solvent mixture. The diastereomeric ratio was determined to be 1.1:1 via crude ^{1}H NMR analysis. The desired compound was obtained as a dense, colorless oil. **^{1}H NMR** (CDCl$_3$, 500 MHz) δ ppm 7.61 (t, J = 7.8 Hz, 2H), 7.41 (d, J = 8.0 Hz, 2H), 3.67-3.61 (m, 1H), 3.33-2.90 (m, 1H), 2.90-2.80 (m, 2H), 2.45-2.1 (m, 2H), 2.07-1.99 (m, 2H), 1.97-1.65 (m, 2H), 1.39 and 1.37 (s, 9H). **^{13}C NMR** (CDCl$_3$, 125 MHz) δ ppm 172.1, 171.9, 145.1, 144.4, 132.7, 129.3, 128.9, 118.9, 111.5, 111.4, 82.0, 81.8, 52.4, 52.4, 47.1, 46.4, 41.9, 41.0, 37.7, 32.6, 32.6, 30.5, 30.4, 28.4, 28.2, 28.2. **FT-IR** (cm^{-1}, neat, ATR) 2936 (w), 2228 (w), 1724 (s), 1368 (m), 1145 (s). **HRMS** (EI) calcd for C$_{18}$H$_{23}$NO$_2$S [M$^+$]: 317.1449, found: 317.1434.
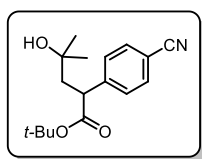
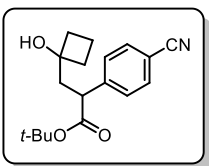**_tert_-Butyl 2-(4-cyanophenyl)-4-hydroxy-4-methylpentanoate, 4.53** (0.109 g, 75%) was prepared according to General Procedure A. The desired

compound was obtained as a white amorphous solid (mp = 105-108 °C). ^{1}**H NMR** (CDCl$_3$, 500 MHz) δ ppm 7.60 (d, *J* = 7.8 Hz, 2H), 7.41 (d, *J* = 7.8 Hz, 2H), 3.79 (d, *J* = 9.5 Hz, 1H), 2.51 (dd, *J* = 14.0, 10.3 Hz, 1H), 1.69 (d, *J* = 14.2 Hz, 1H), 1.59 (s, 1H) 1.37 (s, 9H), 1.26 (s, 3H), 1.24 (s, 3H). ^{13}**C NMR** (CDCl$_3$, 125 MHz) δ ppm 173.2, 146.6, 132.7, 128.8, 119.0, 111.2, 81.8, 70.7, 48.8, 46.7, 30.6, 29.3, 28.1. **FT-IR** (cm^{-1}, neat, ATR) 3452 (br), 2974 (w), 2230 (w), 1726 (s), 1368 (s). **HRMS** (ESI) calcd for C$_{17}$H$_{23}$NO$_3$ [M+H$^+$]: 290.1756, found: 290.1742.
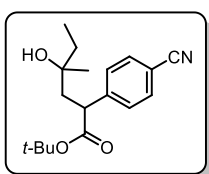
***tert*-Butyl 2-(4-cyanophenyl)-4-hydroxy-4-methylhexanoate, 4.54** (0.145 g, 96%) was prepared according to General Procedure A. The diastereomeric ratio was determined to be 1.5:1 via crude ^{1}H NMR analysis. The desired compound was obtained as a white amorphous solid (mp = 72-74 °C). ^{1}**H NMR** (CDCl$_3$, 500 MHz) δ ppm 7.61-7.58 (m, 2H), 7.41 (d, *J* = 8.2 Hz, 2H), 3.80-3.76 (m, 1H), 2.51-2.42 (m, 1H), 1.68 and 1.62 (dd, *J* = 14.3, 3.2 Hz, 1H) 1.55-1.50 (m, 2H), 1.45 (s, 1H) 1.37 (s, 9H), 1.17 and 1.15 (s, 3H), 0.92 and 0.88 (t, *J*=7.4 Hz, 3H). ^{13}**C NMR** (CDCl$_3$, 125 MHz) δ ppm 173.4 (s), 173.2 (s), 146.8 (m), 146.7 (s), 132.7 (m), 128.8 (s), 119.0 (s), 81.7 (s), 81.7 (s), 72.9 (s), 72.7 (s), 48.6 (s), 48.4 (s), 44.6 (s), 44.4 (s), 36.2 (s), 34.7 (s), 28.1 (s), 26.9 (s), 25.6 (s), 8.7 (s), 8.4 (s). **FT-IR** (cm^{-1}, neat, ATR) 3422 (br), 2974 (w), 2229 (w), 1725 (m), 1368 (m), 1144 (vs). **HRMS** (EI) calcd for C$_{17}$H$_{23}$NO$_3$ [M$^+$]: 289.1678, found: 289.1670.

***tert*-Butyl 2-(4-cyanophenyl)-3-(1-hydroxycyclobutyl)propanoate, 4.55** (0.137 g, 91%) was prepared according to General Procedure A. The desired compound was obtained as a white amorphous solid (mp = 99-101 °C). ^{1}**H NMR** (CDCl$_3$, 500 MHz) δ ppm 7.60 (d, *J* = 8.4 Hz, 2H), 7.42 (d, *J* = 8.4 Hz, 2H), 3.71 (dd, *J* = 9.1, 4.0 Hz, 1H), 2.55 (dd, *J* = 14.6, 9.1, 1H), 2.06-2.02 (m, 2H), 1.93-1.90 (m, 2H), 1.79-1.73

(m, 1H), 1.51-1.43 (m, 3H), 1.36 (s, 9H). ^{13}C NMR (CDCl$_3$, 125 MHz) δ ppm 173.3, 146.4,

132.7, 128.9, 119.1, 111.2, 81.8, 75.2, 48.8, 42.8, 37.2, 35.7, 28.1, 12.5. FT-IR (cm^{-1}, neat, ATR)

3499 (br), 2979 (w), 2229 (w), 1724 (s), 1146 (vs). HRMS (EI) calcd for C$_{14}$H$_{14}$NO$_3$ [M – *t*-Bu$^+$]:

245.1052, found: 245.1058.
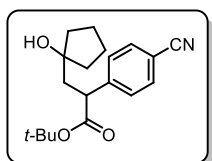
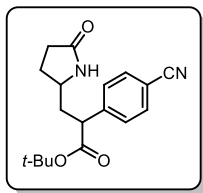***tert*-Butyl 2-(4-cyanophenyl)-3-(1-hydroxycyclopentyl)propanoate, 4.56**
(0.090 g, 57%) was prepared according to General Procedure A. The desired
compound was obtained as a dense, colorless oil. ^{1}H NMR (CDCl$_3$, 500

MHz) δ ppm 7.60 (d, *J* = 8.2 Hz, 2H), 7.42 (d, *J* = 8.4 Hz, 2H), 3.82 (dd, *J* = 9.4, 3.8 Hz, 1H),

2.62 (dd, *J* = 14.4, 9.4 Hz, 1H), 1.82-1.78 (m, 3 H), 1.66-1.60 (m, 3H), 1.48 (d, *J* = 7.1 Hz, 1H),

1.47-1.43 (m, 2H), 1.37 (s, 9H), 1.31 (s, 1H). ^{13}C NMR (CDCl$_3$, 125 MHz) δ ppm 173.32,

146.60, 132.68, 128.88, 119.06, 111.17, 82.18, 81.71, 49.72, 44.76, 41.01, 39.63, 28.09, 23.85,

23.75. FT-IR (cm^{-1}, neat, ATR) 3507 (br), 2965 (w), 2229 (w), 1725 (s), 1146 (vs). HRMS (EI)

calcd for C$_{15}$H$_{15}$NO$_2$ [M – *t*-BuOH$^+$]: 241.1103, found: 241.1096.
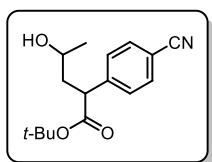
***tert*-Butyl 2-(4-cyanophenyl)-4-hydroxypentanoate, 4.57** (0.098 g, 71%)
was prepared according to General Procedure A using 4 equiv of *tert*-butyl
acrylate. The desired compound was obtained as a colorless oil at 90% purity

with 10% benzophenone catalyst impurity. The diastereomeric ratio was determined to be 1:1 via

crude ^{1}H NMR analysis. ^{1}H NMR (CDCl$_3$, 500 MHz) δ ppm 7.61 (d, *J* = 8.2 Hz, 2H), 7.42 (d, *J*

= 8.2 Hz, 2H), 3.57-3.54 (m, 1H), 2.16 (ddd, *J* = 14.2, 9.6, 6.8 Hz, 1H), 1.85 and 1.83 (dd, *J* =

8.3, 3.4 Hz, 1H), 1.46 (s, 1H), 1.37 (s, 9H), 1.20 (d, *J* = 6.2 Hz, 3H). ^{13}C NMR (CDCl$_3$, 125

MHz) δ ppm 172.8, 145.2, 132.6, 129.2, 119.0, 111.3, 81.7, 66.1, 50.0, 42.3, 28.1, 24.5. FT-IR

(cm^{-1}, neat, ATR) 3425 (br), 2976 (w), 2229 (w), 1724 (s), 1146 (vs). **HRMS** (ESI) calcd for

C$_{16}$H$_{22}$NO$_3$ [M + H$^+$]: 276.1600, found: 276.1586.

***tert*-Butyl 2-(4-cyanophenyl)-3-(5-oxopyrrolidin-2-yl)propanoate, 4.58** (0.112 g, 71%) was prepared according to General Procedure A using 4 equiv of *tert*-butyl acrylate. The diastereomeric ratio was determined to be 1:1 via crude ^{1}H NMR analysis. The desired compound was obtained as a dense, colorless oil. **^{1}H NMR** (CDCl$_3$, 500 MHz) δ ppm 7.63 (d, *J* = 8.4 Hz, 2H), 7.44 and 7.41 (d, *J* = 8.4 Hz, 2H), 6.83 and 6.32 (br s, 1H), 3.63-3.42 (m, 2H), 2.37-2.21 (m, 4H), 1.93-1.84 (m, 1H), 1.80-1.66 (m, 1H), 1.39 and 1.37 (s, 9H). **^{13}C NMR** (CDCl$_3$, 125 MHz) δ ppm 178.49, 178.23, 171.72, 171.60, 144.27, 144.19, 129.05, 128.87, 118.82, 118.77, 111.82, 111.76, 82.53, 82.35, 52.64, 52.50, 49.95, 49.82, 30.26, 30.11, 28.14, 27.79, 27.46. **FT-IR** (cm^{-1}, neat, ATR) 3265 (br), 2978 (w), 2229 (w), 1722 (s), 1690 (vs), 1258 (m), 1145 (vs). **HRMS** (EI) calcd for C$_{18}$H$_{22}$N$_2$O$_3$ [M$^+$]: 315.1630, found: 315.1654.
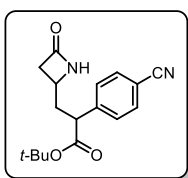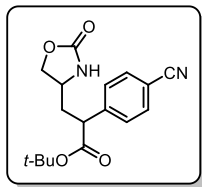

***tert*-Butyl 2-(4-cyanophenyl)-3-(4-oxoazetidin-2-yl)propanoate, 4.59** (0.056 g, 37%) was prepared according to General Procedure A using 4 equiv of *tert*-butyl acrylate. The diastereomeric ratio was determined to be 1:1 via crude ^{1}H NMR analysis. The desired compound was obtained as a dense, colorless oil. **^{1}H NMR** (CDCl$_3$, 500 MHz) δ ppm 7.64 (d, *J* = 8.2 Hz, 2H), 7.41 and 7.39 (d, *J* = 8.3 Hz, 2H) 6.01 and 5.77 (br s, 1H), 3.56 (m, 2H), 3.08 and 3.02 (ddd, *J*=14.9, 4.9, 2.2 Hz, 1H), 2.66 and 2.52 (dd, *J*=14.9, 1.6 Hz, 1H) 2.45-2.40 (m, 1H), 2.05-1.99 (m, 1H), 1.39 and 1.38 (s, 9H). **^{13}C NMR** (CDCl$_3$, 125 MHz) δ ppm 171.42, 171.36, 167.4, 167.3, 144.0, 132.9, 128.9, 118.7, 112.0, 111.9, 82.6, 82.5, 50.6, 50.4, 46.51, 46.49, 44.1, 44.0, 39.1, 38.9, 28.1. **FT-IR** (cm^{-1}, neat, ATR) 3320 (br), 2977

(w), 2229 (w), 1738 (vs), 1722 (vs), 1145 (vs). **HRMS** (ESI) calcd for $C_{17}H_{21}N_2O_3$ [M+H$^+$]: 301.1552, found: 301.1552.

tert-Butyl 2-(4-cyanophenyl)-3-(2-oxooxazolidin-4-yl)propanoate, 4.60 (0.063 g, 40%) was prepared according to General Procedure A using 4 equiv of *tert*-butyl acrylate. The diastereomeric ratio was determined to be 1.1:1 via crude ^{1}H NMR analysis. The desired compound was obtained as a dense, colorless oil.

^{1}H NMR (CDCl$_3$, 500 MHz) δ ppm 7.65 (d, *J* = 8.4 Hz, 2H), 7.40 (d, *J* = 8.2 Hz, 2H), 5.51 (s, 1H), 4.50 (t, *J* = 8.5 Hz, 1H), 4.05 (dd, *J* = 8.8, 6.3 Hz, 1H), 3.94-3.87 (m, 1H), 3.61 (dd, *J* = 9.7, 5.4 Hz, 1H), 2.38 (ddd, *J* = 14.1, 9.6, 4.8 Hz, 1H), 1.92 (ddd, *J* = 13.8, 7.8, 5.4 Hz, 1H), 1.39 (s, 9H). **^{13}C NMR** (CDCl$_3$, 125 MHz) δ ppm 171.3, 159.3 (m), 143.8, 133.0, 128.8, 118.6, 111.9, 83.0, 70.1, 50.9, 49.2, 38.9, 28.1. **FT-IR** (cm^{-1}, neat, ATR) 3311 (br), 2979 (w), 2229 (w), 1755 (vs), 1721 (vs), 1368 (m), 1149 (vs). **HRMS** (EI) calcd for $C_{17}H_{22}N_2O_4$ [M+H$^+$]: 317.1501, found: 317.1498.
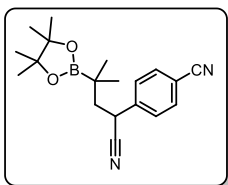
4-(1-Cyano-3-methyl-3-(4,4,5,5-tetramethyl-1,3,2-dioxaborolan-2-yl)butyl) benzonitrile, 4.61 (0.057 g, 35%) was prepared according to General Procedure A using 4 equiv of acrylonitrile. The desired compound was obtained as a dense, colorless oil. **^{1}H NMR** (CDCl$_3$, 500 MHz) δ ppm 7.67 (d, *J* = 8.4 Hz, 2H), 7.50 (d, *J* = 8.2 Hz, 2H), 3.96 (dd, *J* = 10.3, 3.7 Hz, 1H), 2.00 (dd, *J* = 13.9, 10.4 Hz, 1H), 1.75 (dd, *J* = 14.0, 3.7 Hz, 1H), 1.26 (s, 12H), 1.14 (s, 3H), 1.02 (s, 3H). **^{13}C NMR** (CDCl$_3$, 125 MHz) δ ppm 143.5 (s), 133.1 (s), 128.4 (s), 120.9 (m), 118.5 (m), 112.0 (m), 84.0 (s), 47.1 (s), 35.2 (s), 25.4 (s), 25.1 (s), 25.1 (s), 24.9 (s). **^{11}B NMR** (CDCl$_3$, 128.4 MHz) δ ppm 33.7. **FT-IR**

(cm^{-1}, neat, ATR) 2932 (w), 2230 (w), 1317 (m), 1134 (s). **HRMS** (EI) calcd for C$_{19}$H$_{25}$BN$_2$O$_2$ [M$^+$]: 324.2009, found: 324.2006.
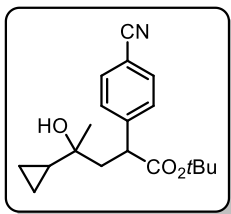
***tert*-Butyl 2-(4-cyanophenyl)-4-cyclopropyl-4-hydroxypentanoate, 4.75** (0.060 g, 38%) was prepared according to General Procedure A. The diastereomeric ratio was determined to be 1.2:1 via ^{1}H NMR. The desired compound was obtained a colorless oil. **^{1}H NMR** (CDCl$_3$, 500 MHz) δ ppm 7.59 (d, *J* = 8.2 Hz, 2H), 7.41 (d, *J* = 8.2 Hz, 2H), 3.98 and 3.83 (dd, *J* = 10.2, 3.2 Hz, 1H), 2.57-2.51 (m, 1H), 1.76 and 1.71 (dd, *J* = 14.4, 3.2 Hz, 1H), 1.36 and 1.35 (s, 9H), 1.24 (br s, 1H), 1.16 and 1.15 (s, 3H), 0.92-0.80 (m, 1H), 0.50-0.24 (m, 4H). **^{13}C NMR** (CDCl$_3$, 125 MHz) δ ppm 173.5, 173.3, 146.75, 146.72, 132.7, 128.8, 119.0, 111.10, 111.08, 81.73, 81.69, 70.7, 70.6, 48.6, 48.5, 46.5, 45.7, 28.04, 28.03, 28.00, 26.5, 22.0, 21.0, 1.4, 1.1, 0.8, 0.3. **FT-IR** (cm^{-1}, neat, ATR) 3520 (br), 2976 (w), 2229 (w), 1724 (m), 1254 (m), 1142 (vs). **HRMS** (ESI) calcd for C$_{19}$H$_{26}$NO$_3$ [M+H$^+$]: 316.1907, found: 316.1893
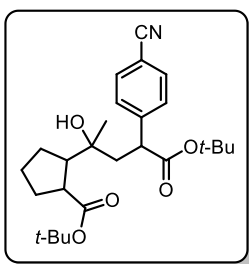

***tert*-Butyl 2-(5-(*tert*-butoxy)-4-(4-cyanophenyl)-2-hydroxy-5-oxopentan-2-yl) cyclopentane-1-carboxylate, 4.76** (0.033 g, 15%) was prepared according to General Procedure A. The diastereomeric ratio was determined to be 1.5:1.2:1 via ^{1}H NMR. The desired compound was obtained a colorless oil. **^{1}H NMR** (CDCl$_3$, 500 MHz) δ ppm 7.60-7.58 (m, 2H), 7.42-7.40 (m, 2H), 3.91 and 3.81 and 3.77 (dd, *J* = 9.6, 3.0 Hz, 1H), 2.75 and 2.67 (q, *J* = 7.8 Hz, 1H), 2.54-2.33 (m, 3H), 1.85-1.68 (m, 3H), 1.66-1.57 (m, 3H), 1.422 and 1.418 and 1.414 (s, 9H), 1.36 (s, 9H), 1.25 (br s, 1H), 1.18 and 1.090 and 1.086 (s, 3H). **^{13}C NMR** (CDCl$_3$,

125 MHz) δ ppm 177.1, 176.9, 176.8, 173.4, 173.2, 173.1, 147.0, 146.7, 146.6, 132.7, 132.6, 129.5, 128.9, 128.8, 128.7, 119.10, 119.06, 119.01, 111.2, 111.1, 111.0, 81.64, 81.58, 81.46, 81.1, 81.0, 80.7, 74.0, 73.8, 73.5, 54.9, 54.0, 53.0, 48.54, 48.52, 48.1, 46.18, 46.16, 46.10, 45.8, 45.3, 42.3, 32.0, 31.6, 31.4, 30.6, 30.0, 29.3, 29.0, 28.7, 28.3, 28.1, 26.4, 26.2, 26.0. **FT-IR** (cm^{-1}, neat, ATR) 3379 (br), 2975 (w), 2229 (w), 1721 (m), 1624 (m), 1142 (s). **HRMS** (ESI) calcd for C$_{26}$H$_{37}$NO$_5$Na [M+Na$^+$]: 466.2569, found: 466.2573
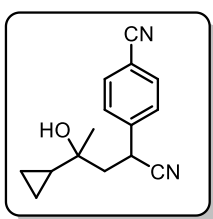
**4-(1-cyano-3-cyclopropyl-3-hydroxybutyl)benzonitrile, 4.77** (0.035 g, 29%) was prepared according to General Procedure A. The diastereomeric ratio was determined to be 1:1 via ^{1}H NMR. The desired compound was obtained a colorless oil. **^{1}H NMR** (CDCl$_3$, 500 MHz) δ ppm 7.68 (d, J = 8.1 Hz, 2H), 7.50 (dd, J = 8.3, 2.7 Hz, 1H), 4.24 and 4.19 (dd, J = 10.2, 3.1 Hz, 1H), 2.35 and 2.31 (dd, J = 14.4, 10.0 Hz, 1H), 1.93 (dt, J = 14.4, 2.8 Hz, 1H), 1.37 and 1.35 (br s, 1H), 1.33 and 1.20 (s, 3H), 1.06-0.87 (m, 1H), 0.60-0.30 (m, 4H). **^{13}C NMR** (CDCl$_3$, 125 MHz) δ ppm 143.1, 142.9, 133.2, 128.5, 128.4, 121.3, 121.2, 118.4, 112.3, 70.4, 70.3, 49.4, 49.0, 32.53, 32.51, 27.5, 27.0, 1.9, 1.1, 0.8. **FT-IR** (cm^{-1}, neat, ATR) 3479 (br), 3006 (w), 2230 (m), 1051 (m). **HRMS** (ESI) calcd for C$_{15}$H$_{16}$N$_2$O [M$^+$]: 240.1263, found: 240.1269
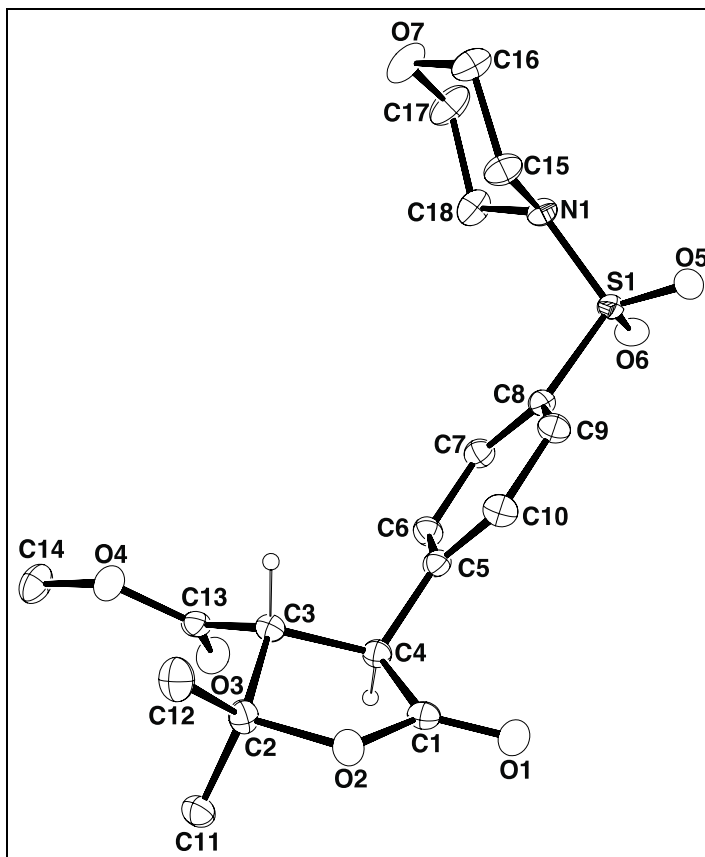
4.6.7. X-ray Structure Determination of 4.44
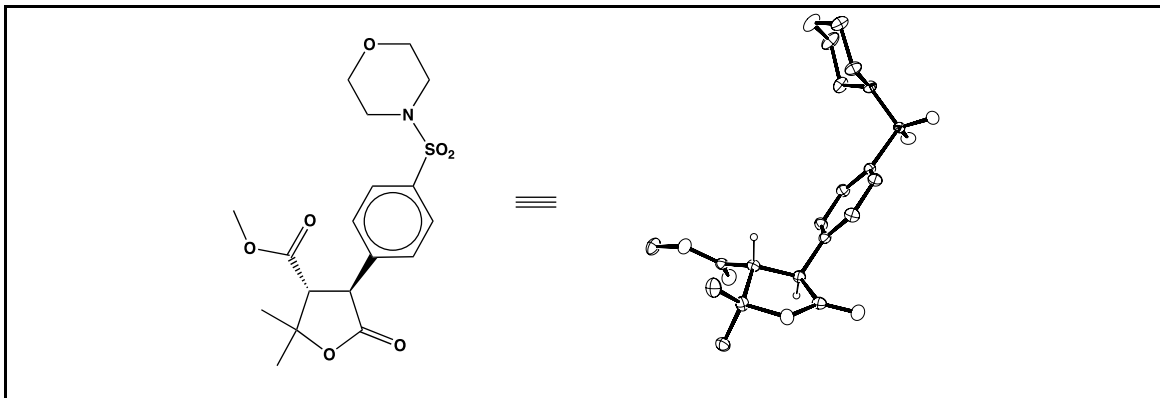
Compound **4.44**, $C_{18}H_{23}NO_7S$, crystallizes in the triclinic space group $P\bar{1}$ with a=8.09480(10)Å, b=9.43630(10)Å, c=12.9539(2)Å, α=83.4470(10)°, β=71.8420(10)°, γ=89.2520(10)°, V=933.80(2)Å^3, Z=2, and d_{calc}=1.413 g/cm^3. X-ray intensity data were collected on a Rigaku XtaLAB Synergy-S diffractometer equipped with an HPC area detector (HyPix-6000HE) and employing confocal multilayer optic-monochromated Cu-Kα radiation (λ=1.54184 Å) at a temperature of 100K. Preliminary indexing was performed from a series of sixty 0.5° rotation frames with exposures of 0.25 seconds for θ = ±49.017° and 1 second for θ = 105.75°. A total of 6594 frames (43 runs) were collected employing ω scans with a crystal to detector distance of 31.6 mm, rotation widths of 0.5° and exposures of 0.05 seconds for θ = ±49.267° and 0.12 seconds for θ = 105.75° and -84.25°.

Rotation frames were integrated using CrysAlisPro, producing a listing of unaveraged F^2 and $\sigma(F^2)$ values. A total of 23403 reflections were measured over the ranges $7.23 \leq 2\theta \leq 149.002°$, $-10 \leq h \leq 10$, $-10 \leq k \leq 11$, $-16 \leq l \leq 16$ yielding 3776 unique reflections (R_{int} = 0.0575). The intensity data were corrected for Lorentz and polarization effects and for absorption using SCALE3 ABSPACK (minimum and maximum transmission 0.5544, 1.0000). The structure was solved by direct methods - ShelXT. Refinement was by full-matrix least squares based on F^2 using SHELXL-2018. All reflections were used during refinement. The weighting scheme used was w=1/[$\sigma^2(F_o^2$)+ (0.0466P)^2 + 0.4863P] where P = (F_o^2 + 2F_c^2)/3. Non-

hydrogen atoms were refined anisotropically and hydrogen atoms were refined using a riding model. Refinement converged to R1=0.0352 and wR2=0.0913 for 3622 observed reflections for which F > 4σ(F) and R1=0.0361 and wR2=0.0921 and GOF =1.038 for all 3776 unique, non-zero reflections and 247 variables. The maximum Δ/σ in the final cycle of least squares was 0.001 and the two most prominent peaks in the final difference Fourier were +0.26 and -0.49 e/Å^3.

ORTEP drawing of the title compound with 50% thermal ellipsoids.

Table 4.10. Summary of Structure Determination of Compound **4.44**

Empirical formula	$C_{18}H_{23}NO_7S$
Formula weight	397.43

Diffractometer	Rigaku XtaLAB Synergy-S (HyPix-6000HE)
Temperature/K	100
Crystal system	triclinic
Space group	$P\bar{1}$
a	8.09480(10)Å
b	9.43630(10)Å
c	12.9539(2)Å
α	83.4470(10)°
β	71.8420(10)°
γ	89.2520(10)°
Volume	933.80(2)Å^3
Z	2
d$_{calc}$	1.413 g/cm^3
μ	1.907 mm^{-1}
F(000)	420.0
Crystal size, mm	$0.26 \times 0.23 \times 0.06$
2θ range for data collection	7.23 - 149.002°
Index ranges	$-10 \leq h \leq 10, -10 \leq k \leq 11, -16 \leq l \leq 16$
Reflections collected	23403
Independent reflections	3776[R(int) = 0.0575]
Data/restraints/parameters	3776/0/247
Goodness-of-fit on F^2	1.038
Final R indexes [I>=2σ (I)]	$R_1 = 0.0352$, $wR_2 = 0.0913$

Final R indexes [all data] $R_1 = 0.0361$, $wR_2 = 0.0921$

Largest diff. peak/hole   0.26/-0.49 eÅ^{-3}

Table 4.11. Refined Positional Parameters for Compound **4.44**

Atom	x	y	z	U(eq)
S1	0.86280(4)	0.77601(3)	0.26642(2)	0.01612(11)
O1	0.09718(13)	0.77736(11)	0.67791(8)	0.0208(2)
O2	0.12196(12)	0.69590(11)	0.84052(8)	0.0189(2)
O3	0.56226(13)	0.95969(10)	0.82922(8)	0.0216(2)
O4	0.61034(13)	0.75102(10)	0.91647(8)	0.0200(2)
O5	0.77918(13)	0.68290(12)	0.21727(8)	0.0230(2)
O6	0.91496(13)	0.91789(11)	0.21441(8)	0.0224(2)
O7	1.32316(14)	0.56074(12)	0.32233(10)	0.0283(3)
N1	1.03833(14)	0.69704(12)	0.27690(9)	0.0165(2)
C1	0.18259(17)	0.76641(14)	0.73925(11)	0.0161(3)
C2	0.24439(17)	0.70522(15)	0.90320(11)	0.0171(3)
C3	0.41979(17)	0.74440(14)	0.81211(10)	0.0148(3)
C4	0.36558(17)	0.82541(14)	0.71917(10)	0.0150(3)
C5	0.48997(17)	0.81144(14)	0.60649(11)	0.0154(3)
C6	0.63072(18)	0.90746(15)	0.56156(11)	0.0176(3)
C7	0.74685(17)	0.89683(15)	0.45837(11)	0.0177(3)
C8	0.72188(17)	0.78857(14)	0.40005(11)	0.0157(3)

304

C9	0.58452(18)	0.69008(15)	0.44422(11)	0.0181(3)
C10	0.46939(18)	0.70264(15)	0.54742(11)	0.0188(3)
C11	0.17981(18)	0.82079(16)	0.97756(11)	0.0209(3)
C12	0.2456(2)	0.55983(16)	0.96569(12)	0.0234(3)
C13	0.53877(17)	0.83201(14)	0.85132(11)	0.0161(3)
C14	0.7173(2)	0.82823(16)	0.96390(13)	0.0245(3)
C15	1.01746(18)	0.55025(15)	0.33226(13)	0.0215(3)
C16	1.19292(19)	0.47995(16)	0.30007(14)	0.0249(3)
C17	1.3396(2)	0.70119(17)	0.26490(15)	0.0291(4)
C18	1.17085(19)	0.77995(16)	0.30134(13)	0.0226(3)

Table 4.12. Positional Parameters for Hydrogens in Compound **4.44**

Atom	*x*	*y*	*z*	U(eq)
H3	0.477903	0.656801	0.787852	0.018
H4	0.357815	0.926747	0.729789	0.018
H6	0.646789	0.979338	0.601253	0.021
H7	0.840094	0.961249	0.428637	0.021
H9	0.570085	0.616921	0.405166	0.022
H10	0.377166	0.637314	0.577447	0.023
H11a	0.181085	0.910419	0.933987	0.031
H11b	0.254191	0.827908	1.021858	0.031
H11c	0.063286	0.797177	1.023878	0.031

H12a	0.134125	0.539482	1.019717	0.035
H12b	0.333722	0.559096	1.001093	0.035
H12c	0.269875	0.488665	0.915928	0.035
H14a	0.808903	0.879658	0.906496	0.037
H14b	0.766764	0.761936	1.007333	0.037
H14c	0.646985	0.894143	1.009241	0.037
H15a	0.934181	0.497165	0.310743	0.026
H15b	0.974644	0.551477	0.410915	0.026
H16a	1.182519	0.385333	0.339966	0.03
H16b	1.228225	0.469556	0.222621	0.03
H17a	1.371284	0.694889	0.186941	0.035
H17b	1.431499	0.753928	0.278273	0.035
H18a	1.138125	0.787847	0.379108	0.027
H18b	1.183475	0.875218	0.262291	0.027

Table 4.13. Refined Thermal Parameters (U's) for Compound **4.44**

Atom	U_{11}	U_{22}	U_{33}	U_{23}	U_{13}	U_{12}
S1	0.01505(17)	0.01998(18)	0.01262(17)	-0.00225(12)	-0.00332(12)	0.00475(12)
O1	0.0189(5)	0.0236(5)	0.0215(5)	-0.0018(4)	-0.0090(4)	-0.0001(4)
O2	0.0157(5)	0.0242(5)	0.0160(5)	0.0002(4)	-0.0042(4)	-0.0048(4)
O3	0.0237(5)	0.0168(5)	0.0250(5)	0.0010(4)	-0.0096(4)	-0.0029(4)
O4	0.0217(5)	0.0178(5)	0.0241(5)	-0.0025(4)	-0.0122(4)	0.0006(4)

O5	0.0183(5)	0.0335(6)	0.0196(5)	-0.0102(4)	-0.0073(4)	0.0052(4)
O6	0.0231(5)	0.0226(5)	0.0165(5)	0.0027(4)	-0.0009(4)	0.0066(4)
O7	0.0219(5)	0.0240(6)	0.0420(7)	0.0055(5)	-0.0172(5)	0.0005(4)
N1	0.0140(5)	0.0157(6)	0.0192(6)	-0.0009(4)	-0.0046(4)	0.0006(4)
C1	0.0160(6)	0.0141(6)	0.0167(6)	-0.0024(5)	-0.0027(5)	0.0013(5)
C2	0.0153(6)	0.0203(7)	0.0155(6)	-0.0009(5)	-0.0050(5)	-0.0034(5)
C3	0.0149(6)	0.0143(6)	0.0143(6)	-0.0019(5)	-0.0030(5)	0.0003(5)
C4	0.0151(6)	0.0144(6)	0.0152(6)	-0.0019(5)	-0.0041(5)	0.0005(5)
C5	0.0146(6)	0.0163(6)	0.0146(6)	0.0002(5)	-0.0041(5)	0.0027(5)
C6	0.0182(6)	0.0177(7)	0.0172(6)	-0.0040(5)	-0.0053(5)	-0.0001(5)
C7	0.0148(6)	0.0185(7)	0.0184(6)	-0.0010(5)	-0.0037(5)	-0.0008(5)
C8	0.0158(6)	0.0172(6)	0.0139(6)	-0.0017(5)	-0.0044(5)	0.0038(5)
C9	0.0193(7)	0.0159(7)	0.0190(7)	-0.0040(5)	-0.0050(5)	0.0011(5)
C10	0.0183(6)	0.0168(7)	0.0192(7)	-0.0010(5)	-0.0031(5)	-0.0021(5)
C11	0.0173(7)	0.0275(7)	0.0163(6)	-0.0041(5)	-0.0026(5)	0.0006(5)
C12	0.0268(8)	0.0216(7)	0.0206(7)	0.0045(6)	-0.0076(6)	-0.0060(6)
C13	0.0139(6)	0.0184(7)	0.0139(6)	-0.0012(5)	-0.0015(5)	0.0023(5)
C14	0.0252(7)	0.0223(7)	0.0320(8)	-0.0032(6)	-0.0174(6)	-0.0006(6)
C15	0.0182(7)	0.0158(7)	0.0290(7)	0.0006(5)	-0.0062(6)	0.0006(5)
C16	0.0206(7)	0.0195(7)	0.0347(8)	-0.0013(6)	-0.0096(6)	0.0038(6)
C17	0.0179(7)	0.0257(8)	0.0432(9)	0.0077(7)	-0.0127(7)	-0.0033(6)
C18	0.0211(7)	0.0181(7)	0.0302(8)	0.0014(6)	-0.0116(6)	-0.0034(5)

Table 4.14. Bond Distances in Compound **4.44**, (Å)

S1-O5	1.4308(11)	S1-O6	1.4340(10)	S1-N1	1.6316(11)
S1-C8	1.7676(13)	O1-C1	1.2008(17)	O2-C1	1.3463(16)
O2-C2	1.4728(16)	O3-C13	1.2095(17)	O4-C13	1.3334(17)
O4-C14	1.4521(17)	O7-C16	1.4270(18)	O7-C17	1.4302(18)
N1-C15	1.4715(17)	N1-C18	1.4673(18)	C1-C4	1.5232(18)
C2-C3	1.5540(18)	C2-C11	1.5170(19)	C2-C12	1.5129(19)
C3-C4	1.5287(18)	C3-C13	1.5134(18)	C4-C5	1.5120(18)
C5-C6	1.3968(19)	C5-C10	1.3895(19)	C6-C7	1.3877(19)
C7-C8	1.3898(19)	C8-C9	1.3916(19)	C9-C10	1.3880(19)
C15-C16	1.517(2)	C17-C18	1.514(2)		

Table 4.15. Bond Angles in Compound **4.44**, (°)

O5-S1-O6	119.85(6)	O5-S1-N1	106.76(6)	O5-S1-C8	107.09(6)
O6-S1-N1	106.66(6)	O6-S1-C8	108.06(6)	N1-S1-C8	107.93(6)
C1-O2-C2	112.02(10)	C13-O4-C14	114.91(11)	C16-O7-C17	110.12(11)
C15-N1-S1	117.09(9)	C18-N1-S1	118.96(9)	C18-N1-C15	112.37(11)
O1-C1-O2	121.80(12)	O1-C1-C4	128.05(12)	O2-C1-C4	110.16(11)
O2-C2-C3	102.76(10)	O2-C2-C11	106.89(11)	O2-C2-C12	107.30(11)
C11-C2-C3	113.65(11)	C12-C2-C3	112.51(12)	C12-C2-C11	112.84(12)
C4-C3-C2	103.81(10)	C13-C3-C2	111.83(10)	C13-C3-C4	112.82(11)
C1-C4-C3	102.88(10)	C5-C4-C1	114.59(11)	C5-C4-C3	113.95(11)

C6-C5-C4	119.64(12)	C10-C5-C4	121.24(12)	C10-C5-C6	119.11(12)
C7-C6-C5	120.75(13)	C6-C7-C8	119.08(12)	C7-C8-S1	120.20(10)
C7-C8-C9	121.08(12)	C9-C8-S1	118.71(10)	C10-C9-C8	119.02(13)
C9-C10-C5	120.93(13)	O3-C13-O4	124.16(13)	O3-C13-C3	124.55(12)
O4-C13-C3	111.26(11)	N1-C15-C16	108.46(11)	O7-C16-C15	111.95(12)
O7-C17-C18	110.95(12)	N1-C18-C17	106.90(12)		

4.6.8. HAT-DCF Control Experiments

Using the same conditions as described in **General Optimization Procedure** a series of control experiments were performed to confirm the role of benzophenone **1** as the active HAT agent and rule out the action of bromide radicals in the mechanism of DCF product formation.

Control Experiment A & B: Using **General Optimization Procedure** with the following modifications: Benzophenone **1** was omitted. Reaction irradiated with 390 nm Kessil Lamp (A) or using twelve 300 nm Rayonet bulb (B).
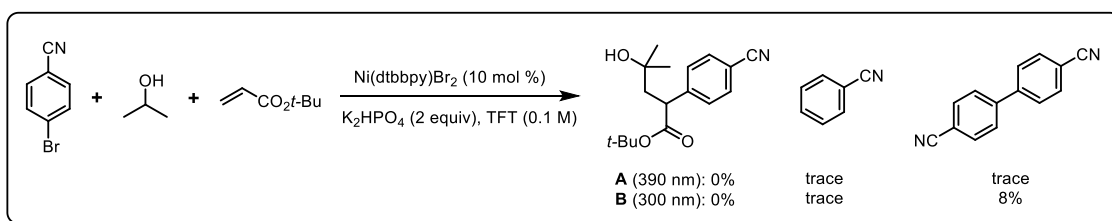
Figure 4.18. Confirming benzophenone catalyst as HAT agent

Control Experiment C: Using **General Optimization Procedure** with the following

modifications: Using 4-iodobenzonitrile and Ni(dtbppy)(NO$_3$)$_2$. Formation of the desired product

in the absence of any bromide source and considering endothermic nature of iodide radical HAT indicates that halogen radicals do not participate in DCF product formation.

HAT-DCF Competition Experiments

General Procedure for Hydroxylation Competition Reactions: To a 4 mL reaction vial with a stir bar was added Ni(dtbbpy)Br$_2$ (0.005 g, 0.01 mmol, 10 mol %), and benzophenone catalyst (0.005 g, 0.02 mmol, 20 mol %). The vial was capped and vacuum filled under argon (x3). A sparged soln of C-H radical precursor/TFT (1:1, 1 mL) was added via syringe to the reaction vial followed by a 1:1 ratio of both alkenes (0.20 mmol each, 2 equiv each). Irradiation was performed with a Kessil® PR160 390 nm lamp at 1.0" from the surface of the reaction vial. The vial was cooled with two fans (Delta compact brushless DC12V fan and household clip fan, see image below) to maintain the temperature on the surface of the vial between 25-34 ºC (measured using Fisherbrand® traceable type-K thermometer). Reactions were carried out to ~25% conversion for accurate measurement of product distribution. The solvent was removed, and the reaction analyzed via ^{1}H NMR using trimethoxybenzene as an internal standard.

General Procedure for Hydroxylation Competition reactions: To a 4 mL reaction vial with a stir bar was added 4-bromobenzonitrile (0.018 g, 0.10 mmol, 1.0 equiv), K$_2$HPO$_4$ (0.035 g, 0.20 mmol, 2.0 equiv), Ni(dtbbpy)Br$_2$ (0.005 g, 0.01 mmol, 10 mol %), and benzophenone catalyst (0.005 g, 0.02 mmol, 20 mol %). The vial was capped and vacuum filled under argon (x3). A sparged solution of C-H radical precursor/TFT (1:1, 1 mL) was added via syringe to the reaction vial followed by the alkene (0.20 mmol, 2 equiv). Irradiation was performed with a Kessil® PR160 390 nm lamp at 1.0" from the surface of the reaction vial. The vial was cooled with two

310

fans (Delta compact brushless DC12V fan and household clip fan, see image below) to maintain the temperature on the surface of the vial between 25-34 ºC (measure using Fisherbrand® traceable type-K thermometer). After 24 h of irradiation the reaction soln was passed through a short plug of Celite/silica gel. The solvent was removed, and the reaction was analyzed via ^{1}H NMR using trimethoxybenzene as an internal standard.

4.7. References

1. Campbell, M. W.; Compton, J. S.; Kelly, C. B.; Molander, G. A. Three-Component Olefin Dicarbofunctionalization Enabled by Nickel/Photoredox Dual Catalysis. *J. Am. Chem. Soc.,* **2019**, *141*, 20069-20078.

2. Guo, L.; Yuan, M. B.; Zhang, Y. Y.; Wang, F.; Zhu, S. Q.; Gutierrez, O.; Chu, L. L. General Method for Enantioselective Three-Component Carboarylation of Alkenes Enabled by Visible-Light Dual Photoredox/Nickel Catalysis. *J. Am. Chem. Soc.,* **2020**, *142*, 20390-20399.

3. Guo, L.; Tu, H. Y.; Zhu, S. Q.; Chu, L. L. Selective, Intermolecular Alkylarylation of Alkenes via Photoredox/Nickel Dual Catalysis. *Organic Letters* **2019**, *21*, 4771-4776.

4. Garcia-Dominguez, A.; Mondal, R.; Nevado, C. Dual Photoredox/Nickel-Catalyzed Three-Component Carbofunctionalization of Alkenes. *Angew. Chem. Int. Ed.,* **2019**, *58*, 12286-12290.

5. Sun, S. Z.; Duan, Y. Y.; Mega, R. S.; Somerville, R. J.; Martin, R. Site-Selective 1,2-Dicarbofunctionalization of Vinyl Boronates through Dual Catalysis. *Angew. Chem. Int. Ed.,* **2020**, *59*, 4370-4374.

6. Zheng, S. L.; Chen, Z. M.; Hu, Y. Y.; Xi, X. X.; Liao, Z. X.; Li, W. R.; Yuan, W. M. Selective 1,2-Aryl-Aminoalkylation of Alkenes Enabled by Metallaphotoredox Catalysis. *Angew. Chem. Int. Ed.,* **2020**, *59*, 17910-17916.

7. Mega, R. S.; Duong, V. K.; Noble, A.; Aggarwal, V. K. Decarboxylative Conjunctive Cross-coupling of Vinyl Boronic Esters using Metallaphotoredox Catalysis. *Angew. Chem. Int. Ed.,* **2020**, *59*, 4375-4379.

8. de Montellano, P. R. O. Hydrocarbon Hydroxylation by Cytochrome P450 Enzymes. *Chem. Rev.,* **2010**, *110*, 932-948.

9. Capaldo, L.; Ravelli, D. Hydrogen Atom Transfer (HAT): A Versatile Strategy for Substrate Activation in Photocatalyzed Organic Synthesis. *Eur. J. Org. Chem.,* **2017**, *15*, 2056-2071.

10. Giese, B. Formation of cc bonds by addition of free-radicals to alkenes. *Angew. Chem.,* **1983**, *22*, 753-764.

11. Shaw, M. H.; Shurtleff, V. W.; Terrett, J. A.; Cuthbertson, J. D.; MacMillan, D. W. C. Native functionality in triple catalytic cross-coupling: sp(3) C-H bonds as latent nucleophiles. *Science* **2016**, *352*, 1304-1308.

12. Jeffrey, J. L.; Terrett, J. A.; MacMillan, D. W. C. O-H hydrogen bonding promotes H-atom transfer from alpha C-H bonds for C-alkylation of alcohols. *Science* **2015**, *349*, 1532-1536.

13. Heitz, D. R.; Tellis, J. C.; Molander, G. A. Photochemical Nickel-Catalyzed C-H Arylation: Synthetic Scope and Mechanistic Investigations. *J. Am. Chem. Soc.,* **2016**, *138*, 12715-12718.

14. Shields, B. J.; Doyle, A. G. Direct C(sp(3))-H Cross Coupling Enabled by Catalytic Generation of Chlorine Radicals. *J. Am. Chem. Soc.,* **2016**, *138*, 12719-12722.

15. Capaldo, L.; Ravelli, D.; Fagnoni, M. Direct Photocatalyzed Hydrogen Atom Transfer (HAT) for Aliphatic C–H Bonds Elaboration. *Chem. Rev.,* **2021**, *122*, 1875–1924.

16. Fan, X. Z.; Rong, J. W.; Wu, H. L.; Zhou, Q.; Deng, H. P.; Da Tan, J.; Xue, C. W.; Wu, L. Z.; Tao, H. R.; Wu, J. Eosin Y as a Direct Hydrogen-Atom Transfer Photocatalyst for the Functionalization of C-H Bonds. *Angew. Chem. Int. Ed.,* **2018**, *57*, 8514-8518.

17. Protti, S.; Ravelli, D.; Fagnoni, M.; Albini, A. Solar light-driven photocatalyzed alkylations. Chemistry on the window ledge. *Chem. Commun.,* **2009**, *47*, 7351-7353.

18. Sarver, P. J.; Bacauanu, V.; Schultz, D. M.; DiRocco, D. A.; Lam, Y. H.; Sherer, E. C.; MacMillan, D. W. C. The merger of decatungstate and copper catalysis to enable aliphatic C(sp(3))-H trifluoromethylation. *Nat. Chem.,* **2020**, *12,* 459-465.

19. Dorman, G.; Nakannura, H.; Pulsipher, A.; Prestwich, G. D. The Life of Pi Star: Exploring the Exciting and Forbidden Worlds of the Benzophenone Photophore. *Chem. Rev.,* **2016**, *116*, 15284-15398.

20. Ferro-Costas, D.; Pendas, A. M.; Gonzalez, L.; Mosquera, R. A. Beyond the molecular orbital conception of electronically excited states through the quantum theory of atoms in molecules. *Phys. Chem. Chem. Phys.,* **2014**, *16*, 9249-9258.

21. Campbell, M. W.; Yuan, M.; Polites, V. C.; Gutierrez, O.; Molander, G. A. Photochemical C–H Activation Enables Nickel-Catalyzed Olefin Dicarbofunctionalization. *J. Am. Chem. Soc.,* **2021**, *143*, 3901-3910.

22. Bolland, J. L.; Cooper, H. R. The photo-sensitized oxidation of ethanol. *Proc. R. Soc. A: Math. Phys. Eng. Sci.,* **1954**, *225*, 405-426.

23. Zhu, D. L.; Young, D. J.; Li, H. X. Carbonyl-Photoredox/Metal Dual Catalysis: Applications in Organic Synthesis. *Synthesis-Stuttgart* **2020**, *52*, 3493-3510.

24. Shen, Y. Y.; Gu, Y. T.; Martin, R. sp(3) C-H Arylation and Alkylation Enabled by the Synergy of Triplet Excited Ketones and Nickel Catalysts. *J. Am. Chem. Soc.,* **2018**, *140*, 12200-12209.

25. Dewanji, A.; Krach, P. E.; Rueping, M. The Dual Role of Benzophenone in Visible-Light/Nickel Photoredox-Catalyzed C-H Arylations: Hydrogen-Atom Transfer and Energy Transfer. *Angew. Chem. Int. Ed.,* **2019**, *58*, 3566-3570.

26. Viehe, H. G.; Janousek, Z.; Merenyi, R.; Stella, L. The captodative effect. *Acc. Chem. Res.,* **1985**, *18*, 148-154.

27. De Vleeschouwer, F.; Van Speybroeck, V.; Waroquier, M.; Geerlings, P.; De Proft, F. Electrophilicity and nucleophilicity index for radicals. *Org. Lett.* **2007**, *9*, 2721-2724.

28. Primer, D. N.; Molander, G. A. Enabling the Cross-Coupling of Tertiary Organoboron Nucleophiles through Radical-Mediated Alkyl Transfer. *J. Am. Chem. Soc.,* **2017**, *139*, 9847-9850.

29. Domingo, L. R.; Perez, P. Global and local reactivity indices for electrophilic/nucleophilic free radicals. *Org. Biomol. Chem.,* **2013**, *11*, 4350-4358.

30. Liakos, D. G.; Guo, Y.; Neese, F. Comprehensive Benchmark Results for the Domain Based Local Pair Natural Orbital Coupled Cluster Method (DLPNO-CCSD(T)) for Closed- and Open-Shell Systems. *J. Phys. Chem. A,* **2020**, *124*, 90-100.

31. Yuan, M. B.; Song, Z. H.; Badir, S. O.; Molander, G. A.; Gutierrez, O. On the Nature of C(sp(3))-C(sp(2)) Bond Formation in Nickel-Catalyzed Tertiary Radical Cross-Couplings: A Case Study of Ni/Photoredox Catalytic Cross-Coupling of Alkyl Radicals and Aryl Halides. *J. Am. Chem. Soc.,* **2020**, *142*, 7225-7234.

32. Gawlita, E.; Lantz, M.; Paneth, P.; Bell, A. F.; Tonge, P. J.; Anderson, V. E. H-bonding in alcohols is reflected in the C alpha-H bond strength: Variation of C-D vibrational frequency and fractionation factor. *J. Am. Chem. Soc.,* **2000**, *122*, 11660-11669.

33. Tian, Y. F.; Liu, Z. Q. H-Bonding-promoted radical addition of simple alcohols to unactivated alkenes. *Green Chem.,* **2017**, *19*, 5230-5235.

34. Duplais, C.; Bures, F.; Sapountzis, I.; Korn, T. J.; Cahiez, G.; Knochel, P. An efficient synthesis of diaryl ketones by iron-catalyzed arylation of aroyl cyanides. *Angew. Chem. Int. Ed.,* **2004**, *43*, 2968-2970.

35. Wang, Q.; Tang, X. Y.; Shi, M. Metal-Free Cross-Coupling of Arylboronic Acids and Derivatives with DAST-Type Reagents for Direct Access to Diverse Aromatic Sulfinamides and Sulfonamides. *Angew. Chem. Int. Ed.,* **2016**, *55*, 10811-10815.

36. Phelan, J. P.; Wiles, R. J.; Lang, S. B.; Kelly, C. B.; Molander, G. A. Rapid access to diverse, trifluoromethyl-substituted alkenes using complementary strategies. *Chem. Sci.,* **2018**, *9*, 3215-3220.

37. Csuk, R.; Dorr, P. Convenient oxidative debenzylation using dimethyldioxirane. *Tetrahedron,* **1994**, *50*, 9983-9988.

38. Lee, C. T.; Yang, W. T.; Parr, R. G. Development of the colle-salvetti correlation-energy formula into a functional of the electron-density. *Phys. Rev. B,* **1988**, *37*, 785-789.

39. Grimme, S.; Antony, J.; Ehrlich, S.; Krieg, H. A consistent and accurate ab initio parametrization of density functional dispersion correction (DFT-D) for the 94 elements H-Pu. *J. Chem. Phys.,* **2010**, *132,* 154104.

40. Weigend, F.; Ahlrichs, R. Balanced basis sets of split valence, triple zeta valence and quadruple zeta valence quality for H to Rn: Design and assessment of accuracy. *Phys. Chem. Chem. Phys.,* **2005**, *7*, 3297-3305.

41. Cossi, M.; Rega, N.; Scalmani, G.; Barone, V. Energies, structures, and electronic properties of molecules in solution with the C-PCM solvation model. *J. Comput. Chem.,* **2003**, *24*, 669-681.

42. *Gaussian 16, Revision C.01*; Gaussian Inc.: Wallingford, CT, 2019.

43. Hellweg, A.; Hattig, C.; Hofener, S.; Klopper, W. Optimized accurate auxiliary basis sets for RI-MP2 and RI-CC2 calculations for the atoms Rb to Rn. *Theor. Chem. Acc.,* **2007**, *117*, 587-597.

44. Neese, F. The ORCA program system. *Wiley Interdisciplinary Reviews-Computational Molecular Science* **2012**, *2* (1), 73-78.

45. *CYLview 1.0b*; Université de Sherbrooke, 2009.

46. Johnson, E. R.; Keinan, S.; Mori-Sanchez, P.; Contreras-Garcia, J.; Cohen, A. J.; Yang, W. T. Revealing Noncovalent Interactions. *J. Am. Chem. Soc.,* **2010**, *132*, 6498-6506.

47. Humphrey, W.; Dalke, A.; Schulten, K. VMD: Visual molecular dynamics. *J. Mol. Graph. Model.,* **1996**, *14*, 33-38.

**Chapter 5. Photochemical C–F Activation Enables Defluorinative Alkylation of
Trifluoroacetates and -Acetamides**

5.1. Introduction

Fluorinated motifs are arguably the most incongruous of all organic functional groups.[1] Though

they possess remarkably unique and desirable characteristics, fluorinated groups still remain one

of the most challenging to install and thus the type of structural motifs that can be accessed is

limited. Despite the pertinent synthetic challenges, a limited suite of fluorinated groups have been

extensively studied in medicinal chemistry. Such fluorinated motifs often exhibit improved

pharmacological/biochemical properties, among the most common of which are:[2]

1. Metabolic stability: replacing oxidatively labile C-H bonds, which decrease oral
   bioavailability, with inert C-F bonds.

2. Increased lipophilicity: the high electronegativity of fluorine causes a reversal in the
   dipole from C-H bonds, resulting in dramatic changes in log *P*.

3. Increased binding affinity: the unique van Der Waals radii and hydrogen bonding
   capabilities of fluorinated functional groups often increase the non-covalent interactions
   between a drug molecule and biological substrate.

Unfortunately, the suite of fluorinated motifs commonly integrated into pharmaceutical

molecules is mainly limited to aryl fluorides and trifluoromethylated arenes because only these

groups have well-established protocols for their installation.[3] The potential applications of alkyl

CF_2-R, CF_2-Y, CFH-R and CFH-Y groups are essentially unexplored because of the daunting

challenge of their synthesis, especially in late-stage functionalization strategies.[4,5] A select range

of methods for the incorporation of alkyl CF_2 and CFH groups have been developed, most of

which rely on harsh reaction conditions and specialized fluorinating reagents.[6] One of the most common methods is electrophilic fluorination of acidic C-H bonds with reagents such as Selectfluor[7] or *N*-fluorobenzenesulfonimide (NFSI).[8] Perhaps the most impressive example of this strategy is in the preparation of the ketolide antibiotic, solithromycin (**Figure 5.1A**).[9] Deprotonation of the acetoacetate starting material (**5.1**) via *tert*-butoxide followed by addition of Selectfluor yielded the tertiary alkyl fluoride intermediate **5.2**, which was taken on to complete the synthesis of the target structure (**5.3**). This acetoacetyl fluoride group was essential for the metabolic stability of this structure. An evident issue associated with this type of reactivity is its poor functional group tolerance, as the strong bases required to deprotonate weakly acidic C-H bonds are not compatible with most acidic and electrophilic groups. In an umpolung approach, diethylaminosulfur trifluoride (DAST)[10] is a nucleophilic fluorinating agent that can activate alcohols, aldehydes, and ketones for addition of fluoride to produce alkyl fluoride motifs. Though applicable in many syntheses, such aminosulfuranes are highly reactive and often facilitate undesired side reactions, as E1 and E2 pathways often predominate over fluoride-mediated substitution. Such nucleophilic fluorination protocols were used in the preparation of a fluoronucleoside, sofosbuvir (**5.7**), which is an FDA-approved hepatitis C RNA-polymerase inhibitor.[11] Conversion of tertiary alcohol **5.4** to alkyl fluoride **5.6** was accomplished via DAST. The isolated yield of **5.6** was particularly low because of the formation of a tertiary carbocation, which predominantly formed E1 elimination byproducts. In a similar manner, exposure of enolizable ketones (e.g., **5.8**) to DAST typically produces the desired *gem*-difluoromethylene (**5.9**) as the major product, but is often complicated by the formation of vinyl fluoride byproducts (**5.10** and **5.11**).[12] Overall, though several protocols exist for the preparation of alkyl fluoride motifs, the conditions employed are not broadly tolerant and often result in numerous side reactions and poor yield.
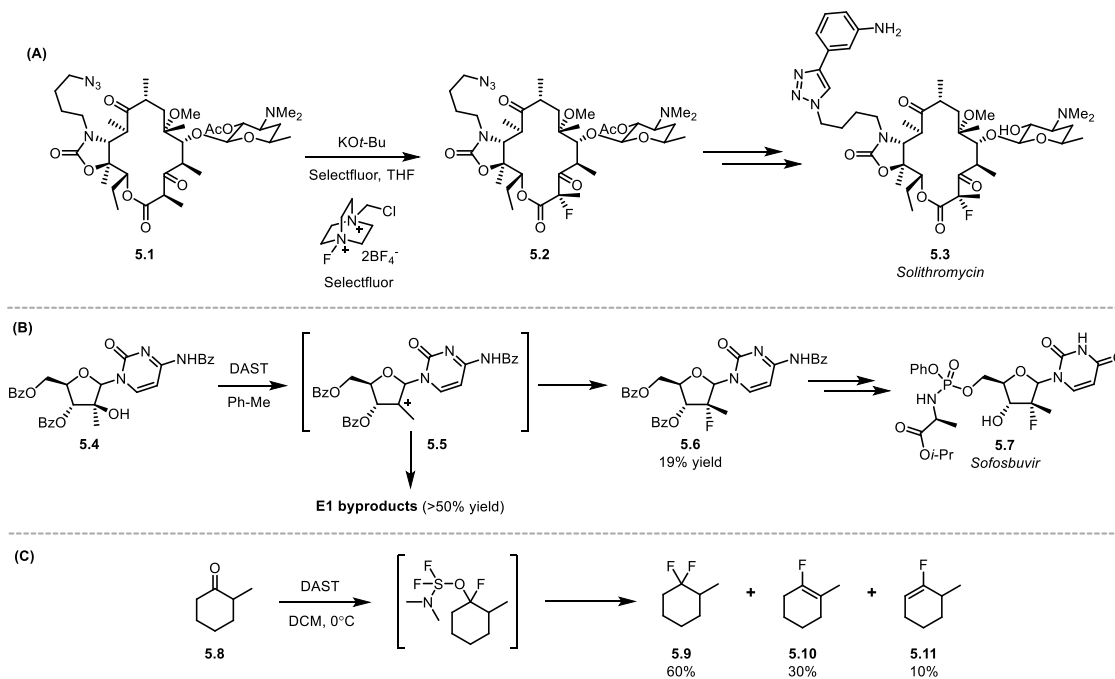
Figure 5.1. Established methods for preparation of -CF$_2$, -CFR and -CFH groups. (**A**) Electrophilic fluorination via Selectfluor in the preparation of Solithromycin. (**B**) Nucleophilic fluorination via DAST in the synthesis of Sofosbuvir. (**C**) Byproduct formation in the nucleophilic fluorination of an enolizable ketone.

The majority of strategies to access alkyl -CF$_2$, -CFR and -CFH motifs involve the fluorination of native functional groups.[13] However, the selective *defluorination* of a trifluoromethyl group remains an underexplored retrosynthetic approach. The selective functionalization of a single C−F bond in a trifluoromethyl group presents a significantly more attractive approach given the diverse array of readily available CF$_3$-containing structures, but also poses a formidable synthetic challenge. At a first approximation this mode of reactivity may appear unfeasible owing to the atypically strong nature of C-F bonds (BDE typically >130 kcal/mol),[14] making them resistant to homolysis or heterolysis. Despite this challenging characteristic, several early strategies accomplished global protodefluorination of trifluoromethylated arenes using stoichiometric reductants and strong Lewis acid activators,

oftentimes with low-valent transition metals.[15-18] Alternatively in the recent past, several strategies for the catalytic reduction of trifluoromethylated arenes to generate benzylic *gem*-difluoromethyl groups have accomplished both protodefluorination as well as defluorinative functionalization.[16-24] Though these reports serve as pioneering examples outlining fundamental mechanistic strategies for C-F bond activation, many pertinent limitations still exist. First, the challenging reduction potential of trifluoromethylated arenes limits the structural diversity to mainly electron-withdrawing aryl- and heteroaryl starting materials. Photoredox strategies offer a controlled kinetic profile in which only catalytic amounts of the reductant are present in the reaction, however, the high reduction potential of even electron-poor benzotrifluorides strictly limits functional group compatibility. Second, the benzylic *gem*-difluorides, though intrinsically valuable scaffolds, have minimal utility as synthetic intermediates, limiting the possibility for further elaboration to diverse chemical structures. Significantly more attractive functional groups are α,α-difluoro esters, which have been used extensively in the development of fluorinated scaffolds. The ester group serves as a versatile synthetic handle, offering a wide array of possible functional group interconversions and allowing the facile incorporation of *gem*-difluoromethylene groups into a limitless array of molecular architectures. The standard method for the retrosynthetic approach of C-CF$_2$ bond formation in α,α-difluoro esters utilizes a α,α-difluoro nucleophilic synthon with a carbon electrophile (Figure 5.2). Bromo- or iododifluoroacetates (**5.12**) are the most common precursors for the corresponding α,α-difluoro organometallic nucleophiles used in copper-mediated Michael addition (**5.12 → 5.13**),[17] Negishi coupling (**5.12 → 5.14**),[18] Reformatsky-type reactions (**5.12 → 5.14**)[19] and other modes of C-CF$_2$ bond formation.
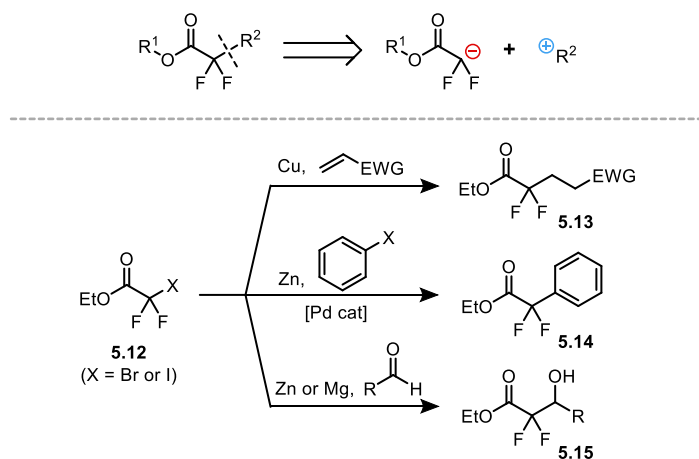
Figure 5.2. Two-electron processes for C-CF$_2$ bond formation in the preparation of α,α-difluoro esters.

In addition to these two-electron mechanisms, bromo- and iododifluoroacetates have also been used as radical precursors that undergo reductive dehalogenation to generate α,α-difluoro ester radicals via stoichiometric reducing metals as well as photoredox catalysis.[20-31] Though each of these serve as useful methods to access alkyl/aryl α,α-difluoro esters, the activation of a commodity, bench-stable starting material, such as ethyl trifluoroacetate ($0.06/mmol), has unquestionable advantages over bromo- and iododifluoroacetates ($2.58−7.15/mmol), which are significantly more expensive. This envisioned strategy could enable the use of trifluoroacetates as bifunctional lynchpins in the synthesis of complex CF$_2$-containing compounds (Figure 1). Following a defluorinative functionalization, the resulting α,α-difluoro ester/carboxylates would offer several potential downstream transformations, allowing chemists to construct highly decorated fluorine-containing molecular scaffolds (Figure 5.3).
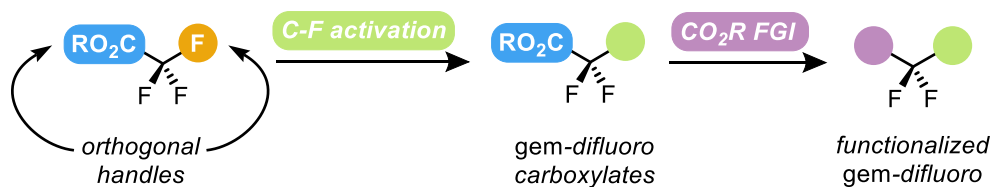
Figure 5.3. C-F functionalization enables the use of trifluoroacetates as bifunctional lynchpins.

321

This concept is not without precedent, as a defluorinative alkylation (DFA) of α-trifluoromethyl carbonyl compounds via boryl radical activation was recently disclosed by Wang and Houk.[21] The proposed mechanism for this transformation relies on a series of well-orchestrated HAT steps. Thermolysis of *tert*-butyl peroxide generates *tert*-butoxy radical, which engages in HAT with a pyridyl-ligated borane (**5.16**). This boryl radical is highly nucleophilic and can perform an inverse addition into an *N*-aryl trifluoroacetamide. This adduct (**5.18**) then undergoes a fragmentation step known as a spin-center shift (SCS). SCS are a subcategory of radical fragmentation/elimination reactions in which the donation of two electrons from a group adjacent to a radical center trigger the 1,2-translocation of the radical center with concerted heterolytic loss of a leaving group.[22] Computational studies of this mechanism suggested that the nitrogen lone pair facilitates the SCS elimination of fluoride promoted by intramolecular hydrogen bonding. The resulting *gem*-difluoro α-amido radical can undergo Giese addition onto activated styrene derivatives. Although novel, the harsh and potentially dangerous conditions required for radical generation (*tert*-butyl peroxide at 120 ℃ in MeCN) and the super-stiochiometric loading of the ligated-borane reductant render it intractable in multi-gram synthesis or late-stage functionalization of complex molecules.

[N] = 4-*N,N*-dimethylaminopyridine
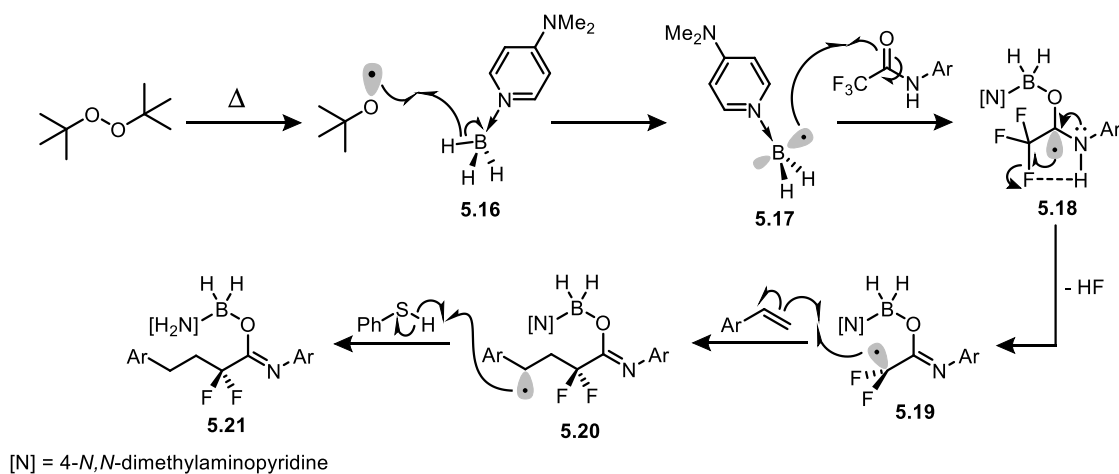
Figure 5.4. Proposed mechanism for DFA via boryl radical activation.

5.2. Initial Reaction Development

We reasoned that photocatalytic HAT may be able to provide an alternative mode of radical generation that would circumvent the harsh reaction conditions required to homolyze the peroxide radical initiator. Initial studies focused on diaryl ketones that serve as a modular, sustainable class of photoactive HAT agents to replace the peroxide radical precursor used in Wang and Houk's report.[23] In this protocol, photoexcitation of the diaryl ketone would access the ketyl diradical, which could engage the amine-ligated borane to access the key boryl radical, which would then proceed through a mechanism similar to Figure 5.4. Our model reaction was designed to achieve DFA of *N*-phenyl trifluoroacetamide and styrene, the standard substrates utilized in Wang and Houk's report. Optimization studies revealed that a large suite of diaryl ketone analogs were all competent HAT catalysts, among which xanthone was the most efficient and commercially available. Further studies revealed that the addition of mildly basic additives such as phosphate and bicarbonate salts improved reactivity, likely because of their ability to function as hydrogen bond acceptors, which assists in the SCS step as suggested by previous computations. Unfortunately, after significant optimization efforts, the reaction still displayed incomplete conversion of the trifluoroacetamide, even in the presence of excess styrene and DMAP-borane. Further increase of the loading of alkene and/or DMAP-borane did not result in complete conversion and was overall detrimental to the yield of the hydroalkylation product (**5.24**). Attempts to apply these conditions to other alkenes resulted in lower yields of the corresponding DFA products with a wide range of byproducts (Figure 5.5). Reaction with 2,3-dihydrofuran converted only half of the starting material and produced both the desired DFA (**5.27**) and analogous protodefluorinated (**5.28**) products. Surprisingly, allyl acetate produced significantly higher yields of the alkylated-protodefluorinated product (**5.31**) and an unexpected double alkylation product (**5.32**). Substituting a trifluoroacetate in place of the trifluoroacetamide

provided only minimal conversion to the desired product and yielded a significant amount of ester hydrolysis.

The incomplete conversion of the trifluoromethyl carbonyl starting materials suggested that the boryl radical addition and/or SCS were the problematic steps in this mechanism. According to calculations by Wang and Houk, the boryl radical addition and defluorinative SCS barriers were significantly high for both trifluoroacetamides and –acetates. We assumed that the elevated temperature used in the previous protocol might be critical for accessing these high energy transition states. Under the optimized conditions in Figure 5.5, increasing the reaction temperature did not assist in starting material conversion and resulted in the formation of additional byproducts. This result was not unreasonable, as excited state lifetimes and temperature typically have an inverse relationship, thus the increased temperature likely had a negative impact on the diaryl ketone HAT step.
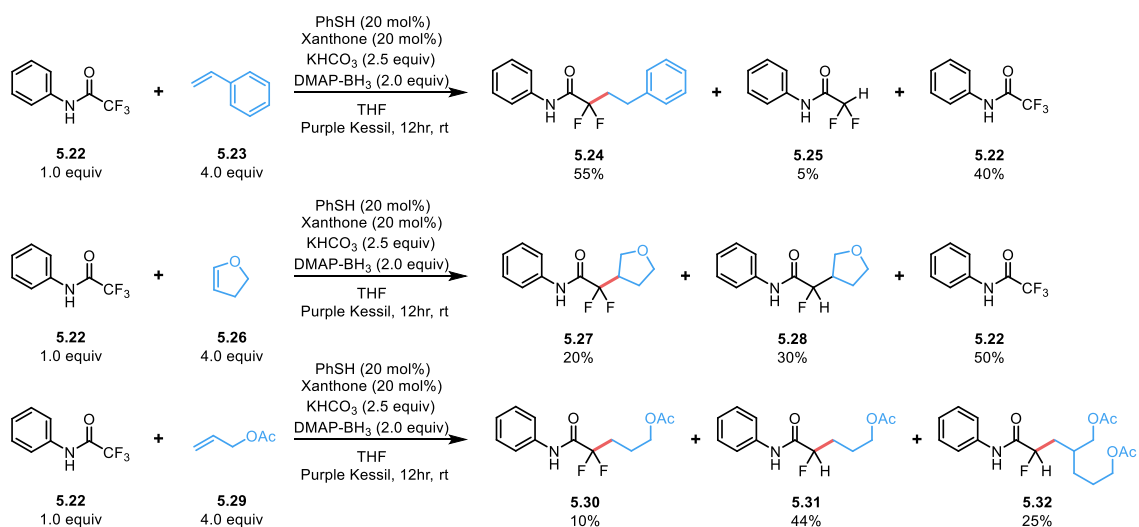
Figure 5.5. Product distribution for DFA of *N*-phenyl trifluoroacetamide via boryl radicals with various alkenes.

Considering the sluggish reactivity observed across a range of structures, we considered whether this mode of photocatalysis was amenable to this transformation. Assuming that the SCS

transition state was the highest barrier in our mechanism, we questioned if a higher energy analog of intermediate **5.18** could be accessed to increase the rate of defluorinative SCS. Preliminary studies by Janata and Giese demonstrated that SCS fragmentation is generally much faster for charged species than their neutral counterparts. Therefore, we reasoned that the corresponding radical anion, generated via single-electron reduction, would undergo a faster defluorinative SCS compared to the neutral intermediate (**5.33**), which was generated via boryl radical addition.

5.33   5.34   5.35   5.36

sluggish SCS, poor DFA yields   *efficient SCS, high DFA yields*
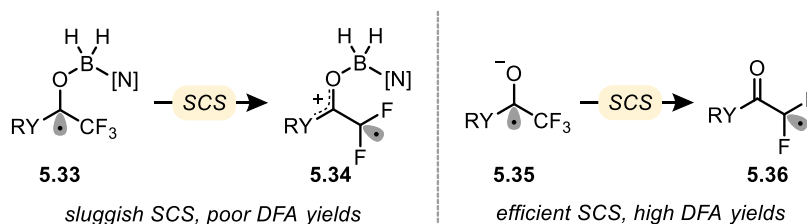
Figure 5.6. Novel approach for defluorinative SCS of trifluoroacetates and –acetamides.

Cyclic voltammetry studies revealed that the reduction potentials of ethyl trifluoroacetate (-2.0 V vs SCE in DMF) and *N*-aryl trifluoroacetamide (> -2.5 V vs SCE in DMF) were beyond the excited state reduction potential of most conventional photocatalysts. Recently, $CO_2^{\bullet-}$ has been identified as a potent reductant (-2.2 V vs SCE in DMF)[24] that can be easily accessed by engaging formate salts in HAT.[25] [26] [27] With this literature precedent it appeared that accessing $CO_2^{\bullet-}$ via formate salts would provide an effective mechanism for single electron reduction of trifluoroacetates to trigger defluorinative SCS. We elected to focus our initial exploration of $CO_2^{\bullet-}$ -mediated defluorinative alkylation focused on trifluoroacetates because of their lower reduction potential and more abundant commercial availability. Given its low cost and volatility, ethyl trifluoroacetate was used in excess, and the olefin served as limiting reagent. Initial attempts to access $CO_2^{\bullet-}$ via HAT with thiyl radicals generated via photocatalytic single electron oxidation as previously described[26] [28] only provided low yields of the desired DFA product and a complex mixture of byproducts. Given these poor results, it became clear that an entirely novel mechanism

would need to be conceived for the $CO_2^{\bullet-}$-mediated DFA of trifluoroacetates. We then envision a mechanism based on direct photochemical HAT via diaryl ketone catalysis (Figure 5.7). Excitation of a diaryl ketone (**5.I**) would access the triplet state diradical (**5.II**), which should readily engage a formate salt (**5.IV**) in a highly exothermic HAT step (formate BDE = 87 kcal/mol, O-H BDE in **5.III** ~ 100 kcal/mol).[14] The resulting $CO_2^{\bullet-}$ (**5.V**) could then perform single electron reduction of trifluoroacetate **5.VI**, producing radical anion **5.VII** and CO_2 as an innocuous byproduct. Radical anion **5.VII** would then undergo defluorinative SCS to access the key *gem*-difluoro radical (**5.VIII**), which would subsequently engage in Giese addition with an electron-rich alkene. Radical Giese adduct **5.IX** would then be quenched via HAT with a thiol (**5.XI**), yielding the DFA product (**5.X**). The concomitant thiyl radical (**5.XII**) would play a critical role in sustaining the reaction mechanism either by engaging in HAT with the formate (inducing a radical chain mechanism that had been previously observed in similar modes of catalysis) or by oxidizing **5.III**, closing the diaryl ketone catalytic cycle.
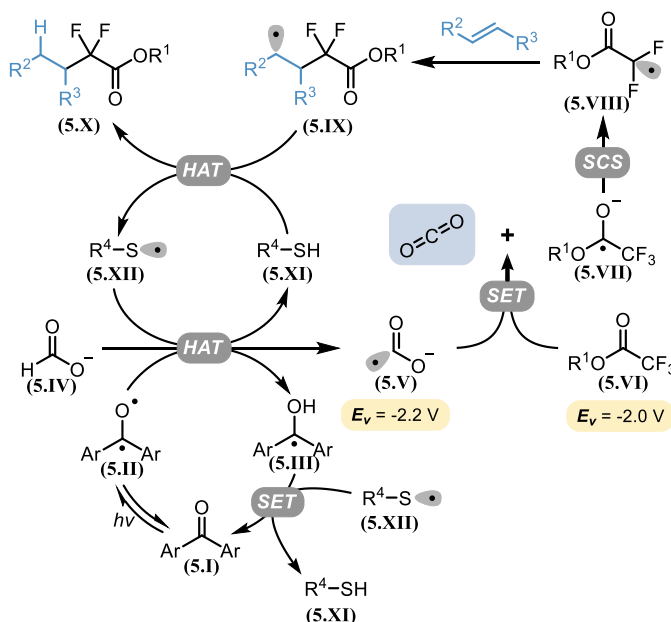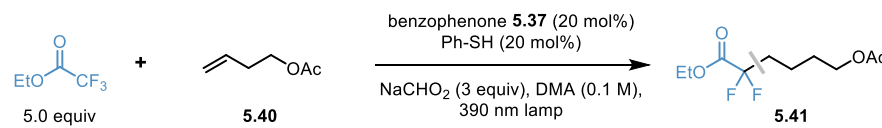
Figure 5.7. Proposed mechanism for diaryl ketone-catalyzed DFA.
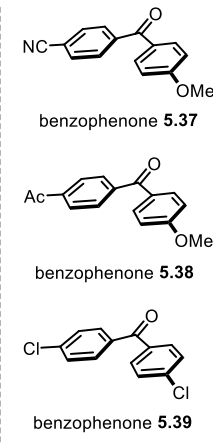
5.4. Results and Discussion

A variety of substituted benzophenones were indeed competent catalysts for this mode of reactivity with our previously developed diaryl ketone, producing the highest yield of the DFA product (Table 5.1, entries 1,3,4). In addition to improved reactivity, this HAT catalyst is able to tolerate a more diverse set of functional groups compared to typical photocatalysts. Consistent with literature precedent, this reaction functioned best in strongly polar, aprotic solvents such as DMSO and DMF. Further optimization revealed that the structure of the thiol had a significant impact on the DFA yield. Assuming that the thiol engages in HAT with the Giese adduct and subsequently with the formate salt, the optimal bond dissociation enthalpy should, in theory, fall between that of the newly formed C−H bond in the product (97−99 kcal/mol) and the formyl C−H bond (88 kcal/mol).[14] A significant decrease in yield was observed when using aryl- (S−H BDE = ∼80 kcal/mol) rather than alkyl thiols (S−H BDE = 87−89 kcal/mol), likely because aryl S−H bond dissociation enthalpies are lower than that of the formyl C−H bond, resulting in inefficient HAT.[14] Sodium outperformed any other alkaline earth metal or organic counterions of the formate salt. Control studies confirmed the necessity of diaryl ketone catalyst, thiol, and light for efficient reactivity (see 5.5 Experimental Section). Additional experiments revealed that the loading of benzophenone **5.37** could be dropped to as low as 1 mol % with only a minimal decrease in yield given the same irradiation time, enabling practical DFA on multigram scale (see 5.5 Experimental Section). Ultimately, these studies demonstrate that this novel strategy of diaryl ketone-mediated HAT is uniquely suited to facilitate the reduction of trifluoroacetates via $CO_2^{\bullet-}$ in the desired DFA.

Table 5.1. Optimization of diaryl ketone-catalyzed DFA

Entry	Variation of Conditions	GCMS P/IS Ratio
1	none	2.77
2	CzIPN instead of benzophenone **5.37**	0.83
3	benzophenone **5.38** instead of **5.37**	2.44
4	benzophenone **5.39** instead of **5.37**	1.52
5	DMSO instead of DMA	4.26
6	DMF instead of DMA	5.22
7	Mes-SH instead of Ph-SH (in DMF)	0.50
8	Cy-SH instead of Ph-SH (in DMF)	6.30
9	LiCHO$_2$ instead of NaCHO$_2$ (in DMF)	2.02
10	KCHO$_2$ instead of NaCHO$_2$ (in DMF)	0.96

CzIPN = 2,4,5,6-tetra(9H-carbazol-9-yl)isophthalonitrile

In the exploration of the scope of alkenes in the DFA of ethyl trifluoroacetate, electron-rich and electron-neutral alkenes were assumed to fare best in the Giese addition with the highly electrophilic *gem*-difluoro radical (**5.VIII**). A wide variety of unactivated, terminally unsubstituted alkenes bearing complex, synthetically applicable and/or pharmaceutically relevant functional groups were well-tolerated under the optimized reaction conditions (**5.42-5.60**). Particularly noteworthy was the good yield observed in the reaction with the FDA-approved antispasmodic agent, Alibendol (**5.59**), which bears an oxidatively sensitive *ortho*-hydroxyanisole motif. A diverse range of alkene-containing natural products underwent the DFA reaction, yielding the desired products in good to excellent yield (**5.54-5.58**). Reaction with (-)-carvone produced a single regioisomer, highlighting the excellent chemoselectivity for Giese addition of the *gem*-difluoro radical into electron-neutral/electron-rich alkenes. This is in sharp contrast to the selectivity observed with nucleophilic alkyl radicals (e.g., *tert*-butyl), which selectively undergo addition into electrophilic alkenes activated by a conjugated electron-withdrawing group.[29] Substitution at the terminus of the alkene did not inhibit the Giese addition, as a range of cyclic

and acyclic internal alkenes underwent DFA with no modification to the standard reaction conditions (**5.61-5.63**). The reaction was not limited to unactivated alkenes, as highly electron-rich alkenes were all amenable to the developed process. Enamines and enamides, though unprecedented Wang and Houk's DFA protocol, demonstrated good to excellent reactivity under diaryl ketone catalysis (**5.64-5.66**). Enol ethers and -acetates were also excellent radical acceptors for the *gem*-difluoro radicals generated in this protocol (**5.67-5.73**). Reaction with an exocyclic hexose produced the desired DFA product as a single diastereomer (**5.67**). Remarkably, a silyl enol ether produced the desired product with no cleavage of the silyl group despite the generation of superstoichiometric fluoride byproducts (**5.70**).

We then sought to expand the protocol to other commercially available α-fluoroesters, (i.e., ethyl difluoroacetate and ethyl pentafluoropropionate) to enable the construction of unique, challenging alkyl fluorinated motifs. A diverse range of alkenes were engaged in hydroalkylation with ethyl difluoroacetate, producing α-monofluoro esters. Ethyl difluoroacetate exhibited sluggish reactivity compared to ethyl trifluoroacetate, likely because of a more challenging reduction potential (−2.9 V vs SCE). However, at increased loadings and extended reaction times, compounds **5.74-5.76**, **5.78** and **5.80** were obtained in good to excellent yield. Ethyl pentafluoropropionate (−2.6 V vs SCE) underwent a single, regioselective defluorinative alkylation with a similar range of alkenes (**5.77**, **5.79**, **5.81**), requiring no alteration of the standard reaction conditions. The compounds accessed via these DFAs serve as exceptionally unique alkyl fluoride structures that have superb potential as synthetic intermediates. The successful DFA of these perfluorinated esters demonstrate that this protocol enables the synthesis of a vast array of alkyl-CF_2, -CFH, -CFCF$_3$, and potentially several other under-explored fluorinated moieties. We anticipate that this protocol will assist in accessing many novel alkyl fluoride groups in pharmaceutical targets that would have been previously unfeasible.

Table 5.2. Scope of alkenes in the DFA of perfluorinated esters
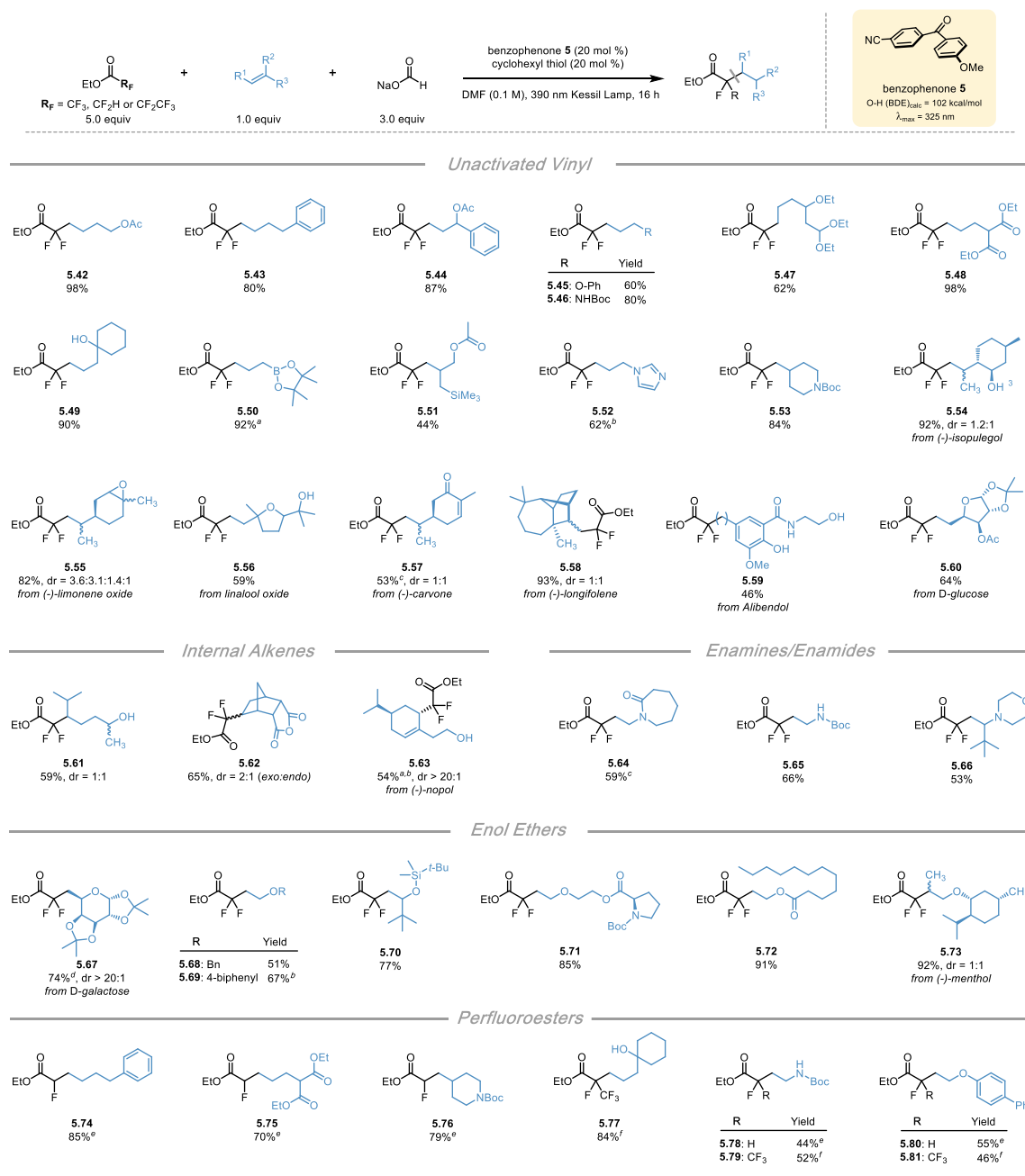
In an effort to expand this protocol beyond trifluoroacetates and enable the C-F activation of other α-trifluoromethyl carbonyl derivatives, the DFA of trifluoromethylacetamides was

330

attempted. A range of secondary- and tertiary trifluoroacetamides with both alkyl and aryl substituents were examined, however, under standard reaction conditions only trace product formation was observed in the case of a secondary *N*-aryl amide (Figure 5.8A). The rationale for this substrate specificity is two-fold. First, computations by Houk and coworkers on the mechanism of the boryl radical-mediated DFA suggest that the presence of an N-H bond significantly lowered the barrier to SCS elimination of fluoride through an intramolecular hydrogen bonding event. It is likely that the current protocol exhibits a similar mechanism, and thus only secondary amides yielded the DFA product because they exhibit a lower-barrier defluorinative SCS. Second, the *N*-aryl trifluoroacetamides display lower reduction potentials compared to their alkyl counterparts, making the reduction via $CO_2^{\bullet-}$ expedient for only the *N*-aryl amides. To identify substrates that would engage in facile SET with $CO_2^{\bullet-}$, secondary trifluoroacetamides bearing electron-withdrawing arenes were incorporated into the DFA protocol. Moderate reactivity was observed with *N*-(4-cyanophenyl)-trifluoroacetamide (**5.88**), which still exhibited a challenging reduction potential (-2.2 V vs SCE). In an effort to accelerate reactivity by decreasing the reduction potential, a suite of Lewis acid additives were examined in the DFA of **5.88**. Application of zinc(II) triflate decreased the reduction potential of **5.88** by 500 mV and provided the highest yield of the DFA product.
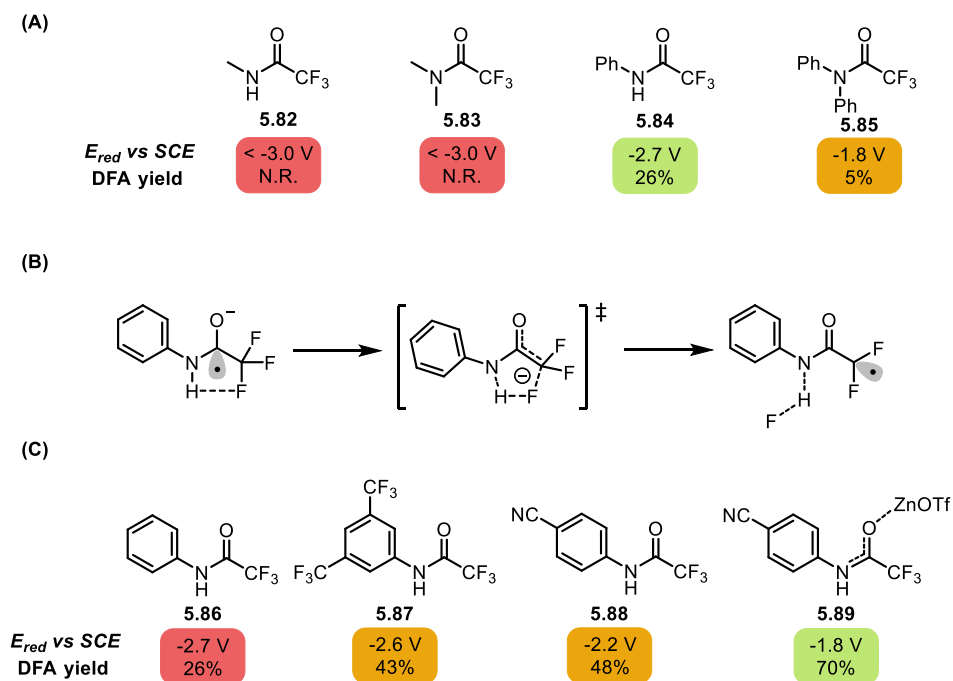
Figure 5.8. Structural optimization for the DFA of trifluoroacetamides. **(A)** The effect of N-substituents on the success of DFA. **(B)** Intramolecular N-H•••F hydrogen bonding interaction in defluorinative SCS of trifluoroacetamides. **(C)** Trend of reduction potential vs DFA yield for various *N*-aryl trifluoroacetamides.

An equally broad range of alkenes was engaged in DFA with a catalytic loading of $Zn(OTf)_2$ and excess **5.88**. Generally speaking, the reaction only consumed one equivalent of **5.88** with only trace protodefluorination, and so the excess, unreacted starting material was easily recovered by crystallization prior to chromatographic purification of the DFA products (% rsm in Table 5.3).

Table 5.3. Scope of alkenes in the DFA of **5.88**
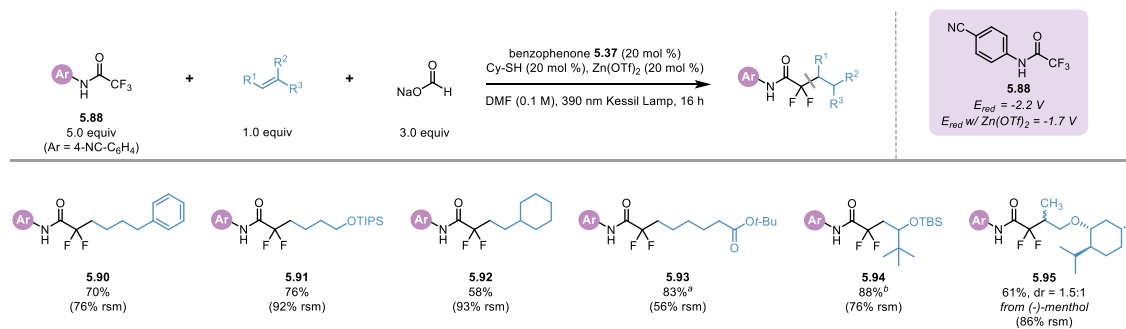
As previously described, the replacement of C-H bonds with C-F bonds in pharmaceutical structures is a common strategy used by medicinal chemists to impart enhanced properties. A particularly unique example is found in the structural analogs of Tafluprost, a prostaglandin analog for the treatment of open-angle glaucoma.[30] Like most prostaglandin derivatives, preliminary structural analogs of Tafluprost contained a C15(*S*)-hydroxy group that participates in critical hydrogen bonding events. Though critical to its pharmacological properties, this allylic alcohol moiety is particularly susceptible to oxidation and ultimately metabolic deactivation. However, replacement of the C15-hydroxy group for a *gem*-difluoromethylene group exhibited equivalent EC$_{50}$ values over a significantly increased half-life as the C-F bonds are not oxidatively labile.
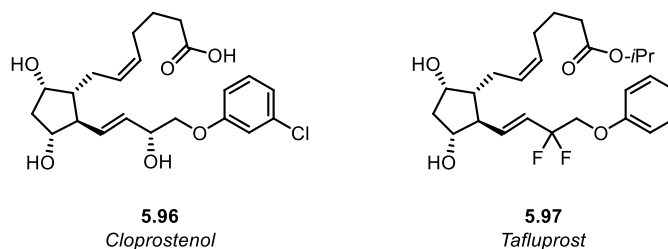
Figure 5.9. Structures of related prostaglandin analogs: Cloprostenol and Tafluprost.

In a similar manner, α-carbonyl oxidation is another common mode of metabolic degradation that is detrimental to a drug's half-life/clearance profile that can be circumvented by exchanging a CH_2 for a CF_2 group.[31] To demonstrate how the developed DFA could provide rapid access to drug structures containing α-difluoromethyl carbonyl motifs, three FDA approved APIs were selected for the synthesis of their difluoro derivatives (Figure 5.10). In each case the starting material alkene (**5.98**, **5.100**, **5.102**) could be prepared via an efficient and high-yielding synthesis. Application of these alkenes in the DFA protocol yielded the desired α,α-difluoroesters in good to excellent yield (**5.99**, **5.101**, **5.103**). Each of these esters could then be readily converted to the API structure. The advantages of this photochemical DFA of unactivated alkenes are evident when juxtaposed with classical approaches using bromo- or iododifluoroacetates, which necessitate unsustainable noble metal catalysis.[32]
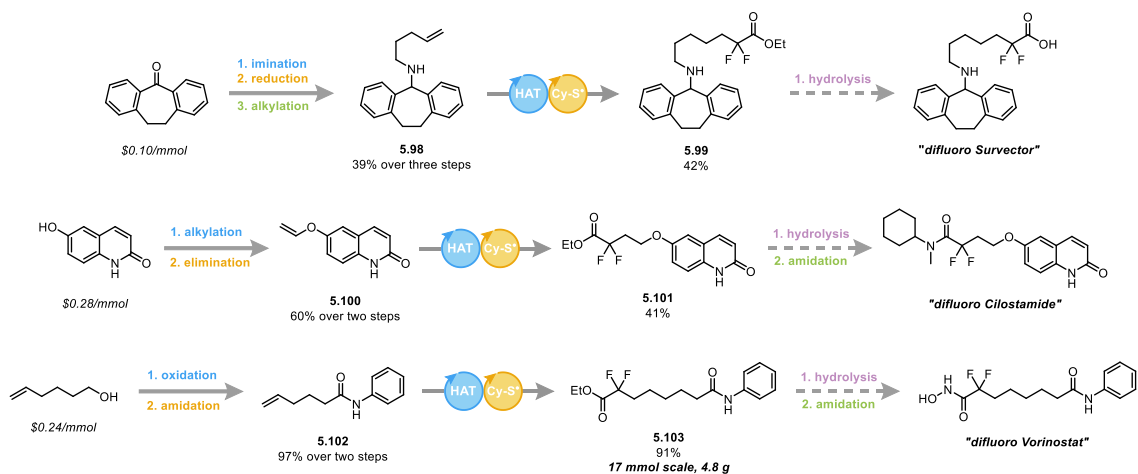
Figure 5.10. Synthesis of difluoro analogs of APIs via alkene DFA

Finally, given literature precedent[27] and highly efficient reactivity that had already been observed in the scope exploration, the scalability of the DFA reaction was probed. Using 4-phenyl-1-butene as a model alkene, the reaction scale was increased 20- and 100-fold with significant lowering of the diaryl ketone catalyst loading in batch with only a minimal decrease in

yield. Importantly, no specialized glassware, equipment, or irradiation source was required, and the reaction was completed within the same time frame as in the small-scale reactions. This is a particularly attractive aspect of this process as most photochemical reaction can only be run on such large scales in a flow-reaction that dramatically increases the exposed surface area for more efficient photon flux. Additionally, the prior trifluoroacetate DFA protocol would have required ~11 grams of di-*tert*-butyl peroxide and ~15 grams of DMAP-BH$_3$ to effect radical defluorination, whereas the current protocol required only ~10 grams of sodium formate, which greatly increases the atom economy and safety of the process. The remarkable catalytic efficiency observed in these large scale reactions strongly suggested a radical-chain process in the proposed mechanism. To verify this, quantum yield experiments were performed that revealed $\boldsymbol{\phi}$ = 4.9, which is in good agreement with previous literature precedent for $CO_2{}^{\bullet-}$-thiol tandem processes. Therefore, we believe that the diaryl ketone is critical for initiation (and likely sustaining) a radical-chain mechanism that is composed of sequential HAT steps with the thiol and formate.
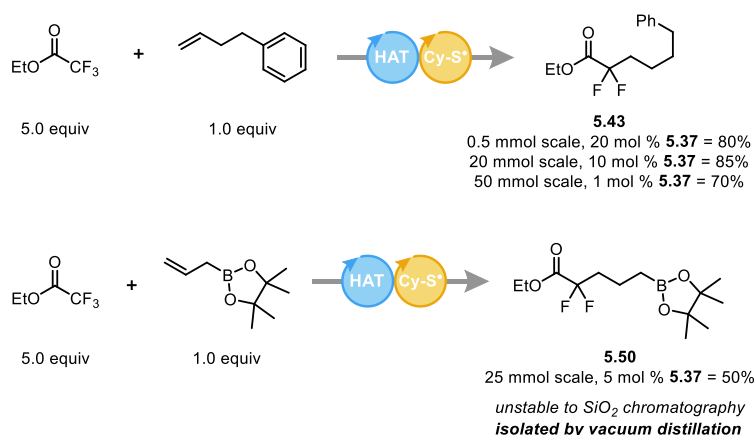
Figure 5.11. Multigram DFA of ethyl trifluoroacetate

We also demonstrated how increased scale allowed more efficient purification methods to be used, such as vacuum distillation, dramatically decreasing the process mass intensity (PMI)[33] for this transformation. In particular, pinacol boronate **5.43** could not be isolated on 0.5 mmol

because it decomposed when exposed to SiO_2 chromatography but was successfully isolated by distillation on 25 mmol scale. The ease of scalability and cost effectiveness of this photochemical transformation make it a remarkably practical method for the multigram preparation of gem-difluoromethylene compounds.

5.4. Conclusion

Overall, the newly developed DFA protocol demonstrated how diaryl ketone catalysis provided a unique mode of reactivity to access $CO_2^{\cdot-}$ to accomplish the defluorinative alkylation of C-F bonds in many α-trifluoromethyl carbonyl groups. This protocol had significant advantages over the previous method, offering a more practical, safe, and scalable reaction set up with a much broader range of substrates that were prepared with markedly higher yields. The mild reaction conditions and broad functional group tolerance make this reaction a prime candidate for the late-stage functionalization of complex molecules. The applicability of this method toward the preparation of fluorinated pharmaceutical structures was demonstrated in the preparation of three difluoro analogs of FDA-approved APIs. The cost effectiveness of all reagents and starting materials, combined with the simple reaction set-up and short irradiation time, make this reaction applicable to multigram scale preparation of fluorinated motifs in organic synthesis.

5.5. Experimental

5.5.1. General Considerations:

All chemical transformations requiring inert atmospheric conditions or vacuum distillation utilized Schlenk line techniques with a dual-bank manifold. *N,N*-Dimethylformamide was distilled over CaH_2, degassed with argon, and stored over 5 Å molecular sieves. All other reagents were purchased and used as received from their respective suppliers unless otherwise

noted. 4-(4-Methoxybenzoyl)benzonitrile (benzophenone **5**) was prepared as outlined in our previous report.[34] Reactions were monitored by ^{1}H NMR, ^{19}F NMR, or TLC using silica gel F254 plates (60 Å porosity, 250 μm thickness). TLC analysis was performed using EtOAc/hexanes and visualized using permanganate stain, ceric ammonium molybdate (Hanessian's) stain, and/or UV light. Flash chromatography was accomplished using an automated system (monitoring at 254 nm and 280 nm in conjunction with an evaporative light scattering detector) with silica cartridges (60 Å porosity, 20-40 μm). Accurate mass measurement analyses were conducted using electron ionization (EI) or electrospray ionization (ESI). The signals were mass measured against an internal lock mass reference of perfluorotributylamine (PFTBA) for EI-GCMS, and leucine enkephalin for ESI-LCMS. The utilized software calibrates the instruments and reports measurements by use of neutral atomic masses. The mass of the electron is not included. IR spectra were recorded using either neat oil or solid products. Data are presented as follows: wavenumber (cm^{-1}) peak shape/intensity (w = weak, m = medium, s = strong, vs = very strong, br = broad). Melting points (°C) are uncorrected. NMR spectra [^{1}H, ^{13}C (^{1}H decoupled), ^{11}B, ^{19}F (^{1}H coupled \nd decoupled)] were obtained at 298 K. ^{1}H NMR (600.4 MHz) chemical shifts are referenced to residual, non-deuterated CHCl$_3$ (δ 7.26), DMSO (δ 2.50) or MeOH (δ 3.31). ^{13}C (^{1}H decoupled) NMR (151 MHz) chemical shifts are reported relative to CDCl$_3$ (δ 77.3), DMSO-d_6 (δ 39.5) or CD$_3$OD (δ 49.1). ^{19}F NMR (471 MHz) spectra are ^{1}H coupled unless otherwise noted. ^{19}F NMR spectra were referenced to either hexafluorobenzene (δ -161.64) or α,α,α-trifluorotoluene (-63.72). Data are presented as follows: chemical shift (ppm), multiplicity (s = singlet, d = doublet, t = triplet, q = quartet, m = multiplet, br = broad), coupling constant J (Hz) and integration.

5.5.2. Preparation of Non-Commercial Starting Materials

The following compounds were prepared according to the established procedures, and all spectral data matched that which was reported in the literature:

tert-Butyl 4-methylenepiperidine-1-carboxylate,[35] (3a*R*,6*S*,6a*R*)-2,2-dimethyl-5-vinyltetrahydro furo[2,3-d][1,3]dioxol-6-yl acetate,[36] 4-(3,3-dimethylbut-1-en-2-yl)morpholine, (3a*R*,5a*R*,8a*S*, 8b*R*)-2,2,7,7-tetramethyl-5-methylenetetrahydro-5H-bis([1,3]dioxolo)[4,5-b:4',5'-d]pyran,[37] *tert*-butyl ((3,3-dimethylbut-1-en-2-yl)oxy)dimethylsilane,[38] (*Z*)-(prop-1-en-1-yloxy)menthol,[39] N-phenylhex-5-enamide.[40]

N-(Pent-4-en-1-yl)-10,11-dihydro-5H-dibenzo[7]annulen-5-amine,

5.98
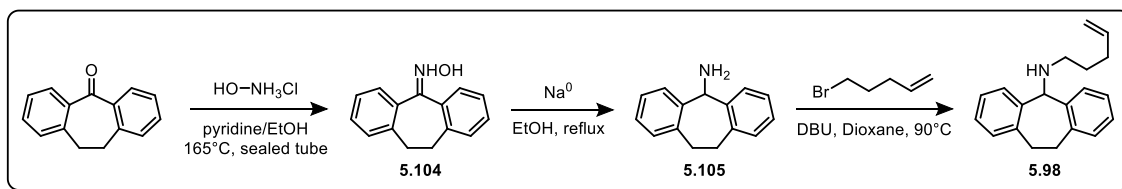
10,11-Dihydro-5H-dibenzo[7]annulen-5-one oxime (5.104): Dibenzosuberone (4.10 g, 19.7 mmol, 1.0 equiv) and hydroxylamine hydrochloride (10.26 g, 147.5 mmol, 7.5 equiv) were added to a 250 mL screw cap tube and dissolved in EtOH/pyridine (4:1, 75 mL). The tube was then tightly capped and heated to 165 °C for 12 h. The reaction was removed from the heating bath and allowed to come to rt before opening the cap. The mixture was then partitioned between aq HCl (100 mL, 2 M) and CHCl₃ (150 mL), and the layers were separated. The aq layer was extracted with an additional portion of CHCl₃ (100 mL), and the combined organic extracts were washed with brine, dried (Na₂SO₄), and the solvent was removed via rotary evaporation to yield a

light brown solid, which was recrystallized from cyclohexane and a minimal amount of CHCl$_3$ to yield the desired product as an off-white powdered solid (2.95 g, 67%). All spectral data matched that reported in the literature.[8]

10,11-Dihydro-5H-dibenzo[7]annulen-5-amine (5.105): 10,11-Dihydro-5H-dibenzo[7]annulen -5-one oxime, **5.104**, (2.70 g, 12.1 mmol, 1.0 equiv) was added to a 250 mL round-bottom flask and dissolved in anhyd EtOH (100 mL), and the reaction solution was heated to a gentle reflux. Solid Na ribbon (~3.4 g, 145 mmol, 12 equiv) was added in small portions while refluxing under air. Each ribbon reacted vigorously on the surface of the soln, and the reaction was judged to be complete when sodium ribbon was added and was not consumed. The reaction was then removed from the heating bath, allowed to return to rt, and slowly quenched with sat. aq NH$_4$Cl (100 mL). The soln was concentrated to approximately half the total volume by rotary evaporation. The resulting soln was diluted with brine (50 mL) and extracted with CHCl$_3$ (3 x 50 mL). The combined organic extracts were dried (Na$_2$SO$_4$), and the solvent was removed via rotary evaporation to yield the desired compound as a tan crystalline solid (2.45 g, 97% yield). All spectral data matched that reported in the literature.[8]

***N*-(Pent-4-en-1-yl)-10,11-dihydro-5H-dibenzo[7]annulen-5-amine, 5.98:** To a 25 mL microwave vial was added 10,11-dihydro-5H-dibenzo[7]annulen-5-amine, **5.105**, (1.08 g, 5.16 mmol, 1.0 equiv). The vial was sealed and placed under an argon atmosphere. Dioxane (5 mL), DBU (1.56 mL, 10.3 mmol, 2.0 equiv) and 5-bromo-1-pentene (920 μL, 7.74 mmol, 1.5 equiv) were each added via syringe. The reaction was then heated to 90 °C for 16 h. The solvent was then removed via rotary evaporation, and the crude material was purified via automated flash silica column chromatography to yield the desired compound as a dense, yellow oil (0.840 g, 59% yield).

¹H NMR (CDCl₃, 600 MHz) δ ppm 7.27 (d, *J* = 8.8, 2H), 7.19-7.10 (m, 6H), 5.77 (ddt, *J* = 16.9, 10.1, 6.7 Hz, 1H), 4.96 (dd, *J* = 17.1, 1.8 Hz, 1H), 4.91 (d, *J* = 10.1 Hz, 1H), 4.81 (s, 1H), 3.78-3.68 (m, 2H), 3.02-2.93 (m, 2H), 2.56 (t, *J* = 7.0 Hz, 2H), 2.07 (q, *J* = 7.2 Hz, 2H), 1.60-1.53 (m, 2H), 1.44 (br s, 1H). **¹³C NMR** (CDCl₃, 151 MHz) δ ppm 140.9, 140.2, 138.9, 130.7, 129.2, 127.6, 126.1, 114.8, 48.2, 32.7, 31.9, 29.8. **FT-IR** (cm⁻¹, neat, ATR) 3270 (w), 3062 (w), 1443 (m). **HRMS** (ESI) calcd for C₂₀H₂₄N [M + H⁺]: 278.1909, found: 278.1916.

6-(Vinyloxy)quinolin-2(1H)-one, 5.100
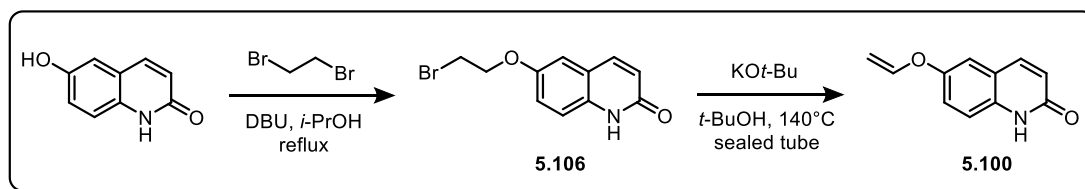
6-(2-Bromoethoxy)quinolin-2(1H)-one, 5.106: 6-Hydroxyquinolin-2(1H)-one (5.00 g, 31.0 mmol, 1.0 equiv) was added to a 250 mL round-bottom flask and dissolved in *i*-PrOH (125 mL). DBU (7.02 mL, 46.5 mmol, 1.5 equiv) and 1,2-dibromoethane (6.71 mL, 77.6 mmol, 2.5 equiv) were added via syringe, and the flask was fitted with a reflux condenser and heated to 110 °C. After 16 h, the reaction had reached approximately 50% conversion, and so an additional portion of DBU (7.02 mL, 46.5 mmol, 1.5 equiv) and 1,2-dibromoethane (6.71 mL, 77.6 mmol, 2.5 equiv) were added via syringe, and the reaction was heated for an additional 16 h. The reaction was then removed from the heat and concentrated to dryness via rotary evaporation. The crude material was then passed through a short silica plug, eluting with EtOAc/EtOH (9:1). The solvent was then removed to yield the desired compound as a light brown powdered solid (3.32 g, 40%). All spectral data matched that reported in the literature.[9]

6-(Vinyloxy)quinolin-2(1H)-one, 5.100: 6-(2-Bromoethoxy)quinolin-2(1H)-one (710 mg, 2.65 mmol, 1.0 equiv) and KO*t*-Bu (1.49 g, 13.2 mmol, 5.0 equiv) were added to a 100 mL screw cap tube and dissolved in anhyd *t*-BuOH (12 mL). The tube was tightly sealed and heated to 140 °C for 16 h. The reaction was then concentrated to dryness via rotary evaporation, and the crude material was passed through a short silica plug, eluting with EtOAc/EtOH (9:1). The solvent was then removed to yield the desired compound as a white powdered solid (491 mg, 99%; mp = 195-205 °C decomp).

^{1}H NMR (DMSO-d_6, 600 MHz) δ ppm 11.72 (s, 1H), 7.86 (d, J = 9.5 Hz, 1H), 7.37 (d, J = 2.7 Hz, 1H), 7.31-7.24 (m, 2H), 6.85 (dd, J = 13.7, 6.0 Hz, 1H), 6.52 (d, J = 9.6 Hz, 1H), 4.70 (d, J = 13.5 Hz, 1H), 4.47 (d, J = 5.8 Hz, 1H). **^{13}C NMR** (DMSO-d_6, 151 MHz) δ ppm 161.6, 150.7, 148.9, 139.6, 135.0, 122.7, 120.9, 119.7, 116.6, 114.1, 94.8. **FT-IR** (cm^{-1}, neat, ATR) 3360 (br), 1661 (vs), 1621 (s), 1427 (m). **HRMS** (ESI) calcd for $C_{11}H_{10}NO_2$ [M + H$^+$]: 188.0712, found: 188.0697.

5.5.3. Optimization of DFA of Ethyl Trifluoroacetate

General Procedure: To a 1-dram, septum cap vial was added diaryl ketone (0.005 g, 0.02 mmol, 0.20 equiv), sodium formate (0.025 g, 0.30 mmol, 3.0 equiv), alkene (0.10 mmol, 1.0 equiv), if solid, and *N*-4-(cyanophenyl)-trifluoroacetamide (0.50 mmol, 5.0 equiv), in the case of Table S6. Anhyd solvent (1.0 mL) was then added, the vial capped, and the reaction soln was sparged with argon for 60 sec. Ethyl trifluoroacetate (0.50 mmol, 5.0 equiv), thiol (0.02 mmol, 0.20 equiv), and alkene (0.10 mmol, 1.0 equiv), if liquid, were added by syringe, and the vial was sealed with Parafilm®. The reaction was then irradiated with a Kessil® PR160-390 nm lamp at a distance of 2 cm. The reaction was cooled with two compact fans ensuring that the surface temperature of the vial did not exceed 35 °C. After 16 h of irradiation, the reaction was quenched slowly with

distilled H_2O (1 mL) and extracted with Et_2O (2 x 2 mL). The combined organic extracts were washed with H_2O (1 mL) followed by brine (1 mL), dried (Na_2SO_4) then decanted, and the solvent was removed via rotary evaporation. The crude reaction material was analyzed by either GCMS using 4,4'-di-*tert*-butylbiphenyl as an internal standard (uncorrected P/IS values) or ^{19}F NMR in CDCl_3 using 5-bromo-3-trifluoromethyl pyridine as an internal standard.

Table 5.4. Optimization of Diaryl Ketone Catalyst

R_1 / R_2 / X	GCMS P/IS ratio
CN / OMe / H,H	2.77
CF_3 / OMe / H,H	2.12
Ac / OMe / H,H	2.44
Cl / Cl / H,H	1.52
F / F / H,H	2.34
OH / H / H,H	2.20
H / H / O	1.95
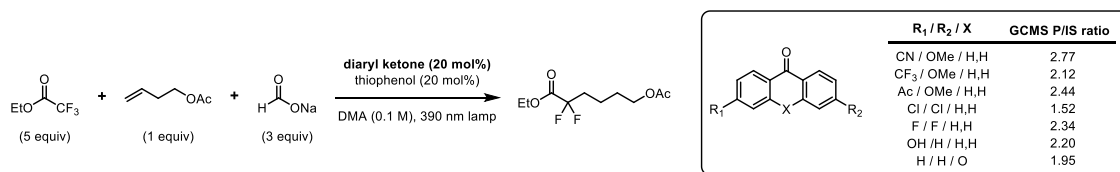
Table 5.5. Optimization of Solvent

solvent	GCMS P/IS ratio
DMA	2.77
DMSO	4.26
DMF	5.22
NMP	2.34
2-Pyrrolidone	2.66
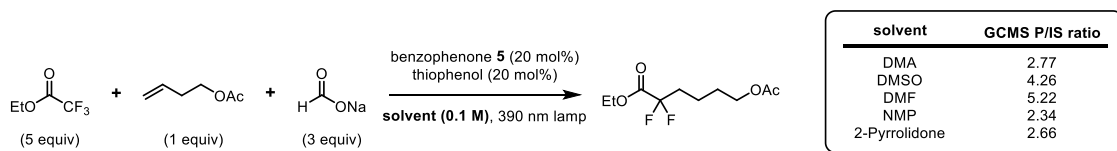
Table 5.6. Optimization of Formate Cation

M^+	GCMS P/IS ratio
Na	5.22
Li	2.02
K	0.96
Cs	1.05
NH_4, NEt_4, NBu_4	< 0.50
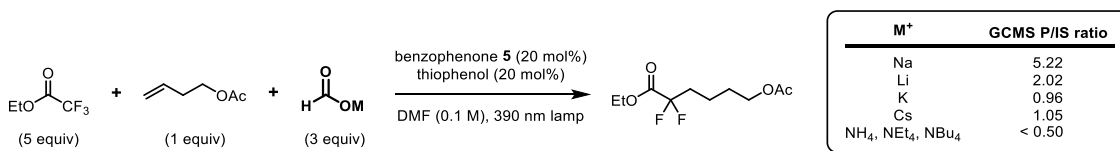
Table 5.7. Optimization of Thiol

thiol	GCMS P/IS ratio
Ph-SH	5.22
Cy-SH	6.30
Mes-SH	< 0.50
TRIP-SH	< 0.50
Mesna	< 0.50
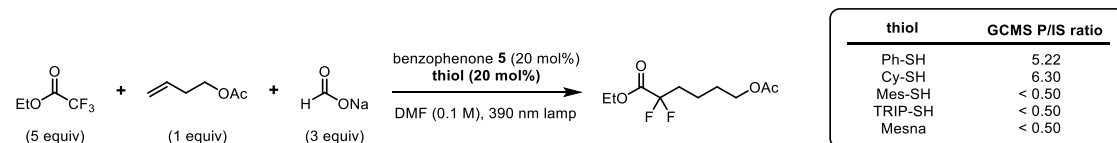
(Mes-SH = 2,4,6-trimethylthiophenol, TRIP-SH = 2,4,6-triisopropylthiophenol, Mesna = sodium 2-mercaptoethanesulfonate)

Table 5.8. Final Optimization Data for DFA of Ethyl Trifluoroacetate
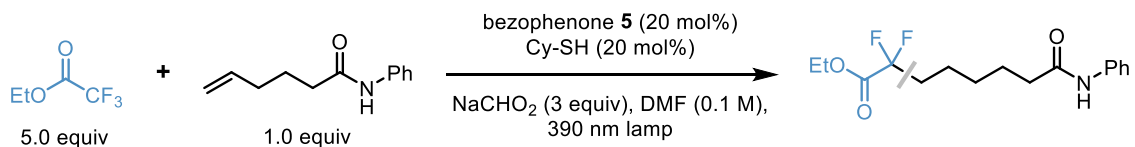
Entry	Variation of Conditions	^{19}F NMR Yield
1	none	99%
2	CzIPN instead of benzophenone **5**	29%
3	DPAIPN instead of benzophenone **5**	61%
4	1 mol% benzophenone **5**	90%
5	w/out benzophenone **5**	42%
6	w/out light	0%
7	(CyS)$_2$ instead of CySH	90%*
8	1 h instead of 16 h	98%
9	"zero precautions"	60%

*additional byproducts present

- CzIPN = 2,4,5,6-Tetrakis(9H-carbazol-9-yl) isophthalonitrile, DPAIPN = 2,4,5,6-Tetrakis(*N,N*-diphenylamino) isophthalonitrile

- In the case of (CyS)$_2$ we observed larger amounts of thiol radical addition to the alkene

- The formation of the desired product in the absence of benzophenone **5** is due to the presence of trace disulfide impurities in commercial cyclohexanethiol that could not be removed.

- "Zero precautions" indicates that non-anhydrous solvent was used, and the reaction was capped under air without sparging.

Table 5.9. Optimization of Lewis Acids for DFA of *N*-(4-cyanophenyl)trifluoroacetamide
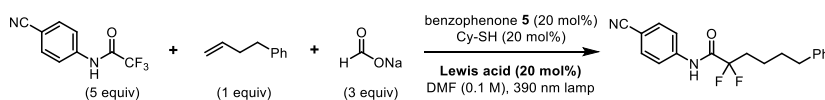
Lewis acid	^{19}F NMR yield
Sc(OTf)$_3$	35%
ZnCl$_2$	72%
Zn(OTf)$_2$	79%
CeCl$_3$	47%
Ti(OMe)$_4$	20%
HfCl$_4$	8%
BF$_3$•Et$_2$O	70%
FeCl$_3$	6%

5.5.4. DFA of Ethyl Trifluoroacetate General Procedure and Compound Characterization Data
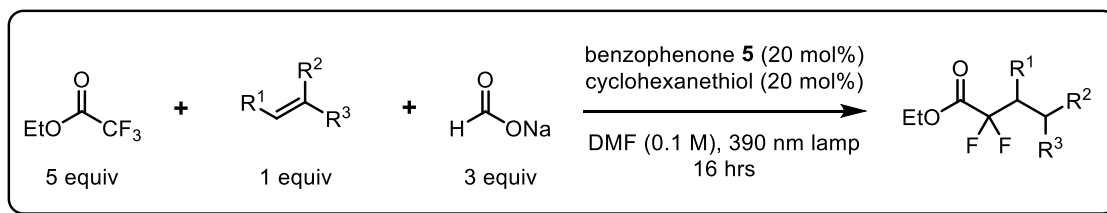
To a 2 dram, septum capped vial was added was added benzophenone **5** (0.024 g, 0.1 mmol, 0.20 equiv), sodium formate (0.102 g, 1.50 mmol, 3.0 equiv) and alkene (0.50 mmol, 1.0 equiv), if solid. Anhyd DMF (5.0 mL) was then added, the vial was capped, and the reaction soln was sparged with argon for 2 min. Ethyl trifluoroacetate (300 µL, 2.50 mmol, 5.0 equiv), cyclohexanethiol (12 µL, 0.10 mmol, 0.20 equiv) and alkene (0.50 mmol, 1.0 equiv), if liquid, were added by syringe, and the vial was sealed with Parafilm. The reaction was then irradiated with a Kessil® PR160-390 nm lamp at a distance of 2 cm. The reaction was cooled with two compact fans, ensuring that the surface temperature of the vial did not exceed 35 °C. After 16 h of irradiation, the reaction was quenched slowly with distilled H_2O (20 mL) and extracted with either Et_2O or EtOAc (2 x 25 mL). The combined organic extracts were washed with H_2O (25 mL) followed by brine (10 mL), dried (Na_2SO_4) then decanted, and the solvent was removed via rotary evaporation. The crude material was then redissolved in CH_2Cl_2 and evaporated onto 5 g of silica to be purified via automated flash silica column chromatography.
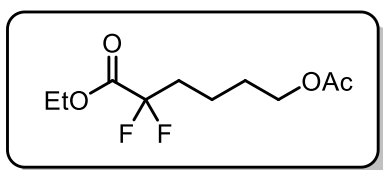
Ethyl 6-Acetoxy-2,2-difluorohexanoate, 5.42 (0.110 g, 98%) was prepared according to General Procedure A. The desired compound was obtained as a dense, colorless oil. [1]**H**

344

NMR (CDCl$_3$, 600 MHz) δ ppm 4.33 (q, *J* = 7.1 Hz, 2H), 4.07 (t, *J* = 6.4 Hz, 2H), 2.13-2.06 (m, 2H), 2.05 (s, 3H), 1.72-1.67 (m, 2H), 1.59-1.54 (m, 2H), 1.35 (t, *J* = 7.1 Hz, 3H). **^{13}C NMR** (CDCl$_3$, 151 MHz) δ ppm 171.4, 164.5 (t, *J* = 31 Hz), 116.4 (t, *J* = 250 Hz), 64.0, 63.1, 34.3 (t, *J* = 23 Hz), 28.3, 21.2, 18.5 (t, *J* = 4.7 Hz), 14.2. **^{19}F NMR** (CDCl$_3$, 471 MHz) δ ppm -107.1 (t, *J* = 15 Hz, 2F). **FT-IR** (cm^{-1}, neat, ATR) 2963 (w), 1725 (m), 1142 (vs), 1075, 726 (m). **HRMS** (EI) calcd for C$_8$H$_{14}$F$_2$O$_3$ [M − CH$_3$CO$^+$]: 196.0911, found: 196.0903.
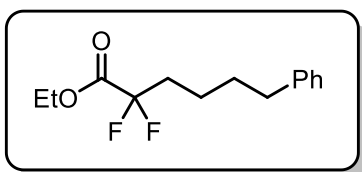
Ethyl 2,2-Difluoro-6-phenylhexanoate, 5.43 (0.102 g, 80%) was prepared according to General Procedure A. The desired compound was obtained as a dense, colorless oil. **^{1}H NMR** (CDCl$_3$, 600 MHz) δ ppm 7.28 (t, *J* = 7.5 Hz, 2H), 7.21 – 7.14 (m, 3H), 4.31 (q, *J* = 7.2 Hz, 2H), 2.63 (t, *J* = 7.7 Hz, 2H), 2.15 – 2.03 (m, 2H), 1.73 – 1.63 (m, 2H), 1.55 – 1.48 (m, 2H), 1.33 (t, *J* = 7.1 Hz, 3H). **^{13}C NMR** (CDCl$_3$, 151 MHz) δ ppm 164.6 (t, *J* = 33 Hz), 142.1, 128.7, 128.6, 126.2, 116.6 (t, *J* = 250 Hz), 63.0, 35.8, 34.6 (t, *J* = 23 Hz), 31.1, 21.4, 14.2. **^{19}F NMR** (CDCl$_3$, 471 MHz) δ ppm -105.8 (t, *J* = 16.8 Hz). **FT-IR** (cm^{-1}, neat, ATR) 2930 (w), 1761 (s), 1178 (s), 1094 (vs). **HRMS** (EI) calcd for C$_{14}$H$_{18}$F$_2$O$_2$ [M$^+$]: 256.1275, found: 256.1288.
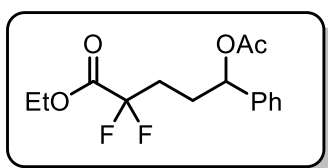
Ethyl 5-Acetoxy-2,2-difluoro-5-phenylpentanoate, 5.44 (0.131 g, 87%) was prepared according to General Procedure A. The desired compound was obtained as a dense, colorless oil. **^{1}H NMR** (CDCl$_3$, 600 MHz) δ ppm 7.38-7.34 (m, 2H), 7.33-7.29 (m, 3H), 5.77 (t, *J* = 6.4 Hz, 1H), 4.31 (q, *J* = 7.1 Hz, 2H), 2.17-1.97 (m, 7H), 1.33 (t, *J* = 7.2 Hz, 3H). **^{13}C NMR** (CDCl$_3$, 151 MHz) δ ppm 170.4, 164.3 (t, *J* = 33 Hz), 139.8, 128.9, 128.6, 126.6, 116.10 (t, *J* = 251 Hz), 74.9, 63.2, 31.0 (t, *J* = 24 Hz), 28.5 (t, *J* = 4.2 Hz), 21.4, 14.2. **^{19}F NMR** (CDCl$_3$, 471 MHz) δ ppm -106.14 (s, 1F), -106.16 (s, 1F). **FT-IR** (cm^{-1}, neat, ATR) 2941 (w), 1737 (s), 1228 (s), 1022 (vs). **HRMS** (EI) calcd for C$_{13}$H$_{15}$F$_2$O$_3$ [M - CH$_3$CO$^+$]: 257.0989, found: 257.0994.
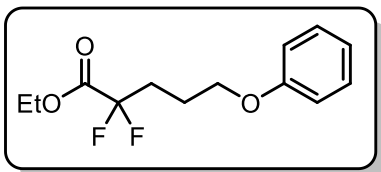
Ethyl 2,2-Difluoro-5-phenoxypentanoate, 5.45 (0.078 g, 60%) was prepared according to General Procedure A. The desired compound was obtained as a dense, colorless oil. **^{1}H NMR** (CDCl$_3$, 600 MHz) δ ppm 7.28 (t, J = 7.7 Hz, 2H), 6.95 (t, J = 7.4 Hz, 1H), 6.89 (d, J = 8.7 Hz, 2H), 4.33 (q, J = 7.2 Hz, 2H), 4.01 (t,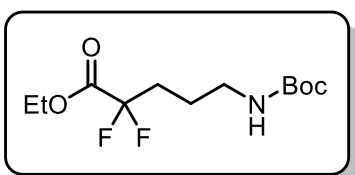 J = 6.1 Hz, 2H), 2.35 – 2.24 (m, 2H), 2.03 – 1.96 (m, 2H), 1.35 (t, J = 7.1 Hz, 3H). **^{13}C NMR** (CDCl$_3$, 151 MHz) δ ppm 164.5 (t, J = 33 Hz), 158.9, 129.8, 121.2, 116.4 (t, J = 251 Hz), 114.7, 66.67, 63.18, 31.7 (t, J = 24 Hz), 22.0 (t, J = 4 Hz), 14.2. **^{19}F NMR** (CDCl$_3$, 471 MHz) δ ppm -106.1 (t, J = 18 Hz, 2F). **FT-IR** (cm^{-1}, neat, ATR) 2936 (w), 1762 (s), 1498 (m), 1243 (vs), 1193 (vs). **HRMS** (EI) calcd for C$_{13}$H$_{16}$F$_2$O$_3$ [M$^+$]: 258.1068, found: 258.1082.

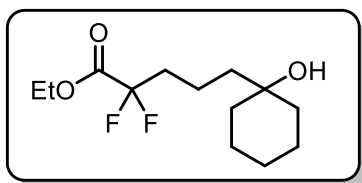**Ethyl 5-((*tert*-Butoxycarbonyl)amino)-2,2-difluoropentanoate, 5.46** (0.112 g, 80%) was prepared according to General Procedure A. The desired compound was obtained as a dense, colorless oil. **^{1}H NMR** (CDCl$_3$, 600 MHz) δ ppm 4.58 (br s, 1H), 4.32 (q, J = 7.1 Hz, 2H), 3.21-3.14 (m, 2H), 2.15-2.04 (m, 2H), 1.72-1.66 (m, 2H), 1.44 (s, 9H), 1.35 (t, J = 7.1 Hz, 3H). **^{13}C NMR** (CDCl$_3$, 151 MHz) δ ppm 164.4 (t, J = 33.2 Hz), 156.2, 116.3 (t, J = 252 Hz), 79.7, 63.2, 40.0, 32.0 (t, J = 24 Hz), 28.6, 22.6, 14.2. **^{19}F NMR** (CDCl$_3$, 471 MHz) δ ppm -105.9 (t, J = 17 Hz, 2F). **FT-IR** (cm^{-1}, neat, ATR) 3410 (br), 2979 (w), 1761 (s), 1689 (vs), 1249 (s), 1168 (vs). **HRMS** (ESI) calcd for C$_8$H$_{13}$F$_2$NO$_4$ [M − *t*-Bu + H$^+$]: 225.0813, found: 225.0824.
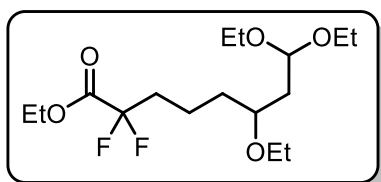
Ethyl 6,8,8-Triethoxy-2,2-difluorooctanoate, 5.47 (0.105 g, 62%) was prepared according to General Procedure A. The desired compound was obtained as a dense, colorless oil. **^{1}H NMR** (CDCl$_3$, 600 MHz) δ ppm 4.63 (dd, J = 7.3, 4.3 Hz, 1H), 4.31 (q, J = 7.1 Hz, 2H), 3.71-

3.57 (m, 2H), 3.54-3.43 (m, 4H), 3.41-3.37 (m, 1H), 2.17-2.00 (m, 2H), 1.80 (ddd, J = 14.2, 8.1,

4.3 Hz, 1H), 1.69 (ddd, J = 14.1, 7.3, 4.5 Hz, 1H), 1.58-1.45 (m, 4H), 1.34 (t, J = 7.1 Hz, 3H),

1.20 (q, J = 7.0 Hz, 6H), 1.16 (t, J = 7.0 Hz, 3H). **^{13}C NMR** (CDCl$_3$, 151 MHz) δ ppm 164.6 (t, J

= 33 Hz), 116.5 (t, J = 250 Hz), 100.9, 75.7, 64.8, 63.0, 61.7, 61.6, 39.0, 34.9 (t, J = 23 Hz), 34.1,

17.6 (t, J = 4.3 Hz), 15.9, 15.7, 15.6, 14.2. **^{19}F NMR** (CDCl$_3$, 471 MHz) δ ppm -105.8 (t, J = 18.2

Hz, 2F). **FT-IR** (cm^{-1}, neat, ATR) 2975 (w), 1766 (m), 1097 (vs), 1059 (vs). **HRMS** (EI) calcd

for C$_{14}$H$_{25}$F$_2$O$_5$ [M − Et$^+$]: 311.1670, found: 311.1676.
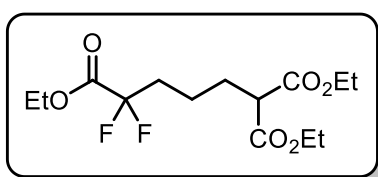
Triethyl   5,5-Difluoropentane-1,1,5-tricarboxylate,   5.48
(0.159 g, 98%) was prepared according to General Procedure
A. The desired compound was obtained as a dense, colorless

oil. **^{1}H NMR** (CDCl$_3$, 600 MHz) δ ppm 4.32 (q, J = 7.1 Hz, 2H), 4.20 (qd, J = 7.2, 3.2 Hz, 4H),

3.32 (t, J = 7.5 Hz, 1H), 2.15-2.04 (m, 2H), 1.98-1.91 (m, 2H), 1.56-1.50 (m, 2H), 1.35 (t, J = 7.1

Hz, 3H), 1.27 (t, J = 7.1 Hz, 6H). **^{13}C NMR** (CDCl$_3$, 151 MHz) δ ppm 169.3, 164.4 (t, J = 33

Hz), 116.2 (t, J = 250 Hz), 63.1, 61.8, 51.9, 34.4 (t, J = 23 Hz), 28.4, 19.7 (t, J = 4.4 Hz), 14.3,

14.2. **^{19}F NMR** (CDCl$_3$, 471 MHz) δ ppm -106.0 (t, J = 16.8 Hz, 2F). **FT-IR** (cm^{-1}, neat, ATR)

2982 (w), 1750 (vs), 1730 (vs), 1252 (m), 1155 (vs), 1097 (vs). **HRMS** (EI) calcd for C$_{14}$H$_{22}$F$_2$O$_6$

[M$^+$]: 324.1384, found: 324.1398.

Ethyl 2,2-Difluoro-5-(1-hydroxycyclohexyl)pentanoate, 5.49
(0.119 g, 90%) was prepared according to General Procedure
A. The desired compound was obtained as a dense, colorless

oil. **^{1}H NMR** (CDCl$_3$, 600 MHz) δ ppm 4.30 (q, J = 7.1 Hz, 2H), 2.10-1.98 (m, 2H), 1.60-1.37

(m, 13H), 1.36-1.19 (m, 5H). **^{13}C NMR** (CDCl$_3$, 151 MHz) δ ppm 164.6 (t, J = 33 Hz), 116.5 (t, J

= 250 Hz), 71.4, 63.0, 41.8, 37.6, 35.2 (t, J = 23 Hz), 26.0, 22.4, 15.5 (t, J = 4.4 Hz), 14.2. **^{19}F**

**NMR** (CDCl$_3$, 471 MHz) δ ppm -105.7 (t, J = 16.8 Hz, 2F). **FT-IR** (cm^{-1}, neat, ATR) 3427 (br),

2930 (m), 1760 (vs), 1187 (m). **HRMS** (EI) calcd for $C_{13}H_{22}F_2O_3$ [M$^+$]: 264.1537, found: 264.1532.
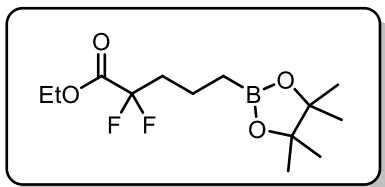
Ethyl 2,2-Difluoro-5-(4,4,5,5-tetramethyl-1,3,2-dioxaborolan -2-yl)pentanoate, 5.50 (3.71 g, 50%) was prepared according to General Procedure A from with the following modification: 25.0 mmol scale with 5.0 mol % of benzophenone catalyst **5** was used. Vacuum distillation (bp = 88-100 °C, 0.3 mm Hg) afforded the title product as a clear, colorless oil. **^{1}H NMR** (CDCl$_3$, 500 MHz) ppm δ 4.31 (q, J = 7.1 Hz, 2H), 2.12-2.02 (m, 2H), 1.63-1.53 (m, 2H), 1.34 (t, J = 7.2 Hz, 3H), 1.23 (s, 12H), 0.82 (t, J = 7.8 Hz, 2H). **^{13}C NMR** (CDCl$_3$, 151 MHz) δ ppm 164.6 (t, J = 33 Hz), 116.5 (t, J = 250 Hz), 83.3, 62.8, 36.9 (t, J = 23 Hz), 24.9, 16.4 (t, J = 4.4 Hz), 14.1 (s). **^{19}F NMR** (CDCl$_3$, 471 MHz) δ ppm -106.8 (t, J = 18.3 Hz, 2F). **^{11}B NMR** (CDCl$_3$, 128 MHz) δ ppm 33.0. **FT-IR** (cm^{-1}, neat, ATR) 2980 (w), 1767 (m), 1372 (s), 1143 (vs). **HRMS** (ESI) calcd for $C_{13}H_{23}BF_2O_4$ [M$^+$]: 293.1736, found: 293.1737.
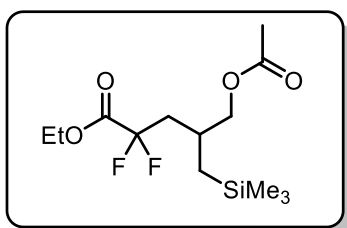
Ethyl 5-Acetoxy-2,2-difluoro-4-((trimethylsilyl)methyl) pentanoate, 5.51 (0.069 g, 44%) was prepared according to General Procedure A. The desired compound was obtained as a dense, colorless oil. **^{1}H NMR** (CDCl$_3$, 600 MHz) δ ppm 4.32 (q, J = 7.1 Hz, 2H), 4.03 (dd, J = 11.0, 4.6 Hz, 1H), 3.89 (dd, J = 11.0, 6.1 Hz, 1H), 2.30-2.22 (m, 1H), 2.21-2.15 (m, 1H), 2.06 (s, 3H), 2.12-1.98 (m, 1H), 1.35 (t, J = 7.2 Hz, 3H), 0.68 (dd, J = 12.4, 6.9 Hz, 2H), 0.04 (s, 9H). **^{13}C NMR** (CDCl$_3$, 151 MHz) δ ppm 171.2, 164.5 (t, J = 33 Hz), 116.4 (t, J = 2.2 Hz), 68.5, 63.2, 39.1 (t, J = 22 Hz), 29.0 (t, J = 3.3 Hz), 21.1, 20.4, 14.2, -0.7. **^{19}F NMR** (CDCl$_3$, 471 MHz, with ^{1}H decoupling) δ ppm -103.2 (d, J = 260.9 Hz, 1F), -104.1 (d, J_{F-F}
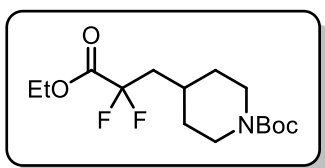
= 260.9 Hz, 1F). **FT-IR** (cm^{-1}, neat, ATR) 3346 (br), 2955 (w), 1742 (s), 1231 (vs), 1042 (m).

HRMS (EI) calcd for C$_{12}$H$_{21}$F$_2$O$_4$Si [M – CH$_3$$^+$]: 295.1177, found: 295.1186.

Ethyl 2,2-Difluoro-5-(1H-imidazol-1-yl)pentanoate, 5.52 (0.072 g, 62%) was prepared according to General Procedure A with the following modificati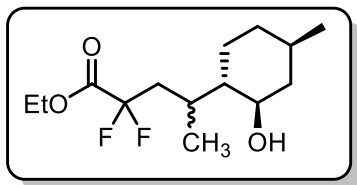ons: 5.0 equiv of sodium formate and 10.0 equiv of ethyl trifluoroacetate were used. The desired compound was obtained as a dense, colorless oil. **^{1}H NMR** (CDCl$_3$, 600 MHz) δ ppm 7.48 (s, 1H), 7.08 (s, 1H), 6.91 (s, 1H), 4.32 (q, J = 7.1 Hz, 2H), 4.03 (t, J = 6.5 Hz, 2H), 2.08-1.99 (m, 4H), 1.34 (t, J = 7.1 Hz, 3H). **^{13}C NMR** (CDCl$_3$, 151 MHz) δ ppm 164.1 (t, J = 32.6 Hz), 137.4, 130.2, 118.8, 115.9 (t, J = 251.0 Hz), 63.4, 46.2, 31.5 (t, J = 23.7 Hz), 23.6 (t, J = 4.0 Hz), 14.2. **^{19}F NMR** (CDCl$_3$, 471 MHz) δ ppm -106.8 (t, J = 16.8 Hz, 2F). **FT-IR** (cm^{-1}, neat, ATR) 2963 (w), 1725 (m), 1142 (vs), 1075, 726 (m). **HRMS** (ESI) calcd for C$_{10}$H$_{14}$F$_2$N$_2$O$_2$ [M$^+$]: 233.1102, found: 233.1108.

***tert*-Butyl 4-(3-Ethoxy-2,2-difluoro-3-oxopropyl)piperidine-1-carboxylate, 5.53** (0.135 g, 84%) was prepared according to General Procedure A. The desired compound was obtained as a dense, colorless oil. **^{1}H NMR** (CDCl$_3$, 600 MHz) δ ppm 4.33 (q, J = 7.1 Hz, 2H), 4.06 (br s, 2H), 2.75-2.65 (br m, 2H), 2.02 (td, J = 17.8, 6.4 Hz, 2H), 1.82-1.76 (m, 1H), 1.74 (d, 2H), 1.45 (s, 9H), 1.36 (t, J = 7.1 Hz, 3H), 1.27-1.15 (m, 2H). **^{13}C NMR** (CDCl$_3$, 151 MHz) δ ppm 164.7 (t, J = 33 Hz), 155.0, 116.4 (t, J = 251 Hz), 79.8, 63.20, 40.9 (t, J = 22 Hz), 32.6, 30.7 (t, J = 3.3 Hz), 28.7, 14.3. **^{19}F NMR** (CDCl$_3$, 471 MHz) δ ppm -103.6 (d, J = 108 Hz, 2F). **FT-IR** (cm^{-1}, neat, ATR) 2925 (w), 1766 (s), 1690 (vs), 1168 (s). **HRMS** (ESI) calcd for C$_{15}$H$_{25}$F$_2$NO$_4$ [M$^+$]: 321.1752, found: 321.1783.

Ethyl **2,2-Difluoro-4-((1S,2R,4R)-2-hydroxy-4-methyl cyclohexyl)pentanoate, 5.54** (0.128 g, 92%) was prepared according to General Procedu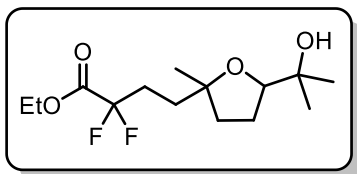re A. The diastereomeric ratio was determined to be 1.2:1 via crude ^{1}H NMR. The desired compound was obtained as a dense, colorless oil. **^{1}H NMR** (CDCl$_3$, 600 MHz) δ ppm 4.32 (q, J = 7.1 Hz, 2H), 3.40 (td, J = 10.4, 4.4 Hz, 1H), 2.44 (q, J = 7.8 Hz, 1H), 2.13-1.94 (m, 3H), 1.68 (d, J = 12.5 Hz, 1H), 1.55 (dq, J = 13.3, 3.4 Hz, 1H), 1.48-1.38 (m, 2H), 1.35 (t, J = 7.2 Hz, 3H), 1.29-1.16 (m, 1H), 1.04 (qd, J = 13.0, 3.5 Hz, 1H), 0.99-0.93 (m, 1H), 0.91 (t, J = 6.8 Hz, 6H), 0.88-0.82 (m, 1H). **^{13}C NMR** (CDCl$_3$, 151 MHz) δ ppm 165.1 (t, J = 33 Hz), 117.5 (dd, J = 252, 250 Hz), 71.0, 63.2, 50.7, 45.0, 37.1 (t, J = 22 Hz), 34.7, 31.9, 26.7 (dd, J = 4.0, 1.7 Hz), 25.1, 22.4, 18.8, 14.2. **^{19}F NMR** (CDCl$_3$, 471 MHz, ^{1}H decoupled) δ ppm -102.9, -103.8 (ABq, J_{AB} = 258 Hz, 2F). **FT-IR** (cm^{-1}, neat, ATR) 3415 (br), 2987 (m), 1766 (s), 1130 (m), 1190 (s). **HRMS** (ESI) calcd for C$_{14}$H$_{25}$F$_2$O$_3$ [M + H$^+$]: 279.1772, found: 279.1742.
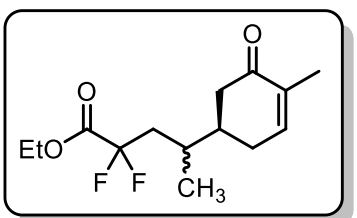

Ethyl **2,2-Difluoro-4-((3R)-6-methyl-7-oxabicyclo[4.1.0] heptan-3-yl)pentanoate, 5.55** (0.108 g, 82%) was prepared according to General Procedure A. The diastereomeric ratio was determined to be 3.6:3.1:1.4:1 via crude ^{1}H NMR. The desired compound was obtained as a dense, colorless oil. **^{1}H NMR** (CDCl$_3$, 600 MHz) δ ppm 4.31 (q, J = 7.2, 2H), 3.17-2.87 (m, 1H), 2.23-1.96 (m, 2H), 1.94-1.53 (m, 5H), 1.51-1.43 (m, 1H), 1.34 (t, J = 7.1 Hz, 3H), 1.29 (d, J = 2.5 Hz, 3H), 1.23-0.96 (m, 2H), 0.96-0.84 (m, 3H). **^{13}C NMR** (CDCl$_3$, 151 MHz) δ ppm 164.79 and 164.78 and 164.76 (t, J = 33 Hz), 116.98 and 116.96 and 116.94 (t, J = 251 Hz), 63.1, 61.04, 60.98, 59.6, 59.5, 58.1, 58.0, 57.80, 57.76, 39.0, 38.9, 38.8, 38.74, 38.69, 38.54, 38.47, 38.46, 38.39, 38.36, 38.33, 38.31, 38.18, 38.16, 34.7, 34.6, 31.50 and 31.4 and 31.2 (t, J = 2.6 Hz), 31.09, 31.07, 31.05, 30.95, 30.6, 30.0, 29.5, 29.4, 29.3, 28.3, 27.8, 26.6,

350

25.5, 24.7, 24.6, 24.1, 23.27, 23.26, 22.7, 21.5, 17.02 (t, *J* = 17 Hz), 16.95, 14.2. ^{19}F NMR (CDCl$_3$, 471 MHz, ^{1}H decoupled) δ ppm -103.4 − -106.5 (m, 2F). FT-IR (cm^{-1}, neat, ATR) 2966 (w), 1765 (s), 1189 (s), 1028 (vs). HRMS (EI) calcd for C$_{14}$H$_{22}$F$_2$O$_3$ [M$^+$]: 276.1537, found: 276.1547.
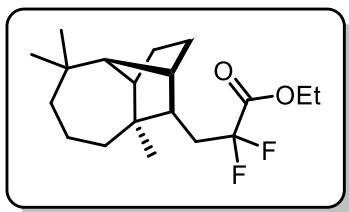

Ethyl 2,2-Difluoro-4-(5-(2-hydroxypropan-2-yl)-2-methyl tetrahydrofuran-2-yl)butanoate, 5.56 (0.087 g, 59%) was prepared according to General Procedure A. The desired compound was obtained as a dense, colorless oil. ^{1}H NMR (CDCl$_3$, 600 MHz) δ ppm 4.33 (q, *J* = 7.2 Hz, 2H), 3.79 and 3.71 (dd, *J* = 8.3, 6.5 Hz and dd, *J* = 8.9, 6.1 Hz, 1H), 2.34-2.08 (m, 2H), 1.92-1.60 (m, 7H), 1.36 and 1.35 (t, *J* = 7.1, 3H), 1.22-1.19 (m, 6H), 1.12-1.10 (m, 3H). ^{13}C NMR (CDCl$_3$, 151 MHz) δ ppm 164.61 and 164.57 (t, *J* = 33 Hz), 116.8 (t, *J* = 250 Hz), 86.0, 85.4, 81.97, 81.92, 71.4, 71.0, 63.2, 63.1, 37.87, 37.86, 33.3 and 32.5 (t, *J* = 3.7 Hz), 30.18 and 30.13 (t, *J* = 23 Hz), 27.8, 27.6, 26.7, 26.6, 26.5, 25.6, 24.5, 24.3, 14.3 (d, *J* = 3.3 Hz). ^{19}F NMR (CDCl$_3$, 471 MHz, ^{1}H decoupled) δ ppm -104.7 − -106.7 (m, 2F). FT-IR (cm^{-1}, neat, ATR) 3460 (br), 2974 (w), 1761 (m), 1183 (s), 1066 (vs). HRMS (EI) calcd for C$_{13}$H$_{21}$F$_2$O$_4$ [M − Me$^+$]: 279.1408, found: 279.1413.
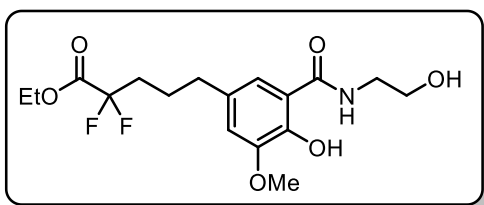

Ethyl 2,2-Difluoro-4-((*R*)-4-methyl-5-oxocyclohex-3-en-1-yl)pentanoate, 5.57 (0.073 g, 53%) was prepared according to General Procedure A with the following modifications: 10.0 equiv of ethyl trifluoroacetate were used. The diastereomeric ratio was determined to be 1:1 via crude ^{1}H NMR. The desired compound was obtained as a dense, colorless oil. ^{1}H NMR (CDCl$_3$, 600 MHz) δ ppm 6.74-6.73 (m, 1H), 4.33 (q, *J* = 7.1, 2H), 2.49-2.42 (m, 1H), 2.37-2.26 (m, 1H), 2.23-2.04 (m, 4H), 1.99-1.81 (m, 2H), 1.77 (t, *J* = 1.2 Hz, 3H), 1.36 (t, *J* = 7.1 Hz, 3H), 1.02 and 1.01 (d, *J* = 3.5 Hz, 3H). ^{13}C NMR (CDCl$_3$, 151 MHz) δ

ppm 200.0, 199.9, 164.6 (t, $J = 33$ Hz), 144.9, 144.8, 135.87, 135.85, 116.64 and 116.63 (t, $J = 251$ Hz), 63.3, 42.2, 40.92, 40.86, 40.7, 38.6 and 38.4 (t, $J = 22$ Hz), 31.4 and 31.3 (t, $J = 2.9$ Hz), 30.1, 28.6, 17.1, 17.0, 15.94, 15.93, 14.26. **^{19}F NMR** (CDCl$_3$, 471 MHz, ^{1}H decoupled) δ ppm -102.9 − -105.0 (m, 2F). **FT-IR** (cm^{-1}, neat, ATR) 2981 (w), 1764 (s), 1674 (vs), 1056 (m). **HRMS** (EI) calcd for C$_{14}$H$_{20}$F$_2$O$_3$ [M$^+$]: 274.1381, found: 274.1376.

Ethyl 2,2-Difluoro-3-((4R,8aS,9R)-4,8,8-trimethyldecahydro-1,4-methanoazulen-9-yl)propanoate, 5.58 (0.152 g, 93%) was prepared according to General Procedure A. The diastereomeric ratio was determined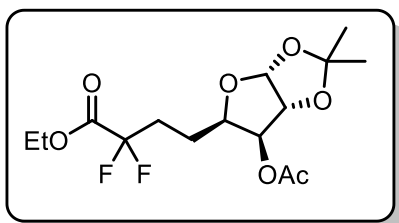 to be 1:1 via crude ^{1}H NMR. The desired compound was obtained as a dense, colorless oil. **^{1}H NMR** (CDCl$_3$, 600 MHz) δ ppm 4.43-4.24 (m, 2H), 2.13-1.93 (m, 4H), 1.73-1.64 (m, 1H), 1.60-1.50 (m, 4H), 1.39-1.29 (m, 10H), 1.00 (s, 3H), 0.94 (s, 3H), 0.77 (s, 3H). **^{13}C NMR** (CDCl$_3$, 151 MHz) δ ppm 165.1 (t, $J = 33$ Hz), 117.4 (t, $J = 250$ Hz), 63.0, 61.6, 45.1, 43.5, 42.7, 40.98, 40.7, 40.3, 33.5, 33.0, 31.2 (t, $J = 22$ Hz), 29.8, 26.2, 24.9, 21.8, 21.3, 14.3. **^{19}F NMR** (CDCl$_3$, 471 MHz, ^{1}H decoupled) δ ppm -102.6, -104.7 (AB, $J_{AB} = 255$ Hz, 2F). **FT-IR** (cm^{-1}, neat, ATR) 2955 (m), 1767 (s), 1087 (vs). **HRMS** (EI) calcd for C$_{19}$H$_{30}$F$_2$O$_2$ [M$^+$]: 328.2214, found: 328.2225.

Ethyl 2,2-Difluoro-5-(4-hydroxy-3-((2-hydroxy ethyl) carbamoyl)-5-methoxyphenyl)pentanoate, 5.59 (0.086 g, 46%) was prepared according to General Procedure A. The desired compound was obtained as a dense, colorless oil. **^{1}H NMR** (CDCl$_3$, 600 MHz) δ ppm 11.21 (s, 1H), 7.34 (s, 1H), 6.96 (s, 1H), 6.77 (s, 1H), 4.30 (q, $J = 7.1$ Hz, 2H), 3.87 (s, 3H), 3.84 (br s, 2H), 3.61 (br s, 2H), 2.73 (br s, 1H), 2.57 (t, $J = 7.6$ Hz, 2H), 2.08-1.97 (m, 2H), 1.81-1.72 (m, 2H), 1.32 (t, $J = 7.1$ Hz, 3H). **^{13}C NMR** (CDCl$_3$, 151 MHz) δ ppm 170.1, 164.6 (t, $J = 33$ Hz), 148.90, 148.87, 131.4,
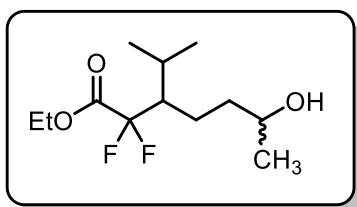
117.8, 116.5 (t, J = 251 Hz), 115.2, 115.0, 63.2, 62.2, 56.4, 42.6, 34.9, 33.9 (t, J = 23 Hz), 23.3 (t, J = 3.9 Hz), 14.1. **^{19}F NMR** (CDCl$_3$, 471 MHz) δ ppm 106.7 (t, J = 18.0 Hz, 2F). **FT-IR** (cm^{-1}, neat, ATR) 3375 (br), 2937 (w), 1760 (m), 1642 (m), 1265 (vs), 1091 (vs). **HRMS** (ESI) calcd for C$_{17}$H$_{24}$F$_2$NO$_6$ [M + H$^+$]: 376.1572, found: 376.1560.

Ethyl 4-((3aR,5R,6S,6aR)-6-Acetoxy-2,2-dimethyltetra hydrofuro[2,3-d][1,3]dioxol-5-yl)-2,2-difluorobutanoate, 5.60 (0.112 g, 64%) was prepared according to General Procedure A. The desired compound was obtained as a dense, colorless oil. **^{1}H NMR** (CDCl$_3$, 600 MHz) δ ppm 5.88 (d, J = 3.8 Hz, 1H), 5.15 (d, J = 2.9 Hz, 1H), 4.51 (d, J = 3.8 Hz, 1H), 4.31 (q, J = 7.1 Hz, 2H), 4.24 (ddd, J = 8.3, 5.2, 2.9 Hz, 1H), 2.36-2.23 (m, 1H), 2.17-2.05 (m, 4H), 1.90-1.79 (m, 1H), 1.76-1.69 (m, 1H), 1.50 (s, 3H), 1.34 (t, J = 7.1 Hz, 3H), 1.30 (s, 3H). **^{13}C NMR** (CDCl$_3$, 151 MHz) δ ppm 170.1, 164.3 (t, J = 33 Hz), 116.1 (t, J = 250 Hz), 112.2, 104.7, 83.9, 78.3, 63.2, 31.6 (t, J = 24 Hz), 26.9, 26.4, 21.0, 20.6, 14.2. **^{19}F NMR** (CDCl$_3$, 471 MHz, ^{1}H decoupled) δ ppm -107.60 (s, 1F), -107.63 (s, 1F). **FT-IR** (cm^{-1}, neat, ATR) 2988 (w), 1745 (m), 1215 (m), 1070 (m). **HRMS** (ESI) calcd for C$_{15}$H$_{22}$F$_2$O$_7$Na [M + Na$^+$]: 375.1231, found: 375.1225.
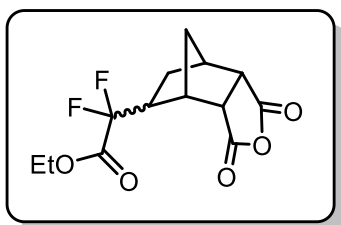

Ethyl 2,2-Difluoro-6-hydroxy-3-isopropylheptanoate, 5.61 (0.083 g, 59%) was prepared according to General Procedure A. The diaste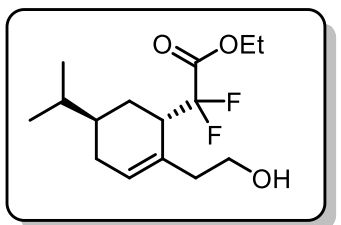reomeric ratio was determined to be 1:1 via crude ^{1}H NMR. The desired compound was obtained as a dense, colorless oil. **^{1}H NMR** (CDCl$_3$, 600 MHz) δ ppm 4.31 (q, J = 7.1 Hz, 2H), 3.79-3.73 (m, 1H), 2.09-2.00 (m, 1H), 1.94-1.88 (m, 1H), 1.74-1.64 (m, 1H), 1.57-1.42 (m, 4H), 1.34 (t, J = 7.1 Hz, 3H), 1.19 (d, J = 6.2 Hz, 3H), 0.99 (d, J =

7.0 Hz, 3H), 0.92 (d, J = 6.9 Hz, 3H). ^{13}C NMR (CDCl$_3$, 151 MHz) δ ppm 165.1 (t, J = 33 Hz), 119.8 and 118.1 (dd, J = 256, 253 Hz), 68.4, 68.2, 63.0, 47.9 and 47.8 (t, J = 20 Hz), 38.9, 38.6, 27.2 (dd, J = 8.5, 4.6 Hz), 23.9, 23.8, 21.8, 20.1 (dd, J = 4.6, 2.5 Hz), 19.9 (dd, J = 4.5, 2.5 Hz), 18.4, 14.2. ^{19}F NMR (CDCl$_3$, 471 MHz, ^{1}H decoupled) δ ppm -104.3 and -104.9 (d, J = 34 Hz, 1F), 109.7 and 110.3 (d, J = 28 Hz, 1F). FT-IR (cm^{-1}, neat, ATR) 3380 (br), 2966 (w), 1759 (s), 1073 (s). HRMS (EI) calcd for C$_{12}$H$_{21}$F$_2$O$_2$ [M − OH$^+$]: 325.1510, found: 235.1519.

Ethyl 2-((3a*R*,4*R*,7*R*,7a*S*)-1,3-Dioxooctahydro-4,7-methanoiso benzofuran-5-yl)-2,2-difluoroacetate, 5.62 (0.094 g, 65%) was prepared according to General Procedure A. The diastereomeric ratio was determined to be 2:1 (exo:endo) via crude ^{1}H NMR.
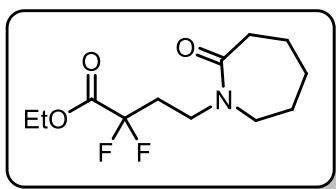
The desired compound was obtained as a dense, colorless oil. The exo diastereomer was fully characterized. ^{1}H NMR (CDCl$_3$, 600 MHz) δ ppm 4.42-4.27 (m, 2H), 3.51-3.42 (m, 2H), 3.01-2.86 (m, 2H), 2.38-2.26 (m, 1H), 1.99 (d, J = 10.8 Hz, 1H), 1.91-1.86 (m, 1H), 1.76 (ddd, J = 14.3, 9.1, 2.6 Hz, 1H), 1.60 (dd, J = 10.9, 2.8 Hz, 1H), 1.36 (t, J = 7.1 Hz, 3H). ^{13}C NMR (CDCl$_3$, 151 MHz) δ ppm 171.3, 170.9, 163.5 (t, J = 33 Hz), 115.7 (t, J = 253 Hz), 63.6, 50.2, 49.2, 41.5 (t, J = 23 Hz), 41.2 (t, J = 2.8 Hz), 41.0 (d, J = 2.4 Hz), 39.8, 27.1 (t, J = 2.9 Hz), 14.2. ^{19}F NMR (CDCl$_3$, 471 MHz, ^{1}H decoupled) δ ppm -111.1 (d, J = 15 Hz, 2F). FT-IR (cm^{-1}, neat, ATR) 2987 (w), 1860 (w), 1780 (s), 1762 (s), 1081 (vs). HRMS (EI) calcd for C$_{13}$H$_{14}$F$_2$O$_5$ [M$^+$]: 288.0809, found: 288.0808.

Ethyl 2,2-Difluoro-2-((1*S*,5*R*)-2-(2-hydroxyethyl)-5-isopropyl cyclohex-2-en-1-yl)acetate, 5.63 (0.078 g, 54%) was prepared according to General Procedure A with the following
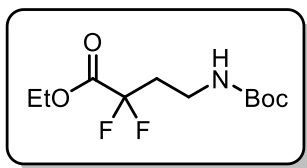
modifications: 5.0 equivalents of sodium formate and 10.0 equivalent of ethyl trifluoroacetate were used. The diastereomeric ratio was determined to be >20:1 via crude ^{1}H NMR. The desired

compound was obtained as a dense, colorless oil. [1]**H NMR** (CDCl$_3$, 600 MHz) δ ppm 5.84 (t, J = 3.0 Hz, 1H), 4.34 (qd, J = 7.1, 2.3 Hz, 2H), 3.74 (dd, J = 7.2, 5.4 Hz, 2H), 2.93 (ddd, J = 16.8, 10.4, 6.1 Hz, 1H), 2.53-2.46 (m, 1H), 2.41-2.34 (m, 1H), 2.16 (td, J = 18.0, 4.9 Hz, 1H), 1.79-1.70 (m, 2H), 1.56-1.47 (m, 2H), 1.40-1.28 (m, 5H), 0.87 (d, J = 6.7 Hz, 6H). **^{13}C NMR** (CDCl$_3$, 151 MHz) δ ppm 164.7 (t, J = 33 Hz), 131.1, 128.5 (d, J = 2.1 Hz), 118.1 (dd, J = 258, 253 Hz), 63.1, 60.9, 41.4 (t, J = 21 Hz), 39.7 (d, J = 3.2 Hz), 34.7 (d, J = 2.7 Hz), 32.6, 29.4, 27.5 (d, J = 6.5 Hz), 20.0, 19.7, 14.3. **^{19}F NMR** (CDCl$_3$, 471 MHz, ^{1}H decoupled) δ ppm -99.6 (d, J = 251 Hz, 1F), -107.2 (d, J = 251 Hz, 1F). **FT-IR** (cm^{-1}, neat, ATR) 3395 (br), 2958 (m), 1760 (m), 1056 (vs). **HRMS** (ESI) calcd for C$_{15}$H$_{24}$F$_2$O$_3$Na [M + Na$^+$]: 313.1591, found: 313.1576.

Ethyl 2,2-Difluoro-4-(2-oxoazepan-1-yl)butanoate, 5.64 (0.078 g, 59%) was prepared according to General Procedure A with the following modifications: 10.0 equiv of ethyl trifluoroacetate were used. The desired compound w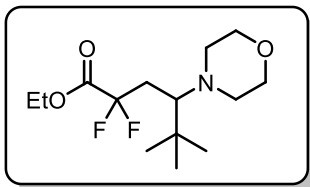as obtained as a dense, colorless oil. **^{1}H NMR** (CDCl$_3$, 600 MHz) δ ppm 4.33 (q, J = 7.1 Hz, 2H), 3.56 (t, J = 7.2 Hz, 2H), 3.37-3.35 (m, 2H), 2.52-2.47 (m, 2H), 2.34 (tt, J = 17.1, 7.3 Hz, 2H), 1.76-1.61 (m, 6H), 1.36 (t, J = 7.1 Hz, 3H). **^{13}C NMR** (CDCl$_3$, 151 MHz) δ ppm 176.2, 164.1 (t, J = 33 Hz), 115.6 (t, J = 251 Hz), 63.3, 50.8, 42.7 (t, J = 5.2 Hz), 37.5, 33.3 (t, J = 23 Hz), 30.2, 28.9, 23.6, 14.2. **^{19}F NMR** (CDCl$_3$, 471 MHz) δ ppm -107.1 (t, J = 15.4 Hz, 2F). **FT-IR** (cm^{-1}, neat, ATR) 2933 (w), 1761 (s), 1641 (s), 1191 (vs). **HRMS** (ESI) calcd for C$_{12}$H$_{20}$F$_2$NO$_3$ [M + H$^+$]: 264.1411, found: 264.1391.

Ethyl 4-((*tert*-Butoxycarbonyl)amino)-2,2-difluorobutanoate, 5.65 (0.353 g, 66%) was prepared according to General Procedure A. The desired compound was obtained as a dense, colorless oil. **^{1}H NMR** (CDCl$_3$, 600 MHz) δ ppm 4.72 (br s, 1H), 4.33 (q, J = 7.2 Hz, 2H), 3.36 (q, J = 6.1 Hz,

2H), 2.30 (tt, J = 16.8, 6.6 Hz, 2H), 1.43 (s, 9H), 1.35 (t, J = 7.2 Hz, 3H). ^{13}C NMR (CDCl$_3$, 151 MHz) δ ppm 164.3 (t, J = 32 Hz), 155.9, 115.9 (t, J = 251 Hz), 79.9, 63.3, 35.1 (t, J = 23 Hz), 34.3, 28.6, 14.2. ^{19}F NMR (CDCl$_3$, 471 MHz) δ ppm -106.71 (t, J = 18.3 Hz, 2F). FT-IR (cm^{-1}, neat, ATR) 3410 (br), 2981 (w), 1762 (s), 1694 (s), 1514 (m), 1166 (s). HRMS (ESI) calcd for C$_{11}$H$_{19}$F$_2$NO$_4$Na [M + Na$^+$]: 297.1180, found: 297.1203.

Ethyl 2,2-Difluoro-5,5-dimethyl-4-morpholinohexanoate, 5.66 (0.078 g, 53%) was prepared according to General Procedure A. The desired compound was obtained as a dense, colorless oil. ^{1}H NMR (CDCl$_3$, 600 MHz) δ ppm 4.34 (qd, J = 7.2, 4.0 Hz, 2H), 3.58-3.50 (m, 4H), 2.83-2.75 (m, 2H), 2.72-2.68 (m, 2H), 2.51-2.48 (m, 1H), 2.48-2.38 (m, 1H), 2.04 (dq, J = 15.7, 1.4 Hz, 1H), 1.36 (t, J = 7.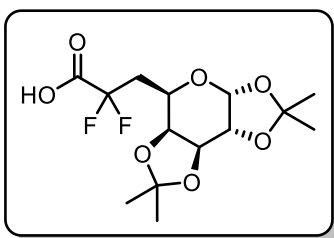1 Hz, 3H), 0.95 (s, 9H). ^{13}C NMR (CDCl$_3$, 151 MHz) δ ppm 164.8 (t, J = 33.0 Hz), 116.7 (dd, J = 247.6, 252.2 Hz), 67.7, 67.3 (dd, J = 5.0, 2.3 Hz), 63.0, 51.3, 38.2, 32.4 (t, J = 23.5 Hz), 28.5, 14.2. ^{19}F NMR (CDCl$_3$, 471 MHz, ^{1}H decoupled) δ ppm -102.1 (d, J = 259 Hz, 1F), -107.7 (d, J = 257 Hz, 1F). FT-IR (cm^{-1}, neat, ATR) 2956 (w), 1767 (m), 1292 (m), 1168 (s). HRMS (EI) calcd for C$_{13}$H$_{22}$F$_2$NO$_3$ [M – CH$_3$$^+$]: 278.1568, found: 278.1561.

2,2-Difluoro-3-((3aR,5R,5aS,8aS,8bR)-2,2,7,7-tetramethyl tetrahydro-5H-bis([1,3]dioxolo)[4,5-b:4',5'-d]pyran-5-yl) propanoic acid, 5.67 (0.135 g, 74%) was prepared according to General Proc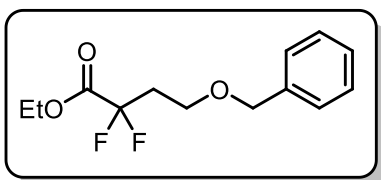edure A. The desired compound was isolated as the corresponding carboxylic acid, a dense, colorless oil, after treatment with 2 M aq NaOH followed by neutralization with conc. HCl and extraction with EtOAc (3 x 10 mL). The diastereomeric ratio was determined to be >20:1 via crude ^{1}H NMR. ^{1}H NMR (CDCl$_3$, 600 MHz) δ ppm 5.16 (d, J = 2.4 Hz, 1H), 4.52 (d, J = 5.2 Hz, 1H), 4.23 (d, J = 1.6 Hz, 1H), 3.89 (dd, J = 9.8, 5.2 Hz, 1H),

3.45 (t, J = 9.9 Hz, 1H), 2.53 (q, J = 12.5 Hz, 1H), 2.42- 2.26 (m, 1H), 1.47 (s, 3H), 1.46 (s, 3H), 1.36 (s, 3H), 1.35 (s, 3H). ¹³C NMR (CDCl₃, 151 MHz) δ ppm 166.6, 114.8 (t, J = 252 Hz), 111.6, 109.7, 96.8, 75.9, 74.5, 72.7, 68.0, 67.9, 37.5 (t, J = 24.3 Hz), 28.2, 28.0, 26.1, 26.0. ¹⁹F NMR (CDCl₃, 471 MHz, ¹H decoupled) δ ppm -103.2 (d, J = 258 Hz, 1F), -108.4 (d, J = 258 Hz, 1F). FT-IR (cm⁻¹, neat, ATR) 3510 (br), 2988 (w), 1768 (m), 1144 (m), 1065 (vs). HRMS (ESI) calcd for $C_{14}H_{20}F_2O_7Na$ [M + Na⁺]: 361.1075, found: 361.1083.
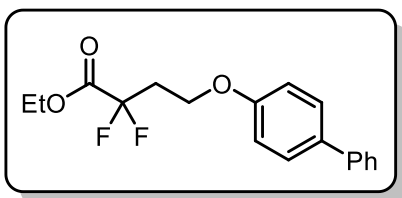

Ethyl 4-(Benzyloxy)-2,2-difluorobutanoate, 5.68 (0.066 g, 51%) was prepared according to General Procedure A. The desired compound was obtained as a dense, colorless oil. ¹H NMR (CDCl₃, 600 MHz) δ ppm 7.37-7.26 (m, 5H), 4.46 (s, 2H), 4.18 (q, J = 7.2 Hz, 2H), 3.66 (t, J = 6.1 Hz, 2H), 2.43 (tt, J = 15.3, 6.1 Hz, 2H), 1.25 (t, J = 7.1 Hz, 3H). ¹³C NMR (CDCl₃, 151 MHz) δ ppm 164.3 (t, J = 32 Hz), 138.0, 128.7, 128.0, 115.6 (t, J = 250 Hz), 73.6, 63.7 (t, J = 6.2 Hz), 63.0, 35.6 (t, J = 24 Hz), 14.1. ¹⁹F NMR (CDCl₃, 471 MHz) δ ppm -105.6 (t, J = 15.4 Hz, 2F). FT-IR (cm⁻¹, neat, ATR) 2983 (w), 1766 (s), 1373 (m), 1228 (m). HRMS (EI) calcd for $C_{13}H_{16}F_2O_3$ [M⁺]: 258.1044, found: 258.1044.


Ethyl 4-([1,1'-Biphenyl]-4-yloxy)-2,2-difluorobutanoate, 5.69 (0.107 g, 67%) was prepared according to General Procedure A with the following modifications: 5.0 equiv of sodium formate and 10.0 equiv of ethyl trifluoroacetate were used. The desired compound was obtained as a white solid (mp = 68-70 °C). ¹H NMR (CDCl₃, 600 MHz) δ ppm 7.56-7.48 (m, 4H), 7.42 (t, J = 7.7 Hz, 2H), 7.31 (t, J = 7.4 Hz, 1H), 6.93 (d, J = 8.6 Hz, 2H), 4.34 (q, J = 7.2 Hz, 2H), 4.22 (t, J = 6.2 Hz, 2H), 2.64 (tt, J = 15.4, 6.2 Hz, 2H), 1.33 (t, J = 7.1 Hz, 3H). ¹³C NMR (CDCl₃, 151 MHz) δ ppm 164.1 (t, J = 32 Hz), 157.9, 140.9, 134.8, 129.0, 128.5, 127.1, 127.0, 115.3 (t, J = 250 Hz), 115.0, 63.3, 61.6 (t, J = 6.2 Hz), 35.1 (t, J = 24 Hz), 14.2. ¹⁹F NMR

(CDCl$_3$, 471 MHz) δ ppm -105.5 (t, J = 15 Hz, 2F). **FT-IR** (cm^{-1}, neat, ATR) 2988 (w), 1773 (vs), 1479 (m), 1229 (s). **HRMS** (EI) calcd for C$_{18}$H$_{18}$F$_2$O$_3$ [M$^+$]: 320.1224, found: 320.1242.
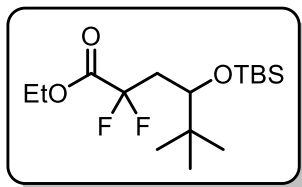
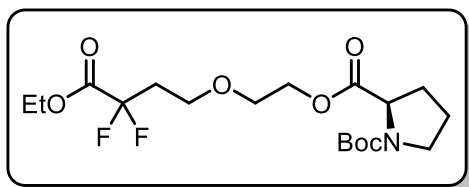**Ethyl 4-((*tert*-Butyldimethylsilyl)oxy)-2,2-difluoro-5,5-dimethylhexanoate, 5.70** (0.130 g, 77%) was prepared according to General Procedure A. The desired compound was obtained as a dense, colorless oil. **^{1}H NMR** (CDCl$_3$, 600 MHz) δ ppm 4.31 (q, J = 7.2 Hz, 2H), 3.70 (dd, J = 4.8, 3.3 Hz, 1H), 2.41 (dddd, J = 27.6, 16.0, 13.6, 3.3 Hz, 1H), 2.07 (dddd, J = 30.0, 16.0, 8.0, 4.7 Hz, 1H), 1.35 (t, J = 7.1 Hz, 3H), 0.89 (s, 9H), 0.87 (s, 9H), 0.08 (s, 3H), 0.07 (s, 3H). **^{13}C NMR** (CDCl$_3$, 151 MHz) δ ppm 163.5 (t, J = 33 Hz), 114.8 (t, J = 251 Hz), 72.5 (d, J = 3.4 Hz), 61.8, 38.4 (t, J = 22 Hz), 35.1, 25.1, 24.6, 17.4, 12.9, 0.0, -5.5. **^{19}F NMR** (471 MHz, CDCl$_3$, ^{1}H decoupled) δ ppm -104.1 (d, J = 258 Hz, 1F), -106.1 (d, J = 258 Hz, 1F). **FT-IR** (cm^{-1}, neat, ATR) 2958 (w), 1769 (m), 1111 (vs), 1083 (vs). **HRMS** (EI) calcd for C$_{15}$H$_{29}$F$_2$O$_3$Si [M – CH$_3$$^+$]: 323.1854, found: 323.1862.

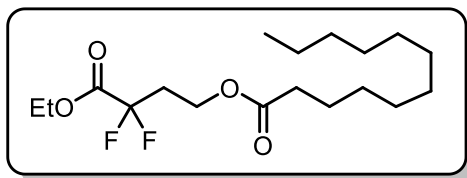**1-(*tert*-Butyl) 2-(2-(4-Ethoxy-3,3-difluoro-4-oxobutoxy) Ethyl) (*R*)-Pyrrolidine-1,2-dicarboxylate, 5.71** (0.174 g, 85%) was prepared according to General Procedure A. The desired compound was obtained as a dense, colorless oil. **^{1}H NMR** (CDCl$_3$, 600 MHz) δ ppm 4.35-4.10 (m, 5H), 3.62 (t, J = 6.2 Hz, 2H), 3.60-3.32 (m, 4H), 2.35 (tt, J = 15.3, 6.2 Hz, 2H), 2.26-2.10 (m, 1H), 1.99-1.88 (m, 2H), 1.87-1.78 (m, 1H), 1.42 and 1.38 (s, 9H), 1.32 (t, J = 7.1 Hz, 3H). **^{13}C NMR** (CDCl$_3$, 151 MHz) δ ppm 173.4, 173.1, 164.10 and 164.08 (t, J = 32 Hz), 154.6, 154.0, 115.4 and 115.3 (t, J = 250 Hz), 80.1, 79.9, 69.2, 64.5 (m), 63.9, 63.8, 63.0, 59.3, 59.0, 46.8, 46.6, 35.4 and 35.3 (t, J = 24, 10.4 Hz), 31.1, 30.1, 28.6, 28.5, 24.5, 23.8, 14.2. **^{19}F NMR** (471 MHz,

CDCl$_3$) δ ppm -106.9 (t, *J* = 16 Hz, 2F). **FT-IR** (cm^{-1}, neat, ATR) 2979 (w), 1749 (s), 1696 (vs), 1392 (vs), 1366 (m). **HRMS** (ESI) calcd for C$_{18}$H$_{29}$F$_2$NO$_7$ [M + Na$^+$]: 432.1810, found: 432.1805.

4-Ethoxy-3,3-difluoro-4-oxobutyldodecanoate, 5.72 (0.159 g, 91%) was prepared according to General Procedure A. The desired compound was obtained as a dense, colorless oil. **^{1}H NMR** (CDCl$_3$, 600 MHz) δ ppm 4.33 (q, *J* = 7.1 Hz, 2H), 4.27 (t, *J* = 6.4 Hz, 2H), 2.45 (tt, *J* = 15.9, 6.4 Hz, 2H), 2.26 (t, *J* = 7.6 Hz, 2H), 1.59 (q, *J* = 8.2, 7.7 Hz, 2H), 1.36 (t, *J* = 7.1 Hz, 3H), 1.26 (d, *J* = 16.3 Hz, 16H), 0.87 (t, *J* = 7.0 Hz, 3H). **^{13}C NMR** (CDCl$_3$, 151 MHz) δ ppm 173.6, 164.0 (t, *J* = 32.4 Hz), 115.1 (t, *J* = 251.0 Hz), 63.3, 57.5 (t, *J* = 5.9 Hz), 34.3, 34.2 (t, *J* = 23.5), 32.2, 29.9, 29.7, 29.6, 29.5, 29.4, 25.0, 23.0, 14.4, 14.2. **^{19}F NMR** (CDCl$_3$, 471 MHz) δ ppm -105.4 (t, *J* = 15.2 Hz, 2F). **FT-IR** (cm^{-1}, neat, ATR) 2925 (m), 1742 (vs), 1096 (vs). **HRMS** (EI) calcd for C$_{15}$H$_{27}$F$_2$O$_2$ [M − CO$_2$Et$^+$]: 277.1979, found: 277.1992.
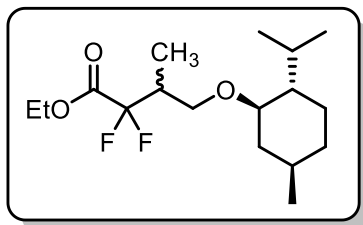

**Ethyl 2,2-Difluoro-4-(((1R,2S,5R)-2-isopropyl-5-methylcyclohexyl)oxy)-3-methylbutanoate, 5.73** (0.146 g, 92%) was prepared according to General Procedure A. The diastereomeric ratio was determined to be 1:1 via crude ^{1}H NMR. The desired compound was obtained as a dense, colorless oil. **^{1}H NMR** (CDCl$_3$, 600 MHz) δ ppm 4.34-4.20 (m, 2H), 3.72 and 3.50 (dd, *J* = 8.9, 7.2 Hz, and dd, *J* = 9.3, 7.0 Hz, 1H), 3.44 and 3.13 (dd, *J* = 9.3, 5.7 Hz and ddd, *J* = 8.9, 6.9, 1.9 Hz, 1H), 2.97 (dtd, *J* = 14.9, 10.6, 4.1 Hz, 1H), 2.70-2.47 (m, 1H), 2.19-2.10 (m, 1H), 2.08-2.02 (m, 1H), 1.68-1.57 (m, 2H), 1.36-1.28 (m, 4H), 1.22-1.12 (m, 1H), 1.10 and 1.08 (d, *J* = 7.0 Hz, 3H), 0.98-0.92 (m, 1H), 0.91 (d, *J* = 6.6 Hz, 3H), 0.88 and 0.87 (d, *J* = 4.0 Hz, 3H), 0.86-0.76 (m, 2H), 0.74 (d, *J* = 7.0, 3H). **^{13}C NMR** (CDCl$_3$, 151 MHz) δ ppm 164.4 and 164.2 (dd, *J* = 33, 14 Hz), 116.9 and 116.7 (dd, *J* = 279, 250 Hz), 80.0, 79.8, 67.7 and 67.2 (dd, *J* = 6.5, 3.4 Hz), 62.8, 62.7, 48.6, 48.5, 40.3, 39.9, 39.6 and

39.32 (t, J = 22 Hz), 34.8, 31.8, 31.8, 25.7, 25.6, 23.5, 23.5, 22.6, 22.6, 21.3, 21.2, 16.4, 16.3, 14.2, 14.2, 10.7 and 10.0 (t, J = 4.5 Hz). **^{19}F NMR** (CDCl$_3$, 471 MHz, ^{1}H decoupled) δ ppm -110.0 and -110.5 (d, J = 146 Hz, 1F), -114.1 and -118.5 (d, J =258 Hz, 1F). **FT-IR** (cm^{-1}, neat, ATR) 2925 (m), 1742 (vs), 1096 (vs). **HRMS** (EI) calcd for C$_{16}$H$_{27}$F$_2$O$_3$ [M − CH$_3$[+]]: 305.1928, found: 305.1951.
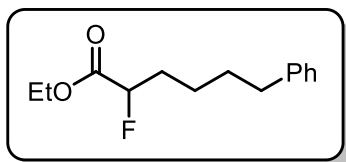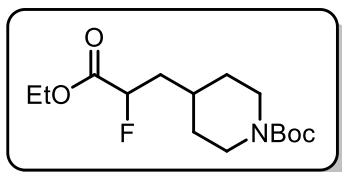

Ethyl 2-Fluoro-6-phenylhexanoate, 5.74 (0.101 g, 85%) was prepared according to General Procedure A with the following modification: ethyl difluoroacetate (5.0 mmol, 10 equiv) was used in place of ethyl trifluoroacetate and the reaction irradiated for 48 hours. The desired compound was obtained as a dense, colorless oil. **^{1}H NMR** (CDCl$_3$, 600 MHz) δ ppm 7.30-7.26 (m, 2H), 7.21-7.16 (m, 3H), 4.88 (ddd, J = 49.8, 6.7, 4.8 Hz, 1H), 4.25 (q, J = 7.1 Hz, 2H), 2.64 (t, J = 7.7 Hz, 2H), 1.98-1.87 (m, 2H), 1.73-1.64 (m, 2H), 1.55-1.49 (m, 2H), 1.30 (t, J = 7.1 Hz, 3H). **^{13}C NMR (**CDCl$_3$, 151 MHz) δ ppm 170.3 (d, J = 24 Hz), 142.4, 128.6, 128.6, 126.1, 89.2 (d, J = 184 Hz), 61.7, 35.9, 32.6 (d, J = 21 Hz), 31.2, 24.3 (d, J = 2.8 Hz), 14.4. **^{19}F NMR** (CDCl$_3$, 471 MHz) δ ppm -192.8 – -193.0 (m, 1F). **FT-IR** (cm^{-1}, neat, ATR) 2933 (m), 1759 (vs), 1738 (vs), 1202 (s). **HRMS** (ESI) calcd for C$_{14}$H$_{20}$FO$_2$ [M + H^{+}]: 239.1447, found: 239.1443.
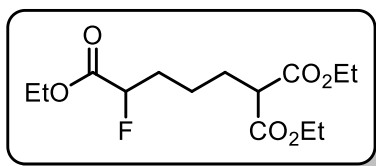
Triethyl 5-Fluoropentane-1,1,5-tricarboxylate, 5.75 (0.106 g, 70%) was prepared according to General Procedure A with the following modification: ethyl difluoroacetate (5.0 mmol, 10 equiv) was used in place of ethyl trifluoroacetate and the reaction irradiated for 48 hours. The desired compound was obtained as a dense, colorless oil. **^{1}H NMR** (CDCl$_3$, 600 MHz) δ ppm 4.88 (ddd, J = 49.1, 7.4, 4.4 Hz, 1H), 4.25 (q, J = 7.1 Hz, 2H), 4.22-4.16 (m, 4H), 3.32 (t, J = 7.5 Hz, 1H), 2.03-1.82 (m, 4H), 1.55-1.48 (m, 2H), 1.30 (t, J = 7.1 Hz, 3H), 1.26 (td, J = 7.1, 1.2 Hz, 6H). **^{13}C NMR** (CDCl$_3$, 151 MHz) δ ppm 170.0 (d, J = 24 Hz), 169.48, 169.46, 88.8 (d, J = 184

Hz), 61.8, 61.7, 52.0, 32.3 (d, *J* = 21 Hz), 28.4, 22.6 (d, *J* = 3.0 Hz), 14.4, 14.3. **¹⁹F NMR** (CDCl₃, 471 MHz) δ ppm -193.1 – 193.4 (m, 1F). **FT-IR** (cm⁻¹, neat, ATR) 2983 (w), 1729 (br and vs), 1271 (s). **HRMS** (ESI) calcd for C₁₃H₂₁FO₆Na [M + Na⁺]: 329.1276, found: 329.1234.
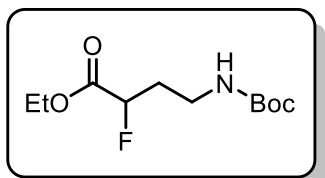

***tert*-Butyl 4-(3-Ethoxy-2-fluoro-3-oxopropyl)piperidine-1-carboxylate, 5.76** (0.120 g, 79%) was prepared according to General Procedure A with the following modification: ethyl difluoroacetate (5.0 mmol, 10 equiv) was used in place of ethyl trifluoroacetate and the reaction irradiated for 48 hours. The desired compound was obtained as a dense, colorless oil. **¹H NMR** (CDCl₃, 600 MHz) δ ppm 4.94 (ddd, *J* = 49.5, 9.3, 3.4 Hz, 1H), 4.24 (q, *J* = 7.1 Hz, 2H), 4.07 (br. s, 2H), 2.68 (br. s, 2H), 1.90-1.81 (m, 1H), 1.81-1.59 (m, 4H), 1.43 (s, 9H), 1.29 (t, *J* = 7.1 Hz, 3H), 1.21-1.07 (m, 2H).**¹³C NMR** (CDCl₃, 151 MHz) δ ppm 170.3 (d, *J* = 24 Hz), 155.0, 87.4 (d, *J* = 185 Hz), 79.6, 61.8, 43.9, 39.1 (d, *J* = 21 Hz), 32.6, 32.5 (d, *J* = 1.9 Hz), 31.5, 28.7, 14.4. **¹⁹F NMR** (CDCl₃, 471 MHz) δ ppm -192.0 – -192.2 (m, 1F). **FT-IR** (cm⁻¹, neat, ATR) 2929 (w), 1739 (m), 1688 (vs), 1447 (s). **HRMS** (ESI) calcd for C₁₄H₂₄FNO₄Na [M + Na⁺]: 326.1644, found: 326.1663.
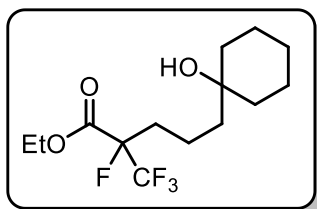
Ethyl 2-Fluoro-5-(1-hydroxycyclohexyl)-2-(trifluoromethyl) pentanoate, 5.77 (0.133 g, 84%) was prepared according to General Procedure A with the following modification: ethyl pentafluoropropionate (2.5 mmol, 5 equiv) was used in place of ethyl trifluoroacetate. The desired compound was obtained as a dense, colorless oil. **¹H NMR** (CDCl₃, 600 MHz) δ ppm 4.35 (q, *J* = 7.2 Hz, 2H), 2.22-2.08 (m, 1H), 2.06-1.97 (m, 1H), 1.72-1.43 (m, 11H), 1.43-1.36 (m, 3H), 1.34 (t, *J* = 7.1 Hz, 3H), 1.28-1.23 (m, 1H). **¹³C NMR** (CDCl₃, 151 MHz) δ ppm 164.9 (d, *J* = 25 Hz), 121.9 (qd, *J* = 285, 29 Hz), 94.1 (dq, *J* = 201, 31 Hz), 71.4, 63.3, 42.0, 37.6 (d, *J* = 56 Hz), 31.8 (d, *J* = 21 Hz), 26.0, 22.4, 16.2 (d, *J* = 2.7 Hz), 14.3. **¹⁹F**

NMR (CDCl$_3$, 471 MHz) δ ppm -79.15 (d, *J* = 7.3 Hz, 3F), -178.47 (ddd, *J* = 27.5, 13.3, 6.9 Hz, 1F). **FT-IR** (cm^{-1}, neat, ATR) 3470 (br), 2933 (m), 1753 (s), 1196 (vs). **HRMS** (EI) calcd for C$_{14}$H$_{22}$F$_4$O$_3$ [M$^+$]: 314.1505, found: 314.1549.

Ethyl 4-((*tert*-Butoxycarbonyl)amino)-2-fluorobutanoate, 5.78 (0.055 g, 44%) was prepared according to General Procedure A with the following modification: ethyl difluoroacetate (5.0 mmol, 10 equiv) was used in place of ethyl trifluoroacetate and the reaction irradiated for 48 hours. The desired compound was obtained as a dense, colorless oil. **^{1}H NMR** (CDCl$_3$, 600 MHz) δ ppm δ 4.96 (ddd, 49, 7.8, 4.0 Hz, 1H), 4.74 (br. s, 1H), 4.29-4.21 (m, 2H), 3.30 (q, *J* = 6.5 Hz, 2H), 2.32-1.91 (m, 2H), 1.42 (s, 9H), 1.30 (t, *J* = 7.1 Hz, 3H). **^{13}C NMR** (CDCl$_3$, 151 MHz) δ ppm 170.0 (d, *J* = 24 Hz), 156.1, 87.5 (d, *J* = 184 Hz), 79.7, 62.0, 36.5 (d, *J* = 4.2 Hz), 32.8 (d, *J* = 20 Hz), 28.6, 14.4. **^{19}F NMR** (CDCl$_3$, 471 MHz) δ ppm -194.1 – -194.5 (m, 1F). **FT-IR** (cm^{-1}, neat, ATR) 3363 (br), 2979 (w), 1742 (m), 1692 (vs), 1272 (s). **HRMS** (EI) calcd for C$_7$H$_{12}$FNO$_4$ [M – *t*Bu$^+$]: 193.0750, found: 193.0743.
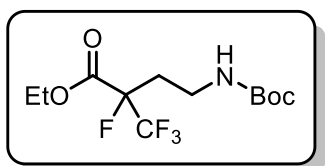

Ethyl 2-Fluoro-5-(1-hydroxycyclohexyl)-2-(trifluoromethyl) pentanoate, 5.79 (0.082 g, 52%) was prepared according to General Procedure A with the following modification: ethyl pentafluoropropionate (2.5 mmol, 5 equiv) was used in place of ethyl trifluoroacetate. The desired compound was obtained as a dense, colorless oil. **^{1}H NMR** (CDCl$_3$, 600 MHz) δ ppm 4.63 (s, 1H), 4.44-4.27 (m, 2H), 3.42-3.16 (m, 2H), 2.59-2.37 (m, 1H), 2.25-2.16 (m, 1H), 1.43 (s, 9H), 1.35 (t, *J* = 7.1 Hz, 3H). **^{13}C NMR** (CDCl$_3$, 151 MHz) δ ppm 164.5 (d, *J* = 25 Hz), 155.6, 121.5 (qd, *J* = 285, 28 Hz), 92.6 (dq, *J* = 201, 32 Hz), 79.8, 63.4, 34.5 (d, *J* = 4.4 Hz), 31.2 (d, *J* = 20 Hz), 28.4, 13.9. **^{19}F NMR** (CDCl$_3$, 471 MHz, ^{1}H decoupled) δ ppm -79.3 (d, *J* = 6.3 Hz, 3F),

179.4 (d, J = 6.3 Hz, 1F). **FT-IR** (cm^{-1}, neat, ATR) 3357 (br), 2981 (w), 1755 (m), 1695 (m), 1199 (vs). **HRMS** (EI) calcd for C$_8$H$_{11}$F$_4$NO$_4$ [M – tBu$^+$]: 261.0624, found: 261.0637.

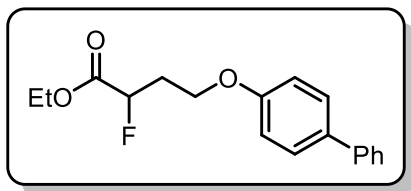**Ethyl 4-([1,1'-Biphenyl]-4-yloxy)-2-fluorobutanoate, 5.80** (0.080 g, 55%) was prepared according to General Procedure A with the following modification: ethyl difluoroacetate (5.0 mmol, 10 equiv) was used in place of ethyl trifluoroacetate and the reaction irradiated for 48 hours. The desired compound was obtained as a colorless solid (mp = 42-44 °C). **^{1}H NMR** (CDCl$_3$, 600 MHz) δ ppm 7.57-7.52 (m, 4H), 7.45-7.40 (m, 2H), 7.31 (tt, J = 7.4, 1.3 Hz, 1H), 7.00-6.96 (m, 2H), 5.20 (ddd, J = 48.8, 8.1, 4.1 Hz, 1H), 4.30 (q, J = 7.1 Hz, 2H), 4.19 (dd, J = 6.7, 5.2 Hz, 2H), 2.60-2.25 (m, 2H), 1.33 (t, J = 7.1 Hz, 3H). **^{13}C NMR** (CDCl$_3$, 151 MHz) δ ppm 169.9 (d, J = 23 Hz), 158.3, 141.0, 134.5, 129.0, 128.5, 127.0, 127.0, 115.1, 86.1 (d, J = 185 Hz), 62.8 (d, J = 3.8 Hz), 62.0, 32.7 (d, J = 21 Hz), 14.4. **^{19}F NMR** (CDCl$_3$, 471 MHz, ^{1}H decoupled) δ ppm -194.5 (s, 1F). **FT-IR** (cm^{-1}, neat, ATR) 2987 (w), 1759 (m), 1739 (s), 1243 (vs). **HRMS** (EI) calcd for C$_{18}$H$_{19}$FO$_3$ [M$^+$]: 302.1318, found: 302.1326.

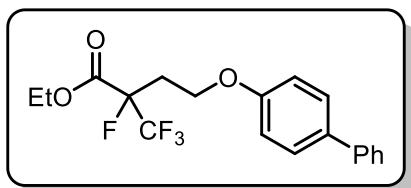**Ethyl 4-([1,1'-Biphenyl]-4-yloxy)-2-fluoro-2-(trifluoro methyl)butanoate, 5.81** (0.085 g, 46%) was prepared according to General Procedure A with the following modification: ethyl pentafluoropropionate (2.5 mmol, 5 equiv) was used in place of ethyl trifluoroacetate. The desired compound was obtained as white crystalline solid (mp = 103-105 °C). **^{1}H NMR** (CDCl$_3$, 600 MHz) δ ppm 7.57-7.49 (m, 4H), 7.42 (t, J = 8.3, 2H), 7.32 (t, J = 7.4 Hz, 1H), 6.91 (d, J = 8.7 Hz, 2H), 4.40-4.33 (m, 2H), 4.23 (td, J = 9.8, 4.3 Hz, 1H), 4.21-4.16 (m, 1H), 2.82 (dddd, J = 33.6, 14.9, 9.8, 5.6 Hz, 1H), 2.47 (ddt, J = 14.9, 8.4, 4.2 Hz, 1H), 1.31 (t, J = 7.2 Hz, 3H). **^{13}C NMR** (CDCl$_3$, 151 MHz) δ ppm 164.4 (d, J =

25 Hz), 157.8, 140.9, 134.8, 129.0, 128.5, 127.1, 127.0, 122.0 (qd, J = 285, 28 Hz), 115.0, 91.7 (dq, J = 202, 32 Hz), 63.4, 61.3 (d, J = 4.7 Hz), 31.3 (d, J = 20 Hz), 14.2. **^{19}F NMR** (CDCl$_3$, 471 MHz, ^{1}H decoupled) δ ppm -79.5 (d, J = 7.8 Hz, 3F), -173.6 – -185.8 (m, 1F). **FT-IR** (cm^{-1}, neat, ATR) 2939 (w), 1774 (vs), 1227 (vs), 1195 (vs). **HRMS** (EI) calcd for C$_{19}$H$_{18}$F$_4$O$_3$ [M[+]]: 370.1192, found: 370.1204.
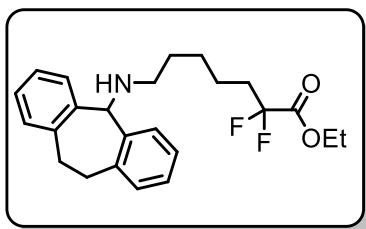
Ethyl 7-((10,11-Dihydro-5H-dibenzo[a,d][7]annulen-5-yl)amino)-2,2-difluoroheptanoate, 5.99 (0.084 g, 42%) was prepared according to General Procedure A. The desired compound was obtained as a dense, colorless oil. **^{1}H NMR** (CDCl$_3$, 600 MHz) δ ppm 7.29-7.24 (m, 2H), 7.18-7.10 (m, 6H), 4.79 (s, 1H), 4.30 (q, J = 7.1 Hz, 2H), 3.76-3.68 (m, 2H), 2.99-2.92 (m, 2H), 2.53 (t, J = 7.0 Hz, 2H), 2.07-1.95 (m, 2H), 1.49-1.40 (m, 5H), 1.38-1.31 (m, 5H). **^{13}C NMR** (CDCl$_3$, 151 MHz) δ ppm 164.7 (t, J = 33.0 Hz), 140.2, 130.7, 129.3, 127.7, 126.1, 116.6 (t, J = 250 Hz), 63.0, 48.5, 34.7 (t, J = 23.2 Hz), 32.6, 30.2, 27.1, 21.6, 14.3. **^{19}F NMR** (CDCl$_3$, 471 MHz) δ ppm -105.7 (t, J = 16.8 Hz). **FT-IR** (cm^{-1}, neat, ATR) 2928 (w), 1760 (m), 1030 (s). **HRMS** (ESI) calcd for C$_{24}$H$_{30}$F$_2$NO$_2$ [M + H^{+}]: 402.2245, found: 402.2246.
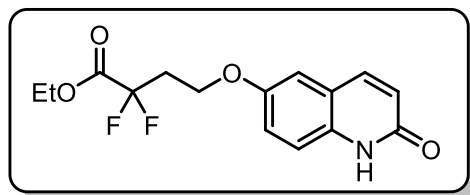
Ethyl 2,2-Difluoro-4-((2-oxo-1,2-dihydroquinolin-6-yl)oxy)butanoate, 5.101 (0.065 g, 42%) was prepared according to General Procedure A. The desired compound was obtained as a white solid (mp = 199-204 °C, decomp). **^{1}H NMR** (DMSO-d_6, 600 MHz) δ ppm 10.17 (s, 1H), 6.85 (d, J = 8.7 Hz, 1H), 6.74 (dd, J = 8.7, 2.8 Hz, 1H), 6.42 (d, J = 2.8 Hz, 1H), 4.24 (q, J = 7.1 Hz, 2H), 4.07-4.00 (m, 2H), 3.79-3.74 (m, 1H), 3.43-3.37 (m, 1H), 2.62-2.52 (m, 2H), 1.18 (t, J = 7.1 Hz, 3H). **^{13}C NMR** (DMSO-d_6, 151 MHz) δ ppm 168.6, 163.1 (t, J = 33 Hz), 153.2, 131.6, 123.1, 116.4,

115.4 (t, J = 250 Hz), 114.0, 113.0, 62.8, 61.4, 44.3, 41.8, 34.0 (t, J = 24 Hz), 27.2, 13.6. ^{19}F

NMR (DMSO-d_6, 471 MHz) δ ppm -103.4 (t, J = 17 Hz, 2F). FT-IR (cm^{-1}, neat, ATR) 3646 (br),

2996 (w), 1761 (m), 1670 (vs), 1253 (m). HRMS (ESI) calcd for $C_{15}H_{16}F_2NO_4$ [M + H$^+$]:

312.1047, found: 312.1050.
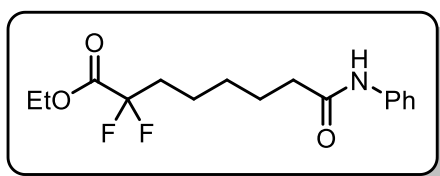
Ethyl 2,2-Difluoro-8-oxo-8-(phenylamino)octanoate, 5.103 (4.801 g, 90%) was prepared according to General Procedure A with the following modification: 17.0 mmol

scale with 5.0 mol % of benzophenone catalyst **5** was used.. The desired compound was obtained

as a white solid (mp = 66-68 °C). ^{1}H NMR (CDCl$_3$, 600 MHz) δ ppm 7.50 (d, J = 8.0 Hz, 2H),

7.32 (t, J = 7.9, 2H), 7.13 (br s, 1H), 7.1 (t, J = 7.4, 1H), 4.32 (q, J = 7.1 Hz, 2H), 2.36 (t, J = 7.4

Hz, 2H), 2.13-2.02 (m, 2H), 1.78-1.73 (m, 2H), 1.56-1.49 (m, 2H), 1.49-1.41 (m, 2H), 1.35 (t, J =

7.2 Hz, 3H). ^{13}C NMR (CDCl$_3$, 151 MHz) δ ppm 171.1, 164.7 (t, J = 33 Hz), 138.1, 129.3, 124.6,

120.0, 116.5 (t, J = 250 Hz), 63.1, 37.6, 34.5 (t, J = 23 Hz), 28.9, 25.3, 21.5 (t, J = 4.3 Hz), 14.3.

^{19}F NMR (CDCl$_3$, 471 MHz) δ ppm -105.8 (t, J = 17 Hz, 2F). FT-IR (cm^{-1}, neat, ATR) 3396

(br), 2930 (w), 1759 (s), 1661 (s), 1599 (s), 1542 (s), 1098 (s). HRMS (ESI) calcd for

$C_{16}H_{21}F_2NO_3Na$ [M + Na$^+$]: 336.1387, found: 336.1385.

5.5.5. General Procedure for DFA of 5.88 and Characterization Data
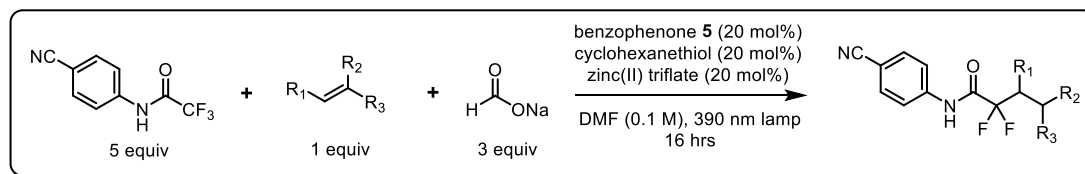
To a 40 mL, septum capped vial was added was added benzophenone **5** (0.048 g, 0.20 mmol, 0.20 equiv), sodium formate (0.204 g, 3.00 mmol, 3.0 equiv), zinc(II) trifluoromethanesulfonate (0.73 mg, 0.20 mmol, 0.20 equiv), *N*-(4-cyanophenyl)-trifluoroacetamide, **5.88** (1.07 g, 5.0 mmol, 5.0 equiv) and alkene (1.0 mmol, 1.0 equiv), if solid. Anhyd DMF (10.0 mL) was then added, the vial was capped, and the reaction solution was sparged with argon for 5 min. Cyclohexanethiol (24 µL 0.20 mmol, 0.20 equiv) and alkene (1.0 mmol, 1.0 equiv), if liquid, were added by syringe, and the vial was sealed with Parafilm. The reaction was then irradiated with a Kessil® PR160-390 nm lamp at a distance of 2 cm. The reaction was cooled with two compact fans, ensuring that the surface temperature of the vial did not exceed 35 °C. After 16 h of irradiation, the reaction was quenched slowly with distilled H$_2$O (40 mL) and extracted with either Et$_2$O or EtOAc (2 x 40 mL). The combined organic extracts were washed with H$_2$O (50 mL) followed by brine (10 mL), dried (Na$_2$SO$_4$), and the solvent was removed via rotary evaporation. The resulting crude solid was then washed with a 2:1 hexanes/Et$_2$O mixture and filtered (2 x 50 mL) to separate the unreacted, crystalline *N*-(4-cyanophenyl)-trifluoroacetamide (typically >90% recovery). The filtrate was then evaporated onto 5 grams of silica be purified via automated flash silica column chromatography.
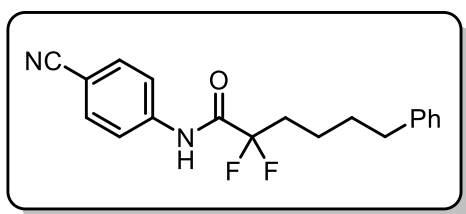
N-(4-Cyanophenyl)-2,2-difluoro-6-phenylhexanamide, 5.90 (0.230 g, 70%) was prepared according to General Procedure B. The desired compound was obtained as a white solid (mp = 73-75 °C). **^{1}H NMR** (CDCl$_3$, 600 MHz) δ ppm 8.12 (s, 1H), 7.74-7.67 (m, 2H), 7.67-7.61 (m, 2H), 7.27-7.23 (m, 2H), 7.18-7.12 (m, 3H), 2.61 (t, *J* = 7.7 Hz, 2H), 2.27-2.12 (m, 2H), 1.72-1.66 (m, 2H), 1.57-1.49 (m, 2H). **^{13}C NMR** (CDCl$_3$, 151 MHz) δ ppm 162.7 (t, *J* = 30 Hz), 142.0, 140.3, 133.7, 128.6 (d, *J* = 7.0 Hz), 126.2, 120.5, 118.6, 118.4 (t, *J* = 254 Hz), 109.1, 35.7, 33.7

(t, J = 23 Hz), 31.1, 21.4 (t, J = 4.1 Hz). **^{19}F NMR** (CDCl$_3$, 471 MHz) δ ppm -106.2 (t, J = 18.5 Hz, 2F). **FT-IR** (cm^{-1}, neat, ATR) 3310 (br), 2897 (w), 2229 (m), 1711 (m), 1596 (s), 1528 (vs). **HRMS** (ESI$^-$) calcd for C$_{19}$H$_{17}$F$_2$N$_2$O [M – H$^-$]: 327.1309, found: 327.1297.
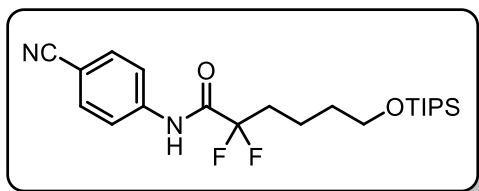
N-(4-Cyanophenyl)-2,2-difluoro-6-((triisopropylsilyl) oxy)hexanamide, 5.91 (0.323 g, 76%) was prepared according to General Procedure B. The desired compound was obtained as a dense, colorless oil. **^{1}H NMR** (CDCl$_3$, 600 MHz) δ ppm 8.10 (br s, 1H), 7.76-7.70 (m, 2H), 7.70-7.63 (m, 2H), 3.74-3.67 (m, 2H), 2.43-1.87 (m, 2H), 1.65-1.58 (m, 4H), 1.09-0.99 (m, 21H). **^{13}C NMR** (CDCl$_3$, 151 MHz) δ ppm 162.8 (t, J = 30 Hz), 140.3, 133.7, 120.4, 118.6, 118.5 (t, J = 256 Hz), 109.1, 62.9, 33.8 (t, J = 23 Hz), 32.5, 18.5 (t, J = 4.4 Hz), 18.3, 12.2. **^{19}F NMR** (CDCl$_3$, 471 MHz) δ ppm -105.4 (t, J = 16.5 Hz, 2F). **FT-IR** (cm^{-1}, neat, ATR) 3396 (br), 2942 (m), 2230 (m), 1717 (m), 1598 (s), 1531 (s). **HRMS** (ESI) calcd for C$_{22}$H$_{35}$F$_2$N$_2$O$_2$Si [M + H$^+$]: 425.2436, found: 425.2445.
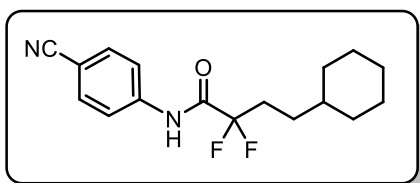
N-(4-Cyanophenyl)-4-cyclohexyl-2,2-difluorobutanamide, 5.92 (0.355 g, 58%) was prepared according to General Procedure B. The desired compound was obtained as a dense, colorless oil. **^{1}H NMR** (CDCl$_3$, 600 MHz) δ ppm 8.16 (s, 1H), 7.74 (d, J = 8.8 Hz, 2H), 7.70-7.59 (d, J = 8.7 Hz, 2H), 2.27-2.08 (m, 2H), 1.74-1.68 (m, 4H), 1.67-1.62 (m, 1H), 1.41 – 1.33 (m, 2H), 1.31-1.08 (m, 4H), 0.96 – 0.85 (m, 2H). **^{13}C NMR** (CDCl$_3$, 151 MHz) δ ppm 162.9 (t, J = 29 Hz), 140.3, 133.7, 120.4, 118.7, 118.8 (t, J = 253 Hz), 109.0, 37.5, 33.2, 31.5 (t, J = 23 Hz), 28.9 (t, J = 3.7 Hz), 26.7, 26.4. **^{19}F NMR** (CDCl$_3$, 471 MHz) δ ppm -106.4 (t, J = 18 Hz). **FT-IR** (cm^{-1}, neat, ATR) 3932 (br), 2924 (m), 2229 (w), 1705 (m), 1596 (s), 1529 (vs). **HRMS** (ESI) calcd for C$_{17}$H$_{21}$F$_2$N$_2$O [M + H$^+$]: 307.1622, found: 307.1627.
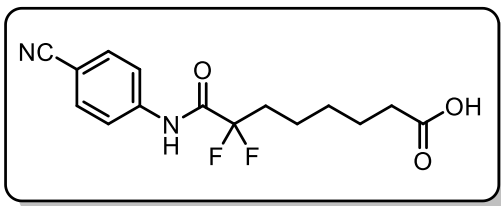
8-((4-Cyanophenyl)amino)-7,7-difluoro-8-oxooctanoic acid, 5.93 (0.258 g, 83%) was prepared according to General Procedure B. The desired compound was obtained as the corresponding carboxylic acid (white solid, mp = 180-182 °C) after treatment with HCl in dioxane (2 M) at 75 °C for 2 h. **¹H NMR** (CD₃OD, 600 MHz) δ ppm 7.91-7.87 (m, 2H), 7.75-7.71 (m, 2H), 2.29 (t, J = 7.4 Hz, 2H), 2.22-2.12 (m, 2H), 1.67-1.59 (m, 2H), 1.57-1.50 (m, 2H), 1.47-1.38 (m, 2H). **¹³C NMR** (CD₃OD, 151 MHz) δ ppm 177.5, 165.3 (t, J = 21 Hz), 143.0, 134.4, 122.3, 119.7, 119.4 (t, J = 252 Hz), 109.3, 35.1 (t, J = 23 Hz), 34.8, 29.8, 25.8, 22.6 (t, J = 4.4 Hz). **¹⁹F NMR** (CD₃OD, 471 MHz) δ ppm -106.8 (t, J = 17.0 Hz, 2F). **FT-IR** (cm⁻¹, neat, ATR) 3285 (v br) 2239 (w), 1718 (m), 1598 (m). **HRMS** (ESI) calcd for $C_{15}H_{17}F_2N_2O_3$ [M + H⁺]: 311.1207, found: 311.1184.

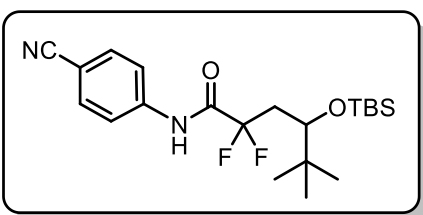**4-((*tert*-Butyldimethylsilyl)oxy)-*N*-(4-cyanophenyl)-2,2-difluoro-5,5-dimethylhexanamide, 5.94** (0.720 g, 75%) was prepared according to General Procedure B. The desired compound was obtained as a dense, colorless oil.

¹H NMR (CDCl₃, 600 MHz) δ ppm 8.14 (br s, 1H), 7.74 (d, J = 8.8 Hz, 2H), 7.67 (d, J = 8.6 Hz, 2H), 3.76 (dd, J = 4.9, 3.2 Hz, 1H), 2.57 (dddd, J = 30.8, 15.7, 12.0, 2.9 Hz, 1H), 2.19 (dddd, J = 31.8, 16.1, 8.1, 5.1 Hz, 1H), 0.90 (s, 9H), 0.89 (s, 9H), 0.09 (s, 6H). **¹³C NMR** (CDCl₃, 151 MHz) δ ppm 162.9 (t, J = 116 Hz), 140.3, 133.7, 120.4, 118.6, 118.0 (t, J_{C-F} = 254 Hz), 109.1, 73.8, 38.7 (t, J = 21.8 Hz), 36.4, 26.4, 26.0, 18.7, -3.0. **¹⁹F NMR** (CDCl₃, 471 MHz) δ ppm -102.55 (ddd, J = 257.0, 31.1, 7.9 Hz, 1F), -104.48 (ddd, J = 257.2, 32.5, 12.1 Hz, 1F). **FT-IR** (cm⁻¹, neat, ATR) 3401 (br), 2957 (m), 2229 (w), 1719 (s), 1532 (s). **HRMS** (ESI) calcd for $C_{21}H_{33}F_2N_2O_2Si$ [M + H⁺]: 411.2279, found: 411.2274.
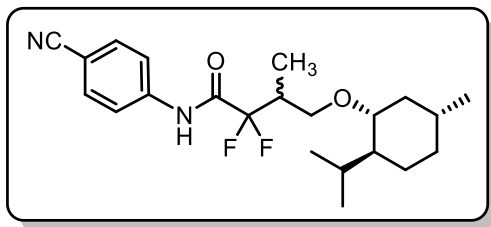
N-(4-Cyanophenyl)-2,2-difluoro-4-(((1R,2S,5R)-2-isopropyl-5-methylcyclohexyl)oxy)-3-methylbutanamide, 5.95 (0.240 g, 61%) was prepared according to General Procedure B. The diastereomeric ratio was determined to be 1.5:1 via crude ^{1}H NMR. The desired compound was obtained as a dense, colorless oil. **^{1}H NMR** (CDCl$_3$, 600 MHz) δ ppm 8.23 and 8.10 (s, 1H), 7.74-7.70 (m, 2H), 7.68-7.65 (m, 2H), 3.77-3.63 (m, 1H), 3.41 and 3.26 (dd, J = 9.7, 5.8 and J = 9.2 and 6.1 Hz, 1H), 3.00-2.94 (m, 1H), 2.88-2.67 (m, 1H), 2.10-1.91 (m, 2H), 1.65-1.45 (m, 2H), 1.33-1.22 (m, 1H), 1.17 and 1.13 (d, J = 7.1 Hz, 3H), 1.07-0.82 (m, 5H), 0.79-0.59 (m, 8H). **^{13}C NMR** (CDCl$_3$, 151 MHz) δ ppm 162.6 (t, J = 35 Hz), 140.7, 140.6, 133.7, 120.2, 120.1, 118.77, 118.75, 108.7, 108.6, 80.2, 80.1, 67.8 and 67.6 (t, J = 4.6 Hz), 48.49, 48.48, 40.4, 40.3, 39.0 and 38.5 (t, J = 22 Hz), 34.8, 34.7, 31.7, 31.6, 25.7, 25.6, 23.32, 23.27, 22.6, 22.5, 21.12, 21.09, 16.3, 16.2, 10.6 and 10.0 (t, J = 4.2 Hz). **^{19}F NMR** (CDCl$_3$, 471 MHz, ^{1}H decoupled) δ ppm -108.0 and -108.6 (dd, J = 76.0, 9.9 Hz, 1F), -114.4 and -119.6 (dd, J = 256.8, 19.6 and J = 254.5, 22.5 Hz, 1F). **FT-IR** (cm^{-1}, neat, ATR) 3315 (br), 2952 (m), 2922 (w), 1717 (m), 1596 (s), 1530 (vs). **HRMS** (ESI) calcd for C$_{22}$H$_{31}$F$_2$N$_2$O$_2$ [M + H$^+$]: 393.2354, found: 393.2359.

5.5.6. Procedure for Large Scale DFA of Ethyl Trifluoroacetate
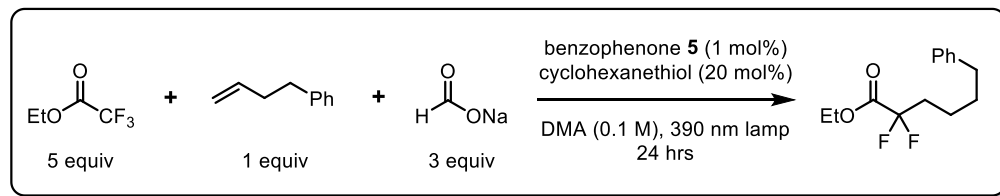
To a 1 L Wheaton standard, wide-mouth bottle was added benzophenone **5** (0.119 g, 0.50 mmol, 0.01 equiv) and sodium formate (10.20 g, 0.15 mol, 3.0 equiv). Anhyd DMF (500 mL) was then added via cannula, the vial sealed with a 24/40 rubber septum, and the reaction solution was sparged with argon for 25 min. Ethyl trifluoroacetate (30 mL, 0.25 mol, 5.0 equiv), cyclohexanethiol (1.20 mL 10.0 mmol, 0.20 equiv), and 4-phenyl-1-butene (6.61 g, 0.05 mol, 1.0 equiv) were added by syringe, and the bottle was sealed with Parafilm. The reaction was then irradiated with two Kessil® PR160-390 nm lamps at a distance of 4 cm. A balloon of argon was then fitted to the reaction (via syringe and 18G needle) for pressure equalization. The reaction was cooled with two compact fans, ensuring that the surface temperature of the vial did not exceed 35 °C (see images below). After 24 h of irradiation, the reaction was quenched slowly with distilled H_2O (250 mL) and extracted with Et_2O (2 x 250 mL). The combined organic extracts were washed with H_2O (250 mL) followed by brine (50 mL), dried (Na_2SO_4), and the solvent was removed via rotary evaporation. The crude material was then purified via short path, high vacuum distillation (bp = 110-114 °C, 0.27 mm Hg) to afford the desired compound as a colorless oil (8.91 g, 0.035 mol, 70%).

Figure 5.12. Reaction set up for large scale DFA.

5.5.7. Quantum Yield Experiments

To confirm the radical chain nature of the DFA mechanism, quantum yield experiments were performed according to the procedure described by Jui *et al*.[27]

Determination of light intensity for 390 nm PR160 Lamp

The photon flux of the light source was determined by standard potassium ferrioxalate actinometry. A 0.15 M soln of potassium ferrioxalate was prepared by dissolving 2.21 g of potassium ferrioxalate hydrate in 30 mL of 0.05 M H_2SO_4. A quenching soln was prepared by dissolving 50 mg of phenanthroline and 11.25 g of NaOAc in 50 mL of 0.5 M H_2SO_4. Both solutions were covered in foil and stored in the dark. A 1 dram septum capped vial was then charged with 2 mL of the ferrioxolate soln and irradiated for 10.0 s with a Kessil PR160 390 nm lamp (100% power) at a distance of exactly 2.0 cm. After irradiation, 0.35 mL of the quenching soln was added to the vial. The soln was then allowed to rest for 30 min in the dark. The

371

absorbance of the soln was measured at 510 nm and compared to that of a non-irradiated standard soln of ferrioxalate. Conversion was calculated using eq 1.

$$\text{mol Fe}^{2+} = \frac{V \times \Delta A}{l \times \varepsilon} \quad \text{(eq 1)}$$

V = final volume of the soln; ΔA = difference in absorbance at 510 nm; l = path length; ε = molar absorptivity of ferrioxalate at 510 nm. The average value of three experiments was 3.707×10^{-6} mol of Fe^{2+}.

The photon flux can then be calculated using eq 2.

$$\text{Photon flux} = \frac{\text{mol Fe}^{2+}}{\phi \times t \times f} \quad \text{(eq 2)}$$

ϕ = quantum yield of ferrioxalate actinometer (1.13 at 390 nm)[11]; t = time ; f = fraction of light absorbed at λ = 390 nm (0.99).[11] The average photon flux was calculated to be 3.31×10^{-7} einsteins s^{-1}

Determination of Quantum Yield for DFA of Ethyl Trifluoroacetate

The quantum yield was determined by irradiating a 0.1 mmol scale DFA reaction using 3-butenyl acetate as the alkene (see General Optimization Procedure) for 10 min. ^{19}F NMR was used to determine the yield (average of three experiments = 27% yield). The quantum yield (ϕ) of the reaction was determined using eq 3.

$$\phi = \frac{\text{mol of product}}{\text{photon flux} \times t \times f} \quad \text{(eq 3)}$$

The fraction of emitted light that is absorbed by benzophenone **5** was determined by integrating the overlap of the absorption of benzopheone **5** and the emission of the PR160 390 nm lamp.
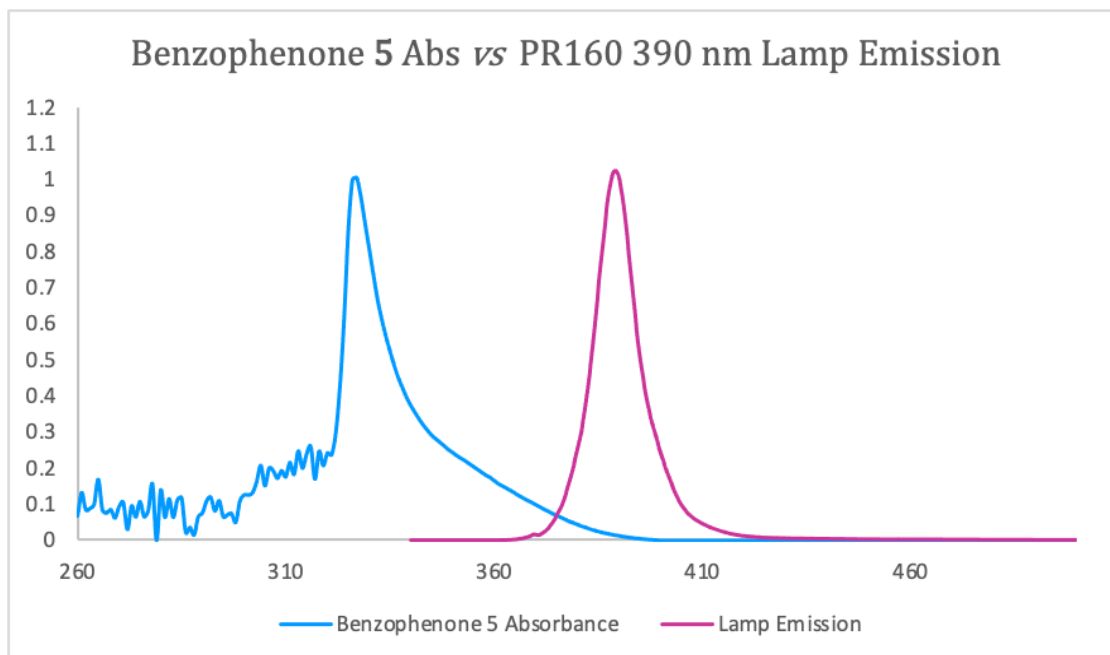
Figure 5.13. Benzophenone **5** absorbance *vs* Kessil Lamp emission.

Based on the overlap between benzophenone **5**'s absorption spectra and the reported emission for the Kessil PR160 390 nm lamp, approximately 5.5% of all light emitted by the lamp is absorbed by benzophenone **5**. The quantum yield was therefore calculated to be 4.94.

$$\phi = \frac{5.40 \times 10^{-5}\ \text{mol}}{3.31 \times 10^{-7}\,\text{E/s} \times 600\ \text{s} \times 0.05} = 4.94$$

5.5.8. Cyclic Voltammetry Studies

Cyclovoltammetry experiments were carried out on a CHI electrochemical workstation using a glassy carbon working electrode, Ag/AgCl pseudoreference electrode, and Pt wire counter electrode. The measurements were taken at room temperature in anhyd DMF containing 0.1 M Bu_4NPF_6 as electrolyte. Voltammograms were calibrated to either $Fe(Cp)_2$ or $Ag(NO_3)$ as internal standards.[12,13]

Ethyl Trifluoroacetate

36 μL (0.30 mmol) of ethyl trifluoroacetate was dissolved in 10 mL of DMF, and 18 mg (0.10 mmol) of $Fe(Cp)_2$ was added as an internal standard. A scan rate of 0.1 V/s was used for the reported voltammogram.

$E_{1/2} = -2.0$ V vs SCE.
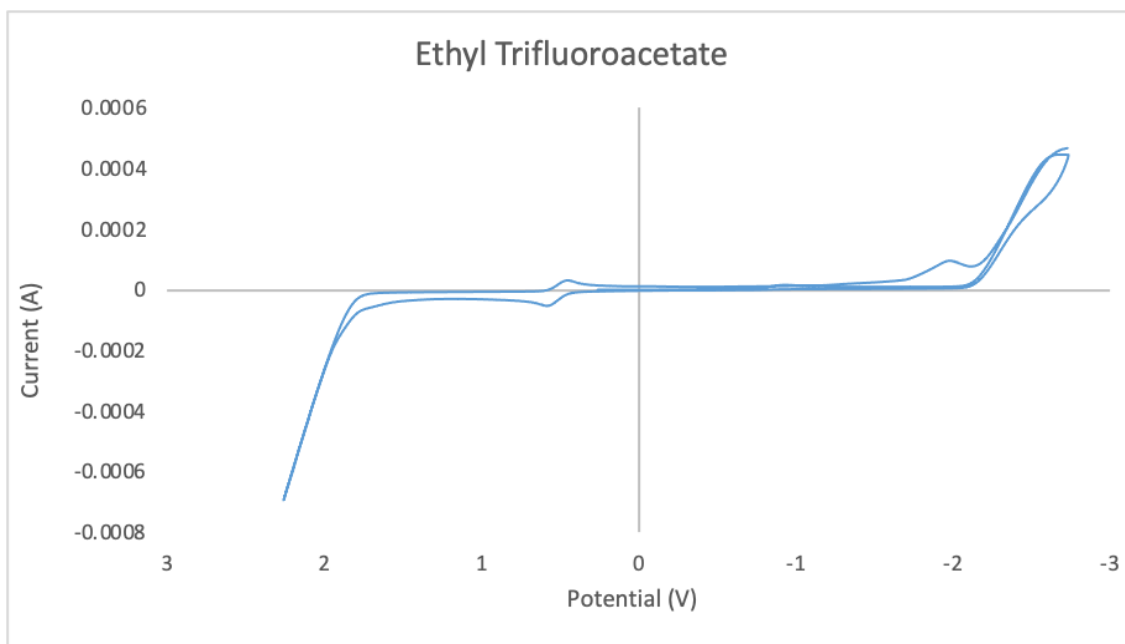
Ethyl Difluoroacetate

35 μL (0.30 mmol) of ethyl difluoroacetate was dissolved in 10 mL of DMF, and 18 mg (0.10 mmol) of Fe(Cp)$_2$ was added as an internal standard. A scan rate of 0.1 V/s was used for the reported voltammogram.

$E_{1/2}$ = -2.9 V vs SCE.

Ethyl Difluoroacetate
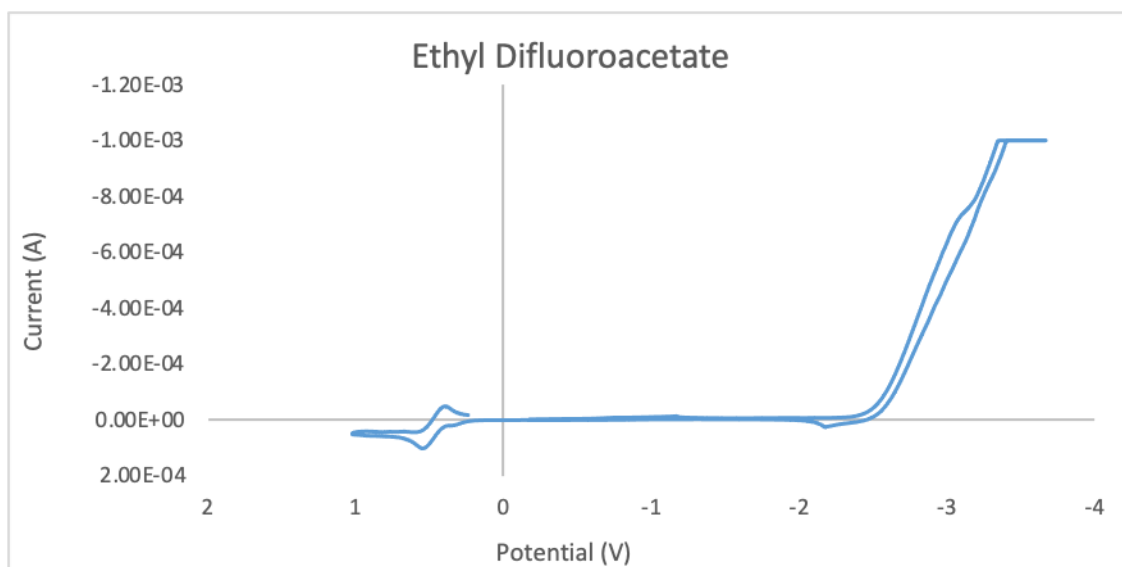
Ethyl Pentafluoropropionate

33 μL (0.30 mmol) of ethyl pentafluoropropionate was dissolved in 10 mL of DMF, and 18 mg (0.10 mmol) of Fe(Cp)$_2$ was added as an internal standard. A scan rate of 0.1 V/s was used for the reported voltammogram.

$E_{1/2}$ = -2.6 V vs SCE.

Ethyl Pentafluoropropionate
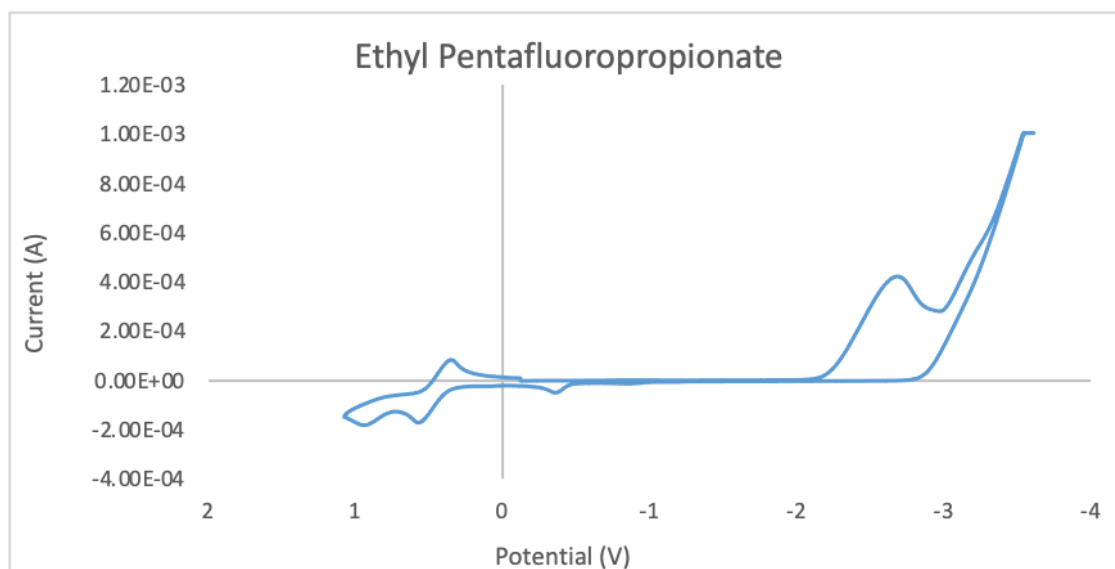
N-(Phenyl)-trifluoroacetamide

56 mg (0.30 mmol) of *N*-(phenyl)-trifluoroacetamide was dissolved in 10 mL of DMF, and 18 mg (0.10 mmol) of Fe(Cp)$_2$ was added as an internal standard. A scan rate of 0.1 V/s was used for the reported voltammogram.

$E_{1/2}$ = -2.7 V vs SCE.

N-Phenyltrifluoroacetamide
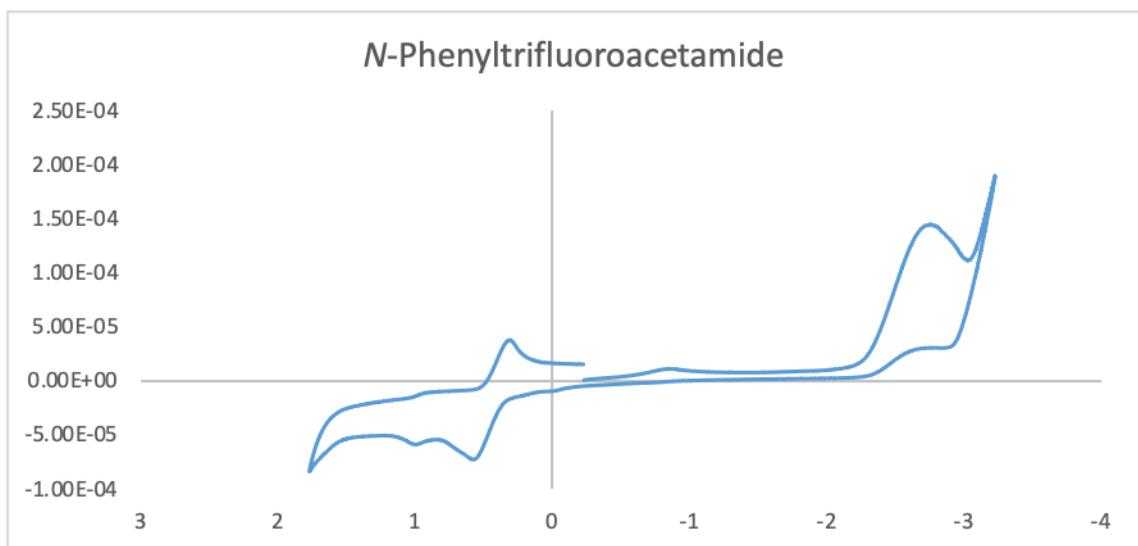
_N_-(3,5-bis(trifluoromethyl)phenyl)-trifluoroacetamide

98 mg of _N_-(phenyl)-trifluoroacetamide was dissolved in 10 mL of DMF, and 18 mg (0.10 mmol) of Fe(Cp)$_2$ was added as an internal standard. A scan rate of 0.1 V/s was used for the reported voltammogram.

$E_{1/2}$ = -2.6 V vs SCE.
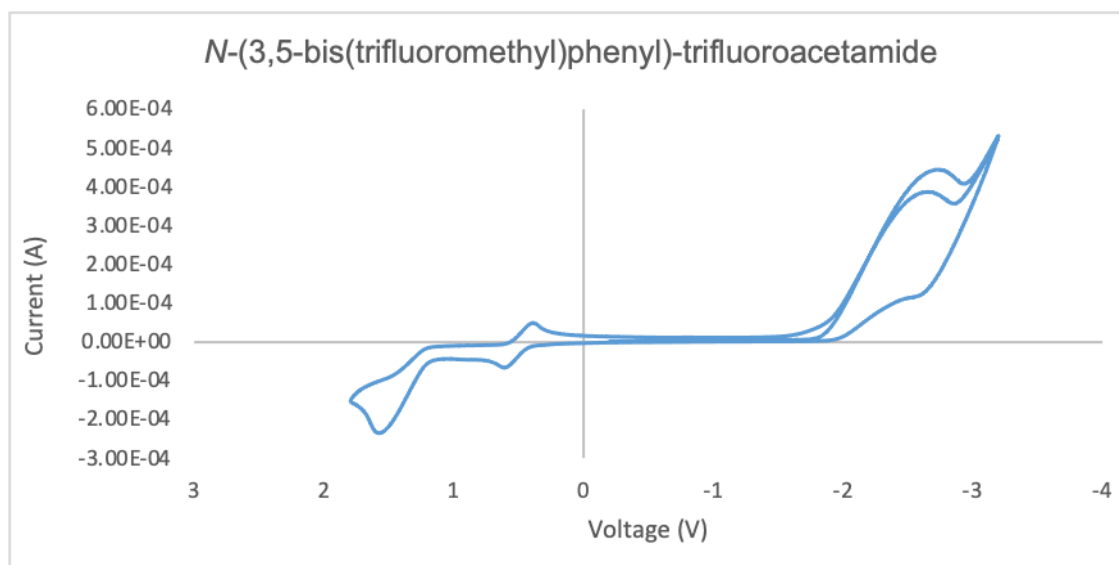
N-(4-Cyanophenyl)-trifluoroacetamide

64 mg (0.30 mmol) of *N*-(4-cyanophenyl)-trifluoroacetamide was dissolved in 10 mL of DMF, and 17 mg (0.10 mmol) of Ag(NO$_3$) was added as an internal standard. After measuring the potential of *N*-(4-cyanophenyl)-trifluoroacetamide, 109 mg (0.30 mmol) of Zn(OTf)$_2$ was added and the measurement was repeated. A scan rate of 0.1 V/s was used for the reported voltammogram.

For *N*-(4-cyanophenyl)-trifluoroacetamide, E$_{1/2}$ = -2.2 V vs SCE

N-(4-cyanophenyl)-trifluoroacetamide
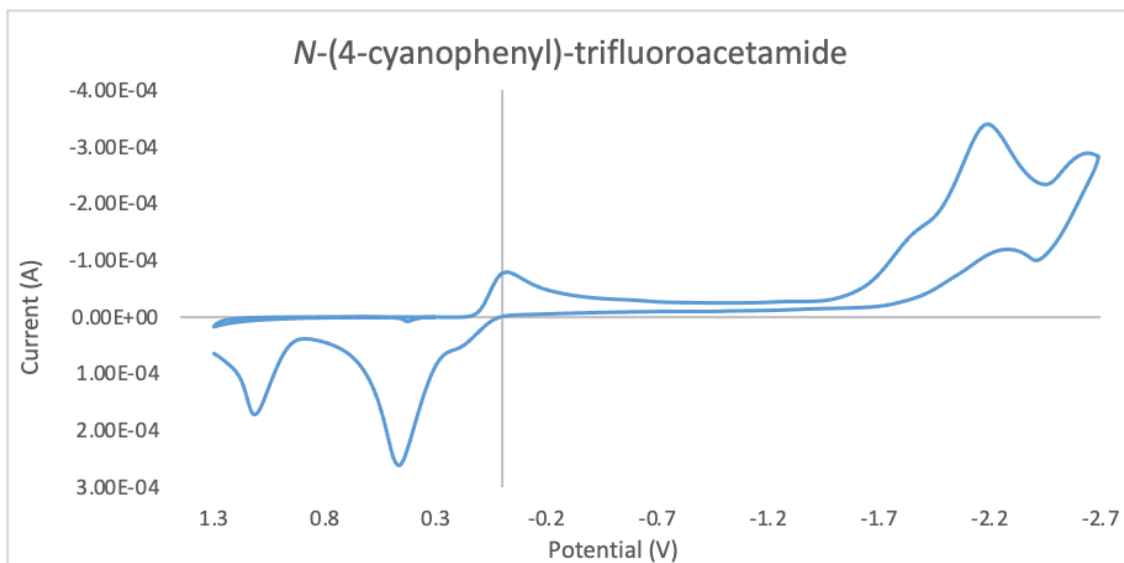
With a 1:1 ratio of *N*-(4-cyanophenyl)-trifluoroacetamide and Zn(OTf)$_2$, E$_{1/2}$ = -1.7 V vs SCE.

N-(4-cyanophenyl)-trifluoroacetamide + Zn(OTf)$_2$
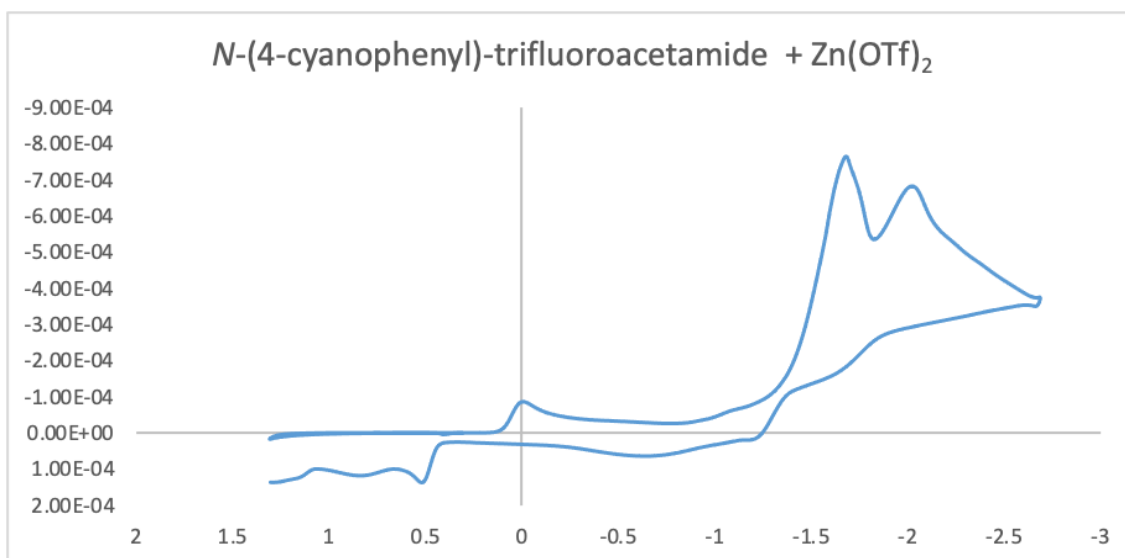
5.6. References

1. Shah, P.; Westwell, A. D. The role of fluorine in medicinal chemistry. *J. Enz. Inhib. Med. Chem.,* **2007**, *22*, 527-540.

2. Bohm, H. J.; Banner, D.; Bendels, S.; Kansy, M.; Kuhn, B.; Muller, K.; Obst-Sander, U.; Stahl, M. Fluorine in medicinal chemistry. *Chembiochem* **2004**, *5*, 637-643.

3. Zhou, Y.; Wang, J.; Gu, Z. N.; Wang, S. N.; Zhu, W.; Acena, J. L.; Soloshonok, V. A.; Izawa, K.; Liu, H. Next Generation of Fluorine-Containing Pharmaceuticals, Compounds Currently in Phase II-III Clinical Trials of Major Pharmaceutical Companies: New Structural Trends and Therapeutic Areas. *Chem. Rev.* **2016**, *116*, 422-518.

4. Meanwell, N. A. Fluorine and Fluorinated Motifs in the Design and Application of Bioisosteres for Drug Design. *J. Med. Chem.,* **2018**, *61*, 5822-5880.

5. Belhomme, M. C.; Besset, T.; Poisson, T.; Pannecoucke, X. Recent Progress toward the Introduction of Functionalized Difluoromethylated Building Blocks onto C(sp(2)) and C(sp) Centers. *Chem. Eur. J.,* **2015**, *21*, 12836-12865.

6. Hu, J. B.; Zhang, W.; Wang, F. Selective difluoromethylation and monofluoromethylation reactions. *Chem. Commun.,* **2009**, *48*, 7465-7478.

7. Nyffeler, P. T.; Duron, S. G.; Burkart, M. D.; Vincent, S. P.; Wong, C. H. Selectfluor: Mechanistic insight and applications. *Angew. Chem. Int. Ed.,* **2005**, *44*, 192-212.

8. Bui, T. T.; Hong, W. P.; Kim, H. K. Recent Advances in Visible Light-mediated Fluorination. *J. Fluor. Chem.,* **2021**, *247*.

9. Fernandes, P.; Martens, E.; Pereira, D. Nature nurtures the design of new semi-synthetic macrolide antibiotics. *J. Antibio.,* **2017**, *70*, 527-533.

10. Middleton, W. J. New fluorinating reagents - dialkylaminosulfur fluorides. *J. Org. Chem.,* **1975**, *40*, 574-578.

11. Sofia, M. J.; Bao, D.; Chang, W.; Du, J. F.; Nagarathnam, D.; Rachakonda, S.; Reddy, P. G.; Ross, B. S.; Wang, P. Y.; Zhang, H. R.; et al. Discovery of a beta-D-2 '-Deoxy-2 '-alpha-fluoro-2 '-beta-C-methyluridine Nucleotide Prodrug (PSI-7977) for the Treatment of Hepatitis C Virus. *J. Med. Chem.,* **2010**, *53*, 7202-7218.

12. Boswell, G. A. Prepn. of vinylene fluoride(s) - by reacting a ketone with a di:substd.-amino-sulphur tri:fluoride, useful as therapeutic agents etc. US4212815-A.

13. Reddy, V. P.; Perambuduru, M.; Alleti, R. Synthetic Approaches to gem-Difluoromethylene Compounds, Advances in Organic Synthesis Modern Organofluorine Chemistry-Synthetic Aspects. Bentham Science Publisher, 2006; pp 327-351.

14. Luo, Y.-R. *Handbook of Bond Dissociation Energies in Organic Compounds*; CRC Press, 2003.

15. Fuchibe, K.; Ohshima, Y.; Mitomi, K.; Akiyama, T. Low-valent niobium-catalyzed reduction of alpha,alpha,alpha-trifluorotoluenes. *Org. Lett.,* **2007**, *9*, 1497-1499.

16. Chen, K.; Berg, N.; Gschwind, R.; Konig, B. Selective Single C(sp(3))-F Bond Cleavage in Trifluoromethylarenes: Merging Visible-Light Catalysis with Lewis Acid Activation. *J. Am. Chem. Soc.,* **2017**, *139*, 18444-18447.

17. Kim, B. C.; Park, A.; An, J. E.; Lee, W. K.; Lee, H. B.; Shin, H. Highly Improved Copper-Mediated Michael Addition of Ethyl Bromodifluoroacetate in the Presence of Protic Additive. *Synthesis-Stuttgart* **2012**, *44*, 3165-3170.

18. Xia, T. T.; He, L.; Liu, Y. H. A.; Hartwig, J. F.; Liao, X. B. Palladium-Catalyzed Cross-Coupling of Ethyl Bromodifluoroacetate with Aryl Bromides or Triflates and Cross-Coupling of Ethyl Bromofluoroacetate with Aryl Iodides. *Org. Lett.,* **2017**, *19*, 2610-2613.

19. Yoshida, M.; Suzuki, D.; Iyoda, M. Practically useful Reformatsky type reactions of chlorodifluoroacetate and bromodifluoroacetate induced by samarium(II) diiodide. *Synth. Commun.,* **1996**, *26*, 2523-2529.

20. Yu, C.; Iqbal, N.; Park, S.; Cho, E. J. Selective difluoroalkylation of alkenes by using visible light photoredox catalysis. *Chem. Commun.,* **2014**, *50*, 12884-12887.

21. Yu, Y. J.; Zhang, F. L.; Peng, T. Y.; Wang, C. L.; Cheng, J.; Chen, C.; Houk, K. N.; Wang, Y. F. Sequential C-F bond functionalizations of trifluoroacetamides and acetates via spin-center shifts. *Science* **2021**, *371*, 1232-1239.

22. Wessig, P.; Muehling, O. Spin-center shift (SCS) - A versatile concept in biological and synthetic chemistry. *Eur. J. Org. Chem.,* **2007**, *14*, 2219-2232.

23. Zhu, D. L.; Young, D. J.; Li, H. X. Carbonyl-Photoredox/Metal Dual Catalysis: Applications in Organic Synthesis. *Synthesis-Stuttgart* **2020**, *52*, 3493-3510.

24. Saveant, J. M.; Nadojo, L.; Lamy, E. Standard potential and kinetic parameters of the electrochemical reduction of carbon dioxide in dimethylformamide. *J. Electroanal. Chem.,* **1977**, *78*, 403-407.

25. Wang, H.; Gao, Y.; Zhou, C.; Li, G. Visible-Light-Driven Reductive Carboarylation of Styrenes with CO_2 and Aryl Halides. *J. Am. Chem. Soc.,* **2020**, *142*, 8122-8129.

26. Chmiel, A. F.; Williams, O. P.; Chernowsky, C. P.; Yeung, C. S.; Wickens, Z. K. Non-innocent Radical Ion Intermediates in Photoredox Catalysis: Parallel Reduction Modes Enable Coupling of Diverse Aryl Chlorides. *J. Am. Chem. Soc.,* **2021**, *143*, 10882-10889.

27. Hendy, C. M.; Smith, G. C.; Xu, Z. H.; Lian, T. Q.; Jui, N. T. Radical Chain Reduction via Carbon Dioxide Radical Anion ($CO_2^{\bullet-}$). *J. Am. Chem. Soc.,* **2021**, *143*, 8987-8992.

28. Vogt, D. B.; Seath, C. P.; Wang, H. B.; Jui, N. T. Selective C-F Functionalization of Unactivated Trifluoromethylarenes. *J. Am. Chem. Soc.,* **2019**, *141*, 13203-13211.

29. Campbell, M. W.; Compton, J. S.; Kelly, C. B.; Molander, G. A. Three-Component Olefin Dicarbofunctionalization Enabled by Nickel/Photoredox Dual Catalysis. *J. Am. Chem. Soc.,* **2019**, *141*, 20069-20078. DOI:

30. Nakajima, T.; Matsugi, T.; Goto, W.; Kageyama, M.; Mori, N.; Matsumura, Y.; Hara, H. New fluoroprostaglandin F-2 alpha derivatives with prostanoid FP-receptor agonistic activity as potent ocular-hypotensive agents. *Bio. Pharm. Bull.,* **2003**, *26*, 1691-1695.

31. Casteels, M.; Foulon, V.; Mannaerts, G. P.; Van Veldhoven, P. P. Alpha-oxidation of 3-methyl-substituted fatty acids and its thiamine dependence. *Eur. J. Biochem.,* **2003**, *270*, 1619-1627.

32. Yin, Z.-B.; Ye, J.-H.; Zhou, W.-J.; Zhang, Y.-H.; Ding, L.; Gui, Y.-Y.; Yan, S.-S.; Li, J.; Yu, D.-G. Oxy-Difluoroalkylation of Allylamines with CO_2 via Visible-Light Photoredox Catalysis. *Org. Lett.,* **2018**, *20*, 190-193.

33. Monteith, E. R.; Mampuys, P.; Summerton, L.; Clark, J. H.; Maes, B. U. W.; McElroy, C. R. Why we might be misusing process mass intensity (PMI) and a methodology to apply it effectively as a discovery level metric. *Green Chem.,* **2020**, *22*, 123-135.

34. Campbell, M. W.; Yuan, M. B.; Polites, V. C.; Gutierrez, O.; Molander, G. A. Photochemical C-H Activation Enables Nickel-Catalyzed Olefin Dicarbofunctionalization. *J. Am. Chem. Soc.,* **2021**, *143*, 3901-3910.

35. Appel, R.; Mayr, H. Quantification of the Electrophilic Reactivities of Aldehydes, Imines, and Enones. *J. Am. Chem. Soc.,* **2011**, *133*, 8240-8251.

36. Nagarapu, L.; Gaikwad, H. K.; Bantu, R.; Manikonda, S. R.; Kumar, C. G.; Pombala, S. Lewis acid-assisted olefin cross-metathesis reaction: an efficient approach for the synthesis of glycosidic-pyrroloquinolinone based novel building blocks of camptothecin and evaluation of their antitumor activity. *Tet. Lett.,* **2012**, *53*, 1287-1291.

37. Zhao, W. J.; Yan, M.; Huang, D.; Ji, S. J. New reaction of enamines with aryldiazoacetates catalyzed by transition metal complexes. *Tetrahedron* **2005**, *61*, 5585-5593.

38. Mereyala, H. B.; Gaddam, B. R. Synthesis of conduritol-a, conduritol-(+)-c and conduritol-(-)-c from d-galactose. *J. Chem. Soc. P. Trans. 1,* **1994**, *15*, 2187-2190.

39. Su, C. C.; Williard, P. G. Isomerization of Allyl Ethers Initiated by Lithium Diisopropylamide. *Org. Lett.,* **2010**, *12*, 5378-5381.

40. Chattopadhyay, S. K.; Ghosh, S.; Sarkar, S.; Bhadra, K. alpha,beta-Didehydrosuberoylanilide hydroxamic acid (DDSAHA) as precursor and possible analogue of the anticancer drug SAHA. *Beilstein J. Org. Chem.,* **2019**, *15*, 2524-2533.

BIBLIOGRAPHY

1. Tomioka, K. Conjugate Addition of Organometallics to Activated Olefins. *ChemInform* **2005**, *36,* 28.

2. Chapdelaine, M. J.; Hulce, M. Tandem Vicinal Difunctionalization: β-Addition to α,β-Unsaturated Carbonyl Substrates Followed by α-Functionalization. *Org. React.,* **1990**, *38*, 227-294.

3. Damon, R. E.; Schlessinger, R. H.; Blount, J. F. A short synthesis of (.+-.)-isostegane. *J. Org. Chem.,* **1976**, *41*, 3772-3773. Luo, F. T.; Negishi, E. Nickel- or palladium-catalyzed cross coupling. 28. A selective synthesis of a mixture of C-15 epimers of (.+-.)-11-deoxyprostaglandin E2 methyl ester. *J. Org. Chem.,* **1985**, *50*, 4762-4766.

4. Domingo, L. R.; Perez, P. Global and local reactivity indices for electrophilic/nucleophilic free radicals. *Org. Biomol. Chem.,* **2013**, *11*, 4350-4358.

5. Giese, B. Formation of C-C bonds by addition of free-radicals to alkenes. *Angew. Chem. Int. Ed.* **1983**, *22*, 753-764.

6. Chatgilialoglu, C.; Ingold, K. U.; Scaiano, J. C. Rate constants and Arrhenius parameters for the reactions of primary, secondary, and tertiary alkyl radicals with tri-n-butyltin hydride. *J. Am. Chem. Soc.,* **1981**, *103*, 7739-7742.

7. Zhang, W. Intramolecular free radical conjugate additions. *Tetrahedron* **2001**, *57*, 7237-7261.

8. Curran, D. P. Comprehensive Organic Synthesis, Vol. 4. Pergamon Press, 1991; pp 715-777.

9. Barton, D. H. R.; McCombie, S. W. A new method for the deoxygenation of secondary alcohols. *J. Chem. Soc., Perkin Transactions,* **975**, 1574-1585.

10. Hu, C. C.; Chen, Y. Y. Chemoselective and fast decarboxylative allylation by photoredox catalysis under mild conditions. *Org. Chem. Front.,* **2015**, *2*, 1352-1355.

11. Schwarz, J.; Konig, B. Metal-free, visible-light-mediated, decarboxylative alkylation of biomass-derived compounds. *Green Chem.,* **2016**, *18*, 4743-4749.

12. Kong, W. G.; Yu, C. J.; An, H. J.; Song, Q. L. Photoredox-Catalyzed Decarboxylative Alkylation of Silyl Enol Ethers To Synthesize Functionalized Aryl Alkyl Ketones. *Org. Lett.* **2018**, *20*, 349-352.

13. Schnermann, M. J.; Overman, L. E. A Concise Synthesis of (-)-Aplyviolene Facilitated by a Strategic Tertiary Radical Conjugate Addition. *Angew. Chem. Int. Ed.,* **2012**, *51*, 9576-9580.

14. Qin, T.; Cornella, J.; Li, C.; Malins, L. R.; Edwards, J. T.; Kawamura, S.; Maxwell, B. D.; Eastgate, M. D.; Baran, P. S. A general alkyl-alkyl cross-coupling enabled by redox-active esters and alkylzinc reagents. *Science,* **2016**, *352*, 801-805.

15. Zheng, C.; Wang, G. Z.; Shang, R. Catalyst-free Decarboxylation and Decarboxylative Giese Additions of Alkyl Carboxylates through Photoactivation of Electron Donor-Acceptor Complex. *Adv. Synth. Catal.,* **2019**, *361*, 4500-4505.

16. Elkhalifa, M.; Elbaum, M. B.; Chenoweth, D. M.; Molander, G. A. Solid-Phase Photochemical Decarboxylative Hydroalkylation of Peptides. *Org. Lett.,* **2021**, ASAP.

17. Sumino, S.; Ryu, I. Hydroalkylation of Alkenes Using Alkyl Iodides and Hantzsch Ester under Palladium/Light System. *Org. Lett.* **2016**, *18*, 52-55.

18. Nguyen, J. D.; D'Amato, E. M.; Narayanam, J. M. R.; Stephenson, C. R. J. Engaging unactivated alkyl, alkenyl and aryl iodides in visible-light-mediated free radical reactions. *Nat. Chem.,* **2012**, *4*, 854-859.

19. Giedyk, M.; Narobe, R.; Weiss, S.; Touraud, D.; Kunz, W.; Koenig, B. Photocatalytic activation of alkyl chlorides by assembly-promoted single electron transfer in microheterogeneous solutions. *Nat. Catal.,* **2020**, *3*, 40-47.

20. Andrews, R. S.; Becker, J. J.; Gagne, M. R. Intermolecular Addition of Glycosyl Halides to Alkenes Mediated by Visible Light. *Angew. Chem. Int. Ed.,* **2010**, *49*, 7274-7276.

21. Giese, B.; Dupuis, J. Diastereoselektive Synthese von C-Glycopyranosiden. *Angew. Chem. Int. Ed.* **1983**, *95*, 8.

22. Aycock, R. A.; Wang, H.; Jui, N. T. A mild catalytic system for radical conjugate addition of nitrogen heterocycles. *Chem. Sci.,* **2017**, *8*, 3121-3125. Aycock, R. A.; Vogt, D. B.; Jui, N. T. A practical and scalable system for heteroaryl amino acid synthesis. *Chem. Sci.,* **2017**, *8*, 7998-8003.

23. ElMarrouni, A.; Ritts, C. B.; Balsells, J. Silyl-mediated photoredox-catalyzed Giese reaction: addition of non-activated alkyl bromides. *Chem. Sci.,* **2018**, *9*, 6639-6646.

24. Wiles, R. J.; Phelan, J. P.; Molander, G. A. Metal-free defluorinative arylation of trifluoromethyl alkenes via photoredox catalysis. *Chem. Commun.,* **2019**, *55*, 7599-7602.

25. Diccianni, J.; Lin, Q.; Diao, T. Mechanisms of Nickel-Catalyzed Coupling Reactions and Applications in Alkene Functionalization. *Acc. Chem. Res.,* **2020**, *53*, 906-919. Green, S. A.; Huffman, T. R.; McCourt, R. O.; van der Puyl, V.; Shenvi, R. A. Hydroalkylation of Olefins To Form Quaternary Carbons. *J. Am. Chem. Soc.,* **2019**, *141*, 7709-7714.

26. Dong, J. Y.; Wang, X. C.; Wang, Z.; Song, H. J.; Liu, Y. X.; Wang, Q. M. Visible-light-initiated manganese-catalyzed Giese addition of unactivated alkyl iodides to electron-poor olefins. *Chem. Commun.,* **2019**, *55*, 11707-11710.

27. Nicewicz, D. A.; MacMillan, D. W. C. Merging photoredox catalysis with organocatalysis: The direct asymmetric alkylation of aldehydes. *Science,* **2008**, *322*, 77-80.

28. Yasu, Y.; Koike, T.; Akita, M. Visible Light-Induced Selective Generation of Radicals from Organoborates by Photoredox Catalysis. *Adv. Synth. Catal.,* **2012**, *354*, 3414-3420.

29. Miyazawa, K.; Koike, T.; Akita, M. Hydroaminomethylation of Olefins with Aminomethyltrifluoroborate by Photoredox Catalysis. *Adv. Synth. Catal.* **2014**, *356*, 2749-2755.

30. Chinzei, T.; Miyazawa, K.; Yasu, Y.; Koike, T.; Akita, M. Redox-economical radical generation from organoborates and carboxylic acids by organic photoredox catalysis. *RSC Adv.,* **2015**, *5*, 21297-21300.

31. Lang, S. B.; Wiles, R. J.; Kelly, C. B.; Molander, G. A. Photoredox Generation of Carbon-Centered Radicals Enables the Construction of 1,1-Difluoroalkene Carbonyl Mimics. *Angew. Chem. Int. Ed.,* **2017**, *56*, 15073-15077.

32. Wu, Z.; Gockel, S. N.; Hull, K. L. Anti-Markovnikov hydro(amino)alkylation of vinylarenes via photoredox catalysis. *Nat. Commun.,* **2021**, *12*, 5956-5965.

33. Huo, H.; Harms, K.; Meggers, E. Catalytic, Enantioselective Addition of Alkyl Radicals to Alkenes via Visible-Light-Activated Photoredox Catalysis with a Chiral Rhodium Complex. *J. Am. Chem. Soc.,* **2016**, *138*, 6936-6939.

34. Gualandi, A.; Matteucci, E.; Monti, F.; Baschieri, A.; Armaroli, N.; Sambri, L.; Cozzi, P. G. Photoredox radical conjugate addition of dithiane-2-carboxylate promoted by an iridium(III) phenyl-tetrazole complex: a formal radical methylation of Michael acceptors. *Chem. Sci.,* **2017**, *8*, 1613-1620.

35. Zhang, S.; Tan, Z. M.; Zhang, H. N.; Liu, J. L.; Xu, W. T.; Xu, K. An Ir-photoredox-catalyzed decarboxylative Michael addition of glyoxylic acid acetal as a formyl equivalent. *Chem. Commun.,* **2017**, *53*, 11642-11645.

36. Bloom, S.; Liu, C.; Kolmel, D. K.; Qiao, J. X.; Zhang, Y.; Poss, M. A.; Ewing, W. R.; MacMillan, D. W. C. Decarboxylative alkylation for site-selective bioconjugation of native proteins via oxidation potentials. *Nat. Chem.,* **2018**, *10*, 205-211.

37. Nakajima, K.; Kitagawa, M.; Ashida, Y.; Miyake, Y.; Nishibayashi, Y. Synthesis of nitrogen heterocycles via alpha-aminoalkyl radicals generated from alpha-silyl secondary amines under visible light irradiation. *Chem. Commun.,* **2014**, *50*, 8900-8903.

38. Remeur, C.; Kelly, C. B.; Patel, N. R.; Molander, G. A. Aminomethylation of Aryl Halides Using α-Silylamines Enabled by Ni/Photoredox Dual Catalysis. *ACS Catal.,* **2017**, *7*, 6065-6069.

39. Nawrat, C. C.; Jamison, C. R.; Slutskyy, Y.; MacMillan, D. W. C.; Overman, L. E. Oxalates as Activating Groups for Alcohols in Visible Light Photoredox Catalysis: Formation of Quaternary Centers by Redox-Neutral Fragment Coupling. *J. Am. Chem. Soc.,* **2015**, *137*, 11270-11273.

40. Slutskyy, Y.; Jamison, C. R.; Lackner, G. L.; Müller, D. S.; Dieskau, A. P.; Untiedt, N. L.; Overman, L. E. Short Enantioselective Total Syntheses of trans-Clerodane Diterpenoids: Convergent Fragment Coupling Using a trans-Decalin Tertiary Radical Generated from a Tertiary Alcohol Precursor. *J. Org. Chem.,* **2016**, *81*, 7029-7035.

41. Abbas, S. Y.; Zhao, P.; Overman, L. E. 1,6-Addition of Tertiary Carbon Radicals Generated From Alcohols or Carboxylic Acids by Visible-Light Photoredox Catalysis. *Org. Lett.* **2018**, *20*, 868-871.

42. Deng, H.-P.; Fan, X.-Z.; Chen, Z.-H.; Xu, Q.-H.; Wu, J. Photoinduced Nickel-Catalyzed Chemo- and Regioselective Hydroalkylation of Internal Alkynes with Ether and Amide α-Hetero C(sp3)–H Bonds. *J. Am. Chem. Soc.,* **2017**, *139*, 13579-13584.

43. Ashley, M. A.; Yamauchi, C.; Chu, J. C. K.; Otsuka, S.; Yorimitsu, H.; Rovis, T. Photoredox-Catalyzed Site-Selective alpha-C(sp(3))-H Alkylation of Primary Amine Derivatives. *Angew. Chem. Int. Ed.,* **2019**, *58*, 4002-4006.

44. Laudadio, G.; Deng, Y. C.; van der Wal, K.; Ravelli, D.; Nuno, M.; Fagnoni, M.; Guthrie, D.; Sun, Y. H.; Noel, T. C(sp(3))-H functionalizations of light hydrocarbons using decatungstate photocatalysis in flow. *Science* **2020**, *369*, 92-98.

45. Lei, G.; Xu, M.; Chang, R.; Funes-Ardoiz, I.; Ye, J. Hydroalkylation of Unactivated Olefins via Visible-Light-Driven Dual Hydrogen Atom Transfer Catalysis. *J. Am. Chem. Soc.,* **2021**, *143*, 11251-11261.

46. Abadie, B.; Jardel, D.; Pozzi, G.; Toullec, P.; Vincent, J. M. Dual Benzophenone/Copper-Photocatalyzed Giese-Type Alkylation of C(sp(3))-H Bonds. *Chem. Eur. J.,* **2019**, *25*, 16120-16127.

47. Tellis, J. C.; Primer, D. N.; Molander, G. A. Single-electron transmetalation in organoboron cross-coupling by photoredox/nickel dual catalysis. *Science,* **2014**, *345*, 433-436.

48. Zuo, Z. W.; Ahneman, D. T.; Chu, L. L.; Terrett, J. A.; Doyle, A. G.; MacMillan, D. W. C. Merging photoredox with nickel catalysis: Coupling of alpha-carboxyl sp(3)-carbons with aryl halides. *Science,* **2014**, *345*, 437-440.

49. Garbarino, S.; Ravelli, D.; Protti, S.; Basso, A. Photoinduced Multicomponent Reactions. *Angew. Chem. Int. Ed.,* **2016**, *55*, 15476-15484.

50. Bohm, H. J.; Banner, D.; Bendels, S.; Kansy, M.; Kuhn, B.; Muller, K.; Obst-Sander, U.; Stahl, M. Fluorine in medicinal chemistry. *Chembiochem* **2004**, *5* (5), 637-643.

51. Meanwell, N. A. Fluorine and Fluorinated Motifs in the Design and Application of Bioisosteres for Drug Design. *J. Med. Chem.,* **2018**, *61*, 5822-5880.

52. Narjes, F.; Koehler, K. F.; Koch, U.; Gerlach, B.; Colarusso, S.; Steinkuhler, C.; Brunetti, M.; Altamura, S.; De Francesco, R.; Matassa, V. G. A designed P-1 cysteine mimetic for covalent and non-covalent inhibitors of HCVNS3 protease. *Bioorg. Med. Chem. Lett.,* **2002**, *12*, 701-704.

53. Zafrani, Y.; Yeffet, D.; Sod-Moriah, G.; Berliner, A.; Amir, D.; Marciano, D.; Gershonov, E.; Saphier, S. Difluoromethyl Bioisostere: Examining the "Lipophilic Hydrogen Bond Donor" Concept. *J. Med. Chem.,* **2017**, *60*, 797-804.

54. Mei, H. B.; Han, J. L.; Klika, K. D.; Izawa, K.; Sato, T.; Meanwell, N. A.; Soloshonok, V. A. Applications of fluorine-containing amino acids for drug design. *Eur. J. Med. Chem.,* **2020**, *186,* 111826.

55. Moschner, J.; Stulberg, V.; Fernandes, R.; Huhmann, S.; Leppkes, J.; Koksch, B. Approaches to Obtaining Fluorinated alpha-Amino Acids. *Chem. Rev.,* **2019**, *119*, 10718-10801.

56. Ulbrich, D.; Daniliuc, C. G.; Haufe, G. Synthesis of alpha,omega-polyfluorinated alpha-amino acid derivatives and delta,delta-difluoronorvaline. *Org. Biomol. Chem.,* **2016**, *14*, 2755-2767.

57. Baba, D.; Fuchigami, T. Electrolytic partial fluorination of organic compounds. Part 61: The first example of direct alpha-fluorination of protected alpha-amino acids. *Tet. Lett.,* **2002**, *43*, 4805-4808.

58. Bailey, P. D.; Baker, S. R.; Boa, A. N.; Clayson, J.; Rosair, G. M. Synthesis of alpha-heterosubstituted glycine derivatives from dihaloethanamides. *Tet. Lett.,* **1998**, *39*, 7755-7758.

59. Kwiatkowski, J.; Lu, Y. X. Asymmetric Michael addition of alpha-fluoro-alpha-nitro esters to nitroolefins: towards synthesis of alpha-fluoro-alpha-substituted amino acids. *Org. Biomol. Chem.,* **2015**, *13*, 2350-2359.

60. Bloom, S.; Liu, C.; Kolmel, D. K.; Qiao, J. X.; Zhang, Y.; Poss, M. A.; Ewing, W. R.; MacMillan, D. W. C. Decarboxylative alkylation for site-selective bioconjugation of native proteins via oxidation potentials. *Nat. Chem.,* **2018**, *10*, 205-211.

61. Vara, B. A.; Li, X. P.; Berritt, S.; Walters, C. R.; Petersson, E. J.; Molander, G. A. Scalable thioarylation of unprotected peptides and biomolecules under Ni/photoredox catalysis. *Chem. Sci.,* **2018**, *9*, 336-344.

62. Wright, T. H.; Bower, B. J.; Chalker, J. M.; Bernardes, G. J. L.; Wiewiora, R.; Ng, W. L.; Raj, R.; Faulkner, S.; Vallee, M. R. J.; Phanumartwiwath, A.; et al. Posttranslational mutagenesis: A chemical strategy for exploring protein side-chain diversity. *Science* **2016**, *354*, 6312.

63. Yang, A.; Ha, S.; Ahn, J.; Kim, R.; Kim, S.; Lee, Y.; Kim, J.; Soll, D.; Lee, H. Y.; Park, H. S. A chemical biology route to site-specific authentic protein modifications. *Science* **2016**, *354*, 623-626.

64. Aycock, R. A.; Vogt, D. B.; Jui, N. T. A practical and scalable system for heteroaryl amino acid synthesis. *Chem. Sci.,* **2017**, *8*, 7998-8003.

65. de Bruijn, A. D.; Roelfes, G. Chemical Modification of Dehydrated Amino Acids in Natural Antimicrobial Peptides by Photoredox Catalysis. *Chem. Eur. J.,* **2018**, *24*, 11314-11318.

66. Liu, Z. L.; Chen, H.; Lv, Y.; Tan, X. Q.; Shen, H. G.; Yu, H. Z.; Li, C. Z. Radical Carbofluorination of Unactivated Alkenes with Fluoride Ions. *J. Am. Chem. Soc.,* **2018**, *140*, 6169-6175.

67. Fukuzumi, S.; Kotani, H.; Ohkubo, K.; Ogo, S.; Tkachenko, N. V.; Lemmetyinen, H. Electron-transfer state of 9-mesityl-10-methylacridinium ion with a much longer lifetime and higher energy than that of the natural photosynthetic reaction center. *J. Am. Chem. Soc.,* **2004**, *126*, 1600-1601.

68. Matsui, J. K.; Primer, D. N.; Molander, G. A. Metal-free C-H alkylation of heteroarenes with alkyltrifluoroborates: a general protocol for 1 degrees, 2 degrees and 3 degrees alkylation. *Chem. Sci.,* **2017**, *8*, 3512-3522.

69. Fleeman, R.; LaVoi, T. M.; Santos, R. G.; Morales, A.; Nefzi, A.; Wemaker, G. S.; Medina-Franco, J. L.; Giulianotti, M. A.; Houghten, R. A.; Shaw, L. N. Combinatorial Libraries As a Tool for the Discovery of Novel, Broad-Spectrum Antibacterial Agents Targeting the ESKAPE Pathogens. *J. Med. Chem.,* **2015**, *58*, 3340-3355.

70. Xin, B. T.; Huber, E. M.; de Bruin, G.; Heinemeyer, W.; Maurits, E.; Espinal, C.; Du, Y. M.; Janssens, M.; Weyburne, E. S.; Kisselev, A. F.; et al. Structure-Based Design of Inhibitors Selective for Human Proteasome beta 2c or beta 2i Subunits. *J. Med. Chem.,* **2019**, *62*, 1626-1642.

71. Venkatraman, S.; Bogen, S. L.; Arasappan, A.; Bennett, F.; Chen, K.; Jao, E.; Liu, Y. T.; Lovey, R.; Hendrata, S.; Huang, Y. H.; et al. Discovery of (1R, 5S)-N- 3-amino-1-(cyclobutylmethyl)-2,3-dioxopropyl -3- 2(S)- (1,1-dim ethylethyl)amino carbonyl amino -3,3-dimethyl-1-oxobutyl -6,6-dimethyl-3 -azabicyclo 3.1.0 hexan-2(S)-carboxamide (SCH 503034), a selective, potent, orally bioavailable hepatitis C virus NS3 protease inhibitor: A potential therapeutic agent for the treatment of hepatitis C infection. *J. Med. Chem.,* **2006**, *49*, 6074-6086.

72. De Vleeschouwer, F.; Van Speybroeck, V.; Waroquier, M.; Geerlings, P.; De Proft, F. Electrophilicity and nucleophilicity index for radicals. *Org. Lett.,* **2007**, *9*, 2721-2724.

73. Parsaee, F.; Senarathna, M. C.; Kannangara, P. B.; Alexander, S. N.; Arche, P. D. E.; Welin, E. R. Radical philicity and its role in selective organic transformations. *Nat. Rev. Chem.,* **2021**, *5*, 486-499.

74. Hu, H.; Lu, Z. Y.; Yang, W. T. Fitting molecular electrostatic potentials from quantum mechanical calculations. *J. Chem. Theo. Comput.,* **2007**, *3*, 1004-1013.

75. Patel, N. R.; Kelly, C. B.; Jouffroy, M.; Molander, G. A. Engaging Alkenyl Halides with Alkylsilicates via Photoredox Dual Catalysis. *Org. Lett.,* **2016**, *18*, 764-767.

76. Wilger, D. J.; Grandjean, J. M. M.; Lammert, T. R.; Nicewicz, D. A. The direct anti-Markovnikov addition of mineral acids to styrenes. *Nat. Chem.,* **2014**, *6*, 720-726.

77. Molander, G. A.; McKee, S. A. Copper-Catalyzed beta-Boration of alpha,beta-Unsaturated Carbonyl Compounds with Tetrahydroxydiborane. *Org. Lett.,* **2011**, *13*, 4684-4687.

78. M. T. Ferreira, P.; L. S. Maia, H.; S. Monteiro, L.; Sacramento, J. High yielding synthesis of dehydroamino acid and dehydropeptide derivatives. *J. Chem. Soc. Per. Trans.,* **1999**, *24*, 3697-3703.

79. Ulbrich, D.; Daniliuc, C. G.; Haufe, G. Halofluorination of N-protected alpha,beta-dehydro-alpha-amino acid esters-A convenient synthesis of alpha-fluoro-alpha-amino acid derivatives. *J. Fluor. Chem.,* **2016**, *188*, 65-75.

80. Devlin, F. J.; Finley, J. W.; Stephens, P. J.; Frisch, M. J. Ab Initio Calculation of Vibrational Absorption and Circular Dichroism Spectra Using Density Functional Force Fields: A Comparison of Local, Nonlocal, and Hybrid Density Functionals. *J. Phys. Chem.,* **1995**, *99*, 16883-16902. =

81. Petersson, G. A.; Allaham, M. A. A complete basis set model chemistry II. open-shell systems and the total energies of the 1st-row atoms. *J. Chem. Phys.,* **1991**, *94*, 6081-6090.

82. Chapdelaine, M. J.; Hulce, M. Tandem Vicinal Difunctionalization: β-Addition to α,β-Unsaturated Carbonyl Substrates Followed by α-Functionalization. *Org. React.,* **1990**, *38*, 227-294.

83. Luo, F. T.; Negishi, E. Nickel- or palladium-catalyzed cross coupling. 28. A selective synthesis of a mixture of C-15 epimers of (.+-.)-11-deoxyprostaglandin E2 methyl ester. *J. Org. Chem.,* **1985**, *50*, 4762-4766.

84. Catellani, M.; Chiusoli, G. P. One-pot palladium-catalyzed synthesis of 2,3-disubstituted bicyclo 2.2.1 heptanes and bicyclo 2.2.1 hept-5-enes. *Tet. Lett.,* **1982**, *23*, 4517-4520.

85. Kosugi, M.; Tamura, H.; Sano, H.; Migita, T. Palladium-catalyzed reaction of organic halides with organotin compounds involving olefin insertion - synthesis of 2,3-di-substituted norboranes. *Tetrahedron,* **1989**, *45*, 961-967.

86. Wu, X.; Lin, H.-C.; Li, M.-L.; Li, L.-L.; Han, Z.-Y.; Gong, L.-Z. Enantioselective 1,2-Difunctionalization of Dienes Enabled by Chiral Palladium Complex-Catalyzed Cascade Arylation/Allylic Alkylation Reaction. *Journal of the American Chemical Society* **2015**, *137* (42), 13476-13479. DOI: 10.1021/jacs.5b08734.

87. Saini, V.; Liao, L. Y.; Wang, Q. F.; Jana, R.; Sigman, M. S. Pd(0)-Catalyzed 1,1-Diarylation of Ethylene and Allylic Carbonates. *Org. Lett.,* **2013**, *15*, 5008-5011.

88. Tasker, S. Z.; Standley, E. A.; Jamison, T. F. Recent advances in homogeneous nickel catalysis. *Nature,* **2014**, *509*, 299-309.

89. Diccianni, J.; Lin, Q.; Diao, T. Mechanisms of Nickel-Catalyzed Coupling Reactions and Applications in Alkene Functionalization. *Acc. Chem. Res.,* **2020**, *53*, 906-919.

90. Lin, B. L.; Liu, L.; Fu, Y.; Luo, S. W.; Chen, Q.; Guo, Q. X. Comparing nickel- and palladium-catalyzed Heck reactions. *Organometal.,* **2004**, *23*, 2114-2123.

91. Qi, X. X.; Diao, T. N. Nickel-Catalyzed Dicarbofunctionalization of Alkenes. *ACS Catal.,* **2020**, *10*, 8542-8556.

92. Derosa, J.; Apolinar, O.; Kang, T.; Tran, V. T.; Engle, K. M. Recent developments in nickel-catalyzed intermolecular dicarbofunctionalization of alkenes. *Chem. Sci.,* **2020**, *11*, 4287-4296.

93. Shrestha, B.; Basnet, P.; Dhungana, R. K.; Shekhar, K. C.; Thapa, S.; Sears, J. M.; Giri, R. Ni-Catalyzed Regioselective 1,2-Dicarbofunctionalization of Olefins by Intercepting Heck Intermediates as Imine-Stabilized Transient Metallacycles. *J. Am. Chem. Soc.,* **2017**, *139*, 10653-10656.

94. Basnet, P.; Dhungana, R. K.; Thapa, S.; Shrestha, B.; Shekhar, K. C.; Sears, J. M.; Giri, R. Ni-Catalyzed Regioselective beta,delta-Diarylation of Unactivated Olefins in Ketimines via Ligand-Enabled Contraction of Transient Nickellacycles: Rapid Access to Remotely Diarylated Ketones. *J. Am. Chem. Soc.,* **2018**, *140*, 7782-7786.

95. Derosa, J.; Tran, V. T.; Boulous, M. N.; Chen, J. S.; Engle, K. M. Nickel-Catalyzed beta,gamma-Dicarbofunctionalization of Alkenyl Carbonyl Compounds via Conjunctive Cross-Coupling. *J. Am. Chem. Soc.,* **2017**, *139*, 10657-10660.

96. Bour, J. R.; Camasso, N. M.; Meucci, E. A.; Kampf, J. W.; Canty, A. J.; Sanford, M. S. Carbon-Carbon Bond-Forming Reductive Elimination from Isolated Nickel(III) Complexes. *J. Am. Chem. Soc.,* **2016**, *138*, 16105-16111.

97. Garcia-Dominguez, A.; Li, Z. D.; Nevado, C. Nickel-Catalyzed Reductive Dicarbofunctionalization of Alkenes. *J. Am. Chem. Soc.,* **2017**, *139*, 6835-6838.

98. Zhao, X.; Tu, H. Y.; Guo, L.; Zhu, S. Q.; Qing, F. L.; Chu, L. L. Intermolecular selective carboacylation of alkenes via nickel-catalyzed reductive radical relay. *Nat. Commun.,* **2018**, *9*.

99. Tu, H. Y.; Wang, F.; Huo, L. P.; Li, Y. B.; Zhu, S. Q.; Zhao, X.; Li, H.; Qing, F. L.; Chu, L. L. Enantioselective Three-Component Fluoroalkylarylation of Unactivated Olefins through Nickel-Catalyzed Cross-Electrophile Coupling. *J. Am. Chem. Soc.,* **2020**, *142*, 9604-9611.

100. Yuan, M. B.; Song, Z. H.; Badir, S. O.; Molander, G. A.; Gutierrez, O. On the Nature of C(sp(3))-C(sp(2)) Bond Formation in Nickel-Catalyzed Tertiary Radical Cross-Couplings: A Case Study of Ni/Photoredox Catalytic Cross-Coupling of Alkyl Radicals and Aryl Halides. *J. Am. Chem. Soc.,* **2020**, *142*, 7225-7234.

101. Primer, D. N.; Molander, G. A. Enabling the Cross-Coupling of Tertiary Organoboron Nucleophiles through Radical-Mediated Alkyl Transfer. *J. Am. Chem. Soc.,* **2017**, *139*, 9847-9850.

102. Fawcett, A.; Pradeilles, J.; Wang, Y.; Mutsuga, T.; Myers, E. L.; Aggarwal, V. K. Photoinduced decarboxylative borylation of carboxylic acids. *Science,* **2017**, *357*, 283-286.

103. Bose, S. K.; Brand, S.; Omoregie, H. O.; Haehnel, M.; Maier, J.; Bringmann, G.; Marder, T. B. Highly Efficient Synthesis of Alkylboronate Esters via Cu(II)-Catalyzed Borylation of Unactivated Alkyl Bromides and Chlorides in Air. *ACS Catal.,* **2016**, *6*, 8332-8335.

104. Noble, A.; Mega, R. S.; Pflasterer, D.; Myers, E. L.; Aggarwal, V. K. Visible-Light-Mediated Decarboxylative Radical Additions to Vinyl Boronic Esters: Rapid Access to gamma-Amino Boronic Esters. *Angew. Chem. Int. Ed.,* **2018**, *57*, 2155-2159.

105. Dick, G. R.; Woerly, E. M.; Burke, M. D. A General Solution for the 2-Pyridyl Problem. *Angew. Chem. Int. Ed.,* **2012**, *51*, 2667-2672.

106. De Vleeschouwer, F.; Van Speybroeck, V.; Waroquier, M.; Geerlings, P.; De Proft, F. Electrophilicity and nucleophilicity index for radicals. *Org. Lett.,* **2007**, *9*, 2721-2724.

107. Parsaee, F.; Senarathna, M. C.; Kannangara, P. B.; Alexander, S. N.; Arche, P. D. E.; Welin, E. R. Radical philicity and its role in selective organic transformations. *Nat. Rev. Chem.,* **2021**, *5*, 486-499.

108. Studer, A. The persistent radical effect in organic synthesis. *Chem. Eur. J.,* **2001**, *7*, 1159-1164.

109. Tutkowski, B.; Meggers, E.; Wiest, O. Understanding Rate Acceleration and Stereoinduction of an Asymmetric Giese Reaction Mediated by a Chiral Rhodium Catalyst. *J. Am. Chem. Soc.,* **2017**, *139*, 8062-8065.

110. Martinez-Botella, G.; Breen, J. N.; Duffy, J. E. S.; Dumas, J.; Geng, B. L.; Gowers, I. K.; Green, O. M.; Guler, S.; Hentemann, M. F.; Hernandez-Juan, F. A.; et al. Discovery of Selective and Potent Inhibitors of Gram-Positive Bacterial Thymidylate Kinase (TMK). *J. Med. Chem.,* **2012**, *55*, 10010-10021.

111. Beckwith, A. L. J.; Schiesser, C. H. Regio-selectivity and stereo-selectivity of alkenyl radical ring-closure - a theoretical-study. *Tetrahedron,* **1985**, *41*, 3925-3941.

112. Fernandez-Mateos, A.; Teijon, P. H.; Clemente, R. R.; Gonzalez, R. R. A Radical Clock for Reactions of Epoxy Derivatives Induced by Titanocene Chloride. *Synlett,* **2008**, (20), 3208-3212.

113. For information on this reactor and its construction see the Photochemical Reactor Design of the Supporting Information of: Remeur, C.; Kelly, C. B.; Patel, N. R.; Molander, G. A. Aminomethylation of Aryl Halides Using α-Silylamines Enabled by Ni/Photoredox Dual Catalysis. *ACS Catal.* **2017**, *7*,6065.

114. Kelly, C. B.; Patel, N. R.; Primer, D. N.; Jouffroy, M.; Tellis, J. C.; Molander, G. Preparation of visible-light-activated metal complexes and their use in photoredox/nickel dual catalysis. *Nat. Prot.* **2017**, *12*, 472.

115. Patel, N. P.; Kelly, C. B.; Siegenfeld, A. P.; Molander, G. A. Mild, Redox-Neutral Alkylation of Imines Enabled by an Organic Photocatalyst. *ACS Catal.* **2017**, *7*, 1766.

116. Phelan, J. P.; Wiles, R. W.; Lang, S. B.; Kelly, C. B.; Molander, G. A. Rapid access to diverse, trifluoromethyl-substituted alkenes using complementary strategies. *Chem. Sci.* **2018**, *9*, 3215.

117. Seebach, D.; Imwinkelried, R; Stucky, G. Optisch aktive Alkohole aus 1,3-Dioxan-4-onen: eine praktikable Variante der enantioselektiven Synthese unter nucleophiler Substitution an Acetal-Zentren. *Helv. Chim. Acta* **1987**, *70*, 448.

118. Rosenau, C. P.; Jelier, B. J.; Gossert, A. D.; Togni, A. Exposing the Origins of Irreproducibility in Fluorine NMR Spectroscopy. *Angew. Chem., Int. Ed.* **2018**, *57*, 9528.

119. Durandetti, M., Maddaluno, J. *Nickel Bromide Bipyridine* in Encyclopedia of Reagents for Organic Synthesis; **2014.**

120. Patterson, S.; Alphey, M. S.; Jones, D. C.; Shanks, E. J.; Street, I. P.; Frearson, J. A.; Wyatt, P. G.; Gilbert, I. H.; Fairlamb, A. H. Dihydroquinazolines as a Novel Class of *Trypanosoma*

brucei Trypanothione Reductase Inhibitors: Discovery, Synthesis, and Characterization of their Binding Mode by Protein Crystallography. *J. Med. Chem.* **2011**, *54*, 6514.

121. Abdelkafi, H.; Michau, A.; Clerget, A.; Buisson, D.-A.; Johannes, L.; Gillet, D.; Barbier, J.; Cintrat, J.-C. Synthesis, Chiral Separation, Absolute Configuration Assignment, and Biological Activity of Enantiomers of Retro-1 as Potent Inhibitors of Shiga Toxin. *ChemMedChem*, **2015**, *10*, 1153.

122. Linstad, E. J.; Vāvere, A. L.; Hu B.; Kempinger J. J.; Snyder S. E.; DiMagno, S.G. Thermolysis and radiofluorination of diaryliodonium salts derived from anilines. *Org. Biomol. Chem.* **2017**, *15*, 2246.

123. Lee, Y.; Silverman, R. B. Catalysis by Amino Acid-Derived Tetracoordinate Complexes: Enantioselective Addition of Dialkylzincs to Aliphatic and Aromatic Aldehydes. *Org. Lett.* **2000**, *2*, 3003.

124. Stone, I. B.; Jermaks, J.; MacMillan, S. N.; Lambert, T. H. The Hydrazine–O_2 Redox Couple as a Platform for Organocatalytic Oxidation: Benzo[*c*]cinnoline-Catalyzed Oxidation of Alkyl Halides to Aldehydes. *Angew. Chem. Int. Ed.* **2018**, *57*, 12494.

125. Choshi, T.; Yamada, S.; Sugino, E.; Kuwada, T.; Hibino, S. Total synthesis of grossularines-1 and -2. *J. Org. Chem.* **1995**, *60*, 5899.

126. Doering, N. A.; Kou, K. G. M.; Norseeda, K.; Lee, J. C.; Marth, C. J.; Gallego, G. M.; Sarpong, R. A Copper-Mediated Conjugate Addition Approach to Analogues of Aconitine-Type Diterpenoid Alkaloids. *J.Org. Chem.* **2018**, *83*, 12911.

127. Barbe, G.; Charette, A. B. Highly Chemoselective Metal-Free Reduction of Tertiary Amides. *J. Am. Chem. Soc.* **2008**, *130*, 18.

128. Yuan, Y.-C.; Kamaraj, R.; Bruneau, C.; Labasque, T.; Roisnel, T.; Gramage-Doria, R. Unmasking Amides: Ruthenium-Catalyzed Protodecarbonylation of N-Substituted Phthalimide Derivatives. *Org. Lett.* **2017**, *19*, 6404.

129. Devine, W.; Woodring, J. L.; Swaminathan, U.; Amata, E.; Patel, G.; Erath, J.; Roncal, N. E.; Lee, P.J.; Leed, S. E.; Rodriguez, A.; Mensa-Wilmot, K.; Sciotti, R. J.; Pollastri, M. P. Protozoan Parasite Growth Inhibitors Discovered by Cross-Screening Yield Potent Scaffolds for Lead Discovery. *J. Med. Chem.* **2015**, *58*, 5522.

130. Goodwin, N. C.; Cianchetta, G.; Burgoon, H. A.; Healy, J.; Mabon, R.; Strobel, E. D.; Allen, J.; Wang, S.; Hamman, B. D.; Rawlins, D. B. Discovery of a Type III Inhibitor of LIM Kinase 2 That Binds in a DFG-Out Conformation. *ACS Med. Chem. Lett.* **2015**, *6*, 53.

131. Fawcett, J. P.; Wang, Y.; Mutsuga, T.; Myers, E. L.; Aggarwal, V. K. Photoinduced decarboxylative borylation of carboxylic acids. *Science* **2017**, *357*, 283.

132. Dai, J.-J.; Zhang, W.-M.; Shu, Y.-J.; Sun, Y.-Y.; Xu, J.; Feng, Y.-S.; Xu, H.-J. Deboronative cyanation of potassium alkyltrifluoroborates via photoredox catalysis. *Chem. Commun.* **2016**, *52*, 6793.

133. Mun, S.; Lee, J.-E.; Yun, J. Copper-Catalyzed β-Boration of α,β-Unsaturated Carbonyl Compounds: Rate Acceleration by Alcohol Additives. *Org. Lett.* **2006**, *8*, 4887.

134. Pulis, A. P.; Blair, D. J.; Torres, E.; Aggarwal, V. K. Synthesis of Enantioenriched Tertiary Boronic Esters by the Lithiation/Borylation of Secondary Alkyl Benzoates. *J. Am. Chem. Soc.* **2013**, *135*, 16054.

135. Campbell, M. W.; Compton, J. S.; Kelly, C. B.; Molander, G. A. Three-Component Olefin Dicarbofunctionalization Enabled by Nickel/Photoredox Dual Catalysis. *J. Am. Chem. Soc.,* **2019**, *141*, 20069-20078.

136. Guo, L.; Yuan, M. B.; Zhang, Y. Y.; Wang, F.; Zhu, S. Q.; Gutierrez, O.; Chu, L. L. General Method for Enantioselective Three-Component Carboarylation of Alkenes Enabled by Visible-Light Dual Photoredox/Nickel Catalysis. *J. Am. Chem. Soc.,* **2020**, *142*, 20390-20399.

137. Guo, L.; Tu, H. Y.; Zhu, S. Q.; Chu, L. L. Selective, Intermolecular Alkylarylation of Alkenes via Photoredox/Nickel Dual Catalysis. *Organic Letters* **2019**, *21*, 4771-4776.

138. Garcia-Dominguez, A.; Mondal, R.; Nevado, C. Dual Photoredox/Nickel-Catalyzed Three-Component Carbofunctionalization of Alkenes. *Angew. Chem. Int. Ed.,* **2019**, *58*, 12286-12290.

139. Sun, S. Z.; Duan, Y. Y.; Mega, R. S.; Somerville, R. J.; Martin, R. Site-Selective 1,2-Dicarbofunctionalization of Vinyl Boronates through Dual Catalysis. *Angew. Chem. Int. Ed.,* **2020**, *59*, 4370-4374.

140. Zheng, S. L.; Chen, Z. M.; Hu, Y. Y.; Xi, X. X.; Liao, Z. X.; Li, W. R.; Yuan, W. M. Selective 1,2-Aryl-Aminoalkylation of Alkenes Enabled by Metallaphotoredox Catalysis. *Angew. Chem. Int. Ed.,* **2020**, *59*, 17910-17916.

141. Mega, R. S.; Duong, V. K.; Noble, A.; Aggarwal, V. K. Decarboxylative Conjunctive Cross-coupling of Vinyl Boronic Esters using Metallaphotoredox Catalysis. *Angew. Chem. Int. Ed.,* **2020**, *59*, 4375-4379.

142. de Montellano, P. R. O. Hydrocarbon Hydroxylation by Cytochrome P450 Enzymes. *Chem. Rev.,* **2010**, *110*, 932-948.

143. Capaldo, L.; Ravelli, D. Hydrogen Atom Transfer (HAT): A Versatile Strategy for Substrate Activation in Photocatalyzed Organic Synthesis. *Eur. J. Org. Chem.,* **2017**, *15*, 2056-2071.

144. Giese, B. Formation of C-C bonds by addition of free-radicals to alkenes. *Angew. Chem.,* **1983**, *22*, 753-764.

145. Shaw, M. H.; Shurtleff, V. W.; Terrett, J. A.; Cuthbertson, J. D.; MacMillan, D. W. C. Native functionality in triple catalytic cross-coupling: sp(3) C-H bonds as latent nucleophiles. *Science* **2016**, *352*, 1304-1308.

146. Jeffrey, J. L.; Terrett, J. A.; MacMillan, D. W. C. O-H hydrogen bonding promotes H-atom transfer from alpha C-H bonds for C-alkylation of alcohols. *Science* **2015**, *349*, 1532-1536.

147. Heitz, D. R.; Tellis, J. C.; Molander, G. A. Photochemical Nickel-Catalyzed C-H Arylation: Synthetic Scope and Mechanistic Investigations. *J. Am. Chem. Soc.,* **2016**, *138*, 12715-12718.

148. Shields, B. J.; Doyle, A. G. Direct C(sp(3))-H Cross Coupling Enabled by Catalytic Generation of Chlorine Radicals. *J. Am. Chem. Soc.,* **2016**, *138*, 12719-12722.

149. Capaldo, L.; Ravelli, D.; Fagnoni, M. Direct Photocatalyzed Hydrogen Atom Transfer (HAT) for Aliphatic C–H Bonds Elaboration. *Chem. Rev.,* **2021**, *122*, 1875–1924.

150. Fan, X. Z.; Rong, J. W.; Wu, H. L.; Zhou, Q.; Deng, H. P.; Da Tan, J.; Xue, C. W.; Wu, L. Z.; Tao, H. R.; Wu, J. Eosin Y as a Direct Hydrogen-Atom Transfer Photocatalyst for the Functionalization of C-H Bonds. *Angew. Chem. Int. Ed.,* **2018**, *57*, 8514-8518.

151. Protti, S.; Ravelli, D.; Fagnoni, M.; Albini, A. Solar light-driven photocatalyzed alkylations. Chemistry on the window ledge. *Chem. Commun.,* **2009**, *47*, 7351-7353.

152. Sarver, P. J.; Bacauanu, V.; Schultz, D. M.; DiRocco, D. A.; Lam, Y. H.; Sherer, E. C.; MacMillan, D. W. C. The merger of decatungstate and copper catalysis to enable aliphatic C(sp(3))-H trifluoromethylation. *Nat. Chem.,* **2020**, *12,* 459-465.

153. Dorman, G.; Nakannura, H.; Pulsipher, A.; Prestwich, G. D. The Life of Pi Star: Exploring the Exciting and Forbidden Worlds of the Benzophenone Photophore. *Chem. Rev.,* **2016**, *116*, 15284-15398.

154. Ferro-Costas, D.; Pendas, A. M.; Gonzalez, L.; Mosquera, R. A. Beyond the molecular orbital conception of electronically excited states through the quantum theory of atoms in molecules. *Phys. Chem. Chem. Phys.,* **2014**, *16*, 9249-9258.

155. Campbell, M. W.; Yuan, M.; Polites, V. C.; Gutierrez, O.; Molander, G. A. Photochemical C–H Activation Enables Nickel-Catalyzed Olefin Dicarbofunctionalization. *J. Am. Chem. Soc.,* **2021**, *143*, 3901-3910.

156. Bolland, J. L.; Cooper, H. R. The photo-sensitized oxidation of ethanol. *Proc. R. Soc. A: Math. Phys. Eng. Sci.,* **1954**, *225*, 405-426.

157. Zhu, D. L.; Young, D. J.; Li, H. X. Carbonyl-Photoredox/Metal Dual Catalysis: Applications in Organic Synthesis. *Synthesis-Stuttgart* **2020**, *52*, 3493-3510.

158. Shen, Y. Y.; Gu, Y. T.; Martin, R. sp(3) C-H Arylation and Alkylation Enabled by the Synergy of Triplet Excited Ketones and Nickel Catalysts. *J. Am. Chem. Soc.,* **2018**, *140*, 12200-12209.

159. Dewanji, A.; Krach, P. E.; Rueping, M. The Dual Role of Benzophenone in Visible-Light/Nickel Photoredox-Catalyzed C-H Arylations: Hydrogen-Atom Transfer and Energy Transfer. *Angew. Chem. Int. Ed.,* **2019**, *58*, 3566-3570.

160. Viehe, H. G.; Janousek, Z.; Merenyi, R.; Stella, L. The captodative effect. *Acc. Chem. Res.,* **1985**, *18*, 148-154.

161. De Vleeschouwer, F.; Van Speybroeck, V.; Waroquier, M.; Geerlings, P.; De Proft, F. Electrophilicity and nucleophilicity index for radicals. *Org. Lett.* **2007**, *9*, 2721-2724.

162. Primer, D. N.; Molander, G. A. Enabling the Cross-Coupling of Tertiary Organoboron Nucleophiles through Radical-Mediated Alkyl Transfer. *J. Am. Chem. Soc.,* **2017**, *139*, 9847-9850.

163. Domingo, L. R.; Perez, P. Global and local reactivity indices for electrophilic/nucleophilic free radicals. *Org. Biomol. Chem.,* **2013**, *11*, 4350-4358.

164. Liakos, D. G.; Guo, Y.; Neese, F. Comprehensive Benchmark Results for the Domain Based Local Pair Natural Orbital Coupled Cluster Method (DLPNO-CCSD(T)) for Closed- and Open-Shell Systems. *J. Phys. Chem. A,* **2020**, *124*, 90-100.

165. Yuan, M. B.; Song, Z. H.; Badir, S. O.; Molander, G. A.; Gutierrez, O. On the Nature of C(sp(3))-C(sp(2)) Bond Formation in Nickel-Catalyzed Tertiary Radical Cross-Couplings: A

Case Study of Ni/Photoredox Catalytic Cross-Coupling of Alkyl Radicals and Aryl Halides. *J. Am. Chem. Soc.,* **2020**, *142*, 7225-7234.

166. Gawlita, E.; Lantz, M.; Paneth, P.; Bell, A. F.; Tonge, P. J.; Anderson, V. E. H-bonding in alcohols is reflected in the C alpha-H bond strength: Variation of C-D vibrational frequency and fractionation factor. *J. Am. Chem. Soc.,* **2000**, *122*, 11660-11669.

167. Tian, Y. F.; Liu, Z. Q. H-Bonding-promoted radical addition of simple alcohols to unactivated alkenes. *Green Chem.,* **2017**, *19*, 5230-5235.

168. Duplais, C.; Bures, F.; Sapountzis, I.; Korn, T. J.; Cahiez, G.; Knochel, P. An efficient synthesis of diaryl ketones by iron-catalyzed arylation of aroyl cyanides. *Angew. Chem. Int. Ed.,* **2004**, *43*, 2968-2970.

169. Wang, Q.; Tang, X. Y.; Shi, M. Metal-Free Cross-Coupling of Arylboronic Acids and Derivatives with DAST-Type Reagents for Direct Access to Diverse Aromatic Sulfinamides and Sulfonamides. *Angew. Chem. Int. Ed.,* **2016**, *55*, 10811-10815.

170. Csuk, R.; Dorr, P. Convenient oxidative debenzylation using dimethyldioxirane. *Tetrahedron,* **1994**, *50*, 9983-9988.

171. Lee, C. T.; Yang, W. T.; Parr, R. G. Development of the colle-salvetti correlation-energy formula into a functional of the electron-density. *Phys. Rev. B,* **1988**, *37*, 785-789.

172. Grimme, S.; Antony, J.; Ehrlich, S.; Krieg, H. A consistent and accurate ab initio parametrization of density functional dispersion correction (DFT-D) for the 94 elements H-Pu. *J. Chem. Phys.,* **2010**, *132,* 154104.

173. Weigend, F.; Ahlrichs, R. Balanced basis sets of split valence, triple zeta valence and quadruple zeta valence quality for H to Rn: Design and assessment of accuracy. *Phys. Chem. Chem. Phys.,* **2005**, *7*, 3297-3305.

174. Cossi, M.; Rega, N.; Scalmani, G.; Barone, V. Energies, structures, and electronic properties of molecules in solution with the C-PCM solvation model. *J. Comput. Chem.,* **2003**, *24*, 669-681.

175. *Gaussian 16, Revision C.01*; Gaussian Inc.: Wallingford, CT, 2019.

176. Hellweg, A.; Hattig, C.; Hofener, S.; Klopper, W. Optimized accurate auxiliary basis sets for RI-MP2 and RI-CC2 calculations for the atoms Rb to Rn. *Theor. Chem. Acc.,* **2007**, *117*, 587-597.

177. Neese, F. The ORCA program system. *Wiley Interdisciplinary Reviews-Computational Molecular Science* **2012**, *2* (1), 73-78.

178. *CYLview 1.0b*; Université de Sherbrooke, 2009.

179. Johnson, E. R.; Keinan, S.; Mori-Sanchez, P.; Contreras-Garcia, J.; Cohen, A. J.; Yang, W. T. Revealing Noncovalent Interactions. *J. Am. Chem. Soc.,* **2010**, *132*, 6498-6506.

180. Humphrey, W.; Dalke, A.; Schulten, K. VMD: Visual molecular dynamics. *J. Mol. Graph. Model.,* **1996**, *14*, 33-38.

181. Shah, P.; Westwell, A. D. The role of fluorine in medicinal chemistry. *J. Enz. Inhib. Med. Chem.,* **2007**, *22*, 527-540.

182. Zhou, Y.; Wang, J.; Gu, Z. N.; Wang, S. N.; Zhu, W.; Acena, J. L.; Soloshonok, V. A.; Izawa, K.; Liu, H. Next Generation of Fluorine-Containing Pharmaceuticals, Compounds Currently in Phase II-III Clinical Trials of Major Pharmaceutical Companies: New Structural Trends and Therapeutic Areas. *Chem. Rev.* **2016**, *116*, 422-518.

183. Belhomme, M. C.; Besset, T.; Poisson, T.; Pannecoucke, X. Recent Progress toward the Introduction of Functionalized Difluoromethylated Building Blocks onto C(sp(2)) and C(sp) Centers. *Chem. Eur. J.,* **2015**, *21*, 12836-12865.

184. Hu, J. B.; Zhang, W.; Wang, F. Selective difluoromethylation and monofluoromethylation reactions. *Chem. Commun.,* **2009**, *48*, 7465-7478.

185. Nyffeler, P. T.; Duron, S. G.; Burkart, M. D.; Vincent, S. P.; Wong, C. H. Selectfluor: Mechanistic insight and applications. *Angew. Chem. Int. Ed.,* **2005**, *44*, 192-212.

186. Bui, T. T.; Hong, W. P.; Kim, H. K. Recent Advances in Visible Light-mediated Fluorination. *J. Fluor. Chem.,* **2021**, *247*.

187. Fernandes, P.; Martens, E.; Pereira, D. Nature nurtures the design of new semi-synthetic macrolide antibiotics. *J. Antibio.,* **2017**, *70*, 527-533.

188. Middleton, W. J. New fluorinating reagents - dialkylaminosulfur fluorides. *J. Org. Chem.,* **1975**, *40*, 574-578.

189. Sofia, M. J.; Bao, D.; Chang, W.; Du, J. F.; Nagarathnam, D.; Rachakonda, S.; Reddy, P. G.; Ross, B. S.; Wang, P. Y.; Zhang, H. R.; et al. Discovery of a beta-D-2 '-Deoxy-2 '-alpha-fluoro-2 '-beta-C-methyluridine Nucleotide Prodrug (PSI-7977) for the Treatment of Hepatitis C Virus. *J. Med. Chem.,* **2010**, *53*, 7202-7218.

190. Boswell, G. A. Prepn. of vinylene fluoride(s) - by reacting a ketone with a di:substd.-amino-sulphur tri:fluoride, useful as therapeutic agents etc. US4212815-A.

191. Reddy, V. P.; Perambuduru, M.; Alleti, R. Synthetic Approaches to gem-Difluoromethylene Compounds, Advances in Organic Synthesis Modern Organofluorine Chemistry-Synthetic Aspects. Bentham Science Publisher, 2006; pp 327-351.

192. Luo, Y.-R. *Handbook of Bond Dissociation Energies in Organic Compounds*; CRC Press, 2003.

193. Fuchibe, K.; Ohshima, Y.; Mitomi, K.; Akiyama, T. Low-valent niobium-catalyzed reduction of alpha,alpha,alpha-trifluorotoluenes. *Org. Lett.,* **2007**, *9*, 1497-1499.

194. Chen, K.; Berg, N.; Gschwind, R.; Konig, B. Selective Single C(sp(3))-F Bond Cleavage in Trifluoromethylarenes: Merging Visible-Light Catalysis with Lewis Acid Activation. *J. Am. Chem. Soc.,* **2017**, *139*, 18444-18447.

195. Kim, B. C.; Park, A.; An, J. E.; Lee, W. K.; Lee, H. B.; Shin, H. Highly Improved Copper-Mediated Michael Addition of Ethyl Bromodifluoroacetate in the Presence of Protic Additive. *Synthesis-Stuttgart* **2012**, *44*, 3165-3170.

196. Xia, T. T.; He, L.; Liu, Y. H. A.; Hartwig, J. F.; Liao, X. B. Palladium-Catalyzed Cross-Coupling of Ethyl Bromodifluoroacetate with Aryl Bromides or Triflates and Cross-Coupling of Ethyl Bromofluoroacetate with Aryl Iodides. *Org. Lett.,* **2017**, *19*, 2610-2613.

197. Yoshida, M.; Suzuki, D.; Iyoda, M. Practically useful Reformatsky type reactions of chlorodifluoroacetate and bromodifluoroacetate induced by samarium(II) diiodide. *Synth. Commun.,* **1996**, *26*, 2523-2529.

198. Yu, C.; Iqbal, N.; Park, S.; Cho, E. J. Selective difluoroalkylation of alkenes by using visible light photoredox catalysis. *Chem. Commun.,* **2014**, *50*, 12884-12887.

199. Yu, Y. J.; Zhang, F. L.; Peng, T. Y.; Wang, C. L.; Cheng, J.; Chen, C.; Houk, K. N.; Wang, Y. F. Sequential C-F bond functionalizations of trifluoroacetamides and acetates via spin-center shifts. *Science* **2021**, *371*, 1232-1239.

200. Wessig, P.; Muehling, O. Spin-center shift (SCS) - A versatile concept in biological and synthetic chemistry. *Eur. J. Org. Chem.,* **2007**, *14*, 2219-2232.

201. Zhu, D. L.; Young, D. J.; Li, H. X. Carbonyl-Photoredox/Metal Dual Catalysis: Applications in Organic Synthesis. *Synthesis-Stuttgart* **2020**, *52*, 3493-3510.

202. Saveant, J. M.; Nadojo, L.; Lamy, E. Standard potential and kinetic parameters of the electrochemical reduction of carbon dioxide in dimethylformamide. *J. Electroanal. Chem.,* **1977**, *78*, 403-407.

203. Wang, H.; Gao, Y.; Zhou, C.; Li, G. Visible-Light-Driven Reductive Carboarylation of Styrenes with CO_2 and Aryl Halides. *J. Am. Chem. Soc.,* **2020**, *142*, 8122-8129.

204. Chmiel, A. F.; Williams, O. P.; Chernowsky, C. P.; Yeung, C. S.; Wickens, Z. K. Non-innocent Radical Ion Intermediates in Photoredox Catalysis: Parallel Reduction Modes Enable Coupling of Diverse Aryl Chlorides. *J. Am. Chem. Soc.,* **2021**, *143*, 10882-10889.

205. Hendy, C. M.; Smith, G. C.; Xu, Z. H.; Lian, T. Q.; Jui, N. T. Radical Chain Reduction via Carbon Dioxide Radical Anion ($CO_2^{\bullet-}$). *J. Am. Chem. Soc.,* **2021**, *143*, 8987-8992.

206. Vogt, D. B.; Seath, C. P.; Wang, H. B.; Jui, N. T. Selective C-F Functionalization of Unactivated Trifluoromethylarenes. *J. Am. Chem. Soc.,* **2019**, *141*, 13203-13211.

207. Nakajima, T.; Matsugi, T.; Goto, W.; Kageyama, M.; Mori, N.; Matsumura, Y.; Hara, H. New fluoroprostaglandin F-2 alpha derivatives with prostanoid FP-receptor agonistic activity as potent ocular-hypotensive agents. *Bio. Pharm. Bull.,* **2003**, *26*, 1691-1695.

208. Casteels, M.; Foulon, V.; Mannaerts, G. P.; Van Veldhoven, P. P. Alpha-oxidation of 3-methyl-substituted fatty acids and its thiamine dependence. *Eur. J. Biochem.,* **2003**, *270*, 1619-1627.

209. Yin, Z.-B.; Ye, J.-H.; Zhou, W.-J.; Zhang, Y.-H.; Ding, L.; Gui, Y.-Y.; Yan, S.-S.; Li, J.; Yu, D.-G. Oxy-Difluoroalkylation of Allylamines with CO_2 via Visible-Light Photoredox Catalysis. *Org. Lett.,* **2018**, *20*, 190-193.

210. Monteith, E. R.; Mampuys, P.; Summerton, L.; Clark, J. H.; Maes, B. U. W.; McElroy, C. R. Why we might be misusing process mass intensity (PMI) and a methodology to apply it effectively as a discovery level metric. *Green Chem.,* **2020**, *22*, 123-135.

211. Appel, R.; Mayr, H. Quantification of the Electrophilic Reactivities of Aldehydes, Imines, and Enones. *J. Am. Chem. Soc.,* **2011**, *133*, 8240-8251.

212. Nagarapu, L.; Gaikwad, H. K.; Bantu, R.; Manikonda, S. R.; Kumar, C. G.; Pombala, S. Lewis acid-assisted olefin cross-metathesis reaction: an efficient approach for the synthesis

of glycosidic-pyrroloquinolinone based novel building blocks of camptothecin and evaluation of their antitumor activity. *Tet. Lett.,* **2012**, *53*, 1287-1291.

213. Zhao, W. J.; Yan, M.; Huang, D.; Ji, S. J. New reaction of enamines with aryldiazoacetates catalyzed by transition metal complexes. *Tetrahedron* **2005**, *61*, 5585-5593.

214. Mereyala, H. B.; Gaddam, B. R. Synthesis of conduritol-a, conduritol-(+)-c and conduritol-(-)-c from d-galactose. *J. Chem. Soc. P. Trans. 1,* **1994**, *15*, 2187-2190.

215. Su, C. C.; Williard, P. G. Isomerization of Allyl Ethers Initiated by Lithium Diisopropylamide. *Org. Lett.,* **2010**, *12*, 5378-5381.

216. Chattopadhyay, S. K.; Ghosh, S.; Sarkar, S.; Bhadra, K. alpha,beta-Didehydrosuberoylanilide hydroxamic acid (DDSAHA) as precursor and possible analogue of the anticancer drug SAHA. *Beilstein J. Org. Chem.,* **2019**, *15*, 2524-2533.